FINAL REPORT

Methods for Estimating Radiation Doses from Short-Lived Gaseous Radionuclides and Radioactive Particles Released to the Atmosphere during Early Hanford Operations

Centers for Disease Control and Prevention
Department of Health and Human Services

November 2002

Note: Support files for this report require Microsoft Excel and Microsoft Access. Click here to download the support files.

Click here to download the entire report. You will require Microsoft Word to read the report, plus Excel and Access to use the support files.

Submitted to the Centers for Disease Control and Prevention
in partial fulfillment of contract number 200-95-0927

"Setting the standard in environmental health"

RAC

Risk Assessment Corporation
417 Till Road, Neeses, SC 29107
Phone 803.536.4883 Fax 803.534.1995

FINAL REPORT

Methods for Estimating Radiation Doses from Short-Lived Gaseous Radionuclides and Radioactive Particles Released to the Atmosphere during Early Hanford Operations

Centers for Disease Control and Prevention
Department of Health and Human Services

November 2002

Contributing Authors

Paul G. Voillequé, MJP Risk Assessment, Inc.
George G. Killough, Hendecagon Corporation
Susan K. Rope, Environmental Perspectives, Inc.

Principal Investigator

John E. Till, PhD., Risk Assessment Corporation

Submitted to the Centers for Disease Control and Prevention
in partial fulfillment of contract number 200-95-0927

SUMMARY

This report describes methods for calculating "worst case[1]" radiation doses from short-lived gaseous radionuclides and radioactive particles that were released to the atmosphere during the early years of operations at the Hanford Reservation near Richland, Washington. The work addresses some concerns that remained following the extensive Hanford Dose Reconstruction (HEDR) project (Farris et al. 1994).[2] The HEDR Project focused on doses to members of the public, located offsite, from releases of various radionuclides, especially ^{131}I, which was determined to be most important. In contrast, the present work addresses possible doses to persons who worked or lived *on* as well as near the Hanford Reservation. Those persons include military personnel stationed on the reservation for protection of the facilities and construction workers who built additional reactors and processing plants after the first facilities began operating in late 1944. Whereas short-lived gaseous radionuclides were not important for offsite residents, they could have been important contributors to dose for onsite workers. In addition, exposure to radioactive particles, the largest of which settled onsite close to the release points, was considered. Primary features of the Hanford Reservation in 1943–1945 are illustrated in Figure S-1.

This report addresses outdoor exposure to radionuclides released to the atmosphere; it does not address exposure to radiation within operational facilities. As requested in the scope of work, we did not design these methods for rigorous dose reconstruction with uncertainty estimation, but rather to perform conservative calculations (i.e., tending to overestimate doses). The work was conducted under a task order agreement between the Centers for Disease Control and Prevention and *Risk Assessment Corporation*.

A first step in the evaluation was to determine the most important radionuclides that should be included. We used a screening procedure that incorporated factors established by the National Council on Radiation Protection and Measurements. The screening factors use the effective dose[3] concept to reflect absorbed doses to all body organs and tissues received from all important atmospheric exposure pathways. The screening procedure used some previously published estimates of amounts of radionuclides released to air from the production reactors. Estimates of releases from fuel processing facilities were based on published processing rates and on processing rates estimated specifically for the screening procedure. In all cases a screening index (the product of the release rate and the screening factor) was computed for each radionuclide and the results were compared.

---

[1] Terminology used in scope of work document. Discussed in other sections of this report, especially Appendix D.

[2] Underlining of references, section numbers, figures, or tables indicates a hyperlink in the electronic version of this report. Clicking on the underlined text will take the reader to the referenced object.

[3] Effective dose (units of rem or mrem) incorporates the absorbed dose received by all organs and tissues (units of rad or mrad), the radiation weighting factors, which address relative biological effectiveness, and the tissue/organ weighting factors, which relate to risk of death from cancer due to radiation exposure.

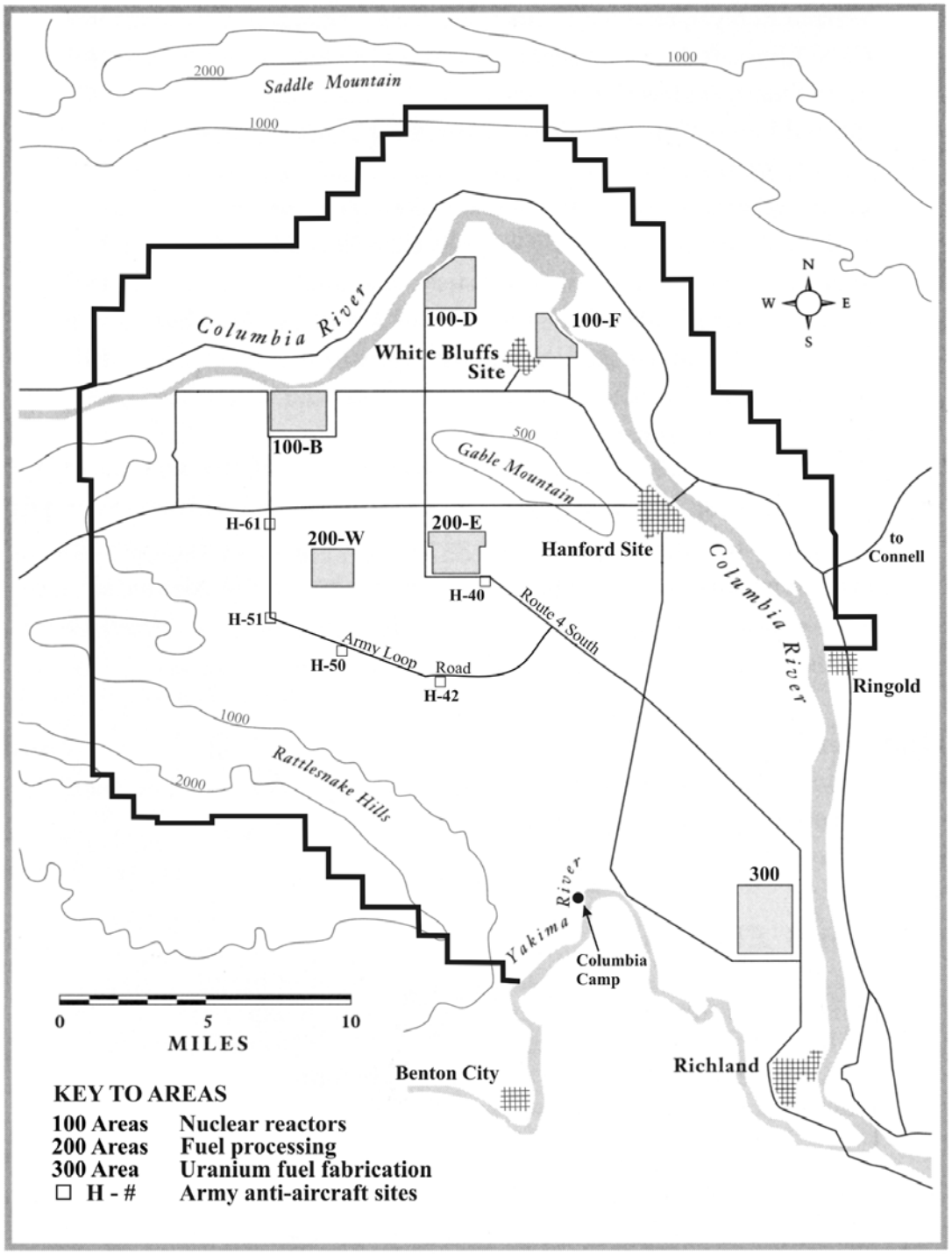

Figure S-1. Primary features of the Hanford Reservation in 1943–1945, then called the "Hanford Engineer Works," adapted from figures in Sanger (1995) and Jones (1985). The dark line shows the outer edge of land acquisition Area B, discussed in Jones (1985). The southeast boundary of the government-occupied land is defined by the Yakima and Columbia Rivers and includes Area C (Richland). The approximate locations of army anti-aircraft sites are based on maps discussed in Section 3.1.2. Contour lines show elevations in feet.

We applied the screening procedure to atmospheric releases from the production reactors (including 10 isotopes of xenon and krypton, seven isotopes of iodine and bromine, ^{41}Ar, ^{14}C, and ^{3}H). For the fuel processing facilities, the initial screening considered 65 particulate radionuclides from which 33 were selected because they were estimated to contribute more than 1 part in a million to the initial total screening index. The fact that the relative amounts of radionuclides released from Hanford facilities varied over time complicated the analyses. Although the largest releases from Hanford facilities occurred during the first years of operation, both military and construction personnel were also working onsite during the 1950s. To assess the effect of different times on the selection of important radionuclides, we repeated the screening procedure for eight separate months distributed over the years 1945 through 1956. For each time, the importance of each radionuclide, relative to iodine-131 (^{131}I) as a reference, was determined and ranked. The overall combined list of key radionuclides,[4] from most to least important, was ^{131}I, ^{41}Ar, ^{95}Zr, ^{137}Cs, ^{144}Ce, ^{239}Pu, ^{95}Nb, ^{106}Ru, ^{103}Ru, ^{134}Cs, ^{91}Y, ^{90}Sr, and ^{141}Ce. These nuclides contributed over 99% of the total screening index during all eight screening comparisons.

Estimates of the monthly releases of these 13 radionuclides were made for the period from December 1944 through February 1956. We evaluated releases from a total of 11 release facilities, four processing facilities in the 200 Areas and seven reactors. Release estimates were developed for ^{41}Ar releases from the reactors and for ^{95}Zr, ^{137}Cs, ^{144}Ce, ^{239}Pu, ^{95}Nb, ^{106}Ru, ^{103}Ru, ^{134}Cs, ^{91}Y, ^{90}Sr, and ^{144}Ce releases from the fuel processing facilities. Others have estimated releases of ^{131}I from those facilities and their values were used. The releases of particulate radionuclides included both routine operational releases and unusual (or episodic) release conditions. The episodic releases occurred when radioactivity that had been deposited on the interior surfaces of fuel processing plant exhaust ventilation systems and stacks was made airborne and discharged to the atmosphere. We used radionuclide processing rates (monthly estimates), release fractions, and effluent treatment modifiers (when appropriate) to estimate the routine operational releases. Each of the contributing factors was uncertain, and the resulting monthly release estimates are presented as statistical distributions of possible values. The 50th and 95th percentiles of the distributions of radionuclide release estimates are included in the report.

There were episodic releases of physically large radioactive particles in the late 1940s and early 1950s. The resulting ground surface deposits were more dense within several miles of the release points. The first releases of these so-called “active particles” were due to corrosion of the exhaust system ductwork by acidic gases during the early years of reprocessing plant operations. Because there were no effluent filtration systems at that time, these episodic releases did not greatly affect the total amount of radioactivity discharged. However, the contaminated corrosion particles were larger than those in routine releases and were deposited around and downwind of the processing plant stacks. Environmental surveys documented the presence of the particles, which contained iron and a mixture of the radionuclides identified above.

The second group of episodic releases of active particles occurred in the 1950s. The key radioactive constituents were ^{103}Ru and ^{106}Ru in large particles released from the REDOX reprocessing facility. A layer of radioactive contamination formed on the lining of the stack by deposition of volatile ruthenium tetroxide and ammonium nitrate. When the layer of

[4] Daughter product radionuclides are not listed here but were included in the methodology.

contaminated ammonium nitrate was disturbed, large radioactive particles were discharged. Although these releases from the stack walls were not well monitored, environmental surveys clearly showed the presence of the released particles in the vicinity and downwind of the stack. Releases of this type occurred during June and September 1952, August 1953, and April–June 1954. Exhaust scrubber system failures also led to unusual releases of ruthenium during March 1952 and January 1954. Other processing activities caused unusual releases in April 1952 and September 1953. We used data collected at the times of these events to estimate "apparent release fractions" for all of them. These "apparent release fractions" were all higher than the release fractions used to estimate routine ruthenium releases. The release estimates are characterized by relatively large uncertainties.

Many measurements of radioactivity in the environment were made during the early years of operation. We compiled the most relevant data and summarized them in Section 4 of this report. While the measurement techniques were not as sensitive or reliable as those used later, the environmental data do provide useful information about affected areas and time periods. The environment near the 200 Areas was most highly contaminated. Radioactivity was mainly spread to the east and southeast of the release points. Concentrations generally decreased rapidly with increasing distance from the contamination sources; however, some of the large particles released from the REDOX facility in 1952–1954 were known to have traveled long distances. After corrective action was taken to reduce particulate releases from REDOX, the number of active particles on the ground decreased due to radioactive decay, weathering, and active measures such as sprinkling, plowing, and seeding. The environmental data indicate that the time periods most affected by releases of large radioactive particles were 1947–1949 and 1952–1955. Iodine releases produced most of the contamination before 1948, whereas releases from the REDOX facility (mainly ruthenium) significantly contributed to environmental contamination during 1952–1955. Large active particles (particularly the large ruthenium flakes) were sometimes visibly discernible from soil and were easily detectable with radiation survey instruments. Physical and radiological measurements of particles collected from contaminated areas helped us define the characteristics of active particles used in the examples in this report.

The primary exposure pathways for persons working and living onsite were inhalation of airborne radionuclides, direct radiation from plumes and material deposited on the ground, and direct physical contact with large active particles. We wrote a computer program called the Hanford Calculator (Hcalc) specifically for this project to implement the environmental transport and dose calculations for airborne releases. Cautious approaches were used that would generally overestimate the radiation doses received. The program can estimate doses at both a working location and a residence on or near the reservation by specifying those geographic coordinates. Hcalc also includes exposure of persons from food chain contamination, which applies to nearby farming areas.

The general strategy followed in this report for avoiding underestimation of exposure and dose is similar to methods used in the 1970s and 1980s for environmental assessments. Calculations deliberately overestimate concentrations of released radionuclides in environmental media by making assumptions that favor this tendency or by altering the underlying models to increase predictions. Although these methods are supported by decades of collective experience, it is usually not possible to prove rigorously that the resulting estimates will never understate dose or risk.

To provide more assurance against underprediction, Appendix D presents stochastic methods that may be applied ad hoc to the results of calculations done with the basic methodology. By taking into account uncertainties in releases and in atmospheric transport of released radionuclides, these methods lead to probability distributions for concentrations of the radionuclides in the air at the location of a designated receptor (which could be an individual breathing the contaminated air or a garden on which radioactive particles deposited). These uncertainty distributions can be propagated into calculated dose and risk, and the use of a high percentile would give confidence that underestimation is correspondingly unlikely (for example, if the 95th percentile were chosen, the probability of underestimation would be 5% or less).

We used the Hcalc program to estimate radiation doses for cumulative airborne releases of radioactive particles and gases from the separations plants and reactors considered in this report. A contour map illustrates the spatial variation in effective dose for a hypothetical person who was continuously present outdoors from January 1, 1945 through December 31, 1961. Although most airborne releases evaluated in this work ended in February 1956, Z Plant releases were evaluated through 1961. Iodine-131 was the primary contributor to dose, and most of those releases occurred before 1950. Ingestion pathways were excluded from this example. The highest cumulative effective dose estimated from this contour map was 6.5 rem for the 17-year period at an onsite location southeast of 200 East (Figure S-2). The dominant radionuclide contributing to the effective dose was ^{131}I. The thyroid was the organ with the highest estimated absorbed dose (120 rad). If a worker had been at that maximum location for 2000 hours per year and spent the rest of the time east of the Hanford Reservation (at the 1.5-rem contour), his cumulative effective dose would have been 2.6 rem (50 rad thyroid dose), or an average of 150 mrem per year (3 rad per year thyroid dose) over the 17 years. The doses are based on the central (50th percentile) estimates for each radionuclide released.

We further illustrated the dose methodology using four example scenarios. The first scenario was a hypothetical member of the armed forces who was assigned for 3 months (April–June 1954) to an army camp called "H-40," which was 4–9 km southeast of the five 200-Area processing plants and 15–18 km from the seven reactors. Although this time period coincided with relatively high releases of the particulate radionuclides, ^{41}Ar and ^{131}I still contribute, respectively, 46% and 32% of the estimated effective dose at this time and place. External exposure from radionuclides in air was the most important pathway (46%), followed by inhalation (41%), and then external exposure from ground deposits of ruthenium and rhodium nuclides (13%). The total effective dose estimated for this 3-month exposure period was 1.8 mrem. Table S-1 also shows absorbed doses (in mrad) to the most highly exposed tissues for this scenario.

A second scenario for evaluating total airborne releases was a construction worker at the PUREX Plant in 200-East Area during the first 3 months of 1954. The worker's residence was in Richland. As in the first onsite worker scenario, ingestion pathways were not included. The two largest organ doses were 11 mrad to thyroid and 3 mrad to lungs (Table S-1). Inhalation was the most important pathway contributing to effective dose (55%), followed by external exposure from ^{41}Ar in air (33%) and external exposure from ground deposits of ruthenium and rhodium nuclides (11%). At this time and place, the particulate radionuclides are relatively important, contributing 34% to the total effective dose, which totaled 1.5 mrem for the 3-month exposure period.

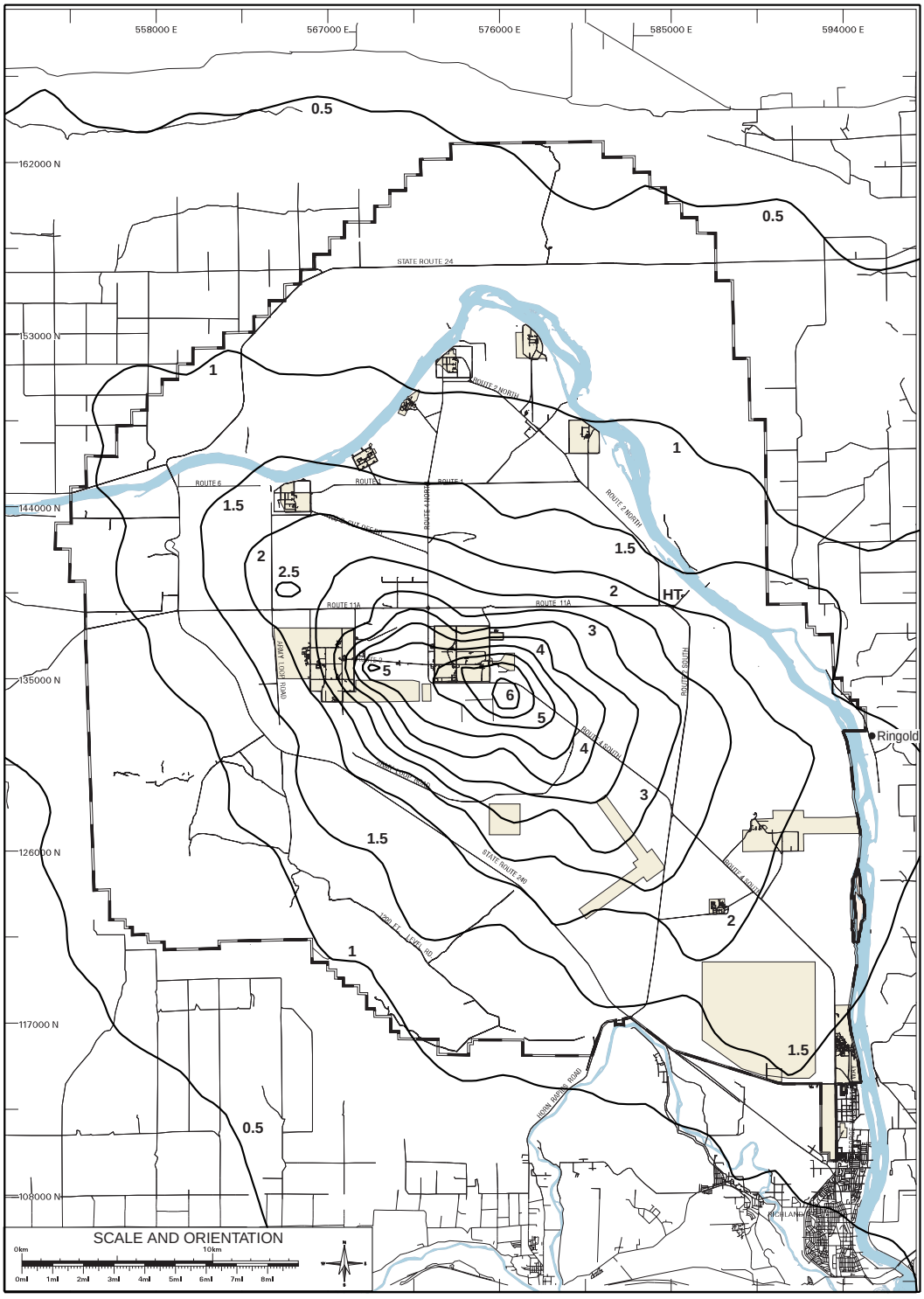

Figure S-2. Contours of committed effective dose (rem) from continuous outdoor exposure to airborne releases from Hanford facilities, 1945–1961. Iodine-131 was the primary contributor to dose, and most of those releases occurred before 1950. Absorbed dose to thyroid (in rad) was about 20 times the effective dose. Ingestion pathways are not included. The notation "HT" shows the location of the old Hanford town site that was closed by March 1945. Base map adapted from the atlas at web site <http://www.bhi-erc.com/dm/hgis/hgis.htm>.

Table S-1. Absorbed Doses to Most Highly Exposed Tissues and Effective Doses for Example Scenarios (Routine Releases)

Exposed person Exposure pathways Duration	Absorbed dose (mrad) to tissues [a]				Effective dose (mrem)
	Thyroid	Lungs	Skin	Bone surfaces	
Soldier, Army encampment H-40 Inhalation, direct radiation, soil ingestion April–June 1954	12	2.0	2.0	1.6	1.8
Construction worker at PUREX Inhalation, direct radiation, soil ingestion January–March 1954	11	3.0	1.3	1.1	1.5
Construction worker at B Plant Inhalation, direct radiation, soil ingestion October 1944–September 1945	12,000	46	29	42	640
Resident of Ringold Inhalation, direct radiation, local diet, soil ingestion January–December 1954	86	3.8	3.8	3.5	6.8

[a] The use of two significant figures to illustrate the results does not imply this degree of precision in these cautious estimates. To obtain absorbed dose in units of Gy and effective dose in units of Sv, multiply values in table by 1×10^{-5}.

The third example illustrates a time of high radioiodine releases when many construction workers were living at the Hanford town site (Figure S-1). The scenario considers a 12-month period, October 1944 through September 1945, when the worker was assumed to be involved with outdoor work at the B-Plant site in 200 East. The residence location was the Hanford town site until it closed (February 1945) and then Richland for the remaining 7 months. There were five Hanford facilities emitting airborne radionuclides during this period: B Reactor, T Plant in 200 West, D Reactor, F Reactor, and B Plant in 200 East. For this example, the T Plant in 200 West is the source of 89% of the total effective dose and the B Plant contributes 11%. Releases from the reactors are insignificant compared to T and B Plant releases at these locations.

Inhalation of ^{131}I contributes 96% of the total effective dose estimate for the B Plant construction worker example, followed by external exposure from ^{131}I on ground (3%) and in air (0.3%). The thyroid is the organ receiving the highest dose (12 rad, or 12,000 mrad), followed by extrathoracic airways (76 mrad) and lungs (46 mrad). Inadvertent ingestion of contaminated soil was considered but is insignificant (0.2% of the total effective dose). The total effective dose (640 mrem) is roughly 400 times higher than the first two scenarios, when the particle releases were *relatively* more important.

The fourth scenario considered exposure of a resident of Ringold during 1954. For this offsite exposure scenario, ingestion of locally produced milk, vegetables, and meat was included. Consequently, ^{131}I is even more important than other radionuclides, compared to scenarios involving exposure onsite, when food pathways were not included. The total effective dose estimate for 1954 was 6.8 mrem, with a thyroid dose of 86 mrad (Table S-1). For comparison, the

annual absorbed dose to the thyroid of a resident of Ringold in 1945 has been estimated to be ~33,000 mrad (Farris et al. 1994).

Possible exposure to the large discrete active particles was estimated from past ground contamination surveys. A computer spreadsheet (called SURVEY) was developed that estimates the likelihood of contact with active particles when working in an area with a certain ground contamination level. A worst-case example calculation is included for a survey technician working outdoors in a highly contaminated area without respiratory protection. The results indicated a 73% chance that a single active particle would have been inhaled during 60 days of work in the area. There was a high probability that an active particle could have been transferred to clothing or skin (depending on protective clothing worn) when working in an area of high ground contamination for even one day. Inadvertent ingestion of large active particles was computed to be a low probability occurrence.

A second scenario using the SURVEY spreadsheet illustrated the probability of contact with an active particle for an offsite resident north of Ringold in 1954. This was a time of high offsite ground contamination from REDOX plant ruthenium particles. In contrast to the onsite survey technician example, there was roughly a 1 in 100 chance of inhalation from ground deposited particles in the entire year and a 2 in 1000 chance of a particle contacting the body during a 16-hour outdoor work day.

Environmental survey data show that workers near the 200 Areas were exposed to much greater concentrations of highly active particles than people in offsite areas. Experimentation with the SURVEY spreadsheet showed that an active particle contamination level of several hundred active particles per 1000 ft^2 of ground surface (or a particle every few ft^2) is necessary before it becomes likely (that is, a >10% chance) that inhalation or body contact would have occurred within a 3-month exposure period. Survey maps, included in Appendix C, show that these particle densities were restricted to onsite areas close to the release points.

A requested feature of the methods developed in this work was the ability to evaluate the sensitivity of the results to various input parameters. For our survey technician example, the most important uncertain assumption affecting the predicted particles inhaled is the resuspension factor during work activities. Other sensitive parameters for inhalation are the ground contamination level, the fraction of airborne particles that are inhalable and the inhalation rate at work. For external contact with active particles, the two most important contributors to uncertainty of the predictions are the contamination level on the ground and the ground-to-body contact probability. The latter was estimated from tracer experiments conducted in the outdoor environment at Hanford. The fraction of the body that is exposed skin is also important for assessing the probability of direct contact with skin as opposed to clothing.

Worker contact with large active particles is difficult to reconstruct. The probability of contact would have varied with location and particle size. Environmental survey data show that workers near the 200 Areas were exposed to much greater concentrations of highly active particles than people in offsite areas. The relatively small number of large active particles, their ill-defined and changing physical shape (particularly the ruthenium flakes), and lack of knowledge of actual activities of workers in the highly contaminated areas make it very difficult to assess past exposures of workers to such particles. In the following tables we summarize bounding estimates for the doses that could have occurred. Table S-2 contains the estimated bounding doses for ingestion and inhalation of a single active particle of two types, the corrosion particles released during the early years of operation of T and B Plants and the ruthenium

particles released during the early 1950s. Although some bioassay measurements were performed on members of the plant workforce in the early years, it seems unlikely that records reflecting internal body contamination due to ingestion or inhalation of radioactive particles during those years have survived to the present time.

Table S-2. Potential Doses (rad)[a] from Inhalation and Ingestion of Active Particles

Type of exposure	Lung	Walls of sections of the GI tract[b]				Bone surfaces	Bone marrow
		Stom	SI	ULI	LLI		
		1940s Active Corrosion Particles					
Inhalation[c]	41	NA	NA	NA	NA	0.34	0.18
Ingestion	NA	0.022	0.040	0.22	0.63	0.46	0.19
		1950s Active Ruthenium Particles					
Inhalation[d]	40	NA	NA	NA	NA	0.046	0.058
Ingestion [e]	NA	3.6	6.2	29	80	1.7	1.7

[a] Note that units in this table are rad, whereas those in Table S-1 are mrad. 1000 mrad = 1 rad.

[b] Abbreviations used: NA = Not applicable; GI = gastrointestinal; Stom = stomach; SI = small intestine; ULI = upper large intestine; LLI = lower large intestine.

[c] Doses from a 5-μCi particle containing a mixture of radionuclides. Dose to the liver: 0.35 rad; doses to adrenals, breast, kidneys, ovaries, spleen, testes, thymus: 0.0081 to 0.14 rad.

[d] Doses from inhalation of a 20-μm particle containing 2.2 μCi of ^{106}Ru. Doses for the adrenals, breast, and thymus: 0.081 to 0.11 rad; doses to the kidneys and liver: 0.040 to 0.053 rad; doses to the bladder wall, ovaries, testes, and uterus: 0.015 to 0.026 rad.

[e] Doses from ingestion of a particle containing 300 μCi of ^{106}Ru.

If skin contact occurred for an appreciable time, the dose rates from these active particles would likely have produced some observable burn or lesion, which could have been documented in medical records. Table S-3 contains dose estimates for body surface contact with the two types of active particles. Doses are estimated for two different depths below the surface; these correspond to the two depths of human skin cells believed to be the most sensitive to damage.

Table S-3. Dose Rates (rad per hour) to Subsurface Tissues from Two Types of Active Particles Located on the Surface

Type of exposure	Dose rate at depth[a]	
	Depth of 0.07 mm	Depth of 0.4 mm
1940s active corrosion particle (5 μCi of mixed fission products on skin surface)	36	12
1950s active ruthenium particle (300 μCi of ^{106}Ru on skin surface)	2400	1300

[a] Dose rates from a "point" source averaged over an area of 1 cm^2.

The usual interpretations of the diffusion and deposition models applied to releases of radioactive particles to the atmosphere construe the airborne plume as a fluid-like continuum, so that any exposure of an individual to the plume, however brief and however small the concentration of radioactivity at the individual's location, must be interpreted to result in a positive (though possibly very small) dose and risk. However, questions are often raised about the validity of these conclusions when the radioactivity is not a gas. If the release is in the form of discrete particles, it is reasonable to ask how likely it is that a potentially exposed person may encounter none of the released radioactive particles at all.

In Appendix E, we furnish some tools for exploring this and similar questions for atmospheric releases of particles from Hanford facilities in the 1940s and 1950s. Based on binomial and Poisson distribution theory, the methods provide a model for estimating the probability that an individual in a specified exposure scenario would have encountered one or more of the released particles (a) on clothing or skin or (b) by inhalation. Appendix E provides examples to guide the reader through the application of the methods to exposure scenarios for incidents of interest during the early years at Hanford.

Table S-4 illustrates the results of such calculations for the unusual ruthenium particle releases from the REDOX Plant, which occurred in March, April, June, and September of 1952; August and September of 1953, and January, April, May, and June of 1954. The probabilities shown are for contact by or inhalation of one or more of the particles released. The columns for maximum potential exposure reflect the assumption that the person is exposed outside throughout the months when the releases occurred, while the last two columns provide estimates for a use factor of 10% during those months. The use factor could reflect a reduced time of exposure or the effect of an indoor location or a combination of the two. The reduction due to the use factor has a proportional effect on the probability of inhalation of one or more particles, but does not appreciably affect the probability of particle contact with the skin or clothing.

Table S-4. Probabilities of Particle Contact with the Body Surface and Particle Inhalation during Unusual REDOX Ruthenium Particle Releases, March 1952–June 1954

	Maximum potential for exposure		Exposure for use factor of 0.1	
Exposure location	Probablility of particle contact[a] with body surface	Probablility of particle inhalation[a]	Probablility of particle contact[a] with body surface	Probablility of particle inhalation[a]
H-61[b]	1.0	0.044	1.0	0.0045
H-51[b]	1.0	0.042	1.0	0.0043
H-42[b]	1.0	0.034	1.0	0.0034
H-40[b]	1.0	0.011	1.0	0.0012
H-50[b]	1.0	0.078	1.0	0.0081
200-E guard tower[c]	1.0	0.014	1.0	0.0014
200-W guard tower[d]	1.0	0.034	1.0	0.0035
Hanford site	1.0	0.0036	0.9997	0.00036
Ringold	1.0	0.0026	0.9860	0.00026
Richland	1.0	0.0048	0.99996	0.00048

[a] Interaction with one or more particles.
[b] Location of military personnel; see Figure S-1.
[c] Tower is located near the southeast corner of 200-E; see Figure S-1.
[d] Tower is located near the center of the east side of 200-W; see Figure S-1.

The results of this work indicate that intakes of ^{131}I by inhalation were the most important component of past exposures of onsite workers to airborne releases of short-lived gases and radioactive particles from Hanford separations plants and reactors. Further refinement of past exposures to other gaseous radionuclides or radioactive particles, beyond what was accomplished by this work, appears unnecessary. The methods developed in this study will provide tools for CDC to answer questions raised by past onsite workers about their radiation exposures.

CONTENTS

FIGURES

TABLES

ACRONYMS

AEC	Atomic Energy Commission
AMAD	Activity Median Aerodynamic Diameter
CDC	Centers for Disease Control and Prevention
C.P.	"Cutie Pie," an instrument used to measure radiation exposure rate
CWS	Chemical Warfare Service
DOE	U.S. Department of Energy
EPA	U.S. Environmental Protection Agency
ERAMS	Environmental Radiation Ambient Monitoring System
GM	Geometric Mean, the central value in a lognormal distribution
G.M.	Geiger-Müeller, a type of radiation detection device or measurement instrument
GSD	Geometric Standard Deviation, the measure of dispersion of a lognormal distribution
HEDR	Hanford Environmental Dose Reconstruction
H.I.	Health Instruments, one of the organizational divisions in the early years at Hanford
ICRP	International Commission on Radiological Protection
ISC	Industrial Source Complex, a type of EPA atmospheric dispersion code
MP	Military Police
NCRP	National Council on Radiation Protection and Measurements
PNL	Pacific Northwest Laboratory
PUREX	Plutonium Uranium Extraction
RAC	*Risk Assessment Corporation*
REDOX	Reduction Oxidation
TSP	Technical Steering Panel
UN	United Nations

PREFIXES, ABBREVIATIONS AND CONVERSIONS FOR UNITS USED IN THIS REPORT

UNIT PREFIXES

multiple	prefix	symbol	fraction	prefix	symbol
10^{12}	tera	T	10^{-2}	centi	c
10^{9}	giga	G	10^{-3}	milli	m
10^{6}	mega	M	10^{-6}	micro	μ
10^{3}	kilo	k	10^{-12}	pico	p
			10^{-15}	femto	f

UNIT ABBREVIATIONS

ACTIVITY

Bq	Becquerel
Ci	curie
dpm[1]	disintegrations per minute
μC	archaic abbreviation for microcurie

EXPOSURE OR DOSE

Gy	gray
Sv	sievert
rep	roentgen equivalent physical
R	roentgen

LENGTH

cm	centimeter
ft	foot
in.	inch
km	kilometer
m	meter
mi	mile

VOLUME

ft^3	cubic feet
L	liter
m^3	cubic meter

TIME

s	second
min	minute
h	hour
d	day
mo	month
yr	year

WEIGHT

g	gram
kg	kilogram

Conversion of Conventional Units to Metric or System International (SI) Units

Multiply	by	To obtain	Multiply	by	To obtain
rad or mrad	0.01	Gy or mGy	ft	0.3048	m
rem or mrem	0.01	Sv or mSv	in.	2.54	cm
Ci	3.7×10^{10}	Bq	mi	1.6094	km
μCi	3.7×10^{4}	Bq	ft^3	28.32	L
pCi	0.037	Bq	ft^3	2.832×10^{-2}	m^3
dpm	0.0167	Bq			

[1] Some field measurements of radioactivity are reported in counts per minute (cpm). The efficiency of the instrument is required to convert to activity.

METHODS FOR ESTIMATING RADIATION DOSES FROM SHORT-LIVED GASEOUS RADIONUCLIDES AND RADIOACTIVE PARTICLES RELEASED TO THE ATMOSPHERE DURING EARLY HANFORD OPERATIONS

1. INTRODUCTION

This report describes methods that can be used to calculate "worst case[1]" doses from short-lived gaseous radionuclides and radioactive particles released to the atmosphere during the early years of operations at the Hanford Reservation near Richland, Washington. Hanford currently occupies 586 square miles of semi-desert land that was withdrawn for government use starting in the spring of 1943 for the secret World War II Manhattan Project. The mission of that project was to produce plutonium for nuclear weapons. The land is mainly in Benton County, but includes parts of Grant, Adams, and Franklin counties. The land withdrawn for the Hanford Reservation contained the three small communities of Hanford, White Bluffs, and Richland, which were evacuated. In the mid-1950s, Richland residents were allowed to purchase their homes, and that community became incorporated as a city of Washington state. At the time the Hanford Reservation was established, Pasco was an important railroad center, and Yakima was a small trade city for agricultural products. The larger cities of Seattle, Tacoma, Olympia, Portland, Boise, and Spokane are more than 100 miles away (Figures 1-1 and 1-2).

Figure 1-1. Location of the Hanford Reservation (shaded area) in the northwestern U.S. (adapted from figure in Sanger [1995]). Richland, Pasco, and Kennewick are called the "Tri-Cities."

[1] Terminology used in scope of work document. Discussed in other sections of this report, especially Appendix D.

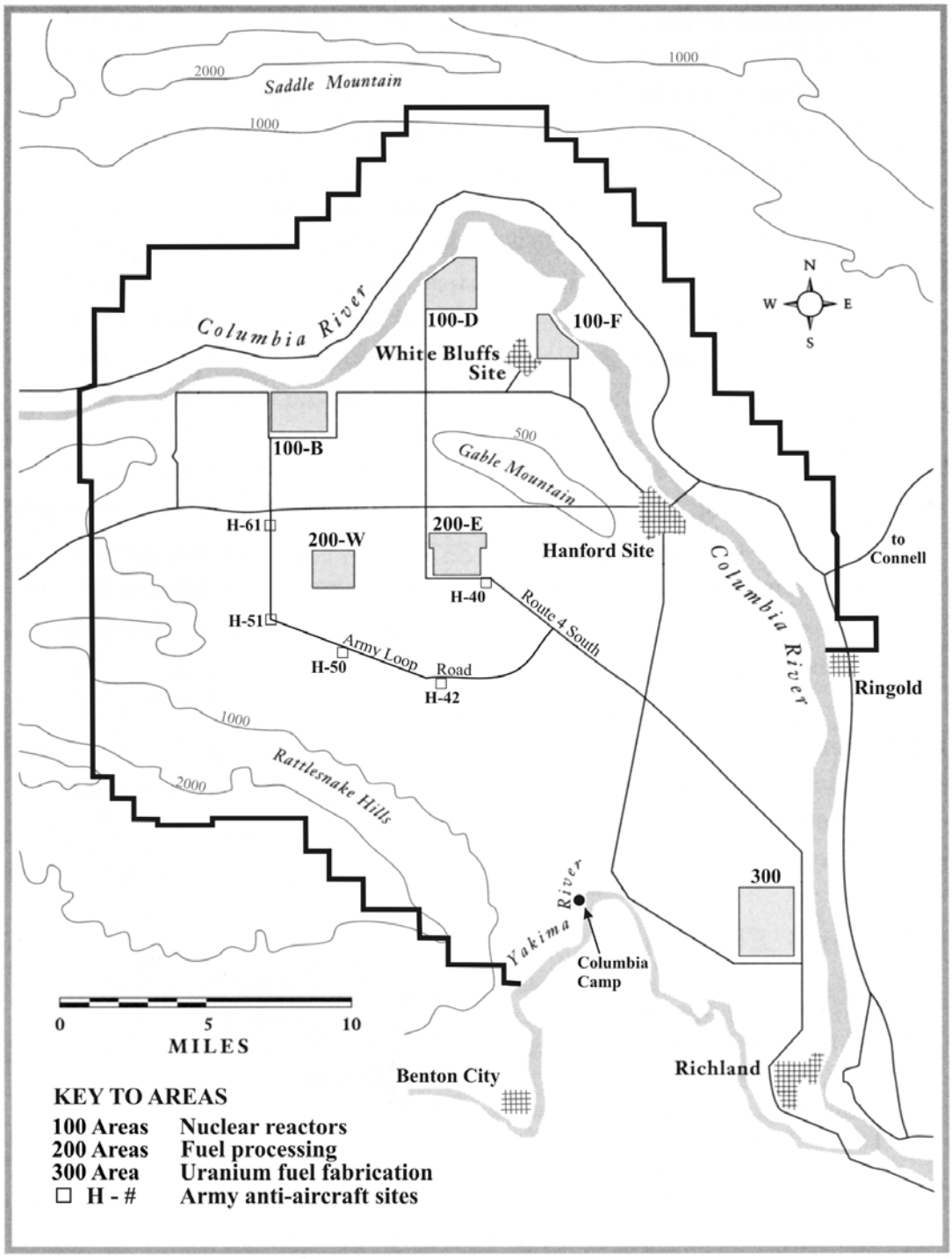

Figure 1-2. Primary features of the Hanford Reservation in 1943–1945, then called the "Hanford Engineer Works," adapted from figures in Sanger (1995) and Jones (1985). The dark line shows the outer edge of land acquisition Area B, discussed in Jones (1985). The southeast boundary of the government-occupied land is defined by the Yakima and Columbia Rivers and includes Area C (Richland). The approximate locations of army anti-aircraft sites are based on maps discussed in Section 3.1.2. Contour lines show elevations in feet.

The methods described in this report address some concerns that remained following the Hanford Environmental Dose Reconstruction (HEDR) Project (Farris et al. 1994). [2] The HEDR Project focused on doses to members of the public, located offsite, from past releases of radionuclides from the Hanford Site. Our study considers possible doses to persons who lived or worked *on* as well as near the reservation boundaries (Figure 1-3). The scope includes outside exposure to airborne releases from Hanford's nuclear facilities, not doses received by workers inside buildings. Also, this work does not address localized fixed sources of radiation near the buildings such as waste tanks, trenches, and spills. Members of military units were located near both the first reactor facilities and fuel processing plants during the early years of operation. Although their numbers decreased dramatically in 1945, construction workers were also present onsite at a number of locations, building reactors, additional processing plants, and other facilities. Thousands of construction workers and others lived at the old Hanford town site until February 1945 (Figures 1-2, 1-3). Section 3.1 includes additional discussion of specific locations and conditions of exposure in the early years of Hanford operations.

The Centers for Disease Control and Prevention (CDC) issued a task order for its contractor, *Risk Assessment Corporation (RAC)*, to develop information and techniques that would help them answer questions from past workers about their radiation exposures. The CDC needed computational tools that would allow them to estimate the doses to the public from these short-lived nuclides and particles and to test the sensitivity of these dose estimates to various input parameters. By CDC's request, the methods should be relatively simple and conservative, that is, tending to overestimate the doses received at a given time and place. Results from these tools are not comparable to those of a rigorous dose reconstruction, nor should they be used as a basis for determining compensation from past radiation exposure or for medical decisions.

There were two types of releases of radioactive materials that were more important for people onsite than for the offsite public. The first was releases of short-lived radionuclides that decayed appreciably in transit to offsite locations. The second type was radioactive particles, the largest of which settled onsite close to the release points. As a demonstration of the dose evaluation techniques, results for example exposure scenarios are presented as part of the report; however detailed evaluation of many scenarios is outside the scope of this work.

This study adds to the growing body of work on the history of the Hanford site. The role of the Hanford facilities in production and separation of plutonium for use in nuclear weapons has been described in histories of the Manhattan Project (Smyth 1945, Groves 1962, Jones 1985, Rhodes 1986, Gosling 1999). Carlisle and Zenzen (1996) have described the importance of the Hanford plutonium production reactors for the United States' nuclear weapons program. A more detailed local history of Hanford activities and their legacy has been published (Gerber 1992a,b). The main processes and facilities for plutonium production have been described (Gerber 1996), and chronicles of individual facilities have been prepared as well (Gerber 1992b, 1993a, 1993b, 1994). Sanger (1995) interviewed over 55 Hanford workers, from top scientists to construction workers, about life and work on the site during World War II. Collections of historical photographs from Manhattan Project sites, including Hanford, have been published (e.g. Fermi and Samra [1995]), and many more are available on the Department of Energy's Internet pages.

[2] Underlining of references, section numbers, Figures, or Tables indicates a hyperlink in the electronic version of this report. Clicking on the underlined text will take the reader to the referenced object.

A tabular chronology of operational changes relevant to this work is included (Table 1-1) after the following historical overview of construction and operations.

Figure 1-3. Onsite workers exposed to airborne releases during the early years of Hanford operations include personnel manning guard towers and posts around facilities (top row), patrol stations at barricades along roadsides and at facility gates (middle left photo), construction workers (middle right), and residents of the Hanford trailer park (lower left) and construction camp (lower right) at the old Hanford town site. The army also manned anti-aircraft sites (see Figure 1-2). See Section 3 of this report for more discussion. *U.S. Department of Energy photos.*

The main features of the first large-scale plutonium production can be summarized simply. The processes had been developed and demonstrated using pilot facilities at a site near Oak Ridge, Tennessee, and the technologies were successfully scaled up to industrial levels at Hanford. Plutonium-239, which is fissionable, was produced by the activation of ^{238}U in large nuclear reactors built at the Hanford site in the last years of World War II. Chemical processing facilities, constructed at the same time, received the irradiated reactor fuel and separated the plutonium product from the uranium and many fission products that were also produced in the reactors. The recovered plutonium nitrate was shipped to the Los Alamos laboratory in New Mexico. There it was converted to metallic form and shaped into the components of the "gadget" that was successfully tested near Alamagordo, New Mexico in July 1945 and the "Fat Man" weapon dropped on Nagasaki, Japan in August of that year.

The first three plutonium production reactors at Hanford were built along the Columbia River at sites called 100-B, 100-D, and 100-F (Figures 1-2, 1-4). These reactors were all operating by March 1945. Following World War II, additional reactors were constructed at other locations along the Columbia River between the original three reactors. The 100-H and 100-DR Reactors began operation in October 1949 and October 1950, respectively. Three more production reactors were completed between November 1952 and April 1955; one was built at 100-C and two were built at 100-K, called K East (KE) and K West (KW). Subsequently, a dual-purpose plutonium production and electricity production reactor was built at 100-N that began operation in 1964.

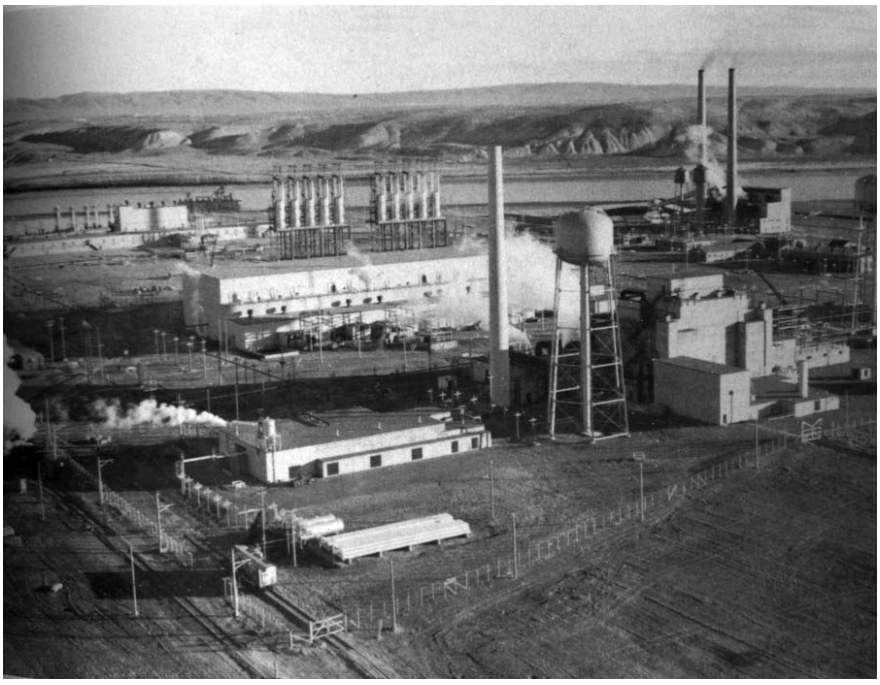

Figure 1-4. 100-F Area in 1944. Initially, three plutonium-producing reactors were built, about six miles apart, on the south bank of the Columbia River. At each site, in addition to the reactor buildings, there were electrical substations, pump stations, water treatment plants, retention basins, and waste processing plants. *Department of Energy photo* from Fermi and Samra (1995).

Also shown in Figure 1-2 are the locations of the fuel processing facilities within the Hanford Reservation, labeled 200-E (east) and 200-W (west). These facilities chemically separated the plutonium from other materials in the fuel that came from the production reactors. The first processing plant, called T Plant, was located in the 200-W Area and began operations in late December 1944 (Figure 1-5). The second plant, B Plant, was in the 200-E Area, and started dissolving irradiated fuel in April 1945. The B Plant was shut down in 1952, while the T Plant operated until February 1956. Two larger plants were built for processing fuel from the growing number of reactors in later years. The REDOX Plant in 200-W began operations in 1952, and in 1956 the PUREX Plant was started up in 200-E. Figure 1-6 illustrates the locations of the four fuel processing plants in the 200 Areas. Also shown in the figure are the Z Plant and U Plant in 200-W. The Z Plant, in which plutonium was processed and fabricated, began operation in 1949. The U Plant processed uranium to produce uranium trioxide for recycling to the reactor fuel production system.

Figure 1-5. Fuel processing (T) Plant in 200–West Area in 1944. Rail cars brought the irradiated uranium slugs from the production reactors in 100 Areas to the separation areas in large vats of water. Here, they were stored in pools of water to allow some of the intense, short-lived radioactivity of the fission products to decay before processing. *Department of Energy photo* from Fermi and Samra (1995).

The fuel processing facilities in the 200 Areas were the principal sources of radionuclides released to the atmosphere. Releases were highest during the earliest operating years, when the war mission was critical and effluent reduction measures had not been implemented. In addition to ongoing routine releases to air, large radioactive particles from corrosion of ductwork in the 1940s and flakes of ammonium nitrate containing radioactive ruthenium in the 1950s settled onto ground surfaces around the fuel processing plants. The amounts released from Hanford facilities over time are discussed in more detail in Section 2 of this report. Releases from the reactors were of greater *relative* importance when the discharges from the processing plants had been reduced by better filtration of the effluents. As the production reactors were closed during the 1960s and early 1970s, processing requirements were reduced. The REDOX Plant was shut down in 1967, and the PUREX plant was shut down in 1972, although it also operated during the 1980s.

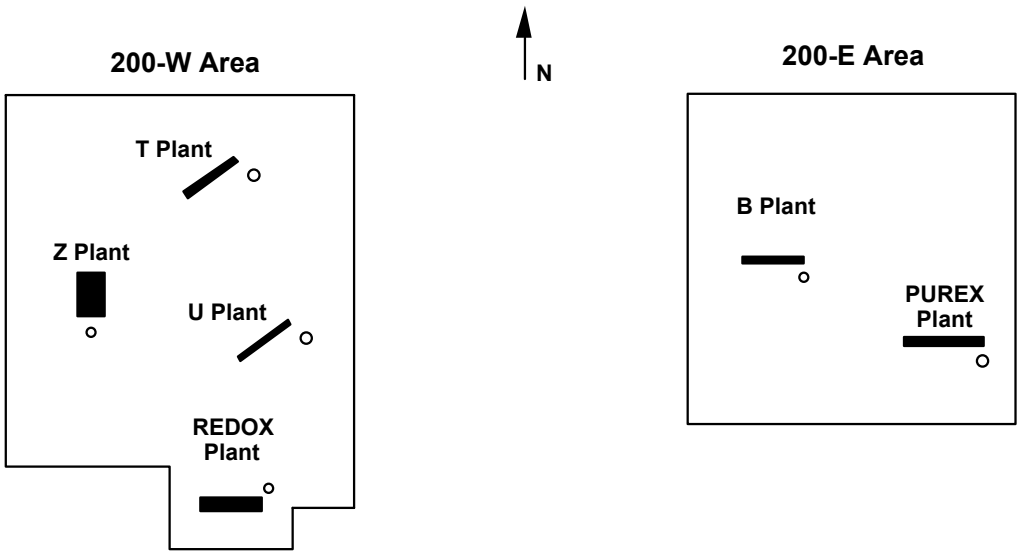

Figure 1-6. Schematic diagram (not to scale) of the 200 Areas at Hanford showing the main fuel processing plants and other large facilities. The small circles show the approximate locations of the 200-ft (61-m) stacks that released airborne wastes from each of the facilities.

Table 1-1. Chronology of Events at Hanford Production Reactors and Fuel Processing Plants[a]

October 1944	Began operations at B Reactor
December 1944	Began operations at D Reactor Began processing fuel at T Plant
March 1945	Began operations at F Reactor
April 1945	Began processing fuel at B Plant
1947	Official end of Manhattan Project (January). The new Atomic Energy Commission became responsible for atomic energy and nuclear weapons. Hanford operations grew due to "cold war" with Soviet Union.
1947–1949	Corrosion of duct work in fuel processing plants (T and B) result in airborne releases of large "active particles"
1948	Sand filters installed at T and B Plants reduce routine releases of radionuclide particles to air; new water scrubbers reduce iodine-131 emissions to air
October 1949	Began operations at H-Reactor
1949	Began processing and fabrication at Z Plant
December 1949	"Green Run" release of iodine-131 to air
1950	Silver reactor filtration installed in T and B Plants reduce iodine-131 emissions to air; new fiberglass filters further reduce particle releases
October 1950	Began operations at DR Reactor
1951	Failure of silver reactor filtration in April and July results in accidental iodine-131 releases
1952	Shut down processing at B Plant Began processing fuel at REDOX Plant
1952–1954	Large particles containing radioactive ruthenium released from REDOX Plant
Summer 1954	Process changes at REDOX Plant reduce ruthenium releases
Nov. 1952–April 1955	Began operations at C, KE, and KW Reactors
1956	Shut down processing at T Plant Began processing fuel at PUREX Plant

[a]Information on airborne effluent control measures from Roberts (1958).

There is not one date that defines the end of the "early years" for this report, although Table 1-1 illustrates reasons why the first decade of Hanford operations contained the highest radionuclide releases. The end of unusual releases of ruthenium particles and the shut-down of T Plant in February 1956 provided a basis for an end year of 1955, and this is the limit of the environmental data evaluation in Section 4. However, depending on the type of information being analyzed and evaluated, the reader will observe various time periods being discussed in this report. For example, as the project progressed, and other questions were raised, consideration was given to some releases over slightly different time periods. The example calculations illustrate doses during periods of high radioactive releases or ground contamination levels.

This report consists of four main sections, besides this introduction. Atmospheric release estimates for short-lived gaseous nuclides and radioactive particles from the Hanford facilities are considered in Section 2 of this report. Screening calculations to identify the most important radionuclides, the main contributors to human radiation exposure, are described first. Detailed estimates of releases are then presented for that set of radionuclides.

Dose calculation techniques, which include methods for a variety of exposure pathways, are described in Section 3. Calculational tools that have been prepared for use by the CDC and the information base that supports them are also described in that part of the report. Section 4 contains descriptions and analyses of the various types of environmental data that were collected during the years of the highest releases from the facilities. Results of both routine monitoring and special studies are discussed and conclusions based upon those measurements are presented.

Section 5 contains results of example dose calculations for exposure scenarios during the early years of operations at Hanford. These scenarios may well represent some of the worst situations that occurred because the times chosen were those when unusually large releases of radioactive particles occurred. They should not be considered to be representative of the full range of possible exposures to military, construction, and other personnel who worked onsite.

Detailed supporting information, including a compendium of documents reviewed during the project, is provided in appendices to the report. Information about the set of documents is also stored in an electronic database that is one of the products of this project.

2. RADIONUCLIDE RELEASES TO THE ATMOSPHERE

2.1 Overview

During the early years of Hanford operations, releases of volatile short-lived radionuclides, particularly ^{131}I, from the processing plants were of greatest concern. Fuel slugs that were irradiated to produce plutonium were removed from the reactors, stored for a time, and then delivered to the processing plants for dissolution and plutonium recovery. In the early years, the time between discharge from the reactor and the start of fuel processing was relatively short. During this period, called the cooling time (or decay time), the amounts of short-lived nuclides were reduced by radioactive decay so smaller quantities would be present when the fuel was dissolved.

Figure 2-1 shows the average fuel decay times during the first years of plutonium production at Hanford (Heeb 1994). This figure provides a general picture of fuel cooling practices at the time. During the first year, many of the average cooling times were less than 40 days and all were less than 55 days. In late 1945, cooling times were increased and that general trend continued over the next two years (Link to Processing Rates.xls). The plot does not reflect cooling times for individual batches of fuel removed from the reactors, but the average for all batches processed during the month.

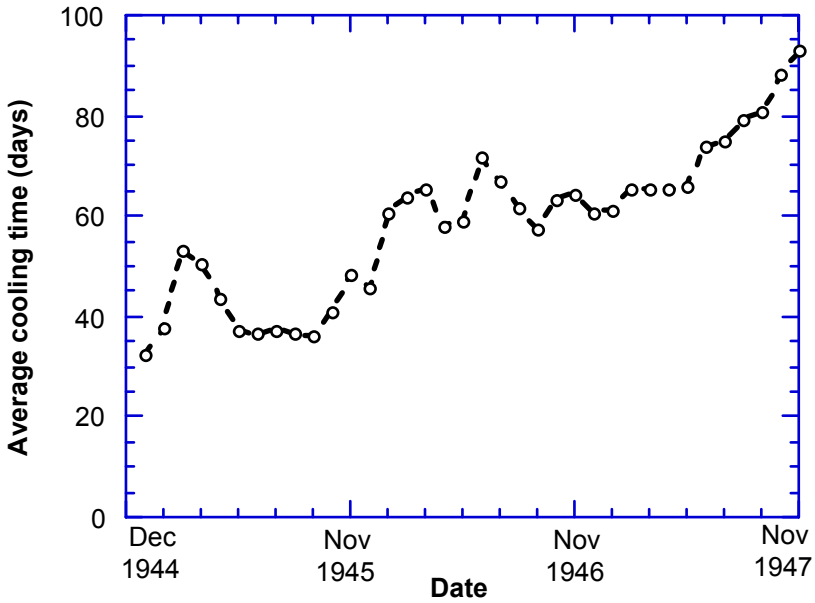

Figure 2-1. Average fuel cooling times prior to processing at Hanford (Heeb 1994).

Iodine-131 has a radiological half-life of 8.04 days and the half-life of ^{133}Xe, a noble gas, is 5.26 days. The shortest average cooling times correspond to four to five half-lives for ^{131}I, meaning that the ^{131}I radioactivity in the fuel would be reduced by a factor of 16–32 (2^4–2^5) during the cooling period. Even after that decay reduction, the monthly amounts of ^{131}I in the fuel dissolved in 1945 exceeded 37 TBq (1000 Ci) and most exceeded 370 TBq (10,000 Ci). Cooling

times of 33 to 38 days diminished the amount of ^{133}Xe in the fuel by a factor that ranged from 32 to 64, but similarly large amounts of ^{133}Xe were also available for release during processing throughout most months of 1945. Other radioiodines and radioactive noble gases, which can be important contributors to dose when a prompt release of gases from irradiated fuel occurs, have shorter half-lives and were substantially reduced by decay prior to fuel dissolution (see Section 2.3). The activities of short-lived particulate radionuclides were similarly reduced.

Table 2-1 lists other radioactive fission products, which have intermediate (30–60 day) and longer half-lives found in particles released during fuel processing activities at Hanford (see Section 4.2.1). The long-lived radionuclide that was the object of Hanford production activities, ^{239}Pu, is also listed. With the exception of ruthenium, which can exist in gaseous form as ruthenium tetroxide (RuO_4), the elements shown in the table are not volatile and were present in waste solutions after fuel dissolution. Various in-plant operations, including steps that oxidized ruthenium, led to releases of these radionuclides. The releases were primarily in particulate form. There were also secondary releases of ruthenium particles from the REDOX Plant stack.

Table 2-1. Radionuclides Found in Particles Released during Hanford Fuel Processing

Elements and radionuclide(s)	Half-life
Strontium	
^{89}Sr	50.5 d
^{90}Sr	29.12 yr
Yttrium, ^{91}Y	58.5 d
Zirconium, ^{95}Zr	64 d
Niobium, ^{95}Nb	35.15 d
Ruthenium	
^{103}Ru	39.3 d
^{106}Ru	368.2 d
Cerium	
^{141}Ce	32.5 d
^{144}Ce	284 d
Cesium, ^{137}Cs	30.0 yr
Plutonium, ^{239}Pu	24065 yr

Comparison of the half-lives listed with the cooling times discussed above shows that decay of short-cooled fuel would have reduced the amounts of ^{103}Ru and ^{141}Ce by only about a factor of two and had an even smaller effect on the amounts of the other radionuclides. Even long cooling times (~100 days) would have had little effect on the amounts of these radionuclides present in the fuel.

Because the elements listed in Table 2-1 are not volatile, releases of the corresponding radionuclides were not generally expected to be as important as ^{131}I to plant operations and public health. When the first processing plants began operating, there were no filtration systems to limit the release of radionuclides. The discovery, in the fall of 1947, of “active particles” in the environment changed expectations about such releases. Stainken (1948) describes key events in

the history of early operations, the active particle contamination found, and actions taken to reduce the releases of active particles.

The next section considers the observed characteristics of the particles that were found in 1947 and the later large releases of ruthenium particles from the REDOX Plant. The results of those measurements help to define the types and magnitudes of exposures to people following releases of radioactivity to the environment.

2.2 Characteristics of Hanford "Active Particles"

The consequences of exposure to radioactive particles depend upon a number of factors. The size of the particle and the chemical form of the radionuclides are both very important, and the amount of radioactivity present is clearly critical to any dose assessment. The studies of "active particles" initially found at Hanford illustrate the types of detective work needed to understand the problem and provide information about important characteristics of those releases. Similar measurements were made in the early 1950s when numerous unexpected releases of radioactive ruthenium particles from the REDOX Plant occurred. Both sets of data help to define the problem of particle exposures.

2.2.1 Characteristics of Particles Released from T Plant and B Plant Stacks

The presence of ground contamination that consisted of many "active particles" or "specks" was discovered near T Plant and B Plant in 1947. Mickelson reported the initial analytical results in late October (HW-7865).[1] The total activities of individual particles ranged up to 2 μCi (74 kBq). The majority of the activity was due to beta particle emission; beta to alpha activity ratios ranged from 83 to about 4100. The primary contributors to the beta particle emission were identified by element (Ce, Y, Sr), but not by isotope. Soon thereafter, Parker reported that additional investigations were underway (HW-7920). These included

- Measurements of the distribution of particles in the environment and the rate of deposition
- Tests to determine the size, chemical makeup, and isotopic composition of the particles
- Estimation of the origin and age of the particles using the test results
- Assays of radioactivity in animals and workers
- Investigation of possible health consequences of exposure to such particles.

Many of the results of these investigations were reported in 1948 by Parker (HW-8624, HW-9259), Thorburn (HW-10261), and Healy (HW-10758). The environmental data have been summarized in Section 4.2.1.

The investigations revealed that the most likely source was release of iron particles from corroding ductwork and the fans in the exhaust systems of the two processing facilities. Analysis of the relationships between beta radioactivity and estimated surface areas and volumes of the particles led to the conclusion that the radionuclides were on the surfaces of the iron particles. This finding and the estimated ages of the particles (100–300 d) both suggested that radionuclides

[1] Throughout this report, references to historical documents produced by the Hanford contractors employ their HW- numbers. This is the most unambiguous and easily traceable method. Appendix A contains both a bibliographic list and a list of the Hanford reports sorted by HW-number.

in the exhaust gases had been deposited on the blowers and other iron surfaces and were subsequently released when the particles of corroded iron were suspended into the stack exhaust air stream. Tests following replacement of corroded components of the exhaust system with stainless steel (the material originally specified) showed that there were two components of the release, the larger corrosion particles and another aerosol composed of smaller diameter particles. It is reasonable to conclude that releases of small particles had been continuous since startup and served as the source of the deposits on the surfaces of the exhaust system (HW-10261).

Data collected during the investigations provide information on the physical characteristics of the particles that were released. The large particles are described as having physical diameters greater than 100 µm, a size that can be described as fine sand.[2] The reported size range for the "active" particles was 20–1500 µm.

The average mass of particles segregated for analysis was reported to be 1 mg, with some masses of particles in this group as low as 0.1 mg (HW-7920). The theoretical density of iron oxide, the principal constituent of these particles, is ~5.2 g cm^{-3}. Raabe[3] suggests that actual physical densities are likely only about 70% of the theoretical value. Following this guide for iron oxide, the effective expected actual particle density would be about 3.6 g cm^{-3}. The physical diameter of a 1-mg iron oxide particle with that density would be ~800 µm. As the text of Parker's report (HW-7920) suggests, the smaller fraction of the distribution was not included in the sample studied in detail.

It must be noted that the observed particles were asymmetrical, rather than spherical, but no estimate of the shape factor was found in the reports. If a default shape factor of 1.5 (ICRP 1993) is assumed and the effective density given above is used, the aerodynamic diameter of a 180 µm particle is estimated to be about 290 µm.

Follow-up reports by Parker (HW-8624, HW-9259) and Thornburn (HW-10261) provide information about cross-sectional sizes of particles, as observed using a microscope. The lengths of the major and minor axes of the observed particles were measured. These were then multiplied

---

[2] The reference here is to the physical diameter of the particle. Other descriptions of particle size are important to the analysis (Hinds 1982, ICRP 1993b). The equivalent volume diameter (d_e) is the diameter of a spherical particle that has the same volume as the particle considered. The aerodynamic diameter (d_{ae}) of a particle is the diameter of a unit density spherical particle that has the same settling velocity as the particle in question. Two properties of the particle are most important in determining its aerodynamic diameter: its shape and its density. The aerodynamic diameter of a spherical particle with density of 3 g cm^{-3} is about 1.73 (the square root of 3) times larger than its physical diameter. Shape factors for non-spherical particles range between one and two. The aerodynamic diameter of a unit density particle with a shape factor of 1.5 is about 1.22 (the square root of 1.5) times smaller than its equivalent volume diameter. These relationships are approximations because a third factor, the Cunningham slip correction factor, may also affect the aerodynamic diameter, particularly when the equivalent volume diameter is less than 1 µm.

In any natural collection of particles or an aerosol, one typically finds a distribution of particle diameters that covers a broad range. Frequently the distribution is lognormal, which means that the logarithms of the diameters are normally distributed. The two parameters that characterize a lognormal distribution of particle diameters are the geometric mean (or median) diameter and the geometric standard deviation (GSD). These quantities are similar to the more familiar mean and standard deviation that describe the central value and the variability of values in a normal ("bell shaped") distribution. The lognormal distribution is asymmetric, and a broader range of particle diameters is indicated by a larger GSD.

[3] Raabe, O. 2000. Ad-hoc review committee, Centers for Disease Control and Prevention. Personal communication with P.G. Voilleque, *Risk Assessment Corporation*. Subject: Review of Task Order 3 report. September 11.

to obtain a quantity that represents an unknown fraction of the actual surface area of the particle. Only the product of the two dimensions is provided in the reports. Frequency plots are presented for 107 particles selected at random and for 68 small particles. Cumulative distributions obtained from the data suggest geometric standard deviations (GSDs) between 2.4 and 2.6 are appropriate for these groups of particles.

If we assume that the reported physical diameter range of 20–1500 µm reflects the 1st and 99th percentiles of a distribution and that the GSD of the distribution is 2.5, then we estimate count median particle diameter of about 180 µm. Calculation of the diameter of average mass using the count median diameter of 180 µm and a GSD of 2.5 using the Hatch-Choate relationship (Hinds 1982) yields a value of 630 µm, somewhat lower than the 800 µm estimated above.

The mean particle size of the smaller aerosol or "mist" was reported to be <5 µm (HW-9864) with some particles <1 µm (HW-9175). If the mean diameter were 3 µm and the GSD of the distribution were 2.5 (as above), the geometric mean particle diameter would be about 2.0 µm. The range of diameters corresponding to the 1st and 99th percentile values would be 0.2–20 µm. The upper tail of the small particle distribution would be comparable to the particle diameters found at the lower end of the distribution of the larger particles described above.

The ratio of the surface area for the 95th percentile diameter of the distribution of large particles to the surface area for the 5th percentile diameter of the distribution of small particles is about 2×10^7. This is broad enough to account for the observed variation in activity per particle of 2.5 pCi to 3.2 µCi (HW-10261). The ratio of those two activities is about 1.3×10^6.

If we take the distribution of physical diameters to be lognormal, with a count median diameter (CMD) of 180 µm and a GSD of 2.5 (as above), we can construct a family of distributions that reflect the properties needed for dispersion, deposition, and dose estimates. In the lower part of Figure 2-2 is a line that illustrates that distribution of physical diameters. The corresponding distribution of aerodynamic diameters, for the estimated density of iron oxide of 3.6 g cm^{-3} and the default shape factor of 1.5, lies just above it. The surface median diameter (SMD) for the distribution, calculated using the Hatch-Choate relationship, is 965 µm; the distribution of surface areas is shown in the upper part of Figure 2-2. It was concluded that the radioactivity was associated with the surfaces of the iron oxide particles, and the distribution of activity would therefore be related to the surface area distribution. We may, as suggested above, associate the highest observed particle activity of 32 kBq (3.2 µCi) with the 95th percentile of the distribution, which leads to the distribution of particle activities (right hand scale in Figure 2-2). For calculational purposes, the aerodynamic size distribution can be subdivided into a number of bins with each reflecting the same percentage of the particles in the distribution. The activity of the particles in a particular aerodynamic size range would be similarly defined.

The estimated median value for the activity distribution in Figure 2-2 is ~0.72 µCi. The mean activity of the large "active particles" is estimated to be about 1.1 µCi. Thus, each curie of a release of large active particles corresponds to a release of about one million particles.

The data on radionuclide composition of the particles are variable and somewhat incomplete. Healy identified three components of the radioactive decay curves for the particles according to half-lives of 30–60 d, about one year, and many years (HW-10758). Healy's decay studies were conducted on samples of particles from air collected from separations plant stacks, from ambient outdoor air, and from vegetation samples in 1945–1947 and are discussed in detail in Section 4.2.1. The following assignments of activities to the three components are considered to be

reasonable and are consistent with Healy's analysis of the decay curves. For the first component: 13% ^{103}Ru, 14% ^{141}Ce, 6% ^{95}Zr, 14% ^{89}Sr, and 23% ^{91}Y; the sum of the activities of these radionuclides is 70% of the total. The second component is estimated to consist of 3% ^{106}Ru and 26% ^{144}Ce-Pr. Because their fission yields and half-lives are comparable, the isotopes ^{90}Sr and ^{137}Cs should contribute about equally to the 1% of activity associated with the longest lived component.

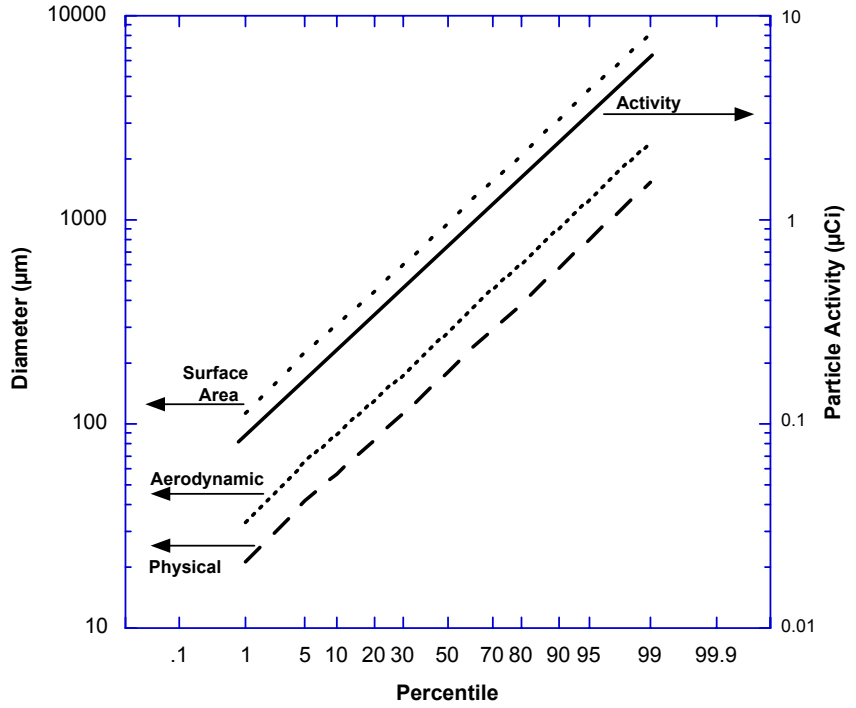

Figure 2-2. Estimated distributions of physical and aerodynamic diameters for large "active particles" together with estimated distributions for particle surface area and activity.

As noted, the particles were principally composed of beta-emitting radionuclides, and the ratio of beta particle to alpha particle emissions was variable. Most of the alpha particle activity was identified as plutonium (^{239}Pu), which was reported to account for 65–96% of the total (HW-7865). The particle with the largest alpha activity contained about 0.7 nCi; the beta activity of that particle was 2 µCi.

2.2.2 Characteristics of Ruthenium Particles Released from the REDOX Stack

The REDOX Plant began start-up testing in January 1952 and operation in February of that year. Although the effluent monitoring system was not installed until June, discovery of radioactive particles in the environment near the plant began soon after start-up, and a series of unplanned particle releases occurred during the next three years. The predominance of radioactive ruthenium isotopes characterized these releases. In July 1954, Ebright prepared a comprehensive account of the particle releases that had occurred (HW-32473). In August, particles were found in offsite areas. Parker wrote a status report to the AEC on the "ground contamination problem" in

September (HW-33068), which includes his assessment of possible consequences of contact with these highly radioactive particles.

In March and April of 1952, particles that contained primarily ruthenium isotopes (^{103}Ru and ^{106}Ru) were found in the environment around the facility. The March release was traced to a scrubber pump failure. The particles found near the end of April were attributed to a release associated with air blown through a process vessel that had been cleaned out. This procedure had been performed several times, and it was concluded that there was environmental evidence for previous releases as well. Other operational activities were identified as possible contributors to particle releases, but the larger releases to come had a very different cause.

A program was established in May 1952 to monitor deposition routinely around the REDOX Plant. In June, large flaky radioactive particles were found around the facility. Some of the particles were quite large, with diameters greater than 10 cm. The principal chemical component was found to be ammonium nitrate and the principal radionuclides were ^{103}Ru and ^{106}Ru. The flakes were fragile, but the residual contamination persisted on the ground. Over time, the radionuclides remained attached to the residual ammonium nitrate matrix or bonded to soil particles.

Many other releases of particles, crystals or flakes contaminated with ruthenium occurred. The most notable ones were in September 1952; August and September 1953; and January, May, and June 1954. The releases in early January 1954 were estimated to be the largest. These provided many opportunities to study the particles that were found in the environment. The age of the particles was estimated using the activity ratio of ^{103}Ru to ^{106}Ru. The observed lower activity of ^{103}Ru was consistent with deposition and holdup on the walls of the stack and release when flakes of the ammonium nitrate, also deposited there, were resuspended into the stack exhaust. A summary table of characteristics of the particles found in the environment is presented in Section 4.2.1.

Measurements performed inside the stack at the REDOX Plant provided information on the size of the primary aerosol for normal conditions, which consisted of relatively small particles. In May 1953, the first measurements indicated a geometric mean physical diameter of 0.2 µm (HW-28780). Four later measurements (December) gave geometric mean diameters that were higher, 0.3 to 0.4 µm (HW-32209). The geometric standard deviations found in the December stack measurements were also greater, ranging from 2.0 to 2.8, compared to 1.6 and 2.5 found in May. The later measurements were more consistent and are considered more reliable. They serve to define a reference aerosol for normal conditions with a geometric mean diameter of 0.35 µm and a geometric standard deviation of 2.5. Diameters corresponding to the 5th and 95th percentiles of this lognormal distribution are 0.077 and 1.6 µm, respectively.

Aerodynamic diameters of the primary ruthenium dioxide particles would be greater than their physical diameters. The theoretical density of RuO_2 is about 7 g cm^{-3}. Following the guide given on page 2-4, we estimate that the actual particle density would be about 4.9 g cm^{-3}. Assuming a default shape factor of 1.5 (ICRP 1993b), the reference aerodynamic diameter is estimated to be about 0.63 µm. The corresponding 5th and 95th percentile aerodynamic diameters are estimated to be 0.14 and 2.9 µm, respectively.

The distributions of particles collected at the inlet to the sand filter were even broader, geometric standard deviations of 2.8 and 3.2 were determined for two samples (HW-32209). These particles were likely formed from the droplets that escaped from the scrubber exhaust. The

observed average geometric standard deviation of ~3 is larger than the estimate made for the primary aerosol in the T Plant and B Plant exhausts (see Section 2.2.1).

Parker's September 1954 status report suggests that the releases from the scrubber failures consisted of larger particles. The releases of primary and most recent concern at that time were the large ruthenium discharge in January due to a scrubber failure (supplemented by a release during stack flushing) and the May release of particles from the interior surface of the stack. Both releases impacted onsite areas and the exposure of military and other personnel onsite (Johnson 1954) as well as the offsite public (HW-33068). The latter reference identifies small particles with typical dimensions of 2 μm, which is larger than the geometric mean diameter measured in the REDOX Plant stack. On the basis of measurements cited above, it is reasonable to assume a geometric standard deviation of ~3 for this particle distribution.

If we take the typical diameter of 2 μm for the scrubber failure aerosol to be the mean value, then the average activity per particle would be about 15 kBq (0.41 μCi). Release of 37 GBq (1 Ci) of radioruthenium during a scrubber failure would involve the release of ~2 million particles (rounded to one significant figure). Most of the radioactivity of these particles would be due to ^{103}Ru.

Characteristics of the secondary aerosols, suspended from the interior surface of the stack, were determined from particles collected in the environment. As noted, some of the contaminated ammonium nitrate flakes collected soon after release were quite large. In contrast to the primary aerosol, which consisted entirely of respirable particles, these big flakes were not even inhalable. After the flakes were broken down in the environment, the active particles were smaller, and inhalable, typically about 100 μm in diameter. In the absence of information, a geometric standard deviation of 3 is assumed for this particle distribution. This choice is considered to be reasonable in view of the other measurements that have been discussed. The largest particles contained up to 200 μCi (7.4 x 10^6 Bq) of ruthenium. On a mass basis the weathered particles were found to be mainly inert; either residual ammonium nitrate or sand was the main component. Some large particles that were found close to the facility produced dose rates in "contact" with survey meter probes that were as high as 20 rad h^{-1} (0.2 Gy h^{-1}) (HW-33068).

Ruthenium particles were measured offsite on several occasions. The release due to the scrubber failure in January 1954 contaminated a narrow strip of land to the northeast, and was detected as far away as Spokane (~200 km) (Figure C-20). A release in May 1954 that produced a strip of contamination in 100-B Area was detected even further north on Wahluke Slope. The discovery that particles had migrated to Richland and other residential areas in August 1954 triggered a broad survey. By early September, contamination had been measured in Richland, Pasco, and Kennewick, all to the southeast; in and around Benton City to the south; on the Wahluke Slope to the north; in Ringold, Mesa, and Connell to the east; and along the approximately north-south line between Ringold and Pasco. Contamination was not found to the northeast in Othello or Lind or in the southwest-west quadrant (Prosser, Sunnyside, Grandview, Yakima) or far (110 km) to the east in Colfax. Appendix C contains ground contamination survey maps for these and other times.

Contemporary soil contamination maps showed particles with diameters greater than 100 μm to be within 4 km of the plant. Maximum deposition densities occurred within about 400 m and were 2–5 particles per 100 m^2. Particles with diameters in the range 3–100 μm were more numerous and were distributed over a much larger area. Near the stack, surface deposition

densities were in the range 100–1000 particles per 100 m^2 for particles of that size. Offsite deposition densities were on the order of one particle per 100 m^2 (Parker 1956b, HW-33068).

Particles found offsite were characterized according to contact dose rate, as measured by instruments. Parker presented results for 288 such particles (HW-33068); the results are given in mrad h^{-1}, traditional units for the time. Contact dose rates for about two-thirds (65.6%) of the particles were in the range 5–50 mrad h^{-1}. About 6% of the measured particle dose rates were lower (1–5 mrad h^{-1}) and about 30% were higher. The percentages of particles exhibiting higher dose rates were: 16% in the range 50–100 mrad h^{-1}, 9.7% in the range 100–200 mrad h^{-1}, 1.7% in the range 200–300 mrad h^{-1}, and 1% greater than 300 mrad h^{-1}. The three most radioactive particles each exhibited a different dose rate: one reading was between 300 and 400 mrad h^{-1}, one reading was 700 mrad h^{-1}, and the last reading was 1400 mrad h^{-1}. It is expected that the observed dose rate was proportional to the ruthenium activity present. Thus, the data on "contact dose rates" provide some information about the activity distribution in the particles. The distribution of reported contact dose rates measured near particles is shown in Figure 2-3. The data suggest that the GSD of the activity distribution was about 3.

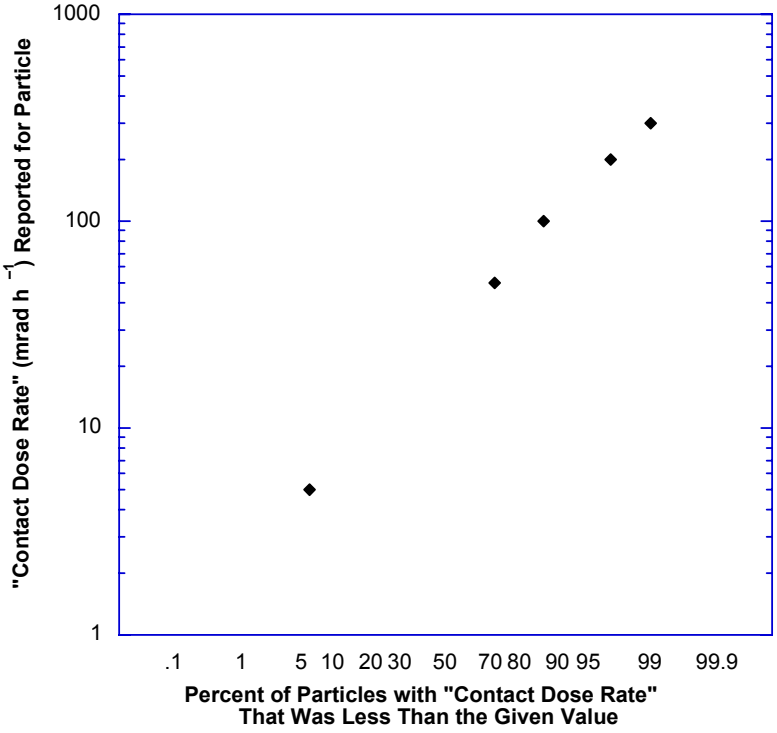

Figure 2-3. Distribution of reported "contact dose rates" for REDOX ruthenium particles found at offsite locations.

The physical size of these offsite particles is not readily determined from the dose rate measurements because the amount of inert material in particular particles is unknown. In general, the particles most likely to be carried great distance by the wind are sufficiently small that they would be in the respirable size range. This generality applies both to stack releases and to particles resuspended from areas of contaminated soil. It does not apply to the releases of flakes

of ruthenium-contaminated ammonium nitrate, whose physical form could allow them to "sail" and transport the contaminant particles over a long distance. Such particles would not be inhalable prior to deposition. The offsite particles that were examined were aged; the time between releases in April–June and the surveys (late August–October) was 2–5 months. In many cases the ammonium nitrate carrier may have disappeared.

Following the method employed for the corrosion particles, we may assign the highest observed particle activity to the 95th percentile of the activity distribution. The GSD of the activity distribution is estimated to be 3, and the median particle activity can be calculated to be about 1.2 MBq (33 μCi). The mean particle activity for this distribution is about 2.2 MBq (60 μCi). A release of 37 GBq (1 Ci) of ruthenium released in the form of flaky particles from the stack wall is estimated to correspond to a release of only ~2 x 10^4 particles (again rounding to one significant figure). Releases of this type occurred several times during the early operation of the REDOX Plant (June and September 1952, August and September 1953, and April, May, and June 1954). A major release in January 1954 appears to have been due to a combination of causes, so the number of particles released at that time was likely higher.

2.3 Screening Calculations to Identify the Most Important Radionuclides

It is apparent from the previous section that the ruthenium isotopes are quite important to onsite human exposure to radioactive particles released to the atmosphere from Hanford plants. The relative importance of other particulate radionuclides is less clear, in part because they received less detailed attention and because measurement capabilities in the early years did not include gamma spectrometry, which would have been a great aid to the particle characterization and other analytical work. Measurements of most short-lived gaseous radionuclides were similarly limited during the early years of operation.

A screening procedure was used to determine the radionuclides that were the most important contributors to radiation dose from early Hanford releases. Historical experience, illustrated by the particle releases discussed above, indicated that processing plant releases would be of greatest interest, but the potential for radionuclide releases from the production reactors must also be considered. The screening process, described below, employed screening factors developed by the National Council on Radiation Protection and Measurements (NCRP) in Report No. 123 (NCRP 1996). For exposure pathways associated with atmospheric releases, the screening factors provide a cautious index of the committed effective dose (Sv) per unit air concentration (Bq m^{-3}). Although designed for releases of long duration, the NCRP screening factors have also been shown to be useful in ranking short-term releases (Meyer et al. 2002).

This screening procedure focused on the question of which radionuclides were most important for assessing doses due to normal operations or common off-normal conditions at the reactors and fuel processing facilities. It does not address the question of which facility contributed most to dose. It is known that releases from processing facilities decreased over time; those changes are reflected in the estimates of releases (Section 2.4). It is beyond the scope of this project to consider the relative importance of individual incidents identified (HW-54636, for example) during the period of interest.

There were four primary pathways by which persons living and working at various locations on the Hanford Reservation were exposed to plant releases. These were inhalation of radionuclides, direct radiation from the plume of airborne material, direct radiation from

radionuclides deposited on the ground following plume passage, and direct radiation from particles that were retained on the body. Exposures via the first three pathways are addressed in the NCRP screening report, but the skin exposure pathway is not. Recommendations regarding "hot particle" exposures were given in NCRP Report No. 106 (NCRP 1989) and, more recently, in NCRP Report No. 130 (NCRP 1999). Both ^{106}Ru and ^{144}Ce decay to unstable radionuclides (rhodium-106 [^{106}Rh] and praseodymium-144 [^{144}Pr], respectively) that emit high-energy beta particles. These radionuclides are primarily responsible for the high dose rates associated with some of the radioactive particles from the fuel processing plants. Yttrium-90 (^{90}Y), produced by the decay of ^{90}Sr, also emits high-energy beta particles, but the contribution was smaller due to the smaller amounts of ^{90}Sr in the particles.

Our screening calculations consider early Hanford radionuclide releases from the production reactors and from the fuel processing facilities. Only very volatile elements, noble gases and halogens, have a substantial potential for release from the operating reactors during normal operations and minor upsets (such as fuel cladding failures). Isotopes of the noble gases krypton and xenon and the halogens iodine and bromine are of greatest interest. All of these isotopes are produced by fission of uranium fuel. Another radioactive noble gas isotope, argon-41 (^{41}Ar) was produced by neutron activation of stable argon in air and discharged from the reactor stacks. Other radionuclides released from the reactors were tritium (^{3}H), which is produced by ternary fission and activation and can be present in hydrogen gas or in water vapor, and the neutron activation product carbon-14 (^{14}C), which also can be present in gaseous forms. Releases from the fuel processing facilities included ^{131}I, ^{133}Xe, and the radionuclides associated with the "active particles" released during Hanford operations. Preliminary screening of releases from the production reactors is described in the next section.

2.3.1 Preliminary Screening of Releases from Production Reactors

The fission product inventory of the Hanford production reactors includes volatile and potentially volatile radionuclides as well as those commonly present in particulate form. Under normal conditions, all these radionuclides were held within the fuel slugs by the cladding that contained the uranium fuel. There were, however, failures of the fuel slug cladding. When such failures occurred, fuel particles were carried from the slug by the cooling water and transported by the cooling water retention pond. Most of the radioactivity releases were to the Columbia River, but the possibility of radioactivity releases to the atmosphere as the result of these failures must also be considered.

Gydesen (1993) performed a detailed review of the failures of fuel cladding that occurred in the Hanford single-pass production reactors between 1944 and 1971 and identified about 2000 such failures. Details about the location of the failed fuel slugs, their irradiation history, and other information documented in plant records was retrieved and presented in the report.

There were also earlier reports that addressed the fuel cladding failure issue. DeNeal (1965) provided data on the number of failures (in all reactors) of fuel and target element cladding per calendar year. Initially, there were few failures: none before 1948, two in that year, none in 1949, and three in 1950. The number of failures of fuel element cladding was much higher in 1951 (102) and remained in the range of 90–250 for each year through 1958. Fewer failures (68–130) occurred in the years 1959–1964. Table 2-2 provides the data for 1948–1958, which includes the period of interest for this study. Failures of target element cladding are not included in Table 2-2.

Table 2-2. Fuel Cladding Failures during 1948–1958

Year	Number of slug cladding failures		Severe ruptures	Severe rupture
	DeNeal (1965)	1959 Report[a]	1959 Report[a]	fraction[a]
1948	2			
1949	0			
1950	3			
1951	102			
1952	142	139	19	0.14
1953	93	49	13	0.27
1954	211	125	20	0.16
1955	242	186	110	0.59
1956	191	165	96	0.58
1957	201	180	60	0.33
1958	174	165	77	0.47

[a] Values estimated from Figure 1 of McCormack and Schwendiman (1959); estimates for years prior to 1952 were not included in the report.

Table 2-2 also includes data on total cladding failures in seven of the years (1952–1958) that were given by McCormack and Schwendiman (1959). Their estimates of the total number of cladding failures were lower than the later totals given by DeNeal (1965). Two categories of fuel cladding failures were considered at that time, based on the work of Healy (1954). The failures that released the most fuel were termed "severe" (usually a side rupture or fragmented element) and "other" (such as a split or end cap failure). At the time, it was assumed that these two types of failures led to releases of 150 g and 9 g of fuel respectively. It was recognized that this assumption was uncertain, but it was considered to lead to overestimates of the fuel release. The number of severe ruptures identified in the years 1952–1958 by McCormack and Schwendiman (1959) is also shown in Table 2-2, and the fraction of the ruptures that were severe is given in the last column.

McCormack and Schwendiman (1959) provided estimates of fuel losses that were based on data from fuel cladding rupture monitors and from discharge basin and river water monitoring for ^{89,90}Sr. Using data from these sources for parts of 1956–1958, they estimated an average fuel loss of 8 gram per rupture, substantially lower than that estimated using the default assumptions established previously.

Jerman et al. (1965) studied the fuel loss from 97 fuel cladding ruptures in 1964. They concluded that fuel losses from two ruptures were as high as 100 g. Losses from 14 other failures were estimated to be 50–75 g; losses from 22 other failures were estimated to be in the range 1-10 g. Losses from the remaining failed slugs were estimated to be 25 g each. From their data, the total fuel loss for that year is estimated to be about 2.7 kg, with an average loss per cladding failure of about 28 g of fuel. This is higher than the average estimated by McCormack and Schwendiman (1959), but lower than predicted by the earlier rough assumptions about fuel loss. They compared predicted releases of ^{131}I to the river from natural uranium in the cooling water and from fuel cladding failures with river monitoring data. Their results for 1964 indicate that about two-thirds of the ^{131}I in fuel released by cladding failures did not reach the river. Based

upon uranium particle size measurements for similar conditions, McCormack and Schwendiman (1959) estimated that gravitational settling of uranium particles in the cooling water retention basin would remove about half of the uranium particles that were transported from the reactor to the basin. Radioactive decay of short-lived nuclides retained in the fuel particles would further reduce the release to the basin and the environment.

The volatile and potentially volatile fission products have relatively short half-lives and reach equilibrium in the reactor fuel in relatively short times, two months at most. A qualitative review of the irradiation times given in Gydesen (1993) suggests that the quantities of these radionuclides in a fuel slug whose cladding failed are likely to have been near equilibrium values. Table 2-3 lists noble gas and halogen radionuclides with half-lives greater than 10 minutes and equilibrium fuel inventories greater than 3.7 TBq. The table includes the radionuclide half-life, the average concentration in reactor fuel, and the atmospheric screening factor for each radionuclide. Complete fission product inventories of Hanford reactor fuels computed for the Hanford Environmental Dose Reconstruction Project were not published; however, Napier (2002b) provided inventories of some radionuclides that he had obtained from ORIGEN computer code runs for Hanford reactors. The fuel concentrations in Table 2-3 were scaled from a pressurized water reactor inventory (Canada 1980) to early Hanford reactor conditions provided by Napier (2002b). Comparison of fuel concentrations for ^{131}I and ^{132}I showed that the scaled concentrations were quite close to values from Napier (2002b); the scaled concentration for ^{133}Xe was about 20 percent lower than the Hanford value.

The radionuclides most likely to be released to the atmosphere following a fuel cladding failure are isotopes of the noble gas elements krypton and xenon, which can more easily escape from the fuel particles by diffusion and will not interact chemically with other constituents of the cooling water. Formation of a halogen gas molecule and subsequent diffusion from a fuel particle is not as rapid, and the probability of escaping from cooling water is much lower. This is because: (1) treatment of the reactor cooling water with 2 ppm sodium dichromate to inhibit corrosion (Walters et al. 1992) provided a large number of Na^+ ions with which the halogens could react chemically to form NaI and NaBr and (2) the partition coefficient (the ratio of the concentration in water to that in air at equilibrium) strongly favors the retention of halogens in the water phase.

Pelletier and Hemphill (1979) reported on the partitioning of radioiodine under various conditions. For a pH of 7, typical of the reactor cooling water (Walters et al. 1992), three measured total iodine partition coefficients ranged from 3500–4900 (average of 4300) for water temperatures between 25 °C and 80 °C (Pelletier and Hemphill 1979). Thus, little (~0.02%, on the basis of partitioning alone) of the radioactive iodine that reached the water from the fuel would escape into the air, and it is not expected that bromine radionuclides would behave in a substantially different manner. Even without considering the effects of chemical reactions with sodium ions, which would further reduce the potential for halogen releases, the noble gases, particularly ^{88}Kr and ^{138}Xe, are seen to be the largest sources of potential dose. Other noble gases (^{87}Kr, ^{135}Xe, ^{135m}Xe, and ^{133}Xe) make smaller contributions to the potential dose from fuel cladding failures.

Table 2-3. Fuel Concentrations and Atmospheric Screening Factors for Radioactive Noble Gas and Halogen Fission Products in Reactor Fuels

Radionuclide	Half-life[a]	Average concentration in fuel (GBq g^{-1})[b]	NCRP screening factor[c] Sv per Bq m^{-3}
^{82}Br	35.34 h	0.00075	1.4×10^{-4}
^{83}Br	2.39 h	0.17	2.4×10^{-7}
^{84}Br	31.8 m	0.31	3.6×10^{-6}
^{83m}Kr	1.83 h	0.17	1.1×10^{-10}
^{85m}Kr	4.48 h	0.39	2.0×10^{-7}
^{87}Kr	76.3 m	0.77	1.0×10^{-6}
^{88}Kr	2.86 h	1.1	5.3×10^{-6}
^{131}I	8.04 d	1.0	2.4×10^{-4}
^{132}I	2.28 h	1.5	1.2×10^{-5}
^{133}I	20.9 h	2.3	4.1×10^{-5}
^{134}I	52.6 m	2.6	6.6×10^{-6}
^{135}I	6.61 h	2.1	2.4×10^{-5}
^{131m}Xe	11.8 d	0.011	1.0×10^{-8}
^{133}Xe	5.25 d	2.2	4.3×10^{-8}
^{133m}Xe	2.19 d	0.069	3.7×10^{-8}
^{135}Xe	9.10 h	0.50	3.0×10^{-7}
^{135m}Xe	15.7 m	0.41	3.7×10^{-7}
^{138}Xe	14.2 m	2.0	2.2×10^{-6}

[a] Abbreviations used here: m = minutes, h = hours, d = days.
[b] Sources of fuel concentration estimates are described in text.
[c] Atmospheric screening factors from Appendix B, NCRP 1996.

Jerman et al. (1965) suggest that cladding failures are more likely to occur in fuel slugs located in the central part of the core, which has the highest neutron flux and power level. In this region, the power level is about 12.5 times the average, and the radionuclide production is similarly elevated. On this basis, the ^{88}Kr concentration in some failed fuel slugs could be ~14 GBq g^{-1}. For an average release of 20 g of fuel in each of 240 failures in a year, an approximate bound on the annual ^{88}Kr release can be estimated to be about 67 TBq by assuming that all the failures were in cladding of slugs from the highest flux region in the core.

Heeb (1994) estimated releases of other radionuclides (^{41}Ar, ^{3}H, and ^{14}C) from the eight Hanford production reactors on the basis of limited historical measurements. Those estimates, shown in Table 2-4, are used for preliminary screening of these reactor releases. The screening factors for the pathways of concern for onsite exposure, inhalation plus direct radiation from airborne radioactivity, are also given in the table. For these nuclides there is no contribution due to direct radiation from surface deposition. The relative importance of these three radionuclides can be estimated by comparing the products of the release rate and the corresponding screening factor. The estimated dose contribution from the noble gas ^{41}Ar is seen to be about 10,000 times greater than that from ^{3}H and about 3,000 times greater than that from ^{14}C.

Table 2-4. Estimated Release Rates from Hanford Reactors and Air Pathway Screening Factors for ^{41}Ar, ^{3}H, and ^{14}C

Radionuclide	Estimated release from all reactors (Bq d^{-1})[a]	Screening factor for inhalation and direct radiation exposure (Sv per Bq m^{-3})[b]
^{41}Ar	1.5×10^{13}	1.5×10^{-6}
^{3}H	5.2×10^{10}	1.4×10^{-7}
^{14}C	4.8×10^{9}	4.5×10^{-6}

[a] Release estimates from Heeb (1994).
[b] Screening factors from Appendix B of NCRP (1996).

The release estimate for ^{41}Ar in Table 2-4 applies only to the period when all eight reactors were operating. This also corresponds to the period of when there were many fuel cladding failures. The estimated annual release of ^{41}Ar at that time was about 5500 TBq, roughly 80 times the estimate for ^{88}Kr given above. The screening factor for ^{88}Kr is about 3.5 times greater than that for ^{41}Ar; overall, the product of release rate and screening factor is more than 20 times higher for ^{41}Ar than for ^{88}Kr.

It is interesting to compare the noble gas releases from the reactors with the noble gas releases from the fuel processing facilities. Releases of ^{41}Ar increased with time as new reactors were brought online. This contrasts with the release history of ^{133}Xe, which decreased over time because longer fuel cooling times were employed. The ^{133}Xe releases were highest in the fall of 1945 (see Section 2.3.2). At that time, there were three reactors operating at three different locations. Heeb (1994) estimated the daily release of ^{41}Ar from each site to be 5.7 TBq. For a reactor operating 90% of the time, the monthly release of ^{41}Ar would be about 155 TBq. The relative importance of that release rate can be compared to the peak monthly ^{133}Xe release rate of 1.6 PBq (Section 2.3.2). The screening factor for ^{41}Ar is about 35 times larger than that for ^{133}Xe, so a simple comparison suggests that even during 1945 the ^{41}Ar release was more important. The comparison is complicated by the fact that the releases occurred at different locations. There may not have been persons exposed at comparable locations downwind from the two locations.

Releases of ^{41}Ar were much more important than other releases from the production reactors and appear to be the most important of all noble gas releases in 1945. Because the ^{41}Ar release rates increased with time and the release rate for ^{133}Xe dropped by more than a factor of ten in 1946 (and further after that; see below), the ^{41}Ar releases are considered the most important noble gas releases throughout the period of interest.

2.3.2 Comparison of Radioactive Gas Releases from Fuel Processing Facilities

The largest radioactivity releases from the fuel processing facilities were of the halogen ^{131}I (Heeb 1994), and it has received the most attention in the studies of past Hanford operations. It serves as a useful point of reference for other radionuclides that were released from the same facilities. The noble gas inventory and potential dose comparisons in the previous section show that ^{133}Xe was the most important noble gas released from the fuel processing plants.

The relative importance of the releases of these two gaseous radionuclides can be assessed in a straightforward way. It is reasonable to expect that nearly all of the ^{133}Xe present in the fuel

elements was released during fuel dissolution. Estimated ^{133}Xe releases are shown in Figure 2-4 for the early years of operation when they were highest. In making the estimates, it was assumed that the average fuel cooling time was appropriate for all the fuel processed. This assumption could lead to an underestimate of releases if the fuel cooling times were highly variable and included significantly shorter cooling periods for some fuel. The increase in fuel element cooling time that began in 1946 caused substantial reductions in the ^{133}Xe releases.

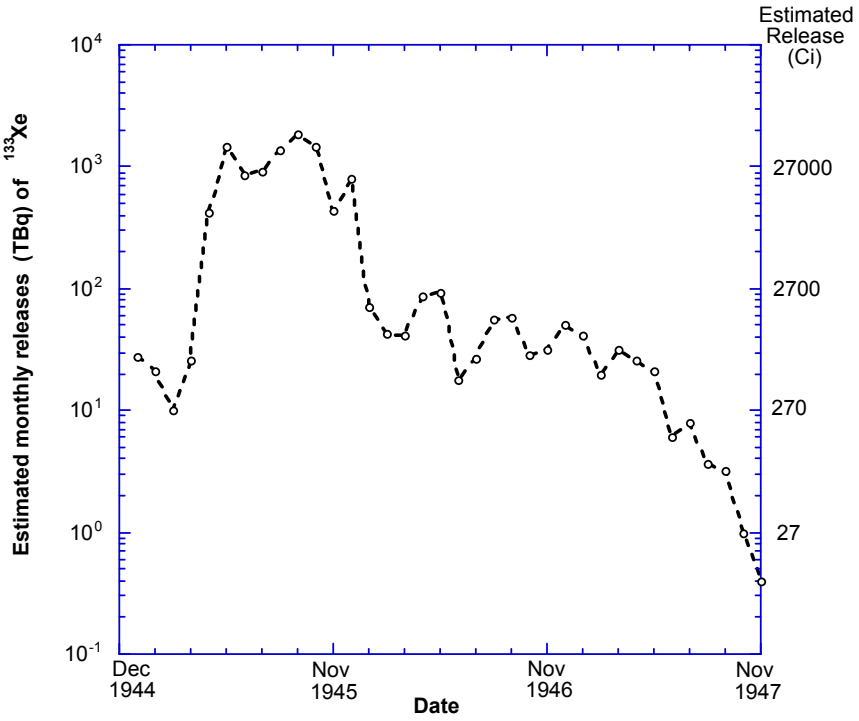

Figure 2-4. Estimated monthly releases of ^{133}Xe during fuel processing at Hanford.

The estimated monthly ^{133}Xe release was highest, about 1.6 PBq (42,000 Ci), in September 1945. In that same month, the release of ^{131}I was estimated (Heeb 1994) to be about 3.3 PBq (89,000 Ci). Screening factors for exposure to atmospheric releases by the inhalation and direct radiation pathways (from the plume and ground deposition) for ^{133}Xe and ^{131}I are 4.3 x 10^{-8} and 2.4 x 10^{-4} Sv per Bq m^{-3}, respectively (NCRP 1996). The ratio of the screening factor for ^{133}Xe to the comparable factor for ^{131}I is about 1.8 x 10^{-4}. The relative dose contributions can be estimated by comparing the products of the release quantities and the screening factors. The conclusion is that, at the peak of the ^{133}Xe releases, its contribution to the dose was more than 10,000 times smaller than that from ^{131}I.

In the next section, we consider the relative importance of many particulate radionuclides, including those (^{89}Sr, ^{90}Sr, ^{91}Y, ^{95}Zr, ^{103}Ru, ^{106}Ru, ^{137}Cs, ^{141}Ce, ^{144}Ce, and ^{239}Pu) associated with "active particles" from early Hanford operations. Those releases are compared with production reactor releases of ^{41}Ar. The estimated releases of ^{131}I from the processing facilities serve as a point of comparison for the screening, which is performed using the NCRP (1996) screening factors.

2.3.3 Screening Comparisons for Fuel Processing and Reactor Releases

Screening calculations to assess the relative importance of various short-lived gases and particulate radionuclides rely on information from several sources. Heeb (1994) provides information on the quantities of several radionuclides in fuels removed from the Hanford reactors, but comprehensive inventories of radionuclides in the fuel were not published. Some inventory data were provided in the river pathway screening report (Napier 1991). Napier (2002b) provided additional inventory estimates for about 30 particulate radionuclides that he had obtained from output files of ORIGEN computer runs made for the HEDR project. These are shown in the first two columns of Table 2-5. The processing rates in Heeb (1994) and the inventory estimates of Napier (2002b) reflect the particular design and operation of the Hanford reactors, which differed from later reactors designed for power production. Heeb (1994) discusses the uncertainties in computed inventories that are related to differences in parameters used in the calculations. For the isotopes that he considered, the maximum uncertainties were about 15%.

Table 2-5. Sources of Inventories for Particulate Radionuclides Considered in Initial Screening Calculation

Inventories obtained from HEDR spreadsheets[a]		Other inventories scaled from PWR estimates[b]	
^{59}Ni	^{234}U	^{85}Sr	^{134}Cs
^{63}Ni	^{235}U	^{86}Rb	^{136}Cs
^{60}Co	^{238}U	^{87}Rb	^{140}Ba
^{89}Sr[c]	^{238}Pu[c]	^{91}Y	^{140}La
^{90}Sr-Y[c]	^{239,240}Pu	^{99}Mo	^{143}Pr
^{93}Zr	^{241}Pu[c]	^{110m}Ag	^{144m}Pr
^{95}Zr[c]	^{239}Np[c]	^{115m}Cd	^{147}Nd
^{95}Nb[c]	^{241}Am	^{119m}Sn	^{147}Pm
^{99}Tc[c]	^{243}Cm	^{123}Sn	^{148}Pm
^{103}Ru[c]	^{244}Cm	^{124}Sb	^{148m}Pm
^{106}Ru-Rh[c]		^{125}Sn	^{149}Pm
^{113m}Cd[c]		^{125}Sb	^{153}Sm
^{132}Te-I[c]		^{125m}Te	^{155}Eu
^{137}Cs[c]		^{126}Sb	^{156}Eu
^{141}Ce[c]		^{127}Sb	^{160}Tb
^{144}Ce-Pr[c]		^{127}Te	^{161}Tb
^{151}Sm[c]		^{127m}Te	^{242}Cm
^{152}Eu[c]		^{129}Te	
^{154}Eu[c]		^{129m}Te	

[a] Data provided by Napier (2002b).
[b] Based upon Canada (1980).
[c] Radionuclides, whose inventories were obtained from both sources and used in inventory comparisons.

Inventories for other particulate radionuclides were obtained from a set of calculations (Canada 1980) for a pressurized water reactor (PWR) that had operated for about 100 days. The inventories were scaled to match the Hanford conditions so the estimates could be compared. Radionuclides in the first two columns of Table 2-5 marked by footnote "c" were obtained from both sources, and were found to be in reasonable agreement. The mean ratio (HEDR to scaled PWR) was 0.84 and the range of ratios was 0.5–1.5. Other particulate radionuclides whose inventories were obtained by scaling the PWR inventory are listed in the last two columns of Table 2-5. The HEDR inventories were preferred for the screening calculations and were used when available; however, use of the scaled PWR inventories was also considered appropriate for our purposes and more than doubled the number of particulate radionuclides that could be screened for possible further evaluation.

Because military and construction personnel were onsite during an extended period and because the releases of radionuclides were not constant over that time, it was decided that a series of screening calculations should be performed to reflect the variety of conditions that were encountered by these people. The initial screening, reflective of the earliest years, was for the month of October 1945. Six other comparisons were made at 18-month intervals (April 1947, October 1948, and so on) and a final comparison was made in February 1956 (rather than in April of that year) because it was the month that the T Plant was shut down.

The initial screening in October 1945 was performed to determine which of the particulate radionuclides was appropriate for further evaluation. For this comparison, three exposure pathways were considered: inhalation, direct radiation from the plume, and external radiation from surface deposits. The screening factors for inhalation and direct radiation from the plume were used directly from the NCRP (1996) tabulation, but those for external radiation from surface deposits of all radionuclides were adjusted to reflect a 3-yr (rather than 30-yr) buildup of the surface deposit to better reflect the duration of very high startup releases from the fuel processing facilities. The three screening factors were summed and the total was used in the screening comparison. Releases of ^{131}I from the fuel processing facilities and releases of ^{41}Ar from the reactors were also included in this comparison; releases of ^{131}I ranked highest and those of ^{41}Ar ranked fifth overall. Thirty-one of the particulate radionuclides each contributed more than 1 part in a million to the total screening index and were kept on the list for further screening. The particulate radionuclides that contributed less than 1 part in a million to the total screening index were not considered in subsequent screening calculations. Table 2-6 contains the list of radionuclides that were retained, their estimated average fuel concentrations after a 30-d cooling period, and the screening factors used for the remaining seven periods. For those periods, the component of the screening factor reflecting direct radiation from surface deposits of the radionuclides was adjusted for a 9-yr period of accumulation.

For each of the seven times considered, a screening index was computed for each radionuclide. That index was the product of the nominal release rate and the screening factor. The importance of each radionuclide at each time was then determined by ranking the values of the screening indices computed for that time.

The nominal release rates for particulate radionuclides were estimated by assuming that an average release fraction of 10^{-7} applied to all of them. This assumption reflects the expectation that the particles were a mixture of the available radionuclides and that the radionuclides did not selectively attach to particles independently. This issue is discussed further in Section 2.4. The ^{41}Ar releases estimated by Heeb (1994) were adjusted for an operating fraction of 0.9 for these

calculations. The estimates for ^{41}Ar considered only the reactor site with the maximum release at each time. Because the releases of ^{41}Ar occurred at differing locations, there is some lack of comparability among the results of the screening calculations, but those differences do not substantially affect the conclusions obtained. For comparison, the mean ^{131}I release estimates made by Heeb (1994) for 1945–1949, and the more recent estimates of Napier (2002a, 2002b) for 1950–1956 were used in the screening calculations.

Table 2-6. Fuel Concentrations and Adjusted Screening Factors for Subsequent Screenings

Radionuclide	Concentration (GBq kg^{-1}) in fuel at 30-d	Adjusted screening factor[a]	Radionuclide	Concentration (GBq kg^{-1}) in fuel at 30-d	Adjusted screening factor[a]
^{60}Co	0.514[b]	9.9 x 10^{-2}	^{140}Ba	847	1.1 x 10^{-3}
^{85}Sr	3.00	1.2 x 10^{-3}	^{140}La	974	1.4 x 10^{-4}
^{89}Sr	935[b]	9.4 x 10^{-5}	^{141}Ce	1940[b]	1.2 x 10^{-4}
^{90}Sr-Y	23.3[b]	2.8 x 10^{-3}	^{143}Pr	930	2.0 x 10^{-5}
^{91}Y	1830	1.2 x 10^{-4}	^{144}Ce-Pr	636[b]	1.4 x 10^{-3}
^{95}Zr	1360[b]	3.5 x 10^{-3}	^{147}Nd	245	7.4 x 10^{-5}
^{95}Nb	1360[b]	9.7 x 10^{-4}	^{147}Pm	94.6	8.2 x 10^{-5}
^{103}Ru	706[b]	7.2 x 10^{-4}	^{148m}Pm	8.99	3.1 x 10^{-3}
^{106}Ru-Rh	82.1[b]	3.8 x 10^{-3}	^{154}Eu	0.173[b]	6.6 x 10^{-2}
^{110m}Ag	0.0680	2.4 x 10^{-2}	^{155}Eu	0.976	3.2 x 10^{-3}
^{127}Te	9.92	7.6 x 10^{-7}	^{156}Eu	10.7	7.1 x 10^{-4}
^{129m}Te	40.5	1.4 x 10^{-4}	^{238}U	0.00489[b]	2.6 x 10^{-1}
^{131}I	80.9[b]	2.4 x 10^{-4}	^{238}Pu	0.0245[b]	5.0 x 10^{-1}
^{134}Cs	4.78	4.0 x 10^{-2}	^{239}Pu	1.04	5.5 x 10^{-1}
^{136}Cs	3.93	1.0 x 10^{-3}	^{241}Pu	4.73	1.0 x 10^{-2}
^{137}Cs	25.9[b]	3.7 x 10^{-2}	^{241}Am	0.000261	5.7 x 10^{-1}

[a] Sum of screening factors factors (Sv per Bq m^{-3}) for inhalation, direct radiation from plume, and direct radiation from deposits on the ground, adjusted for 9-yr period of accumulation; Appendix B of (NCRP 1996).
[b] Derived from (Napier 2002b); other values scaled from Canada (1980).

The top portion of Table 2-7 shows the amount of fuel processed in plants (T, B, or REDOX) that operated during the month and the average time the fuel was held to allow radioactive decay before processing (Heeb 1994) for each of the months considered in the screening calculations. The main body of the table contains the rankings of the radionuclides according to the screening indices calculated for each time period. The last column shows the sum of the individual rankings for each radionuclide. The table shows that ^{131}I was ranked first for seven of the eight periods and that, except for the first period, ^{41}Ar ranked either second or first.

Table 2-7. Fuel Processing Data and Results of Screening Calculations for Selected Times

	Oct 1945	Apr 1947	Oct 1948	Apr 1950	Oct 1951	Apr 1953	Oct 1954	Feb 1955	
FP (Mg)[a]	0.514	0.247	0.304	0.260	0.384	0.657	1.26	2.30	
Decay (d)[b]	41	66	99	98	47	80	111	151	
Radio-nuclide	Rank according to screening index for selected time								Sum[c]
^{41}Ar	10	2	2	2	2	2	2	2	23
^{60}Co	17	16	14	14	16	15	13	13	118
^{85}Sr	27	26	24	24	28	24	24	26	203
^{89}Sr	14	15	16	16	14	17	16	16	124
^{90}Sr-Y	15	14	12	12	15	13	12	10	103
^{91}Y	11	11	11	11	12	11	11	12	90
^{95}Zr	2	3	3	3	3	3	3	3	23
^{95}Nb	3	6	7	7	5	7	7	9	51
^{103}Ru	7	9	10	10	8	9	10	11	74
^{106}Ru-Rh	9	8	8	8	10	8	8	7	66
^{110m}Ag	29	29	26	26	30	27	25	25	217
^{127}Te	33	33	33	33	33	33	33	33	264
^{129m}Te	25	25	25	25	25	25	27	27	204
^{131}I	1	1	1	1	1	1	1	2	9
^{134}Cs	13	10	9	9	11	10	9	8	79
^{136}Cs	28	31	31	31	31	31	31	31	243
^{137}Cs	8	4	4	4	4	4	4	4	36
^{140}Ba	6	12	17	17	9	14	18	23	116
^{140}La	31	31	32	32	32	32	32	32	255
^{141}Ce	12	13	3	13	13	12	15	15	106
^{143}Pr	20	24	28	28	21	26	28	28	203
^{144}Ce-Pr	4	5	5	5	6	5	5	5	40
^{147}Nd	21	27	30	30	23	29	30	30	220
^{147}Pm	22	21	21	21	22	21	20	19	167
^{148m}Pm	18	18	20	20	18	19	21	21	155
^{154}Eu	26	20	19	19	20	20	19	18	161
^{155}Eu	30	23	23	23	27	23	23	22	194
^{156}Eu	24	28	29	29	26	30	29	29	224
^{238}U	32	30	27	27	31	28	26	24	225
^{238}Pu	19	19	18	18	19	18	17	17	145
^{239}Pu	5	7	6	6	7	6	6	6	49
^{241}Pu	16	17	15	15	17	16	14	14	124
^{241}Am	23	22	22	22	24	22	22	20	177

[a] Total amount of fuel processed during month at all plants operating at the time.
[b] Average decay time for fuel processed during the month.
[c] The most important radionuclides are those with the smallest total ranks.

The screening calculations effectively assumed that there were exposed persons at locations with comparable atmospheric dispersion for all of the sources. In fact, persons were located closer to the processing facilities in the 200 Areas than to the various 100 Areas where the ^{41}Ar releases were highest at the times considered. This simplification may have led to overestimation of the contribution of ^{41}Ar and a higher score. On the other hand, only releases from a single site were considered and there are some wind directions that would carry the releases from multiple sites in the same direction. In any case, ^{41}Ar was clearly the most important of the reactor releases and was included in the list of most important nuclides.

The screening calculations also assumed that the releases of particles were from a single location in the 200 Areas. For the times considered, releases occurred at more than one location; however, the screening was designed to select the most important radionuclides released, not the most important release point(s). It should be noted that differences in release locations are considered explicitly in the dose estimation method (Section 3.4) because military personnel were exposed at locations close to the facilities. For those calculations, proper location of the release point(s) is important.

On the basis of these screening results, 13 radionuclides, or radionuclide pairs, (^{131}I, ^{41}Ar, ^{95}Zr, ^{137}Cs, ^{144}Ce-Pr, ^{239}Pu, ^{95}Nb, ^{106}Ru-Rh, ^{134}Cs, ^{103}Ru, ^{91}Y, ^{90}Sr-Y, and ^{141}Ce) were categorized as "most important." The 13 radionuclides listed accounted for more than 99% of the total screening index for all eight periods. Considering only the portion of the screening index due to particulate radionuclides (i.e. not ^{131}I and ^{41}Ar), the eleven radionuclides listed accounted on average for more than 95% of that total, with a range of 92–97% for the eight periods.

2.4 Source Term Development for the Most Important Radionuclides

Each of the radionuclides judged to be among the most important atmospheric releases was discharged at more than one location. The noble gas ^{41}Ar was released from each of the reactor stacks, all located near the Columbia River. The particulate radionuclides were released from facilities in the 200 Areas near the center of the reservation. In the following subsections, the procedures used to estimate releases for the important radionuclides at the individual reactors and processing facilities are described. Monthly information was available for many of the radionuclides of interest (Heeb 1994). Because the duration of exposure for military and other persons on the reservation did not include the entire period considered, monthly processing data were used when available and monthly release estimates were made for all radionuclides. Uncertainties associated with each of the release estimates were incorporated into the calculations and Monte Carlo procedures were used to obtain distributions of release estimates.

The first subsection deals with releases of ^{41}Ar from the reactors. Later subsections deal with releases from the processing facilities.

2.4.1 Releases of ^{41}Ar from Production Reactors

Paas (1953b, 1953d) presented data, obtained in late 1952 and early 1953, on the concentrations of ^{41}Ar in stack effluents from four of the six production reactors then in operation. The limited information from those measurements is presented in Table 2-8; results for individual samples were not given in the referenced documents. The data reported for C Reactor were considered suspect at the time and have not been used in this analysis. The average ^{41}Ar

concentrations found in the effluents from the first three reactors constructed (B, D, and F) are quite similar. Their stack exhaust flow rates were also the same. Higher concentrations were measured in the effluent of DR Reactor, which also had the lowest stack flow rate. The average concentration measured in the H Reactor exhaust was intermediate between the observations at the first reactors and those at DR Reactor. The K Area reactors were not operating at the time of the measurements, but are included in the table to show their stack effluent flow rates, which are similar to those for C Reactor and H Reactor.

The releases from B, D, and F reactors were estimated using a uniform distribution of concentrations between 1 and 39 μCi m^{-3}. That distribution had a mean of 20 μCi m^{-3}, which was the average value measured in the effluents of those three reactors. Releases from DR Reactor were estimated using a uniform distribution with a mean of 80 μCi m^{-3}, the measured average concentration, and bounds of 60 and 100 μCi m^{-3}. The concentrations measured in the H Reactor effluent were used as the basis for estimating releases from the four other reactors (C, H, KE, and KW). A uniform distribution of concentrations between 30 and 66 μCi m^{-3}, which has a mean of 48 μCi m^{-3}, was selected.

In this procedure, effluent concentrations that were measured only for a brief time are used to estimate ^{41}Ar releases over a period of many years. The reactors did not operate continuously, but may have operated throughout any particular month. Examination of detailed reactor operating histories was not attempted. For the calculations of monthly releases, the long-term average on-line fraction of 0.9 was represented as a triangular distribution with bounds of 0.8 and 1.0.

Table 2-8. ^{41}Ar Concentrations Measured in and Effluent Flow Rates for Production Reactor Stacks

Reactor	N[b]	Measured concentration (μCi m^{-3}) of ^{41}Ar[a]		Stack effluent flow rate (m^3 s^{-1})[c]
		Average	Maximum	
B	0	20	39	47
D	4	23	39	47
F	0	17	27	47
DR	11	80	110	40
C	3	<4	<4	64
H	8	48	66	76
KE	[d]	[d]	[d]	67
KW	[d]	[d]	[d]	64

[a] ^{41}Ar concentration data from Paas (1953d).
[b] Number of samples collected (Paas 1953b,d).
[c] Based on flow rates given in Heeb (1994).
[d] The reactor was not operating at the time of the measurements.

Reactor power levels were lower prior to 1951 (Carlisle and Zenzen 1996) and that may have affected the amount of activation (of ^{40}Ar in the air) that occurred. Stack exhaust flow rates also can vary with time and may have been lower during some periods. The concentrations measured in 1952–1953 may have been higher or lower than the long term average values. To reflect these uncertainties, an extrapolation factor was introduced into the calculation. A triangular distribution was assumed with bounds of 0.5 and 1.5 and a mode of 1.

Percentiles from the distributions of monthly releases of ^{41}Ar are presented in Table 2-9. The median and 95th percentiles are contained in an Excel® workbook (Link to Source Terms.xls). Although all of the reactors had individual stacks, three of the 100 Areas had two operating reactors during some periods. Percentiles for the distribution of the sums of release rates for those sites are included in the table and in the spreadsheet.

Table 2-9. Distributions of Monthly Release Estimates for ^{41}Ar from Reactors and Areas

	Percentiles of distributions of release estimates (Ci mo^{-1}) for individual reactors and areas with two reactors				
Reactor	5th	25th	50th	75th	95th
B, D, or F	320	1200	2200	3300	4100
C	4000	5600	7000	8700	11000
B and C[a]	5600	7600	9300	11000	14000
DR	5900	6600	7600	8500	9400
D and DR[b]	7100	8600	9800	11000	13000
H	5700	7000	8600	10000	12000
KE	4200	5900	7400	9100	12000
KW	4100	5600	7000	8700	11000
KE and KW[c]	10000	13000	15000	17000	20000

[a] Both reactors operated in the same area after November 1952.
[b] Both reactors operated in the same area after October 1950.
[c] Both reactors operated in the same area after April 1955.

2.4.2 Releases of Particulate Radionuclides from Fuel Processing Facilities

There were two categories of particle releases from the fuel processing facilities. The first was what may be considered to be from "routine" operations, although the fact that the releases were routine did not mean that they were necessarily small. The "routine" releases were substantially higher during the early years of operations because there were no effluent treatment systems. The second category may be called unusual release conditions. These were times when surprising releases of active and ruthenium particles (Section 2.2) occurred. These two conditions are discussed separately below, followed by estimates of the releases for each of the fuel processing plants.

Routine Operational Releases. Under normal operating conditions, releases of the particulate radionuclides from the fuel processing plants are considered to be generally proportional to the rates at which the radionuclides entered the plants in irradiated fuels that had been discharged from the reactors. Those fuels had been held for varying times to reduce the amounts of short-lived nuclides by radioactive decay. As was illustrated in Figure 2-1, the average fuel cooling times were not constant. Two of the radionuclides considered to be most important (^{103}Ru and ^{141}Ce) were particularly affected by changes in the cooling times because their half-lives are relatively short (Table 2-1). The half-life of ^{95}Nb is also relatively short, but its activity is supported by the decay of ^{95}Zr. Inventories of ^{103}Ru in fuel that was processed after mid-1946 were reduced by the longer cooling times. In general, estimates of the amounts of the particulate radionuclides entering the processing plants are much less affected (when compared

with ^{133}Xe and ^{131}I) by wide variability in periods for which individual batches of fuel were stored before processing.

Heeb (1994) made estimates of radionuclide input to the fuel dissolution process and those are tabulated in his report. The input of ^{103}Ru to the dissolvers during the first 11 years of fuel processing operations is shown in Figure 2-5. The T Plant operated throughout this period. The B Plant operated until June 1952 and the REDOX Plant began operations that year. The general decline in ^{103}Ru input from mid-1946 until the end of 1947 is due, in part, to longer fuel cooling times as well as to a general decline in fuel processing rates. An average fuel cooling time of 456 d led to the sharp drop in the estimated ^{103}Ru input to the REDOX Plant dissolver in May 1955.

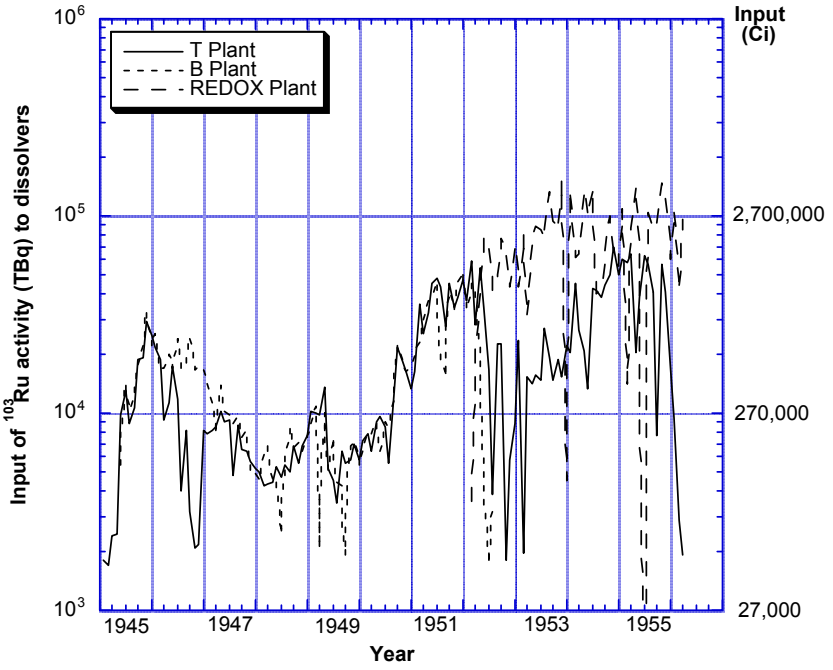

Figure 2-5. Input of ^{103}Ru to the dissolvers at Hanford from startup until closure of T Plant.

Monthly processing rates of ^{90}Sr, ^{103}Ru, ^{106}Ru, ^{131}I, ^{144}Ce, and ^{239}Pu for the T Plant, B Plant, and REDOX Plant dissolvers were compiled for the period December 1944–February 1961 from tables given in the report by Heeb (1994). Processing rates for the other six particulate radionuclides identified as most important by the screening calculations (^{91}Y, ^{95}Zr, ^{95}Nb, ^{134}Cs, ^{137}Cs, and ^{141}Ce) were estimated using the fuel concentrations in Table 2-6, appropriately adjusted for decay, and the fuel processing rates given by Heeb (1994). The fuel processing rates, average fuel decay times, and the tabulated and estimated processing plant input rates are contained in an Excel® workbook (Link to Processing rates.xls).

It is presumed that for normal operations one or more similar processes led to formation of particles that became airborne during fuel processing and were carried in the process vessel exhaust air streams. Data from plant effluent measurements are inadequate to define the processes or to distinguish among alternatives. Although there were multiple contributions to the effluent stream, the most reliable measurements are those of the total activity discharged. The ratio of the radionuclide release to the rate of processing of that radionuclide is defined as its release fraction.

As noted in Section 2.3, the approach taken in this report is to consider that segregation of radionuclides onto different aerosol particles unlikely. The alternative approach of defining a specific release fraction for each radionuclide was taken by Heeb (1994), in spite of the fact that there were only single estimates for ^{90}Sr and ^{144}Ce.

For the purposes of the calculations in this report, estimates of release fractions for monthly periods are most desirable because that is the time scale used for the radionuclide source term estimates. Table 2-10 summarizes release fraction measurements for ^{90}Sr, ^{144}Ce, ^{239}Pu, and ^{106}Ru for various times. When feasible, results given by Heeb (1994) for shorter periods were combined to estimate release fractions more appropriate for monthly release calculations. The table shows that there is a reasonable coherence among the estimates, even though the periods of measurement are rather diverse. Ruthenium estimates for 1961 are of interest because of the greater reliability of the sampling procedure at that time, but they are known to underestimate releases of ruthenium from the REDOX Plant prior to process changes that reduced radioactive ruthenium discharges.

Table 2-10. Measured Release Fractions for ^{90}Sr, ^{144}Ce, ^{239}Pu, and ^{106}Ru

Radionuclide	Dates of measurement	Processing facility	Time interval	N[a]	GM[a]	GSD[a]
^{90}Sr	1957	all	annual	1	1.9×10^{-7}	NA[a]
^{144}Ce	Sept 1958	REDOX	1 month	1	5.25×10^{-7}	NA[a]
^{239}Pu	Oct 1951 to April 1952	T & B Plants	1 week to 3 months	9[b]	1.7×10^{-7}	2.5
^{106}Ru	1961	REDOX[c]	monthly	12[d]	9.5×10^{-8}	1.6
		PUREX	monthly	12[e]	3.3×10^{-7}	2.5
^{103}Ru	1961	REDOX[c]	monthly	11[f]	3.4×10^{-8}	1.6
		PUREX	monthly	11[g]	4.0×10^{-8}	1.8

[a] N = number of measurements; GM = geometric mean; GSD = geometric standard deviation; NA = not applicable.
[b] Range was 2.7×10^{-8} to 1.4×10^{-6}.
[c] Plant process had been modified to avoid the extremely high releases that occurred in 1952–54.
[d] Range was 3.2×10^{-8} to 2.1×10^{-7}.
[e] Range was 4.0×10^{-8} to 1.6×10^{-6}.
[f] One value < 10^{-8} was not included; range was 1.6×10^{-8} to 7.0×10^{-8}.
[g] One value < 10^{-8} was not included; range was 1.4×10^{-8} to 9.2×10^{-8}.

To estimate ruthenium releases, Heeb (1994) chose the values for ^{103}Ru measured at REDOX and PUREX plants in 1961. As can be seen from the table, the estimates for ^{103}Ru are lower than those for ^{106}Ru. The reason(s) for differences between isotopes of the same element are not known, but may be related to decay of the shorter-lived ^{103}Ru in particles residing on surfaces prior to resuspension and release. That phenomenon could also affect the amounts of ^{141}Ce released, but is not likely to greatly affect the releases of most radionuclides considered.

A lognormal distribution of routine release fractions was selected for releases from T Plant and B Plant for periods after the scrubbers and filters were installed. It was characterized by a geometric mean (GM) of 1.4×10^{-7} and a geometric standard deviation (GSD) of 3.2. The

corresponding mean release fraction is 2.8 x 10^{-7}. The release fraction estimates were all obtained after the installation of scrubbers and filters to reduce processing plant effluents. For the early years of operation of T Plant and B Plant, when there was no effluent treatment, the release fraction was increased by an average "effluent treatment modifier" of 150, the mean of a uniform distribution with bounds of 100 and 200. This distribution, the mean of which is larger than the factor of 100 used by Heeb (1994), is a more cautious approach (likely to overestimate releases). Releases from T Plant and B Plant were complicated by releases of active particles, which are discussed in more detail below in connection with the individual plants.

The same release fraction (GM = 1.4 x 10^{-7} and GSD = 3.2) was used to estimate releases of radionuclides other than ^{103}Ru and ^{106}Ru from the REDOX Plant. Ruthenium releases included not only particulate material but the gaseous form RuO_4, which was produced during plant operations. For routine operations between January 1952 and July 1954, when the process modifications were made to reduce releases (HW-32164-Del, HW-34882), a median release fraction of 2.2 x 10^{-6} was adopted for the ruthenium isotopes. The geometric standard deviation of the distribution was assumed to be three, and the corresponding mean release fraction was 4.0 x 10^{-6}. That distribution reflects the range of available release data (which were incomplete) and is considered to be adequate to cover releases that may not have been measured. Release measurements made during the last third of 1954 indicate a lower release fraction following the process changes. Although ruthenium releases were generally undetectable in 1955 and early 1956, the release fraction based on the data of late 1954 (GM = 4.2 x 10^{-7}; GSD = 1.7) was applied to that period as well. This decision may lead to consistent over-prediction of routine releases of ^{103}Ru and ^{106}Ru starting in 1955. Release estimates for the unusual ruthenium releases are described in the REDOX Plant section.

General Procedure for Calculations. Monte Carlo calculations of releases were made for each month from December 1944 through February 1956 for the T, B, and REDOX fuel processing plants in operation during the month of interest. For most months, two plants were operating; however, during the first half of 1952 all three facilities were operating. Calculations of releases from the three plants and their uncertainties were performed independently. A fourth fuel processing plant, the PUREX Plant, operated for only two months during the period December 1944–February 1956, and was not a source of unusual particle releases; releases from that facility were not estimated for this report.

For routine releases, the estimated monthly discharge for a particular radionuclide is the product of several parameters: the monthly processing rate for the radionuclide, the release fraction, the "effluent treatment modifier" when appropriate, and uncertainty factors related to the radionuclide processing rate and the amount of decay that had occurred prior to processing. For releases from a particular plant:

$$Q_i(t) = P_i(t)\ U_{pi}\ U_{di}\ R(t)\ M_{ET} \qquad (2.4.2\text{–}1)$$

where $Q_i(t)$ is the release of radionuclide i (Bq) during month t, $P_i(t)$ is the activity (Bq) of that radionuclide in fuel processed during the same month, U_{pi} and U_{di} are uncertainty factors for the processing rate and decay corrections for the radionuclide, $R(t)$ is the appropriate release fraction for the time, and M_{ET} is the applicable effluent treatment modifier.

Heeb (1994) identified uncertainties in the fuel processing rates, the calculations of radionuclide inventories in the fuel, and in the average fuel cooling times for ^{90}Sr, ^{103}Ru, ^{106}Ru,

^{144}Ce-Pr, and ^{239}Pu. Similar uncertainty estimates were made for the other particulate radionuclides (^{91}Y, ^{95}Zr, ^{95}Nb, ^{134}Cs, ^{137}Cs, and ^{141}Ce) considered here. The uncertainty in decay time is most important for ^{103}Ru and ^{141}Ce. The uncertainty distributions for these factors, the release fraction, and the modifying factor for effluent treatment were all propagated using Monte Carlo methods used to produce distributions of radionuclide release estimates. The uncertainties in processing rates and decay corrections are relatively small, <30%. The uncertainty associated with the release fraction was the most important contributor to the overall uncertainty in the estimated radionuclide releases.

Correlations. The estimates of monthly radionuclide releases from a particular plant ultimately rely upon some common parameters: (a) the monthly fuel processing rate for that plant, (b) the common release fraction for particulate radionuclides, and (c) when applicable, the common factor used to account for the absence of effluent treatment. In the calculations of releases from a particular plant during a particular month, the release fraction (R) and the effluent treatment modifier (M_{ET}), when applicable, are the same for all particulate radionuclides. As a result, the releases of particulate radionuclides from each fuel reprocessing plant, are correlated with one another.

On the other hand, releases from one fuel reprocessing plant are not correlated with those from the other two reprocessing plants. The fuel processing histories differ among plants and were based on historical data describing fuel shipments to the individual facilities. The release calculations for each facility were separate. Thus, the release fraction and modifying factor (when used) were chosen independently for each plant in separate Monte Carlo calculations of radionuclide releases.

Releases from T Plant. Monthly releases for routine operations were estimated throughout the period of operation of T Plant, from late 1944 to early 1956. Beginning in the fall of 1947, the releases of larger "active particles" indicated that operations were no longer "routine." Evidence, discussed in Section 2.2.1, led to the conclusion that the particles were iron based and were due to the corrosion of the exhaust fans and associated carbon steel ductwork. Historical deposition of airborne particles on the surfaces that corroded and attachment of small radioactive particles to the larger iron oxide particles that were airborne were two ways that those particles could be contaminated.

To approximate what may have occurred, it was assumed that an amount of activity equal to the routine release was deposited on duct surfaces continuously from the time of initial hot operation at the plant in December 1944 until September 1947. This led to a predicted deposition of about 7.3 GBq (200 Ci) of ^{144}Ce, about 42 percent of the total activity estimated to have accumulated by the end of August 1947. The estimated deposits of the other beta-gamma-emitting fission products were in the range 0.37–2.6 GBq (10–70 Ci). Calculations showed that the deposits would contain larger fractions of radionuclides with long half-lives (such as ^{90}Sr and ^{137}Cs) that would not decay appreciably while attached to the surface. The estimated ^{90}Sr and ^{137}Cs fractions under the assumed conditions were about five percent; this is about five times larger than the contributions of those isotopes reported when particles found in the environment were analyzed. This suggests that the iron oxide particles were also contaminated by attachment of the small particle aerosol that was routinely discharged to the stack during the period when those larger corrosion particles were being released.

Releases of the surface deposits with corrosion particles were assumed to occur during an 8-month period, starting in September 1947. Fractional releases of the deposits during those months

were taken to be 0.04, 0.08, 0.10, 0.10, 0.10, 0.08, 0.04, and 0.02. In all, it was estimated that a nominal fraction of 54 percent of the total deposit of each radionuclide was carried by corrosion particles in the effluent. The monthly fractions listed were all considered to be uncertain parameters, with uniform distributions ranging from 0.5 to 1.5 times the nominal values. The estimated activity releases from corroding surfaces were added to the "routine" releases for each month during the period. The estimated releases with corrosion particles were 40–60 percent of the "routine" releases. As noted earlier, some of the smaller aerosol particles may also have been attached to the larger corrosion particles, increasing the activity associated with those particles.

Reports by Work, tabulated by Cleavenger and Gydesen (HW-89072), suggest that the large particle releases from T Plant had been substantially reduced by installation of the sand filter and scrubber by April 1948. Releases from the T Plant were estimated to decline gradually after the effluent treatment systems were installed. This pattern is based upon the qualitative information in Cleavenger and Gydesen, and is reflected in the calculations by a gradual decrease over five months (May–September) of the effluent treatment modifier. The decline was described by a reduction from an average value of M_{ET} of 150 in April to 100 in May, and then to 80, 40, 20, and 10 in successive months, reaching 1 in October 1948. A uniform uncertainty distribution of 0.67–1.33 times the nominal value was applied to all values of M_{ET} that were greater than one.

Figure 2-6 illustrates the estimated releases of ^{144}Ce from T Plant. Results of the radionuclide release calculations for all the important radionuclides are tabulated in the spreadsheet labeled T Plant in the source term workbook (Link to Source Terms.xls).

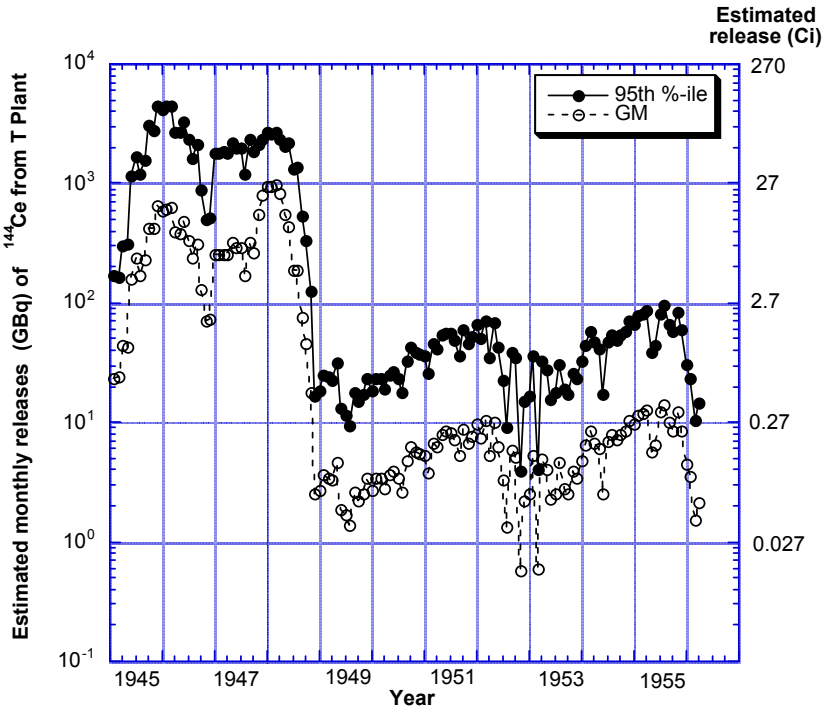

Figure 2-6. Estimated releases of ^{144}Ce from T Plant.

Releases from B Plant. Calculations of particulate radionuclide releases from B Plant are quite similar to those for T Plant. Both routine and larger corrosion particle releases occurred

from B Plant, as described previously. The activity buildup on surfaces that corroded and subsequent releases of that activity were estimated in the same way as for T Plant.

The principal difference between the independent calculations for the two plants is in the estimated releases following installation of effluent filtration and scrubber systems. The qualitative reports tabulated in Cleavenger and Gydesen (HW-89072) indicate that more difficulties with the new effluent treatment systems were experienced at B Plant. To reflect these difficulties and continuing higher releases, the effluent treatment modifier used in the release estimates was reduced more gradually than for T Plant. The assumed sequence of values of M_{ET} is as follows: 150 in May 1948, reduced to 100 in the period June–November, then to 50 for the period December 1948–February 1949, followed by a series of declines to 25, 20, 15, 10, 5, in subsequent months to 1 in August 1949. A uniform uncertainty distribution of 0.67–1.33 times the nominal value was applied to all values of M_{ET} that were greater than one.

Figure 2-7 shows the results of the calculations of releases of ^{95}Zr from B Plant. Results of the B Plant radionuclide release calculations are tabulated in the spreadsheet labeled B Plant in the source term workbook (Link to Source Terms.xls).

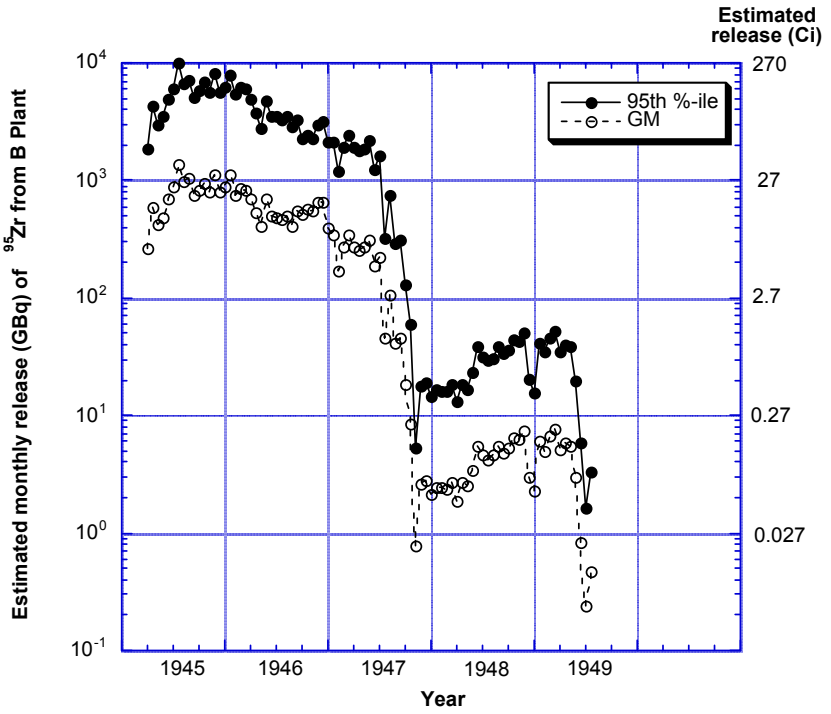

Figure 2-7. Estimated releases of ^{95}Zr from B Plant.

Releases from REDOX Plant. Releases from REDOX Plant during 1952–54 were notable because of the occurrence of several off-normal conditions that resulted in substantial releases of radioactive particles. In qualitative terms, it is clear what led to the unusual particle releases, in which ^{106}Ru and ^{106}Ru were the most important radionuclides.

Releases of ammonia and nitrous oxides from different plant operations were mixed in the exhaust flow and deposits of ammonium nitrate formed on interior surfaces of the plant exhaust

system and stack. In addition, ruthenium releases from the REDOX Plant were elevated due to plant design and operation. An oxidation step in the process yielded the volatile ruthenium oxide, RuO_4. When passing through the offgas lines and the stack, the radioactive ruthenium also deposited on the same surfaces, perhaps simultaneously with the ammonium nitrate under some conditions. Other process activities, such as vessel sparging, led to increased releases of ruthenium particles that also deposited on stack walls and other surfaces as the exhaust gas was transported out of the plant. As a result, there was a deposit of radioactive ammonium nitrate on the walls of the stack. Flakes of this material were resuspended into the stack gas flow and carried to the environment where they caused substantial surface contamination. The particles released were described in Section 2.2.2.

The processes of deposition and resuspension that led to the unusual ruthenium releases occur in other situations as well. Particles in the atmosphere can deposit on the ground or vegetation, either by sedimentation or turbulent diffusion. Part of the deposit can be resuspended, particularly under high wind conditions. There is no indication that it was a change in the stack flow rate that caused resuspension of the contaminated ammonium nitrate, and specific events that caused flakes of material to be released have not been identified. Rough calculations showed that the secondary particle releases could be accounted for by these mechanisms, and the measurements of the $^{103}Ru/^{106}Ru$ activities in the secondary particles clearly showed the aging effect of holdup on the stack wall. Attempts to model the process were hampered by the fact that the releases from the stack wall appeared to be random events. In addition, an empirical deposition velocity, the parameter needed to describe the transfer of gaseous RuO_4 from air to surfaces, was not available.

The particulate radionuclide release calculations for the REDOX Plant are structured like those for the T and B Plants, using monthly tabulations of processing rates and release fraction estimates. To utilize this structure for months when unusual events occurred, "apparent release fractions" (R_{ap}) were estimated for the ruthenium release calculations. Use of these apparent release fractions is a calculational convenience and is not intended to imply that the unusual releases were related to normal plant processes. This simplified approach is used because the actual processes cannot be modeled quantitatively in this project.

There were two main categories of unusual ruthenium releases: those caused by operational events, like scrubber failures, and the release of secondary particles formed on the walls of the ventilation system and stack. The first unusual release was due to a scrubber pump failure in March 1952, before effluent monitoring was routine. Based on the investigation report for the incident (HW-24123) and that for another scrubber failure in 1954 when the monitoring system was operating (HW-30764), a median value of the apparent release fraction was estimated to be 1×10^{-4}. Values of R_{ap} for other unusual releases were estimated similarly, using reports of the event chronology and the findings of investigations (HW-32473, HW-33068, HW-25097, HW-27431, HW-27447, HW-29230). The apparent release fractions are considered to be conservative estimates that may well bias the results on the high side, and that is intentional in view of the nature of the project. The evidence indicates that these releases were relatively brief compared to our monthly source term calculation interval. Thus, in some months, nearly all of the estimated release may have occurred in a few hours or a few days. Table 2-11 provides a summary of the apparent release fraction estimates for unusual ruthenium releases from the REDOX Plant. Geometric standard deviations equal to 3 were chosen for the distributions,

consistent with other decisions about that parameter for the ruthenium releases. We believe that this provides an adequate uncertainty range for the estimates.

Table 2-11. Estimates of "Apparent Release Fractions" for Unusual Ruthenium Releases

Month	Cause of unusual release	Estimated median value for "apparent release fraction"
March 1952	Scrubber failure	1×10^{-4}
April 1952	Vessel sparging operations[a]	4×10^{-6}
June 1952	Flakes from exhaust system surfaces	6×10^{-6}
September 1952	Flakes from exhaust system surfaces	2×10^{-5}
August 1953	Flakes from exhaust system surfaces	2×10^{-5}
September 1953	Plant processes[b]	3×10^{-5}
January 1954	Scrubber failure and stack washing	1×10^{-4}
April 1954	Flakes from exhaust system surfaces	4×10^{-6}
May 1954	Flakes from exhaust system surfaces	1×10^{-5}
June 1954	Flakes from exhaust system surfaces	4×10^{-6}

[a] Probable cause.
[b] Information regarding the cause was not found.

Releases of radionuclides other than ruthenium isotopes were estimated using the distribution of release fractions for routine releases discussed earlier. For the REDOX Plant estimates, the modifying factor M_{ET} was set equal to one because the treatment systems were installed prior to operation.

Figure 2-8 illustrates the estimated median and 95th percentile estimates for releases of ^{106}Ru from the REDOX Plant. Results of all the REDOX Plant radionuclide release calculations are tabulated in the spreadsheet labeled REDOX Plant in the source term workbook (Link to Source Terms.xls).

2.4.3 Releases of ^{239}Pu from Z Plant

One of the radionuclides assigned to the most important category for fuel processing plant releases, ^{239}Pu, was also released from Z Plant. Work in that plant consisted of producing and fabricating metallic plutonium from plutonium nitrate that was recovered by the fuel processing plants. The facility began operation in 1949, and some of the releases occurred at the same time as those addressed in the previous section. In this section, we estimate releases from the Z Plant that occurred during years when available monitoring data were incomplete and the first year (1961) when a complete set of data was found in the records.

Effluents from the plant were passed through high-efficiency particle collection filters, originally the Chemical Warfare System (CWS) type CWS-6. These filters were later replaced by less flammable filters.

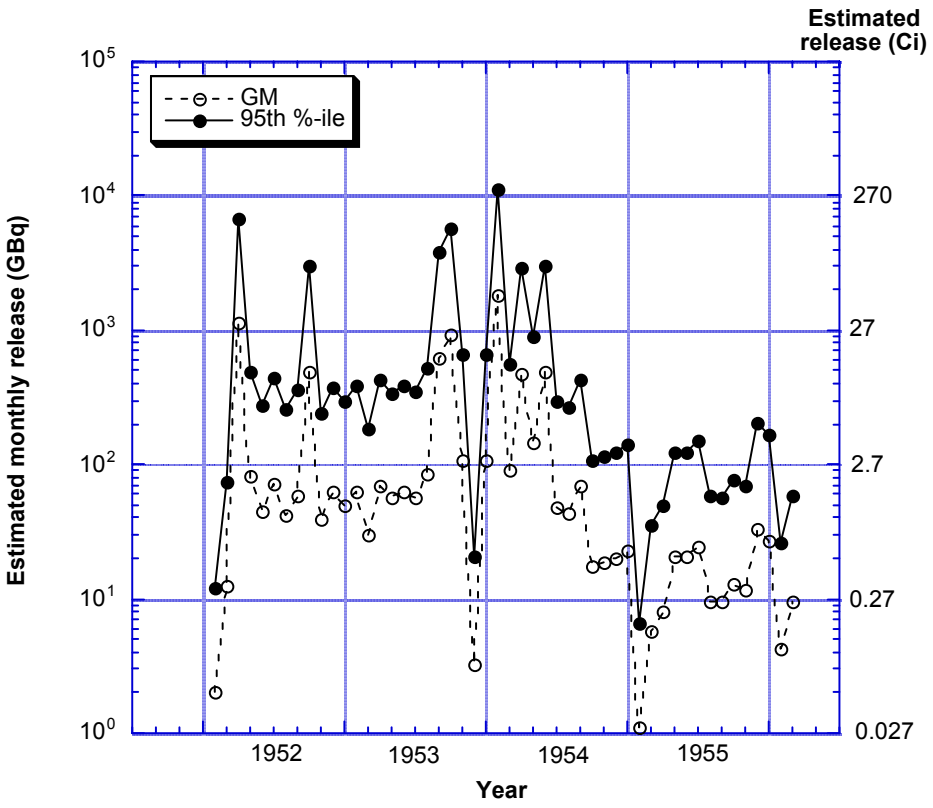

Figure 2-8. Estimated releases of ^{106}Ru from REDOX Plant.

The effluent was sampled on a daily basis. Sampling data for the earliest years of operation have not been located. Postma and Schwendiman (HW-61082) evaluated the Z Plant effluent sampling system in April 1959. They found that the plutonium particles were small, mostly less than 1 μm, and that the sampling system was adequate for particles of that size. Their estimates of the daily release were ~30% lower than those reported by the plant staff for the three days of sampling.

Estimates of monthly releases of ^{239}Pu from Z Plant were located for several months in each of four years, 1957–1960 (Operations Managers 1957a, b; Operations Managers 1958a, b, c, d, e; Operations Managers 1959a, b, c, d, e, f; Operations Managers 1960a, b, c, d, e) and for all months in 1961 (HW-69205). Production data for Z Plant have been deleted from the available monthly reports, except for some coded values. The monthly ^{239}Pu processing rates for the Z Plant were estimated using the ^{239}Pu processing rates for the separations facilities. It was assumed that the ^{239}Pu in all fuel processed was also handled in Z Plant two months after it entered a fuel processing plant. The resulting estimates of monthly production amounts and the effluent monitoring data were used to estimate monthly release fractions of ^{239}Pu for the Z Plant. As before, the release fraction for a month is defined as the ratio of the activity released to the amount processed. Table 2-12 shows, for each year, the number of estimates and the minimum, maximum, and average values of the estimates of the monthly release fractions.

The distributions of release fractions used in calculating Z Plant releases were based upon the available estimates and are described in the last column and footnotes of Table 2-12. The release fractions estimated from monthly effluent releases during 1957 and 1958 were distinctly

higher than the estimates for months in the three subsequent years. Taken together, the nine values were reasonably approximated by a lognormal distribution with a GM of 2 x 10^{-7} and GSD of 1.8. The corresponding mean release fraction is 2.4 x 10^{-7}. The lognormal distribution found for 1957–1958 was assumed to be representative of prior operations as well and was used in calculations of releases for the years 1949–1956. The distributions shown in Table 2-12 for the years 1959–1961 were used to estimate monthly releases during those individual years. For 1959, a loguniform distribution with mean of 3.5 x 10^{-8} was employed. Two of the five monthly release fraction estimates for 1960 were low (1–2 x 10^{-8}) and two were high (1–2 x 10^{-7}), with the fifth one in between. The mean release fraction for the custom distribution that was constructed was 7.2 x 10^{-8}. Release fraction estimates for 1961 were more consistent, and a uniform distribution with mean of 2.2 x 10^{-8} was used in calculations for that year.

Table 2-12. Release Fractions for ^{239}Pu Estimated for Z Plant and Distributions Used in Calculations of Z Plant Releases

Year	Number of estimates	Release fraction estimates			Distribution of release factors used in calculations
		Minimum	Maximum	Average	
1957	4	8.3 x 10^{-8}	2.8 x 10^{-7}	1.6 x 10^{-7}	Lognormal[a]
1958	5	2.0 x 10^{-8}	3.7 x 10^{-7}	2.2 x 10^{-7}	Lognormal[a]
1959	7	1.2 x 10^{-8}	1.0 x 10^{-7}	3.5 x 10^{-8}	Loguniform[b]
1960	5	1.1 x 10^{-8}	1.9 x 10^{-7}	7.5 x 10^{-8}	[c]
1961	12	1.1 x 10^{-8}	3.2 x 10^{-8}	2.2 x 10^{-8}	Uniform[d]

[a] A combined lognormal distribution with GM = 2 x 10^{-7} and GSD = 1.8 was used.
[b] A loguniform distribution with bounds of 1.2 x 10^{-8} and 1.0 x 10^{-7} was used.
[c] A custom distribution with P(1–2 x 10^{-8}) = 0.4, P(2–8 x 10^{-8}) = 0.2, and P(8–20 x 10^{-8}) = 0.4, consistent with the limited data, was used.
[d] A uniform distribution with bounds of 1.1 x 10^{-8} and 3.2 x 10^{-8} was used.

Estimates of monthly releases of ^{239}Pu from the Z Plant were computed in a manner similar to that used for the other processing facilities. As before the uncertainties in quantities and parameters used in the calculations were carried forward, using a Monte Carlo procedure, to obtain distributions of estimates of the releases.

$$Q_{Pu}(t) = P_{Pu}(t)\ U_p\ R_Z(t)\ U_m$$

where $Q_{Pu}(t)$ is the ^{239}Pu release (Bq) in month t, $P_{Pu}(t)$ is the amount of ^{239}Pu (Bq) in fuel processed two months earlier, U_p is the processing uncertainty factor, and $R_Z(t)$ is the applicable Z Plant release fraction for the month. The quantity U_m is a cautious uncertainty factor incorporated into the calculations to account for possible but unknown deficiencies in the effluent monitoring data and their applicability to periods for which data were not found. A triangular distribution with bounds of one and three was used to represent this factor; the mean and mode for this distribution were both two.

Results of the release calculations for the years 1949–1961 are shown in Figure 2-9. The median estimate and the 95th percentile of the distribution are shown for each month during the

period. A gradual increase in the estimated releases with time reflects the increasing plutonium processing rate. The processing rates used in the calculations may be too high because of losses in fuel processing and possible inability for Z Plant to process plutonium at the rate it was provided. This is offset by the fact that the estimated release factors were also computed using processing rates that may also be too high. Any real differences are likely to fall within the uncertainty bounds for the release estimates. Uncertainties in the monthly releases are higher than those indicated for the annual releases. As a point of reference, 3.7 GBq (0.1 Ci) of ^{239}Pu is about 1.6 g of plutonium.

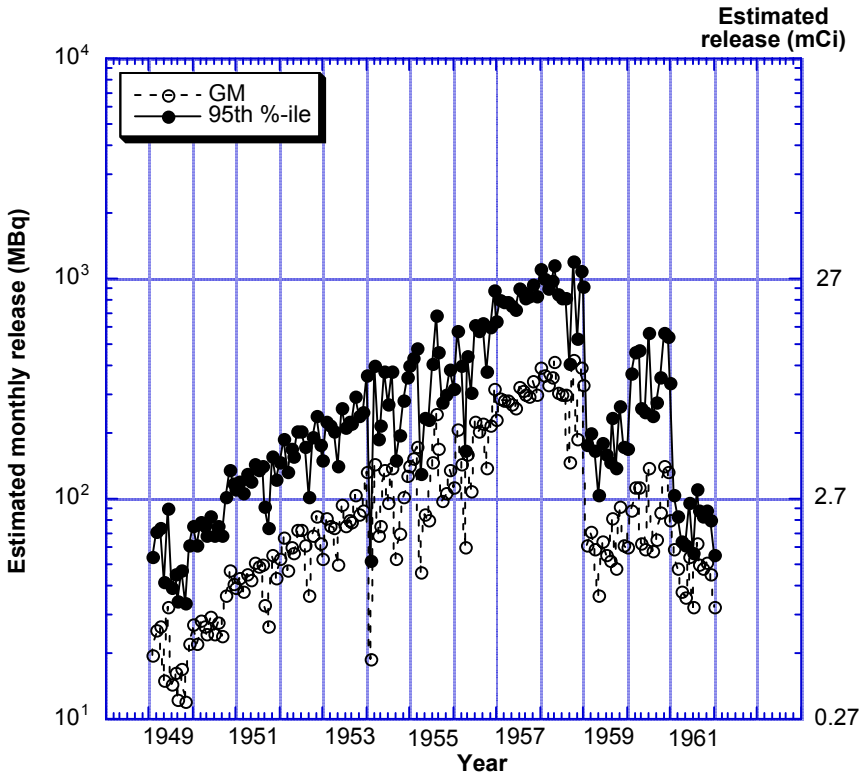

Figure 2-9. Estimated releases of ^{239}Pu from Z Plant.

Mishima and Schwendiman (1973) conducted another investigation of the Z Plant effluent in parts of 1972 and 1973. At that time, they found that the plutonium activity was associated with larger particles having mass median diameters of 3–9 μm. The releases appeared to be uncorrelated with plant operations, so these particles may have been resuspended from surfaces in the ventilation system. In 1972-1973, Mishima and Schwendiman also found that the effluent release estimates made by the plant staff were substantially (2–20 times) lower than those indicated by their own measurements. It was noted in the 1959 investigation (HW-61082) that the sampling system would not be reliable for large aerosols. Also, large particles of iron oxide were found in the effluent air stream in 1959 (HW-61082).

It is not clear what occurred during the interval between 1959 and 1973, but indications are that the deposition-resuspension phenomenon, discussed earlier in the context of the fuel processing plant releases, may also have been a factor affecting releases from the Z Plant. The

environmental monitoring data indicate some elevated concentrations of ^{239}Pu close to the 200 Areas (Section 4). It appears that these were primarily due to releases that occurred after 1961.

The Z Plant ^{239}Pu source term estimates, which include the 95th percentile and median values of the monthly releases, are contained an Excel® spreadsheet (Link to Source Terms.xls).

2.4.4 Releases of ^{131}I from Fuel Processing Plants

Heeb (1994) estimated releases of ^{131}I from the Hanford fuel processing facilities. Those estimates were used in our screening calculations, in which ^{131}I provided a point for comparison. The screening calculations indicated that ^{131}I was a very important component of the exposure, even when all the particulate radionuclides were included.

We noted earlier that variability in cooling times for individual batches of fuel that were processed in a month could affect the inventory estimated using the average fuel cooling time for that month. It was not within the scope of this project to reconstruct those calculations, which would have involved detailed tracing of all fuel processing at Hanford for the years of interest. Warren (1961) reports a broad range of cooling times for fuel processed in 1959–1960. That report also differs from Heeb (1994) in the amounts of ^{131}I charged to the dissolvers, particularly for the REDOX Plant.

In response to review comments (Hoffman et al. 1999) Napier undertook a thorough reinvestigation of the radioiodine releases for years following 1949 and his results (Napier 2002a) were published earlier this year. His estimates, which considered stack monitoring data and environmental measurements starting in 1950, are total monthly releases from all operating plants. Fortunately, we were able to obtain the basic spreadsheets used to calculate the total releases (Napier 2002b) and were able to reconstruct releases from individual processing facilities for most months of interest. In some periods, the breakdown of the total release by facility was not found in the records of monitoring data and the entire release was assigned to a single plant.

The estimates of releases given by Heeb (1994) for December 1944–December 1949 are expressed as the mean values with a coefficient of variation, and Napier (2002a) has used the same method of reporting. We have derived median and 95th percentile estimates from them on the assumption that the distribution of releases is lognormal (Hoffman and Gardner 1983). The estimated median releases for T Plant are shown in Figure 2-10. The vertical scale of the figure is so great that the 95th percentile values are difficult to distinguish from the median values, so they have been omitted from this plot. The estimated 95th percentile values and the medians are both provided in the spreadsheets for each of the processing plants in the source term workbook (Link to Source Terms.xls).

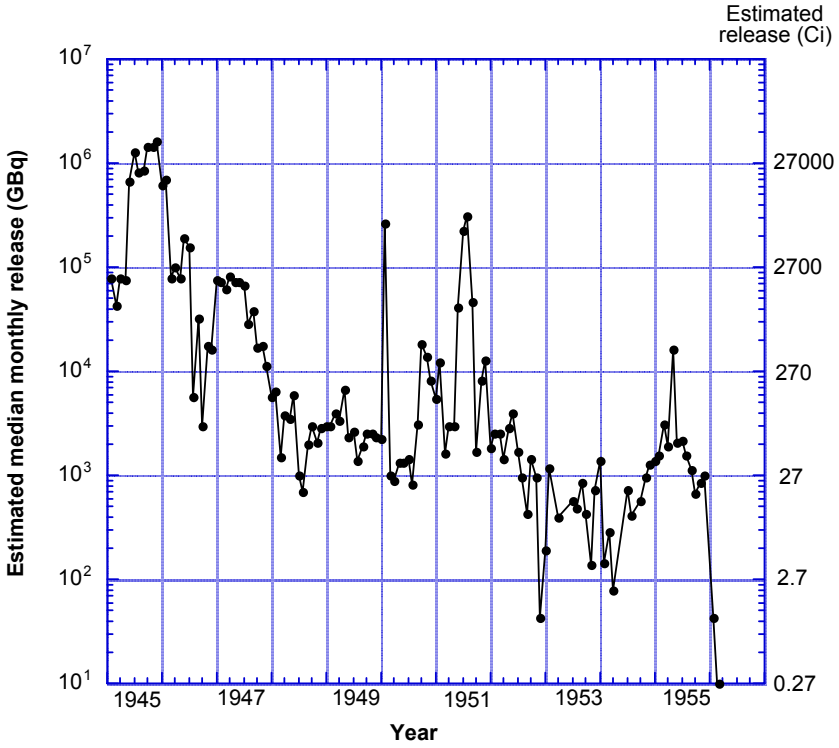

Figure 2-10. Estimated releases of ^{131}I from T Plant; derived from results of Heeb (1994) and Napier (2002a,b).

3. DOSE CALCULATION METHODS

This section presents the methods used to calculate doses from short-lived gaseous radionuclides and radioactive particles released to the atmosphere from past Hanford operations. Once released to air, radioactivity is dispersed into the environment. Exposure pathways describe how the released radioactivity travels from the release point to places where people are located and how those people could have been exposed. An exposure scenario is a description of a person's behavior and location that is used to define parameters needed to calculate dose. Our goal is to describe methods for estimating radiation dose and risk to hypothetical individuals defined by exposure scenarios. Computation of collective dose to a population is outside the scope of this study.

Results of dose calculations for example scenarios are given in Section 5 of this report. Other scenarios may be defined by changing the input to the calculational tools developed for this study. In this way, estimates of doses for other scenarios can be made.

3.1 Pathways and Exposure Scenarios Considered

The scope of this task is the examination of atmospheric releases and pathways. No waterborne releases or pathways are addressed. Atmospheric pathways include direct inhalation of air containing radioactivity, external exposure to radioactivity in air and deposited on the ground, and direct contact of the skin by radioactive particles. In our example calculations, pathways that result in ingestion of contaminated food are considered for persons who resided offsite, but to a lesser extent for those who lived and worked on the reservation. As a practical matter for illustrating the calculational tools being developed, whenever the air-vegetation-cow-milk pathway is included, it dominates the dose estimates for routine releases from Hanford, because of the importance of radioiodine. To our knowledge, there was no production of milk for human consumption from grazing animals on the Hanford Reservation. Further discussion of commercial milk supplies for the Hanford construction camps is included in Section 5.1.3. We do include inadvertent ingestion of soil for all workers, onsite and offsite, to address the contamination of food, for example by dust on the hands or by introduction during food preparation.

3.1.1 Exposure Locations for General Public

As discussed in Section 2, the release points of greatest concern are five fuel processing plants, T Plant, B Plant, Z Plant, the REDOX Plant, and the PUREX Plant, all in the 200 Areas. The 200 Areas were also the source of the highest atmospheric releases of ^{131}I. Based on results of the Hanford Environmental Dose Reconstruction (HEDR) project, the location of the maximally exposed member of the public, off the Hanford Site, was at Ringold, Washington. Ringold is across the Columbia River from the Hanford Site, about 22–29 km (14–18 mi.) in an east to southeast direction from the release points in 200 Areas (Figure 1-2). We have used Ringold as the offsite location in one of the example calculations in Section 5 of this report. Other offsite locations can be defined by entering the appropriate geographic coordinates. We do not recommend using the tools developed beyond ~30 km (~20 mi.) from the center of the release points. A map is also included in this report that shows the relative exposure at locations on and near the Hanford reservation (Figure 5.1).

3.1.2 Exposure Locations for Onsite Personnel

There is no precedent from the HEDR project for defining exposure locations for people on the Hanford Site. The largest radioactive particles released from Hanford facilities were deposited most densely within several kilometers of the release points. Therefore, onsite exposures via direct pathways (such as inhalation) were highest. The scope of this task does not include exposure to workers inside Hanford buildings from releases to the environment; only people outside the buildings are considered. Military forces, construction workers, and contractor security guards are examples of the types of onsite workers that would have been exposed outside (Figure 1-3). In addition, there were personnel involved in environmental monitoring and outdoor research projects, as well as a Federal prison camp in 1944–1947.

It is not within the scope of this project to define where and when various workers or military personnel actually were exposed during Hanford's history. Our charge was to develop a tool to compute dose at a variety of locations where people might have been exposed. However, in order to define the boundaries necessary for that tool, it was useful to review where some of the known exposure locations were. We have chosen known work and residence locations to illustrate the dose results in example calculations in Section 5.

Military Locations. Figure 1-2 in the introduction of this report shows the approximate location of army sites where personnel manned anti-aircraft guns. Those locations were estimated from other maps and documents that are reviewed here. Three army sites were positioned along Army Loop Road within 10 km (6 mi.) to the south and west of 200 Areas (Figure 3-1). A fourth army site (noted as PSN 330, or B Battery) was located about 1 km (0.6 mi.) from the southeast corner of 200-East Area, south of Route 4S (Figure 3-1). PSN 330 was 3.5 km (2.2 mi.) from the B Plant stack in 200-East Area.

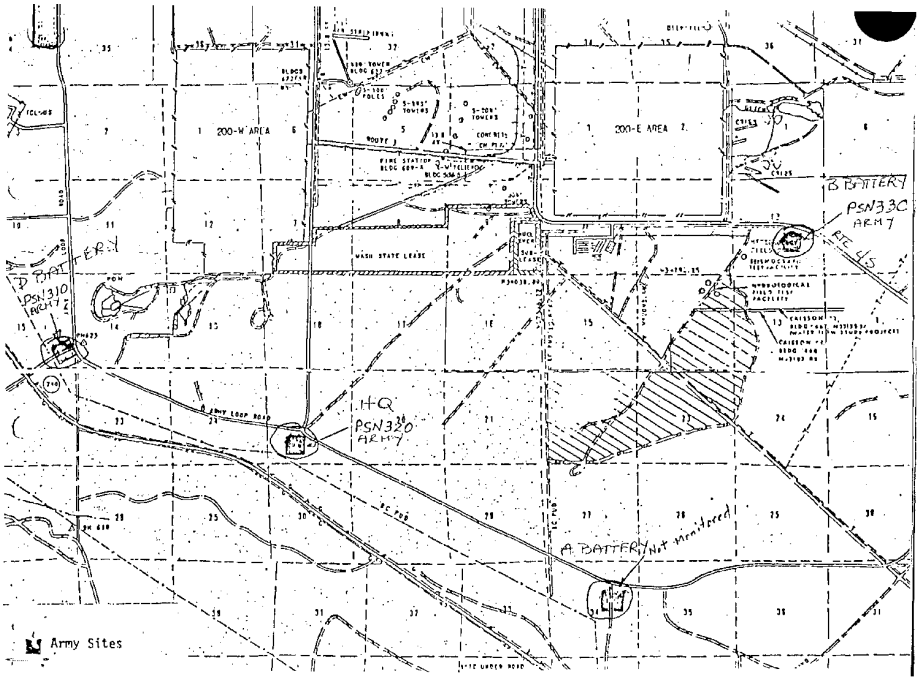

Figure 3-1. Map from unknown source with hand-written names for four army sites: PSN 330 (or B Battery), just southeast of 200-East, and three other sites (A Battery, PSN320, and D Battery [or PSN 310]) south of 200 Areas along Army Loop Road.

At the time an earlier draft of this report was produced, an atlas of the Hanford Site was available on the Internet at http://www.bhi-erc.com/dm/hgis/hgis.htm.[1] The old army sites are identified on the atlas maps as anti-aircraft sites. Figure 3-2 shows the locations of these anti-aircraft sites on a portion of the index map for the atlas. The numbers designating the sites are different (e.g. the old PSN 330 is called H-40), but the locations are the same as shown in Figure 3-1. Changes in the numbers describing these army sites have been confirmed in environmental monitoring reports (Section 4). A fifth anti-aircraft site, H-61, is shown northwest of 200-West Area in Figure 3-2.

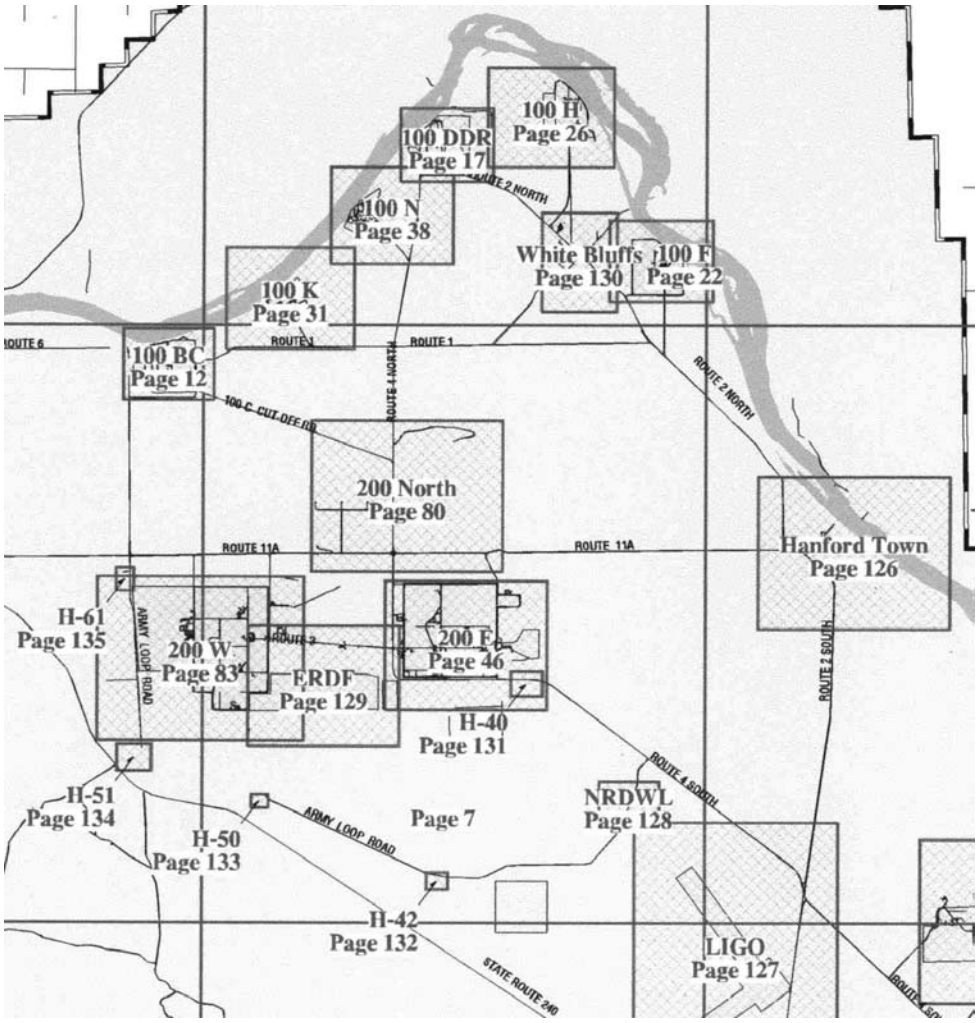

Figure 3-2. Section of index map from the Hanford Site Atlas showing locations of old army sites as "anti-aircraft sites," H-40, H-42, H-50, H-51, and H-61. The "Hanford Town" site was the residence location for thousands of construction and other workers until February 1945 (see next section). Reference to pages on this map note sections of the Hanford Atlas that contain more detailed maps.

[1] The Internet address for the Hanford Geographic Information System is currently http://www.bhi-erc.com/projects/p_m/eis/hgis/hgis.htm. For security purposes, password/user registration is required.

Using more detailed maps from the atlas, the geographic coordinates (Washington State Plane) of these military sites as well as the airborne release points for the reactors and fuel processing plants were obtained. These coordinates are incorporated into the calculational tools developed for the CDC.

Gerber (1992b) describes the conditions and general locations of military units assigned to the Hanford Reservation in the early years. Those involved in constructing and manning the anti-aircraft defenses slept out overnight in tents or hastily built huts and barracks. A small force of Military Police (MPs) and Military Intelligence (Army G-2) personnel guarded the Hanford Reservation at the start-up of plutonium manufacturing in late 1944. In June 1945, the MP numbers were increased to 40 soldiers. Army MPs remained at Hanford until April 1947, when the new Atomic Energy Commission assigned guard duties to company patrolmen of the site contractor, General Electric. In late 1947, with the large production expansion, security concerns increased, and army troops were sent from Fort Lewis near Tacoma to the Hanford complex on prolonged maneuvers. In March 1950, a large convoy arrived at the Hanford Site from Fort Lewis bringing anti-aircraft guns and machine guns. Their headquarters and temporary housing was at North Richland. In 1951, "Camp Hanford"[2] was officially designated by the army. Anti-aircraft guns were replaced by Nike missiles in the next few years. The 1st and 83rd missile battalions, along with support services groups, served at Camp Hanford until the late 1950s, when intercontinental ballistic missiles rendered Hanford's air defense system obsolete and anti-aircraft missiles were no longer effective. The Camp was deactivated in 1960, and the North Richland offices were transferred to the Atomic Energy Commission (AEC) in 1961.

Gerber (1992b) summarizes life at Camp Hanford as described in an army brochure dated April 1955 and titled "83rd AAA Missile Battalion, Camp Hanford Washington" as well as from veterans' accounts. In the earliest years, troops were driven to the sites in vehicles that were open to the air on unpaved roads. After the initial few months of building the gun emplacements, they moved into tents near the gun bunkers. Soldiers did calisthenics in the open every morning and were required to stay out of their tents, near the guns, all day. Conditions could be extremely dusty. There was no protective equipment or clothing issued. Army personnel in the early years got three days leave every 15 days (restricted to the Tri Cities area) and 30 days per year of unrestricted furlough (Gerber 1992b).

Exposure pathways for military personnel on the Hanford Site in 1951 are discussed in a message from the Richland AEC office to the Washington DC office (Shaw 1951). As far as exposure to radioactive emissions from the plant, active particles and atmospheric ^{131}I were their primary concerns. According to Shaw, food sources and handling were under satisfactory control. Drinking water was from plant sanitary water sources and contained only background amounts of radioactive substances. A previous recommendation that military spend no more than a third of the time "in-plant" arose from a desire to follow usual Hanford Plant practice and did not represent a real limitation. The philosophy at the time of early considerations was to permit military personnel to be exposed to airborne particles to the same or lesser degree as Plant

[2] This general term for the entire site military operations should not be confused with the specific "Hanford Camp" at the old Hanford town site, which was closed in February 1945. (See next section of this report.)

personnel. Shaw indicates that most active particles were water soluble and that the number and size of particles had been reduced compared to earlier times.

In addition to the anti-aircraft sites, the army provided site-wide security at various locations including around the perimeters of the nuclear facilities. Interviews in Sanger (1995) include members of the security force during the war years. One indicated that at the peak in July 1944, there were 1395 patrolmen in plant, on boats on the river, and along the perimeter. A former army captain recalls,

> About February of '45, I was sent out to 200 East. We were manning the towers by then, which was operations time. I am trying to recall, we had 225 patrolmen in that one fenced area, where they did the plutonium separation work. We had so many because we were manning the towers[3]. They were wooden structures, right on the fence, with lights. In a short while, we discontinued manning the towers. Instead we had inner road patrols by cars, on the asphalt roads that went inside the fence. (Sanger 1995).

Construction and Operating Personnel Residence Locations. The main residence location for construction workers in the earliest years of Hanford operations was the Hanford town site, also called "Hanford Camp" (Figures 3-2, 1-2, 1-3). In his diaries during work on the Manhattan Project, G.T. Seaborg (1994) describes a visit in May 1944 to the Hanford plant and the onsite Hanford Camp "where the construction workers live in rows of barracks, tents, and trailers stretched out in all directions. We ate in the largest mess hall I have ever been in…there are some 40,000 residing at Hanford." Seaborg also describes all site roads then as "secondary."

Dr. Vincent C. Jones is a World War II veteran and historian on the staff of the U.S. Army Center of Military History since 1955. His book, *Manhattan: The Army and the Atomic Bomb* (Jones 1985) provides insight into the details of the Manhattan Project at Hanford and other sites. His observations were reviewed in the context of the places, people, and conditions of exposure for workers in the wartime construction period (1943-1945) at Hanford.

The support facilities essential to construction and operations of the Manhattan Project facilities had to come first. Scientists had indicated that it would not be safe for plant-operating employees to reside within 10 miles of the reactors or fuel processing facilities. Because these facilities would have to be tested during the latter phases of construction, even construction employees would have to live some distance from them. Engineers favored using sites already occupied by rural villages, where they would be able to take advantage of existing grading, buildings, road networks, and utilities. After considering several plans, it was decided to build a construction camp at Hanford and an operating village at Richland. Hanford was about 6 miles from the nearest process areas. Richland, about 25 miles from the production plant sites, was chosen for the operating community.

Establishing the Hanford construction camp had higher priority than the operating community of Richland. The construction camp started with tents, but eventually there were over 800 barracks, 600 Quonset huts, and a trailer camp with 4,300 people. There were eight mess halls where 50 tons of food was served per meal. In July 1944, Du Pont announced that construction was 98% complete, with nearly 1200 new and remodeled buildings and sufficient

[3] See Figure 1-3 for photographs of towers manned by security personnel.

support facilities to house, feed, and supply the daily necessities of the 51,000 people who, by that time, were living at the construction camp.

Citing historical archive documents, Jones (1985) describes the Hanford construction camp in the 1943–1945 period:

> Newly recruited workers found themselves in what must certainly have been one of the largest temporary communities ever erected. Hundreds of one-story structures, standing in evenly spaced rows along freshly graded streets, filled the generally flat terrain west of the broad Columbia River. The majority of these structures were housing units. At the center were row upon row of wing-type barracks. To the south were hundreds of much smaller hutments. On the north and west stood thousands of family-sized trailers, each positioned on its individual plot. Interspersed at conveniently located intervals were cafeteria buildings. In a triangular-shaped area near the river and between the barracks and the north trailer camp were most of the commercial and administrative buildings, some remodeled from existing structures. Here also were many of the community and recreational facilities—a theater, church, school, hospital, library, and an auditorium-gymnasium. Rising here and there above the low level of most structures were the smoke stacks of heating plants, water and oil storage tanks, and a few trees. Utility lines strung on tall poles lined every street, seeming to bind together the scattered segments of the Hanford camp.

Figure 3-3. View of Hanford construction camp, with barrack hutments in foreground. "Hutments" was a term for the fabricated temporary buildings, which later were referred to as "Quonset huts" because the first of that type in this country had been built at Quonset, Rhode Island. The camp housed some 40,000 workers. The trailer camp was home to another 12,000 residents, including dependents. Hanford Camp was built in 1943 and abandoned in early 1945 when the construction period ended (Sanger 1995).

Hanford was planned as a temporary camp. The minimum amenities of temporary housing were "a chief factor in the continual turnover of construction personnel, which approached an unacceptable rate of 21 percent in the crucial summer of 1944" (Jones 1985). The official photographer at Hanford, Robley Johnson, estimated that he made over 145,000 identification photographs for this revolving-door population (Fermi and Samra 1995). Other discouraging factors were the demoralizing sandstorms, the isolation, and segregated housing. The latter policy precluded families, even husbands and wives, from living together and restricted occupancy on the basis of gender and race.

The trailer camp of the Hanford site (see domestic scene in Figure 1-3) was a reluctantly provided option for those families that would only relocate as a unit. The trailer camp was the largest in the world at the time with 4,000 trailers and some 12,000 residents. Residents recall that it was policed, kept clean, with big bath houses and a school. "These were family people—no riff-raff. Barracks people were totally different." There were a "few houses in real nice shape out on the perimeter of the Hanford camp" that families rented. There were orchards of apples, apricots, peaches, pears, plums, and cherries (Sanger 1995).

Turnover at Hanford was reduced by morale boosters such as recreation halls for both men and women, including bowling alleys, a 4000-seat baseball stadium, softball diamonds, tennis, badminton, volleyball, and horseshoe courts, taverns, nightly motion pictures, and concerts by nationally known entertainment. Wartime residents of Hanford would recall that the camp came to have "a kind of gaiety, a temporary feeling, the mood of a fair or carnival or circus," all enhanced by the continuous playing of music over a public address system (Fermi and Samra 1995).

A timeline in Fermi and Samra (1995) confirms that the Hanford construction camp was closed in February 1945. Also, Sanger (1995) interviewed a past worker whose responsibility it was to "close up Hanford Camp in February of '45." Another noted that the last mess hall closed February 20, 1945 when construction ended. Another wartime worker recalled that by 1946 the camp was dismantled—nothing was left but a few wild goats after the war ended. Nothing but a few faint remnants of the giant camp remain today.

In the 1947 to 1949 expansion period at Hanford, a construction worker enclave was established in North Richland. This included housing in the form of trailers and barracks as well as other facilities. The population of the Tri-Cities region expanded to about 65,000.

If Hanford was the "blue-collar" community, Richland was the "white collar" community during the wartime years. Jones (1985) describes the "operating community" of Richland:

> Richland, with a population of 250, was in early 1943 the center of an agricultural community of some 600 persons who derived their livelihood from farming the irrigated bottomlands near the junction of the Yakima and Columbia Rivers. Most of the commercial and civic structures of the village and some of its homes were built along the axis of a state highway, providing a ready route of access eastward to the important communication centers of Kennewick and Pasco and northward to Hanford and White Bluffs. The original buildings of Richland were of substantial construction, many of them cement or brick. Community services included an underground water system (but no central sewerage system), electricity, and telephones. The roads were chiefly gravel or

packed earth, but some had asphalt surfacing. Surrounding the village center were numerous small farms, planted with orchards or other irrigated crops.

The army turned over the task of converting the farm community of Richland into a home for thousands of plant operating employees to Du Pont and approved architectural engineering firms. Initial estimates for housing needs were repeatedly underestimated and the scope of the community plan grew. Fermi and Samra (1995) states that 17,000 operating personnel, scientists, engineers, and military personnel were housed in Richland during the war. In a fenced-in area at the center of the operating village were the wood-frame buildings of varying size that housed the HEW administrative headquarters. Immediately to the east and southeast of the headquarters and toward the low-lying Columbia River was "downtown" Richland, built around the original commercial center of the village. Here were stores and a variety of service facilities, a hotel for visitors, a theater, churches, a cafeteria, and the dormitories for single men and women. Surrounding downtown on the south, west, and northwest were residential areas, with neighborhood stores and service facilities.

Hanford and Richland were the two largest communities housing Hanford workers during the war, but other communities like Prosser provided a home for workers who would make the commute to the site facilities every day (Sanger 1995). A tent camp in North Richland housed Hanford workers in 1943 and was expanded in later years with permanent housing and trailers.

With respect to working hours, Jones (1985) indicates that approval was given for double work shifts of 9 hours on urgent parts and as much as 10 hours per day, 7 days a week when the fuel processing plants were under construction. These workers would have been exposed to airborne releases from the production reactors starting in October 1944 (Table 1-1). One person interviewed by Sanger (1995) who lived in Prosser worked 10 hours per day, 50 hours per week during the war years. Another indicated, "Most everyone worked 10 hours per day." A concrete worker at 200-East in 1943 recalled working 12 hours per day.

Other relevant comments from wartime Hanford workers recorded by Sanger (1995):

- It was hard to get laundry done. Construction workers would wear their overalls until they couldn't wear them anymore and then they would buy new.
- Mess hall workers recalled riding buses—open, towed by a truck. "We ate more sand in the 40 miles to Hanford—it was endless. We got off the bus and we sank in sand a foot deep. At four o'clock every afternoon the wind would come up and blow that sand. I mean, that sand would sit anywhere from a quarter of an inch to an inch on all of this" (referring to butcher paper over tables in mess halls).
- It was so windy. New hires would get off the bus at Hanford and be on the next one back to Pasco.
- Richland is laid on river pebbles. They bulldozed the place flat, got rid of whatever topsoil there was and brought in silt from the Yakima River Flats. They put 6 inches of this stuff over the town. When the wind blew you wouldn't be able to see across the street. Every morning there was a sand dune under the front door.
- Food at Hanford was prepared by teams of chefs—it was high quality and at reasonable prices. Workers jammed into one of 8 mess halls with a total capacity of 19,500 diners. Fish was fresh and came out of Seattle. First meals were April 21, 1943; last mess hall closed February 20, 1945 "when construction ended."
- Nitric oxide fumes from separations stacks could be "practically brown. We didn't want the wind to be in the direction of the Tri-Cities. If we started dissolving and the wind got bad, we would have to quit. That's before we had sand filters and all kinds of purifiers."

- The people at greatest risk were working in the separations plants. "We did urine tests, at first some were done daily, after that, weekly and then monthly. We were looking for plutonium. Pu did show up, but below the permissible limits." (Du Pont's medical director)

Work locations for construction workers. The work locations for construction workers sometimes brought them close to the important release points for radioactive gases and particles. As opposed to military personnel, however, the construction work force would have spent less time per day near the 200 Areas. There were other construction sites, but 200 Areas probably represent worst-case conditions. For example, the construction site for the PUREX Plant, which began operating in 1956, was about 2 km (1 mi.) from the B Plant stack in 200-East Area and 8 km (5 mi.) from T Plant and REDOX stacks in 200-West Area. The PUREX work location and Richland residence location are used in an example calculation for a construction worker in Section 5. Another example is a survey technician in 200 Areas during a time of high deposition of active particles on ground areas.

Other onsite residence locations. One other onsite residence complex in the early years of Hanford operations was the Columbia Camp on the horn of the Yakima River (Figure 1-2). The Columbia Camp was built for the Federal Prison Industries to house selected prisoners from McNeil Island Federal Penitentiary near Tacoma, Washington. These prisoners, carefully screened as "minimum-custody" offenders with no more than one year to serve, were used to tend and harvest the many orchards confiscated during the government takeover of the Hanford property, while gaining vocational training and rehabilitation. Less than 30% were conscientious objectors. Statistics from the Federal Bureau of Prisons show that a total of 1,300 prisoners served at Columbia Camp with 290 being the maximum at any one time. It was closed in October 1947, having operated since February 1944. Prisoners were transported to the orchards to prune, spray, cultivate, and irrigate and then to harvest the fruit. Fruit was shipped to the McNeil Island Penitentiary, where it was processed (most of it canned) for sale to military services and other government agencies. When the contract ended November 1, 1947, 5,669 tons of fruit had been processed which sold for more than $500,000. Atkinson-Jones next used the camp facilities to house workers while North Richland was constructed. From early 1948 through July 1949 Morrison-Knudsen occupied the camp while constructing and maintaining the Hanford project railroad. The Columbia Camp site was turned over to the Army Corps of Engineers in August 1949 and returned to the Atomic Energy Commission in February 1950. In spring of 1950 the buildings were moved to other locations or sold as excess. The land is now part of Horn Rapids Park.[4]

The methods developed in this work show that the Columbia Camp received somewhat less exposure than the Hanford town site to airborne releases from Hanford facilities (Figure 5-1). An example in Section 5 uses the Hanford town site as a residence location.

[4] The sources for information presented here on the Columbia Camp were cited on Internet site http://allgallery.tripod.com/0000s/ColumbiaCamp.html, and include: "Columbia Camp, Prison Camp in our Midst, 1944-1947," by Jean Carol Davis, The Courier, East Benton County Historical Society, Volume 15, Number 1, February 1993; Tri-City Herald, August 7, 1949, p 1; Pasco News, February 24, 1950, p 13; and "Columbia Camp Revisited," by Jean Carol Davis, The Courier, East Benton County Historical Society, Volume 15, Number 3, October 1993.

3.2 Descriptions of Models

3.2.1 Models of Atmospheric Transport

The models chosen to simulate the transport of released radionuclides through the atmosphere are based on the well-known Gaussian plume model for an elevated point source. The implementation is adapted, in part, from the basic models used in the ISC3 atmospheric dispersion programs (EPA 1995). The fundamental formula, which relates the release rate at the source to the concentration at a receptor location (x, y, z), is

$$C(x,y,z) = \frac{QVD}{2\pi\sigma_y\sigma_z u}\exp\left(-y^2/(2\sigma_y^2)\right) \qquad (3.2.1\text{-}1)$$

where

C = concentration (pCi m^{-3}) at receptor location z m above ground level
Q = release rate (pCi s^{-1})
V = vertical term to account for confinement of the plume between the ground and the mixing lid (see Equation (3.2.1-4))
D = term to adjust for radioactive decay of a released radionuclide or to account for the amount of a radioactive decay product (daughter) formed in transit
σ_y, σ_z = horizontal and vertical Gaussian dispersion coefficients, respectively (m); each parameter is a function of the distance from the source to the receptor location
u = wind speed (m s^{-1}) (usually evaluated at effective release height h)
h = effective release height (m), which may include plume rise from buoyancy or momentum, or entrainment of the plume into a wake cavity in the lee of a building (the vertical term V depends on this parameter); in the present application, h = physical height of release stacks = 61 m
x = distance coordinate from source (m) along plume centerline
y = perpendicular crosswind distance (m) from plume centerline at x to the receptor location at which the concentration is evaluated; if $y = 0$, x is the distance from the source to the receptor.

The horizontal and vertical distributions of concentration about the centerline of the plume are Gaussian, with standard deviations σ_y and σ_z, respectively. These dispersion parameters vary with the horizontal distance from the source to the receptor location, and they are specific to atmospheric stability categories labeled A–F, according to the Pasquill-Gifford scheme (Gifford 1976). For calculating σ_y and σ_z, we have used the parameters and formulas from the ISC3 models (EPA 1995) that approximate the Pasquill-Gifford curves. For σ_y, the equations are

$$\sigma_y(x) = 465.11628\, x \tan(0.017453293(c - d\ln x)) \qquad (3.2.1\text{-}2)$$

where the downwind distance x is in km and the coefficients c and d are taken from Table 3-1. The equation for σ_z is the power formula

$$\sigma_z(x) = ax^b \qquad (3.2.1\text{-}3)$$

with coefficients a and b shown in Table 3-2. Tables 3-1 and 3-2 correspond to Tables 1-1 and 1-2, respectively, of EPA (1995) and the data in them are reprinted here for the convenience of readers.

Table 3-1. Coefficients for Calculating Pasquill-Gifford σ_y (m) As a Function of Distance *x* (km) [a]

Pasquill-Gifford stability category	*c*	*d*
A	24.1670	2.5334
B	18.3330	1.8096
C	12.5000	1.0857
D	8.3330	0.72382
E	6.2500	0.54287
F	4.1667	0.36191

[a]Source: EPA 1995. The formula is given by $\sigma_y(x) = 465.11628\, x \tan(0.017453293(c - d \ln x))$.

The mixing phenomenon represented by the dispersion parameters σ_y and σ_z is assumed to be confined between the ground surface and a mixing height *H*, which increases as energy is added to the system and decreases as the turbulence subsides.

The vertical factor *V* shown in Eq. (3.2.1-1) uses the assumption of reflecting barriers at the mixing lid height *H* (which was assigned an annual average value of 1500 m) and at ground level, so that the plume is confined to the region between, provided the release height *h* is less than *H* (since we use an annual average value of *H*, the release heights considered are all less than *H*). A representation of this scheme is given by an infinite sequence of virtual sources above and below ground level. The result is an infinite series, which may be replaced by a uniform vertical concentration at sufficiently large source-to-receptor distances:

$$V(x,z;h,H) = \exp\left(-\frac{(z-h)^2}{2\sigma_z^2}\right) + \exp\left(-\frac{(z+h)^2}{2\sigma_z^2}\right) + \sum_{p=1}^{4}\sum_{k=1}^{\infty} T_{pk} \quad \text{if } \sigma_z < 1.6H$$
$$= 1/H \quad \text{otherwise} \tag{3.2.1-4}$$

where

$$T_{1k} = \exp\left(-\frac{(H-(2kz-h))^2}{2\sigma_z^2}\right), \quad T_{2k} = \exp\left(-\frac{(H+(2kz-h))^2}{2\sigma_z^2}\right),$$
$$T_{3k} = \exp\left(-\frac{(H-(2kz+h))^2}{2\sigma_z^2}\right), \quad \text{and} \quad T_{4k} = \exp\left(-\frac{(H+(2kz+h))^2}{2\sigma_z^2}\right) \tag{3.2.1-5}$$

.

With $y = 0$, Eqs. (3.2.1-1) through (3.2.1-5) give the concentration C at height z and distance x along the plume centerline. The dichotomy of Eq (3.2.1-4) expresses the approach of the vertical concentration to a constant value at sufficiently great distances from the source; the breakpoint occurs when the vertical dispersion coefficient σ_z (which increases with distance from the source) equals 1.6 times the mixing height.

Table 3-2. Coefficients for Calculating Pasquill-Gifford σ_z (m) as a Function of Distance *x* (km) [a, b]

Pasquill-Gifford stability category	*x* (km)	*a*	*b*
A	<.10	122.8	0.9447
	0.10 - 0.15	158.08	1.0542
	0.16 - 0.20	170.22	1.0932
	0.21 - 0.25	179.52	1.1262
	0.26 - 0.30	217.41	1.2644
	0.31 - 0.40	258.89	1.4094
	0.41 - 0.50	346.75	1.7283
	0.51 - 3.11	453.85	2.1166
	>3.11	c	c
B	<.20	90.673	0.93198
	0.21 - 0.40	98.483	0.98332
	>0.40	109.3	1.0971
C	All	61.141	0.91465
D	<.30	34.459	0.86974
	0.31 - 1.00	32.093	0.81066
	1.01 - 3.00	32.093	0.64403
	3.01 - 10.00	33.504	0.60486
	10.01 - 30.00	36.65	0.56589
	>30.00	44.053	0.51179
E	<.10	24.26	0.8366
	0.10 - 0.30	23.331	0.81956
	0.31 - 1.00	21.628	0.7566
	1.01 - 2.00	21.628	0.63077
	2.01 - 4.00	22.534	0.57154
	4.01 - 10.00	24.703	0.50527
	10.01 - 20.00	26.97	0.46713
	20.01 - 40.00	35.42	0.37615
	>40.00	47.618	0.29592
F	<.20	15.209	0.81558
	0.21 - 0.70	14.457	0.78407
	0.71 - 1.00	13.953	0.68465
	1.01 - 2.00	13.953	0.63227
	2.01 - 3.00	14.823	0.54503
	3.01 - 7.00	16.187	0.4649
	7.01 - 15.00	17.836	0.41507
	15.01 - 30.00	22.651	0.32681
	30.01 - 60.00	27.074	0.27436
	>60.00	34.219	0.21716

[a] Source: EPA 1995.
[b] If the calculated value of F_z exceeds 5000 m, F_z is set to 5000 m.
[c] F_z is equal to 5000 m.

When longer-term averages of concentration are the object, it is common practice to average the concentration over the width of the *wind sector* at distance x and use this sector average in place of the centerline value. Wind data are commonly recorded for a fixed number of directions, or sectors; 16 is the number that corresponds to the data used for these calculations (see section "Meteorological Data" below). The directions are measured clockwise from north and abbreviated according to the compass points N, NNE, NE, ENE, etc. This scheme limits the precision of the wind direction to an angle of 22.5°. Thus, when such wind data are used, the sector average considers variation of the wind direction within the sector, whereas the centerline value would correspond to a wind direction that is always along the sector's centerline. It is usual to specify the sector *from* which the wind blows, so that specifying a wind direction of SW would mean the wind is blowing from the source *toward* the northeast.

Application of the sector averaging procedure to Eq. (3.2.1-1) leads to the following formula:

$$C_j(x,z) = \sqrt{\frac{2}{\pi}}\frac{8QD}{\pi x \sigma_z u}\cdot V_j(x,z;h,H) \qquad (3.2.1\text{-}6)$$

where the index j indicates the stability category (A–F) and (as before) x represents the distance (m) from the source to the receptor. The function V_j (Eq. (3.2.1-4)) depends on the stability category through the vertical dispersion coefficients σ_z. We can now estimate the sector average concentration averaged over all stability classes at distance x from the source and in sector i as

$$\overline{C}_i(x,z) = \sum_{j=\mathrm{A}}^{\mathrm{F}} f_{ij}\cdot C_j(x,z) \qquad (3.2.1\text{-}7)$$

where f_{ij} is the fraction of the time (frequency) for which the wind blows into sector i (or from the sector opposite sector i, in the conventional parlance) during stability conditions of class j. The concentration $C_j(x,z)$ is the sector-averaged value obtained from Eq. (3.2.1-6). The values of the f_{ij} are discussed in the section "Meteorological Data" below.

The factor D of Eq. (3.2.1-1) accounts for radioactive decay of a released radionuclide during its travel from the point of release to the receptor location. In the case of a decay product that is formed during plume travel, D adjusts Eq. (3.2.1-1) so that the concentration represents the decay product. If the travel time is $t = x/u$, where x is the source-to-receptor distance (m) and u is the mean wind speed (m s^{-1}), the factor is

$$D = e^{-\lambda_1 t} \qquad (3.2.1\text{-}8a)$$

for the released radionuclide, and

$$D = \frac{\lambda_2}{\lambda_2 - \lambda_1}\left(e^{-\lambda_1 t} - e^{-\lambda_2 t}\right) \qquad (3.2.1\text{-}8b)$$

for the decay product. The symbols λ_1 and λ_2 (s^{-1}) represent the radioactive decay rate coefficients for the released radionuclide and the decay product, respectively. More complex decay schemes exist, but they are not needed for the Hanford source term.

3.2.2 Models for Deposition

Equation (3.2.1-1) does not account for the depletion of radioactivity concentration in the plume by deposition of material from the air to the ground, or to objects such as plants and buildings. Particles or gas molecules come into contact with the ground as a result of gravitational fall, air turbulence, or molecular diffusion (dry deposition), or as a result of their

association with falling raindrops (wet deposition). These processes are modeled in ways similar to those used in the ISC3 programs (EPA 1995).

Dry Deposition. The total rate of dry deposition is represented by the product of the concentration of radioactivity in the air (Bq m^{-3}) at a reference height (usually 1 m) and a deposition velocity v_d (m s^{-1}). The deposition velocity is interpreted (by analogy with electrical circuit theory) as the reciprocal of a total resistance to deposition. The total resistance is given in terms of component resistances by the formula

$$v_d = \frac{1}{r_{\text{total}}} = \frac{1}{r_a + r_s + r_a r_s v_t} + v_t \qquad (3.2.2\text{-}1)$$

where

r_a = momentum flux resistance associated with atmospheric turbulence above the surface layer (s m^{-1})
r_s = resistance of the surface layer (s m^{-1})
v_t = terminal velocity of particle in gravitational fall (m s^{-1}).

The momentum flux resistance is given by the equation

$$r_a = u / u_*^2 \qquad (3.2.2\text{-}2)$$

where u (m s^{-1}) is the mean horizontal wind speed at the reference height (usually 1 m) and u_* (m s^{-1}) is the friction velocity. The square of the friction velocity is proportional to the slope of the vertical wind speed profile, with a constant of proportionality that varies with atmospheric stability. Empirical representations of the vertical wind speed profile are given for stable, neutral, and unstable air, and these formulas are used to calculate u_* in Eq. (3.2.2-2) (Seinfeld 1986).

A theoretical model for the surface layer resistance is given by

$$r_s = \left[u_*(\text{Sc}^{-2/3} + 10^{-3/\text{St}})\right]^{-1} \qquad (3.2.2\text{-}3a)$$

where the Stokes number St is an increasing function of the particle diameter, and thus the term $10^{-3/\text{St}}$ increases with particle diameter, representing inertial effects. The Schmidt number Sc tends to zero with the particle diameter, and thus the term $\text{Sc}^{-2/3}$ increases without bound as the particle diameter tends to zero. This term expresses deposition by molecular diffusion of the smaller particles. We define the Schmidt and Stokes numbers below, after necessary parameters are introduced.

As an alternative to theoretical models such as the one given by Eq. (3.2.2-3a), Sehmel and Hodgson (1980) have developed an empirical model of dry deposition for which the surface layer resistance is characterized by a regression function of several combinations of the variables that enter into the resistances defined above and other variables that we define or reference below. This regression function was fitted to data from wind tunnel experiments. The functional form is

$$\text{Int}_3 = -\exp(-378.051 + 16.498 \ln \text{Sc} + P \ln \tau^+ - 12.8044 \ln d)$$

where

$$\tau^+ = \text{scaled dimensionless relaxation time} = \frac{\rho_p d^2 u_*^2}{18 \mu_{\text{air}} \nu_{\text{air}}} \times 10^{-8}$$

and

$$P = -11.8178 - 0.28628 \ln \tau^+ + 0.32262 \ln(d / z_0) - 0.33850 \ln(D / (z_0 u_*)).$$

Parameters not defined above are μ_{air} = dynamic viscosity of air = 1.78 × 10^{-4} g s^{-1} cm^{-2}; $\nu_{air} = \mu_{air} / \rho_{air}$ = kinematic viscosity of air (cm s^{-1}), where ρ_{air} = density of air = 1.2 × 10^{-3} g cm^{-3}; D = Brownian diffusivity = $kTC_c / 3\pi\mu_{air} d$ cm^2 s^{-1}, where k = Boltzmann's constant = 1.32 × 10^{-16} erg (molecule K)$^{-1}$, C_c = Cunningham's slip correction factor (see Dennis (1976) for an empirical formulation), T = temperature (296 K was used); and z_0 = roughness length (cm), which is related to roughness of the surface over which the wind moves (Hanna et al. (1982) suggest that $z_0 \approx 1/10$ of the height of the roughness elements). The Schmidt number Sc may now be defined as $\mathrm{Sc} = \nu_{air} / D$ cm^{-1}, and the Stokes number St may be expressed as $\mathrm{St} = d^2 \rho_p \rho_{air} C_c u_*^2 / (18\mu_{air}^2)$ cm. The expression for the surface resistance based on the model of Sehmel and Hodgson (1980) is

$$r_s = \frac{1 - \exp\left((v_t / u_*)\mathrm{Int}_3\right)}{v_t} \quad . \tag{3.2.2-3b}$$

We have applied this model in the calculations for dry deposition rather than the theoretical model of Eq. (3.2.2-3a), although both are available in the source code of HCalc; however, a change in preprocessor instructions and a recompilation of the file drydep.c are necessary to change from one model to the other.

Stokes's law expresses the basic theory of gravitational fall in the following formula for terminal gravitational velocity:

$$v_t = \frac{d^2 g \rho_p}{18\mu_{air}} \tag{3.2.2-4a}$$

where d is the physical diameter of the particle (cm), g is the gravitational acceleration constant (cm s^{-2}), ρ_p is the particle density (g cm^{-3}), and μ_{air} is the dynamic viscosity of air (g s^{-1} cm^{-2}). Stokes's law is modified with Cunningham's slip correction factor to account for the increased mobility of radioactive particles with diameters less than the mean free path of the air molecules. Further detail can be found in Seinfeld (1986). Moreover, the formula loses accuracy as the particle diameter increases beyond about 20 μm. We have used an extension of the theory that avoids this difficulty and includes Eq. (3.2.2-4a) as a special case. We give here a brief outline of the extended theory and our computational method.

The Reynolds number R of air flow around a spherical particle may be defined as

$$R = \frac{Ud\rho_{air}}{\mu_{air}} \tag{3.2.2-4b}$$

where U is the flow velocity (cm s^{-1}) and ρ_{air} is the density of air. (Flows with the same Reynolds number have geometrically similar streamlines, and thus similar dynamic properties, even for different values of the variables of Eq. (3.2.2-4b).) The drag coefficient of the flow, C_D (dimensionless), is defined generically as

$$C_D = \frac{D}{(1/2)\rho_{air} U^2 A} \tag{3.2.2-4c}$$

where D (g cm s^{-2}) is the drag force and $A = \pi d^2 / 4$ (cm^2) is the projected area of the particle. Shifting to coordinates relative to a fixed air medium, in which the particle moves, we put $v = U$ for the velocity of the particle and write the differential equation

$$\frac{dv}{dt} = C_D \frac{3}{4} \frac{\rho_{air} v^2}{\rho_p d} - g \qquad (3.2.2\text{-}4d)$$

which expresses the acceleration of the particle in response to the two competing forces. At steady state, the particle acceleration $dv/dt = 0$, which we substitute into Eq. (3.2.2-4d); then we use Eq. (3.2.2-4b) to eliminate $v = U$. These substitutions lead to

$$R^2 C_D = \frac{4\rho_p d^3 g}{3\mu_{air}} \qquad (3.2.2\text{-}4e)$$

It is possible by experimental means to estimate the drag coefficient C_D as a function of the Reynolds number R. We have used such an experimental curve with Eq. (3.2.2-4e) to express R implicitly as a function of the particle diameter d (Schlichting 1968, Fig. 1.5, curve 2). Solving numerically for R, given d, we then substitute the values of R and d into Eq. (3.2.2-4b) and solve for the velocity U:

$$v_t = U = \frac{\mu_{air} R}{d\rho_{air}} \qquad (3.2.2\text{-}4f)$$

The relationship is linear for $R \le 0.1$ and reduces to the Stokes relationship of Eq. (3.2.2-4a) in that region. For $R > 0.1$ the empirical curve is used with the procedure outlined above. For our calculations, we fitted the digitized logarithmic empirical curve between $R = 0.1$ and $R = 2 \times 10^5$ with a quintic polynomial, i.e.,

$$C_D(R) \sim \exp\left(\sum_{k=0}^{5} c_k r^k\right), \quad r = \ln(R) \qquad (3.2.2\text{-}4g)$$

where the coefficients $c_0, \ldots, c_5$ = 3.247, –0.8498, 0.03937, –0.004372, 9.592×10^{-4}, and -4.789×10^{-5}. After substituting the representation of Eq. (3.2.2-4g) into Eq. (3.2.2-4e), it is still necessary to apply a numerical method to solve the resulting equation for R, given a value of d. We found the FORTRAN nonlinear equation solving routine ZEROIN satisfactory (Forsythe et al. 1977).

The derivation given above uses the formulation of the drag coefficient for an incompressible fluid. For flow velocities less than about 0.3 times the velocity of sound in air (Mach 0.3), the practical effect of compressibility is negligible (Schlichting 1968). The velocity of sound in air is about 34,000 cm s^{-1}, whereas we would rarely, if ever, consider particles of sufficient size and density to achieve a gravitational settling velocity greater than 200 cm s^{-1}.

Wet Deposition. The model for wet deposition is expressed by a scavenging rate coefficient Λ (s^{-1}), which is expressed in terms of rainfall rate R (mm h^{-1}) by the formula

$$\Lambda = \lambda R \qquad (3.2.2\text{-}5)$$

where the factor λ (s^{-1} (mm $h^{-1})^{-1}$) depends on the particle diameter. Our program represents this dependence with a table with entries estimated from the graph of Fig. 1-11 in EPA (1995). Table 3-3 shows the numbers that the program interpolates. With the assumption that the source of the rain is above the plume, the loss rate of radioactivity (Bq m^{-2} s^{-1}) from the plume at distance x from the source and off-centerline distance y is

$$F_{wet}(x, y) = \Lambda \int_0^\infty C(x, y, z)\, dz \qquad (3.2.2\text{-}6)$$

where the concentration $C(x, y, z)$ is given by Eq. (3.2.1-1). With $y = 0$, and using the first two terms of the vertical component V (Eq. (3.2.1-2)), Eq. (3.2.2-6) can be integrated to give

$$F_{\text{wet}}(x) = \frac{QD\Lambda}{\sqrt{2\pi}u\sigma_y}. \qquad (3.2.2\text{-}7)$$

This centerline flux is a conservative estimate of wet deposition rate at distance x from the source.

Table 3-3. Scavenging Rate Parameter (s^{-1} $(mm\ h^{-1})^{-1}$) as a Function of Particle Diameter [a]

Diameter (μm)	0.1	0.2	0.3	0.4	0.6	0.8	1	1.5	2	3	4	6	8	10
$10^4\lambda$ (s^{-1} $(mm\ h^{-1})^{-1}$)	1.7	1.3	0.8	0.6	0.5	0.5	0.45	0.8	1.4	2.2	2.8	4.2	5.1	6.8

[a]Estimated from Fig. 1-11 in EPA 1995.

Plume Depletion. Loss of radioactivity from the plume from deposition processes results in reduced concentrations in air (plume depletion). For both wet and dry deposition, we have applied a technique of source depletion, in which the release rate parameter Q is allowed to decrease with the downwind distance to account for the loss of radioactivity from the plume. In the case of dry deposition, this procedure is based on the differential equation

$$\frac{dQ}{dx} = -v_d \int_{-\infty}^{\infty} C(x, y, z = 0)\, dy \qquad (3.2.2\text{-}8)$$

where the integrand is given by Eq. (3.2.1-1). Making the substitution, with only the first two terms of the vertical component V, we may solve the differential equation and compute the depletion factor as

$$\frac{Q(x)}{Q_0} = \left[\exp \int_0^x \frac{D}{\sqrt{2\pi}\sigma_z \exp(h^2/(2\sigma_z^2))} \right]^{-v_d/u} \qquad (3.2.2\text{-}9)$$

with notations as explained after Eq. (3.2.1-1); Q_0 is the radioactivity release rate at the source (Van der Hoven 1968). The integral is computed numerically. A similar factor for wet deposition is

$$\frac{Q(x)}{Q_0} = e^{-\Lambda x} \qquad (3.2.2\text{-}10)$$

(EPA 1995). For long-term application, this wet depletion fraction would be replaced by

$$\frac{Q(x)}{Q_0} = 1 - f_{\text{precip}} + f_{\text{precip}} e^{-\Lambda x} \qquad (3.2.2\text{-}11)$$

where f_{precip} is the fraction of the time precipitation occurs.

Our computer program will optionally apply the factors of Eqs. (3.2.2-9) and (3.2.2-11) to the prediction of Eq. (3.2.1-7). Not doing so is conservative practice, which will overestimate the air concentration at the receptor location and also the surface soil content from cumulative deposition at that location. In calculations of dose from routine releases, we have followed this conservative practice.

3.2.3 Models for Food Chain Transfer (Vegetables and Animal Products)

Dose from ingestion of radionuclides in garden and animal products as the result of deposition on soil, growing produce, and pasture grass is based primarily on models and parameters of the National Council on Radiation Protection and Measurements (NCRP) screening models (NCRP 1996). These models and parameters are deliberately conservative, in the sense that they deliberately bias the dose estimates upward. These food pathways are primarily applicable to people living off the Hanford Site, although some incidental ingestion of soil may be assumed for workers on the site. Only atmospheric deposition is considered as a source of radioactivity.

Concentrations in vegetation (vegetables and forage) are estimated by the steady state equation

$$C_{\mathrm{veg},i} = C_{\mathrm{a},i} V_{\mathrm{d},i}\ \mathrm{CF}_{\mathrm{veg},i} \Delta_{\mathrm{veg},i}(t_{\mathrm{h}}) \qquad (3.2.3\text{-}1)$$

where

$C_{\mathrm{veg},i}$ = concentration of radionuclide i on the surface and in the tissues of garden vegetables or forage (Bq kg^{-1}),

$C_{\mathrm{a},i}$ = concentration of radionuclide i in the air at surface level (Bq m^{-3}),

$V_{\mathrm{d},i}$ = deposition velocity for radionuclide i (m s^{-1}),

$\mathrm{CF}_{\mathrm{veg},i}$ = concentration of radionuclide i in vegetation per unit deposition on agricultural land (Bq kg^{-1} per Bq m^{-2} d^{-1}), and

$\Delta_{\mathrm{veg},i}(t_{\mathrm{h}})$ = factor for radioactivity depletion due to holdup time (t_{h}) between harvest and consumption of product.

The concentration factor for vegetation is computed as

$$\mathrm{CF}_{\mathrm{veg},i} = \frac{f}{Y}\mathrm{VC}(\lambda_{\mathrm{E},i}, t_{\mathrm{e}}) + \frac{(B_{\mathrm{v}})_i}{P}\mathrm{BC}(\lambda_{\mathrm{B},i}, t_{\mathrm{b}}) \qquad (3.2.3\text{-}2)$$

where

$\mathrm{VC}(\lambda_{\mathrm{E},i}, t_{\mathrm{e}})$ = radiological buildup (Bq d Bq^{-1}) of parent or daughter radionuclide on plant surface, corresponding to effective removal coefficient $\lambda_{\mathrm{E},i}$ (d^{-1}) during growing period t_{e} (d),

$\mathrm{BC}(\lambda_{\mathrm{B},i}, t_{\mathrm{b}})$ = radiological buildup (Bq d Bq-1) of parent or daughter radionuclide in soil, corresponding to effective removal coefficient $\lambda_{\mathrm{B},i}$ (d^{-1}) during deposition period t_{b} (d),

f = interception fraction (dimensionless), i.e., the fraction of deposited radioactivity per unit area of agricultural land that is deposited on and retained by the edible portion of the crop,

Y = crop biomass at harvest (kg m^{-2}),

$\lambda_{\mathrm{E},i}$ = effective rate coefficient for removal of deposited radionuclide i from plant surfaces (d^{-1}); $\lambda_{\mathrm{E},i} = \lambda_{\mathrm{R},i} + \ln 2 / t_{\mathrm{w}}$,

t_{w} = weathering half-life for loss of deposited material from plant surfaces (d),

$(B_{\mathrm{v}})_i$ = element-dependent concentration factor for transfer of the element of radionuclide I to the edible portion of the crop from dry soil (Bq kg^{-1} plant per Bq kg^{-1} soil), and

P = soil mass per unit area of the plow layer (kg m^{-2}),

$\lambda_{B,i}$ = effective removal coefficient for radionuclide i from soil (d^{-1}); $\lambda_{B,i} = \lambda_{R,i} + \lambda_{HL}$,

λ_{HL} = rate coefficient for radioelement removal from soil layer by harvesting and leaching (d^{-1}).

The radiological buildup factors VC and BC have the same mathematical form:

$$\text{VC or BC} = \varphi(L) = L^{-1}(1 - e^{-Lt}) \quad \text{for parent nuclide}$$

$$= \varphi(\lambda_2, L_1, L_2) = \frac{\lambda_2}{L_2 - L_1}\left(\frac{1 - e^{-L_1 t}}{L_1} - \frac{1 - e^{-L_2 t}}{L_2}\right) \quad \text{for daughter nuclide} \tag{3.2.3-3}$$

In the case of a decay chain, indices 1 and 2 correspond to parent and daughter, respectively. For the parent, L corresponds to whichever of the effective removal rate coefficients λ_E or λ_B is applicable; t corresponds to whichever of t_e or t_b is applicable (Eq. (3.2.3-2)). For the daughter, the subscripts on L indicate parent and daughter, and again, L_i corresponds to the appropriate element dependent removal coefficient $\lambda_{E,i}$ or $\lambda_{B,i}$ (plant surface or soil, respectively).

Concentration of radionuclides in locally produced animal products is given by the equation

$$C_{animal,i} = F_{animal,i} C_{forage,i} Q_f \Delta_{animal,i}(t_h) \tag{3.2.3-4}$$

where

$C_{animal,i}$ = concentration of radionuclide i in the animal product (Bq L^{-1} for milk or Bq kg^{-1} for meat),

$F_{animal,i}$ = fraction of the animal's daily intake of radionuclide i that transfers to the milk (d L^{-1}) or meat (d kg^{-1}),

Q_f = feed (kg d^{-1}) consumed by the animal,

$C_{forage,i}$ = concentration of radionuclide i in forage (Bq kg^{-1}) and water (Bq L^{-1}), respectively, that are consumed by the animal; computed with Eqs. (3.2.3-1) and (3.2.3-2),

$\Delta_{animal,i}(t_h)$ = radioactivity depletion factor corresponding to holdup time t_h (d) between milking or slaughter and consumption of the product.

The radioactivity depletion factors $\Delta_{veg,i}(t_h)$ and $\Delta_{animal,i}(t_h)$ take into account the decay chain kinetics for the parent and daughter radionuclides, according to the following scheme:

$$\Delta_1(t) = e^{-\lambda_{R,i} t}$$

$$\Delta_2(t) = e^{-\lambda_{R,2} t} + \frac{\lambda_{R,2}}{\lambda_{R,1} - \lambda_{R,2}}\left(e^{-\lambda_{R,2} t} - e^{-\lambda_{R,1}}\right) \tag{3.2.3-5}$$

where $\lambda_{R,i}$ denotes the radioactive decay rate (d^{-1}) for parent (i = 1) and daughter (i = 2) radionuclides.

The values of the parameters introduced with Eqs. (3.2.3-1)–(3.2.3-5) are shown in Tables 5.1 and 5.2 of NCRP (1996). Tables 3-4 and 3-5 of this report present the relevant values for the Hanford assessment. Table 3-4 gives element-independent parameters; Table 3-5 presents element-dependent parameters for those radioelements included in the data base for this assessment.

Table 3-4. Element-Independent Parameters for Local Crops and Animal Products [a]

Parameter		Footnote	Units	Vegetables	Milk	Beef
V_d	Deposition velocity	b	m d^{-1}	1000	1000	1000
f/Y	Interception fraction /harvest biomass		m^2 kg^{-1}	0.12	2.1	2.1
t_w	Weathering half-life		d	14	14	14
t_e	Exposure time in growing season		d	60	30	30
t_h	Holdup time between production and consumption		d	1	2	7
λ_{HL}	Soil removal coefficient	c	d^{-1}	2.70×10^{-5}	2.70×10^{-5}	2.70×10^{-5}
t_b	Buildup time in soil	d	d	11,000	11,000	11,000
P	Soil mass in root zone		kg m^{-2}	225	225	225
Q_{mf}	Feed for milk cow		kg d^{-1} dry	—	16	—
Q_{ff}	Feed for beef cow		kg d^{-1} dry	—	—	12
F_{ir}	Irrigation rate	e	m d^{-1}	0.002	0.002	0.002

[a] Based on Table 5.1 of NCRP 1996.
[b] Deposition velocity for noble gases is assumed to be zero.
[c] Represents 70-year removal half-time resulting from harvesting and leaching.
[d] Represents 30-year buildup in soil root zone (RAC modified this to 12 years; see text).
[e] 5 L m^{-2} d^{-1} for 150 days per year.

Table 3-5. Element Dependent Transfer Factors for Vegetables, Forage, Milk, and Meat [a]

Element	Fresh vegetables [b]	Dry forage [c]	Milk (d L^{-1})	Beef (d kg^{-1})
Ba	0.01	0.1	0.0005	0.0002
Ce	0.0002	0.1	3×10^{-5}	2×10^{-5}
Cs	0.2	1	0.01	0.05
I	0.02	0.1	0.01	0.04
Nb	0.01	0.1	2×10^{-6}	3×10^{-7}
Pr	0.002	0.1	6×10^{-5}	0.002
Pu	0.001	0.1	1×10^{-6}	0.0001
Rh	0.03	0.2	0.0005	0.002
Ru	0.03	0.2	2×10^{-5}	0.002
Sr	0.3	4	0.002	0.01
Y	0.002	0.1	6×10^{-5}	0.002
Zr	0.001	0.1	6×10^{-7}	1×10^{-6}

[a] Extracted from NCRP1996.
[b] Minimum set at 0.001 to allow for soil ingestion from unwashed vegetables.
[c] Minimum set at 0.1 to account for soil intake by animals.

Consumption rates of 200 kg vegetables yr^{-1}, 100 kg meat yr^{-1}, 300 L milk yr^{-1}, and 365 g soil yr^{-1} are from NCRP (1996).

3.2.4 Uncertainties

At the present stage of this assessment, estimates of dose are calculated deterministically with deliberate overbiasing to provide conservative overestimates. This approach complies with the requests of the Task Order. In general, probability distributions of dose related to parametric uncertainties have not been calculated, except in the estimation of radionuclide releases (Section 2.4). Should such uncertainty distributions of estimated dose be required in the future, Appendix D describes stochastic methods that can be applied retroactively to the output from HCalc to give probability distributions that reflect uncertainties in the releases and atmospheric transport of radionuclides. These distributions will be affected by the overbiased estimates of air concentration used to calculate them, but the effect is that their application would be conservative. For example, if the methods of Appendix D were used to estimate the 95th percentile of a dose, one would expect the probability that the "true" value exceeds this percentile to be less than 5%.

Examples of conservative overbiasing in the deterministic calculations are

(1) neglecting plume rise at the point of release of radionuclides to the atmosphere; this leads to increased estimates of radionuclides in the air and consequently increased deposition on vegetation and soil
(2) neglecting plume depletion caused by wet and dry deposition of airborne radionuclides; this increases estimates of air concentration and deposition
(3) collecting deposited radionuclides in a shallow surface soil layer (5 cm) and neglecting removal by leaching; this predicts higher concentrations of radioactivity in resuspended soil and increases external dose from radioactivity in the soil and from air submersion in the resuspended component (this approach is applied only when the ingestion pathways for local produce and animal products are absent)
(4) assuming a 12-year buildup of radioactivity in the root zone of soil supporting food and forage crops; this period corresponds to the temporal scope of the assessment (the default buildup period of NCRP 1996 is 30 years) and simulates initial levels in the soil commensurate with a fictitious 12-year prior release.

Generic predictions of atmospheric dispersion from a point source using a Gaussian plume model are inherently uncertain when they are applied to specific time intervals and locations. Miller and Hively (1987) give persuasive indications that predictions of annually-averaged air concentrations may be in error by factors of 2 to 10, depending on the distance from the source, the terrain, and the regional meteorology. Should the more pessimistic error apply to this assessment, in the form of an underprediction, it is possible even with overbiasing of the kind reported above that some underestimation of dose could occur. In general, we expect that estimates of dose computed by the deterministic methodology, given the parameters that determine each specific scenario, are higher than actual doses would be for real individuals under the specified conditions of exposure, although this expectation is not generally provable. However, if the stochastic methods of Appendix D are applied to the HCalc estimates of air concentration, the uncertainty for Gaussian plume transport predictions given by Miller and Hively (1987) is taken fully into account as a source of uncertainty and, for example, would be a component in the estimate of the 95th percentile of a calculated dose.

3.3 Supporting Information

3.3.1 Meteorological Data

The meteorological data embedded in the calculation tool are based on continuous monitoring at the Hanford Site during the period 1955–1980. The data were published as joint frequency tables for the atmospheric stability groups: unstable, neutral, stable, and very stable (Stone et al. 1983, Table 50). The tabulated frequencies correspond to the fractions f_{ij} in Equation (6), where i refers to one of 16 wind-direction sectors and j refers to one of the four stability classes that the tabulation provides. We used the value of vertical diffusion coefficient σ_z for Pasquill-Gifford stability class B to correspond to the unstable frequencies in the tabulation (B is thus a surrogate for classes A, B, and C). The tabulated frequencies are also broken down according to six discrete wind speeds, each representing an interval. These wind speeds, converted from the recorded miles per hour to m s^{-1}, are 0.9, 2.7, 4.7, 7.2, 9.6, and 10.7. The last value is based on a greater-than category, but its frequencies are sufficiently small that quibbles about what the best representative value might be can be ignored without fear of significant bias.

The joint frequency tables were based on readings taken at a 60-m instrumentation height, with stabilities based on the temperature gradient between ground level and 60 m. The computer program adjusts the wind speeds to release height for calculating diffusion as a function of plume travel; for deposition calculations, the program adjusts the wind speeds to a 1-m reference height. The profile model used for the adjustments is a simplified power-function version given by Hanna et al. (1982).

3.3.2 Dosimetric Factors

In calculating estimates of equivalent dose to the body organs of exposed individuals on and near the Hanford Site, we have considered several modes of exposure. Dose from radionuclides taken into the body by inhalation of airborne material and ingestion of contaminated soil and foodstuffs constitutes internal dose. Dose coefficients for these two modes have been tabulated by the International Commission on Radiological Protection (ICRP) in the ICRP Database of Dose Coefficients, Workers and Members of the Public, Version 1.0 (distributed by Elsevier Science Ltd). This collection is an extension of ICRP Publications 68 and 72 (ICRP 1994 and ICRP 1996). The dose coefficients for inhalation and ingestion are presented in units of Sv Bq^{-1} (sieverts to the target organ per becquerel of radioactivity taken into the body by inhalation or ingestion). Each dose coefficient is specific to the radionuclide and the target organ. The dose to an organ from inhalation of a radionuclide is the product of the inhalation dose coefficient for the organ and radionuclide, the subject's breathing rate (m^3 s^{-1}), and the time-integrated concentration of the radionuclide in air at the subject's location (Bq s m^{-3}), where the integration is taken over the period of exposure. The dose to an organ from ingestion of a radionuclide is the product of the ingestion dose coefficient for the organ and radionuclide and the subject's cumulative intake of the radionuclide (Bq). The intake is the time integral of the product of the subject's consumption rate of contaminated food (kg per unit time) and the concentration of the radionuclide's radioactivity in the food (Bq kg^{-1}).

Dose from beta and (principally) gamma radiation from airborne radionuclides (air submersion) and from exposure to radioactively contaminated surface soil are the modes of external dose considered here. Dosimetric data for these external exposure modes are given by

Eckerman and Ryman (1993) in Federal Guidance Report No. 12. For both modes, the dose rate conversion factors are presented in units of Sv s^{-1} per Bq m^{-3}. In the case of exposure to contaminated ground, the factors correspond to radioactivity in the top 5 cm of the soil. Each dose rate factor is specific to the radionuclide and the target organ. The dose to an organ from external exposure to an airborne radionuclide is the product of the air submersion dose rate factor for the organ and radionuclide (Sv s^{-1} (Bq m^{-3})$^{-1}$) and the time-integrated concentration of the radionuclide in air at the subject's location (Bq s m^{-3}), where the integration is taken over the period of exposure. The dose to an organ from external exposure to a radionuclide in the top 5 cm of soil is the product of the soil exposure dose rate factor for the organ and radionuclide (Sv s^{-1} (Bq $m^{-3)-1}$) and the time-integrated concentration of the radionuclide in the soil layer at the subject's location, where the integration is taken over the period of exposure.

Highly-contaminated (usually relatively large) individual particles that come into prolonged contact with the skin, or that enter the eye or ear, or that might be ingested or inhaled define a special category of exposure modes that are of interest for the Hanford Site. We refer to these modes collectively as hot particle exposures. Dosimetric information and discussion of so-called deterministic (non-malignant) symptoms that occur soon after exposure are taken from Report No. 130 of the National Council on Radiation Protection and Measurements (NCRP) (NCRP 1999). Further discussion of hot particle methods is given in Sections 3.6 and 5.2.

We note that doses to specific organs given in this report are absorbed dose, with units of gray (Gy). These doses exclude the alpha modifying factor of 20, which occurs only for plutonium among the radionuclides considered here. For ^{239}Pu, absorbed dose in Gy ≈ equivalent dose in Sv divided by 20. Effective dose is presented in Sv; this tissue-risk-weighted measure would be undefined for absorbed dose.

3.4 Description of the Hanford Calculator

The Hanford Calculator (Hcalc) is a computer program designed specifically for estimating dose from radionuclides released to the atmosphere from the Hanford Site. It is less elaborate than general purpose dose or risk estimation programs for radionuclides or chemicals. It contains a limited data base of radionuclides that were selected by screening methods specific to the Hanford Site, and by making some conservative approximations, it avoids extra options and code. It is not provided with a graphic user interface, although it could be fitted with one. It can be compiled and executed in Unix or Windows environments, and it is easily adapted to being executed under the control of script programs (written in Unix shell languages or higher level scripting languages, such as Perl or Python). Appropriate scripts can be developed to introduce Monte Carlo calculations for estimating uncertainty in results that propagate from uncertainties in the source term or in certain parameters. However, many parameters, such as those taken from NCRP (1996), are internal to the program and cannot be replaced by uncertainty distributions.

3.4.1 User's Manual

Hcalc is primarily controlled by a user-prepared ASCII input (.dat) file, which specifies the exposure scenario for an individual on or near the Hanford Site. The program writes its results to an output file (.prt or .out), which is also ASCII and which may be printed, inspected in a text editor, imported into a spreadsheet, or read by a script program. The extensions .dat, .prt, and .out are merely suggestive; the files can be given any names that the operating system permits.

Hcalc is executed from the command line as follows:

```
>hcalc sample.dat sample.prt
```

where ">" indicates the prompt. The file sample.dat is the following (comment lines, starting with "#" can also be used for documentation):

```
# Scenario definition file for the Hanford Calculator (command line
# version). The # symbol introduces a comment. Lines beginning with this
# symbol are ignored by the program. Blank lines are also ignored.
# Separators may be tabs or spaces.

# Keywords are indicated in boldface in this example
# (but the user need not try to indicate boldface).
# Keywords are generally necessary in the indicated order; exceptions are
# the four ingestion specifiers, Vegetables, Meat, Milk, Soil, which may
# be omitted individually or collectively if they are not applicable.

# Begin scenarios (receptors) here. "New_scenario" starts each scenario and
# ends the previous one (except for the first). This example shows only
# one scenario.

# "Title" is required, followed by characters to identify the scenario.

#-----------
New_scenario
#-----------

Title Offsite home east of reactors

# Receptor location (WSP coordinates in meters)
#           East    North
#           ------  ------
Location    591800  146300

# Exposure duration
Duration    Jan 1945    Feb 1956

# Breathing rate (m^3 day^(-1))
Breathing_rate  23

# Hours per day spent outdoors at location
# Note: times outdoors and indoors may add to less than 24 hours, as they
# normally would if the individual spends part of the day
# at an unexposed location.
Outdoors    8
# Hours per day spent indoors at location
Indoors 16

# Contaminated diet (may be omitted if not applicable)
# kg/year for vegetables and meat, and ingested soil, and L/year for milk
Vegetables  200 # kg/y
Meat    100 # kg/y
Milk    300 # L/y
Soil    365 # g/y
```

```
End_scenario

End_file
```

The Hcalc output file corresponding to the input file shown above is too large to exhibit in a single table in this report. Instead, we will extract some individual parts for discussion. The output file begins with names and values of several environmental parameters that can be set by the user in an auxiliary file, hcalc.env. Following this tabulation is a list of the radionuclides released from the plants.

Next is a list of release sources with name, radionuclide, and Washington State Plane coordinates. Here are the first few lines of the table:

```
Table of sources, radionuclides, and coordinates
-------------------------------------------------------
Source ID      Nuclide   Easting (m)    Northing (m)
-------------------------------------------------------
B-Plant        Sr-90     573576         136383
B-Plant        Y-90      573576         136383
B-Plant        Ru-103    573576         136383
B-Plant        Rh-103m   573576         136383
B-Plant        Ru-106    573576         136383
B-Plant        Rh-106    573576         136383
```

Notice that each of these lines has the same name (B-Plant) and location, but a different radionuclide. Each source is specified in its own data file, and the file contains data for a single name, location, and radionuclide. Each line in this file corresponds to a single source data file, or four files in all. Farther down in the table, we find lines for the same radionuclides but a different plant:

```
T-Plant        Sr-90     567696         136877
T-Plant        Y-90      567696         136877
T-Plant        Ru-103    567696         136877
T-Plant        Rh-103m   567696         136877
T-Plant        Ru-106    567696         136877
T-Plant        Rh-106    567696         136877
```

These lines correspond to four more source data files for T-plant. The same radionuclides happen to be released from both plants (though not necessarily in the same amounts). The complete table shows which radionuclides are released from which locations.

The next information in the file is shown in the following display:

```
Scenario #1:
Offsite home east of reactors

Washington State Plane coordinates (meters):
East 591800, North 146300

Source-to-receptor distances (m) and directions (deg)
-----------------------------------------------------------------------
Source              Distance  Direction (deg)  Wind direction
```

```
-----------------------------------------------------------------
B-Plant             20748     61               WSW
T-Plant             25880     69               WSW
REDOX               27194     63               WSW
PUREX               19797     57               WSW
Z-Plant             27494     67               WSW
Reactor-B           26578     86               W
Reactor-C           26537     85               W
Reactor-D           18789     106              WNW
Reactor-DR          18706     105              WNW
Reactor-F           11483     97               W
Reactor-H           15406     114              WNW
Reactor-KE          22573     91               W
Reactor-KW          23113     90               W
-----------------------------------------------------------------
Exposure duration: from Jan 45 through Feb 56

Breathing rate: 23 m^3 day^(-1)
Hours per day in location and outdoors: 8

Hours per day in location and indoors: 16

Vegetable consumption: 200 kilograms per year
Meat consumption: 100 kilograms per year
Milk consumption: 300 liters per year
Soil ingestion: 365 grams per year
```

Most of these entries are echoes of data from the .dat file. The table provides information about the location of the exposed individual (the receptor) relative to the release sources. The angle represents an angle measured clockwise from north about the source location, for example 61º from B-Plant to the receptor. The receptor is downwind from the source when the wind blows *from* the WSW direction. But note that the receptor is located ENE from B-Plant.

The next table in the Hcalc output file is too long to be shown here in its entirety. But its features can be illustrated with the first few lines, which are given below:

```
Table of chi/Q and deposition/Q for scenario
-------------------------------------------
Source ID      Nuclide   s m^(-3)  m^(-2)
-------------------------------------------
B-Plant        Sr-90     6.306E-08 1.24E-11
               Y-90      2.435E-09 1.053E-13
B-Plant        Y-90      6.062E-08 1.194E-11
B-Plant        Ru-103    6.289E-08 1.237E-11
               Rh-103m   4.966E-08 2.301E-12
B-Plant        Rh-103m   1.312E-08 2.861E-12
B-Plant        Ru-106    6.304E-08 1.239E-11
               Rh-106    6.304E-08 3.122E-12
B-Plant        Rh-106    3.158E-29 9.699E-33
```

The tabulated quantities, chi/Q and deposition/Q, are, respectively, radionuclide outdoor air concentration and deposition rate, each normalized to the release rate Q of the radionuclide (with an exception that will be explained). These quantities take into account radioactive decay as the

material moves from the source to the receptor location; they also reflect material loss from the plume if the plume depletion option has been requested. Thus, in the first line of the table, if we assume a release rate for ^{90}Sr from B-plant of Q = 1 Bq s^{-1}, the outdoor air concentration at the receptor location is 6.31×10^{-8} Bq m^{-3}, and the deposition rate is 1.24×10^{-11} Bq m^{-2} s^{-1}.

The exception mentioned above is illustrated by the second line, which does not repeat the name of the plant. This indicates that the ^{90}Y is a decay product of the ^{90}Sr, and this requires a different interpretation of chi/Q and deposition/Q. In this case, each quantity is normalized to the release of the parent radionuclide, ^{90}Sr, and these quantities refer only to the amount of ^{90}Y that forms from the decay of ^{90}Sr *during plume travel*. For example, if the release rate for ^{90}Sr from B-plant is again Q = 1 Bq s^{-1}, the outdoor air concentration of ^{90}Y that formed during plume travel from the source to the receptor is 2.44×10^{-9} Bq m^{-3}, and the deposition rate of that component is 1.05×10^{-13} Bq m^{-2} s^{-1}.

Notice that in the third line of the table, we have another entry for ^{90}Y. This component represents the amount of the decay product that was assumed to be in equilibrium with the ^{90}Sr at the point of release. Thus we have included a separate source for this radionuclide that was released at the same rate as the parent. Notice that the sum of this component and the amount that formed during plume travel ($2.44 \times 10^{-9} + 6.06 \times 10^{-8} = 6.30 \times 10^{-8}$ Bq m^{-3}) is approximately the amount of the parent radionuclide, as it should be if the equilibrium is preserved during plume travel.

The same relationships exist with the chains ^{103}Ru$\rightarrow^{103m}$Rh and ^{106}Ru$\rightarrow^{106}$Rh as shown. Notice that in the last three lines of the table, the component of the decay product ^{106}Rh that formed during plume travel is the same as the parent ^{106}Ru, to the numeric precision shown, and the released component of ^{106}Rh, assumed to be in equilibrium with the parent at the point of release, has decayed to a value many orders of magnitude less than the parent. Rhodium-106 has a half-life of 29.92 s, and thus it quickly approaches secular equilibrium with the parent ^{106}Ru during plume travel, and the released component rapidly decays away.

The next output group begins as follows:

```
Duration of exposure for the scenario: 3.52152E+08 s (134 months)

Exposure matrix for the scenario
```

Time-integrated radionuclide concentrations

Radionuclide	Primary air (Bq s m^(-3))	Resuspended Air (Bq s m^(-3))	Surface soil (Bq s m^(-2))	Fresh vegetables (Bq s kg^(-1))	Milk (Bq s L^(-1))	Meat (Bq s kg^(-1))
Sr-90	6.66E+04	5.26	2.63E+09	5.46E+03	1.29E+07	6.43E+07
Y-90	6.66E+04	0.00852	4.26E+06	80.2	958	8.22E+03
Ru-103	4.01E+06	7.88	3.94E+09	6.74E+04	1.73E+06	1.59E+08
Rh-103m	4E+06	0.00296	1.48E+06	5.61E+04	5.61E+04	5.61E+04
Ru-106	1.15E+06	17.7	8.87E+09	3.02E+04	7.37E+05	7.3E+07
Rh-106	1.15E+06	4.91E-06	2.45E+03	3.02E+04	3.02E+04	3.02E+04

The exposure matrix presents time-integrated concentrations of the indicated radionuclides in air and surface soil. For food products, the quantities represent cumulative intake of radionuclides per unit intake rate (kilogram or liter per second) of the food product. The entries for inhalation (primary air and resuspended air) reflect the breathing rate and attenuation of exposure as a result of time spent indoors.

Dose presentation begins with a table of effective dose estimates, broken down by radionuclide and exposure pathway:

```
Table of committed EFFECTIVE dose (Sv)
```

		Ingestion:		External exposure:	
Radionuclide	Inhalation	Food	Soil	Air	Ground
Sr-90	5.11E-07	9.14E-06	1.7E-08	3.34E-13	1.03E-10
Y-90	1.99E-08	9.64E-11	2.66E-12	8.44E-12	4.72E-12
Ru-103	2.05E-06	3.79E-07	6.66E-10	6.01E-08	4.52E-07
Rh-103m	2.13E-09	4.05E-12	1.3E-15	2.15E-11	2.57E-14
Ru-106	6.89E-06	1.67E-06	1.44E-08	0	0
Rh-106	0	0	0	8.01E-09	1.29E-13

The term "committed" means that the dose rate is integrated from the time of exposure over a period of 50 years; this integration is implicit in the ICRP effective dose coefficients. The entries in the table also represent integration over the period of exposure (134 months in this example), and they take into account the varying levels of exposure during this period.

The zeros for ^{106}Ru in the external exposure columns indicate that this radionuclide is not a gamma emitter, and that external radiation is considered negligible. For ^{106}Rh, however, the zeros are in the inhalation and ingestion columns. Strictly speaking, these columns should contain very small nonzero entries, but the ICRP data base provides no dose coefficients for ^{106}Rh for these exposure modes. With a half-life of about 30 s, very little of the ^{106}Rh in the ambient air would survive the processes of uptake and translocation in the body, whereas the ^{106}Ru taken into the body would rapidly produce an amount of ^{106}Rh corresponding to secular equilibrium of the two radionuclides. Thus, the dose entries for ^{106}Ru (which were computed to include the amount of the daughter that formed within the body) adequately account for ^{106}Rh.

Effective dose is a measure of radiation energy absorbed by all of the body's organs, with the component for each organ weighted by a factor proportional to an estimate of fatal radiogenic cancer risk for irradiation of that organ. Committed absorbed dose (units: gray or Gy) for individual organs and tissues is also tabulated in the output. For effective and equivalent dose, a modifying factor assigns greater weight (a factor of 20) to alpha emissions. This factor is omitted in absorbed dose. For the radionuclides considered in this report, only ^{239}Pu is an alpha emitter and would thus be affected by the distinction. For the other radionuclides, Sv and Gy would be numerically equivalent. The following excerpt from the table of committed absorbed dose to organs omits all columns after the one for ^{106}Rh. If all columns were present, the last one would be a column of totals.

Table of organ absorbed dose (Gy) for each radionuclide

Organ	Sr-90	Y-90	Ru-103	Rh-103m	Ru-106	Rh-106
Adrenals	2.2E-07	6.3E-11	8.4E-07	1.9E-11	1.1E-06	7.4E-09
Bladder Wall	5.0E-07	2.5E-10	7.1E-07	3.1E-11	1.2E-06	7.4E-09
Bone Surface	1.4E-04	1.4E-09	1.0E-06	5.8E-11	1.0E-06	1.3E-08
Brain	2.2E-07	6.3E-11	5.8E-07	1.8E-11	9.8E-07	7.4E-09
Breast	2.2E-07	6.6E-11	8.8E-07	6.7E-11	1.1E-06	8.9E-09
Oesophagus	2.2E-07	6.3E-11	8.7E-07	1.8E-11	1.1E-06	7.4E-09
St Wall	3.0E-07	3.0E-09	8.7E-07	3.4E-09	1.5E-06	7.4E-09
SI Wall	3.7E-07	7.3E-09	1.1E-06	2.2E-09	2.2E-06	7.4E-09
ULI Wall	1.9E-06	3.9E-08	2.4E-06	1.2E-09	8.2E-06	7.4E-09
LLI Wall	7.3E-06	9.1E-08	5.3E-06	2.1E-10	2.2E-05	7.4E-09
Colon	4.3E-06	6.2E-08	3.7E-06	7.9E-10	1.4E-05	7.4E-09
Kidneys	2.2E-07	6.3E-11	7.0E-07	1.8E-11	1.0E-06	7.4E-09
Liver	2.2E-07	1.4E-09	8.0E-07	2.0E-11	1.1E-06	7.4E-09

Muscle	2.2E-07	6.3E-11	7.1E-07	2.2E-11	1.0E-06	7.4E-09
Ovaries	2.2E-07	6.4E-11	1.0E-06	4.7E-11	1.1E-06	7.8E-09
Pancreas	2.2E-07	6.3E-11	8.0E-07	2.3E-11	1.1E-06	7.4E-09
Red Marrow	6.0E-05	1.4E-09	7.8E-07	1.6E-11	1.0E-06	7.5E-09
ET Airways	3.4E-07	1.4E-08	3.4E-06	3.6E-09	2.2E-06	7.4E-09
Lungs	3.2E-06	9.9E-08	1.6E-05	1.4E-08	5.0E-05	7.8E-09
Skin	2.2E-07	3.4E-09	6.3E-07	1.3E-10	9.8E-07	8.4E-08
Spleen	2.2E-07	6.3E-11	7.8E-07	2.0E-11	1.0E-06	7.4E-09
Testes	2.2E-07	6.4E-11	6.6E-07	4.2E-11	1.0E-06	7.8E-09
Thymus	2.2E-07	6.3E-11	8.7E-07	1.8E-11	1.1E-06	7.4E-09
Thyroid	2.2E-07	6.4E-11	6.7E-07	3.1E-11	1.0E-06	7.9E-09
Uterus	2.2E-07	6.3E-11	7.5E-07	2.0E-11	1.0E-06	7.4E-09
Remainder	2.2E-07	2.3E-10	7.1E-07	6.7E-11	1.0E-06	7.4E-09

The “remainder” is not an organ, but rather it consists of all tissues in the body not accounted for by the explicitly tabulated organs.

Although it is not a requirement of the task order, we have included in the program a table of lifetime risk estimates, based on the recent tabulation of factors for a large data base of radionuclides and different exposure pathways in Federal Guidance Report No. 13 (Eckerman et al. 1999). Several lines of this table follow:

Table of mortality risk by exposure pathway

		Ingestion:		External exposure:		
Radionuclide	Inhalation	Food	Soil	Air	Ground	Total
Sr-90	3.76E-08	5.29E-07	9.86E-10	5.51E-14	9.82E-12	5.7E-07
Y-90	2.1E-09	1.41E-11	3.91E-13	6.79E-13	6.59E-13	2.1E-09
Ru-103	1.81E-07	4.41E-08	7.73E-11	3.05E-09	6.25E-08	2.9E-07
Rh-103m	1.75E-10	2.74E-13	8.81E-17	5.79E-13	9.38E-16	1.8E-10
Ru-106	5.95E-07	2.23E-07	1.92E-09	0	0	8.2E-07
Rh-106	0	0	0	4.13E-10	1.85E-14	4.1E-10

Similar remarks to those given previously apply to the zero entries for ^{106}Ru and ^{106}Rh.

This completes our discussion of the output file for this sample calculation.

As it is currently implemented, Hcalc can consider only simple scenarios, with the location and indoor/outdoor parameters referring to the entire period of exposure. However, the program can be executed for multiple input files that are constructed to represent different components of exposure, such as fractions of time spent in different locations on and off the site. The results can then be added to give a composite set of doses. Such multiple runs can be developed into scripts if a large number of calculations are needed for which a uniform pattern can be given. Such extensions are beyond the scope of this report.

The Hcalc program requires some additional files to those already described in order to be executed. The first is a file that must be named `hcalc.env`, and it must be present in the subdirectory that contains the program’s executable module `hcalc.exe`. The following listing shows the version of `hcalc.env` used in the sample calculation:

```
# hcalc.env -- database variables for the Hanford Calculator

# Note: For Windows operating systems, if FILEPATH or METFILE requires
# a path with named directories, use two backslashes where you normally
# would use one (e.g., "\\data\\source\\srclist.dat"). With Unix-type
# systems, use one forward slash (e.g., "/data/source/srclist.dat").

# The variable FILEPATH contains the filename of a list of files that
# define the release sources.
```

```
FILEPATH    srclist.dat

# The variable METFILE names the file with meteorological data
# in the format required for HCALC.
METFILE hanford.met

# The variable Z0 is the roughness length (m) for dry deposition.
# The value .05 m = 5 cm corresponds to uncut grass. The value of Z0
# is roughly one-tenth of the average height of the objects that
# constitute the "roughness."
Z0  .05

# The variable ZI is the height of the mixing layer. The value is
# an annual average for the location.
ZI  1500

UR  SETTING_RURAL

DEPLETE_PLUME   NO

# Parameters for wet deposition. If DEPLETE_PLUME is set to NO,
# these parameters have no effect. PRECIP_MM_PER_H is the average intensity
# of precipitation during periods of measured precipitation.
# PRECIP_H_PER_Y is the average number of hours of
# measurable precipitation per year.
# The figures given were estimated from data in Stone et al.,
# Climatological Summary for the Hanford Area, Rep. PNL-4622 (1983).
PRECIP_MM_PER_H 0.333
PRECIP_H_PER_Y  531

# Parameters for the soil. SURFACE_LAYER_DEPTH must be given in meters
# and represents what is considered resuspendable soil. It also
# affects the estimates of soil ingestion. The BULK_DENSITY parameter
# applies to this layer and is in g cm^(-3). MASS_LOADING_FACTOR
# represents the airborne dust concentration resuspended from soil
# in the near vicinity of the receptor; it is in microgams m^(-3).
# The value given was suggested for generic use
# by Anspaugh, Shinn, Phelps, and Kennedy, Health Physics
# 29: 571-582 (1975).
SURFACE_LAYER_DEPTH 0.05
BULK_DENSITY        1.0
MASS_LOADING_FACTOR 100

# Parameters for building shielding. BLDG_PARTICLE_FRACTION is the fraction
# of airborne particle concentration indoors relative to outdoors.
# BLDG_GAMMA_FRACTION is the fraction of exposure to gamma rays from
# air submersion indoors relative to outdoors.
BLDG_PARTICLE_FRACTION  0.7
BLDG_GAMMA_FRACTION 0.5
```

As with the other input files, "#" indicates a comment (the line is ignored). The file `hcalc.env` sets values of specific "environment" variables for Hcalc. The names of the variables must be

exactly as shown (all capital letters, with the underline character "_" joining words). The value is separated from the name of the variable with one or more spaces or tabs. The comments in the file explain the entries. Notice that two more files are pointed to from within `hcalc.env`: first is `srclist.dat` and second is `hanford.met`. These latter two files, unlike hcalc.env, may have any names that conform to operating system conventions (the names given in `hcalc.env` must be the same as the actual names in the operating system directory). If the files are not in the same directory as the executable module, path strings may be indicated, but note the coventions about slash ("/") and backslash ("\") characters noted in the comments.

The file `srclist.dat` points to the numerous files that contain the source term, that is, the release history of each radionuclide from each location. These files also contain information about release height and particle size distribution. The following display shows `srclist.dat` as it was for the sample calculation:

```
srcdat\\sr90b.txt
srcdat\\y90b.txt
srcdat\\ru103b.txt
srcdat\\rh103mb.txt
srcdat\\ru106b.txt
srcdat\\rh106b.txt
srcdat\\i131b.txt
srcdat\\xe131mb.txt
srcdat\\cs137b.txt
srcdat\\ba137mb.txt
srcdat\\ce144b.txt
srcdat\\pr144b.txt
srcdat\\pu239b.txt
srcdat\\sr90t.txt
srcdat\\y90t.txt
srcdat\\ru103t.txt
srcdat\\rh103mt.txt
srcdat\\ru106t.txt
srcdat\\rh106t.txt
srcdat\\i131t.txt
srcdat\\xe131mt.txt
srcdat\\cs137t.txt
srcdat\\ba137mt.txt
srcdat\\ce144t.txt
srcdat\\pr144t.txt
srcdat\\pu239t.txt
srcdat\\sr90x.txt
srcdat\\y90x.txt
srcdat\\ru103x.txt
srcdat\\rh103mx.txt
srcdat\\ru106x.txt
srcdat\\rh106x.txt
srcdat\\i131x.txt
srcdat\\xe131mx.txt
srcdat\\cs137x.txt
srcdat\\ba137mx.txt
srcdat\\ce144x.txt
srcdat\\pr144x.txt
```

```
srcdat\\pu239x.txt
srcdat\\sr90p.txt
srcdat\\y90p.txt
srcdat\\ru103p.txt
srcdat\\rh103mp.txt
srcdat\\ru106p.txt
srcdat\\rh106p.txt
srcdat\\i131p.txt
srcdat\\xe131mp.txt
srcdat\\cs137p.txt
srcdat\\ba137mp.txt
srcdat\\ce144p.txt
srcdat\\pr144p.txt
srcdat\\pu239p.txt
srcdat\\pu239z.txt
srcdat\\ar41rb.txt
srcdat\\ar41rc.txt
srcdat\\ar41rd.txt
srcdat\\ar41rdr.txt
srcdat\\ar41rf.txt
srcdat\\ar41rh.txt
srcdat\\ar41rke.txt
srcdat\\ar41rkw.txt
```

All source term files are contained in the subdirectory `srcdat`, which is immediately below the subdirectory containing the executable module. Note that under Windows, the double backslash is necessary. In naming the files, we have adopted the scheme of using the element name and mass number (followed possibly by "m" for metastable, in the case of ^{103m}Rh, ^{131m}Xe, and ^{137m}Ba), followed by one or more characters indicating the plant releasing the material (the same radionuclide may be released by more than one plant). The codes are the following:

b	B-Plant
t	T-Plant
x	REDOX
p	PUREX
z	Z-Plant
rb	Reactor B
rc	Reactor C
rd	Reactor D
rdr	Reactor DR
rh	Reactor H
rke	Reactor KE
rkw	Reactor KW

This scheme is quite arbitrary, and these meanings are unknown to the program. It is information in each individual file that informs Hcalc of the name and location of the facility and which radionuclide data the file contains. And each line in srclist.dat tells the program where to find the corresponding source term file. At present, there is a limit of 100 source term files (we are using 61).

We show part of the source term file `.\srcdat\sr90b.txt` (the dot indicates the subdirectory containing the executable module):

```
B-Plant
Sr-90
573576
136383
61
1
4
11/44   0   0
12/44   0   0
1/45    0   0
2/45    0   0
3/45    0   0
4/45    8.6E-02 6.1E-01
5/45    2.5E-01 1.8E+00
6/45    2.2E-01 1.5E+00
```

The first seven lines of a source term file must be in the order indicated. The name "B-Plant" in the first line indicates the name of the plant. It should be shown exactly the same in all files for this plant (including capitalization and presence or absence of the hyphen), because the program groups the plants on the basis of this name. If some are written differently, the output will show a larger number of plants than there really are, corresponding to the number of spelling variants (although the calculated doses will still be correct). In the second line, the name of the radionuclide must be as shown, including capitalization and hyphen. A mistake here will terminate the run if the name is not recognized. The third and fourth lines give the easting and northing coordinates, respectively, of the point of release, in the Washington State Plane (WSP) system (m). The coordinates should be the same for files with the same plant name. If multiple points of release at a given plant are to be considered, variant names should be used to distinguish releases from different locations (this has not been done in the sample calculation). The fifth line gives the release height, for which we use the physical stack height, 61 m. Lines six and seven contain the geometric mean (1 μm) and geometric standard deviation (4), respectively, of the particle size distribution. These parameters are used in the calculation of dry deposition for particulate radionuclides. The program does not use these parameters for noble gases (Ar and Xe) that occur in the source term.

Beyond the seven preliminary lines just discussed are the release entries for the months when the release operated (only eight lines are shown). The date is indicated by the month/year abbreviation. The remaining two numbers per line in this file are, from left to right, the monthly median (50th percentile) and 95th percentile. Only the number in the second column — whatever its interpretation — is read by the program and used as the release. Although the data in the third column are not read by the program, this is a convenient way of storing the additional information. If one were to perform a short-term calculation, using only the 95th percentiles, a new file would have to be prepared with 95th percentiles in the second column (rather than the third).

Note that the lines with zero entries could have been omitted. Similarly, if a line is included with a date outside of the assessment's temporal scope (Oct-45 through Dec-61), the program

ignores it. The lines beyond the first seven are not required to be in temporal order, but we recommend preparing the files that way.

We return finally to the file `hanford.met`, which contains the joint frequency table (JFT) used in the sample calculation and for the assessment generally (Section 3.3.1). The file is as follows:

```
6       // nwsp -- number of windspeed categories
0.894   // windspeed of class 1 (m/s)
2.682   // windspeed of class 2 (m/s)
4.6935  // windspeed of class 3 (m/s)
7.152   // windspeed of class 4 (m/s)
9.6105  // windspeed of class 5 (m/s)
10.728  // windspeed of class 6 (m/s)
61      // height at which windspeed was measured (m)
6       // nstab -- number of stability categories
16      // ndir -- number of directional sectors
A       0             // Relative frequency of Class A stability
N       0             0             0             0             0
NNE     0             0             0             0             0

[ Zeros for all directions NE through WNW ]

NW      0             0             0             0             0
NNW     0             0             0             0             0
TOTAL   0             0             0             0             0
B       0.3125        // Relative frequency of Class B stability
N       0.0205        0.04188       0.01568       0.00448       0.00096       0.00032
NNE     0.01986       0.03292       0.01568       0.008         0.00224       0.00064
NE      0.02178       0.02876       0.00992       0.00416       0.0016        0.00096
ENE     0.01378       0.01948       0.00416       0.00128       0.00032       0.00032
E       0.01474       0.02108       0.00384       0.00064       0             0
ESE     0.01218       0.01916       0.0032        0.00032       0             0
SE      0.0109        0.02172       0.0048        0.00064       0             0
SSE     0.00578       0.01308       0.00384       0.00128       0.00032       0
S       0.00674       0.01532       0.00512       0.00192       0.00064       0.00032
SSW     0.00514       0.01436       0.00992       0.00608       0.0032        0.00256
SW      0.00642       0.01628       0.01728       0.01664       0.00992       0.01184
WSW     0.00514       0.0134        0.01792       0.02176       0.0128        0.01024
W       0.00642       0.01372       0.01184       0.01056       0.00416       0.00288
WNW     0.00674       0.01692       0.0192        0.01984       0.01056       0.0064
NW      0.00994       0.03516       0.0448        0.03136       0.0192        0.01472
NNW     0.01378       0.03836       0.01984       0.00416       0.00096       0.00032
TOTAL   0.17984       0.3616        0.20704       0.13312       0.06688       0.05152
C       0             // Relative frequency of Class C stability
N       0             0             0             0             0             0
NNE     0             0             0             0             0             0

[ Zeros for all directions NE through WNW ]

NW      0             0             0             0             0             0
NNW     0             0             0             0             0             0
TOTAL   0             0             0             0             0             0
```

```
D       0.13          // Relative frequency of Class D stability
N       0.030961538   0.013894231   0.005384615   0.003846154   0.002307692   0.000769231
NNE     0.023269231   0.008509615   0.003846154   0.004615385   0.001538462   0.000769231
NE      0.024038462   0.009278846   0.003076923   0.001538462   0.000769231   0.000769231
ENE     0.020192308   0.007740385   0.002307692   0.000769231   0             0
E       0.024807692   0.008509615   0.002307692   0.000769231   0             0
ESE     0.026346154   0.013125      0.003076923   0.000769231   0             0
SE      0.031730769   0.017740385   0.005384615   0.001538462   0             0
SSE     0.019423077   0.010048077   0.004615385   0.003076923   0.000769231   0
S       0.014807692   0.006971154   0.003076923   0.003846154   0.002307692   0.001538462
SSW     0.010961538   0.005432692   0.004615385   0.005384615   0.005384615   0.004615385
SW      0.010192308   0.006201923   0.006153846   0.01          0.010769231   0.013076923
WSW     0.010961538   0.007740385   0.01          0.016153846   0.012307692   0.006923077
W       0.015576923   0.012355769   0.011538462   0.011538462   0.004615385   0.002307692
WNW     0.015576923   0.018509615   0.031538462   0.033076923   0.019230769   0.013846154
NW      0.024038462   0.036971154   0.056153846   0.041538462   0.024615385   0.022307692
NNW     0.028653846   0.023894231   0.012307692   0.005384615   0.000769231   0
TOTAL   0.331538462   0.206923077   0.165384615   0.143846154   0.085384615   0.066923077
E       0.3158        // Relative frequency of Class E stability
N       0.010548607   0.01080589    0.00569981    0.003483217   0.000633312   0.000316656
NNE     0.006748733   0.005422736   0.003483217   0.003166561   0.001266624   0.000316656
NE      0.006432077   0.004472768   0.002216593   0.001583281   0.001266624   0.000316656
ENE     0.006432077   0.004156111   0.001266624   0.000633312   0.000316656   0
E       0.007698702   0.005422736   0.002216593   0.000633312   0             0
ESE     0.010231951   0.007006016   0.003166561   0.000633312   0             0
SE      0.013081856   0.011439202   0.006333122   0.001899937   0.000633312   0.000316656
SSE     0.007698702   0.007006016   0.006016466   0.004116529   0.001583281   0.000633312
S       0.007065389   0.006056048   0.004433186   0.004749842   0.003166561   0.002216593
SSW     0.005165453   0.004472768   0.006333122   0.007283091   0.006649778   0.009499683
SW      0.004848797   0.006372704   0.009816339   0.015516149   0.015832806   0.015199493
WSW     0.005798765   0.007322673   0.015199493   0.027232426   0.015832806   0.007283091
W       0.007698702   0.013655795   0.032298923   0.042431919   0.01139962    0.002216593
WNW     0.008332014   0.016189044   0.045915136   0.095946802   0.050348322   0.017732742
NW      0.009915294   0.020938885   0.046548448   0.068714376   0.046548448   0.023749208
NNW     0.009281982   0.015555731   0.013932869   0.007283091   0.001266624   0
TOTAL   0.126979101   0.146295123   0.204876504   0.285307156   0.156744775   0.07979734
F       0.2409        // Relative frequency of Class F stability
N       0.0168379     0.017927563   0.00913242    0.00207555    0             0
NNE     0.011026359   0.008795143   0.00498132    0.00249066    0             0
NE      0.010196139   0.006719593   0.0041511     0.00124533    0             0
ENE     0.008120589   0.005474263   0.00332088    0.00083022    0             0
E       0.010611249   0.007134703   0.00290577    0.00083022    0             0
ESE     0.0126868     0.008795143   0.00290577    0             0             0
SE      0.0168379     0.012946243   0.00456621    0.00124533    0             0
SSE     0.012271689   0.012116023   0.0083022     0.00373599    0.00041511    0
S       0.011856579   0.012531133   0.00539643    0.00124533    0.00041511    0
SSW     0.010196139   0.010040473   0.00456621    0.00166044    0.00041511    0.00041511
SW      0.010611249   0.014606683   0.00996264    0.00373599    0.00083022    0.00041511
WSW     0.011441469   0.020833333   0.02241594    0.00996264    0.00124533    0.00041511
W       0.01766812    0.041173724   0.054379411   0.01867995    0.00124533    0
WNW     0.01517746    0.044494604   0.080946451   0.0498132     0.00290577    0
NW      0.01766812    0.039513284   0.070983811   0.061851391   0.00747198    0
NNW     0.01725301    0.027475093   0.02615193    0.0083022     0             0
```

```
TOTAL   0.210460772   0.290577003   0.315068493   0.167704442   0.01494396    0.00124533
```

This file is shown in its near entirety because of the format and the normalization pattern. The frequencies are normalized to add to 1.0 within each stability category, and the frequency for the category as a whole is given at the beginning of the data for the category. For example, Class F occurs with frequency 0.2409. Given that the category is F, the probability that the wind is from the north and the wind speed is in the lowest group (represented by 0.894 m s^{-1}) is 0.0168. But the relative frequency of that stability, direction, and wind speed in general is $0.2409 \times 0.0168 = 4.047 \times 10^{-3}$.

The source of the frequency data (Stone et al. 1983) presented only a single category for "unstable" air. We have assumed that this category is reasonably represented on average by Pasquill-Gifford Class B, and we have assigned zero frequency to categories A and C.

These data were measured at the approximate release height for all sources considered, and we used the wind speed categories as labeled for calculating the plume distances. But for computing deposition velocities, the wind speed labels were adjusted to a height of 1 m, using a power function suggested by Hanna et al. (1982).

The numbers of digits shown in this listing, beyond about four decimals, have no essential significance. They were introduced by renormalization of the original data in a spreadsheet.

3.4.2 Documentation

The Hcalc program is written in C. Object oriented methods have been used in its preparation to improve the organization, to help avoid programming errors, and to facilitate locating and correcting errors that do occur. Although C does not explicitly support object oriented methods (as does C++), it is suitable for their implementation provided the programming is done in a disciplined and methodical manner.

Fairly extensive comments have been included in most of the source code modules, at points where they are believed to be potentially useful to other programmers who might need to correct or modify the program, or to read it for the purpose of answering a question about how it performs some calculation.

The following list of the source files of Hcalc, together with brief summaries of their contents, should provide a starting place for locating parts of the program where specific data are located or particular calculations are performed.

`hcalc.c` — Contains the main program that scans the command line, reads the input file (the scenario descriptions), and oversees the input and processing of the auxiliary files (hcalc.env, the list of source term files, and the file of meteorological frequencies) and the source term files. It coordinates the calculations by using functions contained in other modules. Finally, it writes the output file.

`env.c` — The function defined in this module is invoked from the main program (in hcalc.c) to input the file `hcalc.env`, process the data that it contains, and place the information in the program's data structures, where it can be accessed by the functions that perform the calculations.

`gp.c` — Provides most of the basic functions that perform the atmospheric diffusion calculations, such as calculating the diffusion coefficients σ_y and σ_z, the vertical component of diffusion (V in Eq. (3.2.1-1)), the reduction factors for plume depletion from wet and dry deposition, the wind speed profile function, and the deposition rate and concentration of each

radionuclide in air at each specified location. Some functions in the file have been used in other applications and are not accessed by Hcalc.

`metdata.c` — Contains the functions that input and process the meteorological frequency file and that make the frequencies available to other modules.

`drydep.c` — Contains the functions and data that estimate coefficients for wet and dry deposition.

`golder.c` — Provides auxiliary functions needed by `drydep.c`, which compute ranges of the Monin-Oboukhov parameter corresponding to each Pasquill-Gifford stability category.

`nuclides.c` — Contains the data base for the radionuclides considered for the Hanford assessment, together with functions that provide access to the data from functions in other modules.

`orgdose.c` — Contains the data base for the ICRP organ dose coefficients for each of the radionuclides in the module `nuclides.c`, together with functions to fetch the coefficients for the use of functions in other modules.

`riskfact.c` — Contains the data base for the lifetime risk factors from Federal Guidance Report No. 13 for each of the radionuclides in the module `nuclides.c`, together with functions that enable other functions (in `hcalc.c`) to access the factors.

`srcterm.c` — Provides data and functions related to reading in the source term and making releases available as a function of the source (plant), the radionuclide, and the month.

`expmat.c` — Contains (1) the constructor function for chi-over-Q objects corresponding to each radionuclide-source-receptor combination and (2) the function that uses the chi-over-Q objects to compute the exposure matrix value for each radionuclide and pathway; it also implements the dynamic model for tracking radionuclide concentrations in the surface soil compartment over time. The exposure matrix function is accessed from the main program (in `hcalc.c`) once for each scenario that is analyzed.

`terra.c` — Contains the data base and functions that implement the terrestrial models of NCRP Report No. 123 (NCRP 1996) for each of the radionuclides in the module `nuclides.c`.

`util.c` — Contains miscellaneous utility functions that are used by functions in various modules. Examples are string comparisons, fatal error messages and warnings, and functions that read and format data from input files.

`spline.c` — Contains functions that implement cubic splines for smooth interpolation.

The modules listed above make use of many files with the `.h` extension that are included by the C preprocessor. All but one of these `.h` files have the same name as a `.c` counterpart and contain prototypes for the functions defined in the corresponding `.c` file. The single exception is the file `defs.h`, which contains definitions of symbolic constants that are used by the preprocessor to set array sizes in several of the modules. At present, there are three such constants: `NMONTH` (the maximum number of months a run can cover, 207, which corresponds to Oct-44 through Dec-61); `MAXSRC` (the maximum number of source objects that an analysis can use, 100); and `MAXNUC` (the maximum number of radionuclides the data base in the module nuclides.c can contain, 30). The constants `NMONTH` and `MAXSRC` affect only the module `hcalc.c`; `MAXNUC` affects `expmat.c`, `hcalc.c`, and `srcterm.c`.

3.5 Description of the SURVEY Spreadsheet

The Hanford Calculator models discussed in Sections 3.2–3.4 are used for routine releases of relatively small particles and gases from facility stacks. As discussed in Section 2, there were two notable periods in Hanford operating history when large radioactive particles were released to the environment. These were large corrosion products released from T and B Plants in 1947-1948 and large flakes of ruthenium released from REDOX in 1952-1954.

Hanford personnel identified the releases of these large particles in the past from environmental surveys and effluent monitoring. Effluent monitoring of stack effluents did not pick up all large particle releases, particularly when stacks or ducts were not monitored or when releases occurred from holdup of radioactivity downstream of the sampler. Back-calculating from environmental measurements would be one way to develop a source term for these large particles. This has been done by Hanford personnel and others to estimate the total activity lost to the environment for some short-term release events.

In fulfilling the scope of work for this task, we have concluded that for persons located onsite, direct use of environmental measurements is a preferable method than source term and dispersion analysis to evaluate exposure to large particles after deposition. We believe this approach is likely to produce results closer to what actually happened.[5] We have developed a spreadsheet tool called SURVEY that takes advantage of available environmental measurements of contamination levels. This is a direct way of estimating the probability of past encounters with large radioactive particles in the Hanford environment.

The SURVEY spreadsheet is implemented within a Microsoft® EXCEL 97 spreadsheet. An uncertainty analysis feature within the spreadsheet [Using Crystal Ball version 4.0c (Decisioneering 1996)] will allow the CDC to test the sensitivity of results to a variety of parameters, which was a requested feature. There is flexibility in defining the conditions of exposure, allowing for refinements based on review by the public, past workers, and others. The number of input parameters and their possible range of values illustrate the difficulty in assessing past exposures under a variety of field conditions at different places and times. We have provided recommended values and ranges for parameters based on our review of the historical documents. The basis for those recommendations is established in the following sections.

Evaluation of the historical documents leads us to the following technical judgements relating to the focus of this work. The most important factors that would have affected past exposures to large radioactive particles in the outdoor environment are

- Where a worker was
- When (s)he worked there
- What the contamination level was
- What (s)he did (how the worker's activity affected transfer of contamination to body)
- Type(s) of protective clothing (e.g. long pants, booties, gloves, face mask, respirator).

[5] The SURVEY spreadsheet tool does not incorporate personnel dosimetry data, which might be the most direct way to assess actual past exposures to specific people. These include medical records (which could document skin burns), results of bioassay samples (which can quantify amounts of radionuclides deposited internally), film badge results (to estimate external radiation exposures), and personnel survey (e.g. hand/foot contamination) logs.

A summary of conclusions about the "where, when, and what" of past contamination levels is presented at the end of the environmental data section (4.3). How those data can be implemented using the SURVEY spreadsheet tool is discussed here.

The large particles released from the Hanford separations plants in the 1940s and 1950s deposited on the ground relatively close to the sources, although some were transported long distances. They were measurable as individual particles by radiation detection instruments; many were visible to the naked eye or could be separated by their physical properties. The most important exposure pathways to people following deposition of large particles on the ground were

- External exposure from radioactivity on ground (i.e., no contact or intake of particle)
- Adherence of particle to skin or clothing, resulting in skin dose
- Suspension of particles on ground into air and inhalation of particle, resulting in dose mainly to upper respiratory and GI tract
- Contamination of hands leading to inadvertent ingestion and dose mainly to GI tract.

The SURVEY spreadsheet tool evaluates all these pathways. Input parameters for the spreadsheet are discussed below.

3.5.1 Input Parameters

Particle Deposition Density. The starting point for evaluation of the probability and effects of exposure to large particles is the deposition density of those particles on the ground or surfaces at two locations, the workplace and the residence. For the examples included with this report, the working location is the more contaminated of the two. Deposition density is the number of particles detected per unit area of ground surface. Section 4.1.6 contains a review of available data. In addition, Appendix C contains 22 maps of monthly surveys of large particle contamination on a site-wide or larger scale in the 1950s. Appendix C also includes 19 maps of contamination measured over smaller areas onsite between November 28, 1947 and November 12, 1957. Numerical values are tabulated from these maps in Tables 4-7 through 4-9 for the military camp H-40, for off-project areas, and near the 200 Areas in the 1940s and 1950s.

A factor is included in the spreadsheet to account for particles not detected by the survey instruments used. A factor of 10-100 increase is suggested by comparison of surveys for large active particles released in the 1940s with more sensitive methods (HW-9141; HW-10941). However, if this were done, then the dose assessment from the particles would need to reflect the inclusion of smaller particles and their activity characteristics. We have not made any adjustments to the measured deposition densities for the example calculations included with this report.

Exposure Locations and Duration. The SURVEY spreadsheet computes exposure at two locations, work and residence. The hours per day at work is an input parameter, and the remainder of the day is computed by the spreadsheet for the residence exposure time.

Another input parameter describing worker activity is the exposure duration (working and non-working days). The SURVEY spreadsheet tool is most appropriate when used to evaluate exposures over relatively short periods of time (days to months). The main reason is that the input parameters (environmental contamination levels) did not remain constant over long periods of time. For example, the fragile flakes of ruthenium released from REDOX fractured easily and weathered into soil. Also, radioactive decay is an important reduction factor for depositions of particles containing Ru-Rh and Ce-Pr. During the peak releases from REDOX, the environmental

surveys of particle deposition density were conducted monthly, so there is adequate time resolution in the data for consideration of specific times of exposure. The possible conservatism in using a long exposure duration as input to the SURVEY spreadsheet should be recognized, particularly if the contamination being described by the survey data either decays or weathers rapidly.

Resuspension of Deposited Large Particles. Resuspension is the process whereby previously deposited radioactivity on ground or other surfaces becomes airborne. Healy (1980) distinguishes three main types of resuspension: wind-driven, mechanical disturbance, and local. The last two are most applicable to assessment of exposure of persons in outdoor contaminated areas on the Hanford Site. For wind resuspension, the energy required to dislodge the particles comes from the wind, which disperses particles downwind where they deposit on surfaces at a rate dependent on their properties and the terrain. In contrast, both mechanical and local resuspension result from mechanical disturbance of the soil other than by wind. Such forces could range from the movement of small animals on the surface, through humans walking, to the movement of heavy equipment or plows across the ground. The distinction Healy makes between local and mechanical resuspension is that the exposed person is in the immediate vicinity of the disturbance for local resuspension, whereas the receptor is downwind for mechanical resuspension.

Three main groups of models for estimating airborne concentrations from deposited radioactivity are the resuspension factor, resuspension rate, and mass loading models. There is no question that typical uncertainties in estimating resuspension by any of the methods are many orders of magnitude. The uncertainty analysis features in the SURVEY spreadsheet allow evaluation of the importance of parameters like those describing resuspension. Although Healy (1980) in principle prefers the resuspension rate approach, he acknowledges that the resuspension factor is useful for describing the exposure of the individual causing the disturbance.

There has been a vast amount of research on resuspension at the Hanford Site. It is not within the scope of this task to review all those studies. The wind-driven resuspension of radionuclides routinely released from the Hanford facilities is treated in our Hanford Calculator model using a mass loading approach and a generic mass loading factor of 100 µg m^{-3} (Anspaugh et al. 1975). For the large particles released in 1947-1948 and 1952-1954, we investigated studies whose results were expressed either as a resuspension factor or a resuspension rate. Because these particles are so large and not uniformly distributed over the area of ground or mass of soil, many of the Hanford field experiments on wind-driven resuspension of small particles (and relatively uniform distribution) are not as relevant.

In fact, when the person is in the contaminated area, wind-driven suspension is much less influential in transferring contamination from the ground than the person's activity (Healy 1977; Sehmel 1980). Consequently, we looked for empirical studies that described the transfer of contamination from surfaces to a person working in the contaminated area. An example of the importance of worker activity on suspension is a study by Jones and Pond (1967), who found that a person walking over a contaminated surface in a laboratory suspended up to 250 times as much plutonium nitrate and up to 2500 times as much plutonium oxide as was suspended when there was no movement. A faster rate of walking produced more suspension. Similar, although less dramatic, increases apply to the outdoor environment.

The most relevant studies we reviewed are described here, to provide a basis for the range of values used to describe local resuspension in the SURVEY spreadsheet. In addition, Table 3-6 summarizes the results of these studies as well as others.

Ground-to-Body Transfer: Schwendiman's Tracer-Particle Study. Although published over forty years ago, a study titled "Probability of Human Contact and Inhalation of Particles" (Schwendiman 1958) persists as extremely relevant to this work. It was conducted in the outdoor environment at Hanford, where the importance of large-particle contamination was all too evident, based on the problems around the separations areas in the 1940s and 1950s. In addition, unlike many other resuspension study publications, the results are expressed as the probability of transfer of a particle from the ground to various areas of the body for different activities. Most other resuspension studies result in an estimate of airborne concentration, but further assumptions are needed to translate airborne concentrations to the number of particles contacting the body. As stated above, body contact is an important consideration for these large, high-activity particles.

The tracer particles used by Schwendiman (1958) to simulate radioactive contamination were fluorescent zinc sulfide. Individual particles could be counted under ultraviolet light and magnification. The mean particle diameter was 2 μm and density was 4.1 g cm^{-3}, resulting in an aerodynamic diameter of about 4 μm. Therefore, they are not as large as many of the active particles released from the Hanford separations plants. Schwendiman acknowledges that the particle size distribution of the ZnS is unlikely to be identical to that of radioactive particulates of interest in a given incident. However, he states,

> Being small, they will become airborne more readily, thereby giving a conservative value for the actual probability of contact expected for somewhat larger, perhaps more typical particles. They will also become attached to inert particles of larger size which could also happen in the case of small radioactive particles. Subsequent movement of the trace particle will be influenced by the carrier or host particle. Although the ZnS chosen for these experiments was not an "identical twin" for actual radioactive particles, the simulation is believed to be adequate for the order of magnitude estimates desired.

The conservative bias noted by Schwendiman is consistent with our scope of work. Two types of experiments were conducted:

1. Determination of the particle inhalation probability during operations involving vehicles.
2. Determination of contact probabilities for operations in open field areas such as walking, digging, etc.

The second of these types will be discussed first. Schwendiman states that these experiments were conducted "to estimate the probability of an individual contacting a particle while working in open terrain contaminated with a known number of particles per unit area." The stated purpose of the study and the fact that it was conducted in the Hanford environment highlight its high relevance to our task.

In the contact probability experiments, an area of 100 ft by 100 ft was roped off in wind-blown sandy soil sparsely covered with typical desert growth. A known amount of the ZnS tracer was mixed with sand and distributed uniformly over the plot. Workers performed various tasks in the seeded area. Each wore a strip of double-backed sticky transparent tape on the back of the hands, on the shoulder, overall cuffs, knees, and across the nose-piece of his respirator. After the exposure period, the number of particles on the tapes was determined microscopically.

The tasks performed were

1. Walking through the plot simulating surveying for contamination,
2. Digging a shallow trench,
3. Loading and unloading boxes on a truck driven into the area.

Results are tabulated in the paper and plotted here in Figure 3-4. The measure of "contact probability" is the ratio of the number of particles per square meter per hour on body to the number of particles per square meter on ground surface. Of the areas of the body studied, the contact probability was highest for the cuffs of pants. Of the activities investigated, the highest transfer occurred from walking through the contaminated area. Perhaps a contributing factor to this outcome was the greater surface area of ground that was covered during the walking tests. Walking also resulted in the greatest transfer to areas higher on the body (e.g., the shoulder). Unloading/loading produced the greatest contamination to hands and nose.

In our example calculations presented in this report, we use Schwendiman's contact probability for walking, with a uniform uncertainty distribution between the minimum and maximum value for the five regions of the body measured (0.0017–0.014). For digging, measured values for the five areas of the body ranged from 0.00054 to 0.005. For loading/unloading, the range was 0.0002 to 0.0046. The contact probability is multiplied by the particle deposition density and the surface area of the body to obtain the number of particles contacting the body per hour of work in the area.

The other type of experiment performed by Schwendiman is not as easily applied to the SURVEY spreadsheet, but it is summarized here. The purpose of those experiments was to evaluate the probability of inhalation of a particle during operations involving vehicles. Several situations were simulated:

1. Sweeping a bus in which particles had accumulated
2. Driving a bus in which particles were under the brake pedal
3. Hand-sweeping a bus where particles were placed under the foot pedals
4. Changing a tire that had particles deposited on it.

The inhalation probabilities were highest for sweeping of the bus—3.3×10^{-4} to 6.4×10^{-4} per hour. For tire replacement, the inhalation probabilities ranged from 6×10^{-6} to 2.8×10^{-5}. Contamination of vehicles and roadways was a big problem during the height of ruthenium releases from REDOX (Baumgartner 1954; Ebright 1954; Helgeson 1954; Mobley 1954). Nearly half of the vehicles on the site were surveyed in February and March 1954—20% were found to be contaminated in excess of 100 cpm. The locations contaminated were most often tires and under-surfaces of the vehicles as well as radiators (HW-32473). The contamination was not necessarily predominantly ruthenium—a considerable percentage of rare earth elements was found in some analyses (HW-32473).

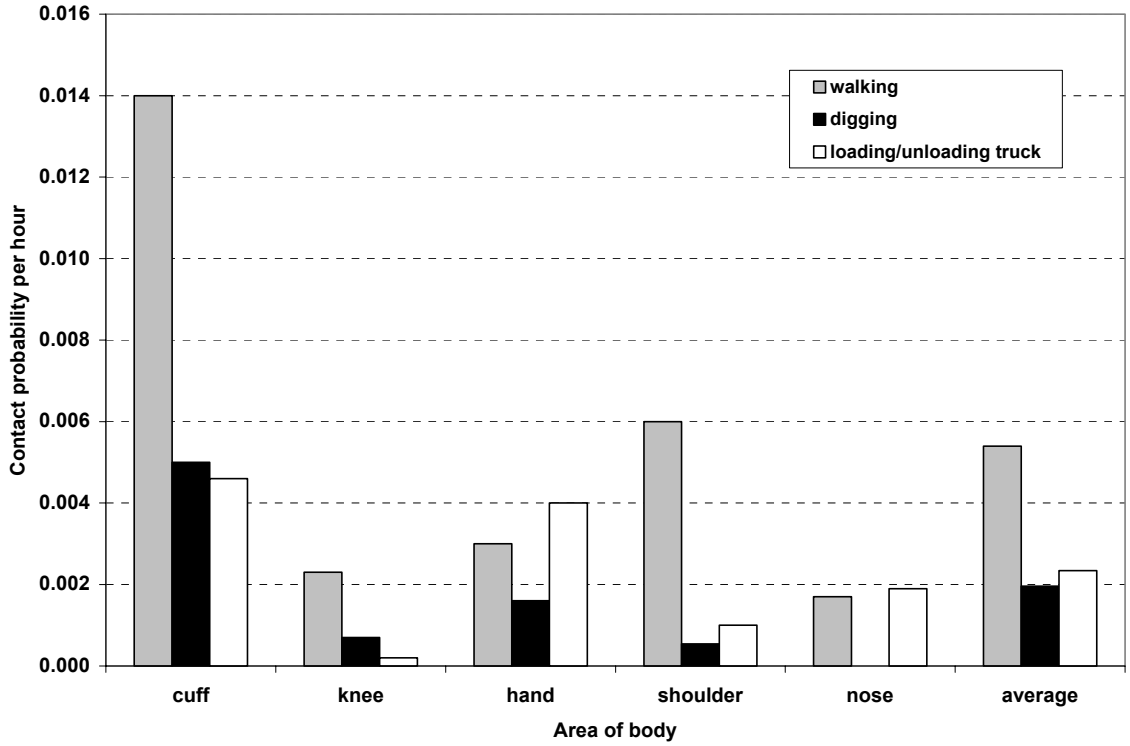

Figure 3-4. Mean probability of transfer of particle from ground to body during various activities (units are particles per square meter per hour on body per particles per square meter on ground surface). Experimental variability errors are presented in the original reference (Schwendiman 1958).

Sehmel's Tracer-Particle Resuspension Studies. In the 1970s, G. A. Sehmel conducted a series of resuspension experiments at Hanford, also using ZnS tracer particles. These studies and others are included in his comprehensive summary of transuranic and tracer simulant resuspension research (Sehmel 1980). As discussed earlier, wind-driven resuspension is not as important as local resuspension for past exposure of persons working in contaminated areas on the Hanford Site. Sehmel summarizes results of local resuspension experiments with ZnS both on cheatgrass areas and on asphalt from vehicular traffic (3/4-ton truck and car) as well as on asphalt by pedestrian traffic.

The disturbance of surface activity caused by a pedestrian in a tracer-contaminated area resulted in 100 times more resuspension than winds of 2-9 miles per hour. Sehmel's results are expressed as a resuspension rate; with units of fraction of the tracer on the ground resuspended per unit time (or per pass, in the case of pedestrian or vehicle movement). We found these units not as applicable to evaluating particle contact with the body as those of Schwendiman (1958).

Resuspension Factors. For evaluating the inhalation of resuspended particles from the air around the person causing the disturbance, the resuspension factor is the best empirical method. The resuspension factor is the airborne concentration (e.g. particles per cubic meter) divided by the surface concentration (e.g. particles per square meter), resulting in units of m^{-1}. Several comprehensive reviews of resuspension factors were obtained and a range of values is illustrated in Table 3-6.

Table 3-6. Contaminant Resuspension Factors during Various Conditions

Contaminant and condition	Value (m^{-1})	Reference
Uranium tetrafluoride, indoors. Suspension enhanced by equipment vibration and air-circulating fans.	Up to 2×10^{-3}	Bailey and Rohr (1953)
Clothes change room, Windscale reprocessing plant	2×10^{-4} to 1×10^{-3}	Brunskill (1967)
Uranium tetrafluoride, normal operations in plant	2.5×10^{-5} to 1.9×10^{-4}	Bailey and Rohr (1953)
Generic value for mechanical resuspension	2×10^{-6} to 1×10^{-3}	Healy (1980) citing Mishima (1964)
Recommended value for guidance purposes, based on review of outdoor experiments	1×10^{-5} to 1×10^{-4}	Stewart (1967)
Recommended value for use in deriving general surface contamination levels, also for plutonium oxide on indoor surfaces	5×10^{-5}	Wrixon et al. (1979); IAEA 1970
Plutonium oxide and nitrate, person walking through laboratory. (No movement resulted in RF of 2×10^{-8}.)	1×10^{-6} to 5×10^{-5}	Jones and Pond (1967)
Fresh deposit of Pu on undisturbed surfaces in semi-arid environments	10^{-6} to 10^{-4}	CEC 1979; Anspaugh, Shinn and Wilson (1974), cited in Healy (1980)
Particulate ^{131}I, digging through rubble of collapsed house	2×10^{-6}	Chamberlain and Stanbury (1951)
Fresh deposit, no disturbance	1×10^{-8} to 2×10^{-6}	Healy (1980) citing Mishima (1964)
Range often used in hazard evaluations	1×10^{-9} to 1×10^{-5}	Sehmel (1980)
Cab of tractor during various agricultural operations in S. Carolina	4×10^{-9} and 2×10^{-7}	Milham et al. (1975), cited in Healy (1977)
Pu at Hanford within the chemical separation areas	6×10^{-10} to 2×10^{-5}	Corley et al. (1976) cited in Sehmel (1980), Table 9
Aged deposit (2-17 years) of Pu on undisturbed surfaces in semi-arid environments	10^{-9} to 10^{-8}	CEC 1979; Anspaugh, Shinn and Wilson (1974), cited in Healy (1980)
^{137}Cs at Hanford in the BC area	4×10^{-11} to 7×10^{-8}	Sehmel (1980), citing Bruns (1976) and Mishima (1973)
Aged deposit, no disturbance	1×10^{-13} to 6×10^{-10}	Healy (1980), citing Mishima (1964)

The uncertainty analysis feature of the SURVEY spreadsheet tool allows us to evaluate the importance of the huge range in resuspension factors on the probability of inhalation of an active particle. For the work location, we recommend (and use in the example calculations) a log-triangular distribution with minimum, likeliest, and maximum values of 2×10^{-6}, 5×10^{-4}, and 1×10^{-3} m^{-1}. For the residence location, we use values that are one-half of those used for the work location, because roughly half that time is spent in little activity (i.e. sleeping).

Other Inhalation Pathway Factors. The SURVEY spreadsheet includes an inhalation rate (m^3 per hour) during work, which is allowed to vary over a range of possibilities, and an inhalation rate at the residence. In our example calculations, the inhalation rate at work is represented by a lognormal distribution with a geometric mean value of 1.5 m^3 h^{-1} [representing light activity such as simple construction or pushing a wheelbarrow (EPA 1985)]. The distribution is truncated on the lower end so the lowest rate (1.1 m^3 h^{-1}) represents light activity such as level walking at 3 mph. The maximum value is 3.8 m^3 h^{-1}, which is reached during activities like stair climbing with a load or chopping with an axe (EPA 1985). Another inhalation pathway factor is the fraction of the suspended particles that were inhalable. This is treated as an uncertain parameter in the SURVEY spreadsheet, with a conservative maximum value of 1.0. The term inhalable means the particle can be inspired through the nose or mouth, it does not mean the particle reaches or deposits in a certain region of the respiratory tract. See Section 3.6 for a review of large particle deposition in various regions of the respiratory tract.

Other Skin Pathway Factors. A number of particles deposited on the body would land on clothing. In a photograph of the Camp Hanford mess hall taken in the summer of 1944, all of the men are wearing long-sleeved shirts and overalls or pants (Seaborg 1994). Table 12.22 of Shleien (1992) shows the surface area of skin represented by different areas of the body. In the SURVEY spreadsheet, both particles contacting the whole body and bare skin are considered. We use a triangular distribution for the fraction of the surface area of the body that is exposed skin. The most likely value considers the hands, forearms and head to be uncovered, which translates to 0.16 of the surface area of the body. The minimum value is only head and hands uncovered (0.10) and the maximum value of 0.33 represents a person wearing knee-length shorts and a sleeveless shirt.

The extent of damage to skin from active particles depends on how long the particle is attached to skin or clothing. Wrixon et al. (1979) states that in practice, contamination on the skin rarely persists for more than a few hours but it can occur. Contamination is most common on the hands and face and can be removed by washing. Jones et al. (1998) obtained retention half-lives of particles deposited on skin that were between 1 and 3 hours. This translates to a mean residence time (= $T_{1/2}$ / ln 2), of 1.4–4.3 hours (Whicker and Schultz 1982).

Inadvertent Ingestion of an Active Particle. The most important exposure pathways for contamination on the skin surface are external irradiation of the skin itself and ingestion of material from the skin (Wrixon et al. 1979; NCRP 1999). For derivation of contamination levels in the working environment, Wrixon et al. (1979) state that it is appropriately cautious to assume that a person ingests all the activity from 10 cm^2 of contaminated skin each working day. Ingestion of contamination from personal clothing was judged unlikely to be significant. This area of skin is 0.3% of the exposed area of skin assumed as our most probable value in the SURVEY spreadsheet. Therefore, we use a transfer fraction of 0.003 particles ingested per particle deposited on the skin with a uniform distribution ranging from 0.002 to 0.005.

3.5.2 SURVEY Spreadsheet Structure and Example Distributions

The SURVEY spreadsheet evaluates exposure to large particles for various pathways by beginning with deposition density of active particles (number per unit ground area) in the person's environment. The output of SURVEY is the number of particles inhaled, ingested, or contacting the body or skin during an exposure period. If the number of particles contacted is much less than one, there is a only a slight probability that contact would have occurred at all under those conditions.

For some places, times, and activities, the probability of contact with an active particle was high. In those cases, the number of particles contacted during the exposure period is greater than one, and a dose/effects assessment is appropriate. Example calculations are given in Section 5 of this report. Also, other conclusions that could be drawn from the SURVEY spreadsheet are discussed.

The structure of the SURVEY spreadsheet is illustrated in Figure 3-5. The distributions and values for uncertain input parameters used in our example calculations are summarized in Table 3-7. The particle deposition density is a custom distribution that depends on the example calculation.

Table 3-7. Distribution Types and Values for Uncertain Input Parameters in the SURVEY Spreadsheet

Parameter	Distribution type	Minimum value	Maximum value	Likeliest or mean value	Mean value in simulation[a]
Fraction of airborne particles that are inhalable	Uniform	0.4	1.0	0.7	0.70
Ground-to-body contact probability	Uniform	0.0017	0.014	0.008	0.0079
Inhalation rate at work ($m^3\ h^{-1}$)	Truncated log-normal	1.1	3.8	1.5	1.7
Resuspension factor at work (m^{-1})	Log-triangular	2×10^{-6}	1×10^{-3}	5×10^{-4}	1.0×10^{-4}
Resuspension factor at residence (m^{-1})	Log-triangular	1×10^{-6}	5×10^{-4}	2.5×10^{-4}	5.1×10^{-5}
Hours per day at work location	Triangular	7	9	8	8
Fraction of surface area of body that is exposed skin	Triangular	0.10	0.33	0.16	0.20
Transfer from skin to ingestion	Uniform	0.001	0.005	0.003	0.003

[a]Mean value in uncertainty analysis simulation after 10,000 trials.

	A	B	C	D	E	F	G	H	I	J	K
1	**SURVEY SPREADSHEET WITH UNCERTAINTY ANALYSIS**										
2											
3	**EXAMPLE CALCULATION FOR ONSITE WORKER DURING PERIOD OF HIGH GROUND CONTAMINATION**										
4											
5	**PART I. INHALATION PATHWAY, RESUSPENSION FACTOR**										
6											
7	**DATA INPUT**	**COMPUTED**									
8	**VALUES**	**VALUES**									
9	5277			ENTER particles per 1000 square feet at working location							
10		56.8		particles per square meter at working location							
11	8			ENTER particles per 1000 square feet at residence							
12		0.081		particles per square meter at residence location							
13	1			Factor for nondetectable particles, default = 1.0.							
14	8			ENTER hours per day at work location							
15		16		hours per day at residence location on a work day							
16											
17	60			ENTER exposure duration (working days)							
18	24			ENTER exposure duration (non-working days)							
19											
20	1.7			inhalation rate during working hours (m^3 per hour)							
21	0.9			inhalation rate during residential hours (m^3 per hour)							
22											
23	-9.23			ln of resuspension factor for local area disturbance during work							
24	-9.90			ln of resuspension factor for general activities at residence location							
25											
26		9.8E-05		exp (ln (resuspension factor for work))							
27		5.0E-05		exp (ln (resuspension factor for residence))							
28											
29		5.5E-03		airborne concentration of particles at work location (particles per cubic meter)							
30		4.0E-06		airborne concentration of particles at residence location (particles per cubic meter)							
31											
32	0.70			Fraction of suspended particles that are inhalable							
33											
34		3.1E+00		particles inhaled at work over exposure period							
35		2.4E-03		particles inhaled at residence on working days over exposure period							
36		1.6E-03		particles inhaled at residence on nonwork days over exposure period							
37		3.1E+00		particles inhaled over exposure period							
38											
39	**PART II. GROUND TO BODY TRANSFER, EMPIRICAL METHOD OF SCHWENDIMAN (1958)**										
40											
41	7.9E-03			particles m^-2 transferred to body m^-2 on the ground, per hour of walking							
42											
43	1.94			surface area of body (m^2)							
44											
45		8.7E-01		particles on body per hour							
46											
47		7		particles on body after 1 work day							
48											
49	0.20			fraction of body that is exposed skin							
50											
51		1.4		particles on skin after 1 work day							
52											
53	**PART III. INADVERTENT INGESTION OF PARTICLE FROM SKIN**										
54											
55	0.003			fractional transfer from skin to ingestion							
56											
57		4.1E-03		particles ingested over 1 work day							
58											

Figure 3-5. Structure of SURVEY spreadsheet. Uncertain input parameters (also called assumptions) are framed in a bold solid border. Uncertain output parameters (also called forecasts) are framed in a dashed border. Link to Survey.xls. The user must have the Crystal Ball® add-on software to access the uncertainty analysis features of this EXCEL workbook.

The formulas for the cells in the spreadsheet survey.xls are reproduced below. The cells are noted by their column and row number (e.g. "B10").

B10 (particles m^{-2} at working location) = A9 (particles per thousand square feet at working location) × 10.76 ft^2 m^{-2} / 1000 ft^2 per thousand square feet

B12 (particles m^{-2} at residence location) = A11 (particles per thousand square feet at residence location) × 10.76 ft^2 m^{-2} / 1000 ft^2 per thousand square feet

B15 (hours per day at residence location on a work day) = 24 h d^{-1} – A14 (hr d^{-1} at work location)

B26 (resuspension factor for work) = exp A23 (ln [resuspension factor for local area disturbance during work])

B27 (resuspension factor for residence) = exp A24 (ln [resuspension factor for general activities at residence location])

B29 (particles m^{-3} air at work location) = B10 (particles m^{-2} ground at work location) × B26 (resuspension factor for work [m^{-1}])

B30 (particles m^{-3} air at residence location) = B12 (particles m^{-2} ground at residence location) × B27 (resuspension factor for residence [m^{-1}])

B34 (particles inhaled at work over exposure period) = B29 (particles m^{-3} air at work location) × A20 (inhalation rate during working hours [m^3 h^{-1}]) × A14 (h d^{-1} at work location) × A17 (working days during exposure period) × A32 (fraction of suspended particles that are inhalable)

B35 (particles inhaled at residence on working days over exposure period) = B30 (particles m^{-3} air at residence location × A21 (inhalation rate during residential hours [m^3 h^{-1}]) × B15 (h d^{-1} at residence on a work day) × A17 (working days during exposure period) × A32 (fraction of suspended particles that are inhalable)

B36 (particles inhaled at residence on non-working days over exposure period) = B30 (particles m^{-3} air at residence location) × 23 m^3 inhaled d^{-1} × A18 (non-working days during exposure period) × A32 (fraction of suspended particles that are inhalable)

B37 (particles inhaled over exposure period) = B34 (particles inhaled at work over exposure period) + B35 (particles inhaled at residence on working days over exposure period) + B36 (particles inhaled at residence on nonworking days over exposure period)

B45 (particles on body per hour) = B10 (particles m^{-2} ground at working location) × A41 (particles m^{-2} transferred to body per m^2 on ground, per hour of walking) × A43 (surface area of body [m^2])

B47 (particles on body after one work day) = B45 (particles on body per hour) × A14 (h d^{-1} at work location)

B51 (particles on skin after one work day) = B47 (particles on body after one work day) × A49 (fraction of body that is exposed skin)

B57 (particles ingested over one work day) = B51 (particles on skin after one work day) × A55 (fractional transfer from skin to ingestion)

3.6 Dosimetry of Highly Radioactive Particles

Persons working and living in contaminated areas were exposed to large "active particles" in several ways. This section addresses exposures when such a particle is inhaled, ingested, or resident on the skin. The first two of these pathways lead to irradiation of several organs and tissues because the radioactivity is distributed in the body after intake.

3.6.1 Estimating Deposition of Large Particles in the Respiratory Tract

Experimental evidence indicates that quite large particles can be inhaled, particularly under windy conditions (not uncommon at Hanford). For still air, the inhalability of particles with aerodynamic diameters in the range of 30–100 μm is estimated from numerous experimental measurements to be about 0.5. The data also show that the inhalability of particles with diameters of 75–90 μm is not greatly different from 1.0 for a wind speed of 9 m s^{-1} and is between 0.7 and 0.9 for a wind speed of 6 m s^{-1} (ICRP 1993b). Unless specific information is available that can be used to make a better estimate, it is assumed that the inhalability of resuspended particles can be as high as one. The SURVEY spreadsheet allows this parameter to range from 0.4 to 1.0 (Table 3.7).

Particles with aerodynamic diameters greater than 10–20 μm are normally not considered respirable, meaning that they are not likely to reach the deep lung (pulmonary region). When such particles are inhaled, they are deposited primarily in the extra-thoracic region of the respiratory tract (nose, naso-orophyrengeal cavities and larynx) and in the larger bronchial airways. Particles deposited in the anterior part of the nose will remain until removed by nose blowing. The clearance half-time for such deposits is estimated to be 17 h. The majority of particles passing beyond the nose or inhaled through the mouth would be deposited in other parts of the extra-thoracic region, with a small fraction reaching the bronchial regions of the lung. These particles will be cleared quickly, swallowed, and will pass through the gastro-intestinal tract. Clearance half-times from the extra-thoracic and upper bronchial region are between 10 and 100 minutes (ICRP 1993b).

The distribution of deposited particles depends on the breathing rate, which is in turn dependent upon the level of physical activity of the exposed person. Table 3-8 shows the effects of activity level and of breathing habits upon deposition fractions for particles with an aerodynamic diameter (d_{ae}) of 20 μm. Tabulations for larger particles were not included in ICRP Publication 66 (ICRP 1993b).

For a reference worker who routinely breathes through the nose, less than one percent of the 20-μm particles are expected to reach the pulmonary region of the lung. The fraction is increased by about a factor of four for a person who habitually breathes through the mouth at the normal rate. The table shows that when the filtering effect of the nasal passages is lost due to mouth breathing, there is also increased deposition in the bronchial region. Information in ICRP Publication 66 (ICRP 1993b) indicates that the fractional depositions in the extra-thoracic cavities do not change rapidly as the particle size increases above 5 μm. Thus, it is reasonable to use the tabled values for those two regions when even larger particles are inhaled. On the other hand, the deposition fractions for the bronchial and pulmonary regions decrease with increasing particle size in the 5 to 20 μm range. Extrapolations suggest that for any particle with an aerodynamic diameter greater than 40 μm, the pulmonary deposition fraction would be less than 0.01, regardless of level of exertion or breathing habit. Bronchial deposition also declines with

particle size, but the decrease is more difficult to project. The bronchial deposition fractions for 20-µm particles given in the table are taken as default values for larger particles.

Table 3-8. Estimates of Particle Deposition in Different Regions of the Respiratory Tract for Various Activities and Breathing Habits (1CRP 1993b)

		Deposition fractions for particles having d_{ae} = 20 µm		
Category	Breathing rate (m^3 h^{-1})	Anterior nasal passages	Naso-oropharynx, larynx (bronchial region)	Pulmonary region
Reference worker				
Nasal intake[a]	1.2	0.32	0.33 (0.01)	0.0072
Oro-nasal intake[b]	1.2	0.13	0.43 (0.06)	0.026
Heavy work				
Nasal intake[a]	1.7	0.29	0.36 (0.02)	0.0065
Oro-nasal intake[b]	1.7	0.12	0.45 (0.06)	0.022
Light exercise[a]	1.5	0.32	0.34 (0.01)	0.0054
Heavy exercise[c]	3.0	0.16	0.44 (0.05)	0.010

[a] Normal nose breather.
[b] Habitual mouth breather.
[c] Normal nasal intake augmented by oral intake.

Table 3-8 shows that most 20-µm particles that are inhaled will be deposited in the upper regions of the respiratory tract. That will also be true for the larger active particles with which we are concerned. The particles that are deposited in the anterior nasal passages will irradiate nearby tissues until they are removed by nose blowing. Such exposures are similar to the situation when the particle is retained on the skin for a time before it is removed by washing or other activities. Most large particles that pass beyond the nose will be promptly cleared from the respiratory tract and swallowed. That type of exposure is thus similar to inadvertent ingestion of an active particle. A very small fraction of inhaled large particles may be deposited in the pulmonary (or alveolar-interstitial) region of the lung. Table 3-8 shows that for a 20-µm particle the chance of this occurring is greater for a person who is taking air in through the mouth, either as the result of habit or because of the level of exertion. The chance of deposition in the deep lung is lower for particles with diameters greater than 20 µm.

3.6.2 Doses from Ingestion

The active particles that were emitted from T Plant and B Plant during the early years of operation contained several radionuclides. The primary contributors and the activity fraction for each of the beta-emitting radionuclides were listed in Section 2.2.1. The alpha-emitting radionuclide ^{239}Pu was also present in the active particles, but the ^{239}Pu activity was much smaller than the total beta activity. The most radioactive particle identified as a result of the survey activities at the time contained a total of 3.2 µCi of beta-emitters. Table 3-9 shows the estimated doses to the most exposed organs and tissues for an ingested particle that contains 5 µCi of beta-

emitters. Doses from ^{239}Pu are included in the totals; it is assumed that the beta to alpha (β/α) particle activity ratio was 100. Estimated doses to most tissues are insensitive to the value of the β/α activity ratio for these particles. Calculations were made for β/α values ranging from 3000 to 100 and showed that only the dose to the liver varied appreciably. The liver dose for β/α = 100 is about 80 percent greater than the dose for β/α = 3000. The dose to bone surfaces also varied somewhat and is about 20 percent greater for a β/α activity ratio of 100. Link to Ingestion.xls.

Table 3-9. Doses from Ingestion of an Active Particle Containing 5 µCi of Beta-Emitters

Organ or tissue	Dose (rad)[a] from ingestion of a 5-µCi[b] particle[c]	Radionuclides that contribute most to the tissue dose
Gastro-intestinal tract		
Stomach wall	0.022	^{137}Cs, ^{144}Ce, ^{106}Ru
Small intestinal wall	0.040	^{144}Ce, ^{137}Cs, ^{106}Ru
Upper large intestinal wall	0.22	^{144}Ce, ^{91}Y, ^{89}Sr
Lower large intestinal wall	0.63	^{144}Ce, ^{91}Y, ^{89}Sr
Bone surfaces	0.46	^{90}Sr, ^{239}Pu, ^{137}Cs, ^{89}Sr
Red marrow	0.19	^{90}Sr, ^{137}Cs, ^{89}Sr
Liver	0.036	^{239}Pu, ^{137}Cs, ^{144}Ce
Kidneys	0.015	^{137}Cs, ^{90}Sr, ^{106}Ru
Bladder wall	0.016	^{137}Cs, ^{90}Sr, ^{106}Ru
Ovaries	0.021	^{137}Cs, ^{95}Zr, ^{103}Ru
Uterus	0.017	^{137}Cs, ^{90}Sr, ^{106}Ru
Testes	0.015	^{137}Cs, ^{90}Sr, ^{106}Ru

[a] Based on dose coefficients given in ICRP Publications 67, 56, and 30 (for ^{89}Sr and ^{91}Y). To obtain doses in gray, divide tabled values by 100.
[b] An activity of 5 µCi corresponds to an activity of 1.85×10^5 Bq.
[c] The ratio of beta- to alpha-particle emissions was assumed to be 100.

Fractional uptake of these elements into blood from the GI tract varies from 5×10^{-4} for Ce and Pu and 1×10^{-4} for Y to 1 for Cs. Values for Zr (0.01), Ru (0.05), and Sr (0.3) are intermediate.

The table shows that the highest dose expected (~0.6 rad) is that to the wall of the lower large intestine. Doses to bone surfaces are nearly as high (~0.5 rad), followed by doses to the wall of the upper large intestine and to red bone marrow (both ~0.2 rad). Doses estimated for the other tissues range from about five to 13 times lower than the bone marrow dose.

Ruthenium-106 was the most important isotope in the highly radioactive particles that were released from the REDOX Plant. Ruthenium-103 was also present, but did not contribute as much to the dose. Highly radioactive particles were reported to contain about 200 µCi (HW-33068). Table 3-10 shows the organ and tissue doses expected from ingestion of a particle containing 300 µCi (11 MBq) of ^{106}Ru. The doses are much higher than those in Table 3-9 because the particle activity considered is substantially greater. The dose distribution reflects only the biokinetic behavior of ^{106}Ru. The largest doses are received by the lower and upper large

intestines. Doses to the small intestine and stomach also exceed doses estimated for the remaining tissues. Link to Ingestion.xls.

Table 3-10. Doses from Ingestion of an Active Particle from REDOX Plant Containing 300 µCi of ^{106}Ru

Organ or tissue	Dose (rad)[a] from ingestion of a 300-µCi[b] particle
Gastro-intestinal tract	
Stomach wall	3.6
Small intestinal wall	6.2
Upper large intestinal wall	29
Lower large intestinal wall	80
Bone surfaces	1.7
Red marrow	1.7
Liver	1.7
Kidneys	1.7
Bladder wall	1.9
Ovaries	1.9
Uterus	1.8
Testes	1.7

[a] Based on dose coefficients given in ICRP (1993a). To obtain doses in gray, divide tabled values by 100.

[b] An activity of 300 µCi particle corresponds to an activity of 1.11×10^7 Bq.

3.6.3 Doses from Inhalation into the Deep Lung

In this section we consider only those particles that reach the pulmonary region of the lung. The probability is small that a particle as large as those observed would reach the deep lung, but the possibility cannot be excluded. The probability of inhalation as a function of location and particle size is discussed further in Appendix E. For these calculations it is assumed that the particle reaches the pulmonary region of the lung and that it is not removed to the gastro-intestinal tract by mucociliary action and swallowing. If it were cleared in that way, the situation would be quite similar to the single particle ingestion case discussed above. Instead, it is assumed that the particle gradually disintegrates into fragments and dissolves, and that the activity enters the blood and is then carried to other body tissues. In effect, single particles are assumed to be cleared in the same way as a collection of small particles.

Table 3-11 contains the estimated doses for such a scenario and a particle containing 5 µCi of beta emitters. The doses were estimated using ICRP dose coefficients for type S material, corrected to reflect the assumed deposition of all the activity in the particle in the deep lung. Estimated doses for particles of absorption types M or S would be lower. Given the assumed exposure conditions, it is not surprising that the estimated dose to the lung is highest, ~40 rad. This dose estimate is based upon standard dose coefficients that assume the presence of many

particles distributed throughout the lung. For a single particle, doses to a small area of the lung would be much higher and doses to other portions would be substantially lower. Doses to bone surfaces and to the liver are also higher than doses to other tissues. Beta-particle irradiation of the tissues in the gastro-intestinal tract, which was very important for the particle ingestion case, is minimal because it is assumed that radioactivity is not swallowed. The doses presented are for a β/α ratio of about 30,000. Smaller β/α ratios lead to a particle that has an aerodynamic diameter greater than 20 μm, and such a particle is unlikely to reach the deep lung. Plutonium-239 accounts for only a small fraction of most tissue doses.

Particles with a β/α ratio of 100 would have aerodynamic diameters greater than 20 μm, unless the ^{239}Pu activity was less than about 0.17 nCi. The corresponding beta activity would be 17 nCi. Inhalation of such a particle would produce doses smaller than those shown in Table 3-11. Link to Ingestion.xls.

Table 3-11. Estimated Doses from Deposition in the Deep Lung of an Active Particle Containing 5 μCi of Beta-Emitters

Organ or tissue	Dose (rad)[a] from inhalation of a 5-μCi[b] particle[c]	Radionuclides that contribute most to the tissue dose
Adrenals	0.12	^{137}Cs, ^{95}Zr, ^{144}Ce
Bladder wall	0.011	^{137}Cs, ^{144}Ce, ^{106}Ru
Bone surfaces	0.34	^{90}Sr, ^{144}Ce, ^{239}Pu
Red bone marrow	0.18	^{90}Sr, ^{144}Ce, ^{137}Cs
Breast	0.12	^{137}Cs, ^{95}Zr, ^{144}Ce
Kidneys	0.043	^{137}Cs, ^{95}Zr, ^{144}Ce
Liver	0.35	^{144}Ce, ^{137}Cs, ^{95}Zr
Lung	41	^{144}Ce, ^{90}Sr, ^{91}Y
Ovaries	0.020	^{137}Cs, ^{144}Ce, ^{95}Zr
Spleen	0.084	^{137}Cs, ^{95}Zr, ^{144}Ce
Testes	0.0081	^{144}Ce, ^{137}Cs, ^{106}Ru
Thymus	0.14	^{137}Cs, ^{144}Ce, ^{95}Zr
Uterus	0.014	^{137}Cs, ^{144}Ce, ^{95}Zr

[a] Based on dose coefficients given in ICRP (1995) and ICRP (1980, 1981) (for ^{91}Y). To obtain doses in gray, divide tabled values by 100.
[b] An activity of 5 μCi corresponds to an activity of 1.85×10^5 Bq.
[c] The ratio of beta- to alpha-particle emissions was assumed to be 30,000.

Estimates of the doses due to inhalation of active ruthenium particles released from the REDOX Plant must also consider particle size. These particles resulted from sequential or co-deposition of ruthenium tetroxide and ammonium nitrate on the walls of the exhaust ventilation system. The effective density of the flakes that were resuspended and released was likely intermediate between the density of ruthenium tetroxide (about 3.3 g cm^{-3}) or ruthenium dioxide (about 2.0 g cm^{-3}) and ammonium nitrate (about 1.7 g cm^{-3}). An effective density of about 3 g cm^{-3} is assumed. Because the particles were generally observed as flakes, a shape factor of two is assumed. For such a particle with an aerodynamic diameter of 20 μm, the equivalent physical diameter is estimated to be about 16 μm.

The mass of a spherical particle with a diameter of 16 μm and a density of 3 g cm^{-3} is about 51 ng. The fraction of the total mass that is ruthenium depends upon the relative amounts of ruthenium oxides and ammonium nitrate, which are unknown. Perhaps about 20 ng would be ruthenium. Of this, most would be the stable isotopes of ^{101}Ru, ^{102}Ru, and ^{104}Ru, all of which have fission yields (^{235}U, thermal neutrons) substantially greater than that of ^{106}Ru (Katacoff 1960). About 3.5% of the mass of ruthenium in these particles would be radioactive (^{103}Ru and ^{106}Ru), with ^{106}Ru accounting for about 95% of that mass. The ^{106}Ru activity of the 20 μm aerodynamic diameter particle under consideration is estimated to be about 2.2 μCi, and the ^{103}Ru activity would be about 1.2 μCi.

Table 3-12 contains the doses estimated for such a particle (ICRP absorption type S) if it deposited in the deep lung. As before, it is assumed that clearance via the bronchial tree does not occur. Link to Ingestion.xls.

Table 3-12. Estimated Doses from Deposition in the Deep Lung of an Active Particle (d_{ae} = 20 μm) from REDOX Plant

Organ or tissue	Dose (rad)[a,b]
Adrenals	0.081
Bladder wall	0.020
Bone surfaces	0.046
Red bone marrow	0.058
Breast	0.097
Kidneys	0.040
Liver	0.053
Lung	40
Ovaries	0.026
Spleen	0.070
Testes	0.015
Thymus	0.11
Uterus	0.020

[a] Based on dose coefficients given in ICRP (1995). To obtain doses in gray, divide tabled values by 100.

[b] The particle is estimated to contain 2.2 μCi (8.1×10^4 Bq) of ^{106}Ru and 1.2 μCi (4.4×10^4 Bq) of ^{103}Ru.

3.6.4 Doses from Contact with Active Particles

The third type of exposure occurs when an active particle remains in contact with the external surface of the body. As noted, the contact could be with the skin or the lining of the anterior nasal passages. Particles may also come into contact with the eyes and ears. In all these situations, the dose received depends directly upon the duration of contact.

In recent years, two different types of "hot particles" have been observed in operating nuclear reactor facilities. These particles generally contain the activation product ^{60}Co in small fragments of metal alloys used in plant piping and valves. Other particles contain fission products associated with small uranium fuel fragments that have escaped into reactor coolant as

the result of fuel cladding failures. This second category of particles is more similar in radionuclide composition to the active particles released from T and B Plants at Hanford, but the mechanism of formation and the content are different. In the last decade, the National Council on Radiation Protection and Measurements has issued two reports that address "hot particle" exposures (NCRP 1989, 1999). The most recent report describes the responses of the skin, ear, eye, respiratory tract, and gastrointestinal tract to high doses from hot particles in some detail. That information could be used when examining individual medical records for indications of extended contact with active particles and ruthenium particles released from Hanford. The report also contains recommendations for medical follow-up in the event such doses occur (NCRP 1999).

The primary contributors to the dose from Hanford particles were energetic beta particles emitted when the radionuclides in the active particles decayed. In the case of the ruthenium particles, the most damaging beta particle emissions come from ^{106}Rh that is produced when ^{106}Ru decays. Table 3-13 shows dose coefficients for two depths below the surface of the skin. The first depth, 0.07 mm, is that at which skin dose has historically been assessed, and represents the range of depths (0.02–0.1 mm) for the basal cells of the skin covering the head and upper body (ICRP 1991). The second (0.4 mm) is approximately the depth of basal cells for the palms and the soles of the feet. There are also radiosensitive cells at that depth beneath the surface on other parts of the body.

Table 3-13. Dose Coefficients for Radionuclides Contained in Hanford Active Particles

Primary radio-nuclide and (decay product)	Fraction of beta activity for T and B Plant particles	Dose coefficient (nGy h^{-1} per Bq cm^{-2})[a]	
		Skin depth of 0.07 mm	Skin depth of 0.4 mm
^{103}Ru	0.13	568	28
^{141}Ce	0.14	1538	169
^{95}Zr (^{95}Nb)	0.06	1288	86
^{89}Sr	0.14	1667	887
^{91}Y	0.23	1669	897
^{106}Ru (^{106}Rh)	0.03	1845	1165
^{144}Ce (^{144}Pr)	0.26	2630	634
^{90}Sr (^{90}Y)	0.05	3133	1384
^{137}Cs	0.05	1432	384

[a] Dose coefficients for distances along the axis of a circular source with area of 1 cm^2 or a point source averaged over that area from Cross et al. (1992). Tabled values include contributions of radioactive decay products. For short exposure times, doses attributed to ^{95}Zr and ^{90}Sr would be overestimated because the half-lives of ^{95}Nb and ^{90}Y are 35.1 d and 64.1 h, respectively.

The dose coefficients in Table 3-13 are derived from the results of Cross et al. (1992) who evaluated doses from small contaminated areas on the skin. They considered a source diameter of 1 cm^2 with a uniform activity distribution and performed Monte Carlo calculations of doses along the axis of the plane circular source. Their calculations are for an air-water interface, which is a reasonable approximation of the air-skin interface. The results are applicable to a

point source whose activity is averaged over the same surface area. The doses estimated are those along a vertical line through the center of the circular area, which extends downward below the skin surface. Doses at distances away from the axis at the same depth would be lower because the distance from the source is larger. As would be expected, the results of Cross et al. (1992) are somewhat lower than those for uniform contamination of the skin (Kocher and Eckerman 1987).

For a Hanford active particle that contained 5 μCi (1.85×10^5 Bq), total dose rates at tissue depths of 0.07 and 0.4 mm are estimated to be 36 rad h^{-1} and 12 rad h^{-1}, respectively. The principal contributors to the dose rate at 0.07 mm are ^{144}Ce-Pr (35%), ^{91}Y (20%), ^{89}Sr (12%), and ^{141}Ce (11%). At the depth of 0.4 mm, the dose rate is due primarily to ^{91}Y (32%),^{144}Ce-Pr (25%),^{89}Sr (19%), and ^{90}Sr-Y (11%). Most of the latter contribution is due to ^{90}Y, and may be overestimated for short exposures. Link to Skin Dose.xls.

Information in Table 3-13 can be used to estimate the skin doses from ruthenium particles released from the REDOX Plant. We again consider a secondary ruthenium particle that contains 300 μCi (1.11×10^7 Bq) of ^{106}Ru. For activity that had a stack residence time of 3 months and release in the spring of 1954, the expected ratio of ^{103}Ru to ^{106}Ru activities is 0.56. Thus, the same particle would also contain about 170 μCi of ^{103}Ru. The estimated dose rate at a skin depth of 0.07 mm below such a particle is about 2400 rad h^{-1}. For a depth of 0.4 mm, the dose rate from such a particle is estimated to be about 1300 rad h^{-1}. Link to Skin Dose.xls.

As noted earlier, long term exposures to such particles have detectable medical consequences. These could occur if the particle were trapped in the nose or ear, near the eye, on the skin, or in a wound. Historically, a few cases were noted among T and B Plant workers, but our limited review suggests that the frequency of detection of lesions on contaminated individuals was generally low. Although there is no doubt that contact with active and ruthenium particles occurred, it appears that either the particle activity was low or the retention periods were relatively brief.

4. HISTORIC ENVIRONMENTAL MONITORING DATA

4.1 Trends in Routine Measurements (1945–1955)

The first processing at 200 Areas began in December 1944 (Table 1-1). Routine sampling of environmental media, principally vegetation, was begun in the latter part of 1945 after the war ended and the secret mission of Hanford was made public. Quarterly reports containing environmental monitoring results were prepared following the first quarter of 1946. They were compilations of weekly and monthly reports and usually contained more analysis and discussion than the other reports. The first annual environmental report was for 1946 (HW-3-5402), but the next did not follow until 1958. For routine environmental monitoring data, we have relied most heavily upon the quarterly environmental reports published during 1945–1955. Appendix B contains a rationale for and description of environmental data sets that were compiled and analyzed.

In the period 1949–1953, routine environmental monitoring continued to expand and it included samples of vegetation and airborne particles throughout the northwest. The occurrence of radioactive particles in the Hanford environs from "a source other than the Hanford Works" (fallout from the atmospheric testing of weapons) was first reported in September 1949. The detection of fallout particles in air samples resulted in an expansion of the routine air sampling program and became an increasingly important aspect of environmental monitoring. Air sampling stations were located as far away from Hanford as Great Falls, Montana; Boise, Idaho; Klamath Falls, Oregon; as well as Seattle and Spokane, Washington.

According to Conklin (1986), surface contamination in the 1940s from Hanford iodine releases, as determined by deposition on vegetation, routinely extended to the southwest as far as the Dalles, to the southeast as far as Walla Walla, and to the northeast as far as Spokane. By 1950, small positive concentrations of ^{131}I continued to be found as far east as Lewiston, Idaho, and west to Hood River, Oregon.

By the mid-1950s, effluent and environmental monitoring included the following media and analyses (Conklin 1986):

- Effluent gases: ^{131}I and $^{103,106}Ru$ from the chemical processing plants; ^{3}H, ^{14}C, ^{35}S from the reactors; total alpha and beta from all plants
- Vegetation: ^{131}I and nonvolatile beta
- Dose rates: ion chambers
- Air: alpha, beta, ^{131}I, particle concentrations
- Liquid effluent to river: beta, selected isotopes, sometimes alpha
- River water: alpha, beta
- Rain: beta
- Drinking water: alpha, beta.

By 1957, a new technique, gamma spectrometry, became available for routine use in analyses of environmental and effluent samples. This permitted individual radionuclide concentrations to be quantified rather than the total (or gross) radioactivity concentration.

Because the highest airborne releases of radioactivity from Hanford facilities occurred before 1956 (see Table 1-1), we have focussed our analyses on data sets compiled from 1945–1955. The following sections summarize the data sets from this time period that we determined were useful for understanding historical particle releases from Hanford. The primary focus of our work is not radioiodine, and consequently specific measurements of that radionuclide in the

environment were not examined. Radioiodine does contribute to measurements of total radioactivity.

4.1.1 Ionization Chambers

Hanf and Thiede (1994) summarizes the early years of radiological monitoring at the Hanford Site (beginning with 1945). The locations and methods are described as determined from review of original documents. No data were compiled in their report; however, it is a good source of the original documents for each year. Some useful general information about early monitoring with ionization chambers at Hanford is excerpted here.

Ambient radiation levels were measured with several types of ionization chambers. These measurements give an indication of what external radiation exposures would have been to people in the areas. The field measurement techniques were basically being developed at the time, and thus were evolving. Early measurement units, called integrons, measured gamma radiation. Hanf and Thiede (1994) discusses reasons why the integron ionization chambers were unreliable in the first three quarters of 1945. Other units, called C type ionization chambers, measured both gamma and some beta radiation. An estimated 15-33% of the beta energy from ^{131}I was transmitted through the walls of the C chambers, which were made from ice cream cartons. In addition, other units called X, S, and M types, were used at various locations around the site and were similar to the C type. According to HW-9871, the M and S chambers were cylindrical ionization chambers with 50% of the wall composed of 1-mil aluminum foil. The foil was thin enough that beta particles would penetrate it (HW-7-4279). The chambers were placed in pairs at the various locations. Because the aluminum on these units was susceptible to scouring by desert sand, they were elevated on stands.

Although there were a confusing number of units[a] used to express external radiation exposure measurements in these early years, the differences between them are not crucial when examining major trends. Radiation exposure measurements were reported in units of milliroentgen (mR) and milliroentgen-equivalent-physical (mrep) through the third quarter of 1953. The roentgen (abbreviated R) is a unit for defining exposure in the air to X or gamma radiation (ionizing radiation). The rep is an outdated unit of absorbed dose and is a measure of the amount of energy deposited in tissue as a result of exposure (in air) to X or gamma radiation. Beginning in the fourth quarter of 1953, data were reported in units of millirad (mrad). The rad is the traditional unit of absorbed dose and represents energy absorbed per unit mass of any absorbing medium from any kind of ionizing radiation. According to Hanf and Thiede (1994), all three of these units are nearly equivalent, as the difference in energy deposited in tissue between all three is very small.

In May and July of 1945, it was felt that most of the positive ionization chamber readings were due to deposited activity on the ground and not atmospheric radiation (HW-7-1115). Exceptions occurred when high readings were found after stack gases were seen to be looping toward ground level under certain meteorological conditions.[b]

Tables in HW-9871 summarize weekly measured radiation levels between September 1945 and September 1946 and monthly levels for 1947 through April 1948. All measurements include

[a] Throughout this section, measurements are given in the conventional units that were used in the original sources. A conversion table to metric or System International (S.I.) units is provided in the introduction.

[b] HW-7-1115 DEL confirms that the effluent fumes from the stack were visible from the presence of brown nitrous compounds. Other reports refer to sampling “in the plume.”

natural background, which was measured by these instruments at about 0.3–0.5 mrep per day. Figure 4-1 is a retouched map from HW-9871 that shows the monitoring locations for C chambers and M and S chambers in May 1948.

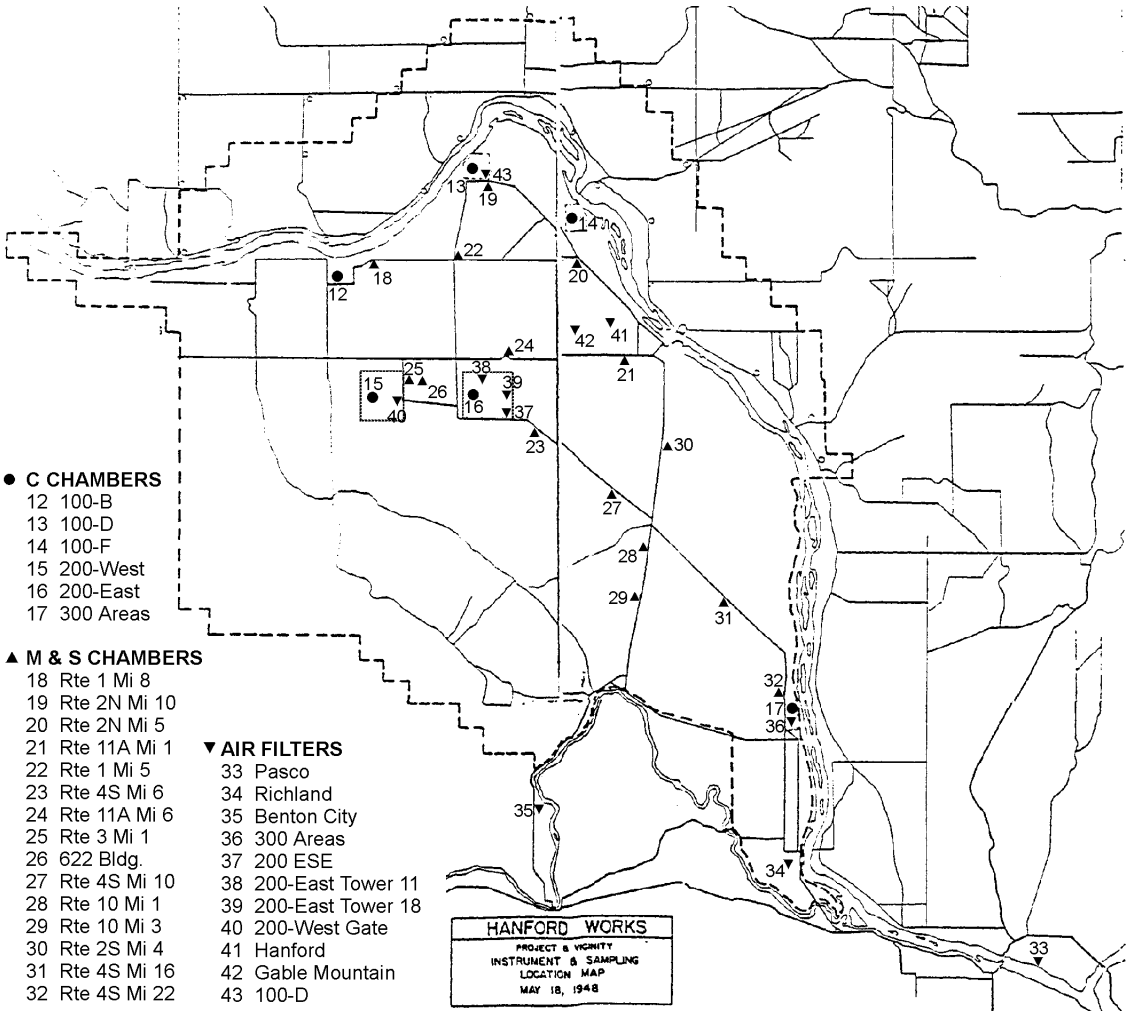

Figure 4-1. Locations for environmental monitoring of airborne radioactivity on the Hanford Works in May 1948. Legibility of the source map (HW-9871) was poor, so the legend and location symbols and numbers were redrawn. Also, river monitoring stations were removed from the original figure.

Figure 4-2 plots C chamber data for two locations on the Hanford Site: 200-E and 100-B. These are location numbers 16 and 12, respectively, in Figure 4-1. The highest value in the tabulations of C chamber results in HW-9871 is 1.9 mrep d^{-1} for the 200-East Area during the week ending June 26, 1946. The excess radiation level near 200-East over this time interval, which can be attributed to releases from operations in that area, averages 0.4 mrep d^{-1}, or around 150 mrep yr^{-1} assuming continuous exposure. The excess was determined by subtracting the value at 100-B from the value at 200-East.

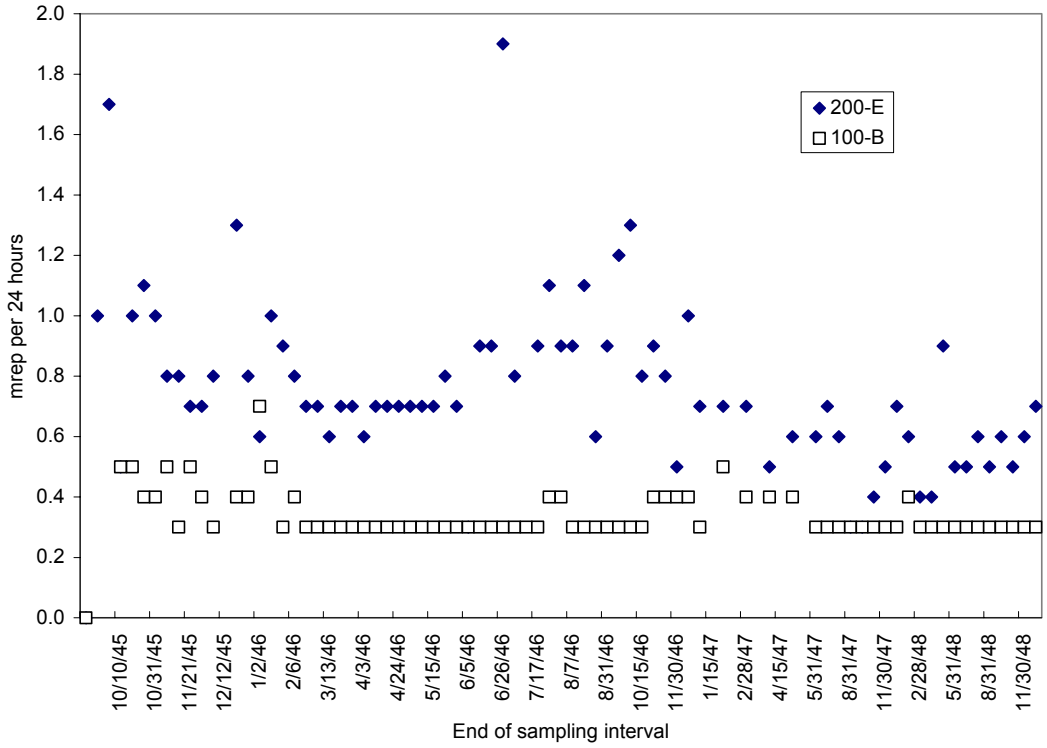

Figure 4-2. Radiation levels measured by detachable C chambers at two locations on the Hanford Site, 1945–1948. Levels at 200-East (separations area) averaged roughly twice those at 100-B (a reactor area). The average level at 100-B was 0.35 mrep per 24 hours, which is within the stated background range of the instrument (0.3–0.5 mrep per 24 hours), and the average level at 200-East was 0.75 mrep per 24 hours (data from HW-9871).

A similar data set was compiled from HW-9871 for the M and S chambers. The exposure rate data for M and S chambers are always reported together in the same table of the Hanford reports, with no separation according to chamber type. Three locations were chosen to illustrate the decrease in radiation levels with distance from the 200 Areas. The locations were 622 building (also called meteorology), which is between 200-West and 200-East Areas; Route 4S, Mile 6; and Route 4S, Mile 10. These locations are numbers 26, 23, and 27 in Figure 4-1. Of the exposure rate chambers in operation at that time, the Route 4S, Mile 6 location was most representative of the military encampment that was SE of 200-East. In addition to these three locations, data were compiled for the Route 1, Mile 8 location (number 18 on Figure 4-1). The Route 1, Mile 8 location represents relatively low exposure to effluents from 200 Areas, based on wind frequency. The M and S chamber data begin 9 weeks earlier (July 1945) than the C chamber data set. Background for these chambers is also stated to be 0.3 to 0.5 mrep d^{-1}.

Figure 4-3 illustrates the annual average M and S chamber results. Sampling frequency was weekly through August 1946, bimonthly through the remainder of 1946, and monthly throughout the remainder of this time period. Excess radiation levels were highest in 1945, averaging 6.5 mrep over background (0.3–0.5 mrep) in a 24-hour period at the Route 4S, Mile 6 location. The maximum reading at the Route 4S, Mile 6 location was 12 mrep d^{-1} for the week ending

October 3, 1945. In 1946, H.M. Parker estimated that the tolerance concentration of ^{131}I on vegetation of 0.2 μCi kg^{-1} might produce 0.04 mrep hr^{-1} (0.96 mrep d^{-1}) (HW-7-5372). Based on this relationship, the amount of ^{131}I on vegetation at Rt 4S, Mile 6 in the latter half of 1945 would have been 1.4 μCi kg^{-1}, assuming most of the exposure rate was from ^{131}I.

There were no locations at which both C chambers and M and S chambers were employed. Examining data from similar areas leads to the conclusion that M and S chambers recorded higher values than C chambers, especially in 1945. This must be due to a greater response of the M and S chambers to ^{131}I.

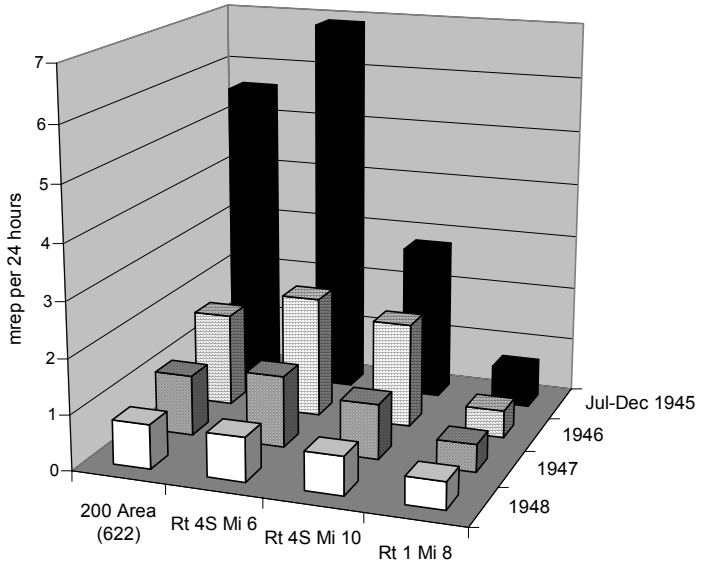

	200 Area (622)	Rt 4S Mi 6	Rt 4S Mi 10	Rt 1 Mi 8
1948	0.8	0.8	0.7	0.5
1947	1.1	1.3	1	0.5
1946	1.7	2.2	1.9	0.5
Jul-Dec 1945	5.6	6.9	2.8	0.7

Figure 4-3. Annual average radiation levels measured at four locations on the Hanford Site by M and S detachable chambers between July 1945 and the end of 1948. Route 4S runs southeast from 200 Areas. Of the locations shown here, the Route 4S, Mile 6 location is most representative of the military encampment that was closest to 200-East. Excess radiation levels were highest in 1945, averaging 6.5 mrep d^{-1} over background (0.3-0.5 mrep d^{-1}) at the Route 4S, Mile 6 location.

A review of the environmental reports through 1955 indicated that the M and S chambers were used at locations of greatest interest to this task. Therefore, we focused only on the M and S chamber exposure rate data for 1949–1955. In the first quarter of 1951, three new M and S-type detachable ionization chamber locations were established in new construction areas and near military encampments (HW-21214). The station near a military camp was at Route 4S, Mile 2.5. In 1952, monitoring at other military installations near 200 Areas began. There was a 32-month period, between April 1952 and November 1954, during which exposure rate monitoring was conducted at four military installations near the 200 Areas as well as in the REDOX area and at the REDOX perimeter. A statistical summary of those results is shown in Table 4-1. Maps locating these military installations are given in Section 3.1.

The exact locations of the REDOX perimeter and REDOX area measurement stations are not specified in the quarterly reports. Table 4-1 clearly shows that exposure rates at the REDOX perimeter are increased during this period of high ruthenium releases (see Section 2.2.2). In addition, the exposure rate measurements at the military installations are higher than the measurements at the upwind location at Route 1, Mile 8. The army camp H-50, which is 3.4 km S of REDOX, shows the largest range of exposure rates. The maximum value there was a monthly average of 5.8 mrad d^{-1} in February 1954. Next most affected were H-61 and H-51, camps to the W of REDOX. Their maximum values were measured in April 1954 and December 1953, respectively.

Table 4-1. Descriptive Statistics for Monthly Average Exposure Rates (expressed as mrep or mrad per day) near the REDOX Plant, at Four Military Installations, and at an Upwind Location (Route 1, Mile 8) between April 1952 and November 1954

Statistic	REDOX perimeter	REDOX area	PSN330 (aka H-40)[a]	PSN 320 (aka H-50)	PSN 310 (aka H-51)	PSN 300 (aka H-61)	Rt. 1, Mi 8
Mean	8.5	1.3	1.1	1.4	1.3	1.5	0.60
Standard Error	2.0	0.11	0.065	0.18	0.14	0.13	0.029
Median	2.9	1.1	0.96	1.1	1.0	1.4	0.60
Standard Deviation	11.6	0.63	0.35	1.0	0.79	0.73	0.16
Range	36.8	2.4	1.4	5.5	3.1	3.6	0.64
Minimum	0.63	0.42	0.53	0.34	0.48	0.58	0.27
Maximum	37.4	2.8	1.9	5.8	3.6	4.1	0.91
Count	32	32	30	31	32	32	32

[a] aka = also known as.

Figure 4-4 illustrates the time period during which the REDOX perimeter station shows elevated exposure rates. The highest monthly average exposure rate was 37 mrad d^{-1} at the REDOX perimeter in May 1954. The average there for the six-month period February–July 1954 was 31 mrad d^{-1}. An outdoor worker on a 40-hour per week schedule would have been exposed to 1.2 rad during this 6-month interval. The closest residence locations to REDOX were army sites H-50, H-51 and H-61. Exposure rates from the beta emissions from ground contamination would have been higher closer to the ground. In January 1955, the most intense ground contamination in the immediate vicinity of REDOX (within 3000 feet of the stacks) had been maintained to about 6 mrad hr^{-1} (144 mrad d^{-1}) at ankle level by the use of water sprinkling which carried the activity into the ground (HW-34882).

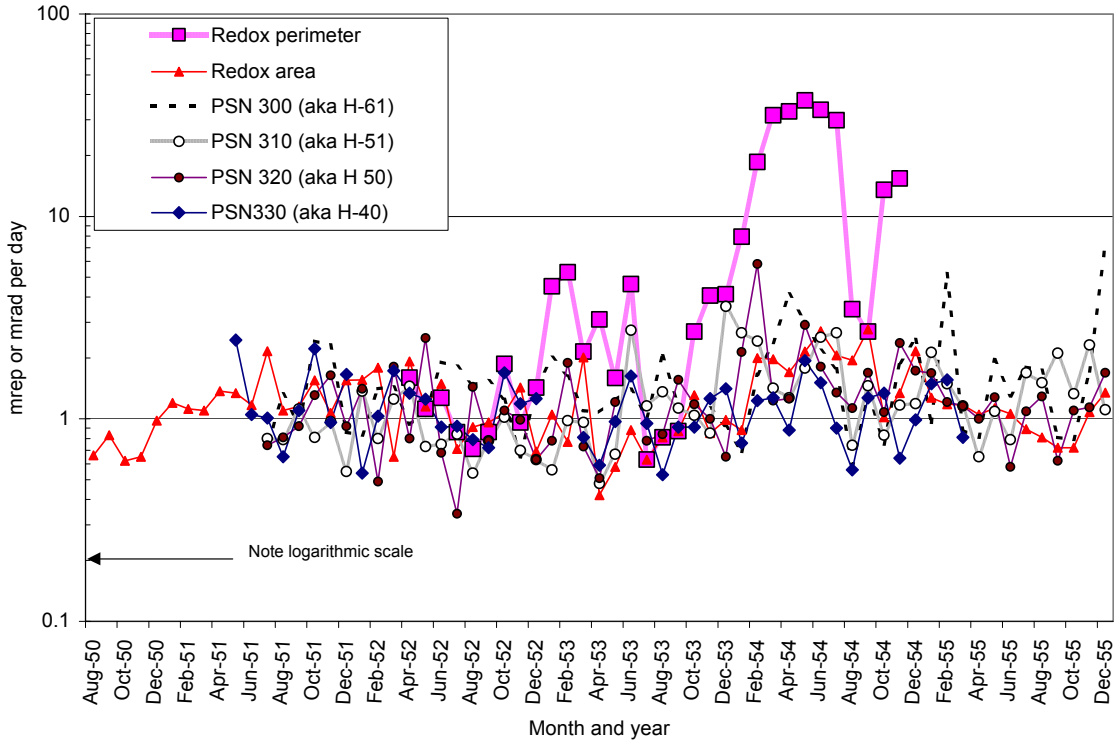

Figure 4-4. Exposure rates measured near the REDOX Plant and at four military installations. Measured exposure rates at the REDOX perimeter are the highest of all environmental stations monitored between 1945 and 1955. Monitoring at the perimeter was discontinued in December 1954, although monitoring continued in the REDOX area.

Figure 4-5 presents a long-term perspective of the time trend in exposure rates at a single location between 200-West and 200-East (the meteorology tower, or 622 building, at Route 1, Mile 3). Exposure rates are highest in 1945 and 1946. Then, exposure rates are relatively low until the 1952–1954 period, believed to be reflecting releases from the REDOX Plant. A similar trend is shown in Figure 4-6 for three locations along Route 4S, SE of the 200 Areas. The upwind location, Route 1, Mile 8, does not appear to be affected much by Hanford releases.

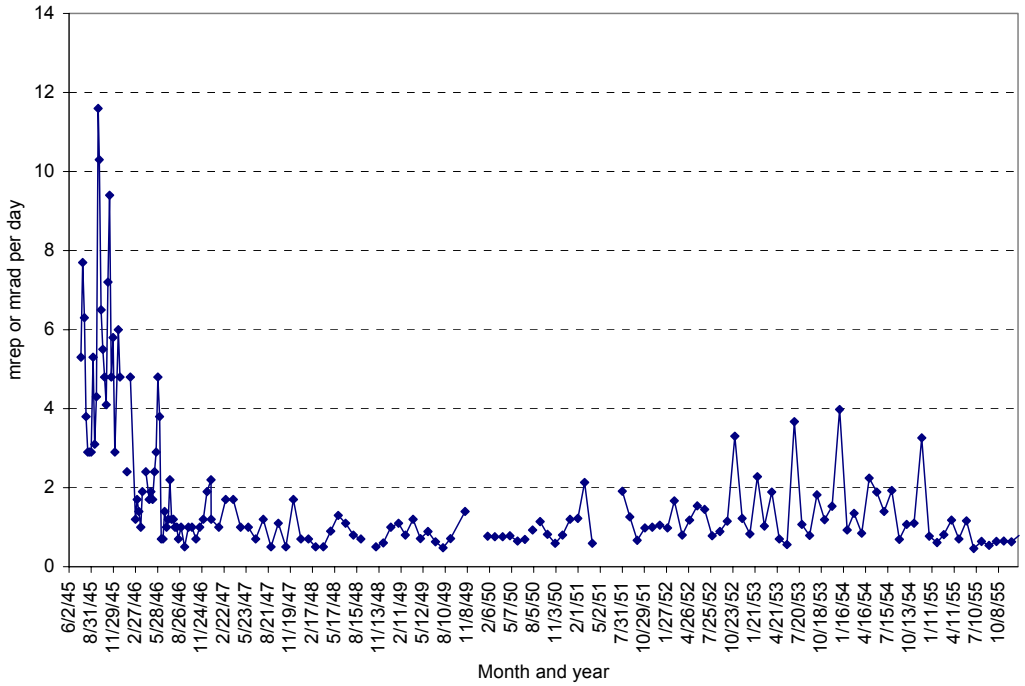

Figure 4-5. Time trend in exposure rates measured at the meteorology station between 200-West and 200-East.

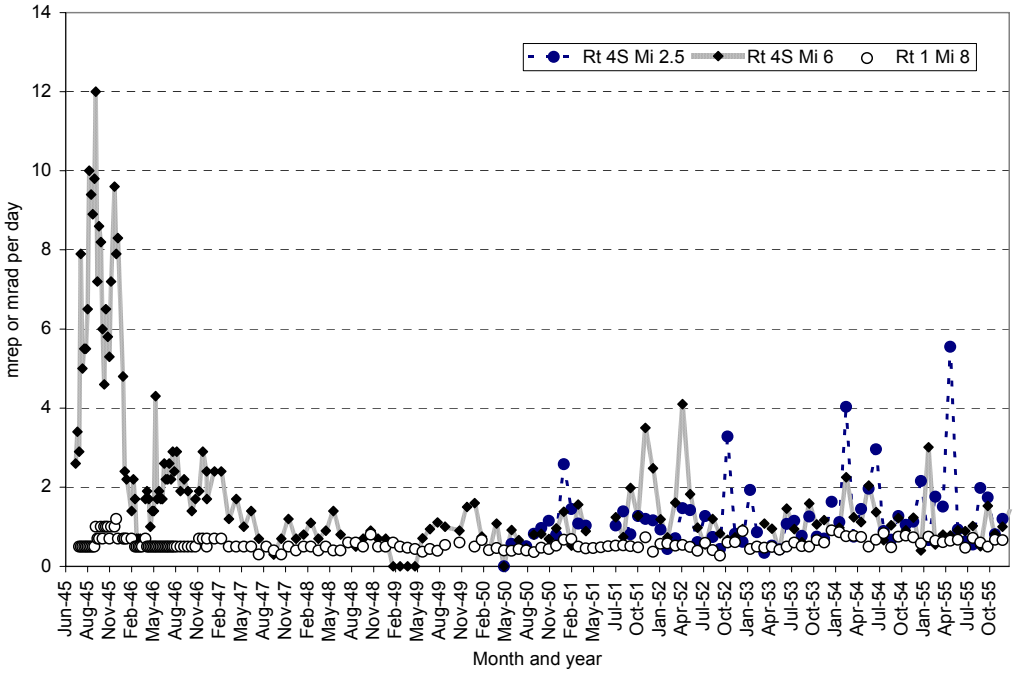

Figure 4-6. Time trend in exposure rates measured at two locations along Route 4S, SE of the 200 Areas, 1945–1955. The military installation PSN330 was between Mile 2.5 and Mile 6 along Route 4S. The sampling location at Route 1, Mile 8 represents an upwind exposure condition.

In summary, all available exposure data using M and S ionization chambers were compiled into electronic spreadsheets for the following 13 locations between July 1945 and December 1955:

- Route 1, Mile 8
- Meterology, Building 622, Route 3, Mile 1
- Route 4S, Mile 2.5
- Route 4S, Mile 6
- Route 4S, Mile 10
- REDOX perimeter
- REDOX area
- Military installations:
  - PSN 300 (aka PSN 61)
  - PSN 310 (aka PSN 51)
  - PSN 320 (aka PSN 50)
  - PSN 330 (aka PSN 40)
  - PSN 42
  - PSN 70.

The data record was essentially continuous throughout this period for four locations: Route 1, Mile 8; Route 3, Mile 1; Route 4S, Mile 6; and Route 4S, Mile 10.

Radiation levels were highest in 1945 and decreased throughout 1946–1948. Maximum exposure rates at the REDOX perimeter in 1954 were higher than any measurements made in 1945–1946. However, measurements made continuously at a location between the 200 Areas (Route 3, Mile 1) throughout the 1945–1955 time period show that exposure rates there were higher in 1945–1946 than in 1952–1954. Measurements were not made at the REDOX perimeter location until about April 1952 (Figure 4-4).

Exposure rate measurements reflect all beta-gamma emitting radionuclides present, including radioiodine, which is not the primary focus of our work. Perhaps the majority of the high exposure rate measured in 1945–1946 was due to 8-day radioiodine. Figure 4-7 illustrates the time trend in iodine and ruthenium releases and exposure rates between the 200 Areas and at the REDOX Plant perimeter. The annual average exposure rate between the 200 Areas is highest in 1945 when iodine releases are highest. However, exposure rates there also increase to 21–25% of the 1945 rate in 1953–1954 when iodine releases are relatively low and ruthenium releases are high. High exposure rates at the REDOX perimeter in 1954 definitely resulted from ruthenium releases (Figure 4-7).

The exposure rate data are useful for this work because they are some of the only historical measurements at locations where military personnel were actually exposed. The time trend also reflects total airborne releases of beta-gamma activity to air from Hanford facilities, which provides a valuable perspective.

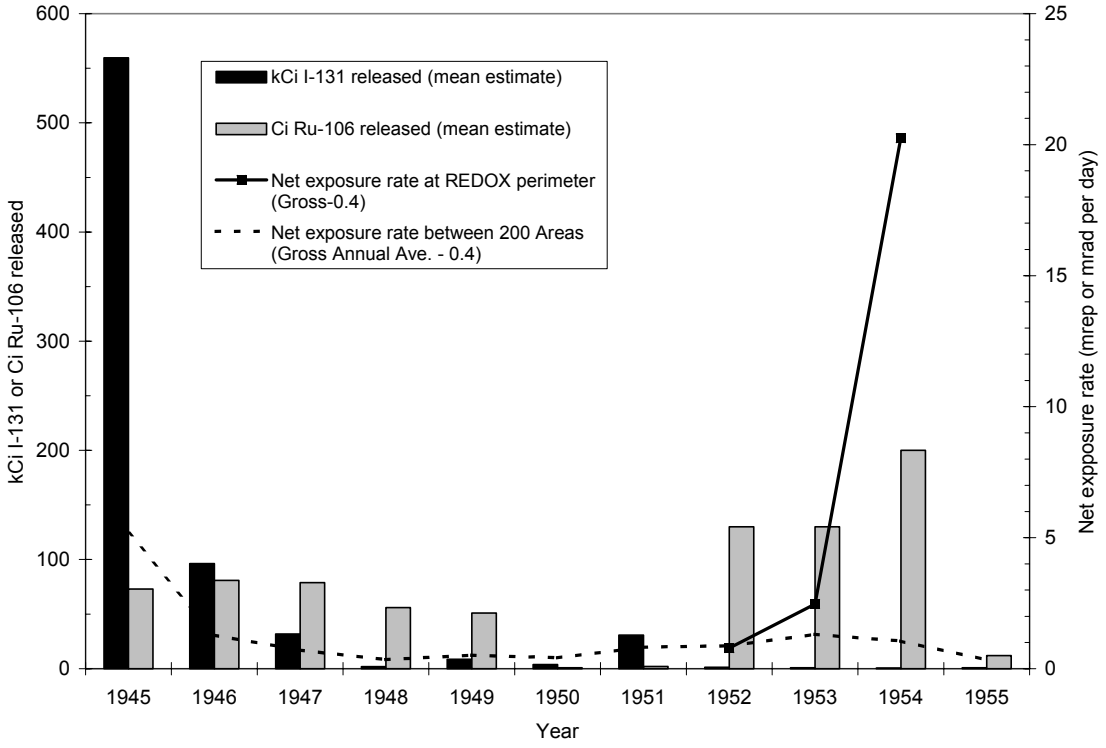

Figure 4-7. Time trends in annual ^{131}I and ^{106}Ru releases to air (see Section 2.4) and net exposure rates between the 200 Areas (Building 622) and at the REDOX Plant perimeter. A measured background exposure rate of 0.4 mrep per day was subtracted from the onsite exposure rate measurements to obtain net exposure rate.

Ground contamination surveys were conducted in the 1950s as part of the investigation of the REDOX ruthenium problem. Data from these surveys were sometimes expressed as dose rates (e.g., mrad per hour) as well as contamination levels in counts per minute. These data are reviewed in Section 4.1.6 of this report.

4.1.2 Air

Beta activity. Document HW-9871 presents summary tables of beta activity collected on ambient (i.e., in the outside environment) air filters for January 1946 through April 1948. Air was sampled continuously through a filter of about 1-1/2 inches diameter at a flow rate of about 2 $ft^3\ min^{-1}$. The filters were counted directly on thin mica-window Geiger counters. The sampling frequency was weekly (HW-12677, HW-13743), and the reporting frequency was monthly. The samplers were located under a protective cupola type roof (HW-13743). At that time, corrections to the measured count rates were made for geometry, collection efficiency, and radioactive decay, with the assumption that all beta activity came from ^{131}I. Data that showed residual long-lived activity after the decay of ^{131}I were not included in this document.

The air filters were not very efficient collectors of iodine. Other methods were used to monitor iodine in air. However, partial collection of iodine by the filters must be considered in interpreting these data. The first quarter 1949 report (HW-14243) states that the CWS filter paper

used in the air monitoring program had been shown to be about 3.5% efficient for gaseous radioiodine. Collections with chemical scrubber solutions showed about 10^{-9} to 10^{-10} μCi ^{131}I per liter of air (0.1–1 pCi m^{-3}) in the 200-West Area at that time. Decay studies in October 1948 (HW-11534) "continued to indicate that most of the activity collected on the air filters was of relatively long half-life material."

The locations monitored by the Hanford contractor for beta activity in air during 1946 and 1947 were Pasco, Richland, Benton City, 300 Areas, 200-ESE, 200-East Tower 11, 200-East Tower 18, 200-West Gate, Hanford, Gable Mountain, and 100-D. The sampling locations are shown in Figure 4-1, included in Section 4.1.1 of this report. The highest measured values of beta activity in air in 1946–1947 were obtained from the 200-East Tower 18 location. The data for Tower 18, 200 ESE, Hanford, and Pasco are illustrated in Figure 4-8. Units of 10^{-10} microcuries per liter, reported in HW-9871, were multiplied by 0.1 to obtain units of pCi m^{-3}, plotted here.

Concentrations of beta activity in air were highest during the first three quarters of 1946, the earliest routine air monitoring data we have located. Monthly average concentrations at 200-East Tower 18 exceeded 100 pCi m^{-3} in 6 of the first 8 months of that year (Figure 4-8). Concentrations at that location had dropped about 100-fold by the first quarter of 1948.

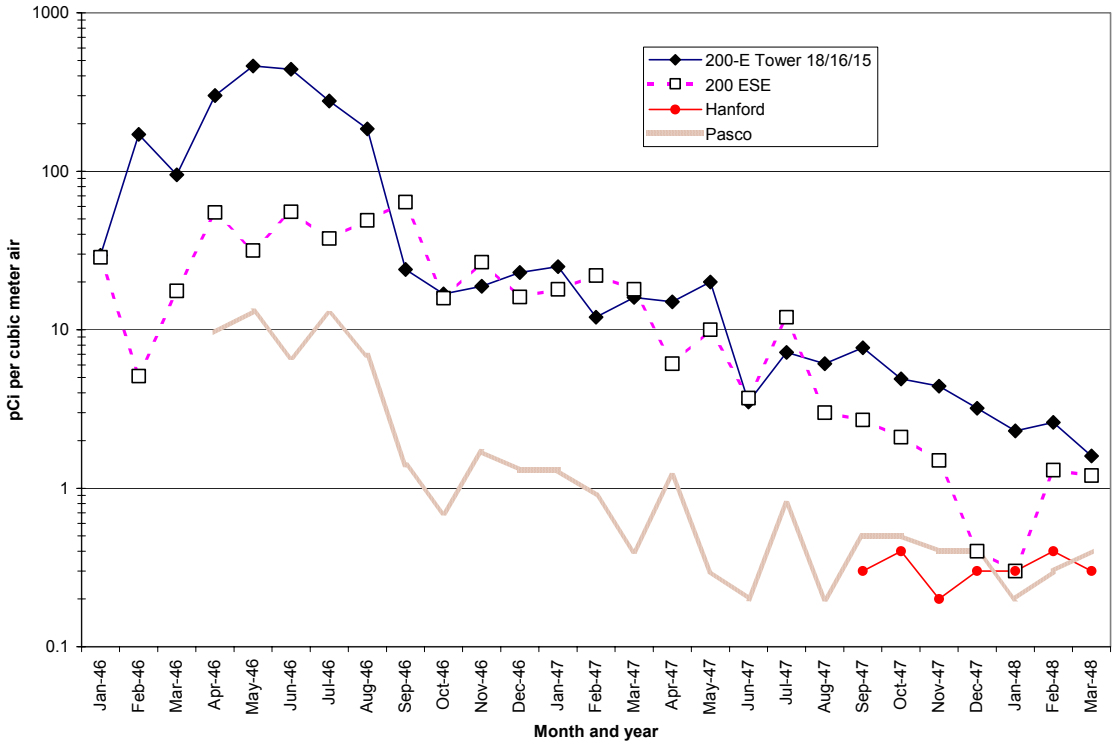

Figure 4-8. Monthly measurements of beta activity in air on and near the Hanford Site, 1946–1948 (data from HW-9871).

Operations began at T Plant in December 1944 and at B Plant in April 1945. We have found no routine air monitoring data for 1945. Document HW-7-1115 states that fumes looped to the ground during three of the first five dissolvings and that concentrations 100 times the permissible limit could occur near the ground for brief periods of time. The tolerance concentration for ^{131}I

in the atmosphere on the site was about 1.0×10^{-13} Ci cm^{-3}, or 100,000 pCi m^{-3} (HW-7-2604).[c] In the first quarter of 1947, the maximum value for air contamination was 1.7×10^{-6} μCi L^{-1} (1700 pCi m^{-3}) obtained using a hand pump filter unit near the 200-West Petrol Building during a period when the smoke fume was looping (HW-3-5511).

HW-8549 reports the results of a statistical analysis of air monitoring data from the third quarter of 1947. Average values are shown in Figure 4-9. No significant difference was found among samples taken at Pasco, Richland, 300 Area, and Hanford. Benton City was significantly higher than these other four locations.

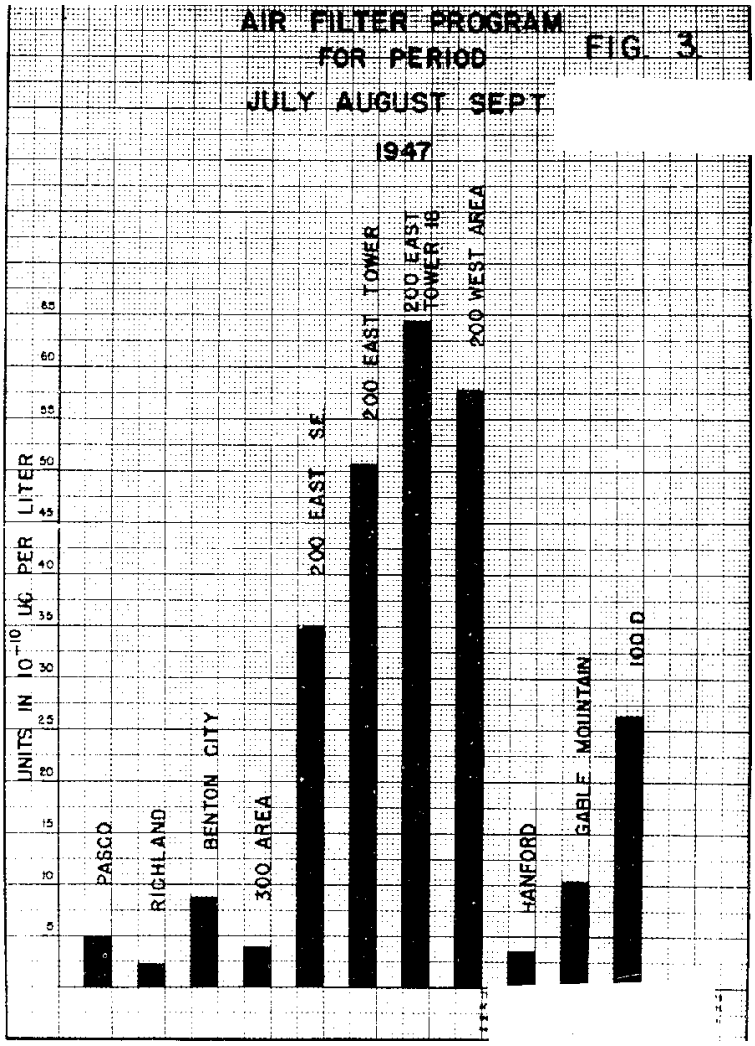

Figure 4-9. Total beta activity in air, third quarter 1947 (from HW-8549).

The air monitoring data set compiled from HW-9871 was continued using data from quarterly reports through 1955. Some of the locations shown in Figure 4-9 were discontinued and other locations were added. In the fourth quarter 1950, a new air monitoring station at the REDOX construction area had some of the highest nonvolatile beta measurements on the site

[c] Using modern dosimetric methods, this concentration equates to an effective dose of 66 mrem d^{-1} assuming 24-hour per day exposure.

(HW-21566). By the end of 1955, the following locations were being monitored for beta activity in air (HW-40871):

- Five locations in 100 areas
- Hanford
- White Bluffs
- 200-East Semi-Works
- 200-West West Center
- 200-West - REDOX
- Gable Mountain
- Military Camp, PSN 50 (later called H-50)
- 200-West East Center
- 300 Area
- 1100 Area
- Pasco
- Benton City
- Riverland.

Figure 4-10 provides a long-term perspective on beta activity in air during the early years of Hanford operations. In general, beta concentrations in air were highest in 1946. An exception was May 1951, when failure of silver reactors[d] in 200-West resulted in a monthly average concentration of 200 pCi m^{-3} at the 200-West Gate (HW-22313).

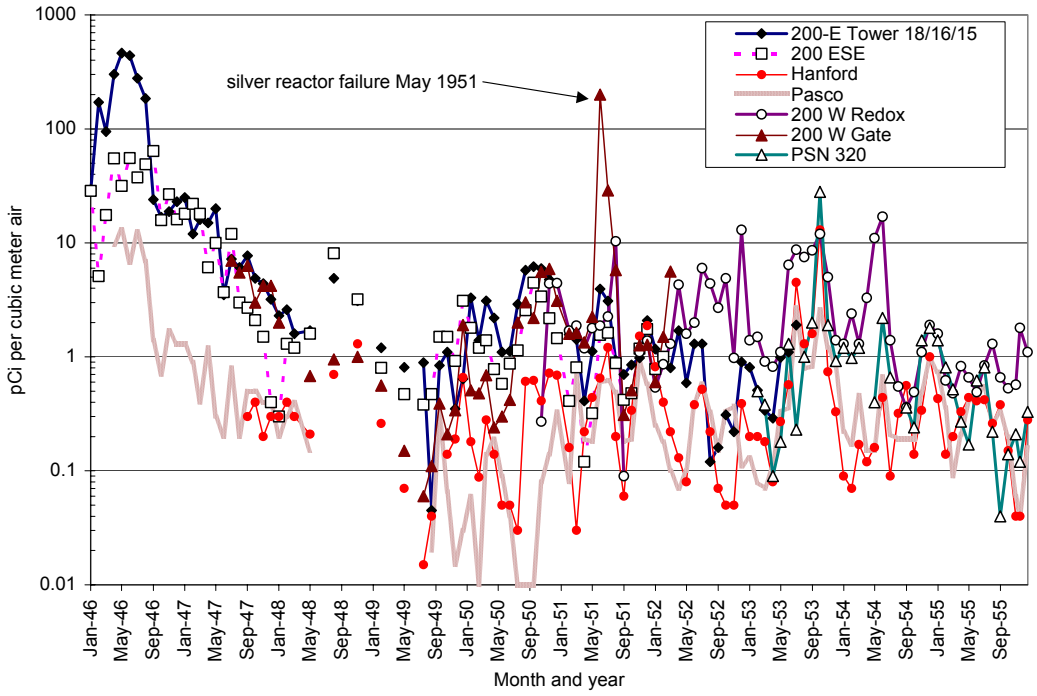

Figure 4-10. Beta activity in air on and near the Hanford Site, 1946 through 1955. Data are monthly averages, except for May 1948–May 1949, which are quarterly.

[d] Effluent control method for radioiodine.

Table 4-2 includes the annual average concentrations calculated from the reported monthly or quarterly data. A weighted average was used in 1948 and 1949 to accommodate both the quarterly and monthly reported values in those 2 years. Figure 4-11 illustrates the same data graphically. The monitoring record at Pasco is the most complete over this time interval. Table 4-3 shows the concentrations measured at the other locations relative to that measured at Pasco.

Table 4-2. Annual Average Concentrations of Beta Activity (pCi m^{-3}) in Air on and near the Hanford Site (1946-1955)

	Location						
Year	200-East Tower 18/16/15	200 ESE	200-West Gate	200-West REDOX	PSN 320	Camp Hanford	Pasco
1946	170	34					6.0
1947	10	8.3	5.0			0.30	0.59
1948	3.0	3.5	0.82			0.64	0.18
1949	0.82	0.97	0.43			0.17	0.085
1950	3.4	1.8	2.0	3.0		0.32	0.093
1951	1.5	0.86	20.5	2.2		0.63	0.41
1952	0.76	1.0	3.6	3.6		0.23	0.24
1953	0.86			4.6	3.1	1.9	0.84
1954				3.5	1.1	0.32	0.38
1955				1.1	0.33	0.28	0.16

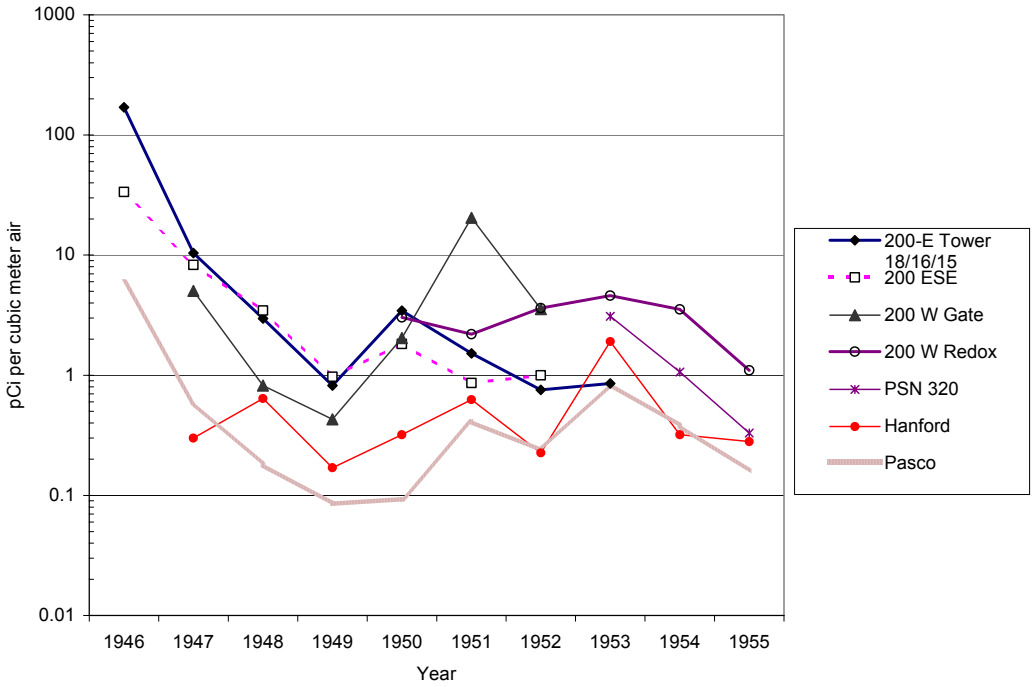

Figure 4-11. Annual average concentrations of beta activity in air at seven locations on and near the Hanford Site, 1946–1955.

Pasco is also a reasonable location to evaluate weapons fallout levels in the 1950s. At that time, fallout from nuclear weapons testing in Nevada and the Pacific sporadically influenced beta activity in air throughout the northwestern United States. Hanford publications that address the fallout issue include HW-20810, HW-22072, HW-28925, and HW-33754. For example, February 1951, May–June 1952, and June 1953 were times during which weapons fallout activity was significant in environmental air samples. In the 1950s, hot spots from weapons fallout were more common than in the 1960s, when larger yield bombs were being tested, which injected their radioactive debris higher into the atmosphere.

Gross beta activity in air at Pasco is compared with measurements made by the National Air Sampling Network in two regions of the United States in 1953–1955 (Figure 4-12). The measurements at Pasco have roughly the same magnitude and trending as the other stations, indicating that at this time, Pasco is a reasonable location to estimate the local background fallout levels for the Hanford area. Weapons fallout continued to increase in the 1960s, reaching a peak at most areas of the United States in 1963. Long-lived radionuclides deposited from weapons fallout in the Hanford area are discussed in Section 4.2.2

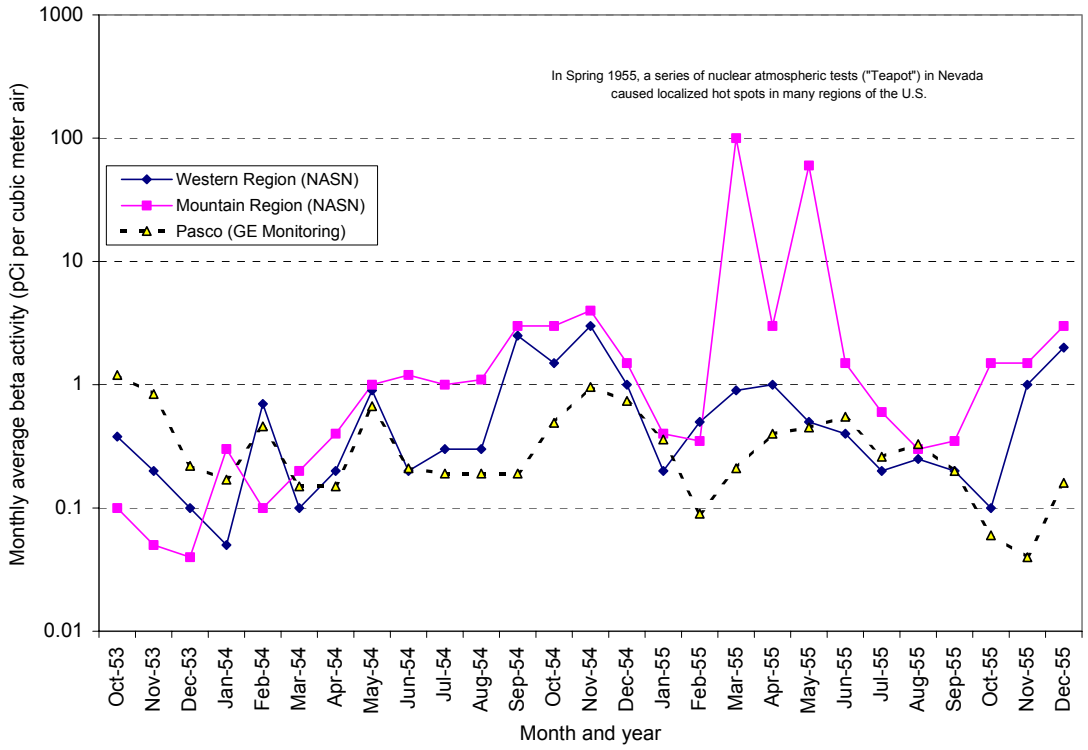

Figure 4-12. Comparison of monthly average concentrations of beta activity in air with measurements made by the National Air Sampling Network at two other regions of the U.S.

In 1946–1950, when fallout was relatively low, gross beta activity in air at Pasco was likely to be mostly from Hanford releases. Annual average concentrations of beta activity in air at the four 200-Area locations were 17 times higher (range 5-37) than those measured in Pasco (Table

4-3). This magnitude comparison agrees with the conclusions presented in HW-7-5372 based on ^{131}I in vegetation in 1945–1946. Those vegetation data, presented in Section 4.1.4 of this report, showed 15–20 times higher concentrations in 200-East Area compared to Richland. Vegetation at Hanford in 1945–1946 was 3 times as contaminated as Richland, which was expected to represent the areas of Benton City and Kennewick as well. Similarly, the average beta concentration in air at Camp Hanford was about 2 times that in Pasco for the period 1947–1955 (Table 4-3). The relatively high ratios in 200-West compared to 200-East for some years are due to specific releases unique to 200-West (e.g. the REDOX Plant releases in 1952 and silver reactor failure in May 1951).

Table 4-3. Annual Average Concentrations of Beta Activity in Air Expressed Relative to Pasco

	Location						
Year	200-East Tower 18/16/15	200 ESE	200-West Gate	200-West REDOX	PSN 320	Camp Hanford	Pasco
1946	28	5.6					1.0
1947	18	14	8.5			0.5	1.0
1948	16	19	4.6			3.6	1.0
1949	9.6	11	5.1			2.0	1.0
1950	37	20	22	33		3.4	1.0
1951	3.7	2.1	50	5.3		1.5	1.0
1952	3.2	4.2	15	15		1.0	1.0
1953	1.0			5.5	3.7	2.3	1.0
1954				9.3	2.8	0.8	1.0
1955				6.9	2.1	1.8	1.0
Average of available years	15	11	18	12	2.8	2.0	1.0

Alpha activity. There was a limited amount of routine monitoring of alpha activity in air by the Hanford contractor during this time period. Reporting of these data began in the second quarter of 1951. A counter geometry correction of 52% and self-absorption correction of 50% were used. Data were reported as quarterly average concentrations. Concentrations as high as 8 femtocuries per cubic meter[e] (fCi m^{-3}) were sometimes reported as less than detectable. The available data through 1955 are plotted in Figure 4-13. The highest quarterly average concentration was 43 fCi m^{-3} in 200-West Area at the end of 1951. In the second quarter of 1956 (HW-44215), alpha activity in air was near the detection limit of 4 fCi m^{-3} except for a weekly maximum at REDOX of 140 fCi m^{-3} after the "plutonium incident on June 18."

In addition to these routine monitoring results, some information from special sampling was located. In the third quarter of 1952, four air filters were taken near REDOX area that contained concentrations of uranium, plutonium, and ruthenium of 0.18, 32, and 1600 fCi m^{-3}, respectively (HW-27510). Other studies also showed that most excess alpha activity in 200 Areas is

[e] A femtocurie, abbreviated fCi, is 10^{-15} Ci, or 1/1000 pCi. This unit is useful for alpha-emitting radionuclides in ambient air because concentrations are lower than beta-emitting radionuclides.

plutonium (HW-9259, HW-10261, HW-15802). In contrast, the alpha contamination in the environment of 300 Areas was more likely to be uranium (HW-12677).

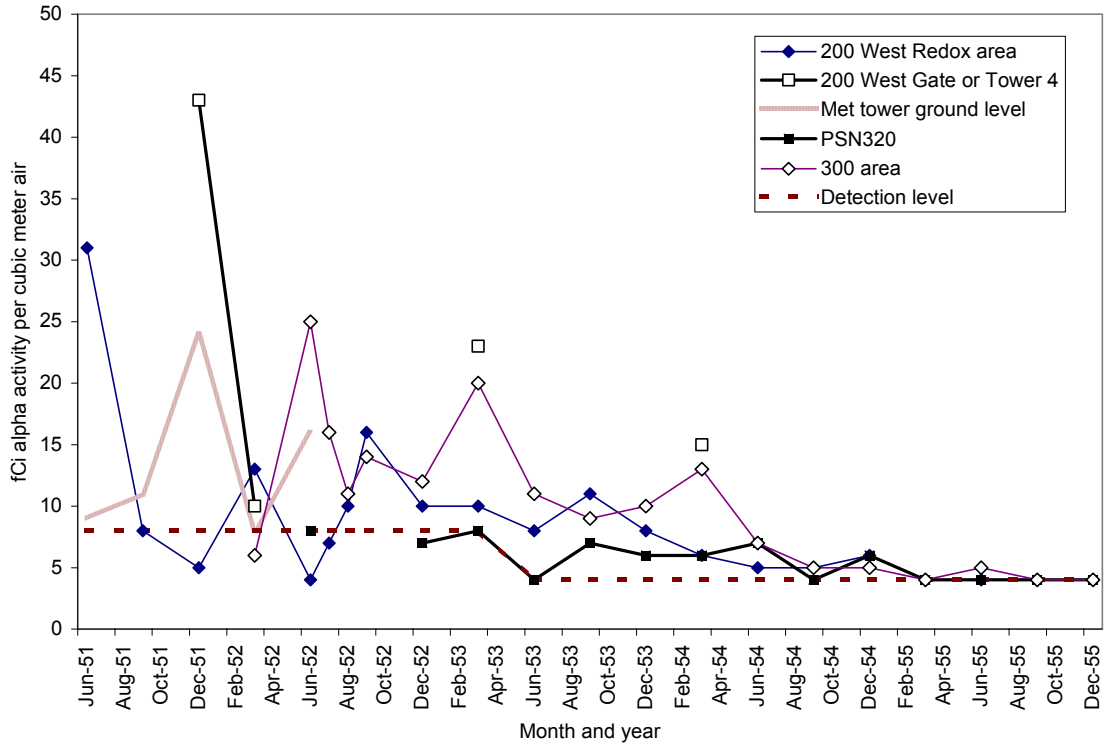

Figure 4-13. Alpha activity in air on the Hanford Site, quarterly averages, 1951–1955.

The uses of the early (1946–1955) air monitoring data for this project are limited by several factors including lack of knowledge about

- Radionuclides present
- The percentage of the measured activity that was from sources other than Hanford
- Information needed to assess data quality.

However, the time and spatial trends are useful as a check on the calculations based on estimated releases and dispersion. Because air sampling devices are inefficient collectors of large particles, the air monitoring data are not as useful as ground contamination surveys for assessing large particle contamination. However, the air monitoring data are more indicative of trends in concentrations of particle sizes that were respirable.

Monitoring of radioactive particle numbers in air samples is discussed in Section 4.1.5 of this report.

4.1.3 Rain

Rain is another medium that was monitored for beta activity in the early years of Hanford operations. As of October 1946, there were 20 permanent rain gauges in operation from which samples were collected once a week if there had been any rain. The rain was evaporated after reducing free iodine with sodium thiosulphate to prevent its loss. The dried sample was counted on a thin mica-window counter. It was assumed that all activity was 8-day radioiodine. However,

the third quarter 1947 report (HW-8549) notes that current experimental evidence indicated the presence of an

> …active filterable substance in some rain samples. Preliminary investigation revealed that filtering of the rain removes most of the activity from the rain; a radiograph of the filter showed that most of the activity was sorbed out on the filter paper; small individual particles which were slightly more active than the overall contamination on the filter were isolated. The exact origin of these particles is not yet known. Decay curves of some of these very active rain samples indicate a relatively long half life.

Similarly, in the first quarter of 1948 (HW-10242), a rain sample collected at Riverland on February 23, 1948, indicated 0.0125 μCi L^{-1} of beta activity that was confined to the filter rather than dissolved in the liquid portion of the sample. The half-life was greater than 8 days expected for radioiodine. The authors state, "This problem is under consideration with the problem of residual longer half-life material found in some air filters and vegetation samples."

In the bimonthly "environs" reports of the Health Instruments Section (HW-7-5042), a maximum onsite and offsite value for radioactivity in rain is given beginning in September 1946. These are the earliest rain data we located. Figure 4-14 illustrates the maximum reported concentrations in 1946 and 1947 for 200-West, 200-East and outlying areas, such as Pasco or Benton City. It is clear that concentrations in the 200 Areas are higher than offsite. On average, beta activity in rain was 26 times higher in 200-West and 11 times higher in 200-East than in outlying areas in 1946–1947. The highest concentration was 0.38 μCi L^{-1} in a sample collected November 15, 1946 in 200-West. There was only one sampling period during this interval in which the outlying area concentration was greater than the onsite concentration.

Beginning in November 1946, a bimonthly average value is also given along with the maximum concentration for the following grouped zones:

- Within 200-West Area
- Within 200-East Area
- Within the 100 Areas
- Intermediate Zone, On Area
- Outlying Zone, Off Area.

Report HW-10242 clarifies these location groupings. All onsite locations *not* within the boundaries of the 200-East, 200-West, or 100 Areas were included in the group called intermediate zone. This intermediate zone, thus, represents exposure locations for military and construction personnel outside individual area boundaries. Locations beyond the Hanford perimeter fence were grouped as the outlying zone. A map of all the locations in January 1948 was included in HW-9496; the map is included as Figure B-1 of this report.

A column chart of average beta activity in rain was included in the third quarter 1947 monitoring report (HW-8549). The influence of 200 Area releases on contamination levels in rain at this time is clear (Figure 4-15).

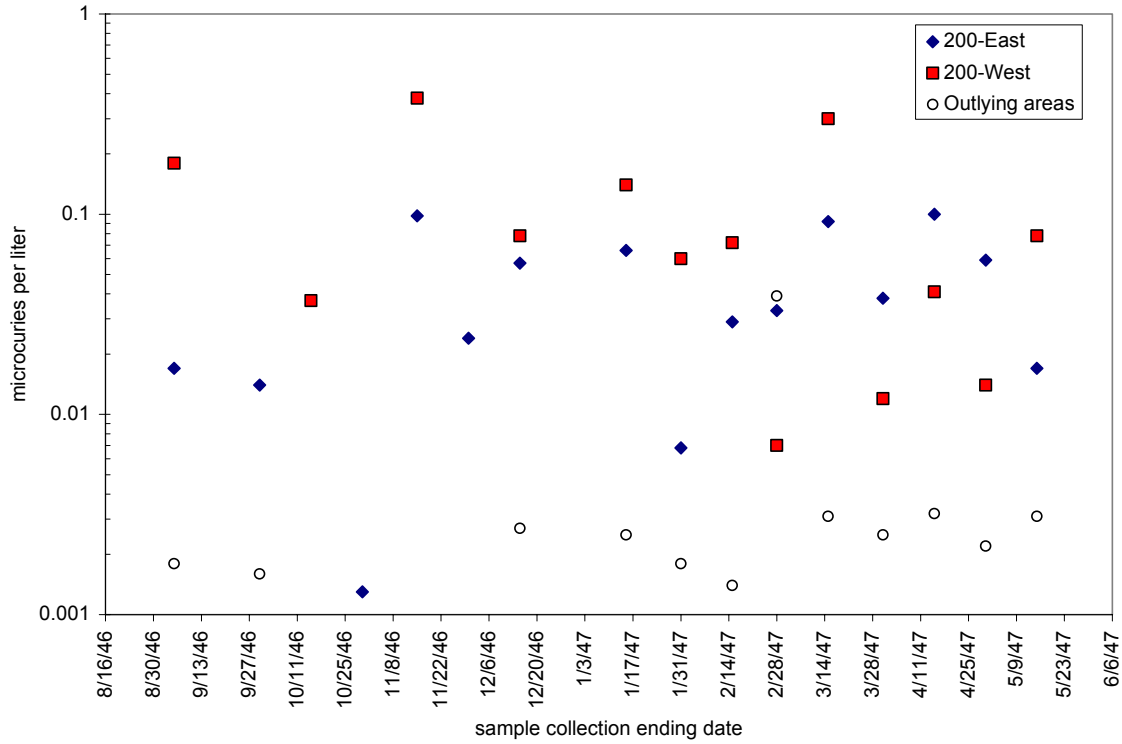

Figure 4-14. Maximum reported concentration of beta activity in rain in 1946 and 1947 at 200-West, 200-East, and outlying areas (e.g., Benton City and Pasco) (data from report HW-7-5042).

Beginning in 1948, the rain data are again presented as numerical values in tables, although as a quarterly average. We compiled the data from 10 locations for 1946–1955 into an Excel spreadsheet. The time trend for five of these locations is shown in Figure 4-16. The rain data show more scatter than the air monitoring data. One reason could be that the air samplers capture relatively small particles, whereas the rain collectors catch all particles including the large active particles. On at least one occasion (June 30, 1952), an active particle was identified as contributing to an unusually high concentration in a rain sample from the Route 4S, Mile 6 location. The October 1948 monthly report states that there were about 100 active particles per rain sample per month in 200-East and 200-West Areas.

Weapons fallout also contributed to large variations in the beta content of precipitation. Known weapons testing fallout events in 1953 and 1954 overlapped with the high ruthenium releases from REDOX, making interpretation of the data difficult. About 1 week after the start of a series of test explosions at the Nevada Proving Ground during the latter part of March 1953, the number of radioactive particles in the atmosphere in the Hanford environs started to show considerable fluctuation (HW-29514). Large amounts of Nevada fallout arrived in late May and early June of 1953. Beta activity in rain was 10 to 1000 times higher after arrival of fallout. Concentrations as high or higher than onsite were measured at remote locations. See HW-28925 for detailed summaries showing the magnitude of the contamination that resulted from this fallout. Fallout contamination of rain was evident again in August and September of 1953 (HW-30174).

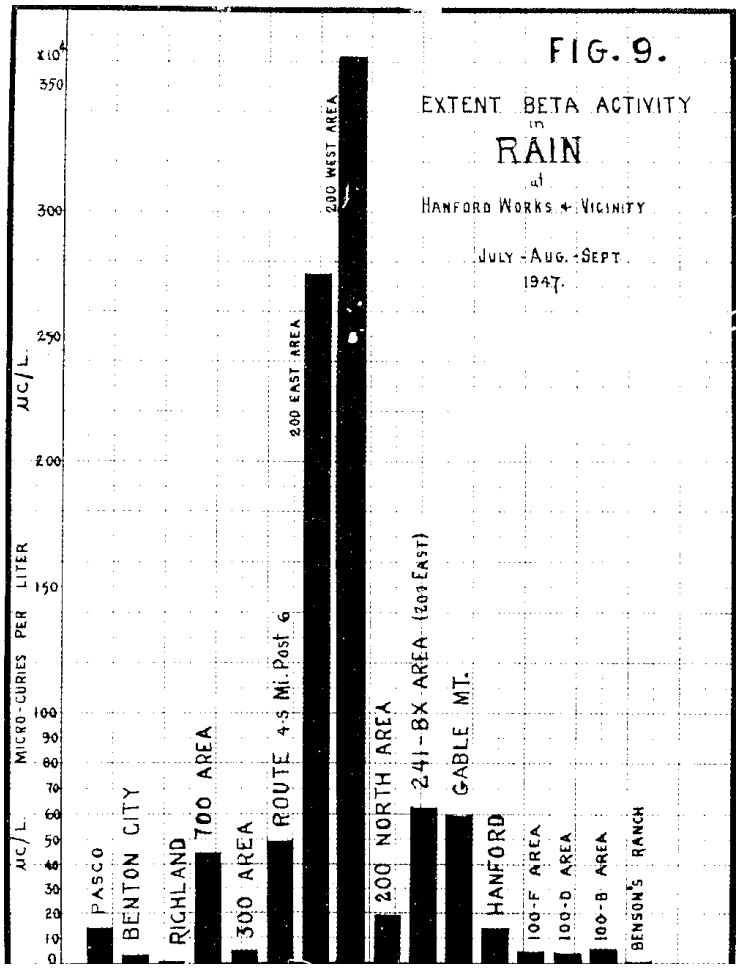

Figure 4-15. Total beta activity in rain, third quarter 1947 (HW-8549).

Annual average concentrations in rain were generated from the reported data (Table 4-4). A time-weighted average was used in 1947 when both bimonthly and quarterly concentrations were reported. The time trend in annual averages for 200-West, 200-East, REDOX, and outlying zone is illustrated in Figure 4-17. The highest annual average concentration of beta activity in rain between 1946 and 1956 was 0.51 μCi L^{-1} in the onsite intermediate zone in 1953. This was highly influenced by Nevada Test Site fallout in an early morning rain on May 26 (HW-29514). The next highest annual average conentration during 1946-1955 was 0.11 μCi L^{-1} from the REDOX area in 1954. This is consistent with the high ruthenium releases that occurred in that year and is 10 times higher than all other locations except 200 West (Table 4-4). The first quarter 1954 environmental report (HW-31818) describes having collected seven snow samples on January 22, 1954. The beta activity concentrations in snow within 2000 ft SE of the REDOX stack were 100 times greater than at the military installation near 200-West.

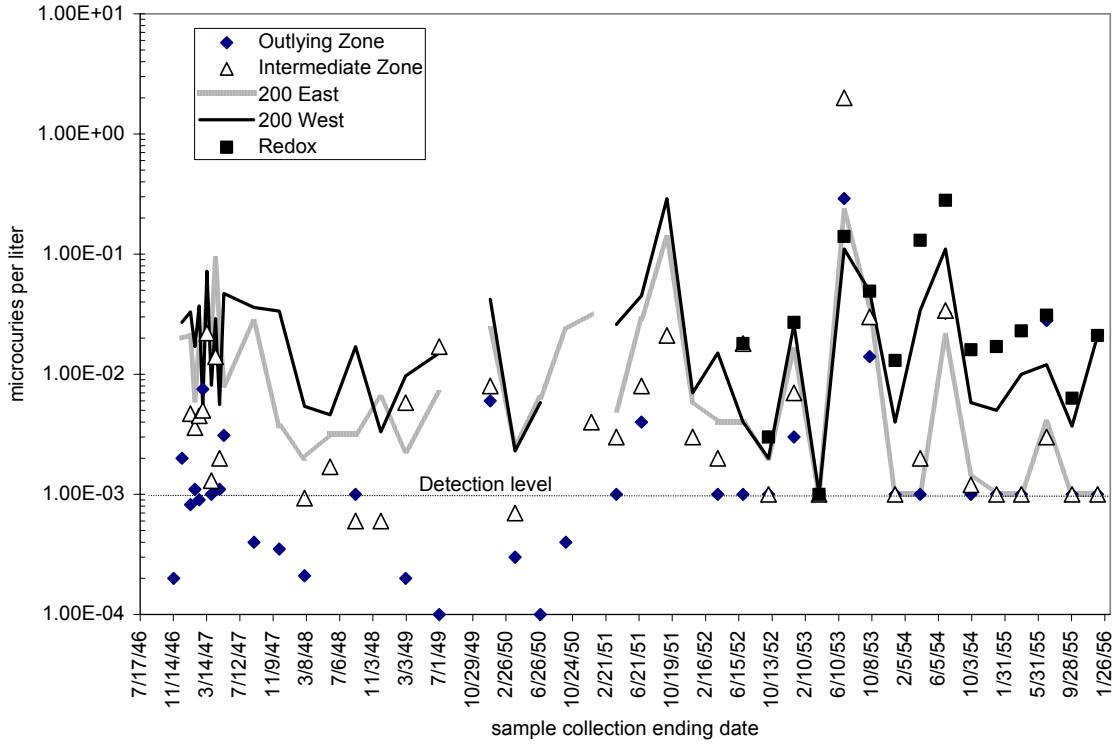

Figure 4-16. Average concentration of beta activity in rain, 1946–1955. Reporting frequency varied from bimonthly to quarterly.

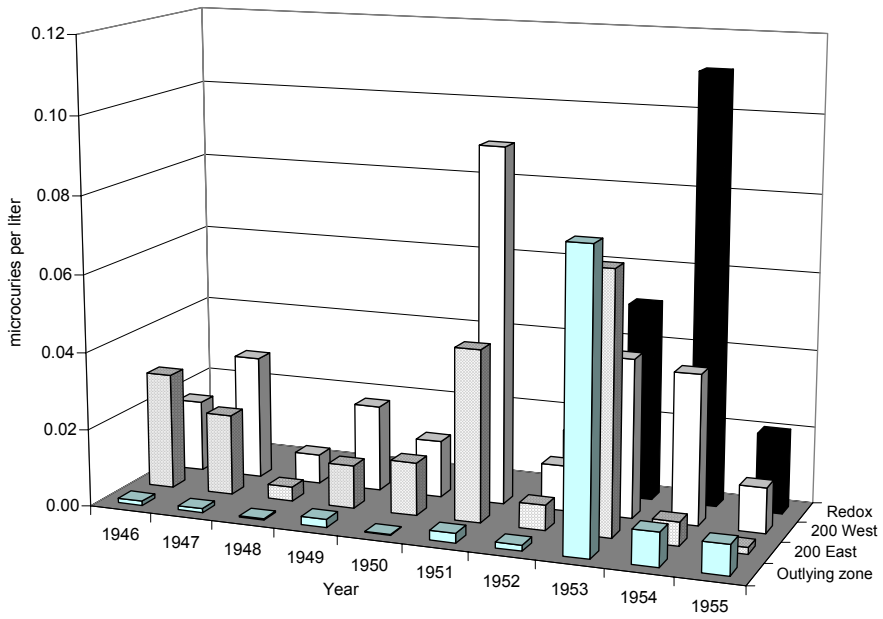

Figure 4-17. Annual average concentrations of beta activity in rain at three onsite locations and offsite (outlying zone), 1946–1955 (data presented in Table 4-4).

The third highest annual average concentration was 0.092 μCi L^{-1} at 200-West in 1951. In 1953, weapons fallout events affected concentrations at most locations, resulting in a higher concentration at outlying areas (0.077 μCi L^{-1}) than onsite. Before 1953, the annual average concentration at outlying areas was barely detectable (≤0.002 μCi L^{-1}).

Overall, in the years 1946–1952, which preceded the effect of significant fallout in rain samples, the annual average concentrations of beta activity in rain of 200-East and 200-West Areas were 25 times higher (range 4–60) than observed in outlying areas. This is in good agreement with the magnitude comparisons made from air and vegetation data. These environmental data give an indication of the relatively greater exposure to Hanford releases for outside workers in the 200 Areas compared to offsite locations.

Table 4-4. Annual Average Concentrations (μCi L^{-1}) of Beta Activity in Rain at 10 Locations on and off the Hanford Reservation, 1946–1955

	Location									
Year	REDOX	200-West	200-East	Inter-mediate zone	Meteor-ology	Rt 4S, Mi 6	Hanford	Pasco	Outlying zone[a]	Richland
1946		0.019	0.030					<0.001	0.001	
1947		0.032	0.021	0.007				0.001	0.001	
1948		0.008	0.004	0.001					<0.001	
1949		0.022	0.011	0.010	0.005		<0.001		0.002	<0.001
1950		0.015	0.016	0.002	0.007	0.001	<0.001	<0.001	<0.001	<0.001
1951		0.092	0.044	0.009		0.007	0.007	0.001	0.003	0.001
1952	0.016	0.012	0.007	0.007	0.005	0.019	0.003	0.002	0.002	0.002
1953	0.051	0.041	0.067	0.508	0.032	0.003	0.008	0.223	0.077	0.009
1954	0.111	0.039	0.006	0.010	0.011	0.011	0.011	0.010	0.009	
1955	0.020	0.012	0.002	0.002	0.001	0.002	0.005	0.001	0.008	

[a]Or Benton City, whichever is listed.

4.1.4 Vegetation

Beta activity. The earliest vegetation monitoring data from the Hanford area are tabulated by month in HW-7-5372 for three locations—200-East, Hanford (the old town site), and Richland—between November 1945 and October 1946. Results were total beta (also called gross beta) activity, decay-corrected as if all activity present were ^{131}I. The first 3 months of this interval show the highest levels of radioactive contamination. The highest monthly average reported value was 30 μCi kg^{-1} in December 1945 in vegetation from 200-East. The authors observed that on average, the 200-East Area was 15 to 20 times as contaminated as Richland, and Hanford was 3 times as contaminated as Richland, which was expected to represent the areas of Benton City and Kennewick as well.

The annual environmental monitoring report for 1946 (HW-3-5402) describes the method of analysis for vegetation: "A one gram sample of the vegetation, taken at these locations, is mounted on cardboard and counted directly with a thin window chamber connected to a scaling unit. Correction is made for the counting geometry, self-absorption in the vegetation, and sample decay for the period between sampling and counting." The fourth quarter 1947 report (HW-9496) states that vegetation samples were taken at least once every 4 weeks from all locations.

Healy (HW-10758) discusses briefly some analytical aspects of vegetation sampling and counting as of 1948. The routine program for analysis of iodine in vegetation began late in 1945. One-gram aliquots of vegetation were mounted in the form of a small pellet about 1-1/2 in. in diameter by using a hand press. Testing using known tracers indicated that a self-absorption factor of 3 should be applied for iodine. The author stated that this factor is probably not applicable to long-lived activity, but he did not indicate if it was still used. In early 1948, the measurement of long-lived activity in vegetation began. This took advantage of the volatility of iodine in hot nitric acid. The remaining mineral salts were plated on a stainless steel plate for beta counting. The counting detector was a 1-in. diameter thin mica window counter contained in a lead pig[f] with 1-1/2-in. walls. Stack samples and air filters were counted on the first shelf below the window, and vegetation samples were counted on the second shelf because of the bulky pellet.

Monthly or biweekly measurements of ^{131}I on vegetation were located for the time interval January 1946 through May 1947 (HW-7-5934, HW-7-5145, HW-7-5301, HW-7-5605, HW-7-5042). Quarterly average concentrations were obtained for the last half of 1947 and 1948 from the quarterly reports. An example of the reporting of the data at this time is shown in Figure 4-18.

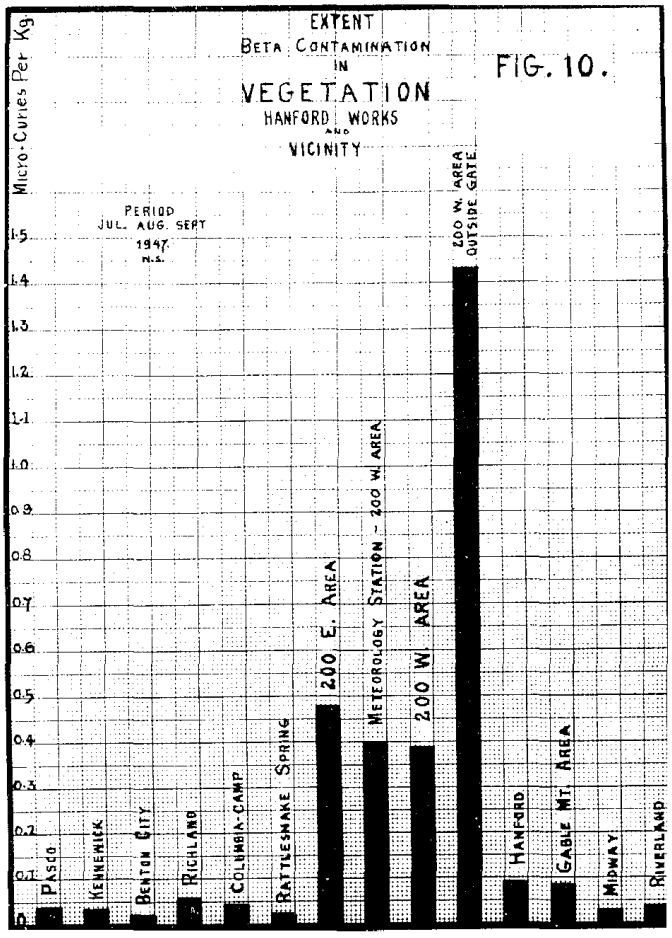

Figure 4-18. Total beta activity in vegetation, third quarter 1947 (from HW-8549).

[f] A shielded container.

Report HW 7-5934 includes a table of ^{131}I concentrations (monthly averages) on vegetation for eight locations (Pasco, Kennewick, Benton City, Columbia Camp, Richland, Gable Mt., Hanford, and Rt. 4S-Mile 4) between January 1946 and March 1947. This report notes that detectable contamination levels (0.05 μCi kg^{-1} or above) were measurable at distances up to 150 and 200 mi from the separations plant stacks. Areas that had levels above the tolerance level[g] of 0.2 μCi kg^{-1} were all within a radius of about 50 mi and included the communities of Pasco, Kennewick, Benton City, and Richland.

Figure 4-19 illustrates the 3-year time trend in ^{131}I concentrations in vegetation from Richland, Hanford, and near 200 Areas. A footnote in report HW-7-5042 in 1947 clarifies that the "near 200 Areas" location group was near Route 4S, Mile 4. This is very near the military camp PSN 330 (see Section 3.1.2). From January 1946 through November 1948, the contamination levels on vegetation at Hanford and Richland are similar (0.29 and 0.22 μCi kg^{-1}), but the location near the military camp at Route 4S, Mile 4 was over 6 times higher (1.6 μCi kg^{-1})

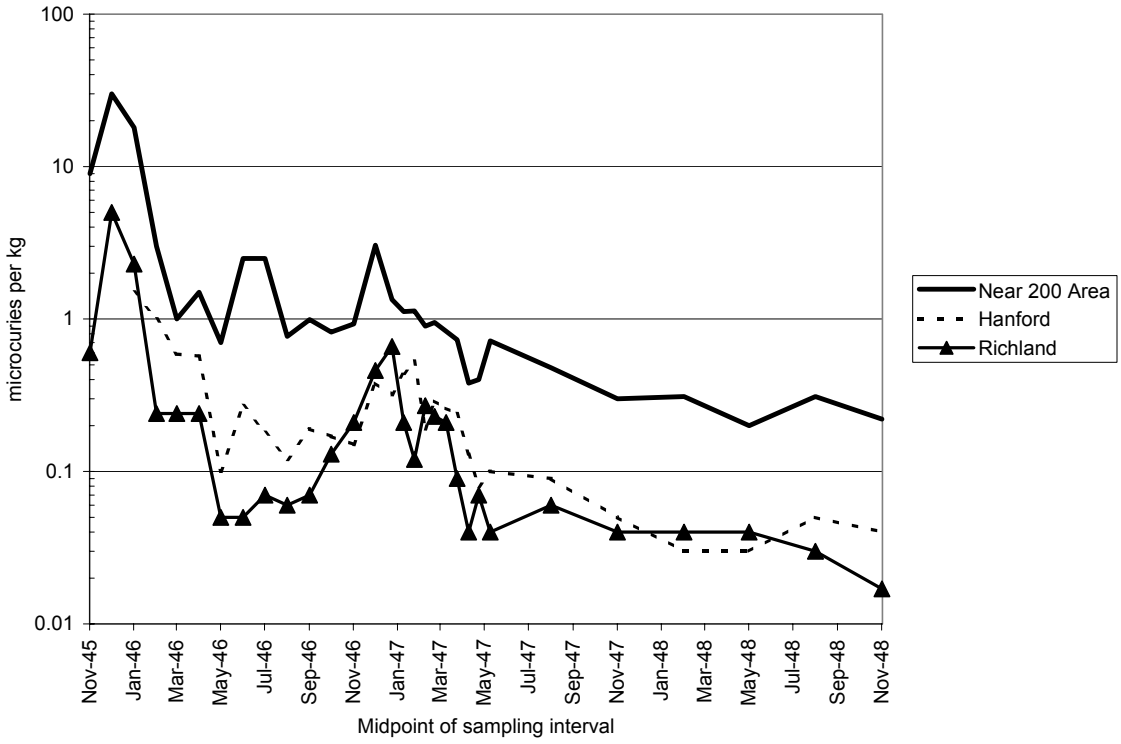

Figure 4-19. Total beta activity on vegetation on and near the Hanford Site, 1945 through 1948. At this time in Hanford history, the iodine was not chemically separated from nonvolatile beta activity in vegetation samples. Counting results were corrected as if all activity present were ^{131}I (data compiled from various Hanford reports).

[g] Provisional "tolerable" contamination level established by H. Parker in January 1946 based on ingestion of ^{131}I by man and animals and limitation of dose to the thyroid of 1 rad per day (HW-7-3217).

To illustrate the spatial differences at this time, average concentrations for calendar year 1946 and the first 5 months of 1947 were computed from monthly and biweekly reported concentrations for seven locations (Figure 4-20). Columbia Camp was a Federal prison camp located along the horn of the Yakima River south of the reservation; it operated between February 1944 and October 1947 (see last part of Section 3.1.2). The Hanford town site was closed before 1946. During 1946, vegetation from all areas in Figure 4-20 contained radioactivity above the tolerance concentration (0.2 μCi kg^{-1}), indicating unacceptable levels of contamination, even by the practices of the time.

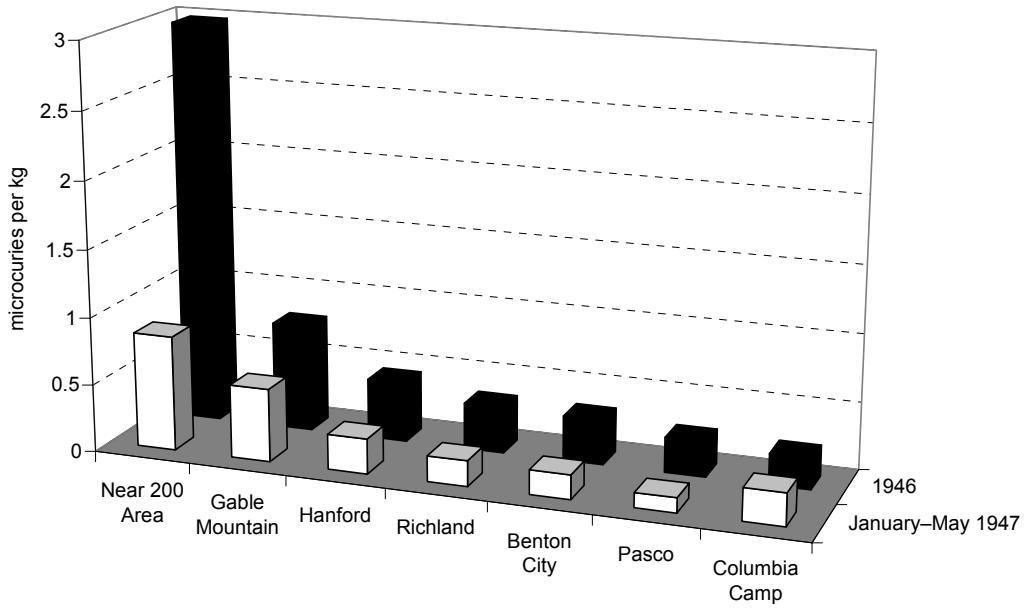

	Near 200 Area	Gable Mountain	Hanford	Richland	Benton City	Pasco	Columbia Camp
January–May 1947	0.85	0.54	0.26	0.19	0.18	0.11	0.24
1946	2.98	0.79	0.44	0.34	0.33	0.26	0.23

Figure 4-20. Comparison of average concentrations of beta activity in vegetation (μCi kg^{-1}) at seven locations in 1946 and 1947. Averages for 1946 were computed from monthly averages reported in HW-7-5934 and HW-7-5372. Averages for January–May 1947 were computed from biweekly concentrations reported in HW-7-5042, with the exception of Columbia Camp and Gable Mountain, which were based on data from HW-7-5934 for January and February only. The natural background concentration is around 0.01 μCi kg^{-1}.

The type of vegetation sampled was not specified and probably varied depending on location. In the first quarter 1947, the statement is made that "in all areas the prevalent vegetation has been sampled," but the vegetation type is not identified (HW-3-5511). One anomalous high-activity sample in October 1948 was stated to be Russian thistle (HW-11534). That month, off-area surveys were "dry weed samples" in one area, whereas live sage, Russian thistle, etc. were taken in other areas. This inconsistency complicates quantitative use of the vegetation monitoring

data. Our objective in examining these data is to obtain general, qualitative trends to complement those from other environmental samples.

Some fraction of the total beta activity on Hanford vegetation during 1945–1948 was due to nonvolatile beta emitters, but most of the contamination in high-activity samples was likely due to iodine. In March 1947, Gamertsfelder stated, "If no more contamination was produced, present levels would decay with a half-life very close to 8 days so that normally undetectable levels (<0.04 μc/kg) would be reached in one to two months" (HW-7-5934).

However, perhaps more residual nonvolatile beta activity was present than was generally recognized at that time. During the following year (1948), techniques were developed to chemically separate the 8-day radioiodine from the nonvolatile beta activity in vegetation before beta counting. Healy (HW-10758) established the half-lives of the longer-lived isotopes on vegetation. The amount of long-lived beta activity (half-life >8 days) on vegetation ranged from <0.02 μCi kg^{-1} in Richland-Kennewick-Pasco areas and 100 Areas to as much as 0.4 μCi kg^{-1} on some samples inside the 200 Areas. Healy's study results are reviewed more thoroughly in Section 4.2.1.

In December 1948, both categories of beta activity (iodine and nonvolatile beta activity) began to be routinely reported for vegetation samples (HW-13743). Reportable detectable levels were 0.002 μCi kg^{-1} for radioiodine and 0.01 μCi kg^{-1} for nonvolatile beta activity. Table 4-5 shows the percentage of total beta activity from nonvolatile beta emitting radionuclides in December 1948. Later studies would show that the naturally occurring beta emitter potassium-40 (^{40}K) was present at concentrations around 0.01 μCi kg^{-1}. Therefore, only three locations nearest the 200 Areas can be viewed as having Hanford-produced beta activity clearly above background in December 1948. At these three locations, the percentage of the total beta activity due to nonvolatile emitters ranged from 38–92% (Table 4-5).

Table 4-5. Percentage of Total Beta Activity from Nonvolatile Beta Emitting Radionuclides in December 1948

	Microcuries per kilogram			
Location	^{131}I	Nonvolatile beta	Total beta	% of total from nonvolatile emitters
Adjacent to 200 Areas	0.072	0.045	0.117	38
Inside 200-East	0.007	0.057	0.064	89
Inside 200-West	0.004	0.046	0.05	92
North of 200 Areas	0.005	0.011	0.016	69
Richland	<0.002	0.013	0.015	>87
Wahluke Slope	0.002	0.012	0.014	86
Hanford	0.002	0.012	0.014	86
South of 200 Areas	0.002	0.011	0.013	85
Pasco	<0.002	<0.01	0.012	a
Kennewick	<0.002	0.010	0.012	>83
Benton City	<0.002	<0.01	0.012	a

[a] Not possible to compute percentage because both values were less than detectable.

About 1500 vegetation samples were collected in the first quarter 1949 (HW-14243) and analyzed for 8-day radioiodine and for beta activity from longer-lived nonvolatile fission

products. The method for determining nonvolatile beta activity in vegetation consisted of digestion of a 1-g sample with nitric acid and hydrogen peroxide, concentration, and transfer to a 1-in. stainless steel plate. Activity was measured with a thin mica-window counter. A yield of 95–100% was obtained for a beta energy of 1.5 MeV. Naturally occurring ^{40}K concentrations were about 10 pCi g^{-1}. The quarterly averages are illustrated in Figure 4-21. As in similar charts presented for other media, concentrations of nonvolatile beta activity in vegetation in 1949 are highest in the 200 Areas, particularly near the 200-West Gate (240 pCi g^{-1}). About 3 mi from this area the activity was about 6 times less, or 20–60 pCi g^{-1} (HW-14243).

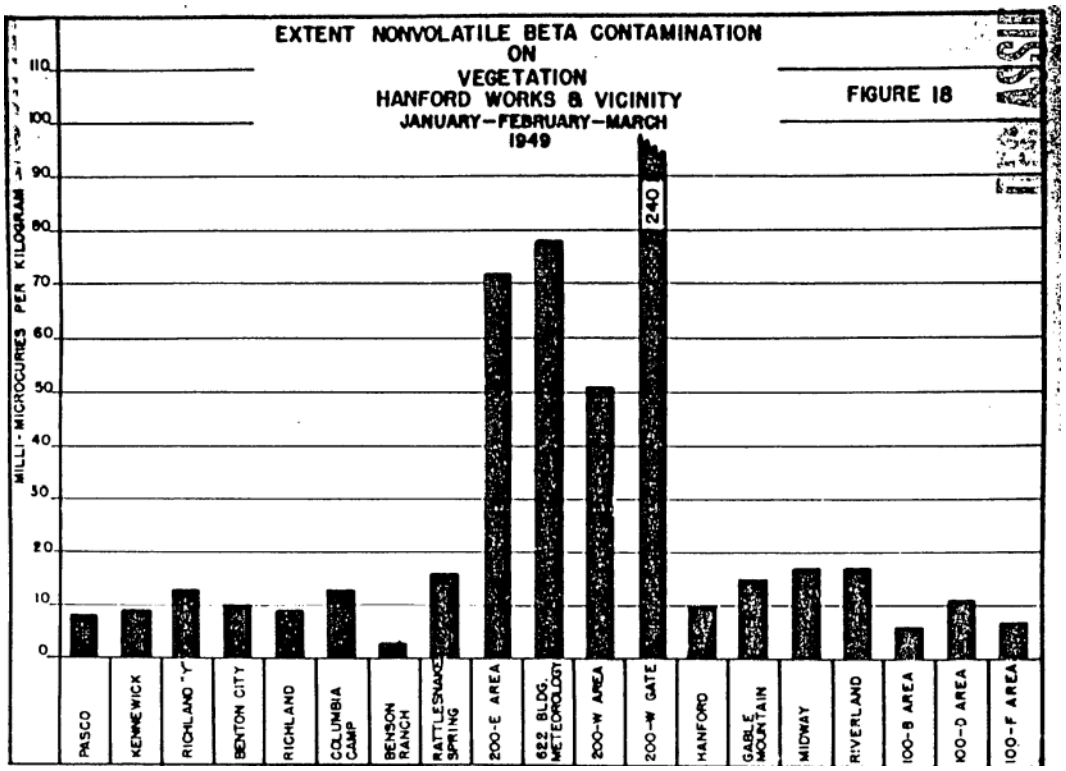

Figure 4-21. Nonvolatile beta activity on vegetation, first quarter 1949 (HW-14243). Millimicrocurie is an archaic unit of radioactivity (10 mμc kg^{-1} is equivalent to 10 picocuries per gram [pCi g^{-1}] or 0.01 μCi kg^{-1}), which is an estimate of the natural beta activity content.

In an effort to determine specific deposition patterns of radioactive effluents near the stacks, a controlled sampling of vegetation began in February 1949. Vegetation samples were taken at half-mile intervals in an area enclosing about 26 mi^2 in and near the separation areas. Results for February and March 1949 are shown as maps, reproduced here as Figure 4-22. Contamination spread of nonvolatile beta activity on vegetation was generally to the east and south of the release points. The isoactivity map for nonvolatile beta activity closely parallels that for iodine (not shown here), although iodine shows more monthly variation.

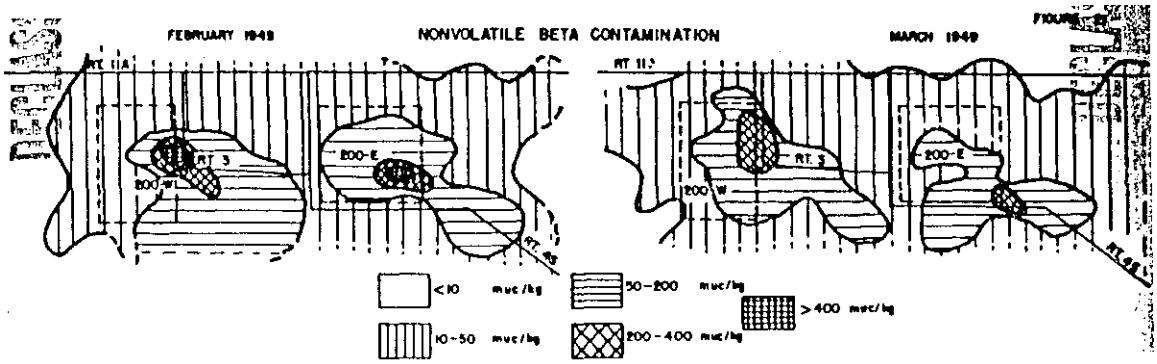

Figure 4-22. Results of "controlled sampling survey" for nonvolatile beta activity on vegetation near the 200 Areas in February and March 1949 (from HW-14243).

A similar isoactivity chart (Figure 4-23) was presented in the second quarter report for 1950 (HW-19454). The deposition pattern of higher activity near the stacks in both 200-West and 200-East is still apparent. However, the absolute amounts of nonvolatile beta activity are not as high in the highest zones, compared with the spring 1949 survey. The units (10^6 μCi/gm) used in 1950 are equivalent to those used in 1949 (mμCi/kg), so the numerical values in the maps in Figures 4-22 and 4-23 can be compared as if the same units were used.

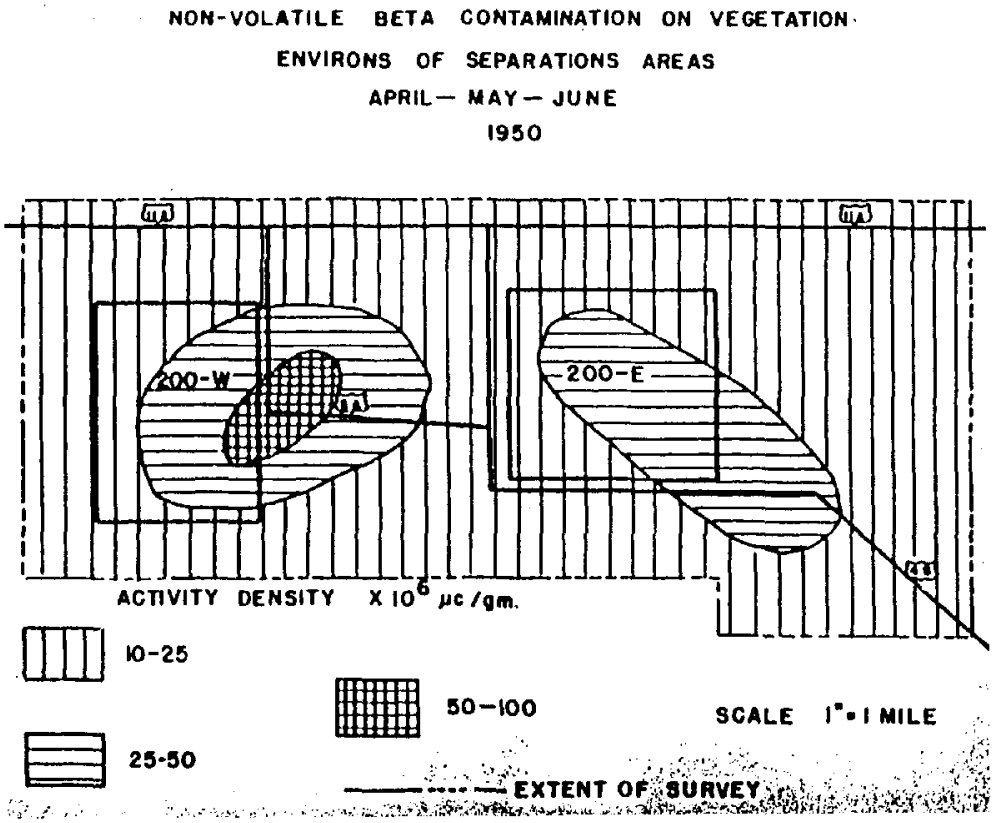

Figure 4-23. Spatial extent of nonvolatile beta contamination on vegetation near 200 Areas, April–June 1950. Highest levels (50–100 × 10^{-6} μCi g^{-1}) were east of the 200-West Area (from HW-19454).

For comparison, a close-in map of ^{131}I activity on vegetation in December 1950 is shown in Figure 4-24. In the area of military camp PSN330 (southeast of 200-East Area off Route 4S, see Figure 3-1), the iodine activity density on vegetation is 250–1000 pCi g^{-1} as opposed to 25–50 pCi g^{-1} of nonvolatile beta emitters. However, in the first quarter of 1950, the iodine content of vegetation was considerably less than shown here for December. Although a silver reactor[h] was installed in the off-gas line of 3-5R in December 1950, which should have reduced iodine emissions to air, dissolving was allowed to take place during the day when dispersion conditions were poor.

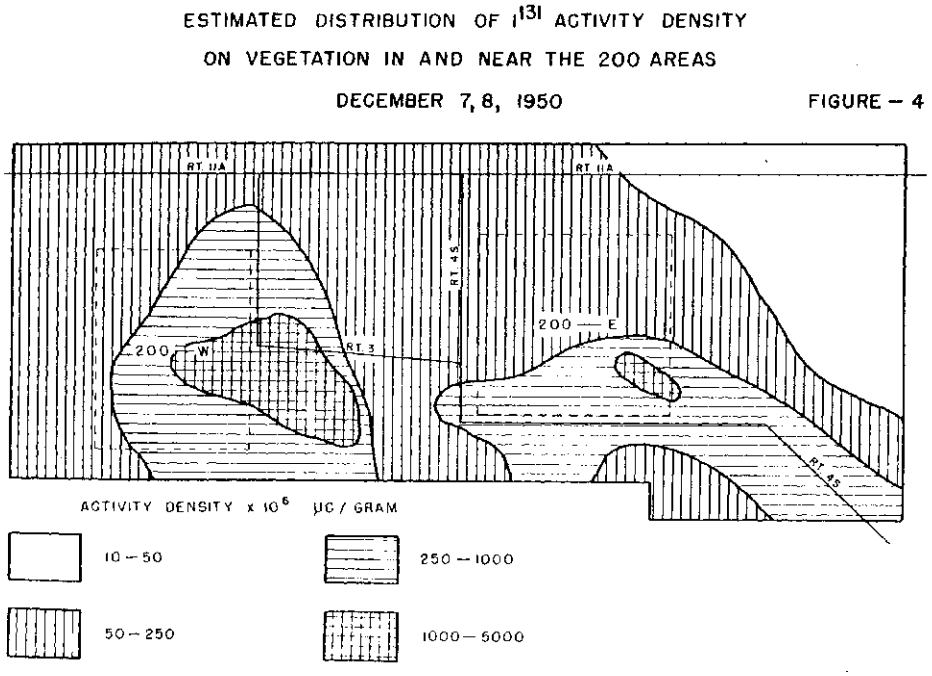

Figure 4-24. Spatial extent of ^{131}I activity on vegetation, December 7–8, 1950 (from HW-21566).

We compiled data for nonvolatile beta activity in vegetation samples from the quarterly reports covering 1949–1955 for nine locations:

- 200-West gate
- Meteorology tower
- Columbia Camp
- Hanford
- Near the 200 Areas
- Richland
- REDOX
- PSN 300-310-320 (military camps)
- 200-West Area.

[h] Effluent control for radioiodine.

The reporting frequency was quarterly until October 1953 and monthly after that. The reportable detection level was 10 pCi g^{-1} (0.01 μCi kg^{-1}). This is also the approximate level of naturally occurring ^{40}K in vegetation. The most complete data sets were for three locations (200-West gate, near the 200 Areas, and Richland), which had at most one missing data point during this time interval. The Columbia Camp and Hanford sampling locations were discontinued after the second quarter 1949 and the fourth quarter 1952, respectively. Monitoring at the plant security sites (military camps) near 200 Areas[i] began in the fourth quarter 1951 and continued through our time period of interest (1955) with only one quarter of missing data. Before that time, we believe that the data from the "near the 200 Areas" sample group is a reasonable representation of levels that would have been present at the military camps. The time trend in nonvolatile beta activity in vegetation from seven locations is illustrated in Figure 4-25.

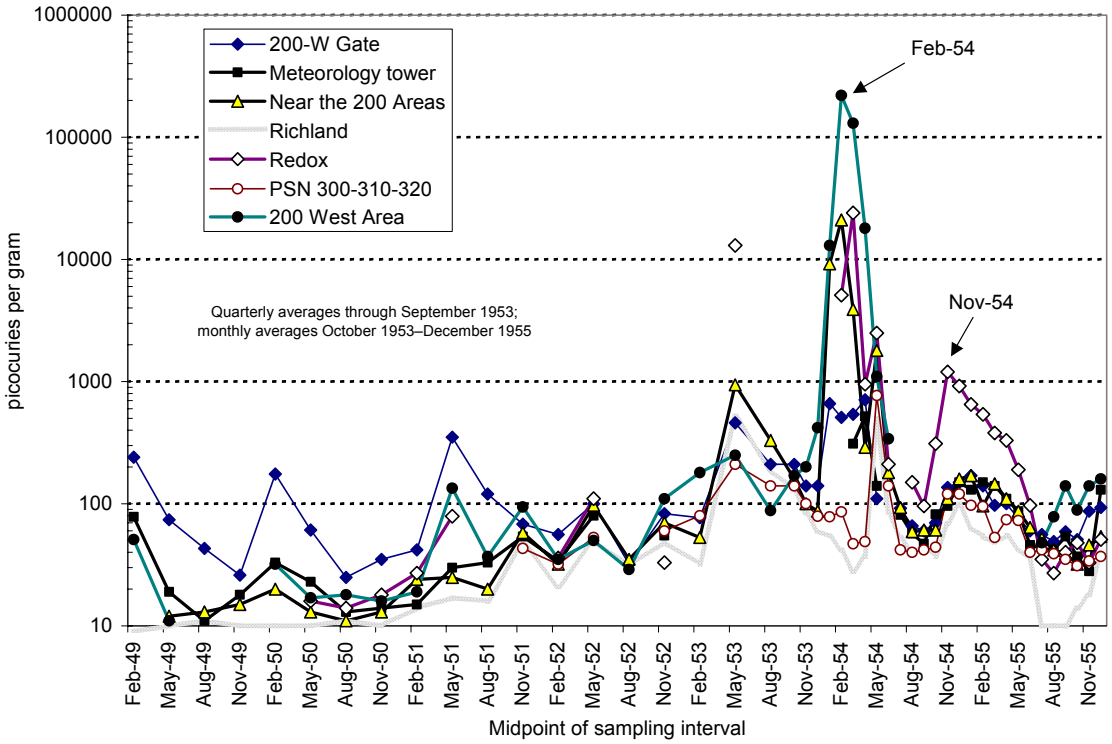

Figure 4-25. Time trend in nonvolatile beta activity on vegetation, 1949–1955. The monthly average reporting frequency beginning October 1953 exaggerates the peak in 1954 somewhat. Quarterly averages were computed for Figure 4-26.

Review of historical documents leads us to the conclusion that fallout from the atmospheric testing of nuclear weapons affected the nonvolatile activity in vegetation in the latter half of the period of data we examined (1945–1955). Based on the spatial patterns in vegetation, as well as other media, weapons fallout was definitely noted during:

[i] Called PSN 300-310-320 in the first part of this time interval and PSN 50-51-61 in the latter part of this time interval. More recently, they are referred to as H-50, H-51, and H-61. However, they are the same sites (see Figures 3-1 and 3-2). The measurement is made on a *composite* of vegetation collected at or near the three military sites.

- First half 1951
- Fourth quarter 1951
- Second quarter 1952
- Second and third quarter 1953
- May 1954
- November–December 1954
- April 1955
- December 1955.

Even with the confounding influence of fallout, the impact of ruthenium releases from REDOX on beta activity in vegetation near the 200 Areas in 1954–1955 is clear (Figure 4-25). The highest reported monthly average concentrations at the nine locations listed above were 220,000 and 130,000 pCi g^{-1} from the 200-West Area in February and March 1954, respectively. Monthly average concentrations near the 200 Areas (previously determined to be Route 4S, Mile 4) were as high as 21,000 pCi g^{-1} in February 1954 and 24,000 pCi g^{-1} in March 1954 near REDOX. A second peak in activity near REDOX occurred in November 1954. The decrease in contamination observed near REDOX in 1955 is believed to be due to radioactive decay and weathering of ruthenium released during 1953–1954.

An extreme example of ruthenium particle contamination of vegetation occurred in September 1954. Inclusion of an active particle or particles of ruthenium/rhodium in a vegetation sample from Route 10, Mile 8, near the southern perimeter of the Hanford Works, resulted in a measured concentration of 330,000 pCi g^{-1}. The monthly average for that location was 110,000 pCi g^{-1}, including that high value and 31 pCi g^{-1} when the high value was excluded from the average.

The "near 200 Areas" location was sampled over the entire 10-year interval, so a long-term trend can be evaluated (Figure 4-26). For a valid perspective, quarterly averages were computed for this plot, although reporting frequency varied from biweekly to quarterly. The peak quarterly average nonvolatile beta activity of 12,000 pCi g^{-1} in the first quarter of 1954 is almost as high as the peak total beta activity concentration of 19,500 pCi g^{-1} in the last quarter of 1945. In 1945, the activity was almost certainly mostly iodine, whereas in 1954, it was probably mostly ruthenium. Weapons fallout was a large component of the nonvolatile beta activity on vegetation in Richland in the 1951–1955 period, whereas in 1945–1948, the total beta activity there was likely influenced by Hanford releases.

Alpha Activity. The second quarter 1951 report (HW-22313) states that spot vegetation samples were analyzed for alpha activity using an ether extraction method, and that results were "negligible." The detection limit then was ~1 pCi g^{-1}. Beginning in December 1951, the quarterly environmental reports include measurements of concentrations of alpha-emitting radionuclides in vegetation. The reporting frequency was monthly through June 1954 and quarterly thereafter. We compiled the data for five locations through December 1955:

- 200-West Gate
- Route 4S, Mile 4
- Route 4S, Mile 6
- 300 Area
- Richland.

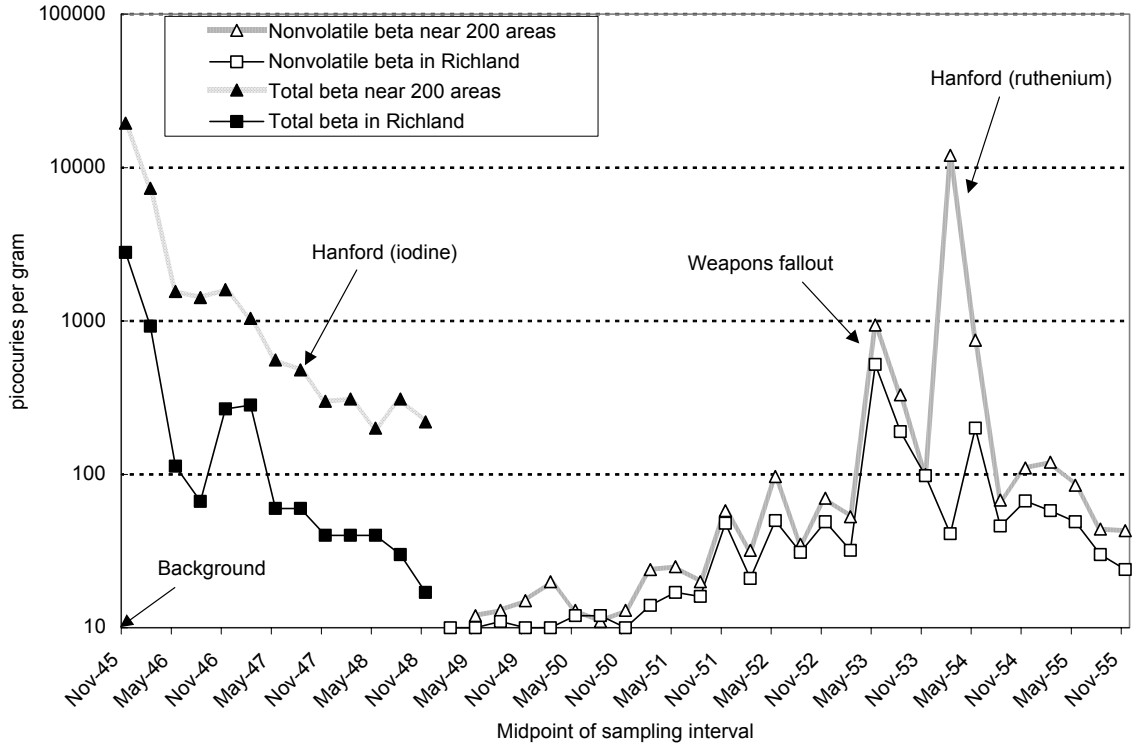

Figure 4-26. Ten-year trend in beta activity in vegetation near the 200 Areas and in Richland. For a valid visual perspective, quarterly averages were generated from the reported data. Thus, peak concentrations are not as high as shown in Figure 4-25.

The alpha measurement data for vegetation are plotted in Figure 4-27. The reportable detection level at this time ranged between 0.05 and 0.1 pCi g^{-1}. The data show significant scatter, and most values are within a factor of 10 of the detection limit. In addition, the contribution of naturally occurring alpha-emitters, such as radium and uranium, is not established. Unlike nonvolatile beta activity, alpha activity concentration in vegetation was not discernibly affected by weapons fallout. The highest values measured were in samples from 300 Area (17 pCi g^{-1} in March 1953) and the 200-West gate (7.8 pCi g^{-1} in January 1954). Because of the work with uranium compounds in 300 Area, the alpha activity there is likely to have been uranium. In January 1955, alpha particle activity on vegetation in the 300 Area was determined by fluorophotometric analysis to be uranium (HW-36506). In contrast, alpha contamination above background present in 200 Areas is more likely to have been plutonium, based on results of analysis of particles emitted from the stacks and located in ground surveys (HW-9259, HW-10261). The concentrations of alpha activity on vegetation near the 200-West gate in the first quarter of 1954 are high, if this was all plutonium. For perspective, plutonium concentrations in soil (an integrator of atmospheric releases) near that area in 1985 ranged up to 0.3 pCi g^{-1} (Figure 4-43).

Before the routine monitoring of total alpha activity in vegetation began, there was some nonroutine sampling and measurement of plutonium in vegetation. Thorburn, in report HEW-7002 dated July 1, 1947, describes the development of a method to determine plutonium in desert flora. It was known that stack gases from Hanford facilities contained not only iodine but other

longer lived beta activity and a low, but significant content of alpha emitting contamination. The possibility of a build-up of alpha contamination was recognized. The method development and detailed procedures are described. The plutonium content of four samples of green leaves taken from one sagebrush plant at location Route 4S, Mile 4 varied from 0.058–0.095 pCi g^{-1}. The plutonium results for nine vegetation samples from four locations in and around the 200 Areas on the site (Tower 18, 4S-4, 3-3, and 200-E BG) ranged from 0.023–0.35 pCi g^{-1}.

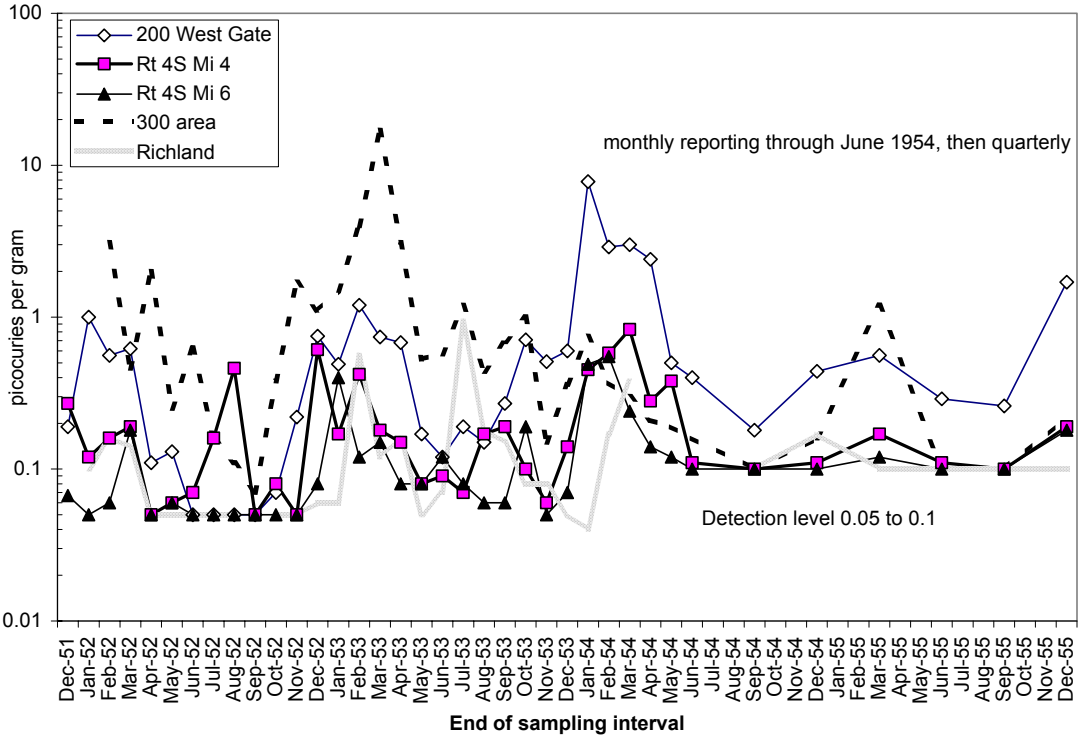

Figure 4-27. Concentrations of alpha activity in vegetation between December 1951 and December 1955.

4.1.5 Particle Counts in Air

Beginning in the fourth quarter of 1948, Hanford's routine environmental reports included data on the number of radioactive particles present in a certain volume of ambient (outside) air (HW-13743). The method used was to expose the air filters from the routine beta air monitoring program to X-ray film for 168 hours and then visually count the spots present on the film. The flow rate of the air samplers was 2 ft^3 min^{-1}, for a total sample volume of about 20,000 ft^3 (570 m^3) per week. The samplers were housed in a vented cupola-type housing; thus, particles collected would be restricted to those whose momentum would permit following the air stream through the vents to the sampler. Generally, large particles would not be efficiently collected.

Other special filter units were also used for determining the concentration of radioactive particles (HW-18615). These filters consisted of an exposed area of approximately 26 $in.^2$ of CWS #6 filter paper through which air was filtered at rates of either 2 or 10 ft^3 min^{-1}. The sampling period was 1 week and exposure to film was as described above.

The first reporting of radioactive particle count data was expressed as the total number of particles collected per month. The highest values were from 200-East. However, beginning in the second quarter 1949, the particle count data were expressed as a concentration (particles per cubic meter). At this time, there were six locations outside in 200-East and vicinity, eight locations in 200-West and vicinity, and nine samples taken from the meteorology tower between 3 and 400 ft above ground level. There also were seven locations near the Hanford perimeter and eight distant off-area locations.

We chose to compile data for one off-area location (Spokane, Washington), one near-perimeter location (Pasco), and three outdoor locations in 200 Areas (Building 222-B [B Plant], Building 222-T [T Plant], and REDOX [if REDOX data were not given, the south gate of 200-West was used]). Monitoring at the REDOX location began in January 1952 and ended at the 222-B location in September 1952. The other locations were monitored continuously from mid-1949 through 1955 (end of our data compilation). During this period, the reportable detectable concentration ranged from 1×10^{-4} to 5×10^{-4} particles per cubic meter air.

The data for these five locations are illustrated in Figure 4-28. The effect of releases from REDOX is evident from the larger number of radioactive particles in air at that location during 1952–1954. The highest monthly average concentration of discrete radioactive particles in air was 3.8 particles per cubic meter in 200 West during September 1953. The highest value at the T-Plant location was also in September 1953, but it was 6 times less (0.6 particles per cubic meter) than the concentration near REDOX that month. Table 4-6 summarizes the data for the 48-month period, January 1952 through December 1955, for the four locations that were being monitored.

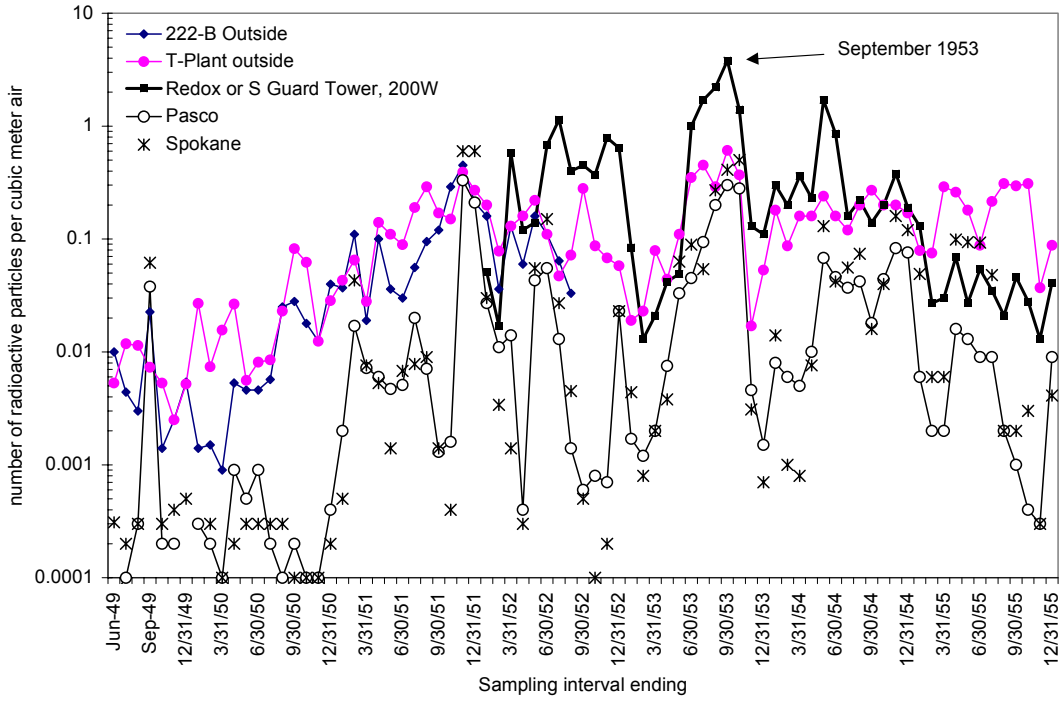

Figure 4-28. Concentration of radioactive particles in air as determined by autoradiography of air filters (data compiled from Hanford monitoring reports).

Table 4-6. Summary Statistics for Concentration of Radioactive Particles in Outdoor Air at Four Locations for the 48-Month Period, January 1952–December 1955

	Monthly average concentration of particles per cubic meter air			
Statistic	REDOX[a]	T-Plant	Spokane	Pasco
Minimum	0.013	0.017	<0.0001	<0.0003
Maximum	3.8	0.61	0.50	0.30
Median	0.15	0.16	0.015	0.0095
Mean	0.45	0.17	0.058	0.035

[a] If REDOX data were not available, the south gate of 200-West Area was used.

These data give an indication of the most important times and possible active particle concentrations in air in outside work locations. Over this interval the median concentration of active particles in air in 200 West was 16 times greater than at Pasco. For a worst case assessment, these particles could all be viewed as respirable. It should be remembered, however, that the air samplers are not efficient collectors of large particles. Therefore, these data do not necessarily reflect the trends in very large particles that settled on ground surfaces. Ground survey data are reviewed in Section 4.1.6.

There were times when nuclear weapons fallout was very likely a primary contributor to the radioactive particle counts, based on the widespread nature of the contamination and the fact that concentrations were comparable or even higher at offsite locations. A clear example of this situation is November–December 1951. Fallout was also probable in May–June 1952, May 1954, and November–December 1954.

Separate reports document specific investigations into radioactive particle concentrations due to weapons fallout. For example, in HW-23517, increased particulate contamination from Nevada bomb tests in the fall of 1951 is documented and discussed. A daily concentration of 8 particles per cubic meter in Klamath Falls, Oregon, was the highest obtained from this type of monitoring during the previous several years. In general, particles were detected between 2 and 5 days after detonation in Nevada. Tabular summaries show the day-to-day trend of particulate contamination at the eight stations that were operated daily (HW-23517). In the second quarter of 1952, weapons fallout also affected particle counts at locations both onsite and offsite (HW-26493). Values in Boise, Idaho, and Great Falls, Montana were as high as 5 to 10 particles per cubic meter over a 1-day period, which were some of the highest concentrations of radioactive particles measured since the inception of the particle monitoring program several years previous. A special survey in a more contaminated zone between Richland and Idaho Falls is summarized in HW-24727. Report HW-28925 discusses fallout in May–June 1953. In the third quarter 1953 (HW-30174), daily monitoring of air showed that particulate contamination was widespread and indicated the origin was a source other than Hanford. Maximum values in excess of 1 particle per cubic meter were observed over 24-hour periods at locations in Oregon, Washington, and Idaho. A value of 8 particles per cubic meter was measured at Walla Walla, Washington, on August 30, 1953.

Because the type of radioactive particles is not characterized by this type of air monitoring, it is impossible to separate definitively the Hanford-released radioactive particles from weapons fallout or naturally occurring radioactive particulates. In conjunction with other environmental data, however, there is little doubt that the high concentrations observed near REDOX in 1952-1954 were caused by releases from that facility.

We examined the data for particle concentrations measured at different heights on the meteorology tower, which was located between 200-West and 200-East. These data add nothing new to the time trend documented by the other stations (e.g., Figure 4-28). In some cases, there was a concentration profile (with height) that was consistent with a release from the 200-ft stack(s) of the processing plants. For example, in October 1950, concentrations were low at 3, 50, and 100 ft; were considerably higher at 150, 200, and 250 ft; and were intermediate in concentration at the 300, 350, and 400-ft levels. In February 1951, the uniform concentration with height was one piece of evidence the authors of the environmental report used to support their belief that most contamination that month was from widespread weapons fallout. However, in general these data are ambiguous, and we did not examine them further.

The particle data from the meteorology tower were used by H.M. Parker in a briefing to the Advisory Committee for Biology and Medicine October 8–9, 1948, on the active particle problem at Hanford Works. A table of data presented to the Advisory Committee was included in the minutes (Gregg 1948) and is included in this report as Figure 4-29. The first four columns of the table are based on monitoring at the meteorology tower, and the rest are believed to be based on ground level air monitoring. Parker appears to be illustrating the calculated inhalation of particles by a person working in the area as well as estimating the number of particles deposited in the 200 Areas per month.

4.1.6 Particle Ground Surveys

Surveys of radioactive particles deposited on outdoor ground surfaces were conducted both routinely and in response to specific contamination events. This section presents what is known about the methods used for ground surveys and discusses the uses and limitations of the data for our task. The survey studies and data are presented in chronological order. Primary sources of information were

- Two contamination maps generated in 1947
- Quarterly environmental reports
- H.M. Parker's 1948 report (HW-9259) on the active particle problem
- Selby and Soldat's 1958 summary report of environmental contamination incidents at Hanford between 1952 and 1957 (HW-54636)
- Overview reports that evaluated ruthenium releases from the REDOX Plant
- Miscellaneous memos.

Memos were important for understanding the active particle releases in the late 1940s because survey data were few and environmental reports were brief. Physical, chemical, and radiological characterization of the particles detected during these ground surveys is discussed in Sections 2.2 and 4.2.1 of this report.

Meteorology Tower

Height above ground	Particles inhaled per month				Particles inhaled per month				Particles deposited in 2DC Areas per mo.
Ft.	July	Aug.	Sept.	Time	200 Area General	200 W Gatehse	Insd Offs.	Insd Op.Gal.	
3	5	5	11	Jan.			-	-	10^7
50	6	3	12	Feb.			-	-	No record
100	10	4	15	Mar.			No	No	5×10^7
150	14	7	26	Apr.		5	prior	prior	8×10^7
200	13	8	35	May	5-10	7	data	data	4×10^8
250	14	7	30	June	5-10	6	-	-	10^9
300	14	8	18	July	10-30	33	10-20	-	4×10^8
350	8	4	20	Aug.	10-30	36	10-20	-	3×10^9
400	6	5	32	Sep.	20-30*	29	10-20	80	10^9

50 - 150
ϕ 80

ϕ per month
7.4×10^8

Notes.

Data reported as for a particular month does not coincide with the exact exposure time, due to lag in radioautography and reporting. This does not affect the argument presented.

Particles inhaled per month are based on the number of particles in the amount of air inhaled by a man working 8 hours per day for 20 days per month in the plant areas. No allowance is made for rejection of large particles or for the exhalation of a fraction of the entering particles.

In residential areas, the inhalation figure is based on a 24-hour day and 30 day month.

* There was one value of 70 here, not mentioned in the presentation.

Figure 4-29. Table of data on active particles in 200 Areas in 1948, presented by H.M. Parker to the Advisory Committee for Biology and Medicine (Gregg 1948).

Methods, Limitations, and Uses of Ground Survey Data. Ground survey results were reported in terms of particle frequencies and radiation instrument readings. Active particle frequencies using Geiger-Müeller (G.M.) meters were complicated because the instruments had difficulty distinguishing two or more particles close together (HW-9259). According to report HW-54636, portable G.M. instrument readings were recorded in units of counts per minute (cpm) per particle. G.M. meter response for energy ranges involved in the ruthenium releases

was approximately 100 cpm per 5000 disintegrations per minute (dpm). The G.M. meter was also used to measure general area contamination not associated with a specific particle (HW-33896).

Instrument readings in units of millirad per hour (mrad h^{-1}) per particle were obtained with Hanford-type "C.P." (Cutie Pie) meters. It is difficult to translate that instrument reading to an amount of radioactivity. According to Selby and Soldat (HW-54636), C.P. meter readings of isolated particles from REDOX were approximately 200 mrad h^{-1} per microcurie (μCi). However, Parker (HW-33068) gives an approximate relationship of 90 mrad h^{-1} survey result for a particle containing 1 μCi ruthenium with an activity ratio of 0.75 ($^{103}Ru/^{106}Ru$).

Some comments on the uses and limitations of the ground survey data are appropriate before presenting our review of the data. One limitation is that the distance from the source to the measuring instrument is not given. Because radiation intensity decreases inversely with the square of the distance from a point source, the distance from the source to the detector is crucial to interpreting the measured value. In our experience, we believe that a technician characterizing a hot particle might have held the instrument close to the particle, perhaps a centimeter or two away. This is sometimes referred to as the dose rate at contact or at ground level. HW-36505 states that surveys for particle numbers represent those particles detectable at ground level using a portable G.M. instrument. In contrast, general area surveys (not measuring a hot particle) with the G.M. meter were probably conducted holding the meter at waist height or about 3 ft above the ground. Because these details are not specified, the ground contamination survey data are best regarded as showing relative trends, rather than providing quantitative measurements that can be related to potential dose to a person.

The number of particles detected with a G.M. instrument was less than that detected using more sensitive techniques such as exposure of film in light-proof envelopes (autoradiography). However, the more sensitive techniques had higher background interference from natural radioactivity. Another limitation is that the ground surveys were a snapshot in time that reflected both past and contemporaneous particle releases. Although helpful for identifying actual conditions that existed, the data would be difficult to compare to predictions of a source term and dispersion assessment.

For the purposes of our work, the ground survey data can be used to represent spatial distribution and time trends in the numbers of large particles. The number of particles in a given work environment is related to the probability that a worker would have come in contact with one of them (see Section 3.5). These large particles represented an external exposure hazard to people, either to the skin (if in contact) or to the whole body, from radiation emanating from the particles on the ground. Under certain conditions, it is possible that even large particles could have been inhaled.

Chronological Review of Survey Data. Health Instrument Section surveyors detected contamination in the form of discrete active particles on the ground in the region of the Hanford separations plants in late September 1947 (HW-9259). Evidence of the radioactive particle problem increased almost daily in October 1947. There were repeated contamination incidents involving footwear, spot contamination over larger ranges, and the isolation of individual particles of high radiation intensity. A pessimistic particle density estimate was one per 4 ft^2 (HW-7865). The necessity for a preventive program became urgent (HW-7865, HW-7920). By mid-October, the general distribution pattern had been investigated such that the T Plant and B Plant stacks were believed to be the source. The problem was thought to have been rapidly developing in the prior several months.

On November 3, 1947, a work order was presented with a memo (HW-7932) to permit installation of (1) a temporary air filter in the 291-T,B Buildings between the existing fans and stacks, (2) a permanent filter system in the 291-T,U,B Buildings between the existing fans and new or revised stacks, and (3) a permanent set of filters in 291-T,U,B Buildings in the individual cell exhaust ducts and the 224-T,U,B Buildings tank vent piping. The results of spot surveys of ground contamination are briefly described. Contaminated areas were within a 1000-ft radius of the stack, quite small, and limited to a maximum surface area of approximately 1 $in.^2$ with essentially no depth. According to the author, the situation "constituted a serious health hazard requiring the utmost expediency in its correction."

On November 25, 1947, a memo (HW-8108) underscores the importance of physical control of the particles at their source, which was not precisely known at the time. The health hazard was viewed as serious; however, it was not practical to subject areas of this size outside the facilities to the same controls as radiation protection zones inside. The amount of radioactivity in and on the particles was enough to cause minor damage to skin or serious damage if deposited internally. Future plans were presented.

On November 28, 1947, a survey map of active particle distribution in 200-East Area was circulated as HW-8430. A scanned image of that map is shown in Figure 4-30. There was no accompanying text with the figure. However, in HW-11082, dated September 1948, this map is referenced as the first comprehensive ground survey for particle contamination. In this report, it is noted that the zone of highest concentration, 5–10 particles per ft^2, covered approximately 50,000 ft^2 (4600 m^2) in the vicinity of the stack. Therefore, about 250,000 to 500,000 particles had been deposited in that highest deposition zone. The average particle in this zone had an activity in the range of 0.05 to 0.5 μCi. The best estimate of the total number of then existing particles was 1.4 million, with a total activity of 100 mCi. There is a cpm range in the legend of the survey map associated with each particle concentration zone. For example, the G.M. count rates in the 5–10 particles per ft^2 zone were 5000–10,000 cpm (Figure 4-31). The G.M. instrument background was about 200 cpm.

A similar map of 200-West was produced (HW-8429) representing particle distribution on December 22, 1947 (Figure 4-31). Note the similar southeastern direction of contamination spread as seen in 200-East. Parker (HW-9259) observed that the heavy and medium contamination zones were more extensive around T Plant (200-West) than around B Plant (200-East). The lowest contamination zone around T Plant was a similar distance downwind but reached further in an upwind direction than around B Plant.

Figures 4-30 and 4-31 show a static picture of ground contamination. By January 20, 1948, a dynamic picture of particle deposition had been obtained by the collection of active particles on rugs maintained on frames 3 ft above the ground with partial wind protection (HW-8624). Typical deposition rates for the three zones around B Plant in 200-East were:

Heavy concentration zone	3–17 particles ft^{-2} mo^{-1}
Medium concentration zone	4 particles ft^{-2} mo^{-1}
Light concentration zone	0.1 to 2.4 particles ft^{-2} mo^{-1}

In September 1948, Parker gives a deposition rate of 40 particles ft^{-2} mo^{-1} close to the stacks. At one mile, the deposition rate could be as heavy, but was typically about 12 particles ft^{-2} mo^{-1}. All these were "sizeable" particles, >5 micron diameter (HW-10941). An inhalation rate of 5-10 particles per month in construction areas was estimated.

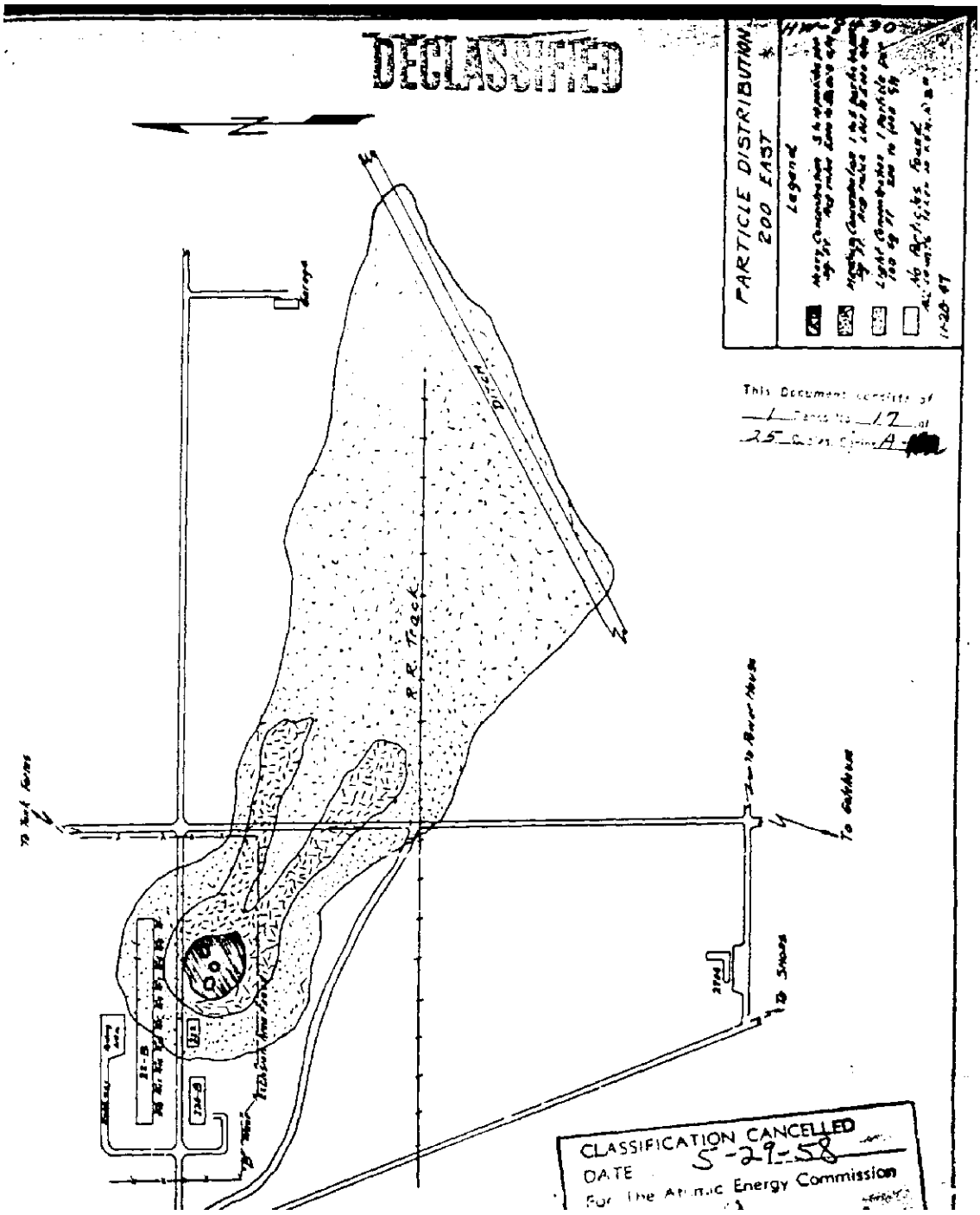

Figure 4-30. Distribution of particles in 200-East, November 28, 1947 (HW-8430). The "heavy concentration" zone around the B Plant stack is 5–10 particles per ft^2 (5000–10,000 cpm). The "medium concentration" zone is 1–5 particles per ft^2 (1000–5000 cpm). The "light concentration" zone is 1 particle per 100 ft^2 or 0.01 particles per ft^2 (200–1000 cpm). The survey results extend about 900 m SE of the B Plant stack, still within the boundaries of 200-East.

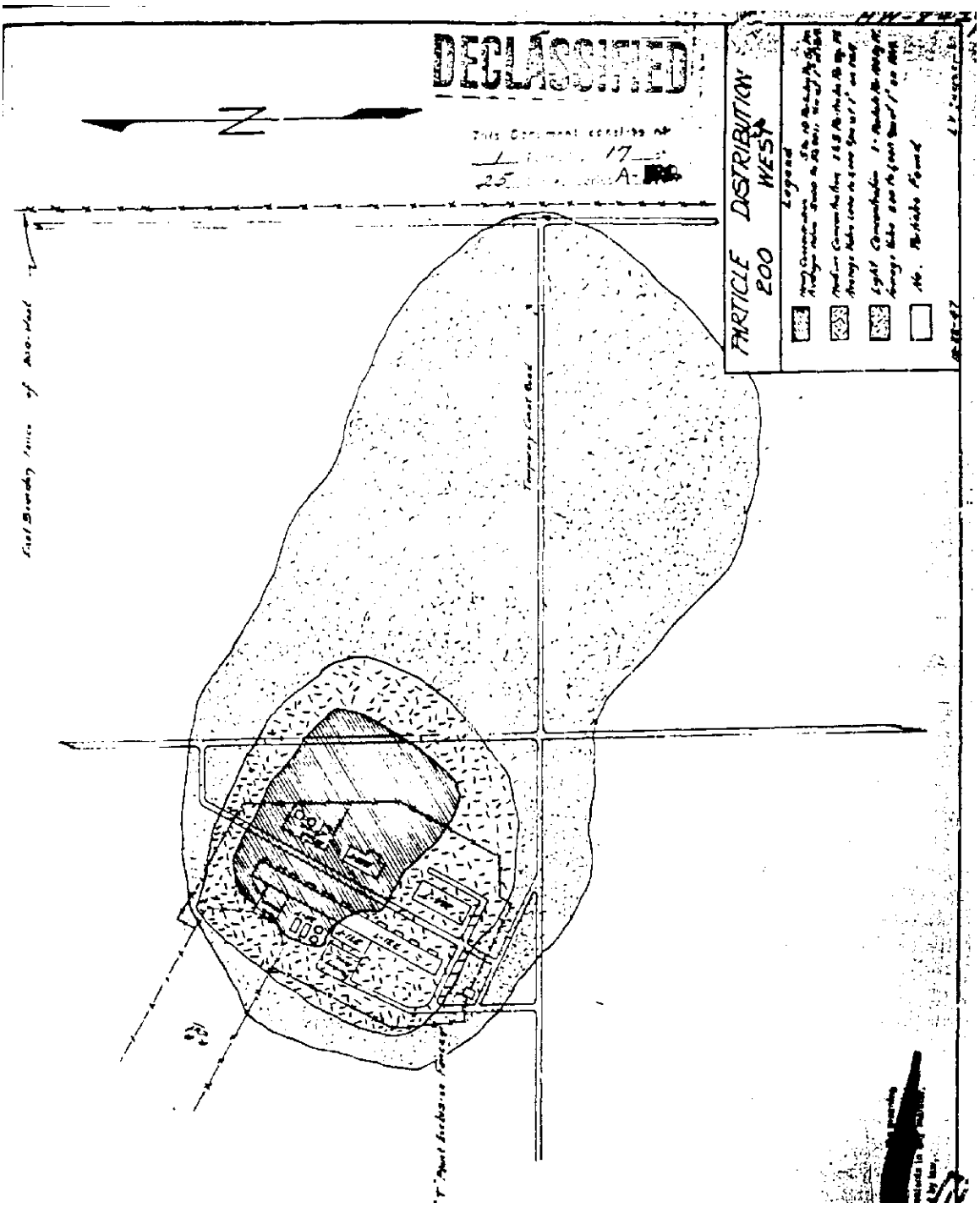

Figure 4-31. Distribution of particles in 200-West, December 22, 1947 (HW-8429). The "heavy concentration" zone around the T Plant stack is 5–10 particles per ft^2 (5000–10,000 cpm). The "medium concentration" zone is 1–5 particles per ft^2 (1000–5000 cpm). The "light concentration" zone is 1 particle per 100 ft^2 or 0.01 particles per ft^2 (200–1000 cpm). The survey results extend about 800 m to the east boundary fence of 200-West.

Given the spatial extent of contamination documented by these maps from 1947, the exposure to active particles was mainly an occupational exposure problem, with the possible exception of construction or other field workers in these areas. According to report HW-20888 (April 1951), military personnel were excluded from the separately fenced areas within the reservation. However, these ground surveys from the late 1940s did not extend to further distances where it is probable that lower concentrations of particles were present. In fact, H.M. Parker (HW-9259) stated that measured deposition was 1–10% of the estimated emission of active particles, meaning that 90–99% of particles were not detected within the surveyed area.

In a memo dated March 10, 1948 (HW-9141), H.M. Parker discusses the contamination on the potential construction sites for the REDOX Plant. Those areas had been surveyed for ground contamination. The proposed test plant site contained no particles detectable by G.M. counter methods. However, what appears to be a potential site for C Plant in 200-East was unsuitable in the author's view because of particle contamination, which averaged 2.5 particles per ft^2 by field survey techniques. The author stated that the particle density would be at least 10 times greater using autoradiographic techniques. The results at the C Plant location are interpreted by Parker as showing a "skip distance" with respect to the B Plant stack. Further detailed surveys were proposed.

In a March 12, 1948, memo (HW-9175), C.N. Gross presents a summary of studies and intended action to achieve decontamination of existing plant ventilating air streams and to design better air cleanup systems. He stated that some of the active particles or droplets involved were small, perhaps less than 1 micron in size. The replacement of fans and ducts in the blower systems for the stacks had reduced the rate of deposition of active particles on the ground around the stacks, but it had not eliminated the deposition. Gross states, "The active material on the ground is picked up by the wind and scattered over a wide area. Complete safety from airborne particles could not be guaranteed inside a radius varying from about 2500 to 5000 feet, depending on prevailing winds."

An April 1, 1948, memo by Parker (HW-9372) poses questions to be addressed by future studies about active particle transport in the environment. Proposals for studies had been prepared by Dr. P.E. Church. A simulated rain experiment had been started. A rough guess by the author (H.M. Parker) of the particle density that could be safely left in place was 0.01 particles per ft^2. A crude estimate of the area contaminated to this degree was 24 mi^2. About 2 mi^2 was believed to be contaminated with 0.1 particles per ft^2 or more.

In a memo dated April 1, 1948, (HW-9476), P.E. Church responded to questions about the transport of the active particles by the wind to other areas of the site and offsite. It is important that the possibility for airborne transport of active particles was recognized at this early date. He did not expect that serious concentrations could be present beyond 2 mi downwind. Their experience was a dilution of a factor of 10,000 within 2000 ft of a ground contamination source. Washing the specks into the ground so that they would not become airborne was suggested, as was maintaining a well irrigated green turf in problem areas.

Report HW-10261 (Thorburn 1948), dated June 11, 1948, documents results of an investigation of the radioactive particles. In the introduction, Thornburn states that the Health Instrument Group from each separations area at the Hanford Works had discovered on the ground and roofs of buildings surrounding the off-gas stacks, "a multitude of small, but extremely contaminated particles." All results of this investigation tended to indicate that the particles were coming from the ductwork fans and surrounding breaching.

A letter from C.M. Patterson (HW-11479) to Dr. John Bowers of the Atomic Energy Commission in November 1948 gave an estimated deposition rate of 10^8 to 10^9 particles per month for the 200 Areas. Extending the area to cover the entire reservation gave an estimate of 10^{10} particles per month. These estimates were obtained by field sampling using systematic survey grids, followed up with "catch frames." Results from off-plant locations showed evidence of particles but were inconclusive. Evidence of particles had been found 170 mi from the stacks, but sufficient quantities for chemical assay had not been collected to determine if they were stack discharge active particles from the Hanford project. Sand filters had been installed as of October 1948, but Patterson (1948) indicated it was too early to evaluate their effectiveness; preliminary tests indicated they were only partially successful.

During the height of the particle releases from REDOX (1952–1954) and later, there were a series of contamination surveys that documented the particle deposition density on ground surfaces. The results were almost always presented as maps illustrating the extent of zones with varying ranges of particle numbers within a certain area of ground surface. These maps are reproduced in Appendix C. Data were extracted from the maps and are presented in tables later in this section. Some general narrative on the surveys is presented below in chronological order.

Donelson (HW-29346) discusses the emission of crystals from the REDOX stack. A third episodic emission of visible particles had recently been observed in the vicinity of the main stack on August 14, 1953; previous episodic emissions had occurred on June 24, 1952, and March 16, 1953. The most recent emission differed from previous instances in that the crystals were larger and carried a greater amount of radioactive material. The largest crystal found was approximately 5 in. long. The highest dose rate reported was 15 rep h^{-1} at the surface. Average crystals were perhaps 1/2 in. in maximum dimension and exhibited dose rates of 300 to 500 mrep h^{-1}. Figure 2 of HW-29346 (Figure C-8) shows the approximate distribution of those visible crystals. Smaller particles, detectable by instruments, were much more frequent and more widely spread than the visible crystals. However, those associated with the recent crystal emission could not be differentiated from those that had fallen previously.

Unusually high ruthenium emission from the REDOX stack in 200-West Area occurred in January 1954. The emission of 260 Ci on the night of January 2 and morning of January 3 represented the highest daily emission of ruthenium since startup of this facility in January 1952 (HW-31818). Failure of the caustic scrubber in the H-cell, 202-S Building was responsible. In addition, about 100 Ci was released between 10:00 a.m. January 5 and 10:30 a.m. January 6. The ruthenium emissions affected the measurements of nonvolatile beta activity on vegetation. A narrow trajectory from the January 2–3 release extended in a northeast direction from the 200-West Area. Contamination of ground surfaces is illustrated in Figure 4-32. The plume to the northeast was from the emission of January 2–3, whereas the one to the north was from the emission of January 5–6. The dose rate in the maximum zone was 500 mrad h^{-1}. Outside the 200-West Area dose rates decreased to values ranging from 25 to 100 mrad h^{-1} over an area several miles removed from the source. Weekly surveys on 100 control plots inside a radius of 6800 ft of the stack were established. In the latter part of the quarter, dose rates did not exceed 10 mrad h^{-1} at locations beyond a radius of 3 mi from the REDOX stack.

Ground contamination resulted in widespread contamination of project vehicles, which became evident in February and March (HW-32473). Nearly half of the vehicles on the site were surveyed and 20% found to be contaminated in excess of 100 cpm. The locations were most often tires and under-surfaces of the vehicles as well as radiators. Later that fall (September-

October 1954), an average of 12% of the vehicles in the REDOX Plant area were still contaminated in spite of water flushing of black-topped road surfaces (HW-33830).

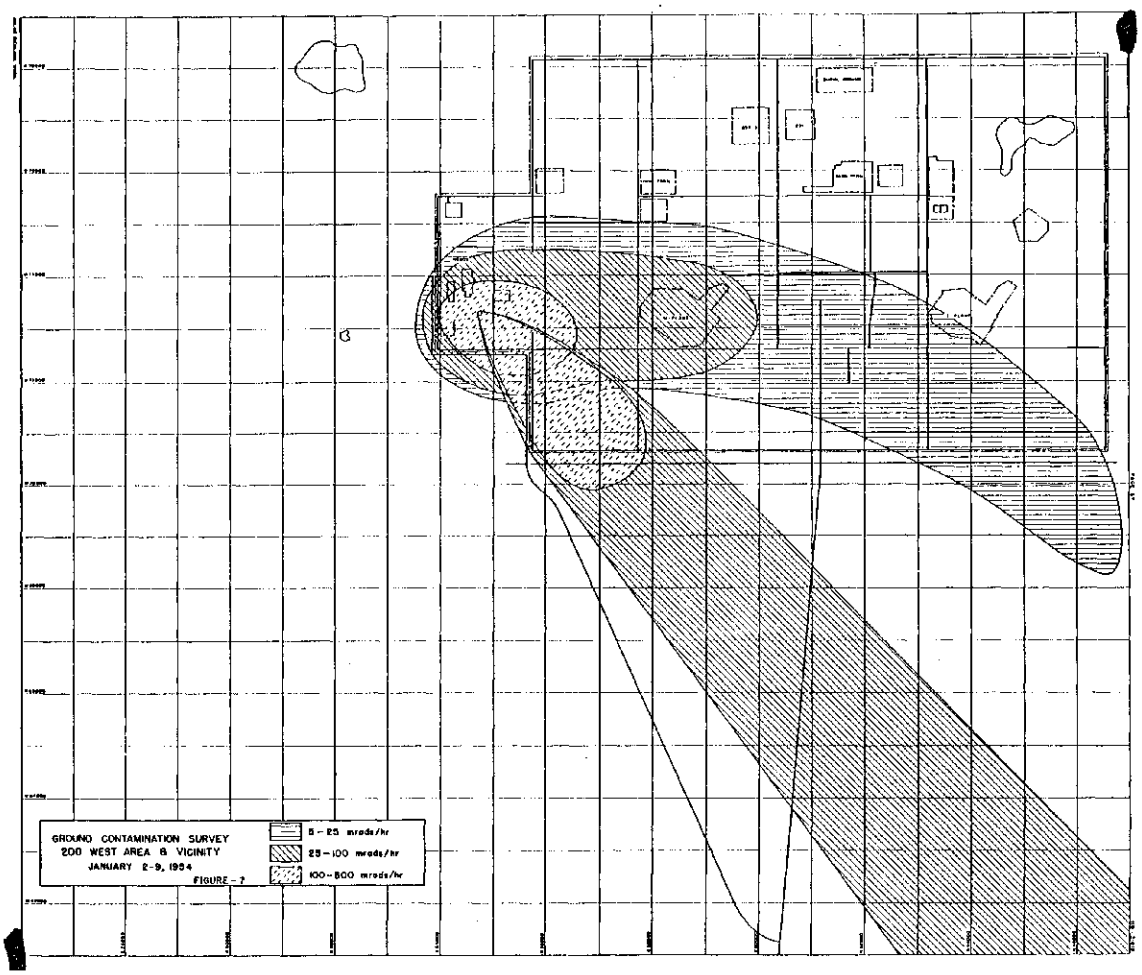

Figure 4-32. Ground contamination survey in 200-West Area and vicinity, January 2–9, 1954, showing trajectories of contamination resulting from episodic releases of ruthenium (Figure 7 from HW-31818) (north is to the right in this figure). Also see Figure C-9 for another schematic of this survey.

In the second quarter of 1954, portable instrument surveys of ground contamination in 200-West Area were conducted on a weekly basis at 100 control plots (HW-33896). Increases in dose rates (mrad per hour) were noted during the month of June 1954. The dose rates measured during the last week of the quarter are shown in this quarterly report as a map (Figure C-15). The survey extended about 2.3 km south of the REDOX stack, not as far as the nearest military encampment along Army Loop Road (3.2 km), (see Section 3.1). However, construction or other field workers could have been in these areas. The contaminating material was identified as ruthenium and rhodium.

The emissions of radioruthenium from the REDOX ventilation stack, of grave concern in early 1954, were substantially reduced after July as a result of the installation and use of additional off-gas decontamination equipment (HW-34882). The most intense ground

contamination in the immediate vicinity of REDOX (within 3000 feet of the stacks) had been maintained to about 6 mrad h^{-1} at ankle level by the use of water sprinkling which carried the activity into the ground. During September 1954, certain areas outside the REDOX exclusion area but within the 200-West Area were plowed to bury contamination and were then planted in rye.

In the third quarter of 1954, generally high ground contamination in the 200-West Area was found to consist of particles with maximum dimensions ranging from a few microns to around 1000 microns (0.1 cm) (HW-36504). The radioactive material present was nearly all ruthenium-rhodium, with dose rates from individual particles being as high as 10 to 20 rad h^{-1} at locations within several thousand feet of the REDOX stack. The activity ratio of ^{103}Ru:^{106}Ru was less than one. The source was definitely REDOX, but the low percentage of ^{103}Ru meant the contamination was not from recently processed fission products.

Environmental surveys made during the third quarter 1954 revealed particles of similar composition to be present throughout the environs as far away as Pendleton, Oregon, and Mesa, Washington. Particle concentrations in the Richland-Benton City areas were on the order of 1 particle per 3000 ft^2 although a somewhat higher concentration was noted on densely vegetated areas. Crop surveys revealed no contamination of fruit, although particles were detected on the ground in some orchards adjacent to the project. Road surveys on the project showed contamination on most highways, with particle frequencies varying from 2 per mile to 30 per mile near the 200-West Area. Most of these particles on the roads were fixed. (We interpret the term "fixed" to be not easily removable contamination, implying that the fragile ammonium nitrate particles had weathered, leaving the ruthenium/rhodium associated with the road surface.)

Report HW-33830 is a progress report for a REDOX particle study conducted in September and October 1954. Although unconfirmed by stack samples, there was every indication that the REDOX stack was continuing to emit radioactive material. Glass wool deposition samples in the stack area continued to show an average of 1000–2000 cpm d^{-1}. These glass wool collectors were mounted horizontally on metal frames with expanded metal tops in the stack area and out to a distance of about 1100 ft from the stack. In addition, a vertical sampler was mounted on one of the legs of the frame generally facing the predominant wind direction. These were normally changed weekly. After October 20, 1954, brownish spots showing uncorrected dose rates (with a C.P. instrument) as high as 150 mrad h^{-1} began to appear on the horizontally mounted deposition samples within 200 ft of the stack. At almost all locations, deposition on the horizontal collector was twice as high as that on the adjacent vertical collector. The one exception was at the railroad cut gate sample station, where the vertical sample was higher and determined to be essentially all cesium. Scans of the particles from the horizontally mounted filter indicated the contamination to be ruthenium with an age of somewhat greater than 200 days since pile discharge.

Surveys of the REDOX area loading docks and surrounding ground showed some new contamination during September 1954 with levels up to 6000 cpm (HW-33830). One particle with an uncorrected dose rate (C.P.) of 7.5 rad h^{-1} was found in the walkway to the exclusion area gate. During October, the deposition sample station mounted on the roof of the REDOX Building indicated positive depositions but of lower magnitude than those around the stack area.

In the routine monitoring report for the fourth quarter 1954, two maps were presented illustrating the results of ground contamination surveys (HW-36505). Abnormal ground contamination continued on the project and in the local environs, with some increases noted during November and December in the vicinity of REDOX. The particle ground contamination

map for September-October is shown in Figure 4-33. (Both maps are included with the entire set of ground contamination survey maps in Appendix C.)

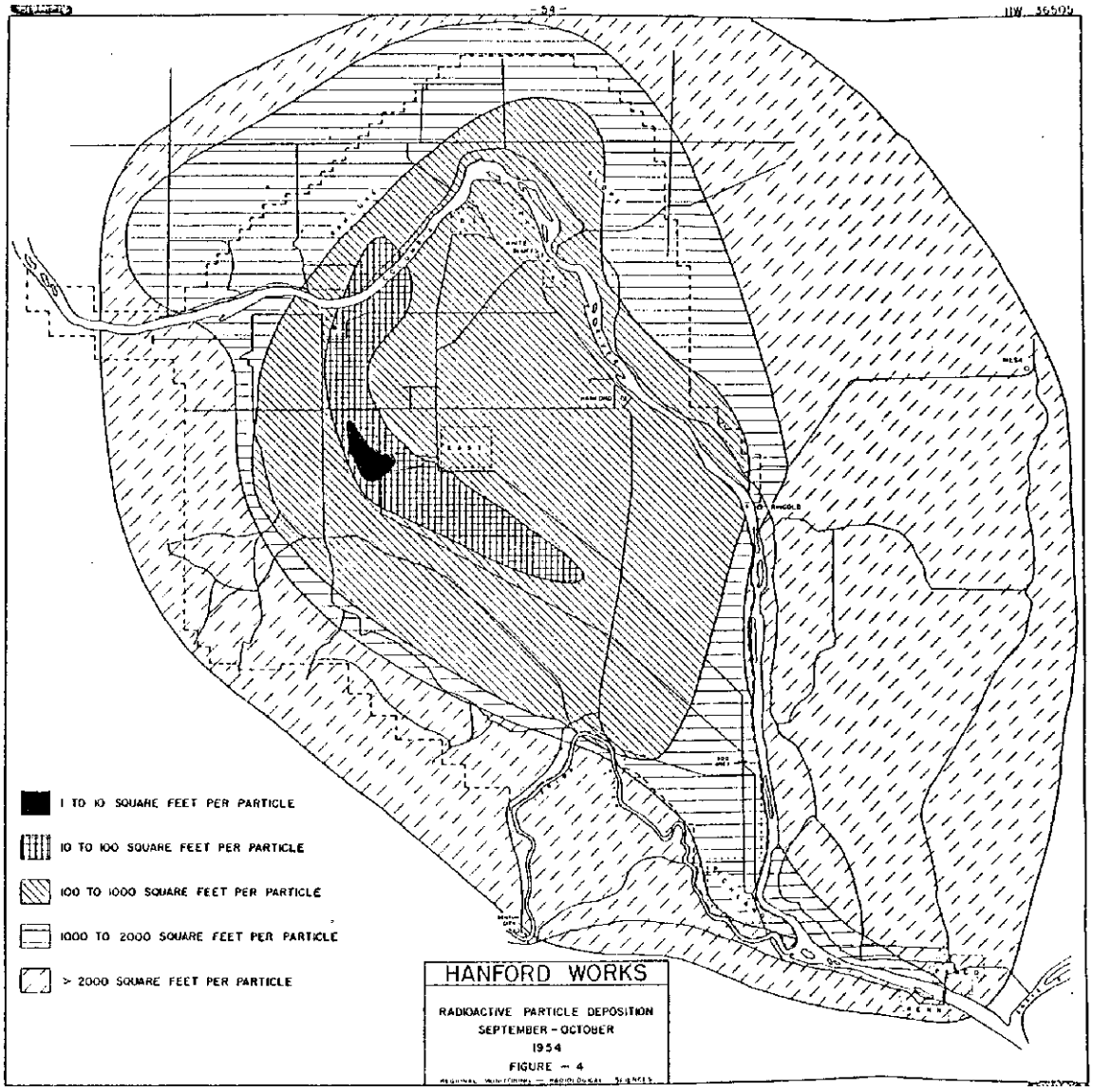

Figure 4-33. Radioactive particle density on the ground, September–October 1954, Figure 4 from HW-36505. The highest contamination zone near 200-West was one particle per 1–10 ft^2. In the lowest zone shown here, one particle was found in an area greater than 2000 ft^2.

The weekly variation in particle concentrations on control plots in the 200-West Area in October–December 1954 is shown in Figure 4-34. The concentrations are expressed relative to the median observed in November, which was a relatively stable period. Concentrations were lowest in October (0.7 relative to November) and highest in early December (1.6 relative to November). All these data represent "those particles detectable at ground level using a portable G.M. instrument."

Measurements of low-activity particles not detectable by portable monitoring instruments were started in the fourth quarter of 1954. The method involved exposure of film in light-proof envelopes to ground surfaces in the area. Concentrations of these low-level particles were found to be on the order of 200 particles per ft^2 at locations adjacent to the 200-West perimeter fence southeast of REDOX, compared to concentrations of less than 10 particles per ft^2 in the 300 Area.

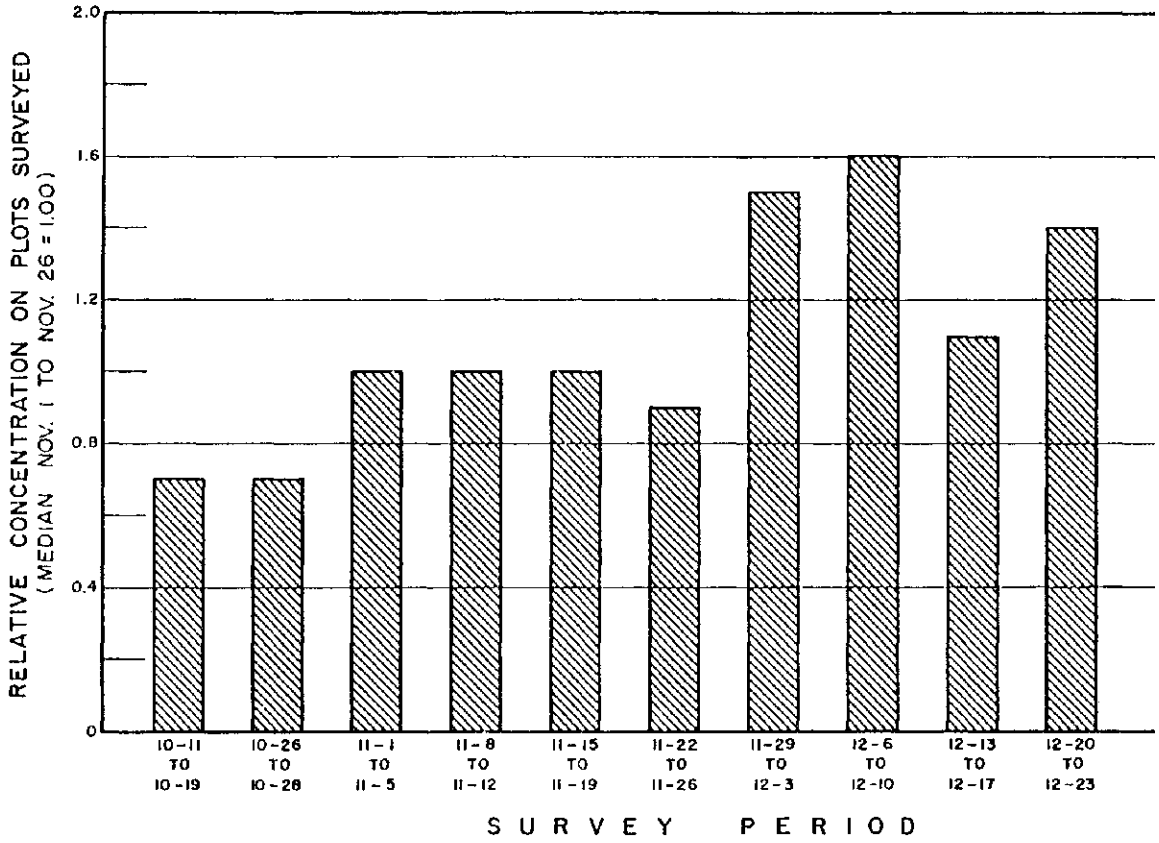

Figure 4-34. Relative concentration of detectable particles on ground survey control plots in 200-West between October 11, 1954, and December 23, 1954, compared to the period November 1–26, 1954 (Figure 6 of HW-36505).

Ground surveys of control plots around REDOX were continued intensively during the first quarter of 1955 (HW-36506). Several particles were found in the surface of the snow in January, indicating that the emission of particulate material was continuing. Following the same procedure as last quarter, the weekly variations in particle concentrations on the control plots were expressed relative to the median observed in November 1954, which was a relatively stable period (Figure 4-35).

Isopleth maps of detectable particle density on the ground were generated for February and March 1955 (not for January because of snow cover). These maps are included in Appendix C. Selected locations in Richland were surveyed showing an average of one particle per 4000 ft^2 in January and one particle per 2000 to 2500 ft^2 in February and March. The detection of particles in January was probably low because of partial snow cover.

Lower-activity particle densities measured in the first quarter 1955 using film in light-proof envelopes varied from 160 particles per ft^2 near REDOX to <3 particles per ft^2 in the vicinity of Richland, Pasco, and Kennewick (HW-36506). Concentrations in the vicinity of T Plant, about 2.8 km north of REDOX, were rather low, on the order of 5–10 particles per ft^2. There is no discussion of the natural background contribution from uranium and thorium series radionuclides. Presumably, natural radioactivity would have also contributed to these lower-activity measurements.

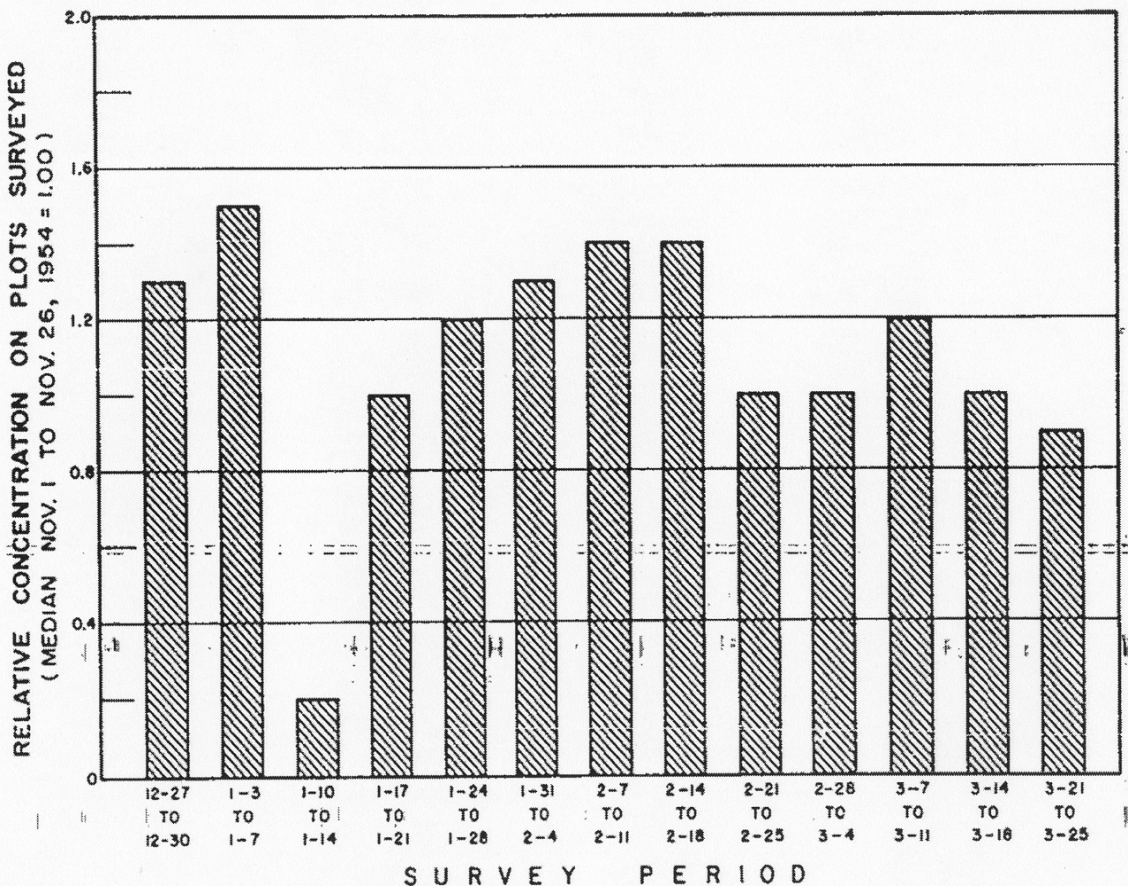

Figure 4-35. Relative concentration of detectable particles on ground survey control plots in 200-West betweeen December 27, 1954, and March 26, 1955, compared to the period November 1–26, 1954 (Figure 4 of HW-36506).

Work continued on determining the best way to measure particle fallout—for example, Hanford scientists experimented with glass wool pads, backed by cardboard, and gummed paper. Comparison of the numbers of particles retained by glass wool pads on the ground and those mounted on frames 2 ft above the ground showed a greater number on the ground, indicating possible movement of active particles at ground level. Gummed paper mounted vertically on telephone poles showed particles in the air as high as 9 ft above the ground (HW-36506).

Ground surveys of control plots around REDOX were continued throughout the second quarter of 1955 at a reduced frequency (HW-38566). The reduction was accomplished by eliminating the two outer rings of existing plots that had contained only a few particles without

any significant changes in number of particles for some time. Again, concentrations are plotted in a column chart relative to the median in November 1954 (Figure 4-36). The relative concentration decreased compared to the previous quarter (index value 1.2 to 0.85).

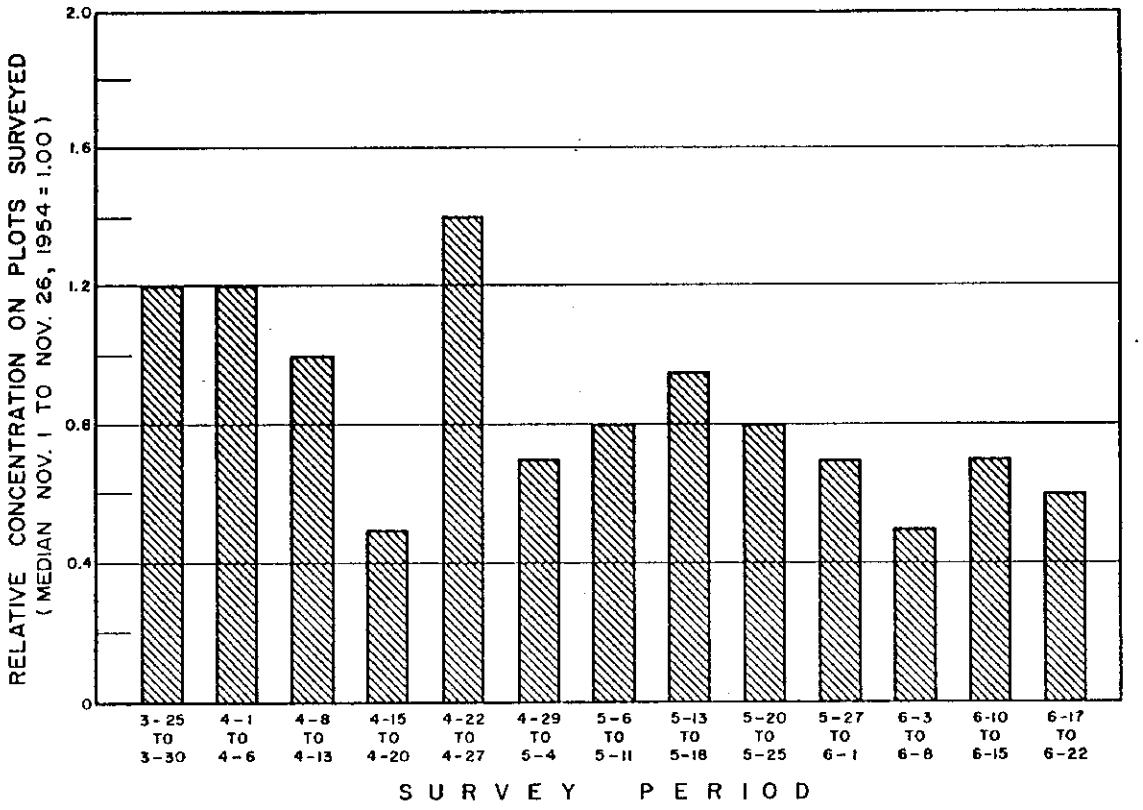

Figure 4-36. Relative concentration of detectable particles on ground survey control plots in 200 West betweeen March 25, 1955, and June 22, 1955, compared to the period November 1-26, 1954 (Figure 4 of HW-38566).

Hanford's Radiological Sciences Department estimated the total number of particles on ground areas from the particle density surveys (HW-38566). During the first 2 weeks of May 1955, they estimated 3.4 million particles detectable by portable instruments on the ground within 1 mi of the REDOX stack. Using the average dose rate per particle measured in the surveys, or approximately 20 mrad h^{-1} and converting this to activity, the total activity represented by this area was 0.7 Ci. This activity estimate was roughly 4 times lower than the 5 million particles representing 2–4 Ci on the ground as of December 17, 1954. (Apparently, the activity per particle differed because the number of particles did not change by a factor of 4.)

The second quarter 1955 report (HW-38566) gave some additional insight into how the sitewide ground contamination maps were generated. It states that ground surveys of 2000 ft^2 were conducted along main roads on and adjacent to the project at 1-mi intervals. The isopleth maps showing particle contamination density for April, May, and June 1955 are included in Appendix C.

Ground surveys of the Tri-City area in the second quarter 1955 produced similar results to the previous quarter, with one particle per 3000–4000 ft^2. Close-in surveys were also performed around reactors in H Area and F Area. Maximum densities around H Area were 16 particles per 100 ft^2. A survey of 10,000 ft^2 on the Wahluke slope located six particles. The maximum dose rate of any one particle was 150 mrad h^{-1}. The particles were composed of mixed fission products. The path of contamination indicated the source to be the 105-H reactor stack; emissions estimates indicated the week of May 3 to May 10, 1955, likely contained the highest releases. At F Area, there was one particle per 2000 ft^2, with the majority in the NE sector of the 100-F Area. The active material in these particles was found to be ruthenium, probably resulting from contamination originating from REDOX in 1954.

In the third quarter 1955 (HW-39429), ground surveys of the control plots around REDOX continued at reduced frequency. The relative index was given as 0.5 compared to 0.85 for the last quarter; however, a column chart of weekly values was not presented. Causes for the decrease are given as radioactive decay, rain, wind, and other meteorological phenomena.

Quarterly ground surveys in the separations areas in 1957 produced estimates of 15 and 5 particles per 1000 square feet for the REDOX and PUREX areas, respectively. Surveys made along roads on the project showed 0 to 2 particles per 1000 square feet. In the Tri Cities areas offsite an average value for 1957 was 15,000 square feet per particle (equivalent to 0.067 particles per 1000 square feet) (HW-89066).

4.1.6.3 Summary of Ground Survey Data. Report HW-54636, by J.M. Selby and J.K Soldat, summarizes incidents at Hanford that resulted in environmental contamination between 1952 and 1957, inclusive. The major problem at 200 Areas during this time interval was the series of ruthenium emissions from REDOX from March 1952 through 1954. Because of the widespread contamination that resulted, extensive surveys of the entire project were performed beginning in the summer of 1954. Over 25 maps in HW-54636, reproduced in Appendix C, illustrate the distribution of ground contamination around 200 Areas. Some maps are sitewide or larger, and some are limited to a smaller area. The sitewide maps are generated from the same data presented in the quarterly reports discussed in the previous subsection of this report. However, they are standardized so that results are expressed in units of particles per 1000 ft^2.

Table 4-7 shows the particle deposition density in the *maximum* zone shown on various survey maps (from Appendix C) as well as the particle deposition density at the H-40 military camp location, 8.9 km east of the REDOX stack (Figure 3-2). It should be mentioned that the military camps H-51 or H-60 are sometimes in the maximum density zone, but the general pattern indicates that H-40 received the greatest deposition. The highest particle deposition densities during the interval July 1954–September 1957 were observed between September 1954 and April 1955 (Table 4-7).

In the text of HW-54636, Selby and Soldat present survey results of the numbers of particles found at some offsite areas during June–September 1954. For ease of use, we converted those results to similar units and then tabulated them along with data from other sources (Table 4-8). Only five active particles were found in an extended survey (1000 ft^2 surveyed every 5 mi) along highways between Wallula, Washington; Lewiston, Idaho; LaGrande, Oregon; Baker, Oregon; Pendleton, Oregon; and back to Wallula. The maximum dose rate from these five particles was 500 mrad h^{-1}. Sixty-six percent of the 288 particles located offsite were within the dose range 5-50 mrad h^{-1} (HW-33068).

Table 4-7. Particle Deposition Density at Military Location H-40 and in the Maximum Reported Contamination Zone from Sitewide Survey Maps

Time interval			Particles per 1000 ft^2[a]	
Beginning	Ending	Source report number	H-40	Maximum zone
7/1/54	8/31/54	HW-54636 Fig 24	10	>100
9/1/54	10/30/54	HW-36505 Fig 4	10	1000
12/1/54	12/31/54	HW-36505 Fig 5	10	1000
2/1/55	2/28/55	HW-36506 Fig 5	10	1000
3/1/55	3/31/55	HW-36506 Fig 6	100	1000
4/1/55	4/30/55	HW-38566 Fig 5	10	100
5/1/55	5/31/55	HW-38566 Fig 6	10	100
6/1/55	6/30/55	HW-38566 Fig 7	10	100
7/1/55	7/31/55	HW-39429 Fig 4	10	100
8/1/55	8/31/55	HW-39429 Fig 5	1	100
9/1/55	9/30/55	HW-39429 Fig 6	10	100
10/1/55	10/30/55	HW-40871 Fig 4	10	>10
11/1/55	11/30/55	HW-40871 Fig 5	10	>10
1/1/56	1/31/56	HW-43012 Fig 4	1	10
3/1/56	3/31/56	HW-43012 Fig 5	1	100
4/1/56	4/30/56	HW-44215 Fig 3	10	100
5/1/56	5/31/56	HW-44215 Fig 4	10	10
6/1/56	6/30/56	HW-44215 Fig 5	10	100
10/1/56	12/31/56	HW-48374 Fig 3	1	10
2/1/57	2/28/57	HW-54636 Fig 35	1	100
4/1/57	4/30/57	HW-54636 Fig 36	1	100
8/1/57	8/31/57	HW-54636 Fig 37	<0.5	10
11/7/57	11/12/57	HW-45636	<5	100

[a] Particles detectable by a G.M. meter at ground level. When a range is presented, the maximum value is shown in this table. For example, a zone of 0.5–1 particles per 1000 ft^2 is shown in this table as 1.

Similarly, Table 4-9 lists the maximum reported contamination levels from close-in surveys that included the 200 Areas but not the entire site. The two surveys in 1947 are included here. The source maps themselves are reproduced in Appendix C. Results in Table 4-9 are expressed four ways: particles per 1000 ft^2, mrad per hour, counts per minute, and disintegrations per minute. The maximum ruthenium-bearing particle density in May 1954 (10 particles per ft^2) was equivalent to the maximum concentration of active corrosion products around the plant stacks in 1947. Because of the different radiological composition of the particles, the equal particle numbers do not necessarily represent the same hazard.

Table 4-8. Particle Deposition Density at Off-Project Areas

Description of location	Source report	Time interval	Particles per 1000 ft^2[a]
Mesa (small sample)	HW-33068	September 1954	1.7
School lawns in Richland	HW-54636	June–September 1954	1.0
Richland - grassy areas	HW-33068	September 1954	0.91
Wahluke Slope	HW-54636	June–September 1954	0.60
Wahluke Slope	HW-33069	September 1954	0.50
Richland	HW-36506	February–March 1955	0.50
Ringold to Pasco	HW-33068	September 1954	0.45
Richland – general	HW-33068	September 1954	0.40
Benton City to Columbia Camp	HW-33068	September 1954	0.40
Benton City to Enterprise	HW-33068	September 1954	0.30
Pasco-Kennewick	HW-33068	September 1954	0.25
Richland	HW-44215	April–June 1956	0.20
North Richland	HW-54636	June–September 1954	0.05–1
Ringold	HW-33068	September 1954	0.18
Connell	HW-33068	September 1954	0.14
Along road between Pasco and Ringold[b]	HW-54636	June–September 1954	0.13
Tri-cities area	HW-48374	October–December 1956	0.07
Tri-cities area	HW-89066	1957	0.067
Twelve orchards east of the project near Ringold	HW-54636	June–September 1954	0.038
Five orchards west of project near Midway	HW-54636	June–September 1954	0.016

[a] Particles detectable by a G.M. meter at ground level.

[b] An area of 1000 ft^2 was surveyed every 0.1 mi.

The PUREX stack was determined to be a source of ground contamination from a survey in July 1957. Table 4-9 values represent the maximum particle deposition density that would have been encountered by construction or field workers in the 200 Areas. It is clear that workers near the 200 Areas were exposed to much greater concentrations of active particles than people in off-project areas (Tables 4-7 through 4-9).

Table 4-9. Maximum Particle Deposition Density from Close-In Surveys That Encompassed the 200 Areas

Time interval			Maximum contamination[a]			
Beginning	Ending	Source report	Particles per 1000 ft^2	mrad h^{-1} per particle	cpm per particle	dpm per particle
11/28/47	11/28/47	HW-8430	10,000		10,000	
12/22/47	12/22/47	HW-8429	10,000		10,000	
3/30/52	5/3/52	HW-54636 Fig 11 and text	4000	800	1000	
6/1/52	6/30/52	HW-54636 Fig 12 and text	3000	600[b]		
7/9/52	7/9/52	HW-54636 Fig 39 and text				200,000[c]
3/1/53	4/30/53	HW-54636 Fig 13		25		
8/14/53	8/14/53	HW-29346 Fig 12 and text	1000[d]	15,000		
8/19/53	8/19/53	HW-54636 Fig 14		20,000		
1/2/54	1/9/54	HW-54636 Fig 16 and text		500[e]	5000[f]	
2/15/54	2/19/54	HW-54636 Fig 17		225		
3/1/54	3/5/54	HW-54636 Fig 18		225		
3/22/54	3/26/54	HW-54636 Fig 19		100		
5/24/54	5/24/54	HW-54636 text	10,000	15,000		
5/25/54	6/10/54	HW-54636 Fig 21 and text		2,000		
5/17/54	5/21/54	HW-54636 Fig 20		100		
6/25/54	6/25/54	HW-33896 Fig 5		950	10,000	
11/1/54	11/30/54	HW-54636 Fig 22	>100			
1/1/55	1/31/55	HW-54636 Fig 23	>100			
6/4/56	6/4/56	HW-54636 Fig 40 and text	1000[g]	450		
10/1/56	12/31/56	HW-48374 text	50			
7/4/57	7/4/57	HW-54636 text		430	20,000[h]	
11/7/57	11/12/57	HW-54636 Fig 41 and text	100	1100	>80,000[i]	

[a] Particles detectable by a G.M. meter at ground level. When a range is presented in the source report, the maximum value is shown in this table. For example, a zone of 5000–10,000 particles per 1000 ft^2 is shown in this table as 10,000.

[b] Text states there was an isolated maximum value of 4000 mrad h^{-1}.

[c] Associated with a fire in the solid waste burial ground. Contamination was alpha activity. Spatial extent was limited.

[d] Visible crystals. Many more were detectable with instruments.

[e] Text states there was an isolated maximum value of 1300 mrad h^{-1}.

[f] On Wahluke Slope following large ruthenium release.

[g] Determined to be large radioactive paint flakes from U Plant duct work, downstream of sand filter.

[h] Associated with PUREX stack releases. Contamination extended about 1500 ft N and NW of the stack.

[i] Associated with burial of very contaminated waste containing ruthenium.

Parker (1956b) summarized the Hanford experiences with respect to dispersion of radioactive particles in a paper presented at a conference in Geneva sponsored by the United Nations in August 1955. Two composite maps (Figures 4-37 and 4-38) illustrate dispersion patterns for an intermediate particle size range of 3-100 microns and for large particles, >100 microns. These largest particles, which could produce damage on skin contact, are restricted to a few kilometers from the source (Figure 4-38).

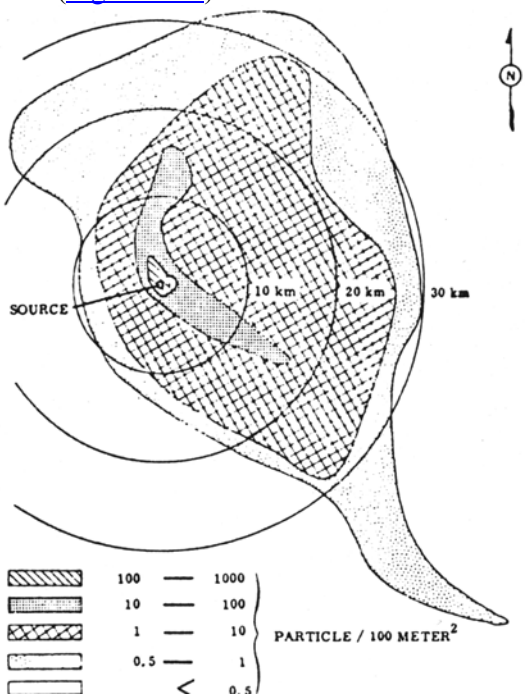

Figure 4-37. Typical distribution of 3–100 micron particles (Parker 1956b).

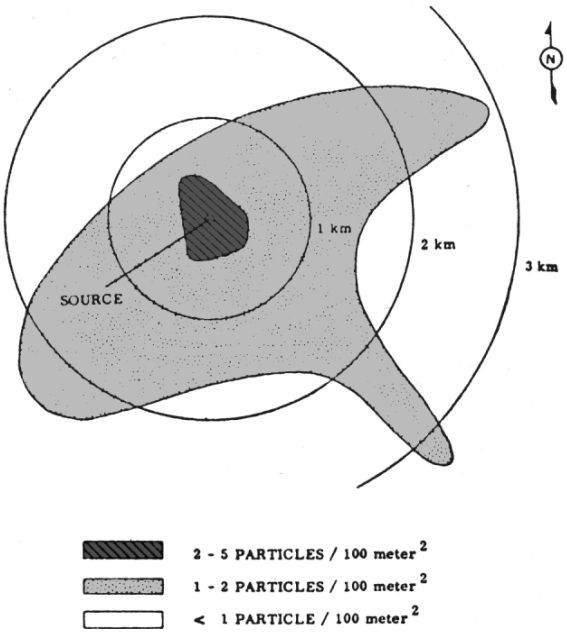

Figure 4-38. Typical distribution of >100 micron particles (Parker 1956b).

Selby and Soldat (HW-54636) used a series of locations selected in mid-1954 to obtain a reproducible time trend for particle survey data for the entire project. Their time trend in particle numbers on the ground of the Hanford project and vicinity is illustrated in Figure 4-39. The second half of 1954 was the most critical time in terms of radioactive ground contamination from the REDOX facility, with a total of 7×10^7, or 70 million particles. Weathering and radioactive decay had reduced those numbers by a factor of 10 by the fall of 1955. Irregularities in the curve after this time were caused by new releases of radioactive particles. For example, about 4 mi^2 in and around the 200-West Area were contaminated with ruthenium following the burial of grossly contaminated equipment on November 6, 1957 (HW-54636). A similar problem was noted in January 1956 (HW-43012).

Weathering of ruthenium into the soil is supported by a study discussed in the fourth quarter 1955 environmental report (HW-40871). An investigation of the penetration of particles into the soil near REDOX indicated that the first 4 in. of soil was heavily contaminated, and that a small number of particles penetrated the soil to at least 6 in. This shows a rapid movement of contamination into the soil column that would have greatly decreased the potential spread to other areas.

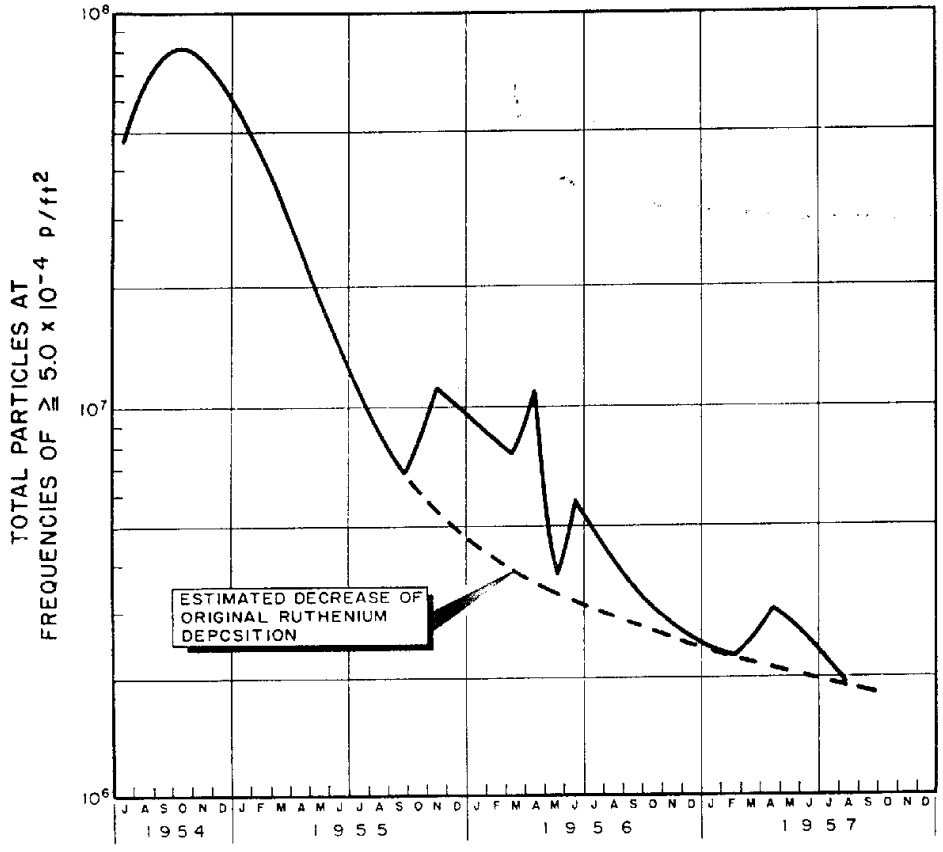

Figure 4-39. Time trend in total radioactive particles on the ground of the Hanford Project and vicinity, July 1954–September 1957, as determined by Selby and Soldat (1958) in HW-54636.

We believe that Figure 4-39, which addresses the total number of detectable radioactive particles in the Hanford environs, may exaggerate the decrease in radioactive particle levels at a single location, e.g., at a construction site near 200 Areas. Our opinion is based on examination of trends in the control plot data that are shown in Figures 4-34 through 4-36. When these data are combined, along with a relative index value stated in the third quarter 1955 report, the trend shown in Figure 4-40 is obtained. First, there is a large amount of scatter in the data that is not reflected in Figure 4-39. Second, the decrease in particle concentration on the control plots is less than that illustrated by Figure 4-39. At most, there was a reduction of a factor of 3 on the control plots (relative index 1.5 to 0.5) between December 1954 and the third quarter of 1955, whereas Figure 4-39 suggests a reduction of about a factor of 7 in the total number of detectable particles over that 9-month interval. A partial explanation may be that the control plots contained particles with some radionuclides that were longer-lived than ruthenium.

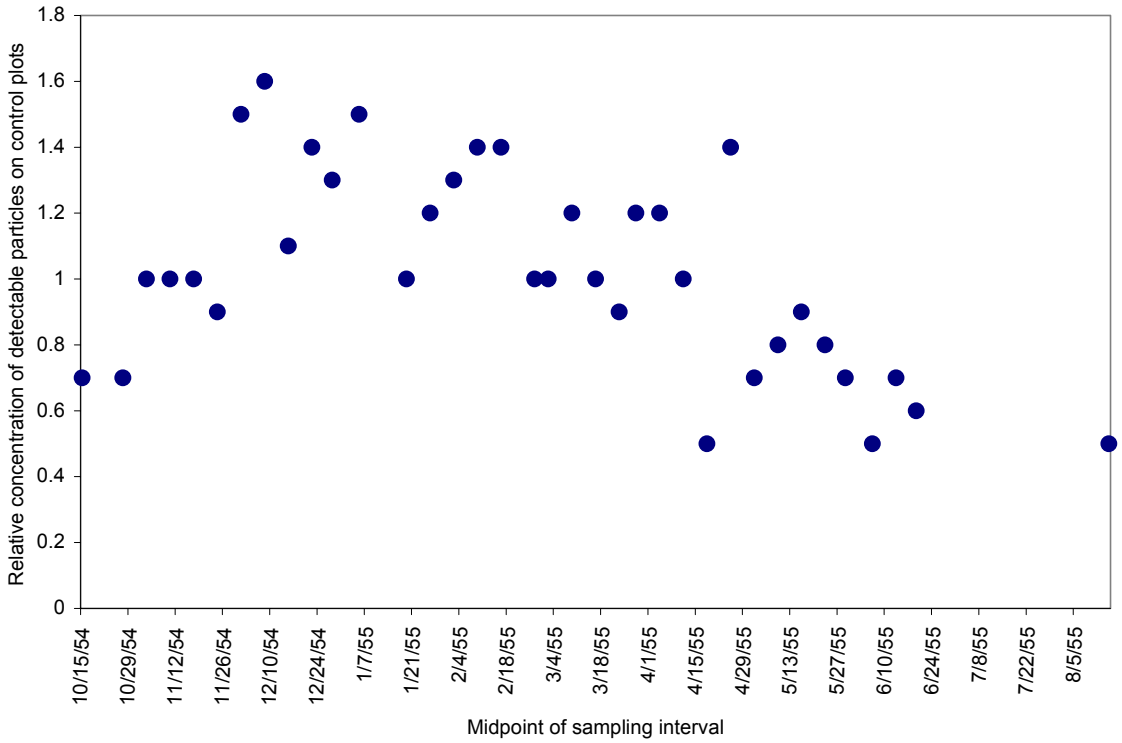

Figure 4-40. Time trend in concentration of detectable radioactive particles on control plots near 200 Areas relative to concentration observed in November 1954.

As with the other environmental monitoring data, weapons fallout in the 1950s must be considered in interpretation of ground survey data. A report by H.M. Parker (HW-33754) provided estimates of total deposition of radioactivity as of the fall of 1954. Total fallout (average over the U.S.) from the Castle series of tests in the Pacific in spring of 1954 amounted to about 100 mCi per square mile as of September 23, 1954. Table 4-10, from HW-33754, shows the maximum deposition density (mCi mi^{-2}) and approximate integrated mCi-days mi^{-2} for various sources between 1946 and 1954. In the text of HW-33754, Parker states that the maximum activity of a single particle was clearly greater for particles from the REDOX area than from fallout. However, the total integrated deposition of radioactivity from fallout from other

sources in the Richland area was about 30% greater than that from Hanford sources, most of which was iodine.

Table 4-10. Deposition Density of Radioactivity from Weapons Fallout and Hanford Processes, 1946 through mid-1954 (HW-33754)

Source	Maximum mCi mi^{-2}	Total mCi-days mi^{-2}
Separations (^{131}I)	~30,000	~340,000
REDOX (Ru)	~20	~10,000
Russia	2,000	~100,000
Pacific	500	~40,000
Nevada	20,000	~170,000
Unknown	4,000	~130,000

4.2 Special Studies of Environmental Contamination

4.2.1 Physical, Chemical, and Radiological Characterization of Particles

Some dose rates measured from particles during ground contamination surveys were presented in the previous section. Table 4-11 summarizes information about the physical, chemical, and radiological properties of radioactive particles associated with Hanford releases between 1945 and 1956. The emphasis here is on characterizing the radioactive particles for the purpose of environmental transport and dosimetry calculations. Minor emphasis is given to release rates or other information for source term development. The emphasis of Section 2.2 is information needed to define source terms. Table 4-11 lists the particle characterization information in chronological order. In addition, the most substantive reports containing information are reviewed in the text in chronological order.

By fall 1947, the term "active particles" was being used in Hanford reports to describe the radioactive particles being found outside on the ground in 200 Areas.

> Recent surveys by the Health Instrument Section have disclosed the presence of many small radioactive spots on ground surfaces in the T an [sic] B plant areas. Investigation has shown that representative samples of the spots when mechanically separated invariably end in a single radioactive particle. Presumably these particles are being dispersed by the T and B plant stacks, although this has not been specifically demonstrated. It is not known whether this phenomenon has existed for a long period of time or is of recent origin. Upon review, existing data suggests a history of this occurrence for approximately six months (HW-7865, dated October 22, 1947).

The particles were found to be widespread throughout the two plant areas. Spots were found around all buildings and extended to and beyond the exclusion area fence. A pessimistic particle density estimate was 1 per 4 ft^2 (HW-7865). However, by the end of October, Parker (HW-7920) estimated a daily particle deposition rate of 1 per ft^2 in the downwind direction and 1 per 4 ft^2 in the upwind direction.

Table 4-11. Physical, Chemical, and Radiological Properties of Radioactive Particles Released from Hanford, 1945–1956

Time interval		Source report	Location of sample	Physical characteristics	Chemical characteristics	Radiological characteristics
Beginning	Ending					
	May 7, 1945	HW-3-2894	Stack samples taken from the T Plant			0.6–0.8 MeV beta presumably from iodine; also 1.5–2.0 MeV beta
1945	1947	HW-10758	Vegetation, processing plant effluent air, and ambient air			See Table 4-13 for radionuclide composition
	August 1947	HW-11082	Outside near T Plant fence	Presence of singular large particles not indicated		Mostly Ce and decay product, Pr
	September 1947	HW-55569	Outside in 200 Areas			Effective half-life of about 300 days. Principal contaminants were (in order): Ce, Y, Sr, Ru, Cs.
	Fall 1947	HW-7865	Outside ground near T, B Plants	Can be mechanically separated from dirt		Total beta activity ranging from 0.5 μCi to 1 μCi. Most of the beta activity was Ce; most alpha was Pu (range 0.07–1.7 nCi)
	Fall 1947	HW-9259	Outside ground near T, B Plants	Color reddish brown; carrier particles >100 μm, range 20 to 1500 μm linear dimensions; small particles, mists, and droplets emitted since operations began	Contain iron oxides; can be separated with magnets	Alpha activity mostly Pu, 1/20 as much U. Beta activity correlated with surface area of particle; mostly Ce (and daughter Pr-144), Y, Sr, Ru, and Cs
	October 1947	HW-7920	Outside ground near T, B Plants	Mass of 0.1 to 1 mg; brown color (different from soil)		0.1 μCi to 1 μCi. T Plant particles 60–90% Ce and up to 15%Y. B Plant 30–55% Ce, 7–20%, Sr and 30–45% Y
October 1947	January 1948	HW-8624	Outside ground near T, B Plants	Physical sizes of 153 large particles ranged from 40 μm to >1 mm. Median 300 μm. No reliable data on very small particles.	Essentially all particles contain enough iron to be separated magnetically	0.0001 to 3 μCi. 30–50% Ce; 10–50% Y; 10–20% Sr

Table 4-11. Physical, Chemical, and Radiological Properties of Radioactive Particles Released from Hanford, 1945–1956

Time interval		Source report	Location of sample	Physical characteristics	Chemical characteristics	Radiological characteristics
Beginning	Ending					
	~March 1948	HW-9175	Processing plant effluent	Some are <1 μm		
	Spring 1948	HW-9864	Processing plant effluent	Mists mean size <5 μm; magnetic specks, density of iron		
	Spring 1948	HW-10261	Ground and roofs surrounding processing plants	Usually less than 500 μm; range 20–1500 μm	High in iron; low carbon and calcium	2.5 pCi to 3.2 μCi beta per particle. Max beta energy 3.0 MeV
	Spring 1948	HW-10261	Processing plant effluent			Beta mostly Ce; alpha mostly Pu
	~September 1948	Gregg 1948	Outside ground	10–1000 μm	Associated with rust	Max 3 μCi beta per particle
July 1948	September 1948	HW-12677	Particles collected by air samplers			1–10 pCi fission products per particle
July 1948	September 1948	HW-12677	Stacks of 314 Building, the Melt Plant, in 300 Area			Mostly uranium
?	1950	HW-15802	Ventilation air of the B Plant before sand filter			100% of alpha was Pu; most of beta was Ce, rare earths, Ru, Zr, Y, and Sr
	April 3, 1952	HW-33068	On survey meter inside car with window open			Particle read 40 rad h^{-1}
	April 29, 1952		Eastern and northern sections of the REDOX area			From 100 cpm at 1 in. to 800 mrad h^{-1} at surface; gross beta activity ranged up to 0.1 μCi per sample

Table 4-11. Physical, Chemical, and Radiological Properties of Radioactive Particles Released from Hanford, 1945–1956

Time interval		Source report	Location of sample	Physical characteristics	Chemical characteristics	Radiological characteristics
Beginning	Ending					
April 1952	June 1952	HW-26493	Particles emitted from REDOX Plant (second, third, and fourth episodic releases on April 3, April 29, and June 24)	Ranged from microscopic translucent hydroscopic crystals adhering to the soil sand, to visible chalky particles varying in shape and size—a few with diameter ~ ½ in. Larger visible particles easily fractured, apparently a conglomerate of microscopic crystals.	Chemically, the composition of the inactive material was mainly ammonium nitrate with a small amount of occluded dust particles	90 to 98% of the total beta activity was Ru; ^{131}I in particulate contamination ranged from 1–5%. Beta particle activity varied in direct relationship with size.
	June 24, 1952	HW-32473	Outside: flakes from fourth episodic release from REDOX	1/64–1/32-in. thick and up to several inches in diameter. Large flaky radioactive particles found near the eastern REDOX exclusion area rapidly disappeared, though activity spots were detectable with survey instruments. Flakes fragile and hydroscopic.	Carrier crystal was predominately ammonium nitrate	Mostly ruthenium
	March 12, 1953	HW-28009	Ambient air near REDOX			36% of beta activity was Ru, 43% rare earths and Y
	Spring 1953	HW-28780	Base (inside) of the REDOX stack	Median particle size about 0.2 μm with GSD of 1.6 during one sample and 2.5 during another		Activity median particle size was 0.6 microns.
August 7, 1953	August 14, 1953	HW-29346 HW-32473	Outside ground southeasterly direction from the REDOX stack	Up to 5 in. (13 cm); average 0.5 in. (1.3 cm); up to 1/2 to ¾-in. thick	Carrier crystals were ammonium nitrate	Max 15 rep h^{-1}; average 300–500 mrep h^{-1} surface. 70% Ru, 25% rare earths and Y, and trace amounts of Sr, Ba, and Zr.

Table 4-11. Physical, Chemical, and Radiological Properties of Radioactive Particles Released from Hanford, 1945–1956

Time interval		Source report	Location of sample	Physical characteristics	Chemical characteristics	Radiological characteristics
Beginning	Ending					
	December 1953	HW-32209	Air entering sand filter of REDOX	Two cascade impactor sample results geometric mean of 0.3 μm (GSD 2.8) and 0.5 μm (GSD 3.2); average particles per cubic meter was 5.3×10^8		
	December 1953	HW-32209	Air at 10-ft level inside REDOX stack	Four cascade impactor sample results ranged from geometric median size 0.3 μm (GSD 2.0) to 0.4 μm (GSD 3.8); average particles per cubic meter, 2.4×10^8		
August 9, 1954	May 18, 1954	HW-33896	Air entering REDOX Plant sand filter			92% of total beta activity was Ru in March; in May, 24% was Ru, 28% rare earths, 14% Zr, and 25% Nb
		HW-33068	General review: input side of process sand filter			Less Ru (80%) and more of the rare earths (10–15%) and Sr (1–2%), compared to particles emitted to the environment
1952	1954	HW-33068	General review: REDOX releases to environment	Primary particles about 2 μm; large secondary particles typically 100 μm.	Carrier base is aggregate of ammonium nitrate, sometimes sand. Inhalable particles were between 40–80% soluble after 36 h in simulated lung fluid. Large particles were 3– 70% soluble after 48 h in simulated gastric juice.	Primary particles up to 5 nCi per particle, dose rate of 0.5 mrad h^{-1}; secondary particles dose rates up to 20 rad h^{-1} and 200 μCi per particle. Ru and Rh activity 98% of the total, with Sr-89 and Sr-90 <0.3%; rare earths plus Y <1.0%; and Zr-95 <0.5%.

Table 4-11. Physical, Chemical, and Radiological Properties of Radioactive Particles Released from Hanford, 1945–1956

Time interval		Source report	Location of sample	Physical characteristics	Chemical characteristics	Radiological characteristics
Beginning	Ending					
	June 1954	HW-32473	Outside ground in 200 Areas	No well-defined relationship between particle size and dose rate. Particles of several thousand square μm were observed. Easily fractured.	Ammonium nitrate present	90% of beta activity was Ru; activity ratio 103:106 was 0.6 to 1.4; one particle with dose rate of 1.2 rad h^{-1} contained 6.3 μCi; another reading 120 mrad h^{-1} had 0.49 μCi; average dose rate per μCi was about 200 mrad h^{-1}
	November 7, 1954	HW-36505	Five particles emitted from REDOX stack	Four of the particles were agglomerates of smaller white crystals with yellow discoloration on some surfaces. One particle was bright yellow without the crystalline appearance.	Ammonium nitrate and iron were found in four particles. The bright yellow particle was mostly calcium and iron.	95% of the beta activity was from Ru/Rh isotopes with the ratio of activity of ^{103}Ru to ^{106}Ru being less than 0.05. Also Sr, rare earths, Zr, Pu.
October 1954	December 1954	HW-36504	Ground surfaces around REDOX	Maximum dimensions ranging from a few μm to ~1000 μm		Nearly all beta was Ru/Rh; Ru-103:Ru-106 ratio less than 1
	December 1954	HW-35542	Ground surfaces around REDOX	Relative to a unit length, the average width was 0.75 +/– 0.14 and the depth was 0.39 +/– 0.18. The density is believed to be about 1.5		
May 29, 1956	June 4, 1956	HW-44215	Outside of U Plant in 200-West Area	Large paint flakes up to 8 in. long, peeled off duct work between sand filter and U Plant stack	Associated with painted stack liner	Alpha and beta

Some of the particles collected in October 1947 were analyzed and showed a total beta activity ranging from 0.5 μCi to 1 μCi. Most of the beta activity near T Plant was cerium (60–90%), with small (<3%) amounts of ruthenium, strontium, zirconium, cesium, yttrium, and columbium.[j] One of the two samples from T Plant showed 15% yttrium. At B Plant, 28–56% of the beta activity was cesium, 32–44% was yttrium, 7–20% was strontium, and <3% was ruthenium and columbium. Plutonium accounted for 65, 70, and 96% of the alpha activity in three samples. Alpha activity per particle ranged from 160 to 3800 dpm (0.07–1.7 nCi) (HW-7865).

Three months later, in January 1948, Parker reported progress on action taken on the spot contamination in the separations plant areas. The physical size distribution of 153 particles is presented in a table for seven size classes ranging from 0.001 to >1.0 mm^2 in area (HW-8624). The area was described by the author as the product of the two principal axes of the particle. The particles were not spherical, but it is useful to estimate an appropriate equivalent spherical size. Using the Crystal Ball uncertainty analysis program (Decisioneering 1996), we determined the median area as 0.071 mm^2, or an equivalent sphere of about 300 microns. The range can be expressed similarly as about 40 microns to >1.1 mm.

Report HW-10261 (Thorburn 1948), dated June 11, 1948, documents results of an investigation of the radioactive particles. Surveys of each separations area had discovered on the ground and roofs of buildings surrounding the off-gas stacks, "a multitude of small, but extremely contaminated particles." The particles were usually less than 0.5 mm in diameter and contained as much as 3 μCi of beta activity. Two possible prime sources were given as

1. Minute droplets from either the dissolver, the process, or stack condensate being blown out of the stack, landing on a small piece of sand and being discovered as a radioactive particle; and
2. The actual breakdown of part of the process system resulting in small particles being blown out of the stack. Examples would be corrosion of the fans resulting in rust particles or stack concrete breakdown producing small pieces of contaminated cement being blown out of the stack.

All results tended to indicate that the particles were coming from the ductwork fans and surrounding breaching. Chemically, the particles were high in iron content. A low carbon and calcium content tended to exclude breakdown of the asphalt-painted cement stack as the source. In addition, the color of the particles was dark, not light like particles from the stack. Analysis of silicon was conducted to test the possibility that small particles were attached to soil.

Physically, the individual particles were relatively small, ranging in diameter from 0.02 mm (20 microns) to 1.5 mm. A size study of 111 particles was conducted. A distribution curve of the results in HW-10261 is shown in Figure 4-41. The average was 0.21 mm^2, and the most likely speck appeared to be in the range of 0.05 to 0.10 mm^2 (equivalent sphere 250–500 μm). The author indicates that the collection of particles of the smallest sizes was undoubtedly limited by visibility. A similar size distribution was obtained for 67 specks with an "area" of less than 0.05 mm^2. For this distribution, the mean speck area was 0.013 mm^2 (130 μm), with the most likely at about 0.002 to 0.004 mm^2 (50–70 μm). All particles appeared rough and granular under a microscope, and at least a spot of rust-brown color was common.

[j] Columbium, symbol Cb, a former name for the element niobium, especially in America (Seaborg 1994).

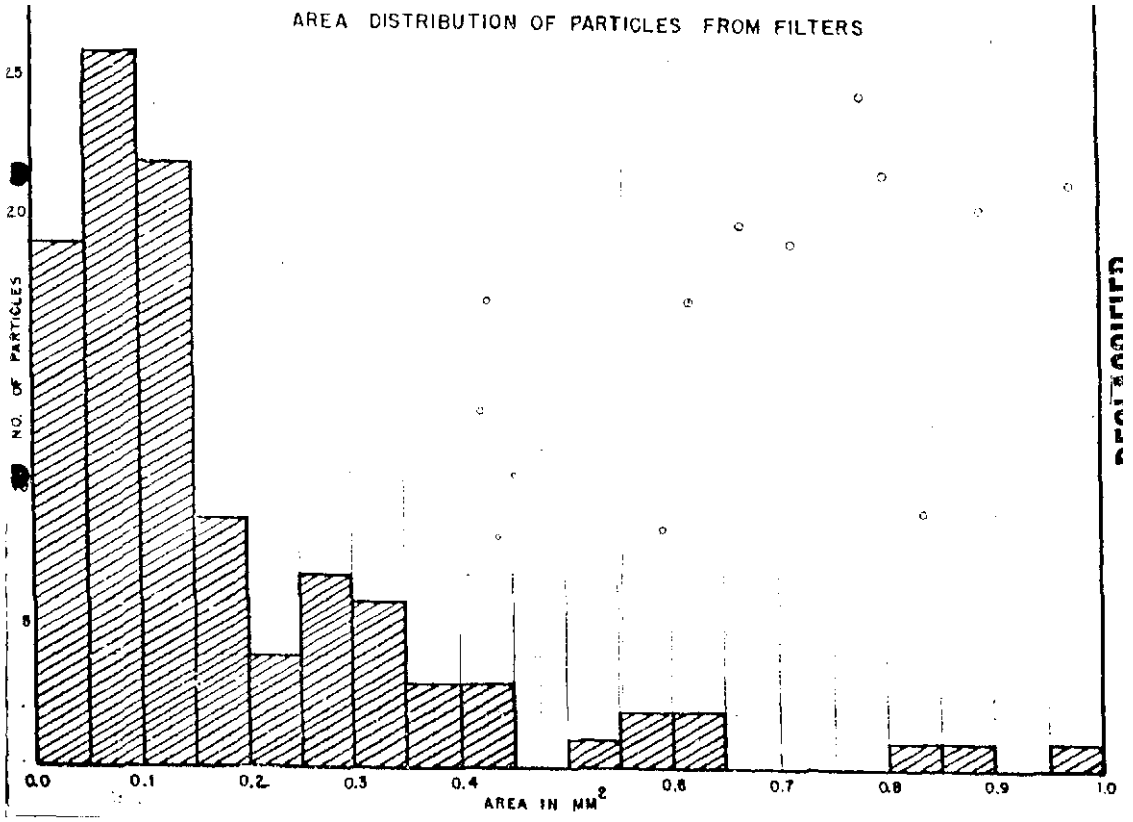

Figure 4-41. Size distribution of particles collected from effluent air filters from 200-Area processing plants in spring 1948 (from HW-10261). The area was computed from the product of the minor and major axes lengths.

Contamination present on the particles was determined. Table III of HW-10261 presents the results for particles collected from a variety of locations, including "new" particles collected directly from the off-gas stream or on a tacky surface. Typical radioanalysis of particles from 200-West and 200-East, as well as stack gases and breech gases from 200-East, indicate the following ranges of activity (expressed as percent of total activity):

Cerium/praseodymium	17–49%
Yttrium	0–28%
Ruthenium/rhodium	0–14%
Strontium	3–10%
Other rare earths[k]	0–12%
Zirconium	0–10%

[k] Rare-earth elements refer to any of the group of chemical elements with atomic number 58 to 71; the name is a misnomer because they are neither rare nor earths; examples are cerium, praseodymium, lanthanum, erbium, and gadolinium.

Iodine	0–7%[l]
Cesium	0–4%
Columbium[m]	0–3%
Tellurium	0–0.7%
Barium	0–0.1%.

Four of the five groups of particles discussed in HW-10261 had alpha activity results. Between 67% and 99.5% of the alpha activity in these active particles was plutonium and between 0.5 and 5% was uranium.

The age of the particles could not be determined by the ratio of different radioelements to each other because of selective volatility and sorption characteristics of different elements. However, insight into the age of the particles could be gained by examining the ratio of different isotopes of the same element, e.g., ^{89}Sr and ^{90}Sr, which behave the same chemically. A spread in age of approximately 200 days (age range 100–300 days) for the active particles was estimated. The isotopic ratio of strontium in the air stream, as determined by filter paper analyses, was lower than any specks, indicating a hang-up of fission products. The author concludes, based on other data as well, that the hold-up occurred on the rust and corrosion of the fans and ductwork.

The total radioactivity of individual particles was determined by direct counting and by analysis of solutions of dissolved particles. A range of 2.5 pCi to 3.2 μCi per particle of beta activity and from <5 dpm to 3800 dpm (2–1700 pCi) per particle of alpha activity was found. The total number of particles analyzed was not given, although 111 specks were picked to test the correlation between particle size and activity. The author indicates that the possibility of even hotter specks exists. Absorption curves with aluminum absorbers indicated beta particles with a maximum energy of 3.0 MeV.

Other special tests are briefly summarized by Thornburn (HW-10261). Feces samples from four men whose work was primarily in the stack area showed no fission product activity. The solubility of a particle in distilled water was found to be zero (no detectable count in dried solution after 24 hours). Several hot spots were found on hand rails and rocks in both separations areas. The spots were dirty yellow in color and appeared to be dried drops. It appeared that larger drops had run down the hand rails before evaporation. The salts from these drops were scraped up and analyzed. One sample was similar to the particulate specks (data presented above); the other contained considerably more strontium (77%). The source and mechanism for this type of contamination was not investigated.

An addendum to HW-10261 indicates that a new stainless steel fan had been inserted into the off-gas system in each of the separations areas. A significant decrease in the number of large (>0.01 mm in diameter) particles was observed in 200-East. The number of smaller particles was about the same, however. Tests were still underway in 200-West, but it appeared so far that there was little change.

HW-10758, *Long-lived Fission Activities in the Stack Gases and Vegetation at the Hanford Works*, published in August 1948 by J.W. Healy, examined releases from 200 Areas. In the

[l] Author states these results are probably low by 5–15%.
[m] Former name for the chemical element niobium. The name is still used occasionally in metallurgy.

context of his report, long-lived means longer half-lives than radioiodine, which had previously received the most attention when studying possible hazards from plant releases. The possibility of more lasting problems with other radionuclides was beginning to be recognized. The main contribution of this work to our task is the apportioning of total long-lived activity into separate isotopes. Healy's composition analysis was done by examining decay curves, which involved counting the same sample (e.g., an air filter) repeatedly over many days and examining the rate of decay. The shape of the curve was analyzed to estimate the composition of the nuclides present. Healy applied this analysis to stack samples, ambient air samples, and vegetation. An example of a decay curve from Healy is shown in Figure 4-42.

The techniques available at the time permitted Healy to separate the possible nuclides present into three broad half-life categories. Table 4-12 shows those categories (with likely isotopes that fall in them) and the composition observed in stack and ambient air samples.

Table 4-12. Composition of Beta Activity (other than Radioiodine) in Hanford Samples from 1945–1947

Type of sample and number (n) of analyses	Half-life category and likely isotopes		
	30–60 days ^{89}Sr, ^{91}Y, ^{95}Zr, ^{103}Ru, ^{141}Ce	275–300 days ^{106}Ru, ^{144}Ce	Long ^{90}Sr, $^{137m}Ba/^{137}Cs$
Stack and ambient air (Healy's summary of all results)[a]	60–80%	30–40%	1–2%
1945 stack air samples (n = 2)	55–59%	40–44%	1%
1947 stack air samples (n = 5)	71%	28%	1%
1945–1947 ambient air filters (n = 9)	Range 52–83% Average 70%	Range 17–46% Average 29%	Range 0.5–2% Average 1%
1945–1947 vegetation (n = 7)	Range 41–71% Average 52%	Range 28–71% Average 46%	Range 1–3% Average 2%

[a] These are the values that Healy states in the summary on page 1 of his report. The values add up to more than 100%. However, in the discussion on page 9 of this report, he says the activity of stack and ambient air samples "averages about 70% of the 30–60 day, about 29% of the 300 day, and about 1% of the long half-life material."

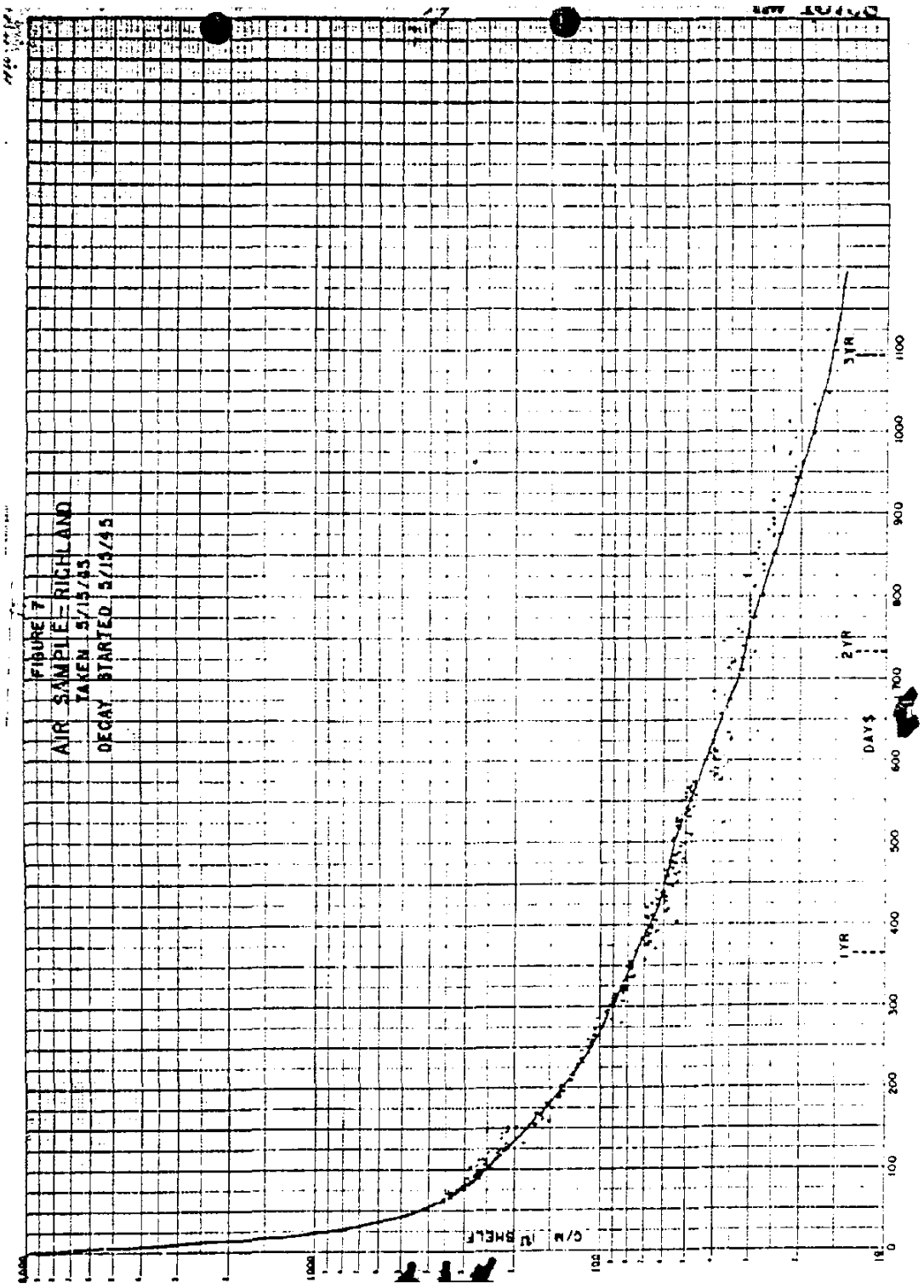

Figure 4-42. Decay curve for air sample from Richland taken May 15, 1945 (HW-10758). The filter sample was counted many times (each dot is a separate count) for a period of time lasting over 3 years. Similar curves are given in Healy for stack air samples and vegetation. By examining the shape of the curve, the composition of the radionuclides present can be estimated.

A single complete fission product analysis was run on a sample of sagebrush from the 200-West gate (HW-10758). The collection date was not given, but it would have had to be before August 1948. The composition was 49% cerium, 19% yttrium, 2% rare earth group, 8% ruthenium, 8% strontium, 3% cesium, and 7% zirconium.[n]

Long-lived beta activity in vegetation collected in 1945–1947 was over 20 times higher (0.4 μCi kg^{-1}) in the 200 Area compared to Richland (<0.02 μCi kg^{-1}). This means that activity measured near the 200 Areas is predominantly from Hanford releases and not some other source. The composition observed in vegetation is shown to have a composition similar to that expected after 3 years exposure to the stack effluent. This confirms that significant releases had been occurring since 1945.

Healy obtained filters from stack samples from T Plant in May 1945 (n = 2) and April 1947 (n = 5). These samples were originally taken to determine the plutonium content of the effluent air, which is reported in another document. Some of these filters had been saved and were used in this study to examine decay curves of the activity collected. Counting of these stack samples began 2 months after collection. In addition to total long-lived activity in microcuries, the percent of the activity in three different half-life groups (55-days, 275-days, and "long") was estimated. The 55-day group, was thought to be possibly ^{89}Sr (55 days), ^{95}Zr (65 days), ^{141}Ce (30 days), ^{91}Y (57 days), and ^{103}Ru (45 days). The 275-day group would include ^{144}Ce (275 days) and $^{104,105}Ru$[o] (1 year). In 1947, 71% of the total was 55-day group, 28% was 275-day group, and 1% was long.[p] In 1945, the composition (same order) was 55–59%, 40–44%, and 1%. The main contribution of the work described in Healy (1948) to our task order objective is the apportioning of total long-lived activity into separate isotopes.

Large particle releases to the environment became a problem again at Hanford in 1952 with the start-up of REDOX. See Table 4-11 for a chronological listing of particle characterization data related to releases from REDOX. In addition to this tabulation, a few source documents are reviewed here.

In the first quarter of 1953, air samples were collected in the visible plume of REDOX effluent at locations within 1 mi of the stack (HW-28009). The measurements were made with a portable, high-volume air sampler (120 cfm for 15 to 60 min) during periods of low atmospheric dispersion. Results showed several values in excess of one particle per cubic meter of air, over 10 times higher than the separation areas and over 100 times higher than in residential areas. Maximum concentrations obtained on February 20 and March 8 were 12 and 4 particles per cubic meter, respectively. The portable air sampler was operated continuously on March 12 for a 9-h period, and the filter was analyzed for beta emitters with the following results (Table 4-13).

On July 22, 1953, Adley et al. published a report of an investigation of particles emitted from the 291-S (REDOX) stack (HW-28780). The study began because of abnormal quantities of airborne particulates in the environs of the separations areas in May 1953. All samples were taken from the base (inside) of the 291-S stack using existing sampling facilities over a short

[n] On page 9 of the report, Healy clarifies which isotopes are likely to be in these elemental categories. Some of the ruthenium, cerium, and strontium would be in the 55-day group, but the majority of the activity after this time should be the longer-lived isotopes.

[o] The author says $^{104,105}Ru$, but is incorrect here. We believe he means to refer to ^{106}Ru for the about 1-year half-life isotope.

[p] Although the author does not give any examples, important fission products in the "long" category would be ^{90}Sr and ^{137}Cs, with half-lives of about 30 years.

time (12-h period). This is an early investigation into REDOX particle size and composition. The radiological focus was on ruthenium. Median particle size was about 0.2 microns, with a geometric standard deviation of 1.6 during one sample and 2.5 during another sample. With respect to radioactivity distribution, the median particle size was 0.6 microns. To clarify, half of the radioactivity was associated with particles >0.6 microns with a count of 28 $\times 10^3$ particles per cubic foot of stack gas. The other half of the activity was associated with particles <0.6 microns with a count of 28 $\times$ 10^6 particles per cubic foot. Ruthenium emitted during coating removal and metal dissolving was believed to become associated with the ammonium nitrate contributed by these operations. The ammonium nitrate crystals that settled around the stack governed the fate of the ruthenium after discharge.

Table 4-13. Composition of Beta Activity in Ambient Air near REDOX, March 12, 1953

Component	Nanocuries per filter	Percent of total beta
Total beta	7	
Zirconium	0.38	5.4
Ruthenium	2.5	35.7
Rare earths and yttrium	3	42.8
Other beta emitters (determined by difference)	1.1	16.0

Donelson (HW-29346) discusses the emission of crystals from the REDOX stack. A third emission of visible particles had recently been observed in the vicinity of the main stack on August 14, 1953; previous emissions had occurred on June 24, 1952, and March 16, 1953. The most recent emission differed from previous instances in that the crystals were larger and carried a greater amount of radioactive material. The largest crystal found was approximately 5 in. long. The highest dose rate reported was 15 rep h^{-1} at the surface. Average crystals were perhaps ½ in. in maximum dimension and exhibited dose rates of 300 to 500 mrep h^{-1}.

The second quarter 1954 environmental report (HW-33896) states that the ruthenium effluent emissions reported for S Plant (REDOX) "do not include any contributions of material sluffing off from the upper stack liner into the effluent." The effluent measurements were taken at a point 20 ft above the base of the stack. During a shutdown in the latter part of June, revisions were made to route more of the process effluent gases through the sand filter to reduce emissions of ruthenium from the stack. Table 4-14 shows measurements of filters at the inlet to the REDOX sand filter in March and May.

Table 4-14. Composition of Beta Activity in Air Entering the REDOX Plant Sand Filter in March and May 1954

	% of total beta activity	
	Filter removed March 9, 1954	Filter removed May 18, 1954
Ruthenium	92	24
Rare earths	2.9	28
Zirconium	1.4	14
Strontium		8
Niobium (assuming equilibrium with zirconium)		25
Total beta activity per filter	550 µCi	1100 µCi

Analyses of five particles emitted from the REDOX stack during the week ending November 7, 1954, revealed that more than 95% of the beta activity was from ruthenium/rhodium isotopes with the ratio of activity of ^{103}Ru to ^{106}Ru being less than 0.05 (HW-36505). Trace activities of strontium, zirconium, and rare-earth elements were also found. Plutonium was found in the only two particles tested for this element, with one particle having 270,000 dpm (0.12 μCi) of plutonium.

4.2.2 Long-lived Radionuclides

In this report, we focus on measurements of radioactivity in the environment during the time period of highest airborne releases from Hanford facilities, before 1955. However, an exception must be made for very long-lived radionuclides, such as plutonium, which were not specifically monitored in the environment during these early years. Plutonium is relatively immobile in the environment, therefore measurements made in more recent times can reflect past releases. Soil is the ultimate sink[q] for long-lived radionuclides such as plutonium and ^{137}Cs in the land environment. Plutonium in air reflects both suspension of contaminated soil and any residual amounts from the atmospheric testing of nuclear weapons or releases from nuclear facilities.

Air. Plutonium was not routinely measured in the U.S. environment until the mid-1960s. Pan and Stevenson (1996) report monitoring data beginning in 1962 that show the time variation of plutonium in surface air at the Pacific Northwest Laboratory (PNL) near Richland, Washington, as well as Chicago, Illinois. Measurements of plutonium in air were taken at the 300 Areas (about 30 km southeast of the 200 Areas, see Figure 1-1) beginning in 1962; this program ended in 1988. Concentrations of plutonium in air decreased over the 1962–1988 period. Monthly average concentrations were highest at the beginning of the period, with maxima around 0.5 fCi m^{-3}. By the mid 1980s, concentrations were <0.01 fCi m^{-3}. Pan and Stevenson conclude that the dominant source of plutonium in the environment has been from fallout resulting from above ground nuclear weapons detonations. The authors suggest that a "post-fallout equilibrium" was achieved around 1984. The average monthly values after 1984 are mostly between 0.0003–0.003 fCi m^{-3} of surface air. Concentrations near Richland were within the range observed in four other U.S. cities through the U.S. Environmental Protection Agency's Environmental Radiation Ambient Monitoring System (ERAMS) network. Those four cities were Portland, Oregon; New York City, New York; Denver, Colorado; and Chicago, Illinois.

Although plutonium in air at Richland and the 300 Areas appears to be mostly weapons fallout, closer to 200 Areas, the Hanford contribution becomes apparent. Whicker et al. (1997) refer to plutonium measurements in air conducted by the Hanford contractor in the 200 Areas between 1978 and 1995. Concentrations within the 200 Areas were elevated above perimeter and distant community locations and ranged up to about 20 fCi m^{-3} at sampler N-165, located near the Z-19 ditch in the 200-West Area. Concentrations at this sampler were considerably higher than the others in 200 Areas, which were typically 0.001–1 fCi m^{-3}. Sehmel (1980) presents a range of airborne plutonium concentrations at on-site Hanford resuspension sites in 1972–1975 that are several orders of magnitude higher than fallout levels. The location between the 200 Areas was the highest, ranging between 3 and 8 fCi m^{-3} in 1972.

[q] A environmental sink is the place where most of the element in question will ultimately end up.

In the years that we studied in detail for this work (1945–1955), only gross alpha activity was measured routinely. The sketchy air monitoring data showed quarterly average concentrations up to 43 fCi m^{-3} in 200-West Area (Figure 4-13), at the end of 1951. During 1951–1955, the highest monthly average concentration of gross alpha activity on vegetation from the 200 Areas occurred in January 1954 near the 200-West Gate (Figure 4-27).

Elevated concentrations of ^{137}Cs and ^{90}Sr were often found in the air of the 200 Areas. For example, in 1976, the maximum concentration of ^{137}Cs found onsite (0.1 fCi m^{-3}) was in 200-West and ^{90}Sr (0.09 fCi m^{-3}) was in 200-East (Fix et al. 1977). It is probable that some of the airborne activity in 200 Areas was from sources other than direct emissions to air, *e.g.* venting of underground tanks, spread of contamination during waste transfers, and fires in open pits. It is beyond the scope of this study to investigate those other sources.

Soil. Poston et al. (1995) reviews concentrations of ^{60}Co, ^{90}Sr, ^{137}Cs, U isotopes, ^{238}Pu, $^{239,240}Pu$, and ^{241}Am in soil (top 2.5 cm) and vegetation collected from 1983 through 1993 during routine surveillance of the Hanford Site. Some study areas on the site contained elevated concentrations compared to other study areas onsite and offsite. The 200-Area soils had slightly elevated ^{90}Sr, ^{137}Cs, ^{238}Pu, $^{239,240}Pu$, and ^{241}Am. A specific region east of the 200-West Gate had historically contained the highest concentrations of these radionuclides. Soil in the 300 Area had a slightly elevated uranium content. Only ^{90}Sr seemed to be decreasing in surface soil over this time interval, attributed to radioactive decay and possibly greater mobility and weathering into the soil. Because of this trend, the ^{90}Sr data from Poston et al. would not be appropriate for estimating exposures to onsite workers in much earlier time periods. However, ^{137}Cs and $^{239,240}Pu$ are tightly bound to soil and the majority of the activity is retained in the upper layer of soil. Although the highest individual sample of ^{137}Cs in soil was from the 200 Areas (28.1 pCi g^{-1}), the highest median concentration was 0.76 pCi g^{-1} from 100 Areas. Plutonium-239,240 concentrations in 65 soil samples from around the 200 Areas ranged from 0.00032–0.83 pCi g^{-1} with a mean of 0.087 and median of 0.014 pCi g^{-1}. Offsite, $^{239,240}Pu$ concentrations in 154 soil samples ranged from 0.00003–0.033 pCi g^{-1} with a mean of 0.010 and median of 0.008 pCi g^{-1}.

Whicker et al. (1997) compared measured plutonium concentrations in air and soil with those predicted from various estimates of plutonium releases from Hanford facilities. The purpose was to help evaluate which of the widely different release estimates was most consistent with environmental measurements. The authors determined that the quality of the environmental data was sufficient for reflecting the general magnitude of past plutonium emissions from Hanford.

Whicker et al. (1997) reference Price (1988) for $^{239,240}Pu$ concentrations in soil with distance downwind of the 200-West Area at Hanford. Concentrations of plutonium in soil at distances less than 1 km from the 200 Areas were 40 times higher than background concentrations from weapons fallout (0.4 pCi g^{-1} vs. 0.01 pCi g^{-1}). By 5 km away, concentrations were indistinguishable from fallout background. There was no statistical change in concentrations between 1983 and 1993 (referencing Poston et al. 1995).

Whicker et al. (1997) concluded that measured concentrations of plutonium in air and soil at the Hanford Site were not consistent with high plutonium release estimates alleged in legal proceedings. They were consistent with releases reconstructed through 1970 during the Hanford Dose Reconstruction Project (Heeb et al. 1996). Weapons fallout is the primary contributor to plutonium in the environment of the Hanford Site, except within a few km of the release points in 200 Areas.

We did our own review of Price (1988), which summarizes the historical record of soil sampling results in the Hanford environs from the late 1950s through 1987. Both routine soil monitoring (begun in 1971) and special-purpose studies are included. The author makes the following general observations:

- Soil sampling has not revealed any gross contamination of the offsite environs from past Hanford operations.
- Some onsite soil sampling locations near facilities have received contamination from past operations at Hanford.
- Results have not indicated a gradual buildup or depletion of contamination after 1971 at any given soil sampling location.
- Results were noted to vary greatly among aliquots analyzed from a single sample or among multiple samples collected at a single location.
- Hanford-derived radionuclides have been difficult to identify in the presence of worldwide fallout, except quite close to areas of contamination.

Radiochemical analyses of routine soil samples collected since 1971 have included ^{90}Sr, ^{137}Cs, ^{238}Pu, and $^{239,240}Pu$ (Price 1988). Americium-241 analyses began in 1982 and uranium in 1973. Some special studies used plutonium isotopic ratios to more accurately determine the source of the contamination. In general, we agree with Price's summary statements highlighted above. In addition, there were some data that give an indication of the exposures to which military and construction workers near 200 Areas could have been exposed (discussed below).

Results from several special studies conducted in 1985 are presented. Nine samples of surface soil (upper 1 in.) were collected onsite east of the 200-West Area. Plutonium contamination was evident. Concentrations of $^{239,240}Pu$ ranged from 0.039 to 0.33 pCi g^{-1} with a mean of 0.095 pCi g^{-1}. The locations and individual results are shown in Figure 4-43. Four samples were also collected within one mile north of the 200-East Area—the $^{239,240}Pu$ concentrations were less than those from 200-West Area, ranging from 0.003 to 0.027 pCi g^{-1} with a mean of 0.019 pCi g^{-1}. However, ^{137}Cs and ^{90}Sr were elevated in those samples north of 200 East, ranging up to 9.3 pCi g^{-1} and 1.2 pCi g^{-1}, respectively. About 10 km southeast of the 200 East Area, at a proposed project site west of the Wye Barricade and east of Highway 240, the $^{239,240}Pu$ concentrations in soil were 0.013-0.019 pCi g^{-1}. This range is about ten times less than measured near the 200 Areas and is probably indistinguishable from fallout, unless more sensitive isotopic ratio techniques were used.

Earlier studies using mass spectrographic analyses of soil samples collected in 1978 and 1982–1984 also showed that the onsite location having the highest amount of Hanford-derived plutonium was near the 200-West Area, at the routine sampling location called "East of 200-West Gate." The offsite location of maximum Hanford-derived plutonium was near Benton City. Results from this study were highlighted in Price (1988) and were reported in their entirety in the 1985 annual environmental monitoring report (Elder et al. 1986).

Price (1988) also presented the results of a special study conducted in February and March 1970. Samples from the upper 0.5-in. soil were collected at onsite and offsite locations and analyzed for plutonium. There was a large degree of variability between replicate samples at the same location and even between aliquots of the same sample. Results are summarized in Figure 4-44. The "200-East Hill" location is the closest to the most exposed military camp for 200-Area

airborne releases. The plutonium concentration in surface soil there in 1970 was 0.12 pCi g^{-1}, about 10 times greater than the concentration from background fallout.

Price's report referenced an earlier Battelle report that analyzed soil sample results for 1971 through 1976 (Miller et al. 1977). The radionuclides analyzed in these samples were various gamma-emitters, plutonium, uranium, and ^{90}Sr. Probability plotting was used to evaluate the Hanford contribution as opposed to widespread sources, mainly fallout from nuclear weapons testing or natural sources. Miller et al. concluded that the few locations impacted by Hanford operations were:

- East of the California Nuclear burial site (^{60}Co)
- Columbia River island near North Richland (^{60}Co)
- East of 200 West area, which showed elevated levels of $^{239,240}Pu$ in soil (0.3 pCi g^{-1}).

As there was only one soil sample in the 200 area, it was not possible for Miller et al. (1977) to determine an excess inventory of plutonium. From the probability plots, the median concentrations of various radionuclides in soils were determined and are presented in Table 3 of that report. The concentrations (pCi g^{-1}) of several radionuclides of interest in this study were: ^{65}Zn, 0.07; ^{90}Sr, 0.13; ^{106}Ru, 0.36; ^{137}Cs, 0.6; $^{144}Ce/Pr$, 0.6; ^{144}Ce, 0.25; and $^{239,240}Pu$, 0.01.

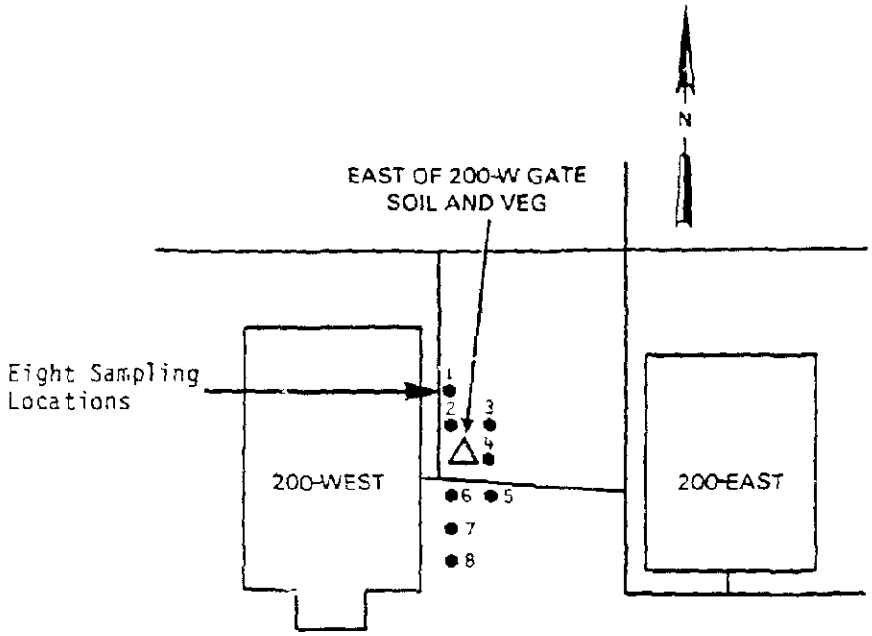

1985 Special Soil Samples - East of 200-West Area

Sample	Concentration, pCi/g					
	Sr-90	Cs-137	Pu-238	Pu-239,240	Am-241	Uranium
1	0.35 ± 0.02	1.6 ± 0.1	0.0009 ± 0.0005	0.072 ± 0.009	0.016 ± 0.016	0.28 ± 0.10
2	0.28 ± 0.02	0.55 ± 0.04	0.0029 ± 0.0006	0.039 ± 0.002	0.005 ± 0.007	0.18 ± 0.07
3	0.44 ± 0.03	1.5 ± 0.1	0.0014 ± 0.0004	0.11 ± 0.01	0.026 ± 0.013	0.43 ± 0.14
4	0.60 ± 0.03	1.4 ± 0.1	0.0014 ± 0.0007	0.12 ± 0.01	0.013 ± 0.013	0.49 ± 0.16
5	0.33 ± 0.02	0.64 ± 0.04	0.0002 ± 0.0002	0.027 ± 0.002	0.001 ± 0.015	0.54 ± 0.18
6	0.30 ± 0.02	1.1 ± 0.1	0.0007 ± 0.0004	0.040 ± 0.003	0.039 ± 0.017	0.54 ± 0.18
7	0.42 ± 0.02	2.2 ± 0.1	0.0011 ± 0.0006	0.073 ± 0.005	0.014 ± 0.017	0.31 ± 0.11
8	0.39 ± 0.02	1.2 ± 0.1	0.0008 ± 0.0004	0.041 ± 0.003	0.002 ± 0.018	0.53 ± 0.11
E of 200-W Gate[a]	0.61 ± 0.12	2.0 ± 0.1	0.0057 ± 0.0009	0.33 ± 0.03	0.023 ± 0.007	0.43 ± 0.14

(a) 1985 results for closest routine sampling location.

Figure 4-43. Results of a special-purpose soil sampling study east of the 200-West Area, August 1985 (Price 1988).

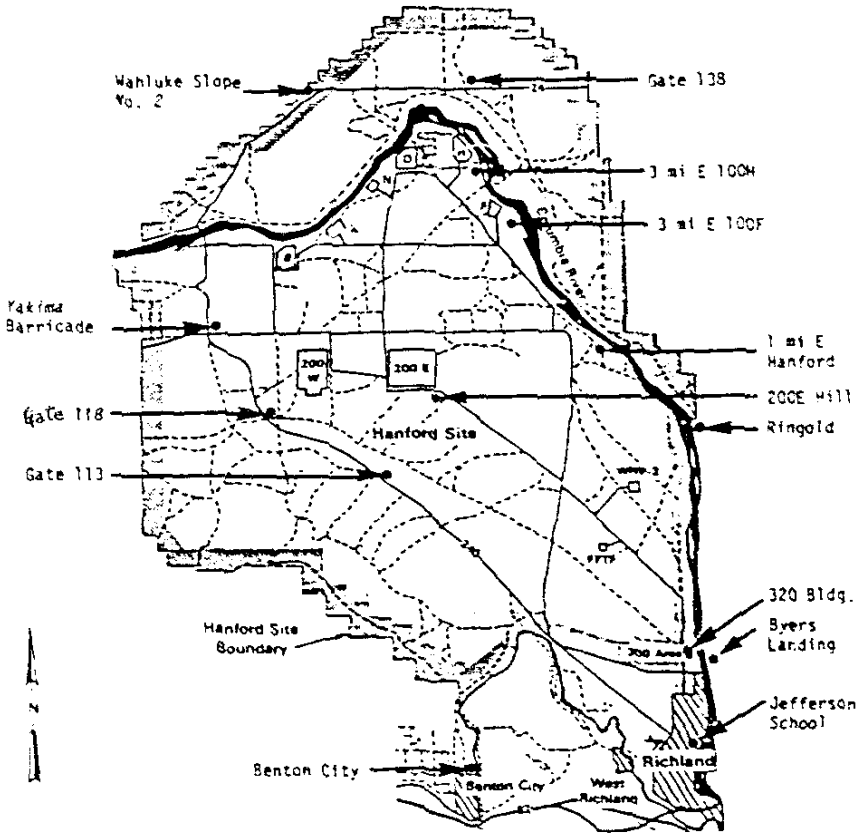

February and March 1970 Special Soil Samples
(0.5 inch deep) - Hanford Environs

Location	Concentration Pu-239,240, pCi/g
200E Hill	0.12 ± 0.01 0.13 ± 0.01(a)
Yakima Barricade	0.028 ± 0.003 0.015 ± 0.002(a) 0.018 ± 0.002(a)
Wahluke Slope No. 2	0.041 ± 0.003
Gate 113	0.040 ± 0.004 0.047 ± 0.004(a)
Jefferson School	0.009 ± 0.002
Benton City	0.009 ± 0.001
Byers Landing Byers Landing	0.004 ± 0.001 0.083 ± 0.009
320 Bldg.	0.012 ± 0.001 0.011 ± 0.001(a)

Location	Concentration Pu-239,240, pCi/g
Gate 118	0.017 ± 0.003
Gate 118	0.019 ± 0.005
Gate 118	0.014 ± 0.001
Gate 118	0.010 ± 0.001
Gate 138	0.031 ± 0.004
Gate 138	0.023 ± 0.002
Ringold	0.027 ± 0.003
1 mi E Hanford	0.049 ± 0.041
3 mi E 100F	0.018 ± 0.003
3 mi E 100F	0.040 ± 0.004
3 mi E 100F	0.017 ± 0.002
3 mi E 100H	0.007 ± 0.001

(a) Separate aliquot from single sample.

Figure 4-44. Sampling locations and results of a special study of ^{239,240}Pu in onsite and offsite surface soils in February-March 1970 (Price 1988).

4.3 Conclusions from Environmental Data: Affected Areas and Times

Any of the environmental data sets we examined for this task could be scrutinized and would be criticized by today's data quality standards. However, taken in total they present a relatively coherent picture of the environmental conditions on the Hanford Reservation where people lived and worked in the first decade of Hanford operations. They are some of the most direct evidence we have to answer the questions raised in this work about onsite exposures. Knowledge of these factors has helped define and develop the tools necessary to estimate radiation doses from short-lived radionuclides and particles released from early Hanford operations.

Several definite but broad conclusions can be made about the most affected areas and times. These conclusions about the "where, when, and what" of past exposures are supported by brief facts listed below. Reference is made to the parts of this section, shown in parentheses, that contain further information.

1. **WHERE. The environment near the 200 Areas was most highly contaminated, and contamination was generally spread to the east and southeast of the release points. Concentrations decreased rapidly with distance from the contaminated sources. However, some of the large particles released were known to have traveled long distances. The data at various locations on and off the site reflect relative contamination levels to which people were exposed.**

- Vegetation in the 200-East Area in 1945 and 1946 was 15–20 times as contaminated with total beta activity as vegetation in Richland. Hanford was 3 times as contaminated as Richland (p. 4-22).
- Long-lived beta activity in vegetation collected in 1945–1947 was over 20 times higher in the 200 Areas compared to levels in Richland (p. 4-68).
- The highest measured values of beta activity in air in 1946–1947 were obtained from 200-East (p. 4-11).
- From January 1946 through November 1948, the contamination levels on vegetation at Hanford and Richland were similar, but the location near the military camp at Route 4S, Mile 4 was over 6 times higher (p. 4-24).
- Annual average concentrations of beta activity in air at four 200-Area locations in 1946–1950 (when fallout was relatively low) were 17 times higher than those measured in Pasco (pp. 4-15 and 4-16).
- Large hot particles near T and B Plants in 1947–1948 were most densely deposited near the release points, with a general spread trending to the SE (pp. 4-40 and 4-41).
- Concentrations of nonvolatile beta activity in vegetation in 1949 were highest in the 200 Areas, particularly near the 200-West Gate. About 3 mi away, the activity concentrations were 6 times lower (p. 4-27). Contamination spread was generally to the east and south of the release points (pp. 4-28 and 4-29).
- In 1946–1952 (before significant fallout), the annual average concentrations of beta activity in rain of 200-East and 200-West Areas were 25 times higher than observed in outlying areas (p. 4-21).
- The beta activity concentrations in snow within 2000 ft SE of the REDOX stack in January 1954 were 100 times greater than at the military installation near 200-West (p. 4-22).

- The army camp H-50, 3.4 km S of REDOX, shows the largest range of external exposure rates from REDOX releases. Next most affected were H-61 and H-51, camps to the W of REDOX (p. 4-6).
- Pasco is a reasonable location to evaluate local weapons fallout levels in the 1950s (p. 4-15).
- During 1952 through 1955, the median concentration of discrete radioactive particles in air was 16 times greater at 200 West than at Pasco (p. 4-35).
- Ground surveys in 1954 revealed particles like those from REDOX as far away as Pendleton, Oregon, and Mesa, Washington (p. 4-45). The density of particles deposited on the ground was much greater onsite than offsite (pp. 4-51 through 4-54).
- Concentrations of plutonium in soil at distances <1 km from the 200 Areas were 40 times higher than regional concentrations from weapons fallout. By 5 km away, concentrations were indistinguishable from fallout in the 1970s and 1980s (p. 4-71). The plutonium concentration in surface soil near an old army camp SE of 200 Areas in 1970 was about 10 times fallout levels (p. 4-72).

2. WHEN. The time periods most affected by releases of large radioactive particles were 1947-1949 and 1952-1955. Iodine releases were highest through 1946.

- Before 1950, annual average radiation levels measured with ionization chambers were highest in 1945, averaging 6.5 mrep d^{-1} over background near a military camp (p. 4-5).
- Concentrations of beta activity in air were highest during the first three quarters of 1946 (earliest data located). Concentrations had decreased 100-fold by the first quarter of 1948 (pp. 4-11 through 4-14).
- The highest annual average concentration of beta activity in rain between 1946 and 1956 was collected from the REDOX area in 1954 (p. 4-21).
- After 1951, maximum monthly exposure rates at three military camps were obtained in December 1953–April 1954 (p. 4-6). A location near a known military camp had a comparable exposure rate in the latter half of 1945 (p. 4-5).
- The highest monthly average concentration of discrete radioactive particles in air occurred in 200 West during September 1953 (p. 4-34). This monitoring began in 1949.
- High REDOX particle densities on the ground were not sustained for long periods of time. Radioactive decay and weathering reduced their impact after 1955 (p. 4-55).

3. WHAT. Iodine-131 dominated onsite environmental measurements before 1948 whereas REDOX releases (mainly ruthenium) dominated in the 1952-1955 interval. Weapons fallout was a confounding factor in the latter time period.

- Spatial trends observed from iodine-dominated data have some similarity to those for other radionuclides.
- Large corrosion-product particles found in 200 areas in 1947–1948 were a mixture of radionuclides (Section 4.2.1). Hanford operations produced localized contamination with a variety of radionuclides, including some long-lived radionuclides like ^{137}Cs, ^{90}Sr, and ^{239}Pu (Section 4.2.2).
- In 1945-1946, areas of high exposure rates were reflecting iodine releases, whereas in 1953 and 1954, REDOX releases were responsible (pp. 4-6, 4-7, 4-10).
- In 1946–1949, gross beta activity in air and vegetation around Hanford was likely to be mostly from Hanford releases, especially iodine. After 1951, beta-emitters in fallout became relatively more important, especially offsite (pp. 4-13 through 4-16, 4-32).

- Isolated hot particles might not be reflected in environmental measurements of radioactivity in air, rain, and vegetation, unless a particle happened to come in close contact with the sample. For example, in June 1952, an active particle was identified as contributing to an unusually high concentration in a rain sample (p. 4-20). A similar event happened with a vegetation sample located near the southern perimeter of the site in September 1954 (p. 4-31).
- Even with the confounding influence of fallout, the impact of ruthenium releases from REDOX on beta activity in vegetation near the 200 Areas in 1954–1955 is clear (p. 4-31).
- Ground surveys located large particle contamination effectively, beginning as early as 1947 around T Plant and B Plant (p. 4-39). Surveys in 1952–1955 document ground contamination from REDOX releases (p. 4-43 through 4-56).
- Contamination with alpha-emitting radionuclides is evident in air, vegetation, and soil around 200 Areas and 300 Area (pp. 4-16, 4-32, 4-70).
- The maximum REDOX particle density on ground areas in May 1954 was similar to the maximum density of active corrosion products in 1947 (p. 4-51).
- Highly active particles of corrosion products and ruthenium flakes were large, limiting the probability of inhalation exposure (Section 4.2.1).

5. EXAMPLE CALCULATIONS

In this section, we provide results of example calculations of radiation doses to people on or near the Hanford reservation for various hypothetical scenarios in the early years of operations. For several examples, the times selected coincide with periods when particle releases from the fuel processing facilities were at or near their highest levels. In contrast, another example takes place during a period of high releases of radioiodine, and a cumulative exposure example also is dominated by dose from radioiodine. Although these results do not reflect a full range of possible exposures to persons who worked and lived onsite during the early years, they are representative of known exposure locations and times. The examples also illustrate the utility of tools developed in this work to evaluate multiple sources and locations of exposure.

The first set of example calculations, presented in Section 5.1, deals with releases from all the facilities and considers a full range of possible exposure pathways. The second set of calculations in Section 5.2 address exposures to large active particles in the Hanford environment.

5.1 Exposures to Releases from All Facilities

Five examples of different exposures to releases from all the facilities are presented in this section. At the times considered, the reactor areas were releasing ^{41}Ar and the processing plants in 200 Areas were releasing particles that contained ^{90}Sr, ^{90,91}Y, ^{95}Zr, ^{103,106}Ru, ^{134,137}Cs, ^{141,144}Ce, and ^{239}Pu and their associated decay products. Iodine-131 was also being released from the fuel processing facilities in the 200 Areas.

As shown in Section 3.4.1, data files for the release of each radionuclide and each point of release contain both the 50th and the 95th percentile for each month's release, where the reference uncertainty distribution is the estimate of the release for the radionuclide, location, and month specified. It is not unreasonable to make deterministic calculations with the medians (50th percentiles) used as nominal values, but one must keep in mind the ambiguous interpretation of the results. In particular, for complex simulations, it is not precisely known what relation such results would have to central statistics (mean or median) of the propagated distribution. The deterministic result could be misleading, in the sense that it might be misinterpreted to be a valid estimate of one of these central statistics.

On the other hand, the uniform use of the 95th percentiles in a deterministic simulation could substantially overestimate the median and mean of the propagated uncertainty distribution. The event that all releases would be as high as their 95th percentiles is extremely improbable, even with the positive correlations that must exist among releases of different radionuclides from the same facility in the same month. Some experimentation could be done with crude calculations of this kind to assess the extent to which they might be presented as conservative estimates. However, we believe the appropriate approach is to develop a set of scripts for Monte Carlo calculations that would sample the joint distribution of the source term with proper allowance for positive correlations. The percentile data that have been computed and stored in the source term files make this the logical next step, although it is beyond the scope of this work.

For the examples given in this section, we have used only the medians from the source term files. We think this procedure is less likely to provide unreasonable results, particularly for longer-term exposures.

The first example gives an over-all impression of the spatial variation of exposure to past Hanford atmospheric releases. Figure 5-1 shows effective dose contours (rem) overlaid on a modern base map of the Hanford site. The dose calculation represents a maximum potential exposure rather than a real one, assuming an adult person is exposed 24 hours per day outdoors from January 1, 1945 through December 31, 1961. Exposure pathways are inhalation and external exposure from radionuclides suspended in the air and deposited on the ground. Ingestion pathways are excluded for this example.

Contributing to the exposure for this example are all radionuclides in the source term data base (those listed in the first paragraph of this section and their decay products) and all release sources (including the Z Plant, which began operations January 1949, and the PUREX Plant, which came on-line January 1956). Iodine-131 contributes the dominant component of the effective dose indicated by the contours in Figure 5-1. Most of the iodine releases occurred before 1950. Radionuclide releases for the simulations were based on median monthly estimates, as discussed above. The smoothed contours were calculated by a kriging method with the Surfer 7 mapping program (Golden Software, Inc., 809 14th Street, Golden, CO 80401-1866, USA).

5.1.1 Army Camp H-40, 1954

An Army encampment called PSN 330 (Figure 3-1), or H-40 (Figure 1-2, Figure 3-2) was close to and downwind from the 200 Areas. This example considers a hypothetical member of the Armed Forces who was assigned to the H-40 station for the months of April through June, 1954. The defined schedule consisted of 15 days' duty on the site, 24 hours per day (assumed to be outside), followed by three days in Richland, 10 hours per day outdoors and 14 hours indoors, for five cycles (total of 90 days). This period coincided with relatively high releases of the particulate radionuclides. This location is 3.7 km SE from B Plant, 9.1 km ESE from T Plant, 8.9 km E from REDOX Plant, and at distances ranging from 15 to 18 km generally S and SE from the reactors.

Table 5-1 shows the estimated absorbed dose to each ICRP-defined organ for the following nuclide components: ^{41}Ar, ^{131}I+^{131m}Xe, particles, and total. Examination of the results shows that the thyroid is the organ receiving the largest dose (12 mrad), nearly all of which is due to releases of ^{131}I. The lungs and skin were the organs that were estimated to receive the next largest doses (2 mrad). Particulate radionuclides contributed 60% and 34% of the total organ dose to lungs and skin, respectively.

Table 5-2 shows effective dose for the same nuclides. Use of the effective dose facilitates showing the most important exposure pathways and radionuclides. The results for each nuclide are broken down by inhalation, ingestion, and external exposure modes. Inadvertent ingestion of soil at a rate of one gram per day is included to address the general dusty conditions and possible transfer of contamination from hands or other surfaces to food. Although this time period coincided with relatively high releases of the particulate radionuclides, ^{41}Ar and ^{131}I still contribute, respectively, 46% and 32% of the estimated effective dose at this time and place. External exposure from radionuclides in air was the most important pathway (46%), followed by inhalation (41%), and then external exposure from ground deposits of ruthenium and rhodium nuclides (13%). The total effective dose estimated for this 3-month exposure period was 1.8 mrem.

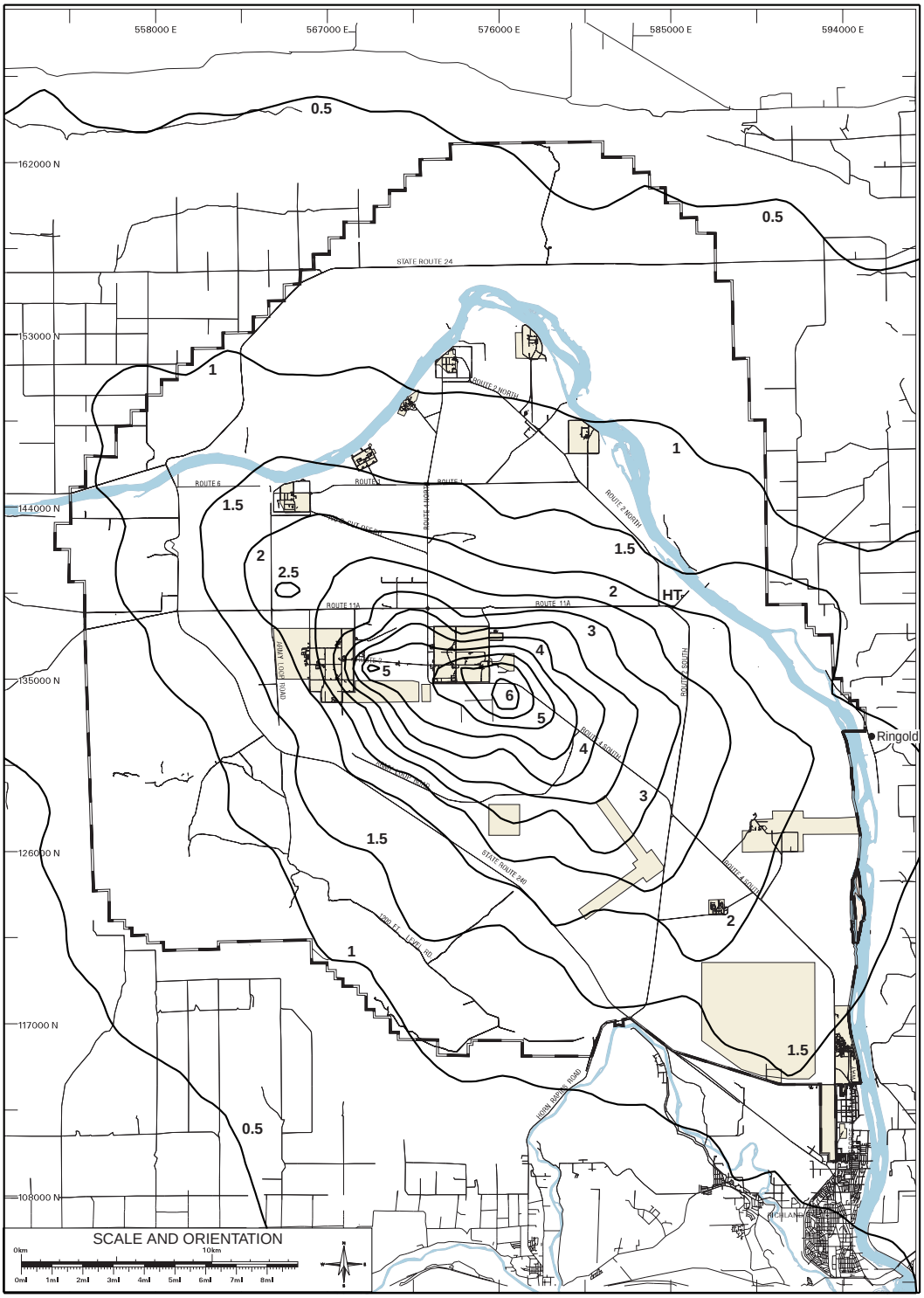

Figure 5-1. Contours of committed effective dose (rem) from continuous outdoor exposure to airborne releases from Hanford facilities, 1945–1961. Iodine-131 was the primary contributor to dose, and most of those releases occurred before 1950. Absorbed dose to thyroid (in rad) was about 20 times the effective dose. Ingestion pathways are not included. The notation "HT" shows

the location of the old Hanford town site that was closed by March 1945. Base map adapted from the atlas at web site <http://www.bhi-erc.com/dm/hgis/hgis.htm>.

Table 5-1. Committed Absorbed Dose to Organs for Armed Forces Member at Camp H-40, April through June 1954

Organ	Dose (mrad[a]) from each radionuclide or set of radionuclides			
	^{41}Ar	^{131}I + ^{131m}Xe	Particles	Total
Adrenals	7.6×10^{-1}	3.1×10^{-2}	2.1×10^{-1}	1.0
Bladder wall	7.6×10^{-1}	4.9×10^{-2}	2.1×10^{-1}	1.0
Bone surface	1.1	5.9×10^{-2}	3.7×10^{-1}	1.6
Brain	7.6×10^{-1}	3.3×10^{-2}	2.0×10^{-1}	1.0
Breast	8.9×10^{-1}	3.6×10^{-2}	2.3×10^{-1}	1.2
Esophagus	7.6×10^{-1}	3.3×10^{-2}	2.1×10^{-1}	1.0
Stomach wall	7.6×10^{-1}	3.2×10^{-2}	2.1×10^{-1}	1.0
Small intestine wall	7.6×10^{-1}	3.1×10^{-2}	2.1×10^{-1}	1.0
Upper large intestine wall	7.6×10^{-1}	3.2×10^{-2}	2.4×10^{-1}	1.0
Lower large intestine wall	7.6×10^{-1}	3.2×10^{-2}	3.1×10^{-1}	1.1
Colon	7.6×10^{-1}	3.2×10^{-2}	2.7×10^{-1}	1.1
Kidneys	7.6×10^{-1}	3.1×10^{-2}	2.1×10^{-1}	1.0
Liver	7.6×10^{-1}	3.1×10^{-2}	2.8×10^{-1}	1.1
Muscle	7.6×10^{-1}	3.3×10^{-2}	2.1×10^{-1}	1.0
Ovaries	7.8×10^{-1}	3.5×10^{-2}	2.3×10^{-1}	1.1
Pancreas	7.6×10^{-1}	3.1×10^{-2}	2.1×10^{-1}	1.0
Red marrow	7.8×10^{-1}	3.3×10^{-2}	2.3×10^{-1}	1.1
Extrathoracic airways	7.6×10^{-1}	7.9×10^{-2}	2.5×10^{-1}	1.1
Lungs	8.1×10^{-1}	5.0×10^{-2}	1.2	2.0
Skin	1.3	4.2×10^{-2}	6.7×10^{-1}	2.0
Spleen	7.6×10^{-1}	3.1×10^{-2}	2.1×10^{-1}	1.0
Testes	7.8×10^{-1}	3.4×10^{-2}	2.3×10^{-1}	1.1
Thymus	7.6×10^{-1}	3.3×10^{-2}	2.1×10^{-1}	1.0
Thyroid	8.1×10^{-1}	11	2.0×10^{-1}	12
Uterus	7.6×10^{-1}	3.2×10^{-2}	2.0×10^{-1}	1.0
Remainder	7.6×10^{-1}	3.3×10^{-2}	2.1×10^{-1}	1.0

[a]To obtain dose in units of Gy, multiply values in table by 1×10^{-5}.

Table 5-2. Committed Effective Dose to Armed Forces Member at Camp H-40, April through June 1954

	Dose (mrem[a]) from particular exposure pathways					Total dose	
		Ingestion		External exposure			
Nuclides	Inhalation	Food	Soil	Air	Ground	(mrem)	%
^{41}Ar	0	[b]	0	8.1×10^{-1}	0	8.1×10^{-1}	45.5
^{90}Sr/^{90}Y	7.8×10^{-4}	[b]	1.5×10^{-3}	1.5×10^{-8}	3.6×10^{-4}	2.6×10^{-3}	0.1
^{91}Y	2.5×10^{-3}	[b]	7.0×10^{-6}	3.5×10^{-7}	2.4×10^{-5}	2.6×10^{-3}	0.1
^{95}Zr/^{95}Nb	1.6×10^{-3}	[b]	4.3×10^{-6}	6.2×10^{-5}	6.7×10^{-3}	8.4×10^{-3}	0.5
^{103}Ru/^{103m}Rh	1.4×10^{-2}	[b]	7.3×10^{-5}	5.0×10^{-4}	7.3×10^{-2}	8.8×10^{-2}	4.9
^{106}Ru/^{106}Rh	1.0×10^{-1}	[b]	1.5×10^{-3}	1.4×10^{-4}	7.3×10^{-2}	1.8×10^{-1}	9.9
^{131}I/^{131m}Xe	5.5×10^{-1}	[b]	1.1×10^{-3}	2.0×10^{-3}	3.0×10^{-2}	5.8×10^{-1}	32.4
^{134}Cs	1.2×10^{-5}	[b]	1.8×10^{-5}	5.3×10^{-7}	2.3×10^{-3}	2.3×10^{-3}	0.1
^{137}Cs/^{137m}Ba	5.0×10^{-5}	[b]	6.6×10^{-4}	1.2×10^{-6}	4.7×10^{-2}	4.8×10^{-2}	2.7
^{141}Ce	6.8×10^{-4}	[b]	7.2×10^{-7}	2.7×10^{-6}	1.1×10^{-4}	7.8×10^{-4}	<0.1
^{144}Ce/^{144}Pr	1.9×10^{-2}	[b]	1.7×10^{-4}	5.4×10^{-6}	2.7×10^{-3}	2.1×10^{-2}	1.2
^{239}Pu	4.3×10^{-2}	[b]	4.1×10^{-4}	1.4×10^{-11}	2.1×10^{-7}	4.3×10^{-2}	2.4
Particles[c]	1.8×10^{-1}	[b]	4.4×10^{-3}	1.0×10^{-3}	2.1×10^{-1}	4.0×10^{-1}	22.3
Total	7.3×10^{-1}	[b]	5.5×10^{-3}	8.2×10^{-1}	2.4×10^{-1}	1.8	100
%	40.8	[b]	0.3	45.7	13.2	100	

[a] To obtain dose in units of Sv, multiply values in table by 1×10^{-5}.
[b] Food pathways were not evaluated for onsite examples in this report, although onsite workers could have consumed contaminated food produced locally. The dose from food pathways is dominated by ^{131}I and is illustrated in the last scenario, resident of Ringold.
[c] "Particles" includes all the radionuclides listed except ^{41}Ar and ^{131}I/^{131m}Xe.

5.1.2 PUREX Plant Construction Worker, 1954

For a construction worker at the PUREX site in 200-East Area, we consider the months January through March, 1954. The worker is assumed to be on-site for 10 hours each day and in Richland for 14 hours each night (for 7 days exposure per week). The work location is 1.8 km ESE from B Plant, 7.9 km E from T Plant, 7.8 km E from REDOX Plant, and at distances ranging from 12 to 16 km generally S and SE from the reactors. Ingestion of food was not included; however inadvertent ingestion of soil was included.

Table 5-3 shows the estimated absorbed dose to each ICRP-defined organ for the following nuclide components: ^{41}Ar, ^{131}I + ^{131m}Xe, particles, and the total. The two largest organ doses were 11 mrad to thyroid and 3 mrad to lungs. Table 5-4 shows effective dose for individual nuclides, broken down by inhalation, ingestion, and external exposure modes. Inhalation was the most important pathway (55%), followed by external exposure from ^{41}Ar in air (33%) and external exposure from ground deposits of ruthenium and rhodium nuclides (11%). At this time and place, the particulate radionuclides are relatively important, contributing 34% to the total effective dose, which totaled 1.5 mrem for the 3-month exposure period.

Table 5-3. Committed Absorbed Dose to Organs for PUREX Plant Construction Worker, January through March 1954

Organ	Dose (mrad) from each radionuclide or set of radionuclides			
	^{41}Ar	$^{131}I + {}^{131m}Xe$	Particles	Total
Adrenals	4.9×10^{-1}	1.5×10^{-2}	1.9×10^{-1}	7.0×10^{-1}
Bladder wall	4.9×10^{-1}	3.1×10^{-2}	1.8×10^{-1}	7.0×10^{-1}
Bone surface	7.2×10^{-1}	2.9×10^{-2}	3.2×10^{-1}	1.1
Brain	4.9×10^{-1}	1.7×10^{-2}	1.8×10^{-1}	6.8×10^{-1}
Breast	5.6×10^{-1}	1.8×10^{-2}	2.1×10^{-1}	8.0×10^{-1}
Esophagus	4.9×10^{-1}	1.7×10^{-2}	1.9×10^{-1}	7.0×10^{-1}
Stomach wall	4.9×10^{-1}	1.6×10^{-2}	1.9×10^{-1}	7.0×10^{-1}
Small intestine wall	4.9×10^{-1}	1.5×10^{-2}	2.0×10^{-1}	7.0×10^{-1}
Upper large intestine wall	4.9×10^{-1}	1.5×10^{-2}	2.6×10^{-1}	7.6×10^{-1}
Lower large intestine wall	4.9×10^{-1}	1.5×10^{-2}	4.1×10^{-1}	9.2×10^{-1}
Colon	4.9×10^{-1}	1.5×10^{-2}	3.3×10^{-1}	8.3×10^{-1}
Kidneys	4.9×10^{-1}	1.4×10^{-2}	1.8×10^{-1}	6.8×10^{-1}
Liver	4.9×10^{-1}	1.5×10^{-2}	2.3×10^{-1}	7.4×10^{-1}
Muscle	4.9×10^{-1}	1.7×10^{-2}	1.8×10^{-1}	6.8×10^{-1}
Ovaries	5.0×10^{-1}	1.7×10^{-2}	2.0×10^{-1}	7.2×10^{-1}
Pancreas	4.9×10^{-1}	1.5×10^{-2}	1.9×10^{-1}	6.9×10^{-1}
Red marrow	5.0×10^{-1}	1.7×10^{-2}	2.1×10^{-1}	7.3×10^{-1}
Extrathoracic airways	4.9×10^{-1}	5.9×10^{-2}	3.2×10^{-1}	8.6×10^{-1}
Lungs	5.0×10^{-1}	3.2×10^{-2}	2.4	3.0
Skin	8.0×10^{-1}	2.1×10^{-2}	4.5×10^{-1}	1.3
Spleen	4.9×10^{-1}	1.5×10^{-2}	1.9×10^{-1}	6.8×10^{-1}
Testes	5.0×10^{-1}	1.7×10^{-2}	2.0×10^{-1}	7.2×10^{-1}
Thymus	4.9×10^{-1}	1.7×10^{-2}	1.9×10^{-1}	7.0×10^{-1}
Thyroid	5.1×10^{-1}	9.8	1.8×10^{-1}	11
Uterus	4.9×10^{-1}	1.5×10^{-2}	1.8×10^{-1}	6.8×10^{-1}
Remainder	4.9×10^{-1}	1.7×10^{-2}	1.8×10^{-1}	6.8×10^{-1}

[a]To obtain dose in units of Gy, multiply values in table by 1×10^{-5}.

Table 5-4. Committed Effective Dose to PUREX Plant Construction Worker, January through March 1954

	Dose (mrem[a]) from particular exposure pathways					Total dose	
		Ingestion		External exposure			
Nuclides	Inhalation	Food	Soil	Air	Ground	(mrem)	%
^{41}Ar	0	[b]	0	5.1×10^{-1}	0	5.1×10^{-1}	33.1
^{90}Sr/^{90}Y	5.1×10^{-4}	[b]	2.1×10^{-3}	9.4×10^{-9}	2.0×10^{-4}	2.8×10^{-3}	0.2
^{91}Y	1.3×10^{-3}	[b]	9.9×10^{-6}	1.6×10^{-7}	1.4×10^{-5}	1.3×10^{-3}	0.1
^{95}Zr/^{95}Nb	8.1×10^{-4}	[b]	6.2×10^{-6}	2.9×10^{-5}	3.9×10^{-3}	4.7×10^{-3}	0.3
^{103}Ru/^{103m}Rh	6.6×10^{-2}	[b]	2.2×10^{-4}	2.2×10^{-3}	8.5×10^{-2}	1.5×10^{-1}	9.9
^{106}Ru/^{106}Rh	2.4×10^{-1}	[b]	2.2×10^{-3}	3.2×10^{-4}	4.2×10^{-2}	2.9×10^{-1}	18.6
^{131}I/^{131m}Xe	5.0×10^{-1}	[b]	1.2×10^{-3}	1.7×10^{-3}	1.3×10^{-2}	5.2×10^{-1}	33.4
^{134}Cs	5.8×10^{-6}	[b]	2.6×10^{-5}	2.3×10^{-7}	1.3×10^{-3}	1.4×10^{-3}	0.1
^{137}Cs/^{137m}Ba	2.4×10^{-5}	[b]	9.1×10^{-4}	5.2×10^{-7}	2.6×10^{-2}	2.7×10^{-2}	1.7
^{141}Ce	3.6×10^{-4}	[b]	1.1×10^{-6}	1.3×10^{-6}	6.0×10^{-5}	4.2×10^{-4}	<0.1
^{144}Ce/^{144}Pr	1.2×10^{-2}	[b]	2.8×10^{-4}	3.2×10^{-6}	1.8×10^{-3}	1.4×10^{-2}	0.9
^{239}Pu	2.5×10^{-2}	[b]	5.6×10^{-4}	7.4×10^{-12}	1.1×10^{-7}	2.6×10^{-2}	1.6
Particles[c]	3.5×10^{-1}	[b]	6.3×10^{-3}	2.3×10^{-3}	1.6×10^{-1}	5.2×10^{-1}	33.6
Total	8.5×10^{-1}	[b]	7.5×10^{-3}	5.2×10^{-1}	1.7×10^{-1}	1.5	100
%	54.9	[b]	0.5	33.4	11.2	100	

[a] To obtain dose in units of Sv, multiply values in table by 1×10^{-5}.
[b] Food pathways were not evaluated for onsite examples in this report, although onsite workers could have consumed contaminated food produced locally. The dose from food pathways is dominated by ^{131}I and is illustrated in the last scenario, resident of Ringold.
[c] "Particles" includes all the radionuclides listed except ^{41}Ar and ^{131}I/^{131m}Xe.

5.1.3 B Plant Construction Worker, 1944-1945

This example illustrates a time of high radioiodine releases when workers were living at the Hanford town site (Figure 1-2). The scenario considers a 12-month period, October 1944 through September 1945. The person works outdoors at the B-Plant site in 200 East during the entire 12 months. The residence location is the Hanford town site through February 1945, when the Hanford town site was closed. The worker's residence is Richland for the remaining 7 months. There are five Hanford facilities emitting airborne radionuclides during this period: B Reactor, T Plant in 200 West, D Reactor, F Reactor, and B Plant in 200 East. Start-up times for these five sources are shown in Table 5-5.

Table 5-5 includes the estimated effective dose from the five operating Hanford sources at the three locations (work and two residences). Although many people lived at the Hanford town site, it was closed before the large releases of radioactive iodine occurred (Figure 5-2). During the 12 months of this example, which was designed as a maximum condition for a Hanford construction worker, only 0.9% of the total dose was received while at the Hanford residence location, while 27% was received while in residence at Richland and 72% while on the B Plant job site in 200 East. For this example, the T Plant in 200 West is the source of 89% of the total dose and the B Plant contributes 11%. (For other work and residence locations at this and other times, the source contributions would be different.) Releases from the reactors are insignificant

compared to T and B Plant releases at these locations. The example illustrates the utility of the tools developed during this work to evaluate multiple sources and locations of exposure.

Table 5-5. Committed Effective Dose (mrem[a]) to B-Plant Construction Worker, October 1944 through September 1945

	Locations of exposure				
Radionuclide sources (start-up month/year)	Work location (B Plant)	Hanford residence (Oct 1944-Feb 1945)	Richland (residence Mar-Sept 1945)	All locations	Percentage from source
B Reactor (Oct 1944)	4.1×10^{-1}	5.0×10^{-2}	1.6×10^{-2}	4.8×10^{-1}	0.1
T Plant (Dec 1944)	460	5.4	100	570	89.3
D Reactor (Dec 1944)	6.3×10^{-2}	4.2×10^{-2}	3.9×10^{-3}	1.1×10^{-1}	<0.1
F Reactor (Mar 1945)	3.6×10^{-2}	0	5.3×10^{-3}	4.1×10^{-2}	<0.1
B Plant (Apr 1945)	0	0	68	68	10.7
All sources	460	5.5	170	640	100.0
Percentage at location	72.0	0.9	27.1	100.0	

[a]To obtain dose in units of Sv, multiply values in table by 1×10^{-5}.

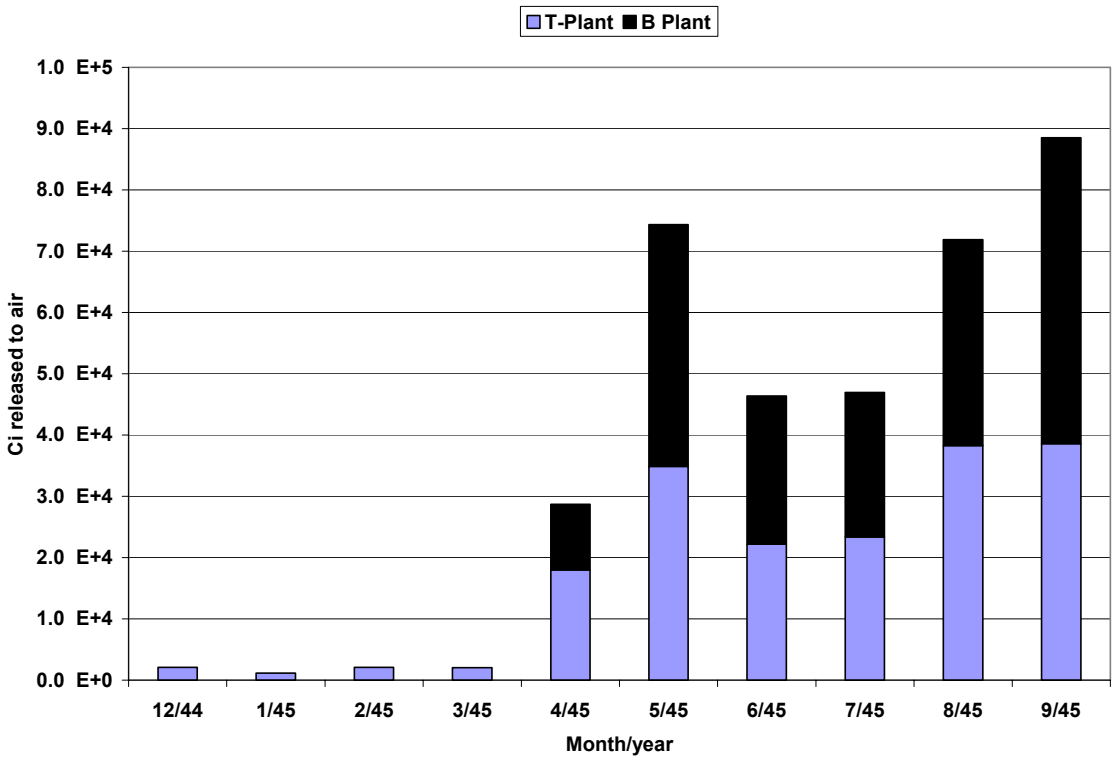

Figure 5-2. Median monthly releases of ^{131}I to air from T and B Plants, December 1944 through September 1945. This source term is illustrated here to help interpret results for the B Plant construction worker example. See Section 2 for further details on releases of radionuclides to air from Hanford facilities.

This example illustrates the importance of radioiodine releases in 1944-1945, even without food pathways. Inhalation of ^{131}I contributes 96% of the total effective dose estimate followed by

external exposure from ^{131}I on ground (3%) and in air (0.3%). The thyroid is the organ receiving the highest dose (12 rad, or 12,000 mrad), followed by extrathoracic airways (76 mrad) and lungs (46 mrad). Inadvertent ingestion of contaminated soil was considered but is an insignificant contributor (0.2% of the total effective dose). The total effective dose (640 mrem) is roughly 200 times higher than the other short-term examples in this report (Sections 5.1.1 and 5.1.2), when the particle releases were *relatively* more important (in 1954).

Including contaminated food pathways in any of these three examples would further increase the importance of radioiodine as well as the overall dose estimate because of the effective transfer of iodine to the milk of dairy cows grazing on fresh pasture. Deonigi et al. (1994) state

> During the 1945-1951 time period, Morning Milk (later Carnation), located in Sunnyside[1], was the exclusive commercial milk supplier to the Hanford construction camps on the Hanford Reservation. Morning Milk and the Yakima Dairyman's Association (later Darigold) were also the only suppliers of commercial milk to the burgeoning town of Richland until 1950. In 1950 the smaller and more local commercial milk operations began to carve into the market shares of (then) Carnation and Darigold. Twin City Creamery came under new ownership and began its first deliveries to Richland in 1949. Later, operations in Walla Walla began delivering to the Tri-Cities area. Commercial milk in the Prosser-Benton City area was marketed by Hulbert Dairy in Benton City and two operations in Prosser. Later in the 1950s, Hulbert Dairy opened dairy stores in the Tri-Cities.

It is clearly outside our scope of work to reconstruct the extent of contamination of food and resulting dose for workers on the Hanford Reservation. On the other hand, it is obvious that the milk pathway in particular is important whether the person works on the reservation or not. In our final example of exposures to releases from all facilities (Section 5.1.4), an offsite resident is assumed to consume milk from a cow that grazes just east of the site near Ringold.

5.1.4 Member of the Public, Resident of Ringold, 1954

We estimated the dose to a member of the public at Ringold, east of the Site, resulting from a year's exposure throughout 1954. The individual is assumed to spend 10 hours per day outdoors at this location and 14 hours indoors. Annual intakes of locally produced food are as follows: 200 kg of vegetables, 100 kg of meat, and 300 L of milk. The food intake and inhalation rates chosen are appropriate for an adult.

The calculation conservatively assumes year-round availability of contaminated food, although realistically the grazing pathway would not be available in winter. The residence location is 22 km ESE from B Plant, 28 km E from T Plant and REDOX Plant, and at distances ranging from 21 to 33 km generally SE and ESE from the reactors.

Table 5-6 shows the estimated absorbed dose to each ICRP-defined organ for the following nuclide components: ^{41}Ar, ^{131}I + ^{131m}Xe, particles, and the total. The thyroid is the organ that is

[1] Eastern part of Yakima County, Washington State.

estimated to receive the largest dose (86 mrad), which is over 20 times higher than the estimated dose to the lung.

Table 5-6. Absorbed Dose to Organs for One-Year (1954) Resident of Ringold

Organ	Dose (mrad[a]) from each radionuclide or set of radionuclides			
	^{41}Ar	^{131}I + ^{131m}Xe	Particles	Total
Adrenals	1.8	3.7×10^{-2}	2.5×10^{-1}	2.1
Bladder wall	1.8	1.7×10^{-1}	2.4×10^{-1}	2.2
Bone surface	2.7	7.6×10^{-2}	7.0×10^{-1}	3.5
Brain	1.8	5.4×10^{-2}	2.3×10^{-1}	2.1
Breast	2.1	4.4×10^{-2}	2.7×10^{-1}	2.4
Esophagus	1.8	5.6×10^{-2}	2.4×10^{-1}	2.1
Stomach wall	1.8	7.8×10^{-2}	2.6×10^{-1}	2.1
Small intestine wall	1.8	3.7×10^{-2}	2.8×10^{-1}	2.1
Upper large intestine wall	1.8	4.3×10^{-2}	4.5×10^{-1}	2.3
Lower large intestine wall	1.8	5.6×10^{-2}	8.7×10^{-1}	2.7
Colon	1.8	4.9×10^{-2}	6.4×10^{-1}	2.5
Kidneys	1.8	3.6×10^{-2}	2.4×10^{-1}	2.1
Liver	1.8	3.7×10^{-2}	3.4×10^{-1}	2.2
Muscle	1.8	5.2×10^{-2}	2.4×10^{-1}	2.1
Ovaries	1.9	4.0×10^{-2}	2.7×10^{-1}	2.2
Pancreas	1.8	3.9×10^{-2}	2.4×10^{-1}	2.1
Red marrow	1.9	4.7×10^{-2}	4.1×10^{-1}	2.3
Extrathoracic airways	1.8	1.2×10^{-1}	3.3×10^{-1}	2.3
Lungs	1.9	7.1×10^{-2}	1.9	3.8
Skin	3.0	5.0×10^{-2}	7.3×10^{-1}	3.8
Spleen	1.8	3.7×10^{-2}	2.4×10^{-1}	2.1
Testes	1.9	3.8×10^{-2}	2.6×10^{-1}	2.2
Thymus	1.8	5.6×10^{-2}	2.4×10^{-1}	2.1
Thyroid	1.9	84	2.3×10^{-1}	86
Uterus	1.8	3.9×10^{-2}	2.4×10^{-1}	2.1
Remainder	1.8	5.1×10^{-2}	2.4×10^{-1}	2.1

[a]To obtain dose in units of Gy, multiply values in table by 1×10^{-5}.

Table 5-7 shows the effective dose for individual nuclides with the contributions due to inhalation, ingestion, and external exposure pathways. Because the individual was assumed to consume locally produced food, those food pathways are most important (52% of the total), and ^{131}I is the most important radionuclide (63% of the total). The particulate radionuclides (mainly ruthenium and rhodium) and ^{41}Ar make up 9% and 28%, respectively, of the total effective dose estimate of 6.8 mrem for 1954. For comparison, the annual absorbed dose to the thyroid of a resident of Ringold in 1945 has been estimated to be ~33,000 mrad (Farris et al. 1994), or ~1600 mrem, over 200 times higher than this estimate for 1954. This is because of the much larger release of radioiodine to air in 1945. Farris' dose estimate for an offsite resident in 1945 is nearly

three times higher than our annual B Plant construction worker example, which included parts of 1944 and 1945 and did not include food pathways (Section 5.1.3).

Table 5-7. Committed Effective Dose to One-Year (1954) Resident of Ringold

	Dose (mrem[a]) from particular exposure pathways					Total dose	
		Ingestion		External exposure			
Nuclides	Inhalation	Food	Soil	Air	Ground	(mrem)	%
^{41}Ar	0	0	0	1.9	0	1.9	28.1
^{90}Sr/^{90}Y	1.1×10^{-3}	1.9×10^{-2}	2.1×10^{-3}	1.9×10^{-8}	3.5×10^{-4}	2.2×10^{-2}	0.3
^{91}Y	3.1×10^{-3}	7.8×10^{-4}	1.1×10^{-5}	3.7×10^{-7}	2.8×10^{-5}	3.9×10^{-3}	0.1
^{95}Zr/^{95}Nb	2.0×10^{-3}	8.0×10^{-7}	6.9×10^{-6}	6.5×10^{-5}	7.8×10^{-3}	9.9×10^{-3}	0.1
^{103}Ru/^{103m}Rh	3.8×10^{-2}	6.9×10^{-3}	9.7×10^{-5}	1.2×10^{-3}	7.0×10^{-2}	1.2×10^{-1}	1.7
^{106}Ru/^{106}Rh	1.6×10^{-1}	3.8×10^{-2}	2.3×10^{-3}	1.9×10^{-4}	7.8×10^{-2}	2.8×10^{-1}	4.1
^{131}I/^{131m}Xe	7.9×10^{-1}	3.5	1.3×10^{-3}	2.4×10^{-3}	2.7×10^{-2}	4.3	63.3
^{134}Cs	1.7×10^{-5}	2.0×10^{-3}	2.4×10^{-5}	6.1×10^{-7}	2.2×10^{-3}	4.3×10^{-3}	0.1
^{137}Cs/^{137m}Ba	6.8×10^{-5}	1.1×10^{-2}	9.0×10^{-4}	1.4×10^{-6}	4.6×10^{-2}	5.8×10^{-2}	0.8
^{141}Ce	7.9×10^{-4}	5.5×10^{-6}	1.1×10^{-6}	2.7×10^{-6}	1.2×10^{-4}	9.2×10^{-4}	<0.1
^{144}Ce/^{144}Pr	2.6×10^{-2}	1.9×10^{-4}	2.6×10^{-4}	6.5×10^{-6}	3.0×10^{-3}	2.9×10^{-2}	0.4
^{239}Pu	6.0×10^{-2}	1.6×10^{-5}	5.6×10^{-4}	1.6×10^{-11}	2.1×10^{-7}	6.0×10^{-2}	0.9
Particles[b]	2.9×10^{-1}	7.7×10^{-2}	6.2×10^{-3}	1.4×10^{-3}	2.1×10^{-1}	5.8×10^{-1}	8.6
Total	1.1	3.6	7.5×10^{-3}	1.9	2.3×10^{-1}	6.8	100
%	15.9	52.4	0.1	28.2	3.4	100	

[a] To obtain dose in units of Sv, multiply values in table by 1×10^{-5}.
[b] "Particles" includes all the radionuclides listed except ^{41}Ar and ^{131}I/^{131m}Xe.

5.2 Probability of Exposure to Large Particles Deposited on Ground Surfaces

The SURVEY spreadsheet tool (Section 3.5) was used to evaluate the exposure to large radioactive particles deposited on ground surfaces. Results of two example calculations are discussed below. The first example is a field survey technician working in the 200 Areas in 1947 and the second is an offsite resident near Ringold in 1954. These are times of high ground contamination from corrosion of T and B Plant duct work and ruthenium from REDOX Plant.

5.2.1 Onsite Survey Technician, 1947

The first example calculation is a maximum exposure condition for a hypothetical field worker such as an environmental survey technician. This person's work required walking in the contaminated areas of ground around the T Plant and B Plant stacks. The deposition density of active particles at the work location was based on the surveys conducted there in 1947. This contamination level was represented in the SURVEY spreadsheet by a custom distribution in which half the area had a deposition density of 5-10 particles ft^{-2} and the other half had a density of 1-5 particles ft^{-2}. These ranges represent the heavy and medium density zones measured in 1947 and mapped in Figures 4-30 and 4-31. The ground surveys in 1947 did not extend to

residence areas. However, the lowest deposition density measured around the stacks was 0.01 particles ft^{-2} (Figures 4-30 and 4-31). For this example, we assumed the particle deposition density at the residence location was 0.005-0.01 particles ft^{-2}. The exposure duration at work in this example was 8 hours per day, 5 days per week, for 12 weeks, or 60 working days. The distributions of the uncertain input assumptions were presented in Table 3-7.

The SURVEY spreadsheet provides four predictions: the number of particles inhaled during the exposure period, the number of particles contacting the body or skin during one work day, and the number of particles ingested inadvertently from contaminated skin in a day. Table 5-8 includes the percentiles that describe the uncertainty distributions for these predictions for the onsite survey technician.

Table 5-8. Percentiles for Predicted Contact with Large Active Particles from Ground Surfaces in 200 Areas: Onsite Survey Technician in 1947

Percentile of distribution	Estimated number of particles			
	Inhaled during exposure period[a]	Contacting body during 1 work day	Contacting skin during 1 work day	Ingested during 1 work day
0%	0.01	0.3	0.04	0.00009
10%	0.30	2	0.3	0.0008
20%	0.63	3	0.5	0.0012
30%	1.2	4	0.7	0.0017
40%	1.9	5	0.9	0.0023
50%	**3.0**	**6**	**1.1**	**0.0029**
60%	4.4	7	1.3	0.0037
70%	6.7	9	1.7	0.0048
80%	10	11	2.2	0.0065
90%	17	14	2.9	0.0092
100%	91	24	7.3	0.031

[a]Sixty working days within a 3-month period in 1947.

The median estimate (50^{th} percentile) is 3 particles inhaled in this 3-month period. The uncertainty distribution allows us to express the certainty (or probability) that a single particle would have been encountered. There is a 73% certainty that a single resuspended particle would have been inhaled during the 60 work days. The SURVEY spreadsheet does not address the fraction of particles inhaled that would have been exhaled without deposition. (See Section 3.6 for a discussion of deposition of particles in the respiratory tract following inhalation.) If the particles were large, the probability of deposition in the deep lung would be low, and the particle is likely to have been either blown from the nose or cleared from the upper respiratory tract and ingested.

The SURVEY spreadsheet addresses the pathways of exposure from contaminated ground surfaces. Inhalation of active particles directly from the airborne plume from the stacks would be in addition to the inhalation of resuspended particles predicted by SURVEY. During times when active particles were being released in large quantities, direct inhalation from the plume would have been more important than resuspension, if the person were in the contaminated plume. For example, H.M. Parker estimated (reported in Gregg 1948) that a person working outside in the

200 Areas would have the potential to inhale between 5 and 30 active particles per month between May and September 1948 (Figure 4-29). See Section 5.3 for additional discussion of the probability of exposure to large particles in the direct plume of air.

The example calculation assumes no respiratory protection was used. From the site memos and reports at the time, we know that respiratory protection was used in some of the most highly contaminated outdoor areas (HW-11348, HW-55569, HW-8624). However, respiratory protection was generally not provided to construction workers nor to guards in outside areas (HW-8624, U.S. Senate Committee on Governmental Affairs 1989). Construction work in 1947–1948 was prohibited in areas of high particle concentration although there was no absolute limit at which this cut-off was made (HW-11348).

In contrast to inhalation, the external contact pathways are computed based on a single working day because of the likelihood that removal of clothing and washing of skin would occur. This exposure duration might be appropriately lengthened for another scenario (e.g. a person in an Army camp). However, the spreadsheet does not incorporate the retention of the particle on clothing or skin, so the predicted estimates represent even brief contact of a particle with the body. As discussed in Section 3.5.1, the persistence of particulate contamination on the body is rarely more than a few hours.

The median estimate is 6 particles contacting the body per work day (Table 5-8). Using the predicted uncertainty distributions, there is a 99% certainty that at least one particle would have contacted the body and a 54% certainty that one particle would have contacted exposed skin during one working day. No attempt has been made to reconstruct the type of protective clothing that might have been worn by the worker. The results illustrate the high probability of body contact with active particles in these highly contaminated areas. Section 3.6 discusses dosimetric results for the skin in the case of a particle that remains attached to the body for a certain length of time.

In contrast to inhalation and body contact, the inadvertent ingestion of an active particle from contamination on the skin is a low-probability event (Table 5-8). Even the 90th percentile estimate is 0.009 particles ingested from contaminated skin in a work day. However, another mechanism for exposure of the GI tract is clearance of a large inhaled particle from the upper respiratory tract and subsequent swallowing (Section 3.6).

A requested feature of the computational tools developed in this work was the ability to evaluate the sensitivity of the results to various input parameters. Table 5-9 illustrates the sensitivity of the four predictions in the survey technician example to ten uncertain input assumptions. Sensitivity is the amount of uncertainty in a prediction that is a result of both the uncertainty (probability distribution) and the model sensitivity of an assumption. Model sensitivity is the overall effect that a change in an assumption produces in the prediction. This effect is solely determined by the formulas in the spreadsheet model. Sensitivity is measured by the rank correlation coefficient between the assumption and prediction cells of the spreadsheet (Decisioneering 1996).

The most important input assumption affecting the predicted particles inhaled is the resuspension factor used when the person is working at the contaminated area (Table 5-9). The next most important is the particle deposition density at the work location, followed by the fraction of the activity that is inhalable and the inhalation rate at work. The hours per day spent at the work location and the conditions at the residence location are relatively unimportant.

Table 5-9. Sensitivity[a] of SURVEY Predictions to Ten Input Assumptions: Onsite Survey Technician (1947) Example

Input assumption	Estimated number of particles			
	Inhaled	Contacting body	Contacting skin	Ingested
Particle deposition density at work location	0.36	0.72	0.68	0.61
Particle deposition density at residence location	<0.02	<0.02	<0.02	<0.02
Fraction of airborne particles that are inhalable	0.15	b	b	b
Ground-to-body contact probability	b	0.65	0.62	0.55
Inhalation rate at work (m^3 h^{-1})	0.14	b	b	b
Resuspension factor at work (m^{-1})	0.89	b	b	b
Resuspension factor at residence (m^{-1})	<0.02	b	b	b
Hours per day at work location	<0.02	0.03	0.03	0.03
Fraction of surface area of body that is exposed skin	b	b	0.29	0.25
Transfer from skin to ingestion	b	b	b	0.44

[a]Values in table are the rank correlation coefficients for each prediction. The rank correlation coefficient is a measure of the sensitivity of the predicted value to the assumption (Decisioneering 1996). A larger correlation coefficient indicates that the assumption has a greater effect on the prediction. See Table 3-7 for distributions of input assumptions.
[b]Prediction does not depend on this input assumption.

For external contact with active particles, the two most important contributors to uncertainty of the predictions are the particle deposition density at the work location and the ground-to-body contact probability (Table 5-9). The fraction of the body that is exposed skin is important for the predicted contact with skin as well as inadvertent ingestion. Again, conditions at the residence location and the hours per day spent at work are relatively unimportant.

Because the number of particles potentially encountered is small, there are a large number of dose outcomes, depending on where the active particle deposits in the body and the activity per particle. The reader is referred to Sections 3.6.2 and 3.6.3, which contain dose consequences resulting from ingestion and inhalation of highly radioactive particles like some of those released in the past from Hanford.

5.2.2 Offsite Resident North of Ringold, 1954

Our second example for exposure to large particles deposited on the ground is for an offsite resident north of Ringold in 1954. This is a time of high ground contamination from REDOX Plant ruthenium particles. Generally, the particle deposition densities at offsite areas from REDOX releases were less than 1 particle per 1000 ft^2 (Table 4-8). However, in September–October 1954, there was an offsite area east of the site and north of Ringold that had particle deposition densities of 1-10 particles per 1000 ft^2 (Figure 4-33, equivalent to 100 to 1000 ft^2 per particle). By December 1954, the particle deposition density there was 2-20 times less, at >2000 ft^2 per particle (Figure C-23, equivalent to <0.5 particles per 1000 ft^2). In this example, we conservatively assume that the particle deposition density at the person's residence and work location was 1-10 particles per 1000 ft^2 for a 3-month period and was 0.5-1.0 particles per 1000 ft^2 for the remainder of the year. The other assumption distributions are the same as described for the onsite worker example, with the exception that the duration of the work day is 16 hours (range 15-17) rather than 8.

Table 5-10 presents the percentiles for the predicted contact with large active particles offsite in 1954. In contrast to the onsite worker example, there are no values greater than one, indicating low probability of contact at these particle densities. Examining the median values, there was roughly a 1 in 100 chance of inhalation of a particle during the year and a 2 in 1000 chance of a particle contacting the body during a 16-hour work day. The chance of inadvertent ingestion of a particle in a work day was one in a million.

Table 5-10. Percentiles for Predicted Contact with Large Active Particles from Ground Surfaces: Offsite Resident in 1954

Percentile of distribution	Estimated number of particles			
	Inhaled during exposure period	Contacting body during 1 work day	Contacting skin during 1 work day	Ingested during 1 work day
0%	1×10^{-4}	3×10^{-4}	4×10^{-5}	5×10^{-8}
10%	2×10^{-3}	8×10^{-4}	1×10^{-4}	4×10^{-7}
20%	4×10^{-3}	1.2×10^{-3}	2.2×10^{-4}	5×10^{-7}
30%	6×10^{-3}	1.6×10^{-3}	2.9×10^{-4}	7×10^{-7}
40%	8×10^{-3}	2.0×10^{-3}	3.7×10^{-4}	9.6×10^{-7}
50%	$\mathbf{1 \times 10^{-2}}$	$\mathbf{2.3 \times 10^{-3}}$	$\mathbf{4.5 \times 10^{-4}}$	$\mathbf{1.2 \times 10^{-6}}$
60%	1.5×10^{-2}	2.8×10^{-3}	5.4×10^{-4}	1.6×10^{-6}
70%	2×10^{-2}	3×10^{-3}	6.8×10^{-4}	2×10^{-6}
80%	3×10^{-2}	5×10^{-3}	1×10^{-3}	3×10^{-6}
90%	6×10^{-2}	1×10^{-2}	3×10^{-3}	7×10^{-6}
100%	6×10^{-1}	5×10^{-2}	1×10^{-2}	5×10^{-5}

Experimentation with the SURVEY spreadsheet leads us to conclude that an active particle density of several hundred particles per 1000 ft^2 (or only a few ft^2 per particle) is necessary before it becomes likely (that is, >10% chance) that inhalation or body contact would have occurred within a 3-month exposure period. Survey maps show that these particle densities were restricted to onsite areas close to the release points (Appendix B).

5.3 Probability of Interaction with Particles Released from Processing Facilities

The previous section addressed the probability of exposure to large active particles after they had been deposited on ground surfaces. This section discusses the probability of interactions with radioactive particles during an airborne release from one of the fuel processing facilities.

The usual interpretations of the diffusion and deposition models applied to releases of radioactive particles to the atmosphere construe the airborne plume as a fluid-like continuum, so that any exposure of an individual to the plume, however brief and however small the concentration of radioactivity at the individual's location, must be interpreted to result in a positive (though possibly very small) dose and risk. However, questions are often raised about the validity of these conclusions when the radioactivity is not a gas. If the release is in the form of discrete particles, it is reasonable to ask how likely it is that a potentially exposed person may encounter none of the released radioactive particles at all.

In Appendix E, we furnish some tools for exploring this and similar questions for atmospheric releases of particles from Hanford facilities in the 1940s and 1950s. Based on binomial and Poisson distribution theory, the methods provide a model for estimating the probability that an individual in a specified exposure scenario would have encountered one or more of the released particles (a) on clothing or skin or (b) by inhalation. Appendix E provides examples to guide the reader through the application of the methods to exposure scenarios for incidents of interest during the early years at Hanford.

An extended example examines the unusual release from the REDOX plant in March 1952 due to a scrubber failure. From the estimated activity released and the average activity per particle, it was estimated that 290 million ruthenium-bearing particles were discharged. The probability of surface contact (skin or clothing) with one or more particles in Richland was 1.00; however the probability of inhalation of one or more particles was relatively small, 1.4×10^{-3}. Although the difference may seem surprising, the analysis given in Appendix E shows that the results are consistent.

A second example considers the cumulative probability of interaction with one or more of the particles released in a series of events. Table 5-11 illustrates the results of calculations for the unusual ruthenium particle releases from the REDOX Plant, which occurred in March, April, June, and September of 1952; August and September of 1953, and January, April, May, and June of 1954. For each event, the number of particles was estimated using the estimated activity and the average activity per particle released, discussed in Section 2.2.2. The number of particles released per unit activity depends upon the type of particle and the nature of the event. The probabilities shown are for contact by or inhalation of one or more of the particles released. The columns for maximum potential exposure reflect the assumption that the person is exposed outside throughout the months when the releases occurred, while the last two columns provide estimates for a use factor of 10% during those months. The use factor could reflect a reduced time of exposure or the effect of an indoor location or a combination of the two. The reduction

due to the use factor has a proportional effect on the probability of inhalation of one or more particles, but does not appreciably affect the probability of particle contact with the skin or clothing.

Table 5-11. Probabilities of Particle Contact with the Body Surface and Particle Inhalation during Unusual REDOX Ruthenium Particle Releases, March 1952–June 1954

	Maximum potential for exposure		Exposure for use factor of 0.1	
Exposure location	Probablility of particle contact[a] with body surface	Probablility of particle inhalation[a]	Probablility of particle contact[a] with body surface	Probablility of particle inhalation[a]
H-61[b]	1.0	0.044	1.0	0.0045
H-51[b]	1.0	0.042	1.0	0.0043
H-42[b]	1.0	0.034	1.0	0.0034
H-40[b]	1.0	0.011	1.0	0.0012
H-50[b]	1.0	0.078	1.0	0.0081
200-E guard tower[c]	1.0	0.014	1.0	0.0014
200-W guard tower[d]	1.0	0.034	1.0	0.0035
Hanford site	1.0	0.0036	0.9997	0.00036
Ringold	1.0	0.0026	0.9860	0.00026
Richland	1.0	0.0048	0.99996	0.00048

[a] Interaction with one or more particles.
[b] Location of military personnel; see Figure 1-2.
[c] Tower is located near the southeast corner of 200-E; see Figure 1-2.
[d] Tower is located near the center of the east side of 200-W; see Figure 1-2.

Hanford scientists and outside advisors made similar attempts, some very simple and some more developed, to evaluate the probability of inhalation of active particles. Table 5-12 is a summary of estimates made during 1948-1954. This list is not exhaustive, but does give perspective and an indication of awareness of the problem at the time. The different estimates reflect the fact that there are many more small-diameter, low-activity particles per unit activity release than there are for large active particles. The differences between the small and large particle components of the releases from the T and B Plants in the 1940s are discussed in Section 2.2.1. Note also that the estimates based upon measured numbers of particles in air samples are much lower than the more theoretical calculations.

The last entry in Table 5-12 gives a probability of inhalation of 1–2 particles per year in the TriCities, roughly comparable to Richland in the extended example in Appendix E, for a particle release rate of 840 million particles per day. The release rate of 9700 particles per second (see footnote e to Table 5-12), or 840 million in a day, is about three times larger than the March 1952 scrubber release. Adjusting for the number of particles and the greater period of exposure, the result in Table 5-12 is roughly comparable to the calculation in Appendix E, although this may be fortuitous considering the differences in the methods.

Table 5-12. Contemporaneous Estimates of Probability of Inhalation of Active Particles

Time of exposure	Place and condition of exposure	Estimate of active particle inhalation	Source
January 1948	T and B Plant areas, heavy concentration zone (see Figures 4-30 and 4-31)	One "warm" particle (up to 0.1 μCi) in 4-6 d and 1 "hot" particle (>0.1 μCi) in 2-3 mo[a,b]	HW-8624
January 1948	T and B Plant areas, light concentration zone (see Figures 4-30 and 4-31)	One warm particle (see entry above) in 1-3 mo and 1 hot particle in 27 mo[a]	HW-8624
May-Sept 1948	200 Areas, general, outside	5-30 particles mo^{-1}	Gregg 1948[c]
April-Sept 1948	200 West gatehouse	5-36 particles mo^{-1}	Gregg 1948[c]
July-Sept 1948	Residential areas	10-20 particles mo^{-1}	Gregg 1948[c]
Sept 1948	Inside canyon operating gallery (200 Area plant), "comparable with that outside the buildings"	80 particles mo^{-1}	Gregg 1948, HW-11348
Sept 1948	200 Areas	30 "sizeable" particles (~5 μm) mo^{-1}	HW-10941
Sept 1948	Construction areas	5-10 "sizeable" particles (~5 μm) mo^{-1}	HW-10941
Sept 1948	Spokane, Mullen Pass, and Mt. Rainier (100-200 miles away)	1-3 particles mo^{-1}	HW-11348
October 1948	Inside buildings at 200 Areas	50 particles mo^{-1}	HW-11479
March 1949	200 Areas	1-5 particles mo^{-1} [d]	HW-12689
1951	Military sites, maximum location based on air sampling	1 particle inhaled and retained in about 100 d, usually $<3 \times 10^{-4}$ μCi/particle	Shaw 1951
Nov 1954	Nearest army camp, 1.6 km from source [e]	15 particles yr^{-1}	HW-32209
Nov 1954	Tri Cities [e]	1-2 particles yr^{-1}	HW-32209

[a] Parker (HW-8624) computed these estimates based on two separate methods: (1) measured deposition of particles to rugs on platforms and back-calculation of air concentration from particle settling velocity and (2) dilution of stack gases of 1:100 in heavy zone and 1:1000 in light zone. Exposure time 10 hours per day, 5 days per week; inhalation rate 1 cubic meter per hour. Air sampling gave much lower probability estimates: one warm particle in 41–94 months in the heavy concentration zone.

[b] Refers to "adopted policy of wearing masks in the T and B Plant Areas" being justified by these calculations. One of 3500 Martindale type filters worn to date contained 4 active particles, and the rest were "essentially clean." Seventy seven Comfo respirators worn in zones of heavy contamination showed no discrete active particles.

[c] See Figure 4-29 for table of data presented by H.M. Parker and included in Gregg (1948). Based on air sampling and exposure time of 8 hours per day, 20 days per month for work locations and 24 hours per day, 30 days per month for residential areas.

[d] Report HW-12689 refers to Health Instruments monthly reports of the time for this estimate of probability of inhalation. This report presents results from sputum samples taken from volunteers working strenuously for 45 min without masks in the vicinity of the separation stacks. No active particles were detected.

[e] From proposed PUREX Plant, based on experience at REDOX Plant, of emission rate of 9700 particles s^{-1} with activity $>10^{-3}$ μCi/particle. Emission rate of particles $> 10^{-2}$ μCi/particle was 50 times less. Inhalation rate used was 7300 m^3 yr^{-1} (representative of continuous exposure).

Relatively few personnel contacts with particles were identified in the reports we reviewed. A 1954 report mentions three known cases where an active particle was lodged against the skin, for example behind a belt or sock (HW33068). Ebright (HW-32473) specifically mentions a waist are skin burn on April 23, 1954 to a construction employee in a non-radiation area near the REDOX Plant and an incident on June 7, 1954 of a particle (with a contact reading of 1.3 rad h^{-1}) lodged in an employee's sock. It is the larger more active particles that were likely to have been reported and detected, while body surface contacts with the more numerous low-activity particles may have gone unnoticed.

Application of the methods provided in Appendix E depends upon the amount of information available for a particular scenario of personnel exposure. For persons exposed to specific events, the investigation could also include the examination of detailed meteorological data at the time of occurrence, a refinement that has not been considered here.

APPENDIX A

BIBLIOGRAPHY

Document Database

A document database was established to keep track of documents reviewed that were relevant to this Task Order. As stated in the scope of work, this database is a required deliverable for this work. Microsoft® Access 97 is the software used. The fields in the database are:

- Document Date (month/day/year)
- Title
- Authors
- Citation (This is often the HW or other report number. Otherwise, a journal volume and number, etc.)
- Description (This field was used for internal RAC communications. It is not an abstract of the source; rather it contains notes relevant to this task order. It may be blank.)
- Copies to (for RAC tracking purposes)
- Hanford Reading Room Number

Most documents are available for review in the Hanford reading room and can be located there by their accession number, which is included in our database. In addition, when this report was released in January 2001, the Department of Energy maintained a site on the Internet <http://www2.hanford.gov/declass/d20pydeclass.asp> called the Hanford Declassified Document Retrieval System (DDRS). At the time of final revision of this report in 2002, the address for the DDRS was http://www2.hanford.gov/DDRS/. Of the HW- reports referenced in this report, over 97% could be read online and downloaded or printed from this site. We are aware that the DOE Internet site has not been operational and cannot state that it will operate continuously in the future. The reading room should be continuously maintained.

There are more than 300 documents in the database. At least one of these documents (HW-89072) is a compilation of material extracted from over 150 other weekly or monthly reports.

In our reference call-outs in the text of this report, we use the HW- number for those reports issued by the Hanford contractor. Early on in the review of documents, using the HW- number was judged to be prudent, to avoid the possible mix-ups associated with the multiple documents produced in the same year by the same author (e.g. Parker 1948a, 1948b, 1948c, etc.). In addition, the author's name was sometimes illegible on these old documents, whereas at least one page would clearly show the HW- number. Use of the HW- number also permits identification of the document in the database (in the citation field) without uncertainty. Another unambiguous number is the Hanford reading room accession number. However, this is not useful at other library locations, and not all documents we used were in the Hanford reading room. If that number is desired, it can be obtained from the database.

There are two listings in this appendix—Table A-1 is a complete bibliography of the database contents, sorted alphabetically by author. Table A-2 is a list of the HW- reports, ordered by HW- number. This table allows the reader of the hard-copy version of this report to locate the

author and date of HW reports cited in the text. Further information (such as the Hanford reading room number) can then be obtained by referring to the author-ordered listing.

Table A-1. Complete Bibliographic List of Documents by Sorted by Author

Adley, F.E. 1948. *Report of a Study of the Fate of 200 Area Stack Gases*. HW-9864. Hanford Reading Room Number 1088. May 21.

Adley, F.E. 1950. *Natural Atmospheric Particulate Background at the Hanford Works*. HW-29698. Hanford Reading Room Number 8810. December 19.

Adley, F.E., J.J. Fuquay, W.E. Gill, R.E. Scott, and D.E. Wisehart. 1954. *Redox Stack Gas Particulates*. HW-32209. Hanford Reading Room Number 4998. November 10.

Adley, F.E., W.E. Grill, H.B. Perry, R.H. Scott, and D.E. Wisehart. 1953. *Particulates Emitted by 291-S Stack*. HW-28780. Hanford Reading Room Number 4990. July 22.

AEC-GE Study Group for the Economic Development of Richland. 1964a. *Catalog of Hanford Buildings and Facilities, 100 Areas*. GEH-26434-100. Hanford Reading Room Number 7756. April.

AEC-GE Study Group for the Economic Development of Richland. 1964b. *Catalog of Hanford Buildings and Facilities, 200 Areas*. GEH-26434-200. Hanford Reading Room Number 7755. April.

Andersen, B.V. 1956. November Monthly Report Regional Monitoring. One page memo to A.R. Keene. December 3.

Andersen, B.V. 1957. December Monthly Report Regional Monitoring. One page memo to A.R. Keene. January 3.

Andersen, B.V. 1958a. *Regional Monitoring - Data Summary (1957)*. HW-89066. Hanford Reading Room Number 1163. March.

Andersen, B.V. 1958b. *Regional Monitoring Activities September, 1958*. HW-57644. Hanford Reading Room Number 7347. October.

Andersen, B.V., M.W. McConiga, and J.K. Soldat. 1956. *Radioactive Contamination in the Hanford Environs for the Period July, August, September 1956*. HW-46726. Hanford Reading Room Number 1144. December 7.

Andersen, B.V., M.W. McConiga, and J.K. Soldat. 1957. *Radioactive Contamination in the Hanford Environs for the Period October, November, December 1956*. HW-48374. Hanford Reading Room Number 1146. February 25.

Andersen, B.V. and J.K. Soldat. 1955. *Radioactive Contamination in the Hanford Environs for the Period July, August, September 1955*. HW-39429. Hanford Reading Room Number 1137. October 10.

Andersen, B.V. and J.K. Soldat. 1956a. *Radioactive Contamination in the Hanford Environs for the Period January, February, March 1956*. HW-43012. Hanford Reading Room Number 1140. May 28.

Andersen, B.V. and J.K. Soldat. 1956b. *Radioactive Contamination in the Hanford Environs for the Period October, November, December 1955*. HW-40871. Hanford Reading Room Number 1138. February 6.

Andersen, B.V. and J.K. Soldat. 1956c. *Radioactive Contamination in the Hanford Environs for the Period April, May, June 1956*. HW-44215. Hanford Reading Room Number 1141. August 7.

Anonymous. 1949. *Radioactive Contamination*. HAN-25408 1/2 Manager's Data Book June 1949 Edition Volume II. Hanford Reading Room Number 9866. May 28.

Anonymous. 1951. *Radioactive Contamination in the Environs of the Hanford Works for the Period April, May, June, 1951*. HW-22313. Hanford Reading Room Number 1112. October 8.

Anonymous. 1986. *Highlights of Historical Documents 1943–1948; 1949–1953; 1954–1957; 1958–1961; 1962–1965; 1966–1969; 1970–1973; 1974–1977; 1978–1981; 1982–1985.* Hanford Reading Room Number 18107. February 26.

Anspaugh, L.R., J.H. Shinn, P.L. Phelps, and N.C. Kennedy. 1975. "Resuspension and Redistribution of Plutonium in Soils." *Health Physics* 29:571-582.

Apple, R.S. 1946. *Activities Discharged Into the Atmosphere*. HW-7-4275. Hanford Reading Room Number 8579. June 18.

Backman, G.E. 1965. *Summary of Environmental Contamination Incidents at Hanford, 1958–1964*. HW-84619. Hanford Reading Room Number 1205. April 12.

Bailey, J.C. and R.C. Rohr. 1953. *Airborne Contamination Resulting from Transferable Contamination on Surfaces*. K-1088. U.S. Atomic Energy Commission, Washington, D.C.

Baumgartner, W.V. 1954. *Radiation Monitoring Unit Investigations of the Radioactive Particles found in the 200-West Area*. HW-33857. Hanford Reading Room Number 5002. November 18.

Bell, R.S. 1947. *Active Particle Investigation—200 Areas: Establishment of Physical Control*. HW-8108. Hanford Reading Room Number 8108. November 26.

Botsford, C.W. 1945. *Study of Calibration of Victoreen Integrons*. HW-7-2271. Hanford Reading Room Number 7488. July 25.

Brodsky, A. 1990. "Resuspension Factors and Probabilities of Intake of Material in Process (Or 'Is 10^{-6} a Magic Number in Health Physics?')". *Health Physics* 39: 992–1000.

Browne, W.G. 1955. *T Emission Problem - Bismuth Phosphate Plant*. HW-36112. Hanford Reading Room Number 1131. April 6.

Brunskill, R.T. 1967. "The Relationship between Surface and Airborne Contamination." *Surface Contamination*. Symposium proceedings, Gatlinburg, Tennessee, 1964. Pergamon Press, Oxford.

Burger, L.L. 1989. *Fission Product Iodine During Early Hanford-Site Operations: Its Production and Behavior During Fuel Processing, Off-Gas Treatment and Release to the Atmosphere.* PNL-7210 HEDR. Hanford Reading Room Number 8160. December.

Bustad, L.K. and J.L. Terry. 1986. *Basic Anatomical, Dietary, and Physiological Data for Radiological Calculations*. HW-41638. Hanford Reading Room Number 1139. February 24.

Canada, R.G. 1980. *NSAC EPRI ORIGEN Code Calculation of TMI-2 Fission Product Inventory*. R-80-012. Technology for Energy Corporation, Knoxville, Tennessee.

Cantril, S.T. and J.W. Healy. 1945. *Iodine Metabolism with Reference to I-131*. HW-7-2604. Hanford Reading Room Number 4898. October 22.

Carlisle, R.P. and J.M. Zenzen. 1996. *Supplying the Nuclear Arsenal, American Production Reactors, 1942–1992*. Johns Hopkins University Press, Baltimore, Maryland.

Chamberlain, A.C. and G.R. Stanbury. 1951. *The Hazard from Inhaled Fission Products in Rescue Operations after an Atomic Bomb Explosion*. AERE HP/R-737.

Christy, J.T. 1953. *200 Area Monthly Reports for 1952*. HAN-61662-DEL. Hanford Reading Room Number 9892.

Church, P.E. 1948. *Meteorological Information*. HW-9476. Hanford Reading Room Number 11313. April.

Cleavenger, P.M. and S.P. Gydesen. 1989. *Stack Gas Disposal Extracts: March 1947–January 1952*. HW-89072. Hanford Reading Room Number 8820. October.

Clukey, H.V. 1954. *Ventilation for Radiation Protection at Redox*. HW-32319. Hanford Reading Room Number 9264. January 7.

Conklin, A.W. 1986. *Overview of Historical Documents*. Office of Radiation Protection, State of Washington Department of Social and Health Services. Hanford Reading Room Number 10709. September 22.

Cross, W.G., N.O. Freedman, and P.Y. Wong. 1992. "Beta Ray Dose Distributions from Skin Contamination." *Rad. Prot. Dos*. 40: 149–168.

Decisioneering, Inc. 1996. *Crystal Ball: Forecasting and Risk Analysis for Spreadsheet Users*. Aurora, Colorado.

DeLong, C.W. 1950. *Collection and Analysis of Active Particles*. HW-15802. Hanford Reading Room Number 10669. January 27.

DeNeal, D.L. 1965. *Historical Events–Reactors and Fuels Fabrication*. RL-REA-2247. General Electric, Hanford Atomic Products Operation, Richland.

Denham, D.H., E.I. Mart, and M.E. Thiede. 1993. *Conversion and Correction Factors for Historical Measurements of Iodine-131 in Hanford-Area Vegetation 1948–1951*. PNWD-2176 HEDR. Hanford Reading Room Number 12948. September.

Deonigi, D.E., D.M. Anderson, and G.L. Wilfert. 1994. *Commercial Milk Distribution Profiles and Production Locations*. Hanford Environmental Dose Reconstruction Project. PNWD-2218 HEDR. Batelle Pacific Northwest Laboratories, Richland, Washington. April.

Dockum, N.L. and J.W. Healy. 1955. *Spot Diameter Method of Quantitative Autoradiography of Ru106 Particles in Lung Tissue*. HW-36760. Hanford Reading Room Number 5016. March 15.

DOE (U.S. Department of Energy). 1998. *Radionuclide Air Emissions Report for the Hanford Site, Calendar Year 1998*. DOE/RL-98-33. Available at internet address <www.hanford.gov> or from Office of Scientific and Technical Information, Springfield, Virginia.

DOE. 1999. *Hanford Site Atlas*. Internet address <http://www.bhi-erc.com/dm/hgis/hgis.htm>.

Donelson, R.N. 1953. *Emission of Crystals from Redox Stack*. HW-29346. Hanford Reading Room Number 8494. September 5.

Duncan, J.P. 1994. *Overview of Vegetation Monitoring Data*. PNWD-2235 HEDR. Hanford Reading Room Number 13782. March.

Ebright, D.P. 1953a. *Radiological Sciences Department Investigation Radiation Incident, Class I, No. 225*. HW-27431. Hanford Reading Room Number 6967. March 16.

Ebright, D.P. 1953b. *Radiological Sciences Department Investigation Radiation Incident, Class I, No. 246*. HW-27447. Hanford Reading Room Number 6965. March 16.

Ebright, D.P. 1953c. *Radiological Sciences Department Investigation, Radiation Incident, Class I, No. 299*. HW-29230. August 25.

Ebright, D.P. 1954. *A History of the Redox Ruthenium Problem*. HW-32473. Hanford Reading Room Number 1127. July 16.

Eckerman, K.F. and J.C. Ryman. 1993. *External Exposure to Radionuclides in Air, Water, and Soil*. Federal Guidance Report No. 12. Report EPA-402-R-93-081. Office of Radiation and Indoor Air, U.S. Environmental Protection Agency, Washington, D.C.

Eckerman, K.F., R.W. Leggett, C.B. Nelson, J.S. Puskin, and A.C.B. Richardson. 1999. *Cancer Risk Coefficients for Environmental Exposure to Radionuclides*. Federal Guidance Report No. 13. Report EPA-402-R-99-001, Office of Radiation and Indoor Air, U.S. Environmental Protection Agency, Washington, D.C.

Elder, R.E., A.W. Conklin, G.W. Egert, D.D. Brekke, and W.L. Osborne. 1986. *Rockwell Hanford Operations Environmental Surveillance Annual Report, Calendar Year 1985*. Hanford Reading Room Number 4329. May.

Dennis R. (Ed.) 1976. *Handbook on Aerosols*. Report TID-26608, Technical Information Center, Energy Research and Development Administration.

EPA (U.S. Environmental Protection Agency). 1985. *Methodology for Characterization of Uncertainty in Exposure Assessments*. EPA/600/8-85-009. Washington, DC.

EPA (U.S. Environmental Protection Agency). 1995. *User's Guide for the Industrial Source Complex (ISC3) Dispersion Models*. EPA-454/B-95-003b, Office of Air Quality Planning and Standards Emissions, Monitoring, and Analysis Division, Research Triangle Park, North Carolina.

Essig, T.H. and R.B. Hall. 1966. *Environmental Status of the Hanford Project—1965 Annual Summary*. BNWL-CC 913. Hanford Reading Room Number 1210. November 8.

Essig, T.H. and R.B. Hall. 1967. *Environmental Status of the Hanford Reservation for December, 1966*. BNWL-CC-637 12. Hanford Reading Room Number 1221. March 20.

Farris, W.T., B.A. Napier, P.W. Eslinger, T.A. Ikenberry, D.B. Shipler, and J.C. Simpson. 1994. *Atmospheric Pathway Dosimetry Report, 1944–1992*. PNWD-2228 HEDR. Hanford Reading Room Number 13631. October.

Fermi, R. and E. Samra. 1995. *Photographs from the Secret World of the Manhattan Project.* Harry N. Abrams, Inc., New York.

Fix, J.J. and P.J. Blumer. 1977. *Radiochemical Analyses of Game Birds Collected from the Hanford Environs 1971–1975*. BNWL-2089. Hanford Reading Room Number 1263. July.

Fix, J.J., P.J. Blumer, and P.E. Bramson. 1977. *Environmental Status of the Hanford Site for CY-1976*. BNWL-2246. Hanford Reading Room Number 168. May.

Forsythe G.E., M.A. Malcolm, and C.B. Moler. 1977. *Computer Methods for Mathematical Computations*. Prentice-Hall, Inc., Englewood Cliffs, New Jersey.

Foster, R.F. and I.C. Nelson. 1961. *Evaluation of Radiological Conditions in the Vicinity of Hanford for 1960*. HW-68435. June 1.

Foster, R.F. and R.H. Wilson. 1965. *Evaluation of Exposure from Multiple Environmental Sources in the Environs of the Hanford Plant*. BNWL-SA-53. Hanford Reading Room Number 4248. June 8.

Fuquay, J.J. and C.E. Elderkin. 1965. *Recent Hanford Diffusion Results Significant for Estimating Pollution Potential*. BNWL-SA-429. Hanford Reading Room Number 4251. November 23.

Fuquay, J.J. and C.L. Simpson. 1963. *Use of Meteorological Measurements for Predicting Dispersion from Releases Near Ground-Level*. HW-SA-3176. Hanford Reading Room Number 4696. October.

Gamertsfelder, C.C. 1946. H.I. *Report on the 200 Areas and Environs for the Week Ending January 9, 1945*. HW-7-3194. Hanford Reading Room Number 7161. January 11.

Gamertsfelder, C.C. 1947. *Effects on Surrounding Areas Caused by the Operations of the H.E.W*. HW-7-5934. Hanford Reading Room Number 7104. March 11.

Gamertsfelder, C.C. 1951. *Measurement of Beta Radiation in Field Situations*. HW-21121. Hanford Reading Room Number 7280.

General Electric. 1952. *Analysis of Radioactive Material Found in 200 Area*. HW-24885. Hanford Reading Room Number 8423. July.

Gerber, M.S. 1992a. *Legend and Legacy: Fifty Years of Defense Production at the Hanford Site*. WHC-MR-0293, Revision 2. Hanford Reading Room Number 10879. September.

Gerber, M.S. 1992b. *On the Home Front, The Cold War Legacy of the Hanford Nuclear Site*. Lincoln and London: University of Nebraska Press. Hanford Reading Room Number 12232.

Gerber, M.S. 1993a. *A Brief History of the PUREX and UO_3 Facilities*. WHC-MR-0437. Westinghouse Hanford Company, Richland, Washington. Hanford Reading Room Number 13107. November.

Gerber, M.S. 1993b. *Multiple Missions: The 300 Area in Hanford Site History*. WHC-MR-0440. Westinghouse Hanford Company, Richland, Washington. Hanford Reading Room Number 13120. September.

Gerber, M.S. 1994. *A Brief History of the T Plant Facility at the Hanford Site*. WHC-MR-0452, Addendum 1. Westinghouse Hanford Company, Richland, Washington. Hanford Reading Room Number 13937. May.

Gerber, M.S. 1996. *The Plutonium Production Story at the Hanford Site: Processes and Facilities History*. WHC-MR-0521. Westinghouse Hanford Company, Richland, Washington. Hanford Reading Room Number 18228. June.

Gifford, F.A. 1976. "Turbulent Diffusion-Typing Schemes: A Review." *Nuclear Safety* 17 (1): 71.

Gilbert, R.O., E.I. Mart, D.L. Strenge, and T.B. Miley. 1994. *Uncertainty and Sensitivity Analysis of Historical Vegetation Iodine-131 Measurements in 1945–1947*. PNWD-1978 HEDR. Hanford Reading Room Number 13564. March.

Gill, W.E. 1955. *Penetration of Respiratory Protective Equipment by Ruthenium at Building 202-S*. HW-35043. Hanford Reading Room Number 5007. February 21.

Gill, W.E. and D.E. Wisehart. 1954. *A Study of Certain Properties of Ruthenium Compounds found in the REDOX Process*. HW-32175. Hanford Reading Room Number 10905. June 23.

Gill, W.E., D.E. Wisehart, and F.E. Adley. 1952. *291 Stack Gas Particulates Interim Report*. HW-24932. Hanford Reading Room Number 8503. July 3.

Gosling, F.G. 1999. *The Manhattan Project: Making the Atomic Bomb.* United States Department of Energy, History Division. Report DOE/MA-0001-01/99.

Greager, O.H. and W. Cready. 1948. Stack Gas Decontamination—Separations Plants. HW-8667. Hanford Reading Room Number 4913. January 27.

Gregg, A. 1948. "Minutes: Advisory Committee for Biology and Medicine. Twelfth Meeting Held at Hanford Operations Office, Richland, Washington, October 8-9, 1948." Hanford Reading Room Number 10727. December 9.

Gross, C.N. 1948. *Stack Gas Decontamination, Separation Plants: Development of Decontamination Systems*. HW-9175. Hanford Reading Room Number 6400. March 12.

Groves, L.R. 1962. *Now It Can Be Told*. Harper and Brothers, New York.

Gydesen, S.P. 1992a. *Declassifications Requested by the Technical Steering Panel of Hanford Documents Produced 1944–1960*. PNWD-2024 HEDR. Hanford Reading Room Number 11857. September.

Gydesen, S.P. 1992b. *Documents Containing Operating Data for Hanford Separations Processes, 1944–1972*. PNWD-2028-HEDR. Hanford Reading Room Number 11858. September.

Gydesen, S.P. 1993. *Fuel-Element Failures in Hanford Single-Pass Reactors 1944–1971*. PNWD-2161 HEDR. Hanford Reading Room Number 12759. July.

Haller, W.A. and R.W. Perkins. 1967. "Organic Iodine-131 Compounds Released from a Nuclear Fuel Chemical Processing Plant." *Health Physics* 13: 733–738.

Hanf, R.W., J.P. Duncan, and M.E. Thiede. 1993. *Iodine-131 in Vegetation Collected Near the Hanford Site: Concentration and Count Data for 1948–1951*. PNL-2177 HEDR. Hanford Reading Room Number 12964. September.

Hanf, R.W. and M.E. Thiede. 1994. *Environmental Radiological Monitoring of Air, Rain, and Snow on and near the Hanford Site, 1945–1957*. PNWD-2234 HEDR. Hanford Reading Room Number 13783. March.

Hanna, S.R., G.A. Briggs, and R.P. Hosker, Jr. 1982. *Handbook on Atmospheric Diffusion*. DOE/TIC-11223 (DE82002045). Technical Information Center, U.S. Department of Energy. Available from National Technical Information Service (NTIS), Springfield, Virginia.

Harmon, M.K. 1955. Addendum to HW-34882, "Technical Appraisal of Redox Ruthenium Problems and their Resolution." HW-35496. Hanford Reading Room Number 10899. February 24.

Healy, J.W. 1945. *Special Studies Reports for Weeks Ending 5-20-45 through 12-30-45*. HW-3-2894-del. Hanford Reading Room Number 7509. July 27.

Healy, J.W. 1947. *The Trend of Contamination Observed in the Air, the Columbia River, Vegetation, and Waste at the HEW for the Period 3/25/47 to 6/30/47*. HW-7317. Hanford Reading Room Number 1083. August 12.

Healy, J.W. 1948. *Long-lived Fission Activities in the Stack Gases and Vegetation at the Hanford Works*. HW-10758. Hanford Reading Room Number 1091. August 17.

Healy, J.W. 1949. *Your Reference CWI*. HW-15234. Hanford Reading Room Number 4943. November 29.

Healy, J.W. 1954. *Operation of Both Sides of Reactor Effluent Retention Basins*. HW-31059. March 3.

Healy, J.W. 1955. *A Preliminary Estimate of Wind Pickup and Impaction of Particles*. HW-35542. Hanford Reading Room Number 5009. March.

Healy, J.W. 1977. *An Examination of the Pathways from Soil to Man for Plutonium*. LA-6741-MS. Los Alamos Scientific Laboratory, Los Alamos, New Mexico. April.

Healy, J.W. 1980. "Review of Resuspension Models." In *Transuranic Elements in the Environment*. Edited by W.C. Hanson. DOE/TIC-22800. Hanford Reading Room Number 6200. pp. 209–235.

Healy, J.W. and C.C. Gamertsfelder. 1946. *H.I. Environs Reports—Sept. 1946 thru May 1947*. HW-7-5042. Hanford Reading Room Number 5608. September 18.

Healy, J.W. and L.C. Schwendiman. 1950. *Counter Calibrations in the Health Instrument Methods Group*. HW-18258. Hanford Reading Room Number 7946. July.

Healy, J.W., R.C. Thorburn, and Z.E. Carey. 1951. *H.I. Control Laboratory Routine Chemical Procedures*. HW-20136. Hanford Reading Room Number 2471. July 15.

Heeb, C.M. 1991. *Uncertainties in Source Term Calculations Generated by the Origen2 Computer Code for Hanford Production Reactors*. PNL-7223 HEDR. Hanford Reading Room Number 8185. March.

Heeb, C.M. 1993. *Iodine-131 Releases from the Hanford Site, 1944 through 1947, Volume 1 - Text. Volume 2 - Data*. PNWD-2033 HEDR. Hanford Reading Room Number 11852. March.

Heeb, C.M. 1994. *Radionuclide Releases to the Atmosphere from Hanford Operations, 1944–1972*. PNWD-2222 HEDR. Hanford Reading Room Number 13197. May.

Heeb, C.M. and S.P. Gydesen. 1994. *Sources of Secondary Radionuclide Releases from Hanford Operations*. PNWD-2254 HEDR. Hanford Reading Room Number 13929. May.

Heeb, C.M., S.P. Gydesen, J.C. Simpson, and D.J. Bates. 1996. "Reconstruction of Radionuclide Releases from the Hanford Site, 1944–1972." *Health Physics* 71 (4): 545–555.

Heeb, C.M. and L.G. Morgan. 1991. *Iodine-131 in Irradiated Fuel at Time of Processing from December 1944 Through December 1947*. PNL-7253 HEDR. Hanford Reading Room Number 9696. March.

Helgeson, G.L. 1954. *Redox Particle Study, Progress Report Sept. 1, 1954 to Oct. 28, 1954*. HW-33830. Hanford Reading Room Number 8954. November 22.

Hill, O.F., J.M. Smith, G.B. Barton, G.L. Helgeson, W.C. Schmidt, W.G. Browne, A.J. Waligura, K.L. Adler, W.N. Carson, Jr., and W.M. Harty. 1955. *Symposium on Iodine Problem*. HW-39073. Hanford Reading Room Number 1136. August 3.

Hilst, G.R. 1951. *The Determination of Probable Trajectories for Airborne Wastes Emitted in the Hanford Works Area*. HW-20502. Hanford Reading Room Number 4972. February 26.

Hinds, W.C. 1982. *Aerosol Technology, Properties, Behavior, and Measurement of Airborne Particles.* John Wiley & Sons, New York.

Hoffman, F.O. and R.H. Gardner. 1983. "Evaluation of Uncertainties in Environmental Radiological Assessment Models." *Radiological Assessment: A Textbook on Environmental Dose Assessment*, J.E. Till and H.R. Meyer (eds.). NUREG/CR-3332, ORNL-5968. p. 11-1–11--55.

Hoffman, F.O. Nair, S.K. and Wichner, R. 1999. *Review of HEDR Source Term for the Atmospheric Release of I-131.* Senes Oak Ridge, Inc., Oak Ridge, Tennessee.

Honstead, J.F. 1952. *Monitoring Survey -- Richland to Arco, Period May 9-11, 1952*. HW-24727. Hanford Reading Room Number 4375. June 20.

Honstead, J.F. 1968. *Evaluation of Radiological Conditions in the Vicinity of Hanford, January–June 1967*. BNWL-665. Hanford Reading Room Number 3923.

IAEA (International Atomic Energy Agency). 1970. *Monitoring of Radioactive Contamination on Surfaces*. Technical Report Series No. 120. IAEA, Vienna.

ICRP (International Commission on Radiological Protection). 1980. Limits for Intakes of Radionuclides by Workers. ICRP Publication 30, Part 2. Pergamon Press, Oxford, England.

ICRP. 1981. Limits for Intakes of Radionuclides by Workers. ICRP Publication 30, Supplement to Part 2. Pergamon Press, Oxford, England.

ICRP. 1989. *Age-dependent Doses to Members of the Public from Intake of Radionuclides: Part 1*. ICRP Publication 56. Pergamon Press, Oxford, England.

ICRP. 1991. *Recommendations of the International Commission on Radiological Protection*. ICRP Publication 60. Pergamon Press, Oxford, England.

ICRP. 1993a. *Age-dependent Doses to Members of the Public from Intake of Radionuclides: Part 2, Ingestion Dose Coefficients*. ICRP Publication 67. Pergamon Press, Oxford, England.

ICRP. 1993b. *Human Respiratory Tract Model for Radiological Protection*. ICRP Publication 66. Pergamon Press, Oxford, England.

ICRP. 1994. "Dose Coefficients for Intakes of Radionuclides by Workers." ICRP Publication 68. *Annals of the ICRP 23(4)*. Elsevier Science Ltd., Oxford.

ICRP. 1995. *Age-dependent Doses to Members of the Public from Intake of Radionuclides: Part 4, Inhalation Dose Coefficients*. ICRP Publication 71. Pergamon Press, Oxford, England.

ICRP. 1996. "Age-Dependent Doses to Members of the Public from Intake of Radionuclides: Part 5, Compilation of Ingestion and Inhalation Dose Coefficients." ICRP Publication 72. *Annals of the ICRP 26(1)*, Elsevier Science Ltd, Oxford.

Irish, E.R. 1955. *Technical Appraisal of Redox Ruthenium Problems and Their Resolution*. HW-34882. Hanford Reading Room Number 8429. January 21.

Jenne, D.E. and J.W. Healy. 1950. *Dissolving of Twenty Day Metal at Hanford ("Green Run Report")*. HW-17381-DEL. Hanford Reading Room Number 7294. May.

Jerman, P.C., W.N. Koop, and F.E. Owen. 1965. *Release of Radioactivity to the Columbia River from Irradiated Fuel Element Ruptures*. RL-REA-2160. General Electric, Hanford Atomic Products Operation, Richland.

Johnson, W.E. 1954. "Undue Contamination in Construction Areas." Letter from General Manager, General Electric to D.F. Shaw, Manager, AEC Hanford Operations Office. June 8.

Jones, A., P. Mansfield, and K. Bell. 1998. "Implications of Deposition on Skin for Accident Consequence Assessments." *Radiological Protection Bulletin* No. 207: 9–14. England. November.

Jones, I.S. and S.F. Pond. 1967. "Some Experiments to Determine the Resuspension Factor of Plutonium from Various Surfaces." *Surface Contamination*. Symposium proceedings, Gatlinburg, Tennessee, 1964. Oxford: Pergamon Press.

Jones, V.C. 1985. *United States Army in World War II. Special Studies. Manhattan: The Army and the Atomic Bomb*. Center of Military History, United States Army, Washington, D.C.

Junkins, R.L., E.C. Watson, I.C. Nelson, and R.C. Henle. 1960. *Evaluation of Radiological Conditions in the Vicinity of Hanford for 1959*. HW-64371. May 9.

Katacoff, S. 1960. "Fission-product Yields from Neutron-Induced Fission." *Nucleonics* 18:201–208.

Kiel, G.R. 1954. *Review of REDOX Plant Head-End Treatment*. Deleted version of Hanford report HW-32164. June 17.

Kocher, D.C. and K.F. Eckerman. 1987. "Electron Dose-rate Conversion Factors for External Exposure of the Skin from Uniformly Deposited Activity on the Body Surface." *Health Physics* 53: 135–141.

Kornberg, H.A. 1956. *Biology Research—Annual Report 1955*. HW-41500. Hanford Reading Room Number 4428. February 16.

Kornberg, H.A. and J.F. Kline. 1949. *Test Sputum Survey for Radioactive Particles in the 200 Areas*. HW-12689. March 1.

Lapple, C.E. 1948. *Interim Report—August 2, 1948–October 11, 1948, 200 Area Stack Contamination*. HDC-743. General Electric Company. Hanford Reading Room Number 8150. October 11.

Lapple, C.E. 1949. *Stack Contamination—200 Areas*. HDC-978. Hanford Reading Room Number 4892. January 25.

Lindberg, B.G. 1952a. *Radiological Sciences Department Investigation Radiation Incident, Class I, No. 199*. HW-24123. Hanford Reading Room Number 6964. March 25.

Lindberg, B.G. 1952b. *Radiological Sciences Department Investigation Radiation Incident, Class I, No. 206*. HW-25097. Hanford Reading Room Number 6966. June 20.

Lindberg, B.G. 1954. *Radiological Sciences Department Investigation Radiation Incident, Class I, No. 333*. HW-30764. Hanford Reading Room Number 4993. January 28.

MacCready, W.K. 1947. *Installation of Air Filters—200 Areas*. HW-7932. Hanford Reading Room Number 4906. November 3.

Maider, J.E. 1954a. *Redox Plant—Ruthenium Contamination Control*. HW-32056. Hanford Reading Room Number 10907. June 7.

Maider, J.E. 1954b. *Redox Plant—Ruthenium Contamination Control*. HW-31417. Hanford Reading Room Number 10889. April 9.

Mart, E.I., D.H. Denham, and J.E. Thiede. 1993. *Conversion and Correction Factors for Historical Measurements of Iodine-131 in Hanford-Area Vegetation, 1945–1947*. PNWD-2133 HEDR. Hanford Reading Room Number 13322. December.

McConnon, D. 1962. *The Status of Gaseous Effluent Monitoring at HAPO December 1961*. HW-69205-REV. Hanford Reading Room Number 3955. August 27.

McCormack, J.D. and L.C. Schwendiman. 1959. *Significance of Rupture Debris in the Columbia River*. HW-61325. August 17.

Meyer, K.R., H.J. Mohler, J.W. Aanenson, and J.E. Till. 2002. *Identification and Prioritization of Radionuclide Releases from the Idaho National Engineering and Environmental Laboratory*. RAC Report No. 3-CDCTask Order 5-2000-Final. Risk Assessment Corporation, Neeses, South Carolina. October 8.

Mickelson, M.L. 1947. *Preliminary Report on Existing Active Particle Hazard—200 Areas*. HW-7865. Hanford Reading Room Number 3944. October 22.

Miller C.W. and L.M. Hively. 1987. "A Review of Validation Studies for the Gaussian Plume Atmospheric Dispersion Model." *Nuclear Safety* 28 (4): 522–531.

Miller, C.W. and J.M. Smith. 1996. "Why Should We Do Environmental Dose Reconstructions?" *Health Physics* 71 (4): 420–424.

Miller, M.L., J.J. Fix, and P.E. Bramson. 1977. *Radiochemical Analyses of Soil and Vegetation Samples Taken from the Hanford Environs, 1971–1976*. BNWL-2249. Hanford Reading Room Number 1265. June.

Mishima, J. and L.C. Schwendiman. 1973. *Characterization of Radioactive Particles in the 234-5Z Building Gaseous Effluent*. BNWL-B-309. Battelle, Pacific Northwest Laboratories. Hanford Reading Room Number 9845. December.

Mobley, W.N. 1954. *Discussion of Ruthenium Problem in Redox Plant*. HW-30809. Hanford Reading Room Number 10891.

Napier, B.A. 1991. *Selection of Dominant Radionuclides for Phase I of the Hanford Environmental Dose Reconstruction Project*. Pacific Northwest Laboratory Report PNL-7231 HEDR. July.

Napier, B.A. 2002a. "A Re-evaluation of the ^{131}I Atmospheric Releases from the Hanford Site." *Health Physics* 83: 204–226.

Napier, B.A. 2002b. Personal communication with P. Voillequé of unpublished information from Hanford Environmental Dose Reconstruction Project files.

NCRP (National Council on Radiation Protection and Measurements). 1989. *Limit for Exposure to "Hot Particles" on the Skin*. NCRP Report No. 106. Bethesda, Maryland. December 31.

NCRP. 1996. *Screening Models for Releases of Radionuclides to Atmosphere, Surface Water, and Ground*. NCRP Report No. 123. Bethesda, Maryland. January 22.

NCRP. 1999. *Biological Effects and Exposure Limits for "Hot Particles."* NCRP Report No. 130. Bethesda, Maryland. December 10.

Nelson, I.C. and V.W. Thomas, Jr. 1977. "Plutonium in Human Lung in the Hanford Environs." In BNWL-SA-5855. Presented at the 4th International Congress of the International Radiation Protection Association, April 24–30, 1977, Paris, France. Hanford Reading Room Number 3940. April 24.

Office of Human Radiation Experiments. 1995a. *Human Radiation Studies: Remembering the Early Years*. *Oral History of Health Physicist Carl C. Gamertsfelder, Ph.D*. DOE/EH-0467. Hanford Reading Room Number 17183. September.

Office of Human Radiation Experiments. 1995b. *Human Radiation Studies: Remembering the Early Years*. *Oral History of Health Physicist William J. Bair, Ph.D*. DOE/EH-0463. Hanford Reading Room Number 16917. June.

Office of Human Radiation Experiments. 1995c. *Human Radiation Studies: Remembering the Early Years. Oral History of John W. Healy*. DOE/EH-0455. Hanford Reading Room Number 16687. May.

Operation Managers. 1957a. *Chemical Processing Department Monthly Report for October, 1957*. Deleted version of Hanford report HW-53449. November 22.

Operation Managers. 1957b. *Chemical Processing Department Monthly Report for November, 1957*. Deleted version of Hanford report HW-53967. December 23.

Operation Managers. 1958a. *Chemical Processing Department Monthly Report for December, 1957*. Deleted version of Hanford report HW-54319. January 21.

Operation Managers. 1958b. *Chemical Processing Department Monthly Report for January, 1958*. Deleted version of Hanford report HW-54821. February 21.

Operation Managers. 1958c. *Chemical Processing Department Monthly Report for February, 1958*. Deleted version of Hanford report HW-55215. March 21.

Operation Managers. 1958d. *Chemical Processing Department Monthly Report for March, 1958*. Deleted version of Hanford report HW-55571. April 21.

Operation Managers. 1958e. *Chemical Processing Department Monthly Report for October, 1958*. Deleted version of Hanford report HW-58051. November 21.

Operation Managers. 1958f. *Chemical Processing Department Monthly Report for November, 1958*. Deleted version of Hanford report HW-58305. December 22.

Operation Managers. 1959a. *Chemical Processing Department Monthly Report for March, 1959*. Deleted version of Hanford report HW-59849. April 20.

Operation Managers. 1959b. *Chemical Processing Department Monthly Report for June, 1959*. Deleted version of Hanford report HW-60915. July 22.

Operation Managers. 1959c. *Chemical Processing Department Monthly Report for July, 1959*. Deleted version of Hanford report HW-61366. August 21.

Operation Managers. 1959d. *Chemical Processing Department Monthly Report for September, 1959*. Deleted version of Hanford report HW-62179. October 21.

Operation Managers. 1959e. *Chemical Processing Department Monthly Report for October, 1959*. Deleted version of Hanford report HW-62593. November 20.

Operation Managers. 1959f. *Chemical Processing Department Monthly Report for November, 1959*. Deleted version of Hanford report HW-62864. December 21.

Operation Managers. 1960a. *Chemical Processing Department Monthly Report for January, 1960*. Deleted version of Hanford report HW-63706. February 22.

Operation Managers. 1960b. *Chemical Processing Department Monthly Report for August, 1960*. Deleted version of Hanford report HW-63706. September 21.

Operation Managers. 1960c. *Chemical Processing Department Monthly Report for September, 1960*. Deleted version of Hanford report HW-66958. October 21.

Operation Managers. 1960d. *Chemical Processing Department Monthly Report for October, 1960*. Deleted version of Hanford report HW-67252. November 21.

Operation Managers. 1960e. *Chemical Processing Department Monthly Report for November, 1960*. Deleted version of Hanford report HW-67459. December 21.

Overbeck, W.P. 1948. *Location of Redox Test Unit*. HW-9091. Hanford Reading Room Number 4916. March 5.

Paas, H.J. 1951a. *Radioactive Contamination in the Environs of the Hanford Works for the Period July, August, September, 1951*. HW-23133. Hanford Reading Room Number 1113. December 29.

Paas, H.J. 1951b. *Radioactive Contamination in the Environs of the Hanford Works for the Period October, November, December, 1950*. HW-21566. Hanford Reading Room Number 1109. July 13.

Paas, H.J. 1952a. *Radioactive Contamination in the Environs of the Hanford Works for the Period April, May, June, 1952*. HW-26493. Hanford Reading Room Number 1118. December 15.

Paas, H.J. 1952b. *Radioactive Contamination in the Environs of the Hanford Works for the Period January, February, March, 1952*. HW-25866. Hanford Reading Room Number 1117. October 15.

Paas, H.J. 1952c. *Radioactive Contamination in the Environs of the Hanford Works for the Period October, November, December, 1951*. HW-24203. Hanford Reading Room Number 1114. April 22.

Paas, H.J. 1953a. *Radioactive Contamination in the Environs of the Hanford Works for the Period July, August, September, 1952*. HW-27510. Hanford Reading Room Number 1119. April 15.

Paas, H.J. 1953b. *Radioactive Contamination in the Environs of the Hanford Works for the Period October, November, December, 1952*. HW-27641. Hanford Reading Room Number 1120. April 20.

Paas, H.J. 1953c. *Radioactive Contamination in the Hanford Environs for the Period April, May, June 1953*. HW-29514. Hanford Reading Room Number 1123. October 2.

Paas, H.J. 1953d. *Radioactive Contamination in the Hanford Environs for the Period January, February, March 1953*. HW-28009. Hanford Reading Room Number 1121. May 22.

Paas, H.J. 1953e. *Radioactive Contamination in the Hanford Environs for the Period July, August, September 1953*. HW-30174. Hanford Reading Room Number 1124. December 5.

Paas, H.J. 1953f. *Radioactive Particles in the Hanford Environs November-December 1952*. HW-28300. Hanford Reading Room Number 1122. June 22.

Paas, H.J. 1954a. *Radioactive Contamination in the Hanford Environs for the Period January, February, March 1954*. HW-31818. Hanford Reading Room Number 1126. May 10.

Paas, H.J. 1954b. *Radioactive Contamination in the Hanford Environs for the Period October, November, December 1953*. HW-30744. Hanford Reading Room Number 1125. January 29.

Paas, H.J., R.E. Adley, P.L. Eisenacher, D.L. Reid, J.J. Fuquay, and D.E. Jenne. 1953. *Radioactive Particle Fallout in the Hanford Environs from Nevada Nuclear Explosions, Spring 1953*. HW-28925. Hanford Reading Room Number 2533. August 4.

Paas, H.J. and G.E. Pilcher. 1954. *Radioactive Contamination in the Hanford Environs for the Period April, May, June 1954*. HW-33896. Hanford Reading Room Number 1130. November 24.

Paas, H.J. and W. Singlevich. 1950a. *Radioactive Contamination in the Environs of the Hanford Works for the Period April, May, June, 1949*. HW-17434 del. Hanford Reading Room Number 1099. April 3.

Paas, H.J. and W. Singlevich. 1950b. *Radioactive Contamination in the Environs of the Hanford Works for the Period April, May, June, 1950*. HW-19454. Hanford Reading Room Number 1105. November 24.

Paas, H.J. and W. Singlevich. 1950c. *Radioactive Contamination in the Environs of the Hanford Works for the Period January, February, March, 1950*. HW-18446. Hanford Reading Room Number 1102. July 28.

Paas, H.J. and W. Singlevich. 1950d. *Radioactive Contamination in the Environs of the Hanford Works for the Period July, August, September 1949*. HW-18615. Hanford Reading Room Number 1103. August 30.

Paas, H.J. and W. Singlevich. 1950e. *Radioactive Contamination in the Environs of the Hanford Works for the Period October, November, December, 1949*. HW-17003 DEL. Hanford Reading Room Number 1098. March 2.

Paas, H.J. and W. Singlevich. 1951a. *Radioactive Contamination in the Environs of the Hanford Works for the Period January, February, March, 1951*. HW-21214. Hanford Reading Room Number 1108. June.

Paas, H.J. and W. Singlevich. 1951b. *Radioactive Contamination in the Environs of the Hanford Works for the Period July, August, September, 1950*. HW-20700. Hanford Reading Room Number 1106. April 6.

Paas, H.J. and C.W. Thomas. 1952. *Report of Particle Contamination—October-December 1951*. HW-23517. Hanford Reading Room Number 4982. February 15.

Pan, V. and K.A. Stevenson. 1996. "Temporal Variation Analysis of Plutonium Baseline Concentration in Surface Air from Selected Sites in the Continental US." *Journal of Environmental Radioactivity* 32 (1): 239–257. March.

Parker, H.M. 1945. *Monthly Reports—H.I. Section—for 1945*. HW-7-1228. Hanford Reading Room Number 7513. January 27.

Parker, H.M. 1946a. *H.I. Section Report for October 1946*. HW-7-5301. Hanford Reading Room Number 8730. November 4.

Parker, H.M. 1946b. *H.I. Section Report for September 1946*. HW-7-5145. Hanford Reading Room Number 8729. October 3.

Parker, H.M. 1946c. *Some Considerations on the Habitability of the Hanford Camp Site*. HW-7-5372. Hanford Reading Room Number 7750. November 19.

Parker, H.M. 1946d. *Tolerable Concentration of Radio-Iodine on Edible Plants*. HW-7-3217. Hanford Reading Room Number 1080. January 14.

Parker, H.M. 1947a. *Action Taken on the Spot Contamination in the Separations Plant Areas*. HW-7920. Hanford Reading Room Number 4356. October 30.

Parker, H.M. 1947b. *H.I. Section Report for December 1946*. HW-7-5605. Hanford Reading Room Number 8731. January 3.

Parker, H.M. 1948a. *Action Taken with Respect to Apparent Enhanced Active Particle Hazard*. HW-11348. Hanford Reading Room Number 8493. October 25.

Parker, H.M. 1948b. *Further Comments on Report ARSC-8*. HW-10941. Hanford Reading Room Number 8806. September 7.

Parker, H.M. 1948c. *Meteorological Consultation March 19, 1948*. HW-9372. Hanford Reading Room Number 11312. April.

Parker, H.M. 1948d. *Progress Report on "Action Taken on the Spot Contamination in the Separations Plant Areas."* HW-8624. Hanford Reading Room Number 4912. January 20.

Parker, H.M. 1948e. *Review of the Stack Discharge Active Particle Contamination Problem*. HW-9259. Hanford Reading Room Number 1086. March 22.

Parker, H.M. 1948f. *Spot Contamination on Potential Building Sites*. HW-9141. Hanford Reading Room Number 4918. March 10.

Parker, H.M. 1950. *Feasibility of Reduction of Cooling Time—Separations Process*. HW-18409. Hanford Reading Room Number 1101. July 25.

Parker, H.M. 1951. *Components of Radiation Exposure of Military Personnel within the Hanford Reservation*. HW-20888. Hanford Reading Room Number 9386. April 20.

Parker, H.M. 1954a. *Control of Ground Contamination*. HW-32808. Hanford Reading Room Number 6401. August 19.

Parker, H.M. 1954b. *Fallout Comparisons*. HW-33754. Hanford Reading Room Number 1129. November 10.

Parker, H.M. 1954c. *Radiological Sciences Report, Research & Development Activities July—September, 1954*. HW-33437. Hanford Reading Room Number 4414. October 10.

Parker, H.M. 1954d. *Status of Ground Contamination Problem*. HW-33068. Hanford Reading Room Number 1128. September 15.

Parker, H.M. 1955a. *Radiological Sciences Report, Research & Development Activities January - March, 1955*. HW-36301. Hanford Reading Room Number 4416. April 10.

Parker, H.M. 1955b. *Radiological Sciences Report, Research & Development Activities October—December, 1954*. HW-34408. Hanford Reading Room Number 4006. January 10.

Parker, H.M. 1956a. "Radiation Exposure Experience in a Major Atomic Energy Facility." *Proceedings of the International Conference on the Peaceful Uses of Atomic Energy, Geneva, Switzerland, 8 August—20 August, 1955. Volume 13 Legal, Administrative, Health and Safety Aspects of Large-Scale Use of Nuclear Energy*. United Nations, New York. p 266–269.

Parker, H.M. 1956b. "Radiation Exposure from Environmental Hazards." *Proceedings of the International Conference on the Peaceful Uses of Atomic Energy, Geneva, Switzerland, 8 August - 20 August, 1955. Volume 13 Legal, Administrative, Health and Safety Aspects of Large-Scale Use of Nuclear Energy*. United Nations, New York. p 305-310.

Parker, H.M. and C.C. Gamertsfelder. 1945. *Weekly H.I. Reports on 200 Area and Environs for 1-5-45 thru 2-13-46 (#1 thru 58)*. HW-7-1115. Hanford Reading Room Number 7509. January 8.

Patterson, C.M. 1946. Manual of Standard Procedures, Site Survey (Special Studies). HW-7-4279. May 1.

Patterson, C.M. 1947a. *#143 - H.I. Report on the 200 Areas and Associated Laboratories for the Week Ending October 1, 1947*. HW-7695. Hanford Reading Room Number 4904. October 2.

Patterson, C.M. 1947b. *#140 - H.I. Report on the 200 Areas and Associated Laboratories for the Week Ending September 10, 1947*. HW-7539. Hanford Reading Room Number 4903. September 10.

Patterson, C.M. 1947c. *H.I. Report on the 200 Areas and Associated Laboratories for the Week Ending August 27, 1947*. HW-7405. Hanford Reading Room Number 11242. August 28.

Patterson, C.M. 1948. *Contamination in the 200 Areas*. HW-11479. Hanford Reading Room Number 4927. November 5.

Pelletier, C.A. and R.T. Hemphill. 1979. *Nuclear Power Plant Related Iodine Partition Coefficients.* NP-1271. Electric Power Research Institute, Palo Alto, California. December.

Perkins, R.W. 1964. "Physical and Chemical Forms of I-131 from Fallout and Chemical Processing Plants." *In Hanford Radiological Sciences Research and Development Annual Report for 1963*. HW-81746. January.

Perkins, R.W., C.A. Thomas, and J.M. Nielsen. 1964. *Airborne Radionuclide Measurements and Physical Characteristics Determination*. HW-SA-3742. Hanford Reading Room Number 7761. October 15.

Philipp, L.D. and E.M. Sheen. 1965. *Aerial and Ground Gamma Survey Monitors*. BNWL-62.

Pilcher, G.E., J.K Soldat, and Z.E. Carey. 1955. *Radioactive Contamination in the Hanford Environs for the Period July, August, September 1954*. HW-36504. Hanford Reading Room Number 1132. April 20.

Postma, A.K. and L.C. Schwendiman. 1959. *Radioactive Particles in the 234-5 Building Ventilation Exhaust*. HW-61082. Hanford Reading Room Number 13453. July 13.

Poston, T.M., E.J. Antonio, and A.T. Cooper. 1995. *Radionuclide Concentrations in Terrestrial Vegetation and Soil On and Around the Hanford Site, 1983 Through 1993*. PNL-10728. Hanford Reading Room Number 16934. August.

Price, K.R. 1988. *A Review of Historical Data on the Radionuclide Content of Soil Samples Collected from the Hanford Site and Vicinity*. PNL-6734. Hanford Reading Room Number 7102. November.

Ramsdel, J.V. and K.W. Burk. 1989. *Atmospheric Transport Modeling and Input Data for Phase I of the Hanford Environmental Dose Reconstruction Project*. PNL-7199-HEDR. Hanford Reading Room Number 8159. December.

Ramsdell, J.V. Jr., C.A. Simonen, K.W. Burk, and S.A. Stage. 1996. "Atmospheric Dispersion and Deposition of ^{131}I Released from the Hanford Site." *Health Physics* 71 (4): 568–577.

Regional Radiation Measurements Unit. 1955a. *Radioactive Contamination in the Hanford Environs for the Period April, May, June 1955*. HW-38566. Hanford Reading Room Number 1135. August 9.

Regional Radiation Measurements Unit. 1955b. *Radioactive Contamination in the Hanford Environs for the Period January, February, and March 1955*. HW-36506. Hanford Reading Room Number 1134. May 15.

Regional Radiation Measurements Unit. 1955c. *Radioactive Contamination in the Hanford Environs for the Period October, November, December 1954*. HW-36505. Hanford Reading Room Number 1133. April 29.

Rhodes, R. 1986. *The Making of the Atomic Bomb*. Simon & Schuster, New York.

Roberts, R.E. 1957. *CPD - Waste Storage and Experience*. HWN-1991. Hanford Reading Room Number 9899. July 26.

Roberts, R.E. 1958. *History of Airborne Contamination and Control—200 Areas*. HW-55569 RD. Hanford Reading Room Number 1162. April.

Roos, L.D. 1947. *Particle Distribution 200-East*. HW-8430. Hanford Reading Room Number 4910. November 28.

Sanger, S.L. 1995. *Working on the Bomb: An Oral History of WWII Hanford*. Edited by Craig Wollner. Continuing Education Press, Portland State University, Portland, Oregon.

Schlichting H. 1968. *Boundary-Layer Theory*, Sixth Edition. McGraw-Hill Book Company, New York.

Schmidt, W.C. 1957. *Treatment of Gaseous Effluents*. HW-49549 A. Hanford Reading Room Number 4447. April 10.

Schwendiman, L.C. 1954a. *An Application of Fluorescent Pigment to the Measurement of Particle Inhalation Probabilities*. HW-32292. Hanford Reading Room Number 4999. July.

Schwendiman, L.C. 1954b. *Evaluation of Routine REDOX Stack Sampling Procedures and Radiochemical Analysis*. HW-32262. Hanford Reading Room Number 8964. July.

Schwendiman, L.C. 1954c. *Standard Practices Counting Manual*. HW-30492. Hanford Reading Room Number 3498. January 4.

Schwendiman, L.C. 1958. "Probability of Human Contact and Inhalation of Particles." *Health Physics* 1: 352–356. Hanford Reading Room Number 1164.

Seaborg, G.T. 1994. *The Plutonium Story: The Journals of Professor Glenn T. Seaborg 1939-1946.* Edited by G.L. Kathren, J.B. Gough, and G.T. Benefiel. Battelle Memorial Institute, Battelle Press, Columbus, Ohio.

Sehmel, G.A. 1980. "Transuranic and Tracer Simulant Resuspension." In *Transuranic Elements in the Environment*. Edited by W.C. Hanson. DOE/TIC-22800. Hanford Reading Room Number 6200. pp. 236–287.

Sehmel, G.A. and W.H. Hodgson. 1980. A Model for Predicting Dry Deposition of Particles and Gases to Environmental Surfaces," in *Implications of Clean Air Amendments of 1977 and of Energy Considerations for Air Pollution Control.* Symposium Series #196, vol. 76, American Institute of Chemical Engineers Symposium Series.

Seinfeld, J. 1986. *Atmospheric Chemistry and Physics of Air Pollution*. John Wiley and Sons, New York.

Selby, J.M. and J.K. Soldat. 1958. *Summary of Environmental Contamination Incidents at Hanford 1952—1957*. HW-54636. Hanford Reading Room Number 1157. January 25.

Seymour, F.P. 1946. *A Study of Total Amounts of Active Waste Released in All Manners by the H.E.W. Process to Date*. HW 7-5463 del. Hanford Reading Room Number 1082. December 5.

Shaw, D.F. 1951. *Radiation Dosage of Military Personnel in Hanford Area*. Message to R.W. Cook, U.S. Atomic Energy Commission. Washington, D.C. April 23.

Shipler, D.B., B.A. Napier, W.T. Farris, and M.D. Freshley. 1996. "Hanford Environmental Dose Reconstruction Project—An Overview." *Health Physics* 71 (4): 532–544.

Shleien, B. 1992. *The Health Physics and Radiological Health Handbook*. Silver Spring, Maryland: Scinta, Inc.

Singlevich, W. 1947. *The Trend of Contamination in the Air, Columbia River, Rain, Sanitary Water, Vegetation, and Wastes, at the Hanford Works and Vicinity for the Period July, August, September, 1947*. HW-8549. Hanford Reading Room Number 8578.

Singlevich, W. 1948a. *H.I. "Environs" Report for Month of October, 1948*. HW-11534. Hanford Reading Room Number 4928.

Singlevich, W. 1948b. *Radioactive Contamination in the Columbia River and in the Air and Radiation Levels Measured in the Air at Hanford Works and Vicinity for 1945, 1946, 1947, and Early 1948*. HW-9871. Hanford Reading Room Number 1089. May 24.

Singlevich, W. 1948c. *Radioactive Contamination in the Environs of the Hanford Works and Vicinity for the Period January–February–March 1948*. HW-10242 del. Hanford Reading Room Number 1090. June 10.

Singlevich, W. 1948d. *Radioactive Contamination in the Environs of the Hanford Works for the Period April - May - June, 1948*. HW-11333. Hanford Reading Room Number 8575. October 15.

Singlevich, W. 1948e. *The Trend of Contamination in the Air, Columbia River, Rain, Sanitary Water, Vegetation, and Wastes, at the Hanford Works and Vicinity for the Period October, November, December, 1947*. HW-9496. Hanford Reading Room Number 8577.

Singlevich, W. 1949a. *H.I. "Environs" Report for Month of March, 1949*. HW-12948. Hanford Reading Room Number 5611. April.

Singlevich, W. 1949b. *Radioactive Contamination in the Environs of the Hanford Works and Vicinity for the Period July, August, September, 1948*. HW-12677 del. Hanford Reading Room Number 1094. March 10.

Singlevich, W. 1951. *Radioactive Particles in the Atmosphere January 1951–March 1951*. HW-20810. Hanford Reading Room Number 4370. April 12.

Singlevich, W. and H.J. Paas. 1949a. *Radioactive Contamination in the Environs of the Hanford Works for the Period January, February, March, 1949*. HW-14243 del. Hanford Reading Room Number 1096. December 23.

Singlevich, W. and H.J. Paas. 1949b. *Radioactive Contamination in the Environs of the Hanford Works for the Period October, November, December, 1948*. HW-13743 del. Hanford Reading Room Number 1095. June 22.

Smyth, H.D. 1945. *A General Account of the Development of Methods of Using Atomic Energy for Military Purposes Under the Auspices of the United States Government, 1940–1945*. U.S. Government Printing Office. August.

Soldat, J.K. 1966. *Evaluation of Environmental Radiation Exposures in the Vicinity of Hanford*. BNWL-SA-1606. Hanford Reading Room Number 4277. June 15.

Stainken, F.A.R. 1948. *Primary Report on the Chronology of the Separations Plant Stack Discharge Active Particle Contamination Problem at Hanford Works*. HW-11082. Hanford Reading Room Number 7432. September 15.

Stevenson, C.G. 1950. *Hanford Codes and Jargon*. HW-18223. Hanford Reading Room Number 9384. July 3.

Stewart, K. 1967. "The Resuspension of Particulate Material from Surfaces." *Surface Contamination*. Symposium proceedings, Gatlinburg, Tennessee, 1964. Pergamon Press, Oxford.

Stohr, J. 1995. *Hanford Atmospheric Particulate Releases Preliminary Review, 1944–1954. Technical Steering Panel of the Hanford Environmental Dose Reconstruction Project, Special Report*. Hanford Reading Room Number 17821. December.

Stone, W.A., J.M. Thorp, O.P. Gifford, and D.J. Hoitink. 1983. *Climatological Summary for the Hanford Area*. PNL-4622. Hanford Reading Room Number 1293. June.

Strenge, S.A. et al. 1993. *Interim Report on the Meteorological Database*. PNWD-2090 HEDR. Hanford Reading Room Number 12359.

Sturges, D.G. 1951. "High Offsite Particle Counts." Letter to R.W. Cook with data table. August.

Syers, J.K., M.L. Jacksoh, V.E. Berkheiser, R.N. Clayton, and R.W. Rex. 1969. "Eolian Sediment Influence on Pedogenesis during the Quaternary." *Soil Science* 107: 421–427.

Technical Steering Panel. 1994a. *Summary: Radiation Dose Estimates from Hanford Radioactive Material Releases to the Air and the Columbia River*. Hanford Reading Room Number 13629. April 21.

Technical Steering Panel. 1994b. *Technical Steering Panel Combined Annotated Bibliography, July 1988–May 1994*. Hanford Environmental Dose Reconstruction Project. Hanford Reading Room Number 10962. October.

Technical Steering Panel. 1995a. *Declassification: Plan, Procedure, Findings. Hanford Environmental Dose Reconstruction Project*. Hanford Reading Room Number 18145. December.

Technical Steering Panel. 1995b. *Recommendations for Completion and Closure of the Hanford Environmental Dose Reconstruction Project*. Hanford Environmental Dose Reconstruction Project. Hanford Reading Room Number 17817. December.

Technical Steering Panel. 1995c. *Releases from Miscellaneous Hanford Facilities. Hanford Environmental Dose Reconstruction Project*. Hanford Reading Room Number 17816. December.

Technical Steering Panel. 1995d. *Source Term Subcommittee, May 1988–September 1994.* Hanford Environmental Dose Reconstruction Project. Hanford Reading Room Number 17153. December.

Thiede, M.E., D.J. Bates, E.I. Mart, and R.W. Hanf. 1994. *A Guide to Environmental Monitoring Data, 1945–1972*. PNWD-2226 HEDR. Hanford Reading Room Number 13930. May.

Thomas, C.W. and D.M. Polinsky. 1956. *Tabulation of the Isotopic Counting Correction Factors and Decay Schemes*. HW-18258-APP. Hanford Reading Room Number 8025. November 16.

Thomas, C.W., J.A. Young, N.A. Wogman, and R.W. Perkins. 1968. *Measurement and Behavior of Airborne Radionuclides Since 1962*. BNWL-SA-1739. Hanford Reading Room Number 4278. April.

Thompson, R.C., M.H. Weeks, O.L. Hollis, J.E. Ballou, and W. D. Oakley. 1956. *Physiological Parameters for Assessing the Hazard of Exposure to Ruthenium Radioisotopes*. HW-41422. Hanford Reading Room Number 10782. March.

Thompson, R.C., O.L. Hollis, and W.D. Oakley. 1956. *Evaluation of Biological Hazards from Ruthenium Particulates. I. Studies of Percutaneous Absorption, Gastrointestinal Absorption, and Gastrointestinal Holdup*. HW-41519. Hanford Reading Room Number 5043. March.

Thorburn, R.C. 1947. *Detection of Plutonium in Desert Flora*. HW-7002 or HEW-7002 DE87 003659. Hanford Reading Room Number 4902. July.

Thorburn, R.C. 1948. *Radioactive Particle Investigation*. HW-10261. Hanford Reading Room Number 8241. June 11.

Thorburn, R.C. 1951. *A Report of Particle Contamination February 20, 1951 to August 15, 1951*. HW-22072. Hanford Reading Room Number 1111. August 31.

Tomlinson, R.E. and F.J. Leitz. 1954. *Ruthenium in the Purex Process*. HW-33479. Hanford Reading Room Number 8424. October.

Turner, L.D. 1947a. *The Trend of Contamination Observed in the Air, Columbia River, and Vegetation, at the Hanford Engineer Works for 1946*. HW-3-5402 (some pages labelled "3-5406"). Hanford Reading Room Number 1077. March 27.

Turner, L.D. 1947b. *The Trend of Contamination Observed in the Air, the Columbia River, Vegetation, and Waste at the Hanford Engineer Works for the Period January 1, 1947 to March 25, 1947*. HW-3-5511. Hanford Reading Room Number 1078. May 9.

Uebelacker, D.L.. 1960. *The Source of Activity Contained in Radioactive Fallout from the Redox 291-S Stack*. HW-67520. Hanford Reading Room Number 2475. December 9.

Uebelacker, D.L. 1961. *Filter Efficiencies and Activity Level of the Off-gas System for the Redox Multipurpose Dissolver*. HW-70844. Hanford Reading Room Number 8974. August 24.

U.S. Senate Committee on Governmental Affairs. 1989. *Early Health Problems of the U.S. Nuclear Weapons Industry and Their Implications for Today*. 101st Congress 1st Session S. Prt. 101-63, U.S. Government Printing Office, Washington, D.C. Hanford Reading Room Number 10728. December.

Van der Hoven, I. 1968. "Deposition of Particles and Gases." Section 5-3 in *Meteorology and Atomic Energy 1968*. Edited by D. Slade. Report TID-24190, U.S. Atomic Energy Commission, Office of Information Services. Available from National Technical Information Service (NTIS), Springfield, Virginia.

Walters, W.H., R.L. Dirkes, and B.A. Napier. 1992. *Literature and Data Review for the Surface-Water Pathway: Columbia River and Adjacent Coastal Areas*. PNWD-2034 HEDR. November.

Warren, J.H. 1961. *Control of I-131 Releases to Atmosphere*. HW-68392. Hanford Reading Room Number 7777. February 6.

Whicker, F.W., T.E. Hakonson, and J. Mohler. 1997. *Environmental Plutonium at Hanford: A Review of Literature and Monitoring Data*. Prepared for Kirkland and Ellis, Chicago, Illinois. May 31.

Whicker, F.W. and V. Schultz. 1982. *Radioecology: Nuclear Energy and the Environment, Volume I.* CRC Press. Boca Raton, Florida:

Wolman, A., P. Drinker, L. Gilbertson, G.R. Hill, H.F. Johnstone, E.P. Stevenson, and W.P. Yant. 1948. *A Progress Report on the Activities of the Stack Gas Problem Working Group*. HAN-19910. October 19.

Wooldridge, C.B. 1968. *Environmental Surveillance in the Vicinity of Hanford for January, 1968*. BNWL-778 1. Hanford Reading Room Number 2410. April 15.

Work, J.B. 1946. *Disposal of Separation Plant Off-Gases*. HW-7-5520-Del. Hanford Reading Room Number 7172. December 18.

Work, J.B. 1948. *Decontamination of Separation Plant Ventilation Air*. HW-11529. Hanford Reading Room Number 8238.

Wrixon, A.D., G.S. Linsley, K.C. Binns, and D.F. White. 1979. *Derived Limits for Surface Contamination*. NRPB-DL2. National Radiological Protection Board, Harwell, England. November.

Zahn, L.L. 1953. *Review of Exhaust Ventilation Air Filtration Requirements for Purex*. HW-30337. Hanford Reading Room Number 9078. December 23.

Zahn, L.L. 1954. *Facilities Required for Correction of Ammonium Nitrate Emission Problem at Redox*. HW-30935. Hanford Reading Room Number 8825. March 17.

Zuerner, L.V. 1947. *Particle Distribution 200-West*. HW-8429. Hanford Reading Room Number 6399. December 22.

Table A-2. List of HW Reports Sorted by HW- Number

CITATION	DATE	AUTHORS	TITLE	READING ROOM NUMBER
HW-10242 del	6/10/48	Singlevich, W.	Radioactive Contamination in the Environs of the Hanford Works and Vicinity for the Period January - February - March - 1948	1090
HW-10261	6/11/48	Thorburn, R.C.	Radio-active Particle Investigation	8241
HW-10758	8/17/48	Healy, J.W.	Long-lived Fission Activities in the Stack Gases and Vegetation at the Hanford Works	1091
HW-10941	9/7/48	Parker, H.M.	Further Comments on Report ARSC-8	8806
HW-11082	9/15/48	Stainken, F.A.R.	Primary Report on the Chronology of the Separations Plant Stack Discharge Active Particle Contamination Problem at Hanford Works	7432
HW-11333	10/15/48	Singlevich, W.	Radioactive Contamination in the Environs of the Hanford Works for the Period April - May - June, 1948	8575
HW-11348	10/25/48	Parker, H.M.	Action Taken with Respect to Apparent Enhanced Active Particle Hazard	8493
HW-11479	11/5/48	Patterson, C.M.	Contamination in the 200 Areas	4927
HW-11529	11/10/48	Work, J.B.	Decontamination of Separation Plant Ventilation Air	8238
HW-11534	11/3/48	Singlevich, W.	H.I. "Environs" Report for Month of October, 1948	4928
HW-12677 del	3/10/49	Singlevich, W.	Radioactive Contamination in the Environs of the Hanford Works and Vicinity for the Period July, August, September, 1948	1094
HW-12689	3/1/49	Kornberg, H.A. and J.F. Cline	Test Sputum Survey for Radioactive Particles in the 200 Areas	
HW-12948	4/1/49	Singlevich, W.	H.I. "Environs" Report for Month of March, 1949	5611
HW-13743 del	6/22/49	Singlevich, W. and H.J. Paas	Radioactive Contamination in the Environs of the Hanford Works for the Period October, November, December, 1948	1095
HW-14243 del	12/23/49	Singlevich, W. and H.J. Paas	Radioactive Contamination in the Environs of the Hanford Works for the Period January, February, March, 1949	1096
HW-15234	11/29/49	Healy, J.W.	Your Reference CWI	4943
HW-15802	1/27/50	DeLong, C.W.	Collection and Analysis of Active Particles	10669
HW-17003 DEL	3/2/50	Paas, H.J. and W. Singlevich	Radioactive Contamination in the Environs of the Hanford Works for the Period October, November, December, 1949	1098
HW-17381-DEL	5/1/50	Jenne, D.E. and J.W. Healy	Dissolving of Twenty Day Metal at Hanford ("Green Run Report")	7294
HW-17434 del	4/3/50	Paas, H.J. and W. Singlevich	Radioactive Contamination in the Environs of the Hanford Works for the Period April, May, June, 1949	1099
HW-18223	7/3/50	Stevenson, C.G.	Hanford Codes and Jargon	9384
HW-18258	7/1/50	Healy, J.W. and L.C. Schwendiman	Counter Calibrations in the Health Instrument Methods Group	7946
HW-18258-APP	11/16/56	Thomas, C.W. and D.M. Polinsky	Tabulation of the Isotopic Counting Correction Factors and Decay Schemes	8025

HW-18409	7/25/50	Parker, H.M.	Feasibility of Reduction of Cooling Time - Separations Process	1101
HW-18446	7/28/50	Paas, H.J. and W. Singlevich	Radioactive Contamination in the Environs of the Hanford Works for the Period January, February, March, 1950	1102
HW-18615	8/30/50	Paas, H.J. and W. Singlevich	Radioactive Contamination in the Environs of the Hanford Works for the Period July, August, September 1949	1103
HW-19454	11/24/50	Paas, H.J. and W. Singlevich	Radioactive Contamination in the Environs of the Hanford Works for the Period April, May, June, 1950	1105
HW-20136	7/15/51	Healy, J.W. et al.	H.I. Control Laboratory Routine Chemical Procedures	2471
HW-20502	2/26/51	Hilst, G.R.	The Determination of Probable Trajectories for Airborne Wastes Emitted in the Hanford Works Area	4972
HW-20700	4/6/51	Paas, H.J. and W. Singlevich	Radioactive Contamination in the Environs of the Hanford Works for the Period July, August, September, 1950	1106
HW-20810	4/12/51	Singlevich, W.	Radioactive Particles in the Atmosphere January 1951--March 1951	4370
HW-20888	4/20/51	Parker, H.M.	Components of Radiation Exposure of Military Personnel within the Hanford Reservation	9386
HW-21121	4/20/51	Gamertsfelder, C.C.	Measurement of Beta Radiation in Field Situations	7280
HW-21214	6/1/51	Paas, H.J. and W. Singlevich	Radioactive Contamination in the Environs of the Hanford Works for the Period January, February, March, 1951	1108
HW-21566	7/13/51	Paas, H.J.	Radioactive Contamination in the Environs of the Hanford Works for the Period October, November, December, 1950	1109
HW-22072	8/31/51	Thorburn, R.C.	A Report of Particle Contamination February 20, 1951 to August 15, 1951	1111
HW-22313	10/8/51	Anonymous	Radioactive Contamination in the Environs of the Hanford Works for the Period April, May, June, 1951	1112
HW-23133	12/29/51	Paas, H.J.	Radioactive Contamination in the Environs of the Hanford Works for the Period July, August, September, 1951	1113
HW-23517	2/15/52	Paas, H.J. and C.W. Thomas	Report of Particle Contamination--October-December 1951	4982
HW-24123	3/25/52	Lindberg, B.G.	Radiological Sciences Department Investigation Radiation Incident, Class I, No. 199	6964
HW-24203	4/22/52	Paas, H.J.	Radioactive Contamination in the Environs of the Hanford Works for the Period October, November, December, 1951	1114
HW-24727	6/20/52	Honstead, J.F.	Monitoring Survey -- Richland to Arco, Period May 9-11, 1952	4375
HW-24885	7/1/52	General Electric	Analysis of Radioactive Material Found in 200 Area	8423
HW-24932	7/3/52	Gill, W.E. et al.	291Stack Gas Particulates Interim Report	8503
HW-25097	6/20/52	Lindberg, B.G.	Radiological Sciences Department Investigation Radiation Incident, Class I, No. 206	6966
HW-25866	10/15/52	Paas, H.J.	Radioactive Contamination in the Environs of the Hanford Works for the Period January, February, March, 1952	1117

HW-26493	12/15/52	Paas, H.J.	Radioactive Contamination in the Environs of the Hanford Works for the Period April, May, June, 1952	1118
HW-27431	3/16/53	Ebright, D.P.	Radiological Sciences Department Investigation Radiation Incident, Class I, No. 225	6967
HW-27447	3/16/53	Ebright, D.P.	Radiological Sciences Department Investigation Radiation Incident, Class I, No. 246	6965
HW-27510	4/15/53	Paas, H.J.	Radioactive Contamination in the Environs of the Hanford Works for the Period July, August, September, 1952	1119
HW-27641	4/20/53	Paas, H.J.	Radioactive Contamination in the Environs of the Hanford Works for the Period October, November, December, 1952	1120
HW-28009	5/22/53	Paas, H.J.	Radioactive Contamination in the Hanford Environs for the Period January, February, March 1953	1121
HW-28300	6/22/53	Paas, H.J.	Radioactive Particles in the Hanford Environs November-December 1952	1122
HW-28780	7/22/53	Adley, F.E. et al.	Particulates Emitted by 291-S Stack	4990
HW-28925	8/4/53	Paas, H.J. et al.	Radioactive Particle Fallout in the Hanford Environs from Nevada Nuclear Explosions, Spring 1953	2533
HW-29230	8/25/53	Ebright, D.P.	Radiological Sciences Department Investigation, Radiation Incident, Class I, No. 299.	
HW-29346	9/5/53	Donelson, R.N.	Emission of Crystals from Redox Stack	8494
HW-29514	10/2/53	Paas, H.J.	Radioactive Contamination in the Hanford Environs for the Period April, May, June 1953	1123
HW-29698	12/19/50	Adley, F.E.	Natural Atmospheric Particulate Background at the Hanford Works	8810
HW-30174	12/5/53	Paas, H.J.	Radioactive Contamination in the Hanford Environs for the Period July, August, September 1953	1124
HW-30337	12/23/53	Zahn, L.L.	Review of Exhaust Ventilation Air Filtration Requirements for Purex	9078
HW-30492	1/4/54	Schwendiman, L.C.	Standard Practices Counting Manual	3498
HW-30744	1/29/54	Paas, H.J.	Radioactive Contamination in the Hanford Environs for the Period October, November, December 1953	1125
HW-30764	1/28/54	Lindberg, B.G.	Radiological Sciences Department Investigation Radiation Incident, Class I, No. 333	4993
HW-30809	2/8/54	Mobley, W.N.	Discussion of Ruthenium Problem in Redox Plant	10891
HW-30935	3/17/54	Zahn, L.L.	Facilities Required for Correction of Ammonium Nitrate Emission Problem at Redox	8825
HW-31417	4/9/54	Maider, J.E.	Redox Plant -- Ruthenium Contamination Control	10889
HW-31818	5/10/54	Paas, H.J.	Radioactive Contamination in the Hanford Environs for the Period January, February, March 1954	1126
HW-32056	6/7/54	Maider, J.E.	Redox Plant - Ruthenium Contamination Control	10907
HW-32164	6/17/54	Kiel, G.R.	Review of REDOX Plant Head-End Treatment. (Deleted version.)	
HW-32175	6/23/54	Gill, W.E. and D.E. Wisehart	A Study of Certain Properties of Ruthenium Compounds found in the REDOX Process	10905
HW-32209	11/10/54	Adley, F.E. et al.	Redox Stack Gas Particulates	4998

HW-32262	7/1/54	Schwendiman, L.C.	Evaluation of Routine REDOX Stack Sampling Procedures and Radiochemical Analysis	8964
HW-32292	7/1/54	Schwendiman, L.C.	An Application of Fluorescent Pigment to the Measurement of Particle Inhalation Probabilities	4999
HW-32319	1/7/54	Clukey, H.V.	Ventilation for Radiation Protection at Redox	9264
HW-32473	7/16/54	Ebright, D.P.	A History of the Redox Ruthenium Problem	1127
HW-32808	8/19/54	Parker, H.M.	Control of Ground Contamination	6401
HW-3-2894-del	12/31/45	Healy, J.W.	Special Studies Reports for Weeks Ending 5-20-45 through 12-30-45	7509
HW-33068	9/15/54	Parker, H.M.	Status of Ground Contamination Problem	1128
HW-33437	10/10/54	Parker, H.M.	Radiological Sciences Report, Research & Development Activities July - September, 1954	4414
HW-33479	10/14/54	Tomlinson, R.E. and F.J. Leitz	Ruthenium in the Purex Process	8424
HW-33754	11/10/54	Parker, H.M.	Fallout Comparisons	1129
HW-33830	11/22/54	Helgeson, G.L.	Redox Particle Study, Progress Report Sept. 1, 1954 to Oct. 28, 1954	8954
HW-33857	11/18/54	Baumgartner, W.V.	Radiation Monitoring Unit Investigations of the Radioactive Particles found in the 200-West Area	5002
HW-33896	11/24/54	Paas, H.J. and G.E. Pilcher	Radioactive Contamination in the Hanford Environs for the Period April, May, June 1954	1130
HW-34408	1/10/55	Parker, H.M.	Radiological Sciences Report, Research & Development Activities October - December, 1954	4006
HW-34882	1/21/55	Irish, E.R.	Technical Appraisal of Redox Ruthenium Problems and Their Resolution	8429
HW-35043	2/21/55	Gill, W.E.	Penetration of Respiratory Protective Equipment by Ruthenium at Building 202-S	5007
HW 3-5402 (some pages "3-5406")	3/27/47	Turner, L.D.	The Trend of Contamination Observed in the Air, Columbia River, and Vegetation, at the Hanford Engineer Works for 1946	1077
HW-35496	2/24/55	Harmon, M.K.	Addendum to HW-34882, "Technical Appraisal of Redox Ruthenium Problems and their Resolution"	10899
HW-3-5511	5/9/47	Turner, L.D.	The Trend of Contamination Observed in the Air, the Columbia River, Vegetation, and Waste at the Hanford Engineer Works for the Period January 1, 1947 to March 25, 1947	1078
HW-35542	3/1/55	Healy, J.W.	A Preliminary Estimate of Wind Pickup and Impaction of Particles	5009
HW-36112	4/6/55	Browne, W.G.	I-131 Emission Problem - Bismuth Phosphate Plant	1131
HW-36301	4/10/55	Parker, H.M.	Radiological Sciences Report, Research & Development Activities January - March, 1955	4416
HW-36504	4/20/55	Pilcher, G.E. et al.	Radioactive Contamination in the Hanford Environs for the Period July, August, September 1954	1132
HW-36505	4/29/55	Regional Radiation Measurements Unit	Radioactive Contamination in the Hanford Environs for the Period October, November, December 1954	1133
HW-36506	5/15/55	Regional Radiation Measurements Unit	Radioactive Contamination in the Hanford Environs for the Period January, February, and March 1955	1134
HW-36760	3/15/55	Dockum, N.L. and J.W. Healy	Spot Diameter Method of Quantitative Autoradiography of Ru106 Particles in Lung Tissue	5016

HW-38566	8/9/55	Regional Radiation Measurements Unit	Radioactive Contamination in the Hanford Environs for the Period April, May, June 1955	1135
HW-39073	8/3/55	Hill, O.F. et al.	Symposium on Iodine Problem	1136
HW-39429	10/10/55	Andersen, B.V. and J.K. Soldat	Radioactive Contamination in the Hanford Environs for the Period July, August, September 1955	1137
HW-40871	2/6/56	Andersen, B.V. and J.K. Soldat	Radioactive Contamination in the Hanford Environs for the Period October, November, December 1955	1138
HW-41422	3/1/56	Thompson, R.C. et al.	Physiological Parameters for Assessing the Hazard of Exposure to Ruthenium Radiioisotopes	10782
HW-41500	2/16/56	Kornberg, H.A.	Biology Research - Annual Report 1955	4428
HW-41519	3/1/56	Thompson, R.C. et al.	Evaluation of Biological Hazards from Ruthenium Particulates. I. Studies of Percutaneous Absorption, Gastrointestinal Absorption, and Gastrointestinal Holdup	5043
HW-41638	2/24/56	Bustad, L.K. and J.L. Terry	Basic Anatomical, Dietary, and Physiological Data for Radiological Calculations	1139
HW-43012	5/28/56	Andersen, B.V. and J.K. Soldat	Radioactive Contamination in the Hanford Environs for the Period January, February, March 1956	1140
HW-44215	8/7/56	Andersen, B.V. and J.K. Soldat	Radioactive Contamination in the Hanford Environs for the Period April, May, June 1956	1141
HW-46726	12/7/56	Andersen, B.V. et al.	Radioactive Contamination in the Hanford Environs for the Period July, August, September 1956	1144
HW-48374	2/25/57	Andersen, B.V. et al.	Radioactive Contamination in the Hanford Environs for the Period October, November, December 1956	1146
HW-49549 A	4/10/57	Schmidt, W.C.	Treatment of Gaseous Effluents	4447
HW-53449 deleted version	11/22/57	Operation Managers	Chemical Processing Department Monthly Report for October, 1957	11451
HW-53967 deleted version	12/23/57	Operation Managers	Chemical Processing Department Monthly Report for November, 1957	11453
HW-54319 deleted version	1/21/58	Operation Managers	Chemical Processing Department Monthly Report for December, 1957	11662
HW-54636	1/25/58	Selby, J.M. and J.K. Soldat	Summary of Environmental Contamination Incidents at Hanford 1952--1957	1157
HW-54821 deleted version	2/21/58	Operation Managers	Chemical Processing Department Monthly Report for January, 1958	11663
HW-55215 deleted version	3/21/58	Operation Managers	Chemical Processing Department Monthly Report for February, 1958	7182
HW-55569 RD	4/1/58	Roberts, R.E.	History of Airborne Contamination and Control -- 200 Areas	1162
HW-55571 deleted version	4/21/58	Operation Managers	Chemical Processing Department Monthly Report for March, 1958	11458
HW-57644	10/7/58	Andersen, B.V.	Regional Monitoring Activities September, 1958	7347
HW-58051 deleted version	11/21/58	Operation Managers	Chemical Processing Department Monthly Report for October, 1958	11358
HW-58305 deleted version	12/22/58	Operation Managers	Chemical Processing Department Monthly Report for November, 1958	11361
HW-59849 deleted version	4/20/59	Operation Managers	Chemical Processing Department Monthly Report for March, 1959	11778

HW-60915 deleted version	7/22/59	Operation Managers	Chemical Processing Department Monthly Report for June, 1959	11773
HW-61082	7/13/59	Postma, A.K. and L.C. Schwendiman	Radioactive Particles in the 234-5 Building Ventilation Exhaust	13453
HW-61366 deleted version	8/21/59	Operation Managers	Chemical Processing Department Monthly Report for July, 1959	11667
HW-62179 deleted version	10/21/59	Operation Managers	Chemical Processing Department Monthly Report for September, 1959	11658
HW-62593 deleted version	11/20/59	Operation Managers	Chemical Processing Department Monthly Report for October, 1959	11765
HW-62864 deleted version	12/21/59	Operation Managers	Chemical Processing Department Monthly Report for November, 1959	11469
HW-63706 deleted version	2/22/60	Operation Managers	Chemical Processing Department Monthly Report for January, 1960	11761
HW-64371	5/9/60	Junkins, R.L. et al.	Evaluation of Radiological Conditions in the Vicinity of Hanford for 1959	108
HW-66646 deleted version	9/21/60	Operation Managers	Chemical Processing Department Monthly Report for August, 1960	11650
HW-66958	10/21/60	Operation Managers	Chemical Processing Department Monthly Report for September, 1960	11770
HW-67252 deleted version	11/21/60	Operation Managers	Chemical Processing Department Monthly Report for October, 1960	12076
HW-67459	12/21/60	Operation Managers	Chemical Processing Department Monthly Report for November, 1960	12078
HW-67520	12/9/60	Uebelacker, D.L.	The Source of Activity Contained in Radioactive Fallout from the Redox 291-S Stack	2475
HW-68392	2/6/61	Warren, J.H.	Control of I-131 Releases to Atmosphere	7777
HW-68435	6/1/61	Foster, R.F. and I.C. Nelson	Evaluation of Radiological Conditions in the Vicinity of Hanford for 1960	109
HW-69205-REV	8/27/62	McConnon, D.	The Status of Gaseous Effluent Monitoring at HAPO December 1961	3955
HW-7002 or HEW-7002 DE87 003659	7/1/47	Thorburn, R.C.	Detection of Plutonium in Desert Flora	4902
HW-70844	8/24/61	Uebelacker, D.L.	Filter Efficiencies and Activity Level of the Off-gas System for the Redox Multipurpose Dissolver	8974
HW-7-1115	1/8/45	Parker, H.M. and C.C. Gamertsfelder	Weekly H.I. Reports on 200 Area and Environs for 1-5-45 thru 2-13-46 (#1 thru 58)	7509
HW-7-1228	1/27/45	Parker, H.M.	Monthly Reports -- H.I. Section -- for 1945	7513
HW-7-2271	7/25/45	Botsford, C.W.	Study of Calibration of Victoreen Integrons	7488
HW-7-2604	10/22/45	Cantril, S.T. and J.W. Healy	Iodine Metabolism with Reference to I131	4898
HW-7317	8/12/47	Healy, J.W.	The Trend of Contamination Observed in the Air, the Columbia River, Vegetation, and Waste at the HEW for the Period 3/25/47 to 6/30/47	1083
HW-7-3194	1/11/46	Gamertsfelder, C.C.	H.I. Report on the 200 Areas and Environs for the Week Ending January 9, 1945	7161
HW-7-3217	1/14/46	Parker, H.M.	Tolerable Concentration of Radio-Iodine on Edible Plants	1080
HW-7405	8/28/47	Patterson, C.M.	H.I. Report on the 200 Areas and Associated Laboratories for the Week Ending August 27, 1947	11242
HW-7-4275	6/18/46	Apple, R.S.	Activities Discharged Into the Atmosphere	8579

HW-7-4279	5/1/46	Patterson, C.M.	Manual of Standard Procedures, Site Survey (Special Studies)	
HW-7-5042	9/18/46	Healy, J.W. and C.C. Gamertsfelder	H.I. Environs Reports -- Sept. 1946 thru May 1947	5608
HW-7-5145	10/3/46	Parker, H.M.	H.I. Section Report for September 1946	8729
HW-7-5301	11/4/46	Parker, H.M.	H.I. Section Report for October 1946	8730
HW-7-5372	11/19/46	Parker, H.M.	Some Considerations on the Habitability of the Hanford Camp Site	7750
HW-7539	9/10/47	Patterson, C.M.	#140 - H.I. Report on the 200 Areas and Associated Laboratories for the Week Ending September 10, 1947	4903
HW 7-5463 del	12/5/46	Seymour, F.P.	A Study of Total Amounts of Active Waste Released in All Manners by the H.E.W. Process to Date	1082
HW-7-5520-Del	12/18/46	Work, J.B.	Disposal of Separation Plant Off-Gases	7172
HW-7-5605	1/3/47	Parker, H.M.	H.I. Section Report for December 1946	8731
HW-7-5934	3/11/47	Gamertsfelder, C.C.	Effects on Surrounding Areas Caused by the Operations of the H.E.W	7104
HW-7695	10/2/47	Patterson C.M.	#143 - H.I. Report on the 200 Areas and Associated Laboratories for the Week Ending October 1, 1947	4904
HW-7865	10/22/47	Mickelson, M.L.	Preliminary Report on Existing Active Paricle Hazard -- 200 Areas	3944
HW-7920	10/30/47	Parker, H.M.	Action Taken on the Spot Contamination in the Separations Plant Areas	4356
HW-7932	11/3/47	MacCready, W.K.	Installation of Air Filters -- 200 Areas	4906
HW-8108	11/26/47	Bell, R.S.	Active Particle Investigation -- 200 Areas: Establishment of Physical Control	8108
HW-81746	1/1/64	Perkins, R.W.	Physical and Chemical Forms of I-131 from Fallout and Chemical Processing Plants	4638
HW-8429	12/22/47	Zuerner, L.V.	Particle Distribution 200-West	6399
HW-8430	11/28/47	Roos, L.D.	Particle Distribution 200-East	4910
HW-84619	4/12/65	Backman, G.E.	Summary of Environmental Contamination Incidents at Hanford, 1958-1964	1205
HW-8549	12/28/47	Singlevich, W.	The Trend of Contamination in the Air, Columbia River, Rain, Sanitary Water, Vegetation, and Wastes, at the Hanford Works and Vicinity for the Period July, August, September, 1947	8578
HW-8624	1/20/48	Parker, H.M.	Progress Report on "Action Taken on the Spot Contamination in the Separations Plant Areas"	4912
HW-8667	1/27/48	Greager, O.H. and W. Cready	Stack Gas Decontamination -- Separations Plants	4913
HW-89066	3/1/58	Andersen, B.V.	Regional Monitoring - Data Summary (1957)	1163
HW-89072	10/1/89	Cleavenger, P.M. and S.P. Gydesen	Stack Gas Disposal Extracts: March 1947-January 1952	8820
HW-9091	3/5/48	Overbeck, W.P.	Location of Redox Test Unit	4916
HW-9141	3/10/48	Parker, H.M.	Spot Contamination on Potential Building Sites	4918
HW-9175	3/12/48	Gross, C.N.	Stack Gas Decontamination, Separation Plants: Development of Decontamination Systems	6400
HW-9259	3/22/48	Parker, H.M.	Review of the Stack Discharge Active Particle Contamination Problem	1086
HW-9372	4/1/48	Parker, H.M.	Meteorological Consultation March 19, 1948	11312
HW-9476	4/1/48	Church, P.E.	Meteorological Information	11313

HW-9496	3/20/48	Singlevich, W.	The Trend of Contamination in the Air, Columbia River, Rain, Sanitary Water, Vegetation, and Wastes, at the Hanford Works and Vicinity for the Period October, November, December, 1947	8577
HW-9864	5/21/48	Adley, F.E.	Report of a Study of the Fate of 200 Area Stack Gases	1088
HW-9871	5/24/48	Singlevich, W.	Radioactive Contamination in the Columbia River and in the Air and Radiation Levels Measured in the Air at Hanford Works and Vicinity for 1945, 1946, 1947, and Early 1948	1089
HWN-1991	7/26/57	Roberts, R.E.	CPD - Waste Storage and Experience	9899
HW-SA-3176	10/1/63	Fuquay, J.J. and C.L. Simpson	Use of Meteorological Measurements for Predicting Dispersion from Releases Near Ground-Level	4696
HW-SA-3742	10/15/64	Perkins, R.W. et al.	Air-borne Radionuclide Measurements and Physical Characteristics Determination	7761

APPENDIX B

ENVIRONMENTAL MONITORING DATA AND LOCATIONS

B-1. General Discussion of Environmental Data Compilations

The environmental data analysis performed for this work was exploratory in nature. We wanted to see what, if any, use the data might have to help understand past airborne releases of radioactive materials from Hanford facilities, particularly for locations near the release points where military, construction, and other onsite workers were exposed. It was a useful qualitative exercise. See Section 4.3, "Conclusions from Environmental Data: Affected Areas and Times." It was not unexpected that the data specificity and sensitivity were not adequate for validation of dispersion of estimated releases. The historic data are crude by modern standards and are more useful for illustrating trends over space and time than for accurate or precise measurement at any one place and time. The scope of work emphasized radionuclides other than ^{131}I, consequently those environmental data were not examined.

The monitoring locations and times selected for compilation were based on the data available and our judgment about which would be productive. Not all locations were included in our data compilations. For each type of monitoring, we chose a small group of locations (typically less than 8) that produced a broad coverage of the Hanford site, represented a low-exposure location, were near worker exposure locations, or were in high impact locations (based on the magnitude of concentrations measured). Preference was given to locations with a long record of monitoring. However, many locations chosen did not have a complete data record over the entire time period.

The electronic worksheets of environmental data are provided to the Centers for Disease Control staff for their use and discretionary distribution. Although every effort was made to assure accuracy, there is a possibility of data transcription errors, due to source report illegibility or human error. The original documents are the definitive sources.

B-2. Description of Content of Data Spreadsheets

The name and content of each separate EXCEL workbook of environmental data are listed below with the individual worksheets, in the order they appear in the workbook. The overall order of the workbooks listed below is the order of presentation in Section 4 of this report.

WORKBOOK: exposure.xls

- Worksheet "C Chamber data" contains measurements of exposure rates using C Chambers at locations 16 (200-East) and 12 (100-B) for September 1945 through December 1948 and the difference between the two locations.
- Worksheet "Figure 4-2" is self-explanatory.
- Worksheet "M&S and C data" contains exposure rate measurements using a C Chamber at 200-E and an M&S Chamber at Route 4S, Mile 6 between July 1945 and April 1948.
- Worksheet "Chart M&S and C" contains a plot of data in the previous worksheet.

- Worksheet "ratio M&S to C" contains a chart of the ratio of data in the previous chart. The conclusion from this and the previous two worksheets is presented in the text immediately preceding Figure 4-3.
- Worksheet "M&S Chambers data" contains measurements of exposure rates at 13 onsite locations using M & S Chambers between July 1945 and December 1955. Data for 8 of the locations begin in 1950.
- Worksheet "Figure 4-3" is self-explanatory.
- Worksheet "Figure 4-4" is self-explanatory.
- Worksheet "Figure 4-5" is self-explanatory.
- Worksheet "Figure 4-6" is self-explanatory.
- Worksheet "exposure statistics" includes the raw data and computations for Table 4-1. Note that the data are a subset of that in worksheet "M&S Chambers data."
- Worksheet "Figure 4-7" is self-explanatory.
- Worksheet "data for Fig 4-7" contains the data to produce the previous worksheet's chart. It computes annual average exposure rates at the meteorology (622) monitoring location between the 200 Areas for 1945 through 1955 and subtracts a background exposure rate estimate to obtain net exposure rates. Annual average exposure rates for REDOX perimeter for 1953 through 1955 are entered directly from other calculations, as are the mean release quantities for ^{131}I and ^{106}Ru from all plants for 1945 through 1955.

WORKBOOK: air.xls

- Worksheet "airbeta" contains beta activity on air filters from seven locations: 200-E Tower 18/16/15, 200 ESE, Hanford, Pasco, 200W Redox, 200 W Gate, and PSN 320 between January 1946 through 1955. Original units are converted to pCi m^{-3} in the worksheet. The worksheet also computes annual averages (absolute [Table 4-2] and relative to Pasco [Table 4-3]).
- Worksheet "monthly46-48" is Figure 4-8.
- Worksheet "monthly46-55" is Figure 4-10.
- Worksheet "beta ann ave" is Figure 4-11.
- Worksheet "air alpha" contains alpha activity on air filters at five onsite areas (200 W REDOX area, 200 W Gate or Tower 4, Met tower ground level, PSN 320, and 300 area) between June 1951 and December 1955.
- Worksheet "alpha chart" is Figure 4-13.

WORKBOOK: air bkg.xls

- Worksheet "Background" contains monthly beta activity on particulate air filters between October 1953 and December 1955 at Pasco, and the Western and Mountain Regions of the National Air Sampling Network.
- Worksheet "Bkg Chart" is Figure 4-12.

WORKBOOK: rain.xls

- Worksheet "maxima chart" is Figure 4-14.
- Worksheet "maxima data" is the source for Figure 4-14. It contains maximum concentrations of beta activity in rain at six onsite locations and "outlying areas" between September 1946 and May 1947.

- Worksheet "average chart" is Figure 4-16.
- Worksheet "data average" contains the concentrations of beta activity in rain from 10 onsite and offsite locations between November 1946 and December 1955. The data provide the basis for Figure 4-16. Annual averages are computed at cell W6.
- Worksheet "annual averages" sorts data in the previous worksheet for Table 4-4.
- Worksheet "annual average chart" is Figure 4-17.

WORKBOOK: veg.xls

- Worksheet "1945–1948 chart" is Figure 4-19.
- Worksheet "total beta 1940s" contains results of beta activity in vegetation (including iodine) at 11 locations on and offsite for the three-year period November 1945–November 1948.
- Worksheet "ave40chart" is Figure 4-20.
- Worksheet "averages 40s" contains data for Figure 4-20.
- Worksheet "nonvolatile beta" contains nonvolatile beta activity concentrations in vegetation from nine locations from February 1949 through December 1955.
- Worksheet "NVB chart" is Figure 4-25.
- Worksheet "longterm chart 48-55" is Figure 4-26.
- Worksheet "longterm data 48-55" contains data for Figure 4-26.
- Worksheet "alpha" contains average alpha activity concentrations in vegetation from five locations in original units of 10^{-8} μCi g^{-1} (and converted to pCi g^{-1}) for a 3-year period, December 1951 through 1955.
- Worksheet "alpha chart" is Figure 4-27.

WORKBOOK: particle.xls

- Worksheet "particles per volume" includes particle concentrations in air from five locations for June 1949 through December 1955 and the summary statistics presented in Table 4-6.
- Worksheet "49-55 chart" is Figure 4-28.
- Worksheet "met tower" contains particle concentrations in air from nine heights between 5 and 400 feet on the meteorology tower from May 1949 through December 1955. These data were not used or presented in this report.
- Worksheet "vertical chart" is a plot of the data in worksheet "met tower."
- Worksheet "particle numbers" contains the number of active particles on air filters at four locations between September 1948 and June 1949. These data were not used in this report.

WORKBOOK: groundsurveys.xls

- Worksheet "H-40" contains the data presented in Table 4-7.
- Worksheet "conversions" contains formulas to convert data presented in units of 'ground area per particle' to units of 'particles per ground area' and vice versa.
- Worksheet "relative chart" is Figure 4-40.
- Worksheet "relative Index" contains data for Figure 4-40.

B-3. Maps

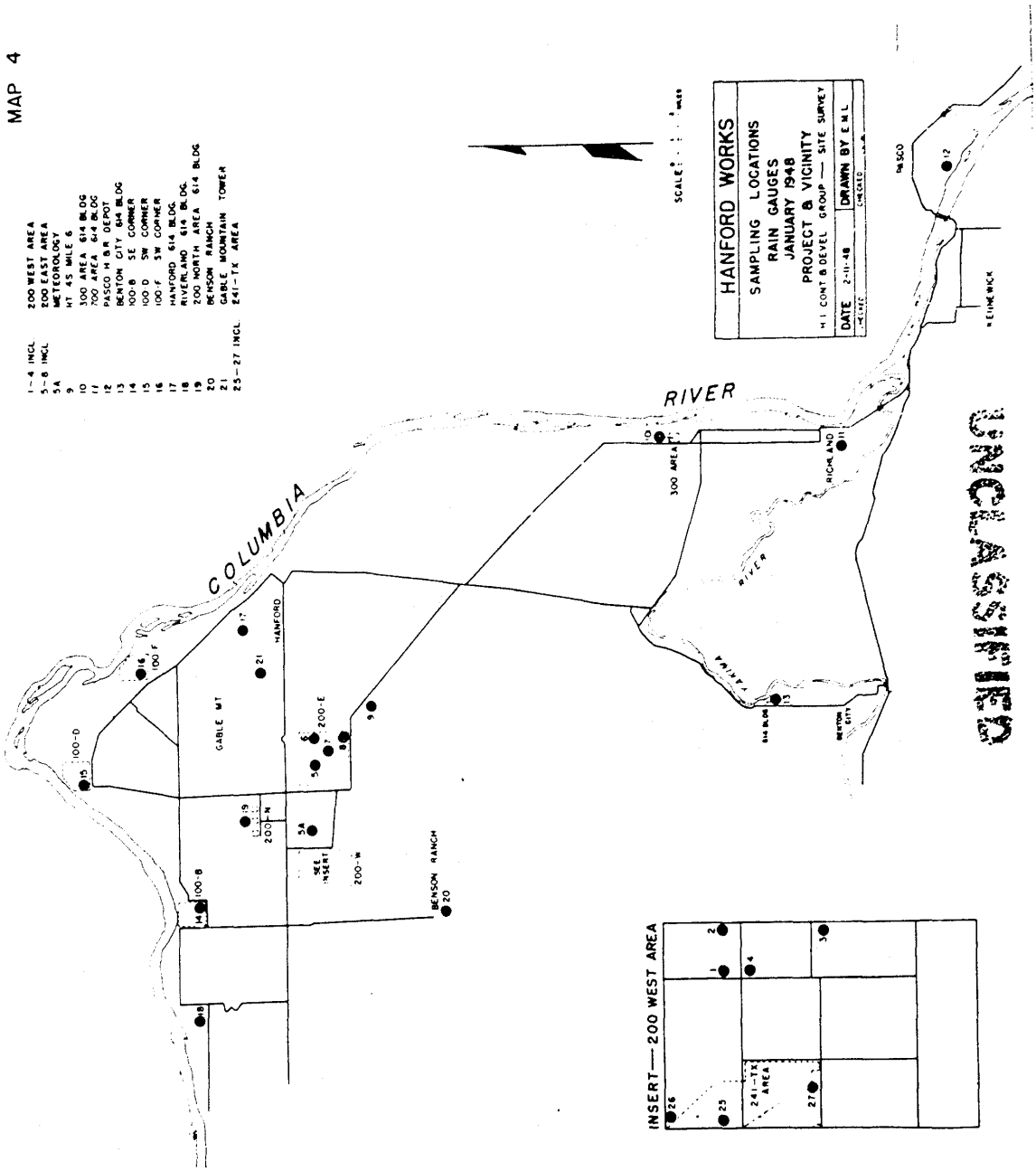

Figure B-1. Locations of rain gauges in January 1948. These samples were analyzed for beta activity. Map from HW-9496.

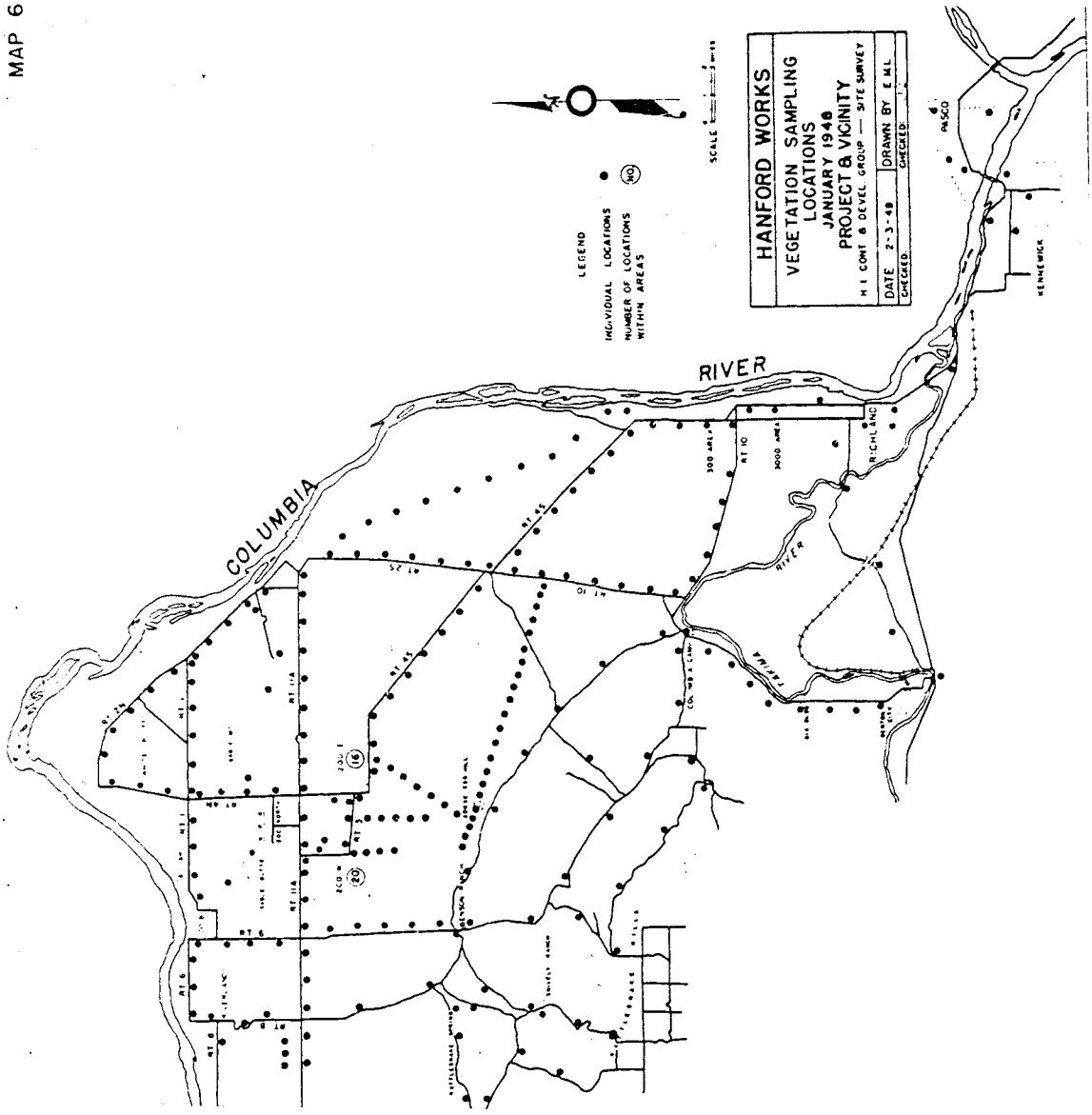

Figure B-2. Locations of vegetation sampling in January 1948. These samples were analyzed for total beta activity. Map from HW-9496. Note location of Columbia Camp along the northern bend of the Yakima River.

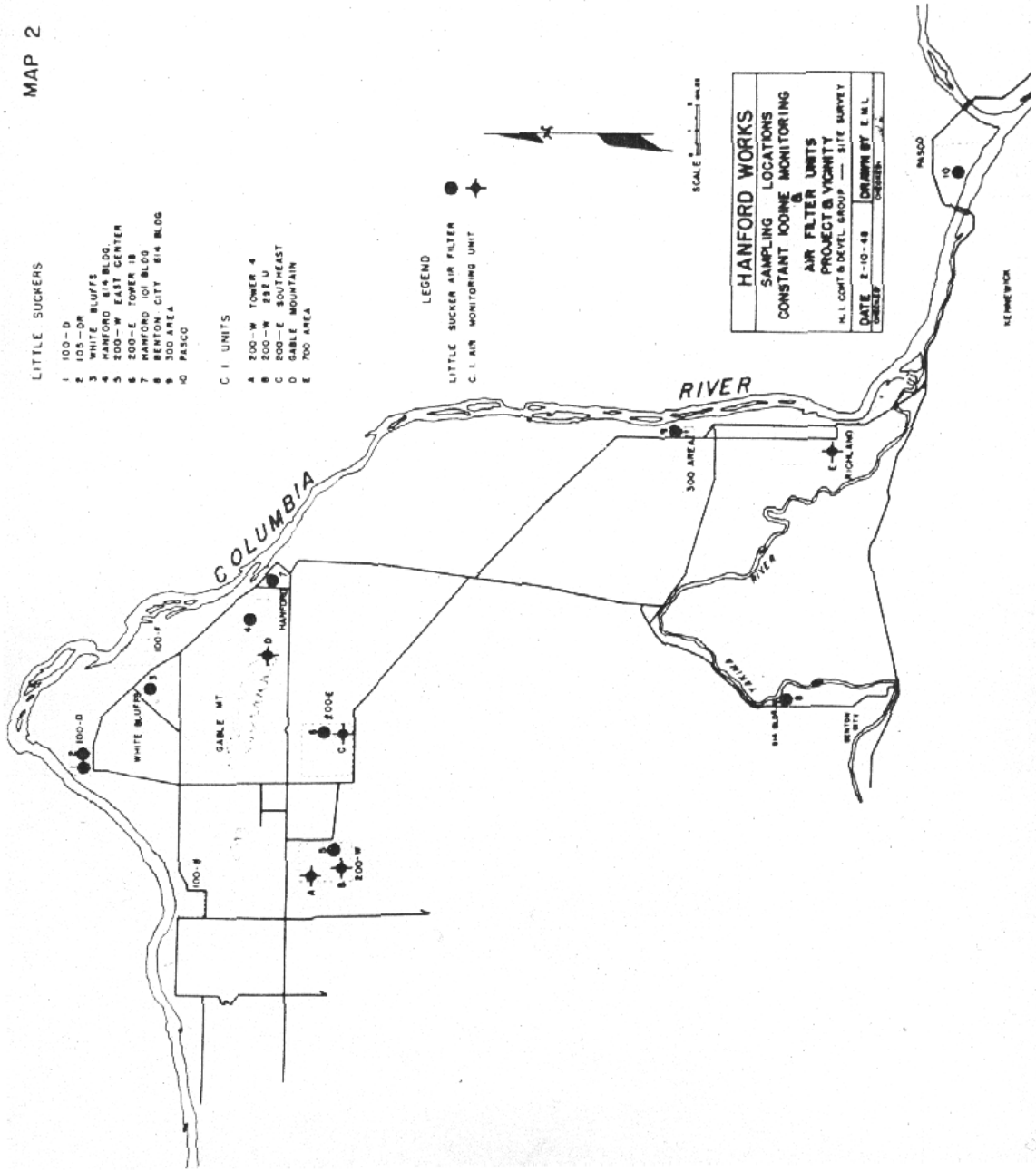

Figure B-3. Locations of air sampling in January 1948. Map from HW-9496.

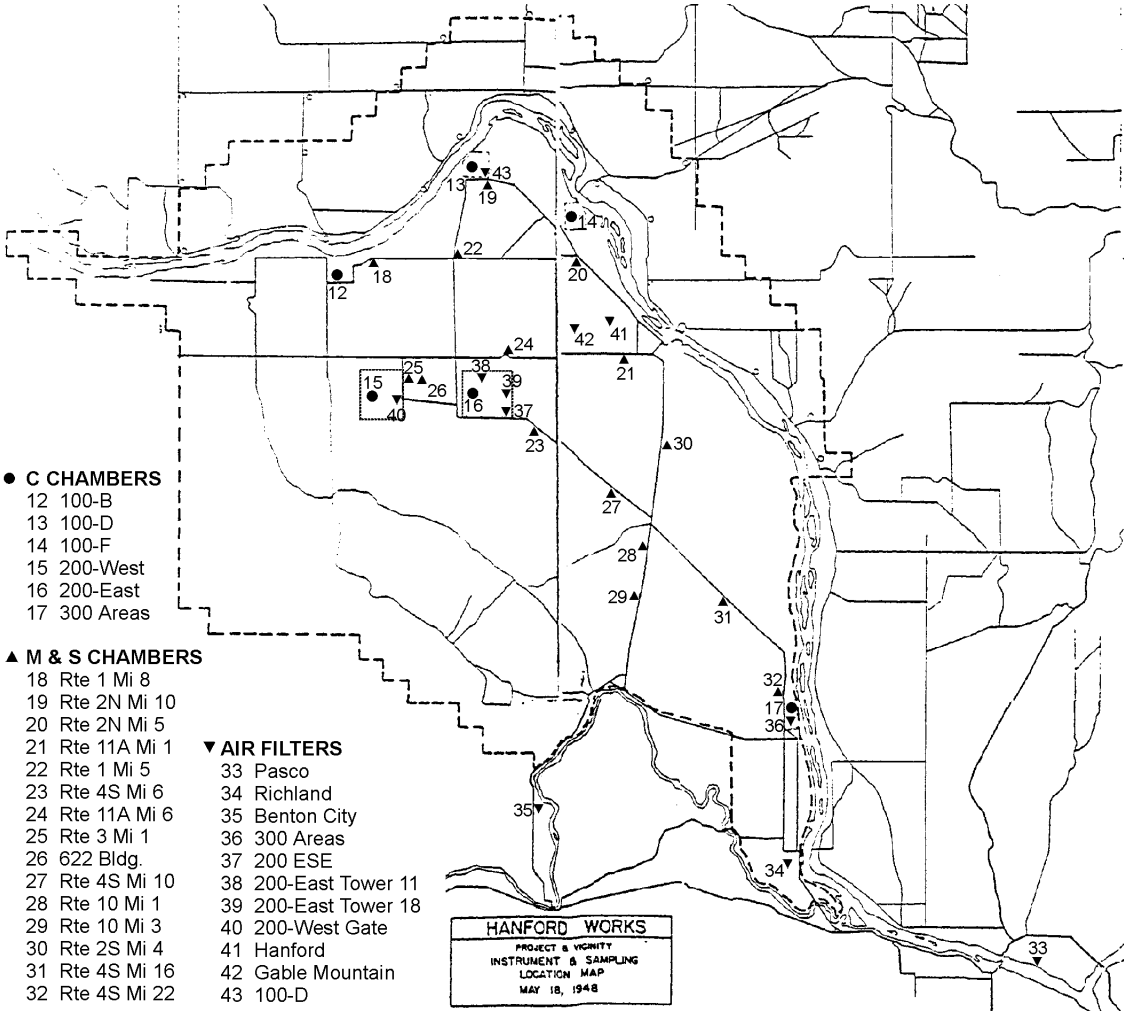

Figure B-4. Locations for environmental monitoring of airborne radioactivity on the Hanford Works in May 1948. Legibility of the source map (HW-9871) was poor, so the legend and location symbols and numbers were redrawn. Also, river monitoring stations were removed from the original figure.

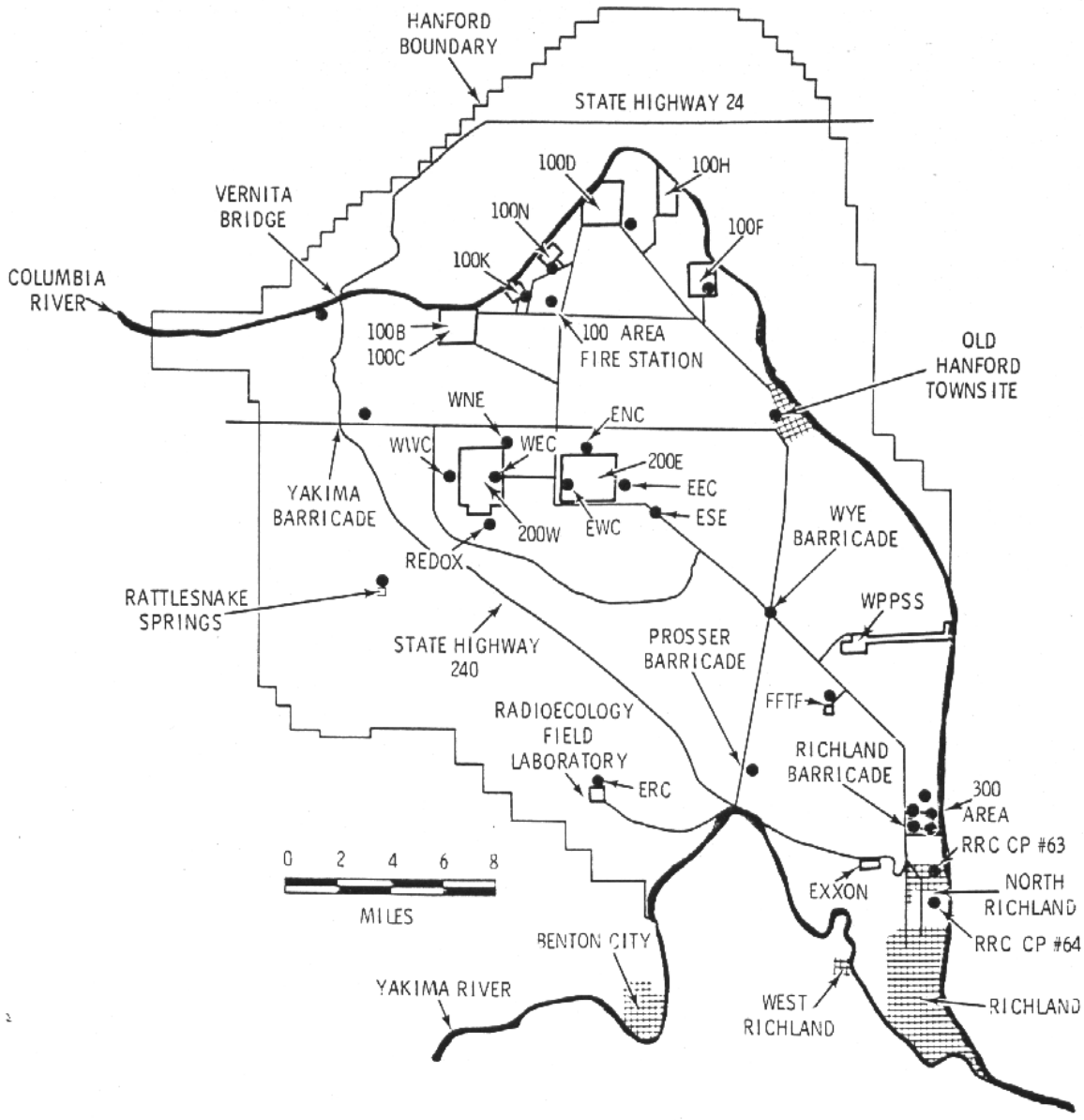

Figure B-5. Onsite and North Richland air monitoring locations in 1976 (Fix et al. 1977).

APPENDIX C

MAPS OF SPATIAL EXTENT OF PARTICLE CONTAMINATION ON GROUND AND VEGETATION

C-1. INTRODUCTION

This appendix contains a number of maps that illustrate the spatial extent of radioactive particle contamination on ground and vegetation of the Hanford Works in the 1940s and 1950s. Some key maps are also reproduced in the main text. The order is chronological within two parts, close-in surveys and site-wide (or larger) surveys. Brief notations are given in the figure captions; however, most discussion is provided in the main text. Because the scope of this task order does not emphasize radioiodine (^{131}I), similar maps for that nuclide are not reproduced here, although many are available.

C-2. CLOSE-IN SURVEYS

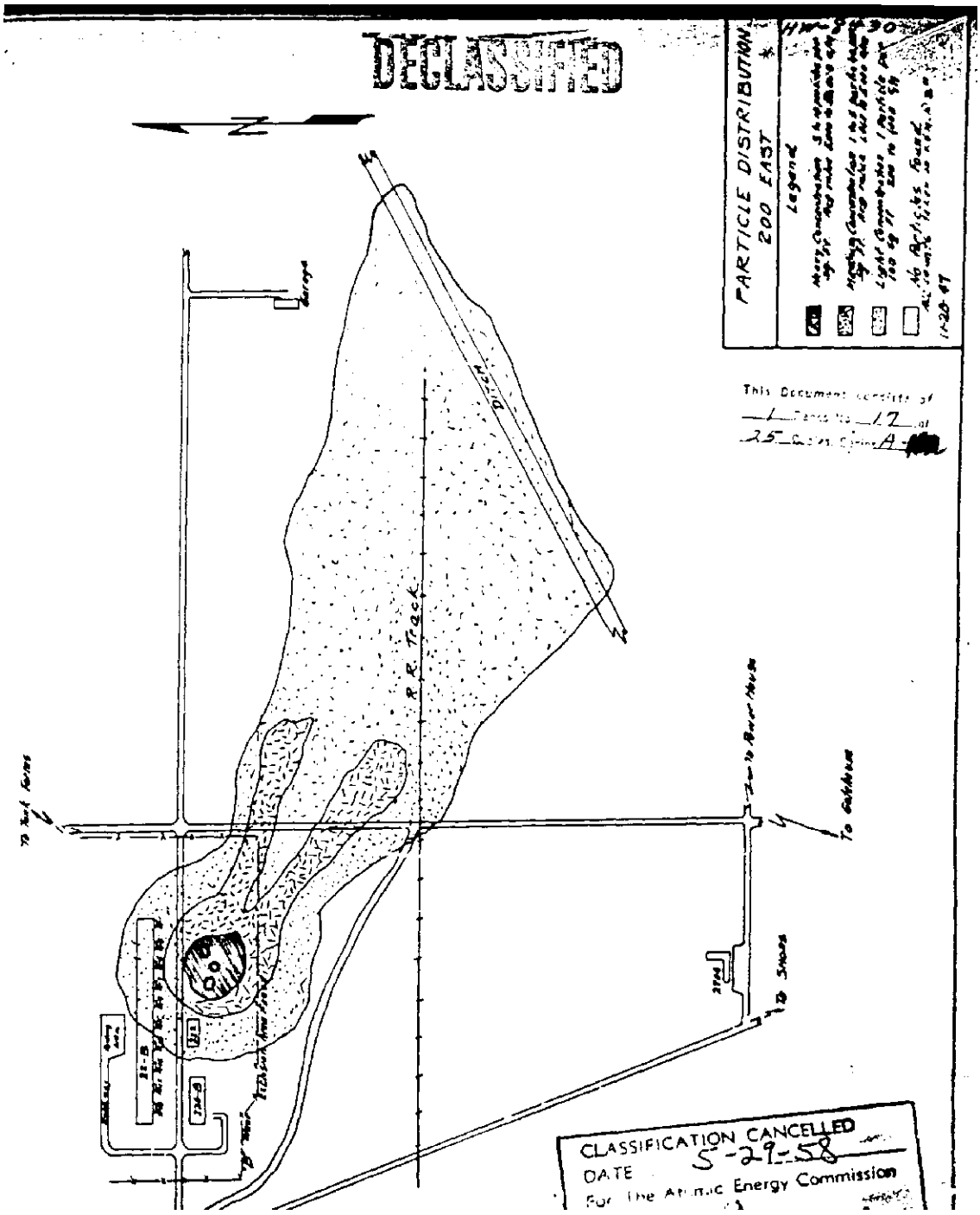

Figure C-1. Distribution of particles in 200-East, November 28, 1947 (HW-8430). The "heavy concentration" zone around the B Plant stack is 5–10 particles per ft^2 (5000–10,000 cpm). The "medium concentration" zone is 1–5 particles per ft^2 (1000–5000 cpm). The "light concentration" zone is 1 particle per 100 ft^2 or 0.01 particles per ft^2 (200–1000 cpm). The survey results extend about 900 m SE of the B Plant stack, still within the boundaries of 200-East.

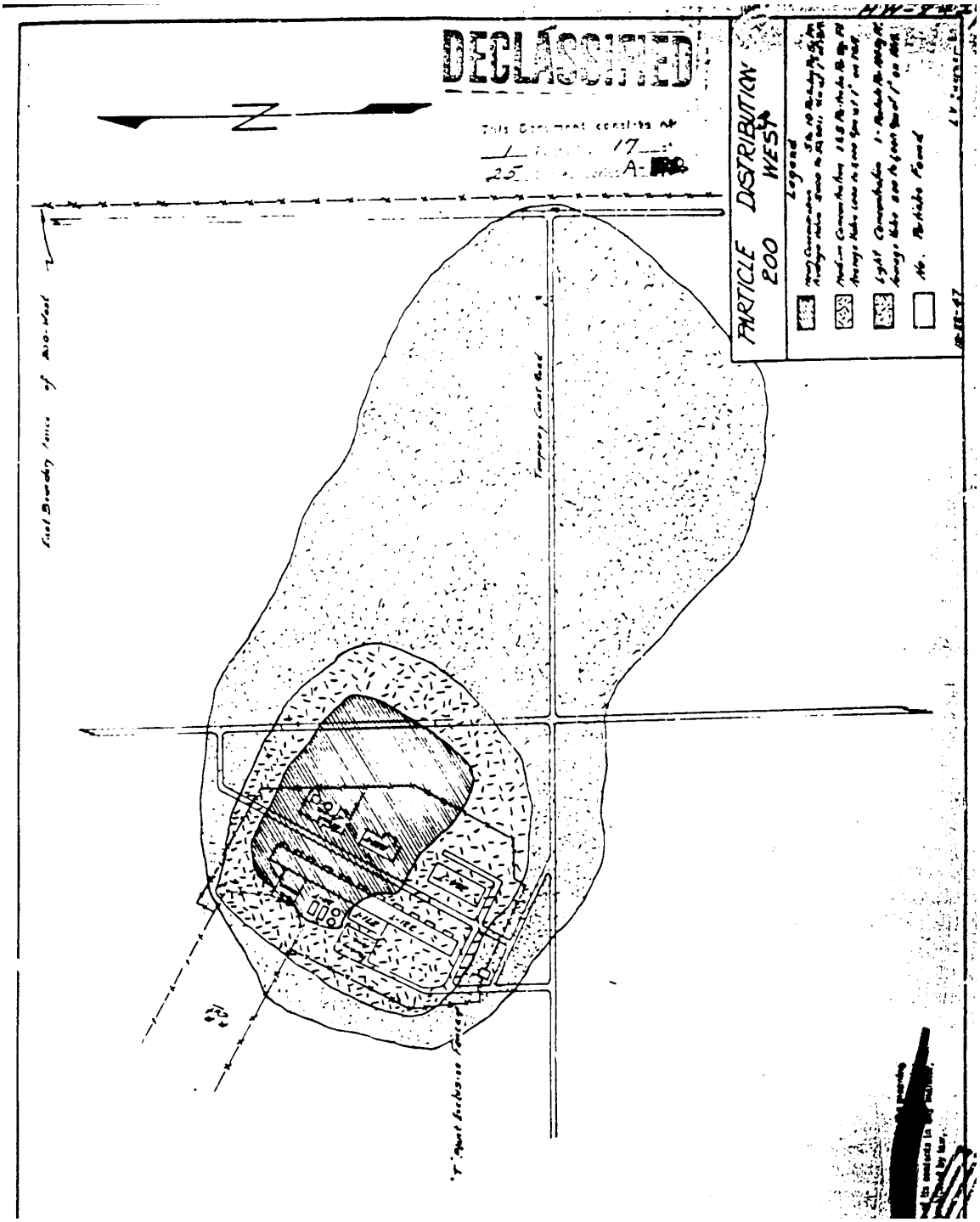

Figure C-2. Distribution of particles in 200-West, December 22, 1947 (HW-8429). The "heavy concentration" zone around the T Plant stack is 5–10 particles per ft^2 (5000–10,000 cpm). The "medium concentration" zone is 1–5 particles per ft^2 (1000–5000 cpm). The "light concentration" zone is 1 particle per 100 ft^2 or 0.01 particles per ft^2 (200–1000 cpm). The survey results extend about 800 m to the east boundary fence of 200-West.

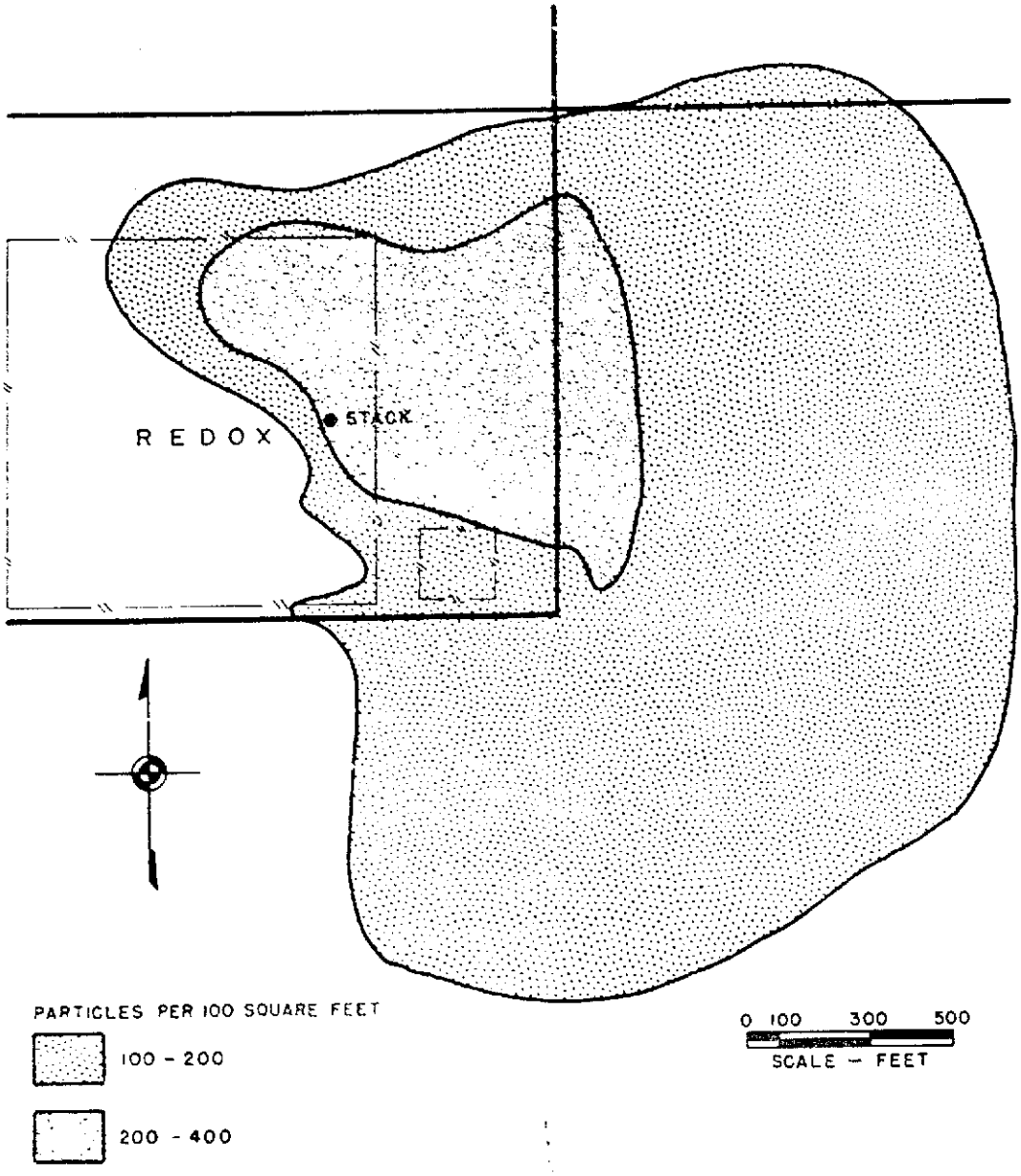

FIGURE – 11
GROUND CONTAMINATION PATTERN
200 WEST
MARCH 30 – MAY 3, 1952

Figure C-3. Ground contamination pattern in 200-West, March 30–May 3, 1952. Figure 11 from Selby and Soldat (1956), HW-54636.

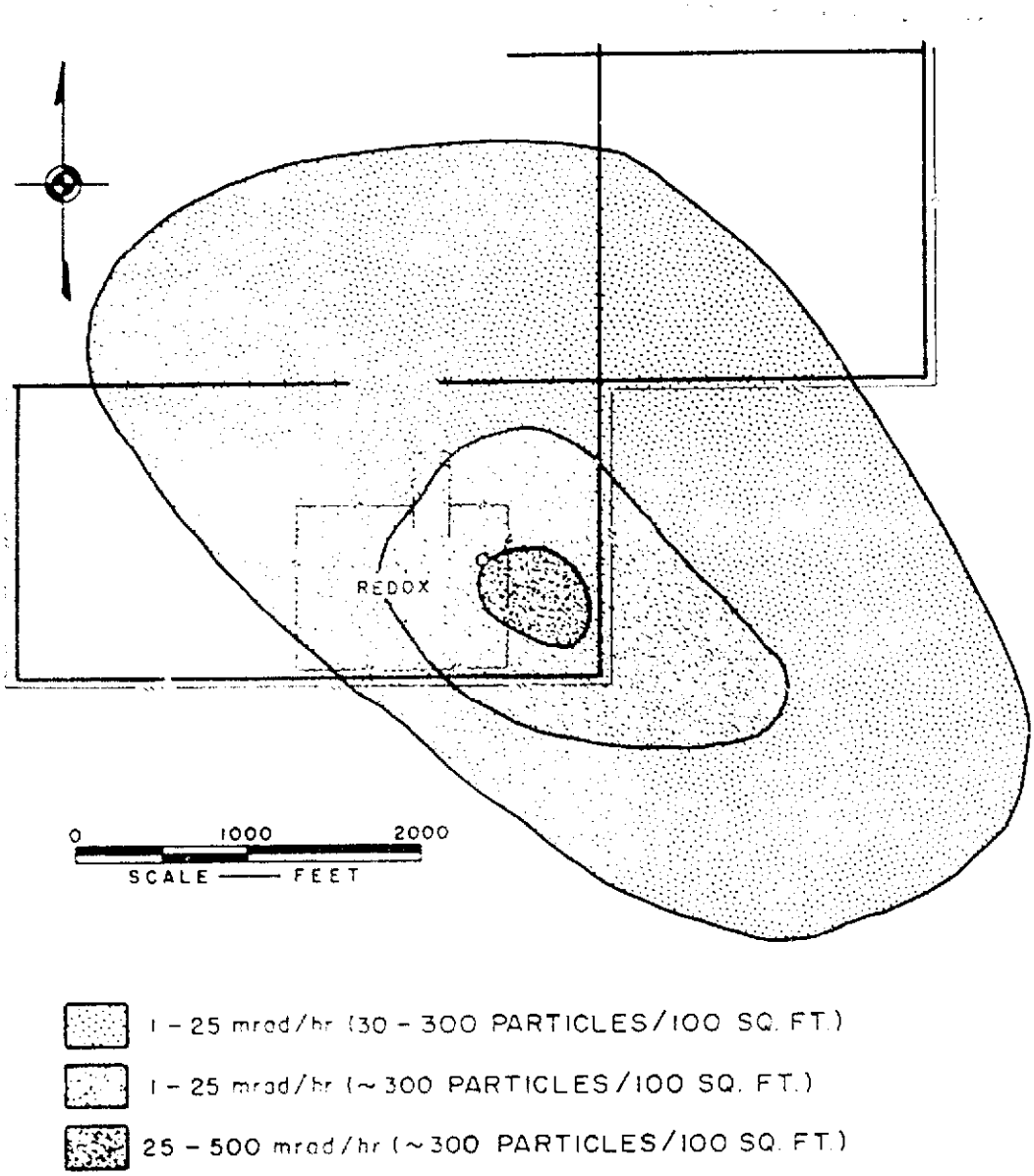

Figure C-4. Ground contamination pattern in 200-West, June 1952. Figure 12 from Selby and Soldat (1956), HW-54636.

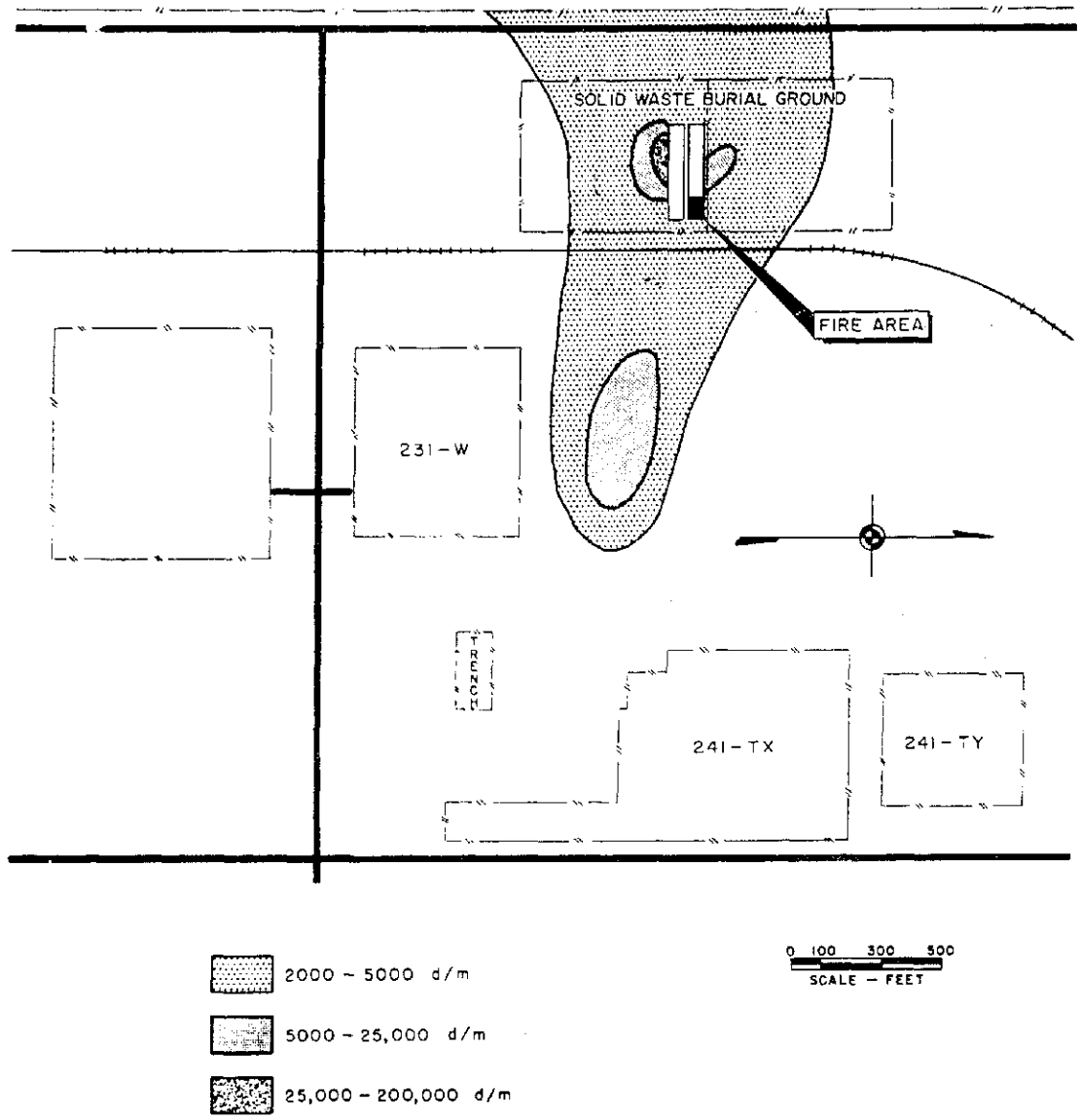

FIGURE - 39
GROUND CONTAMINATION PATTERN
200 WEST
JULY 9, 1952

Figure C-5. Ground contamination pattern in 200-West, July 9, 1952. Figure 39 from Selby and Soldat (1956), HW-54636.

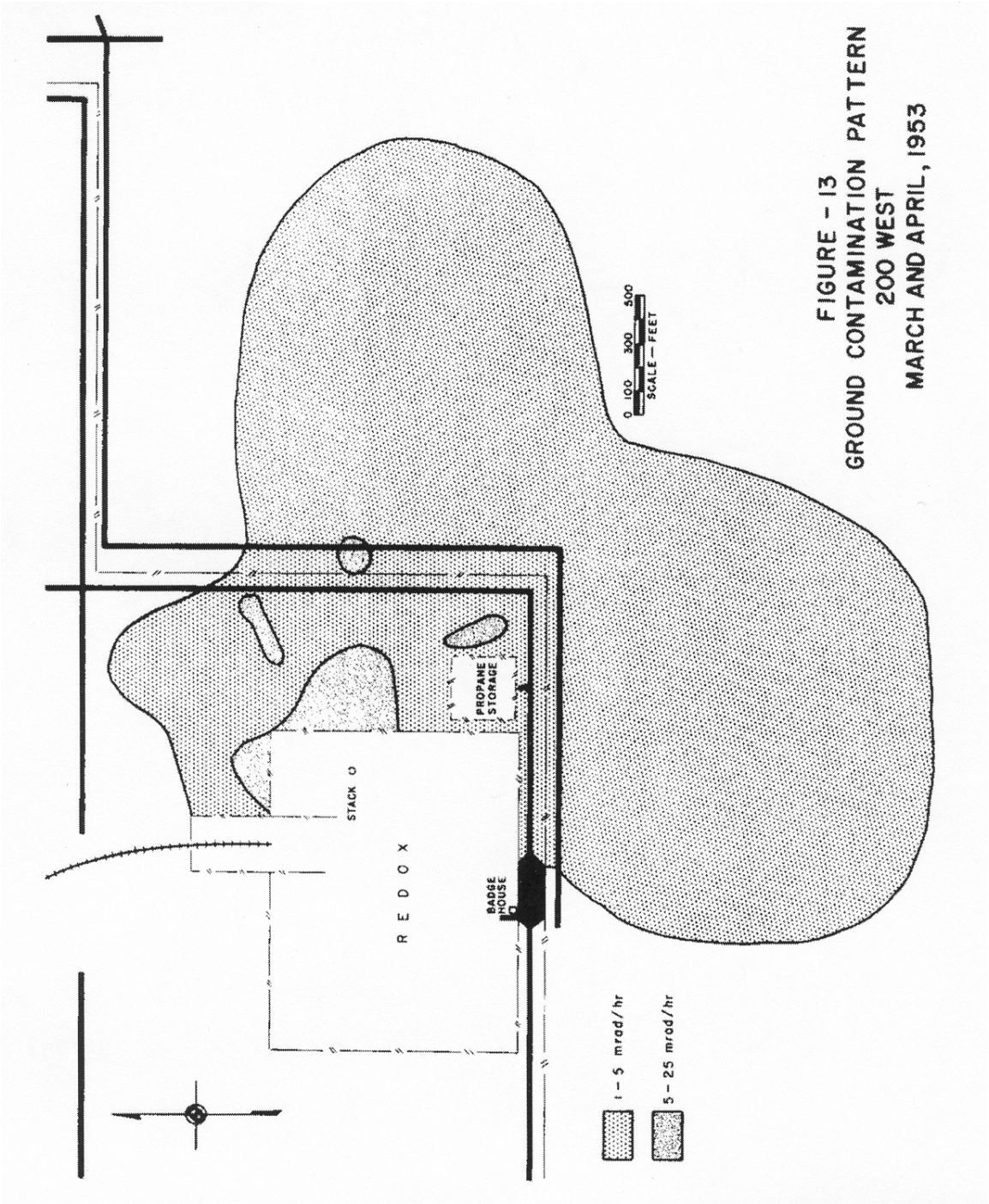

Figure C-6. Ground contamination pattern in 200-West, March and April 1953. Figure 13 from Selby and Soldat (1956), HW-54636.

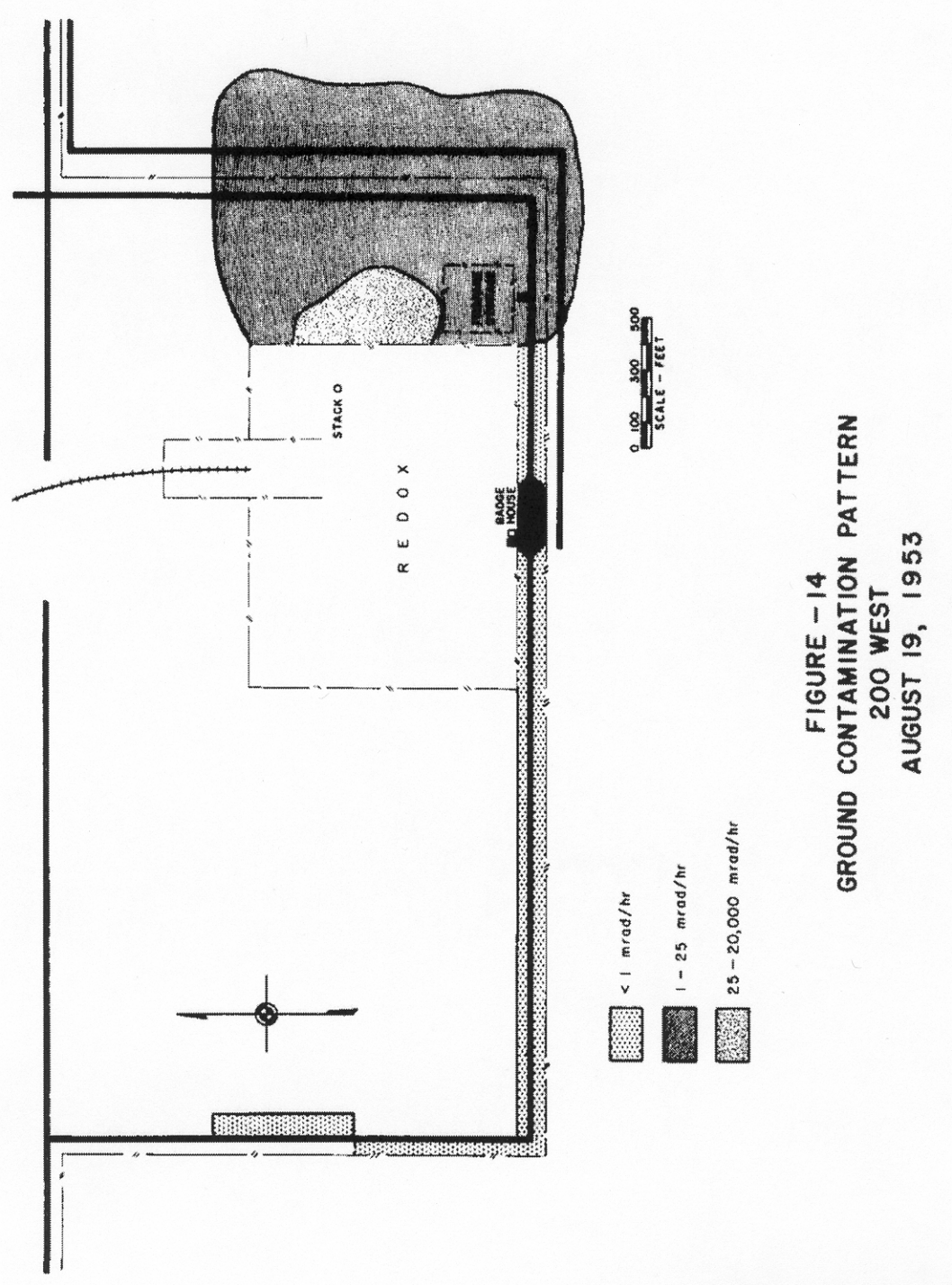

Figure C-7. Ground contamination pattern in 200-West, August 19, 1953. Figure 14 from Selby and Soldat (1956), HW-54636.

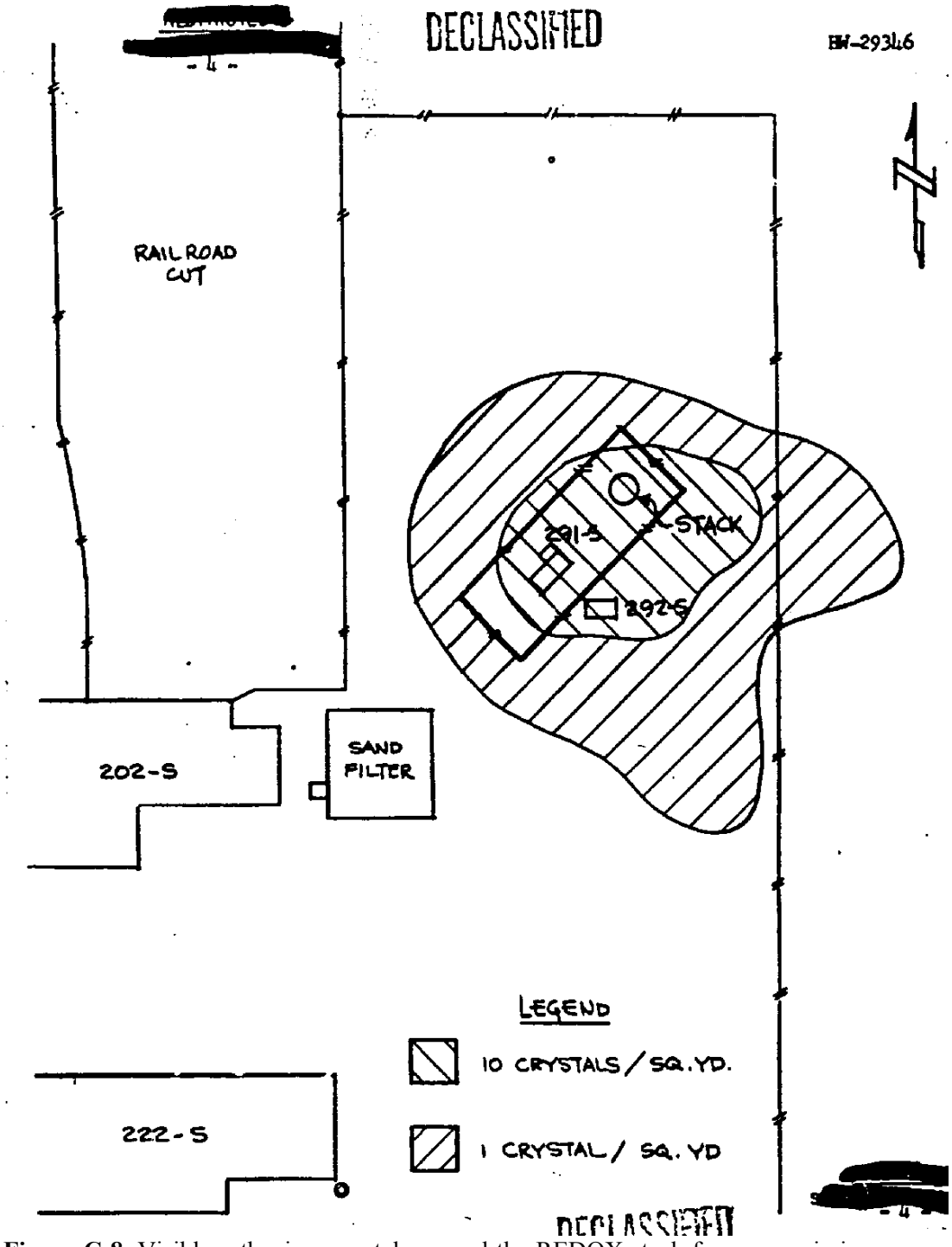

Figure C-8. Visible ruthenium crystals around the REDOX stack from an emission that occurred August 14, 1953 (HW-29346). Finer particles, detectable by instruments, were much more frequent and more widely spread than the visible crystals.

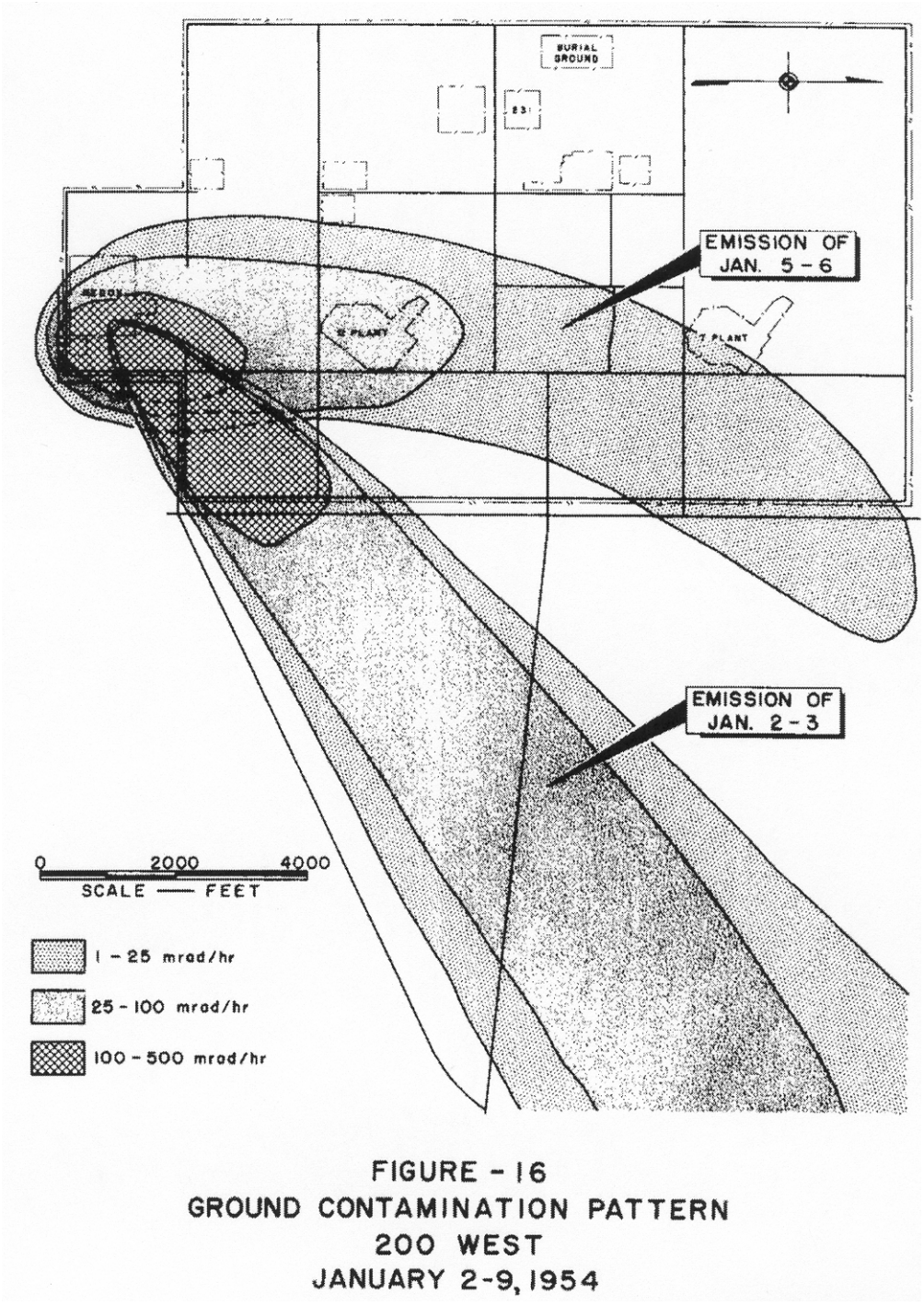

Figure C-9. Ground contamination pattern, 200-West, January 2-9, 1954. Figure 16 from Selby and Soldat (1956), HW-54636.

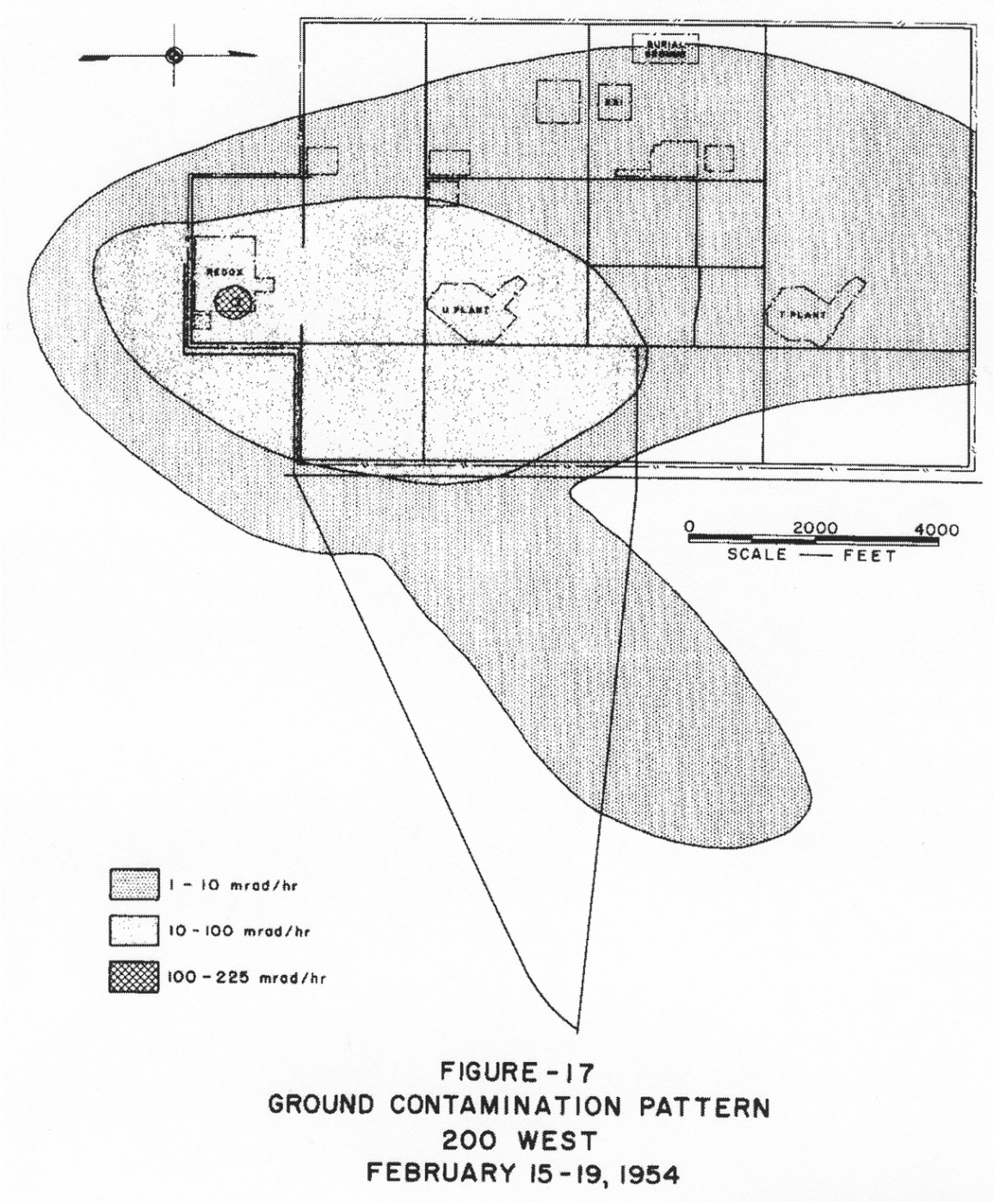

Figure C-10. Ground contamination pattern, 200-West, February 15-19, 1954. Figure 17 from Selby and Soldat (1956), HW-54636.

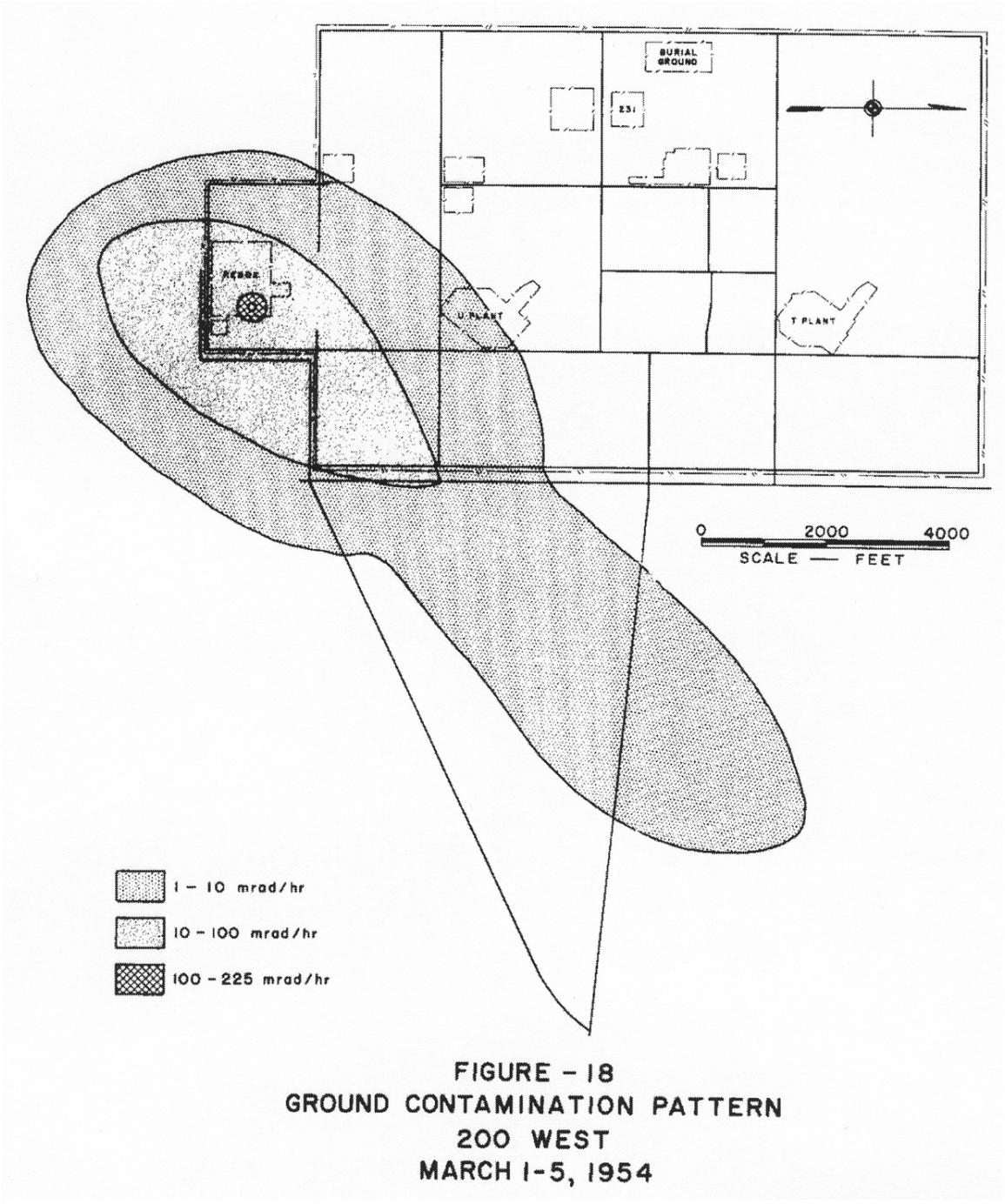

Figure C-11. Ground contamination pattern, 200-West, March 1-5, 1954. Figure 18 from Selby and Soldat (1956), HW-54636.

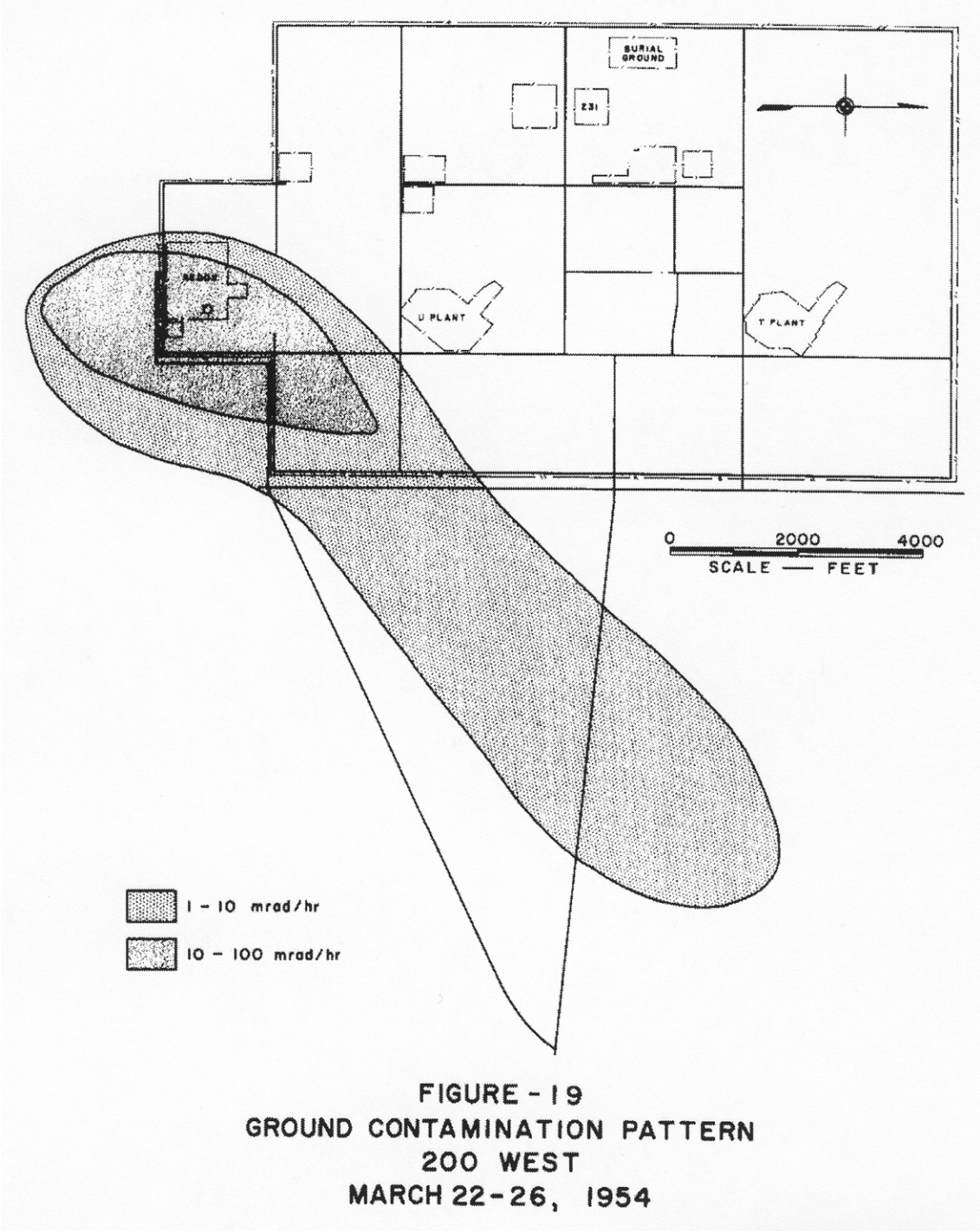

Figure C-12. Ground contamination pattern, 200-West, March 22-26, 1954. Figure 19 from Selby and Soldat (1956), HW-54636.

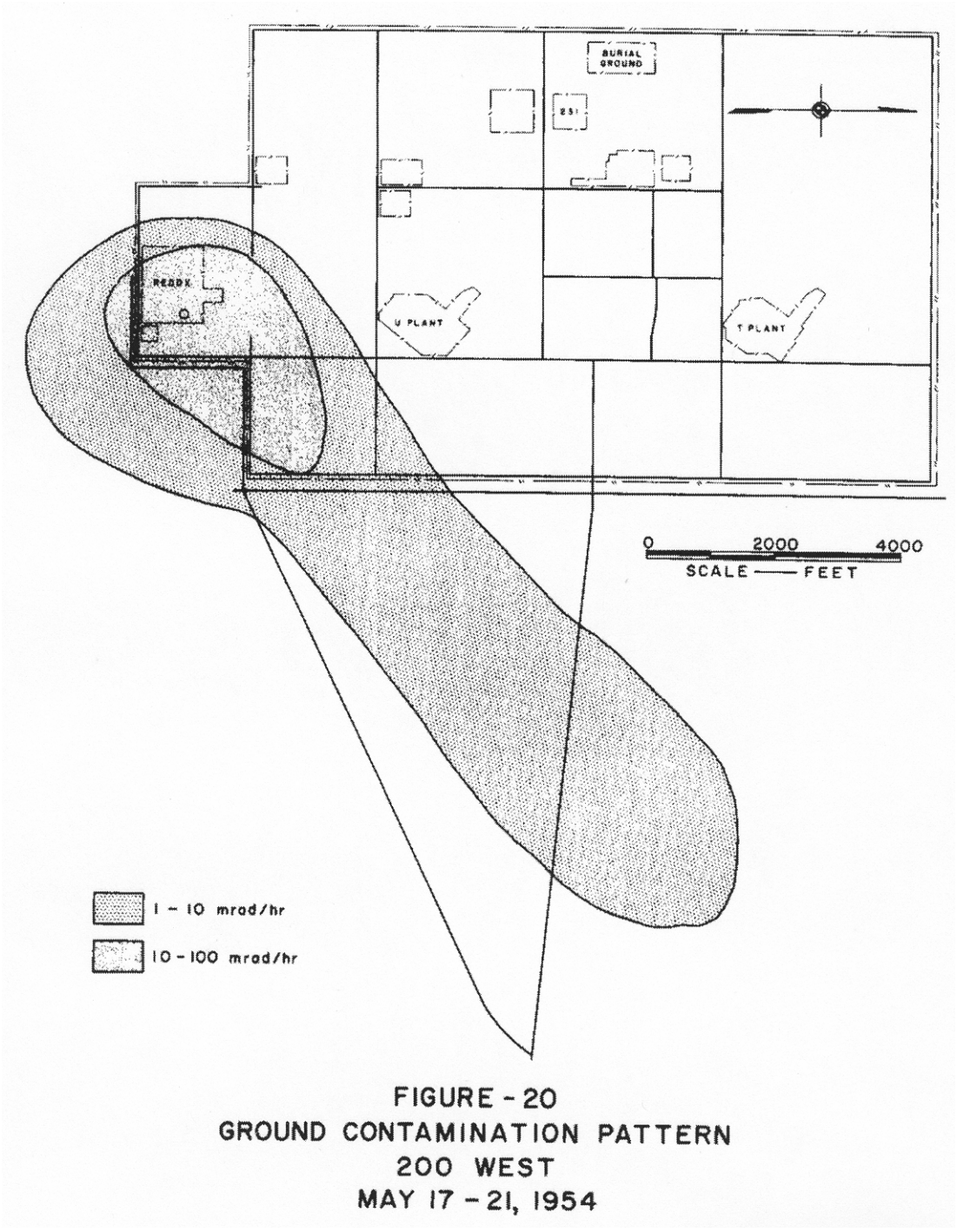

Figure C-13. Ground contamination pattern, 200-West, May 17-21, 1954. Figure 20 from Selby and Soldat (1956), HW-54636.

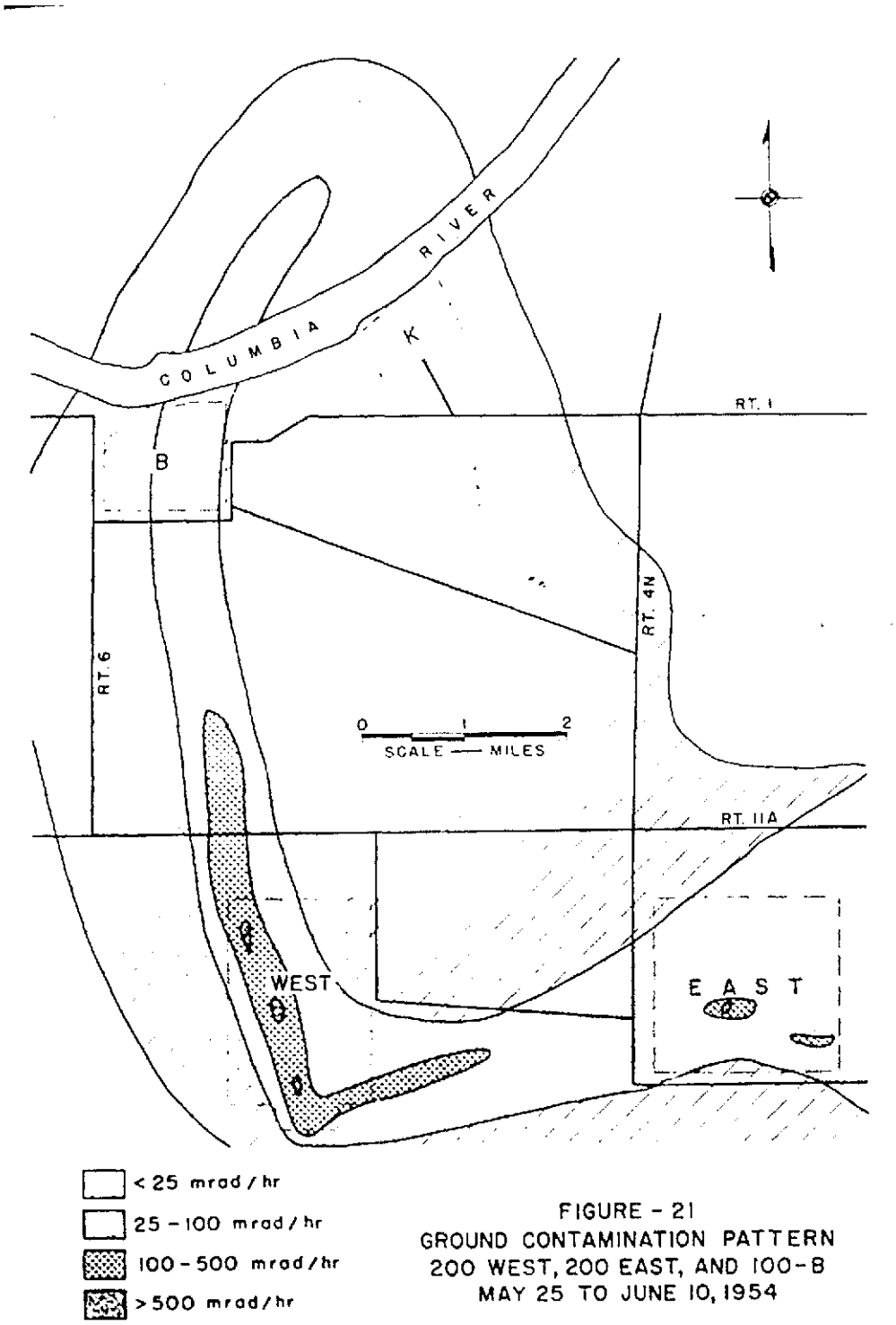

Figure C-14. Ground contamination pattern in 200-West, 200-East, and 100-B, May 25 to June 10, 1954. Figure 21 from Selby and Soldat (1956), HW-54636.

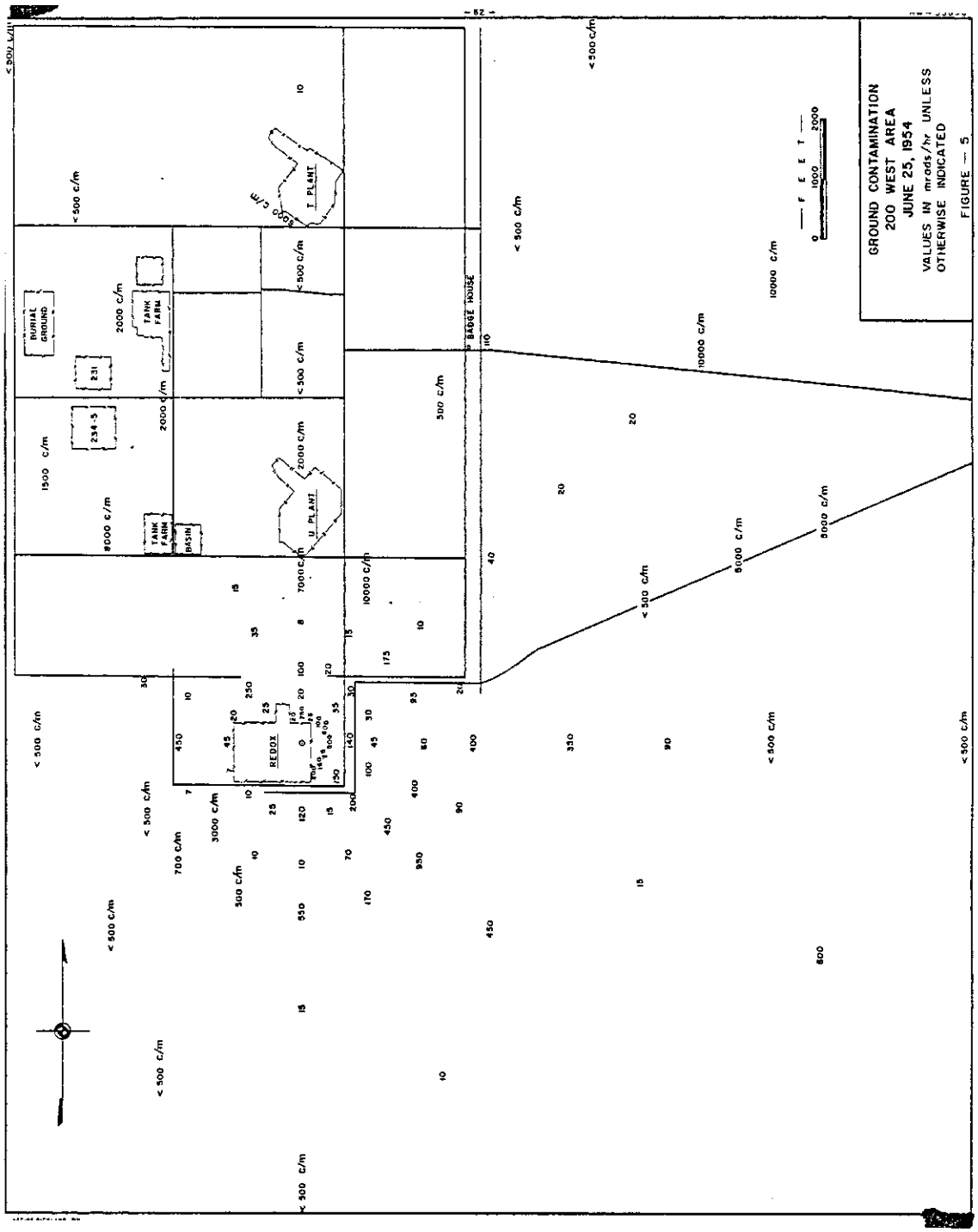

Figure C-15. Ground contamination in 200-West Area, June 1954. Reproduced from Figure 5 of HW-33896. This survey did not extend as far as the nearest military encampment. Values are either cpm general area contamination or mrads h^{-1} from active particles. The highest values are 950 mrad h^{-1} at 2700 ft SE of the stack and 10,000 cpm 3000 ft NNE of the stack.

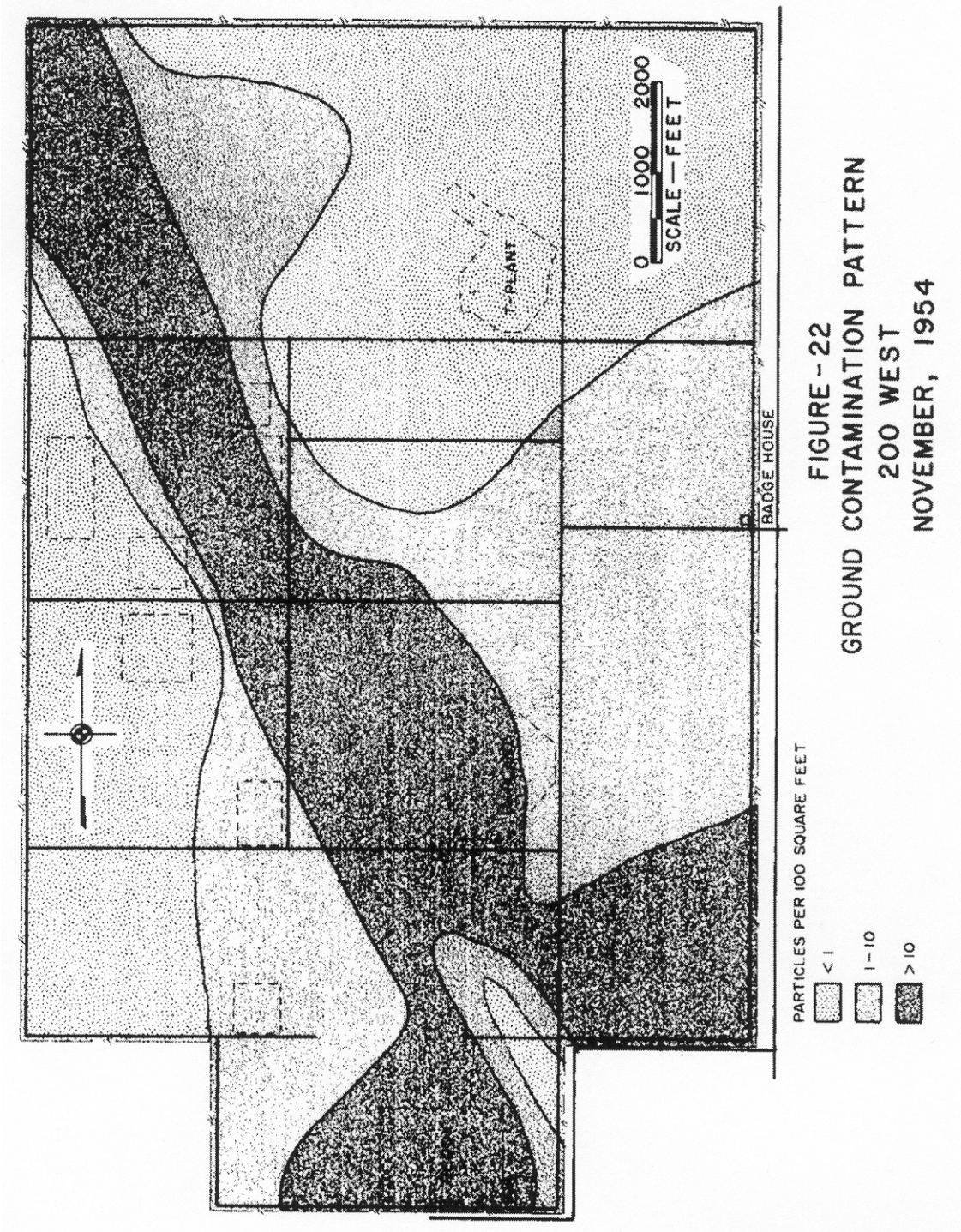

Figure C-16. Ground contamination pattern, 200-West, November 1954. Figure 22 from Selby and Soldat (1956), HW-54636.

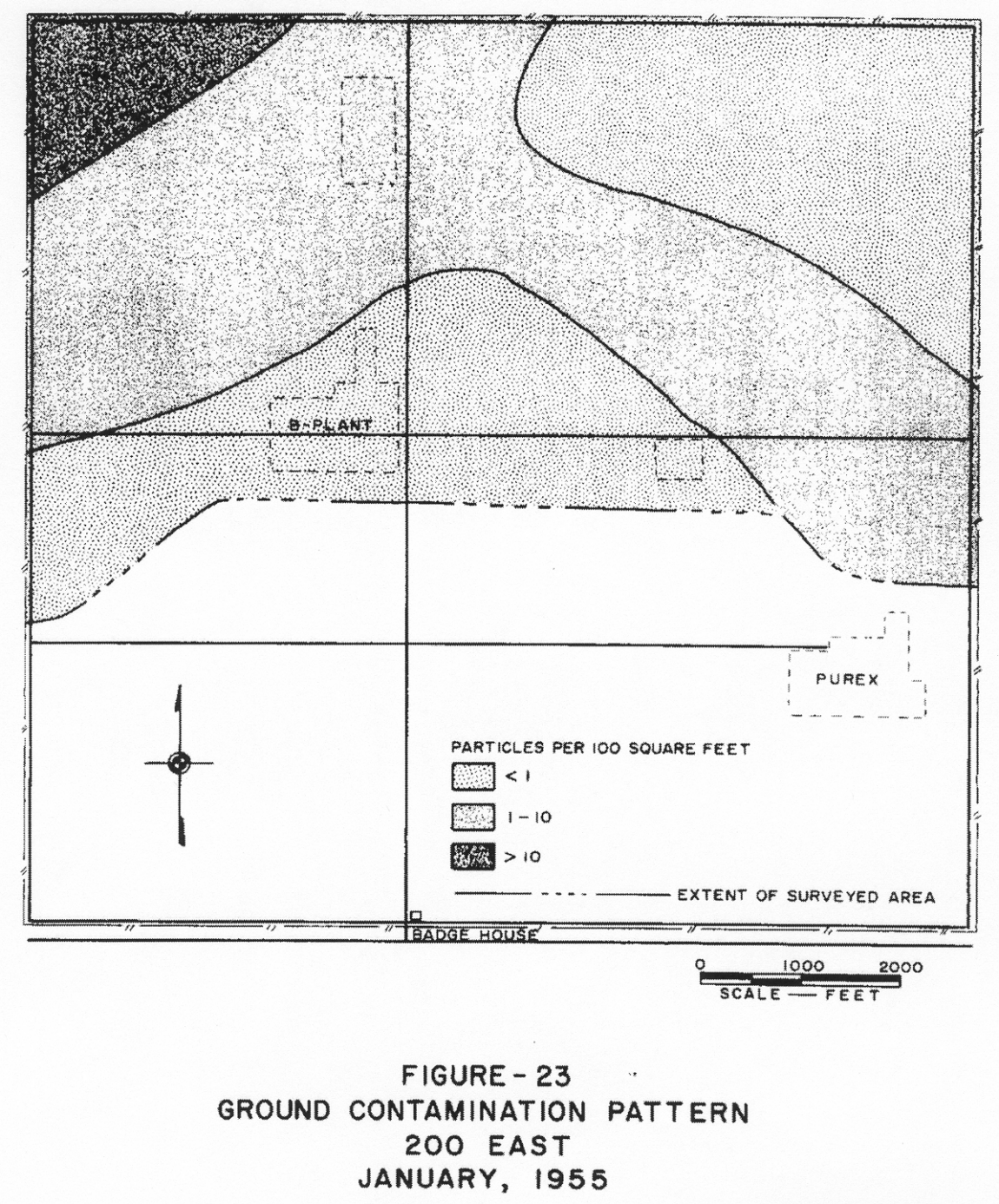

Figure C-17. Ground contamination pattern, 200-East, January 1955. Figure 23 from Selby and Soldat (1956), HW-54636.

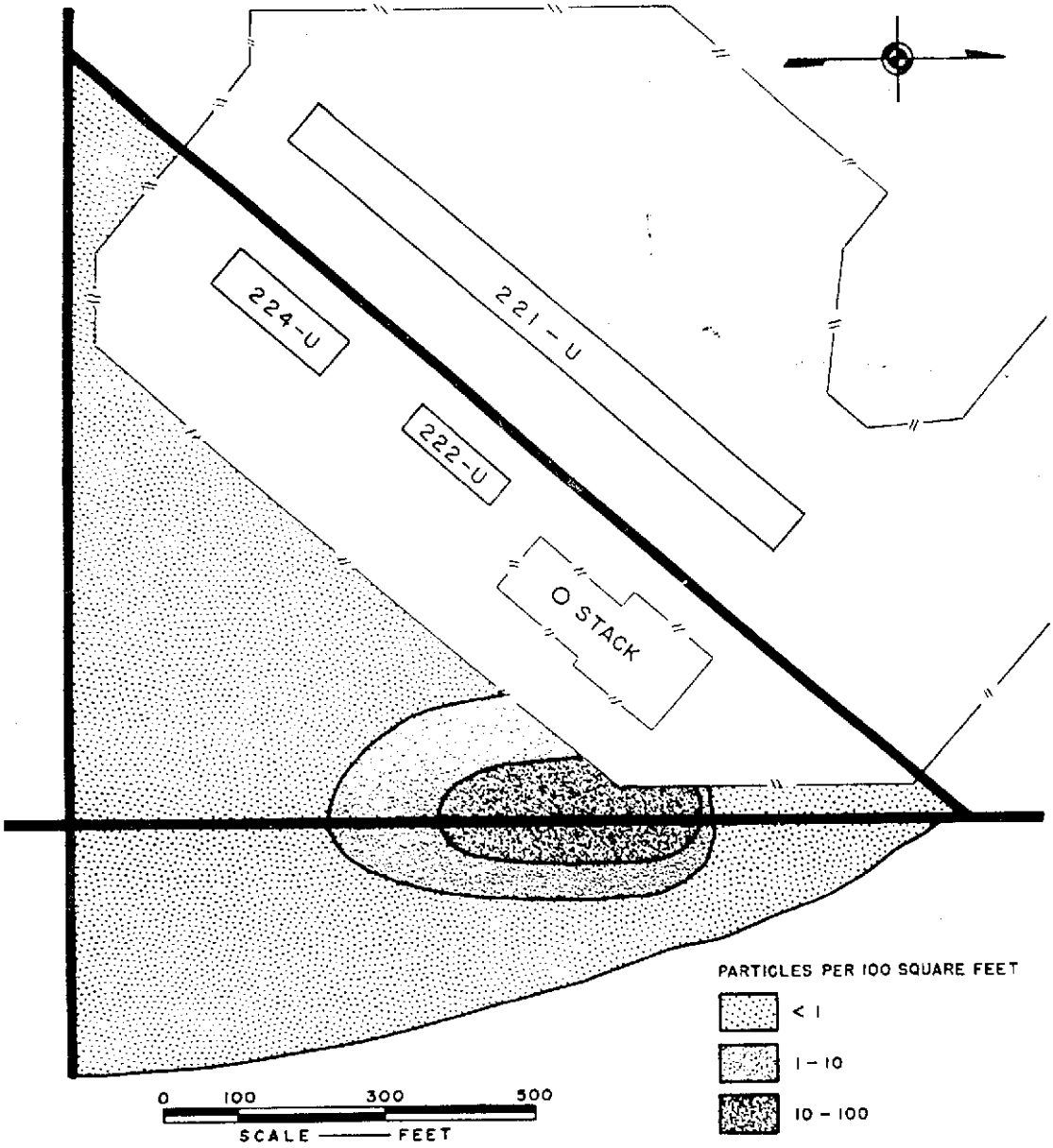

FIGURE - 40
GROUND CONTAMINATION PATTERN
200 WEST
JUNE 4, 1956

Figure C-18. Ground contamination pattern, 200-West, June 4, 1956. Figure 40 from Selby and Soldat (1956). HW-54636.

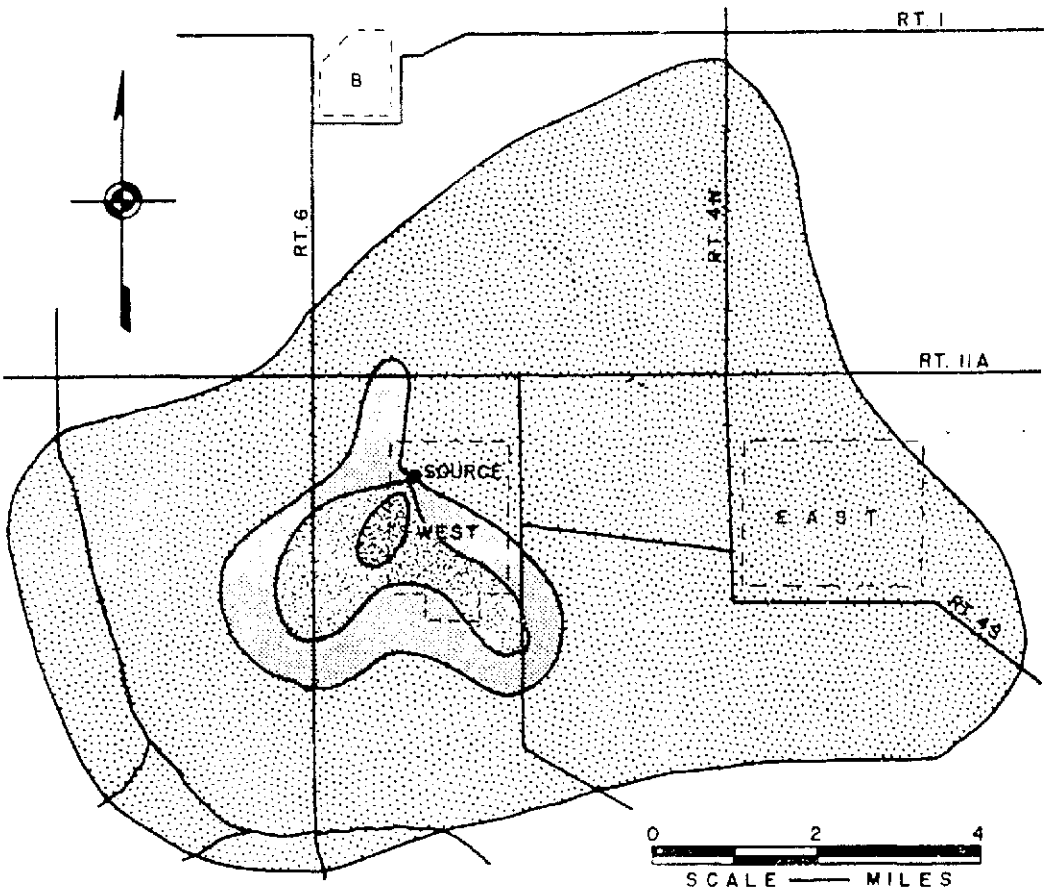

FIGURE - 41
GROUND CONTAMINATION PATTERN
200 WEST AREA & VICINITY
NOVEMBER 7-12, 1957

Figure C-19. Ground contamination pattern, 200-West Area and vicinity, November 7-12, 1957. Figure 41 from Selby and Soldat (1956), HW-54636.

C-3. SITE-WIDE (OR LARGER) SURVEYS

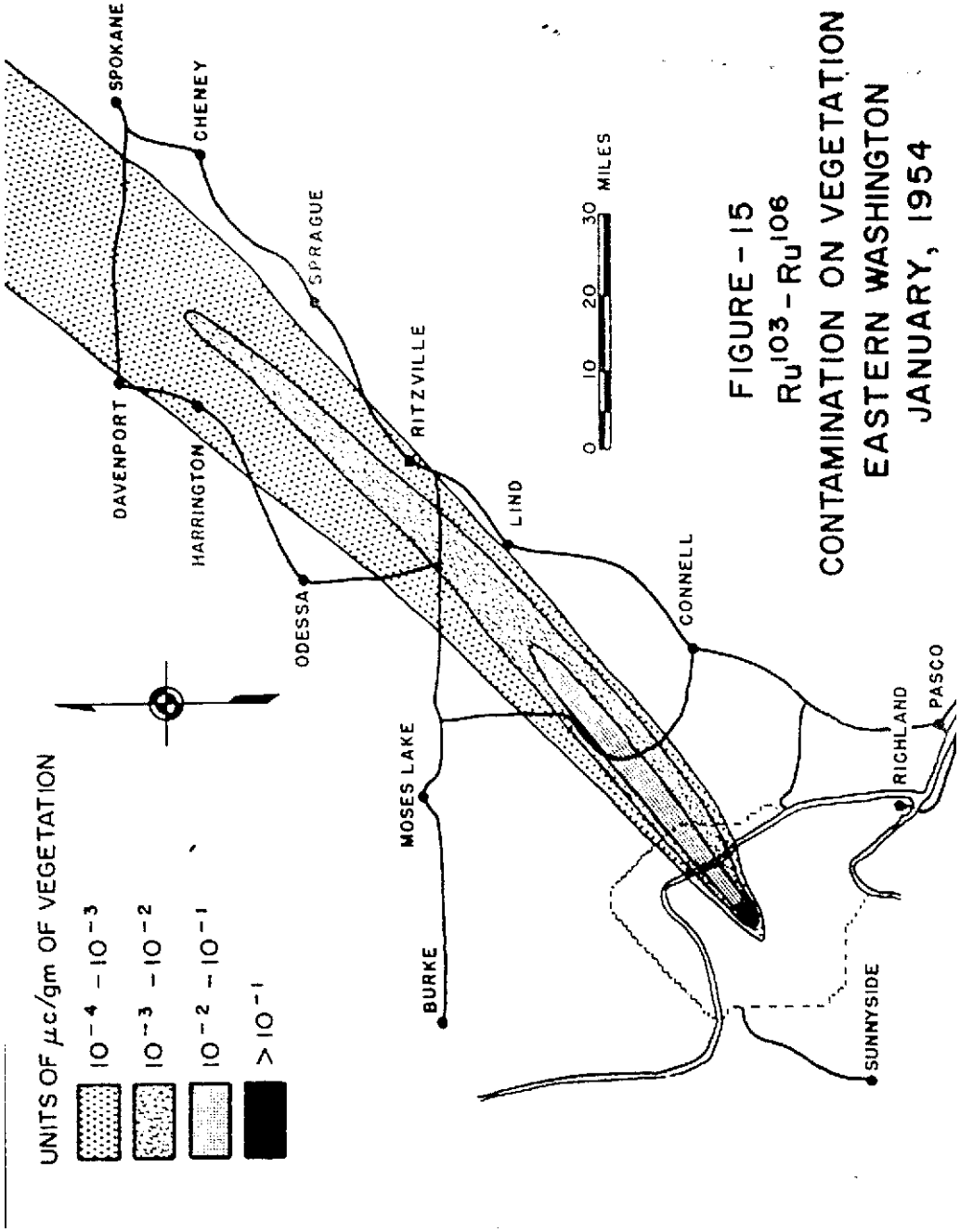

Figure C-20. Ruthenium contamination on vegetation of Eastern Washington, January, 1954. Figure 15 from Selby and Soldat (1965), HW-54636.

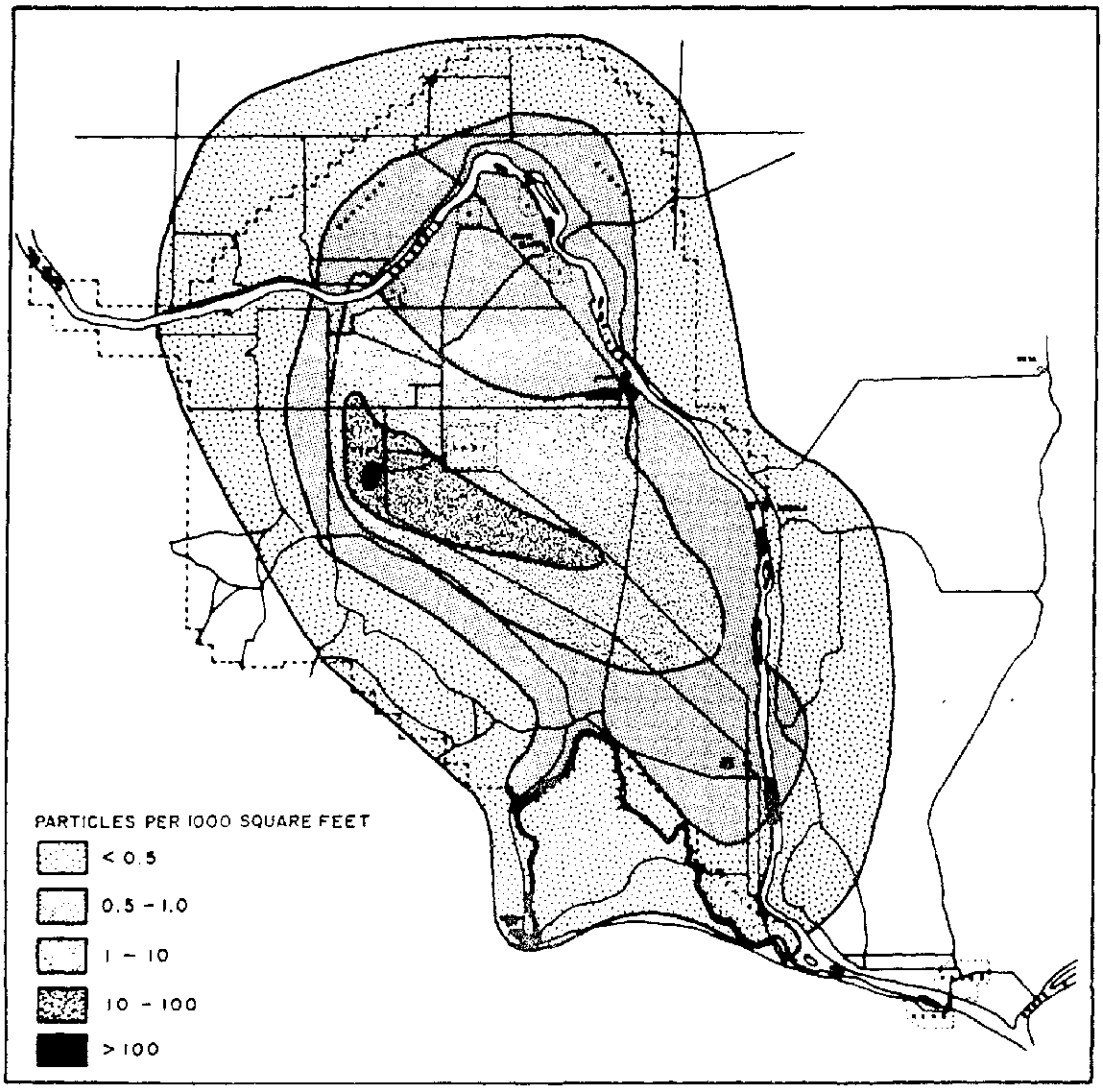

FIGURE 24

GROUND CONTAMINATION PATTERN
HANFORD AND VICINITY
JULY AND AUGUST, 1954

Figure C-21. Ground contamination pattern, Hanford and vicinity, July and August, 1954. Figure 24 from Selby and Soldat (1965), HW-54636.

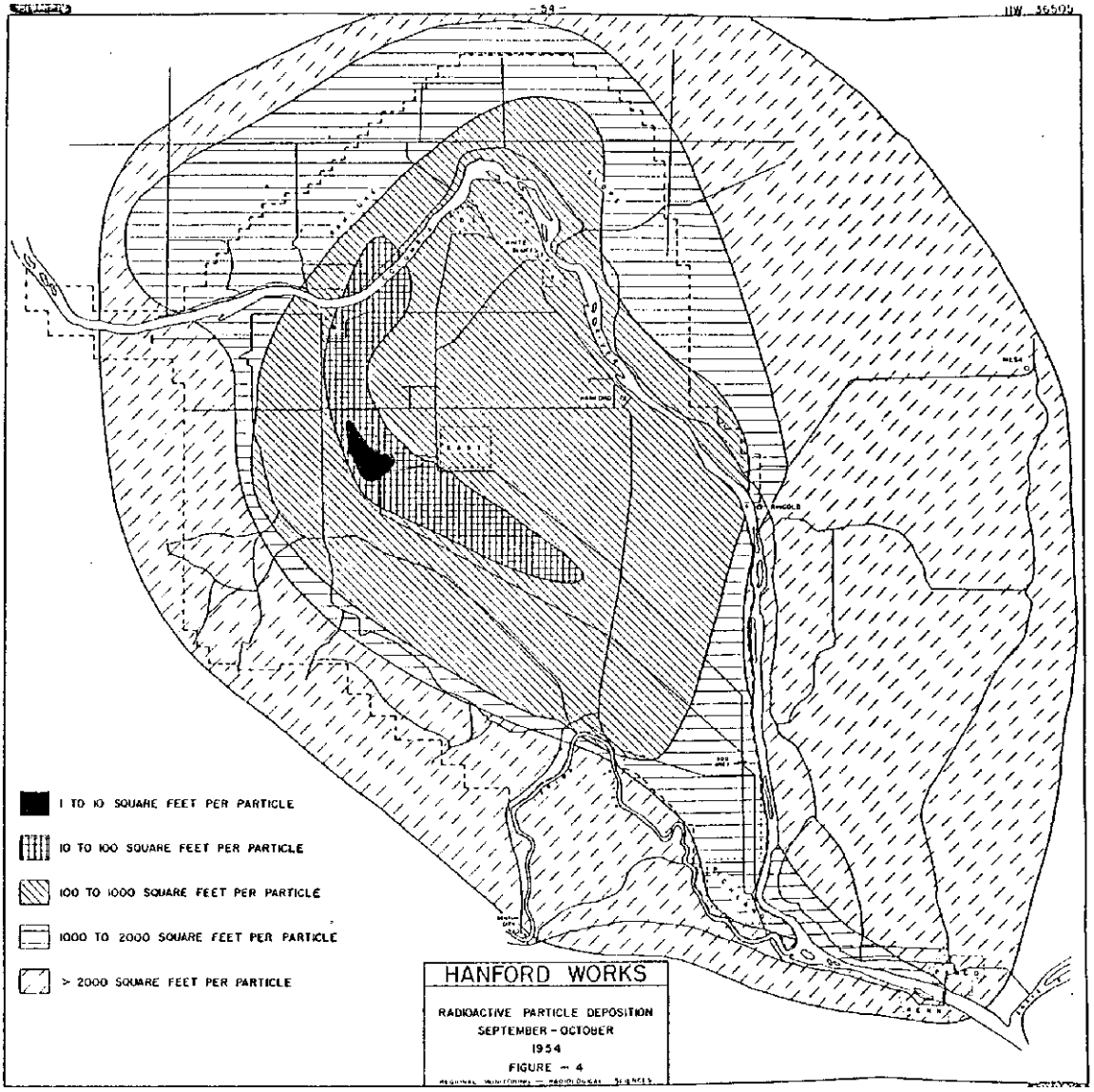

Figure C-22. Radioactive particle deposition on and around the Hanford site, September-October 1954. Figure 4 from HW-36505. The highest contamination zone near 200-West was one particle per 1-10 square feet. In the lowest zone shown here, one particle was found in an area greater than 2000 square feet.

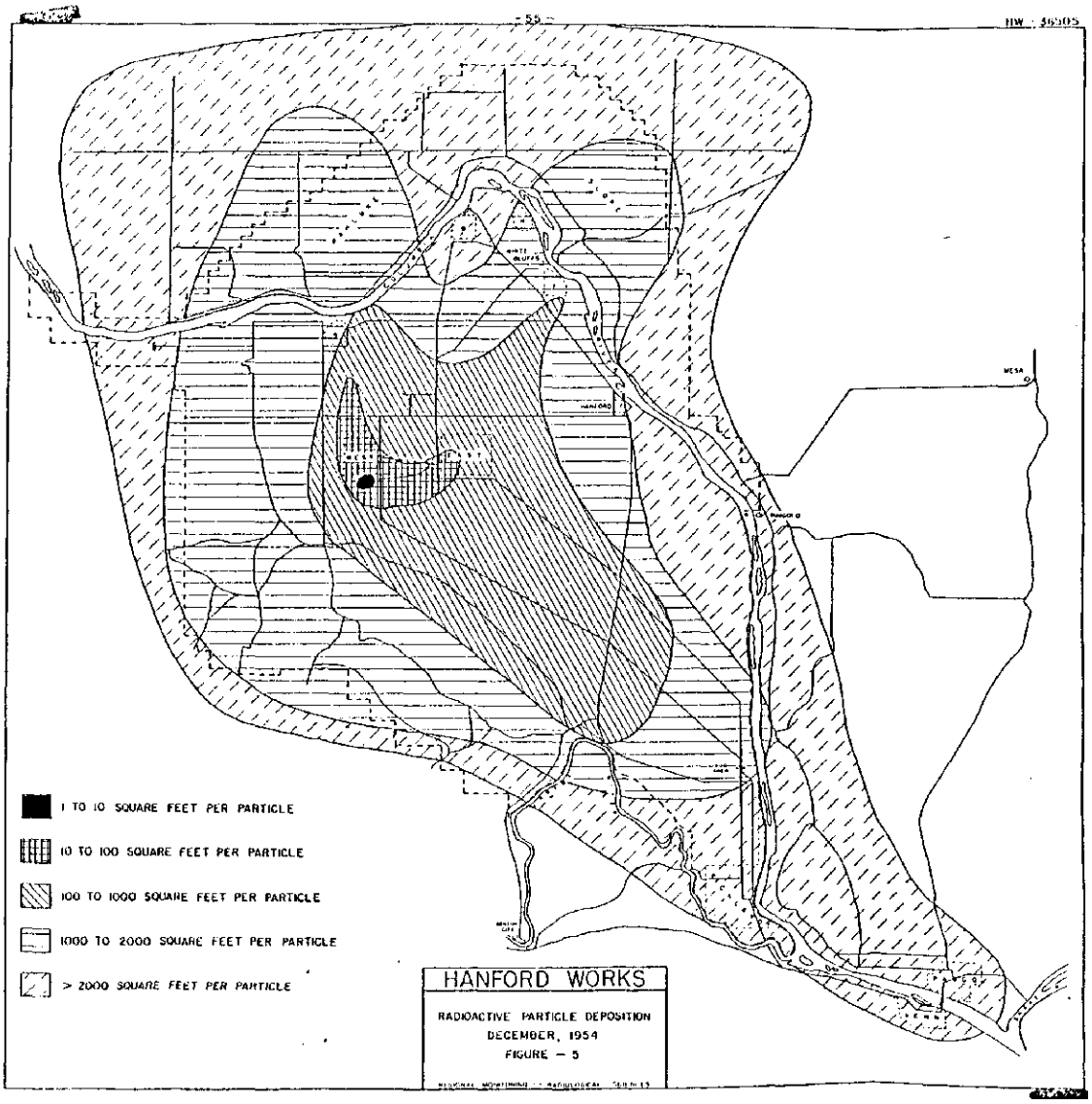

Figure C-23. Radioactive particle deposition density on and around the Hanford site, December 1954. Figure 5 from HW-36505.

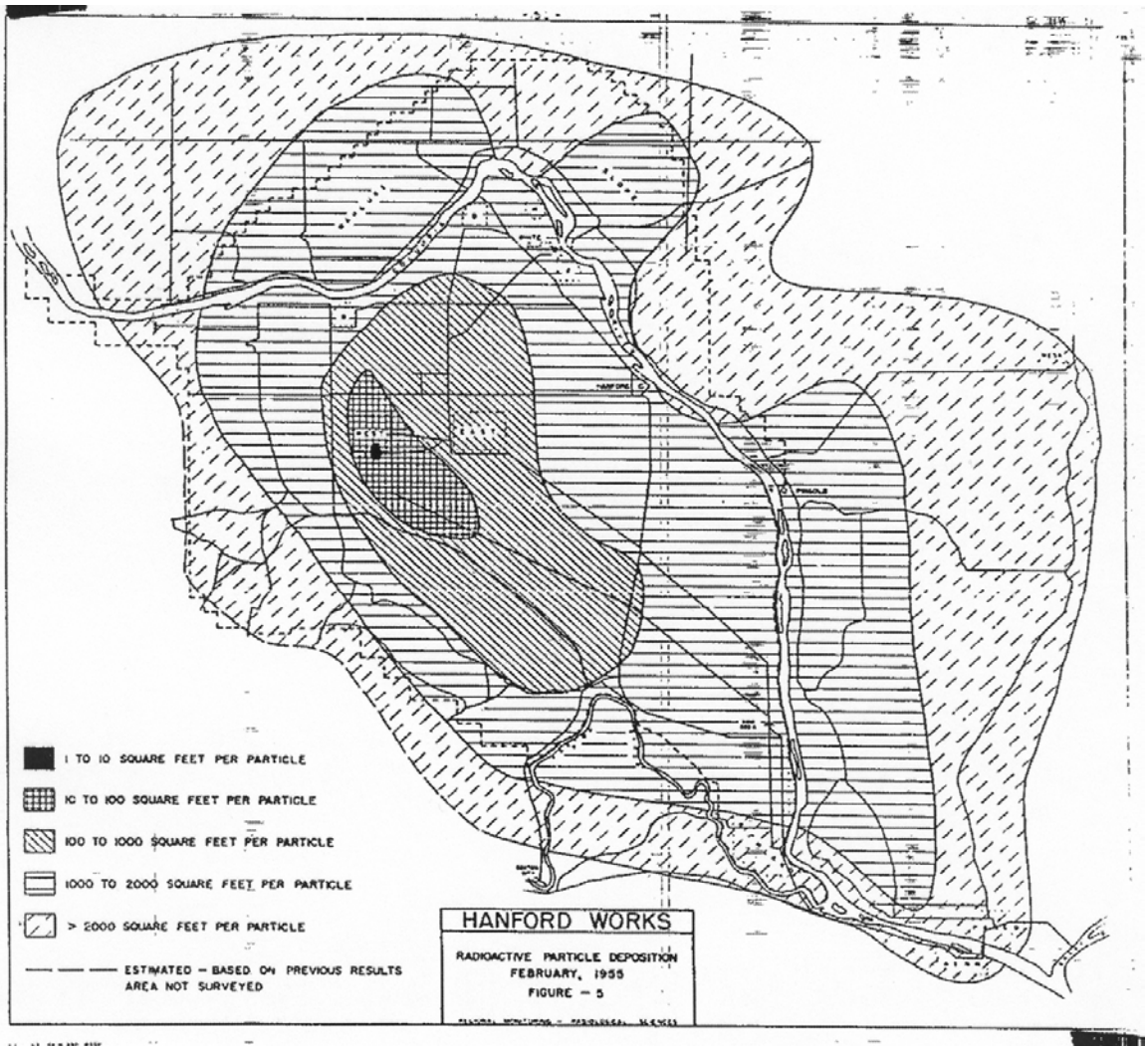

Figure C-24. Radioactive particle deposition density on and around the Hanford site, February 1955. Figure 5 from HW-36506.

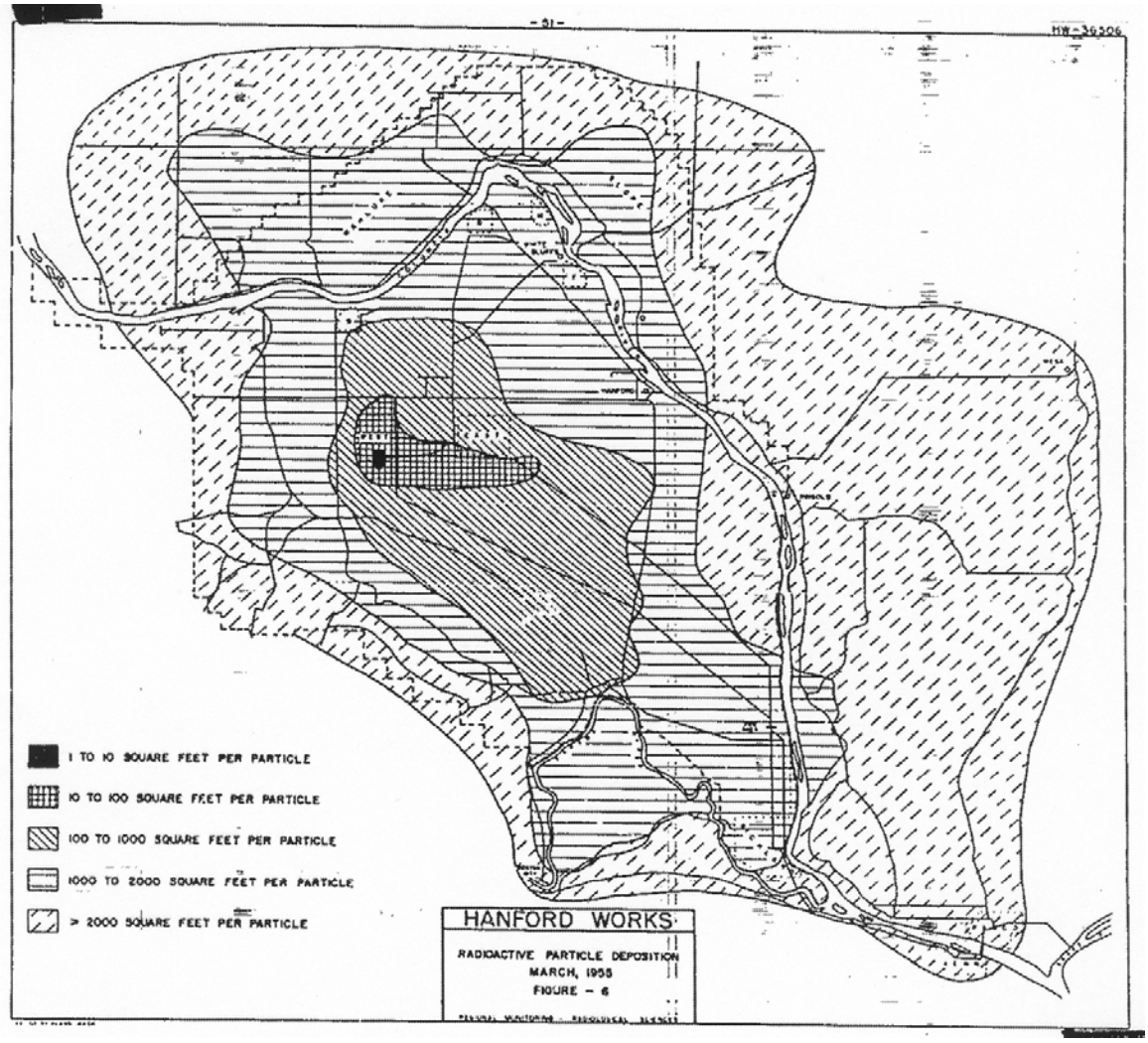

Figure C-25. Radioactive particle deposition density on and around the Hanford site, March 1955. Figure 6 from HW-36506.

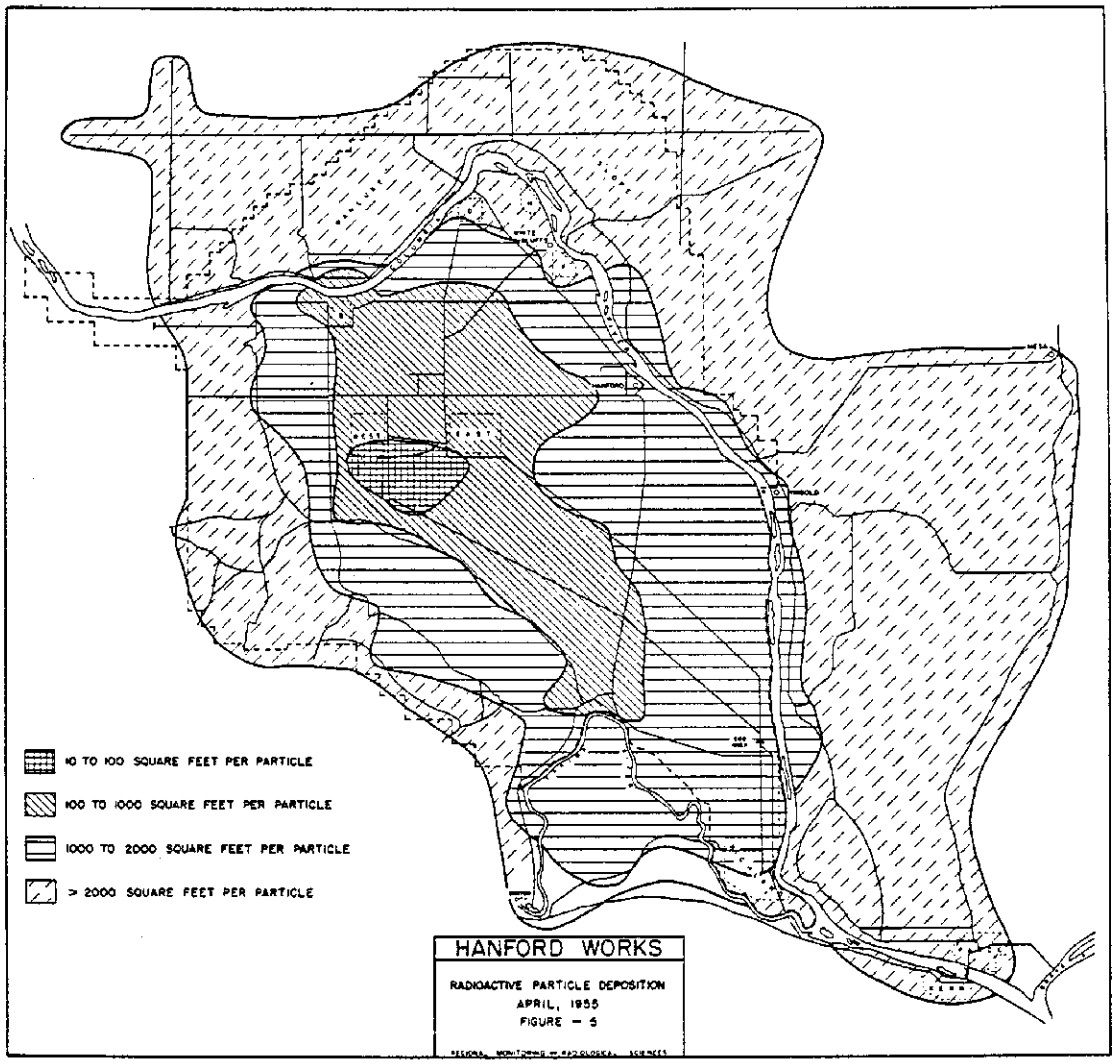

Figure C-26. Radioactive particle deposition density on and around the Hanford site, April 1955. Figure 5 from HW-38566.

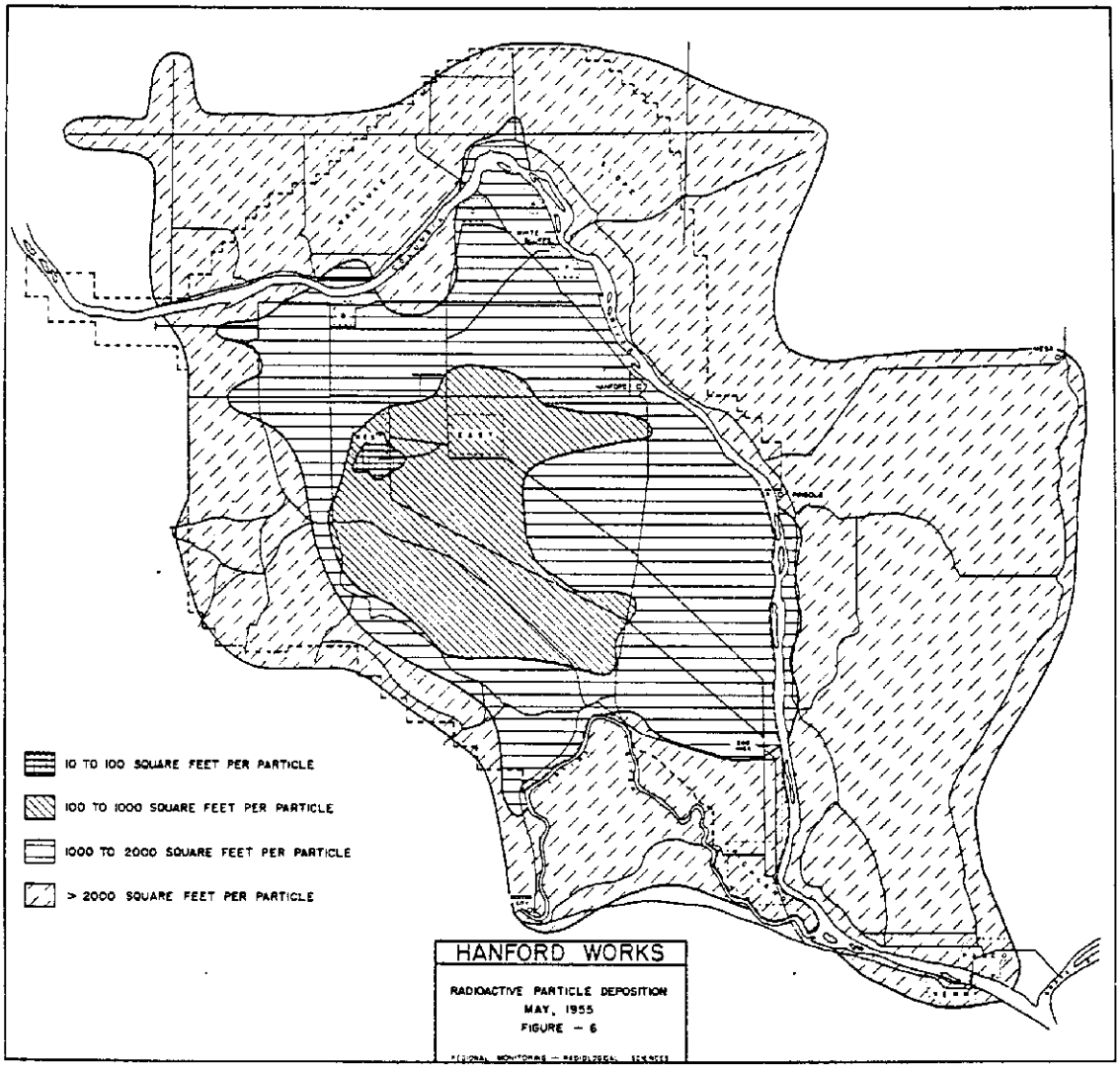

Figure C-27. Radioactive particle deposition density on and around the Hanford site, May 1955. Figure 6 from HW-38566.

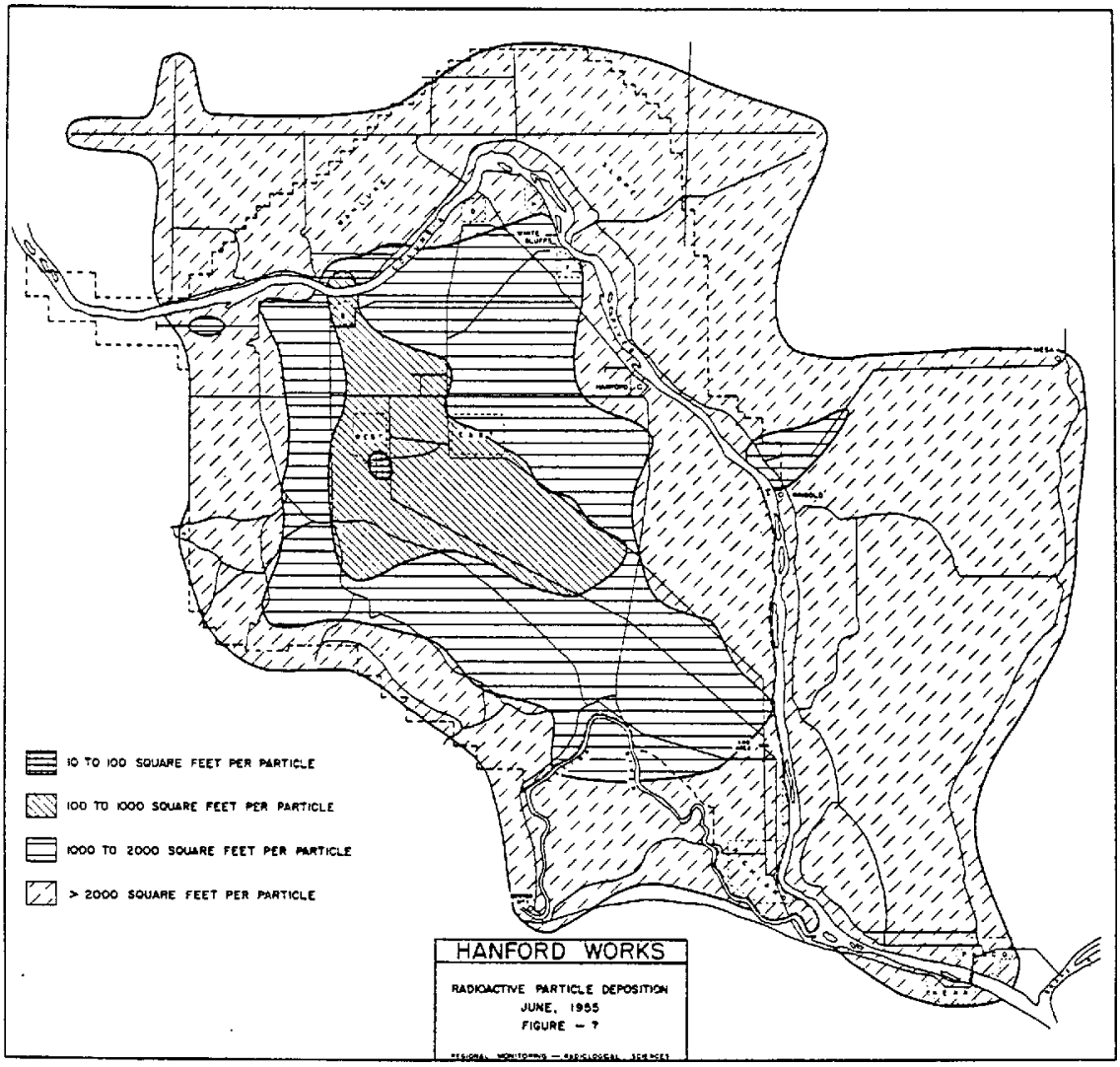

Figure C-28. Radioactive particle deposition density on and around the Hanford site, June 1955. Figure 7 from HW-38566.

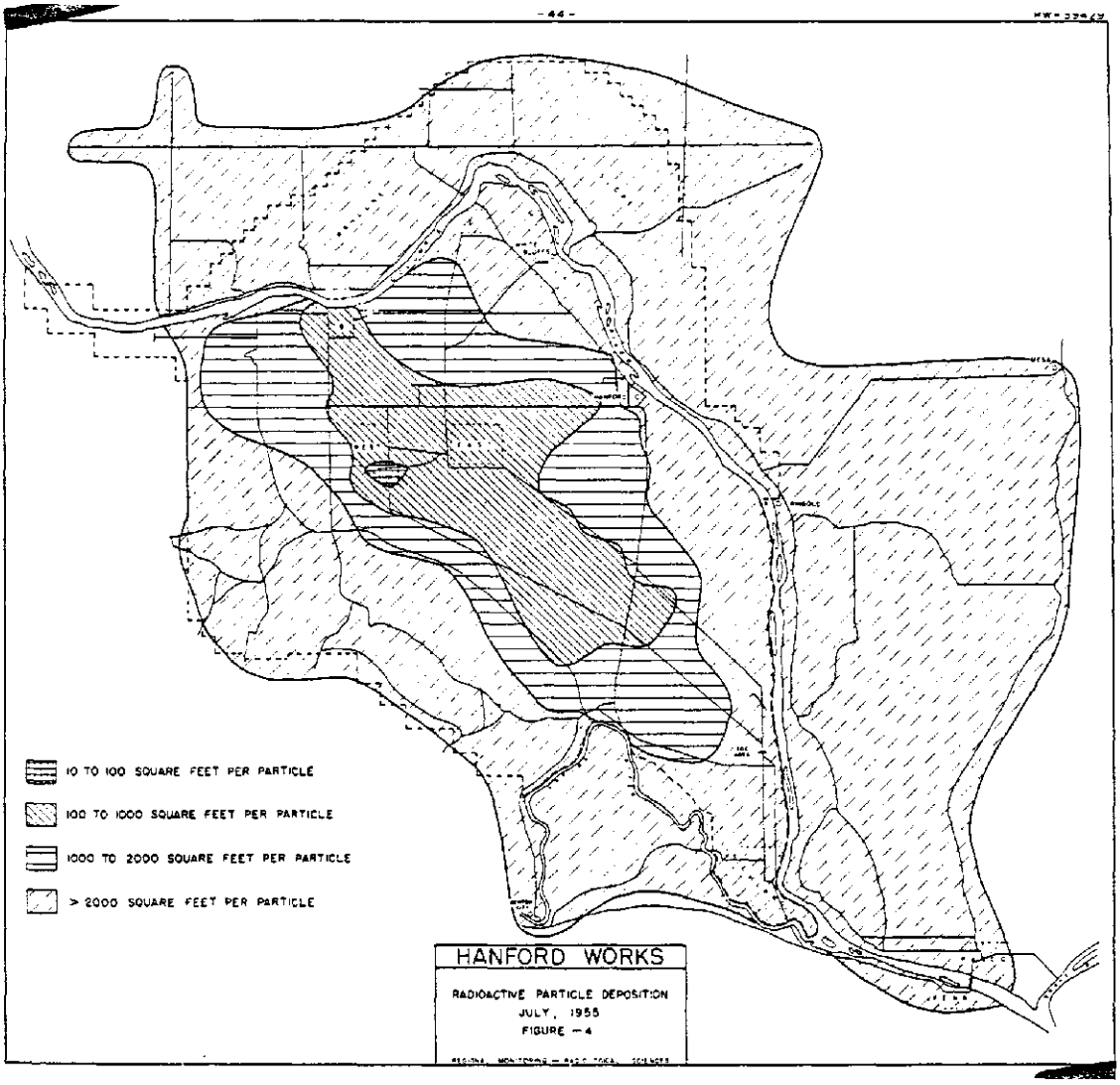

Figure C-29. Radioactive particle deposition density on and around the Hanford site, July 1955. Figure 4 from HW-39429.

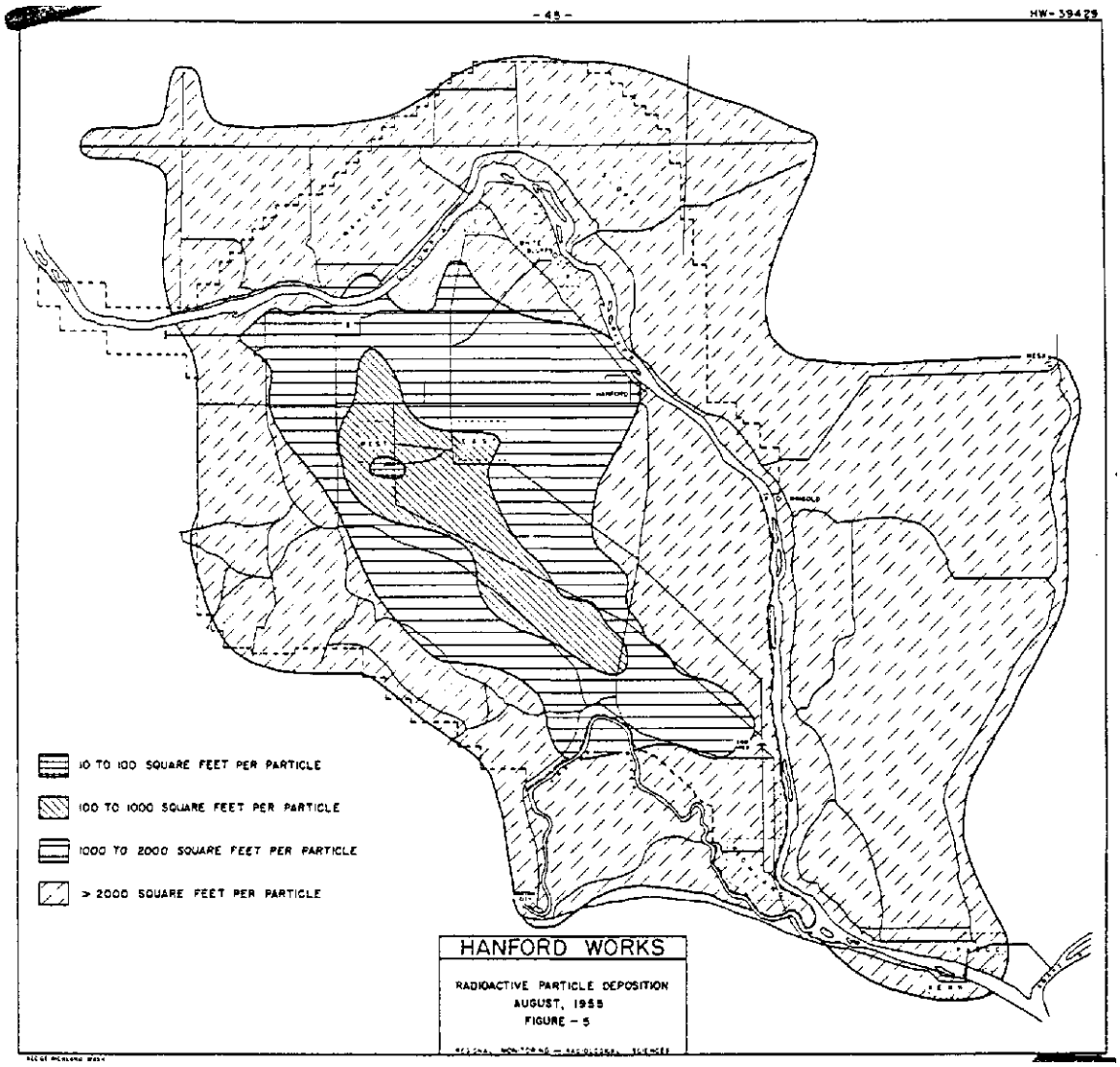

Figure C-30. Radioactive particle deposition density on and around the Hanford site, August 1955. Figure 5 from HW-39429.

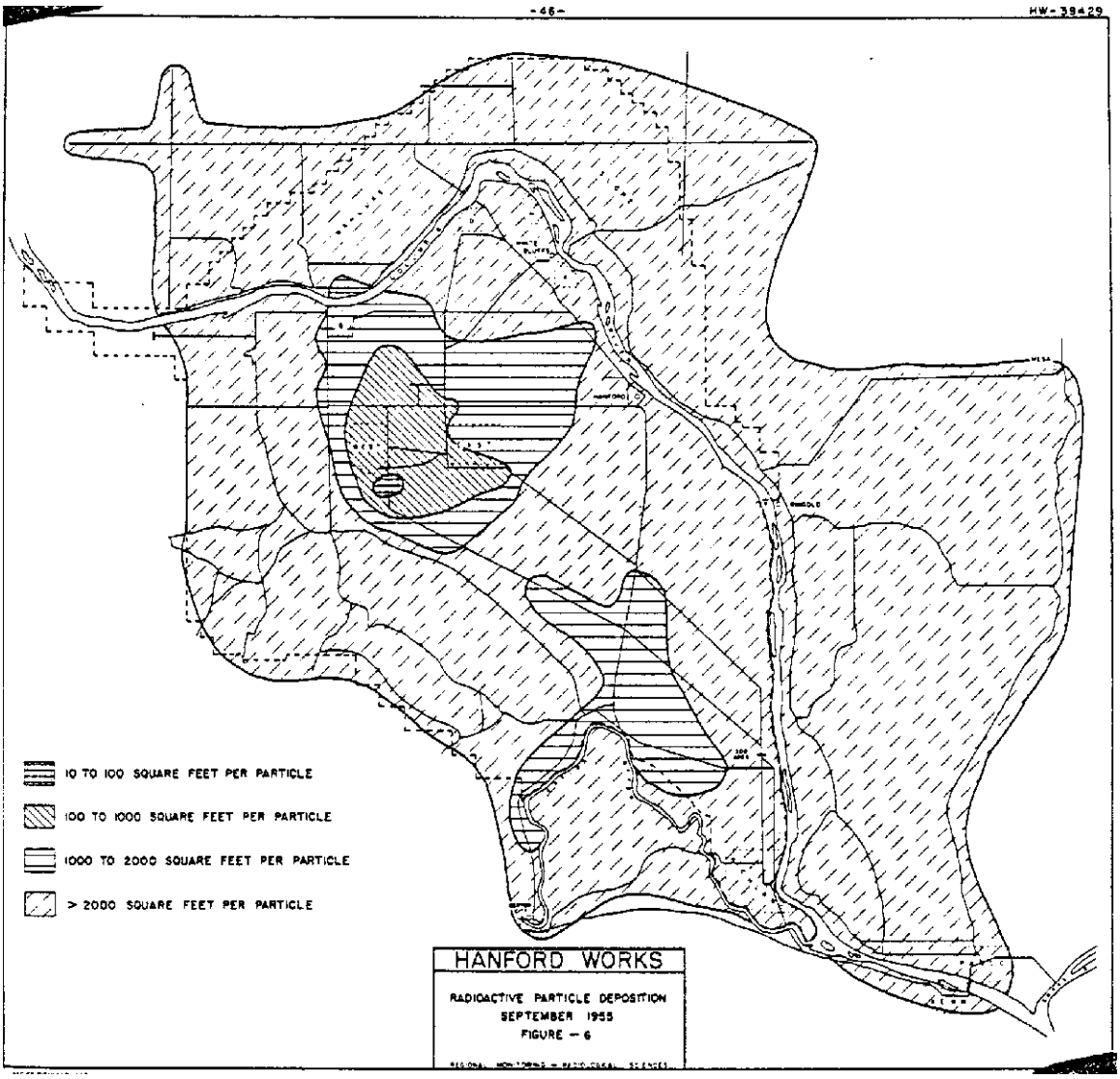

Figure C-31. Radioactive particle deposition density on and around the Hanford site, September 1955. Figure 6 from HW-39429.

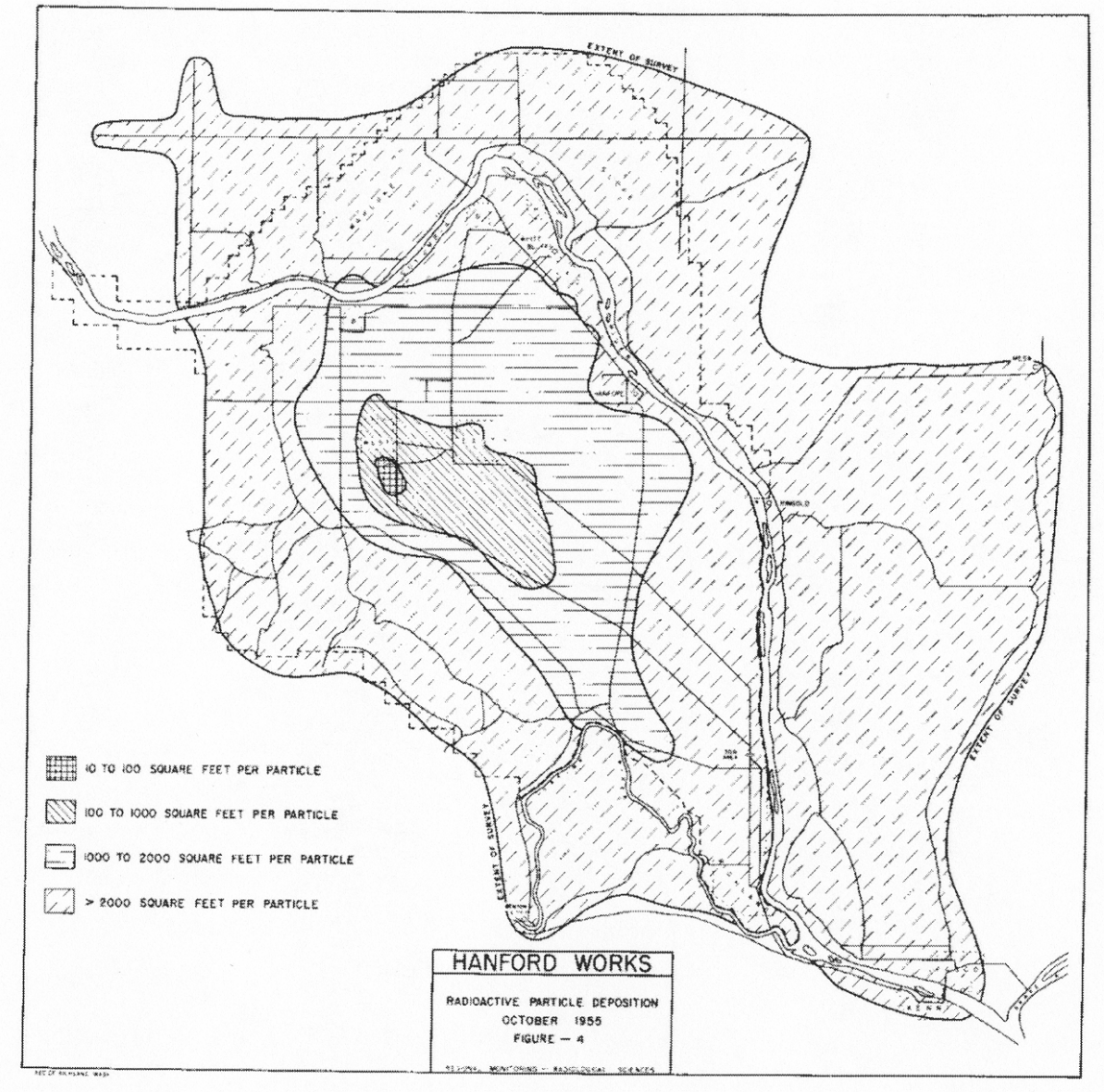

Figure C-32. Radioactive particle deposition density on and around the Hanford site, October 1955. Figure 4 from HW-40871.

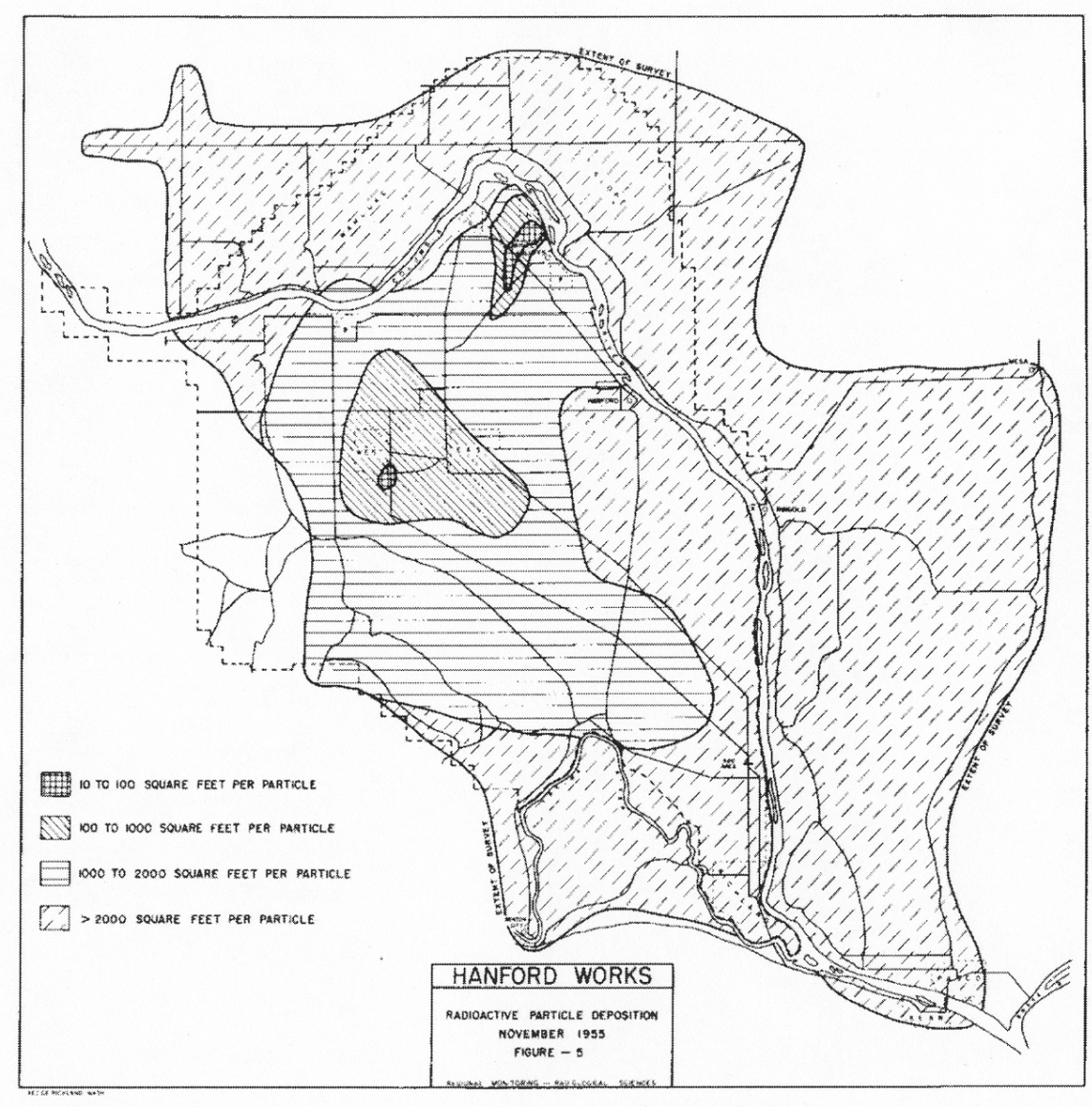

Figure C-33. Radioactive particle deposition density on and around the Hanford site, November 1955. Figure 5 from HW-40871.

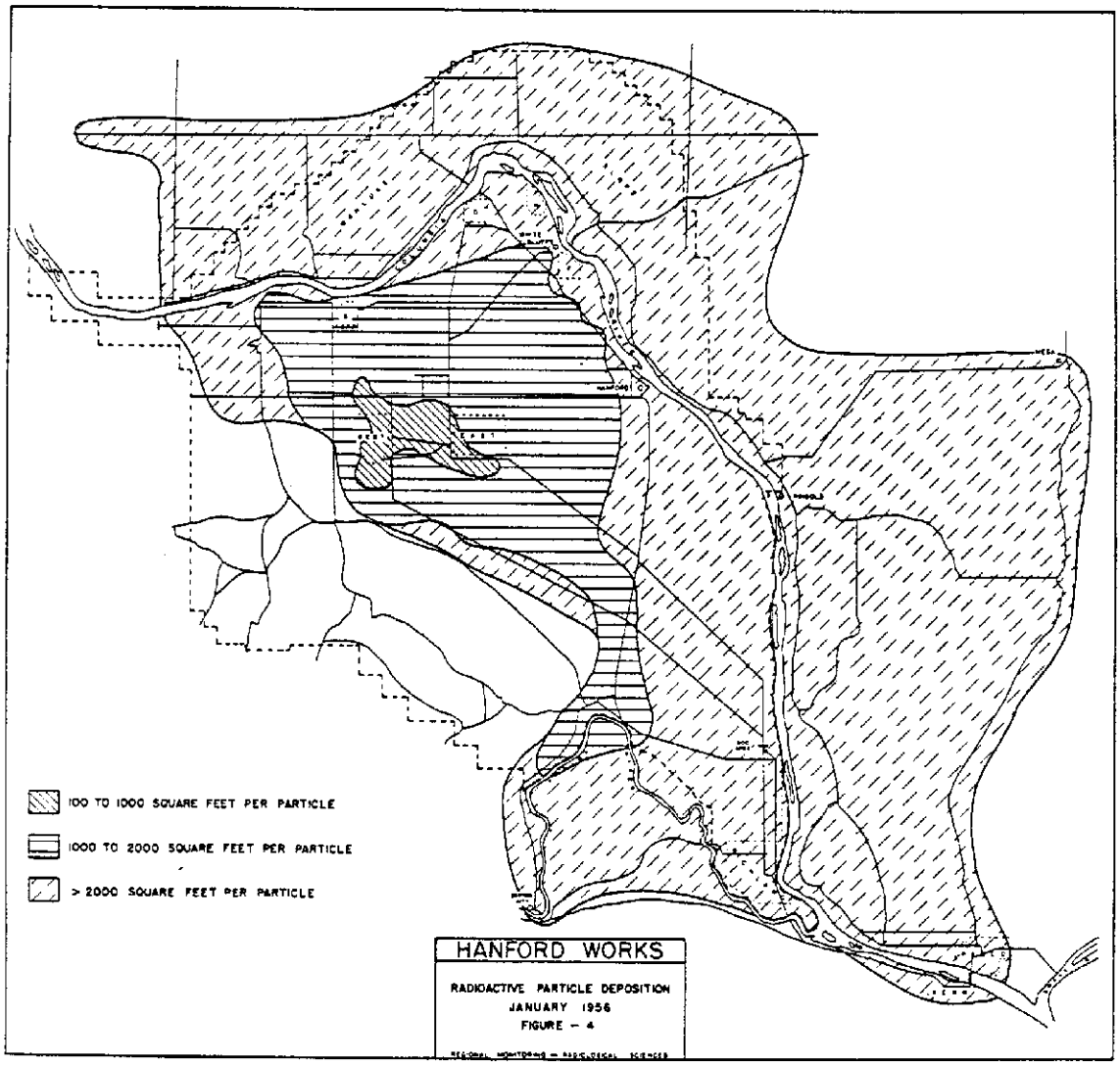

Figure C-34. Radioactive particle deposition density on and around the Hanford site, January 1956. Figure 4 from HW-43012.

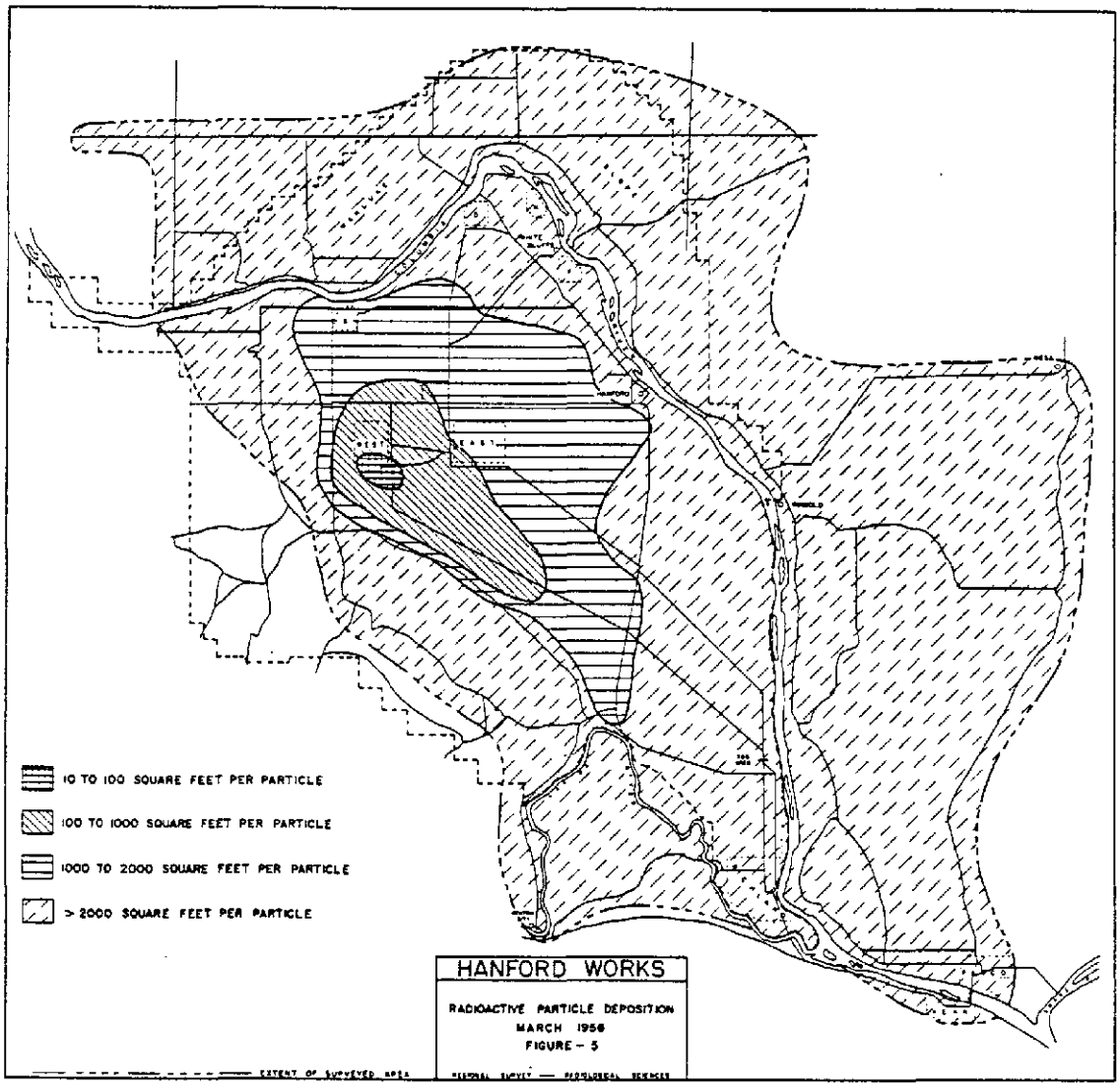

Figure C-35. Radioactive particle deposition density on and around the Hanford site, March 1956. Figure 5 from HW-43012.

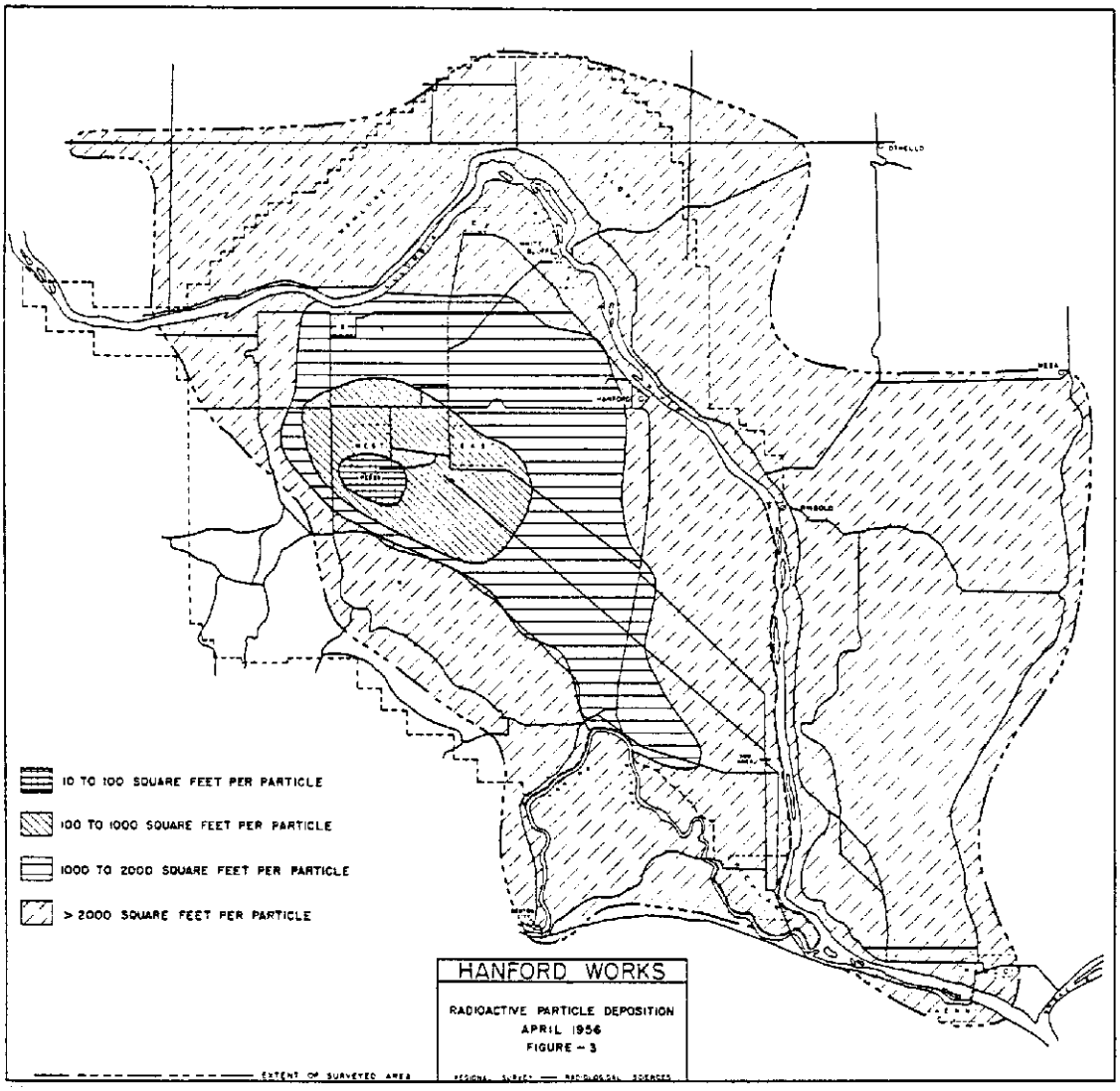

Figure C-36. Radioactive particle deposition density on and around the Hanford site, April 1956. Figure 3 from HW-44215.

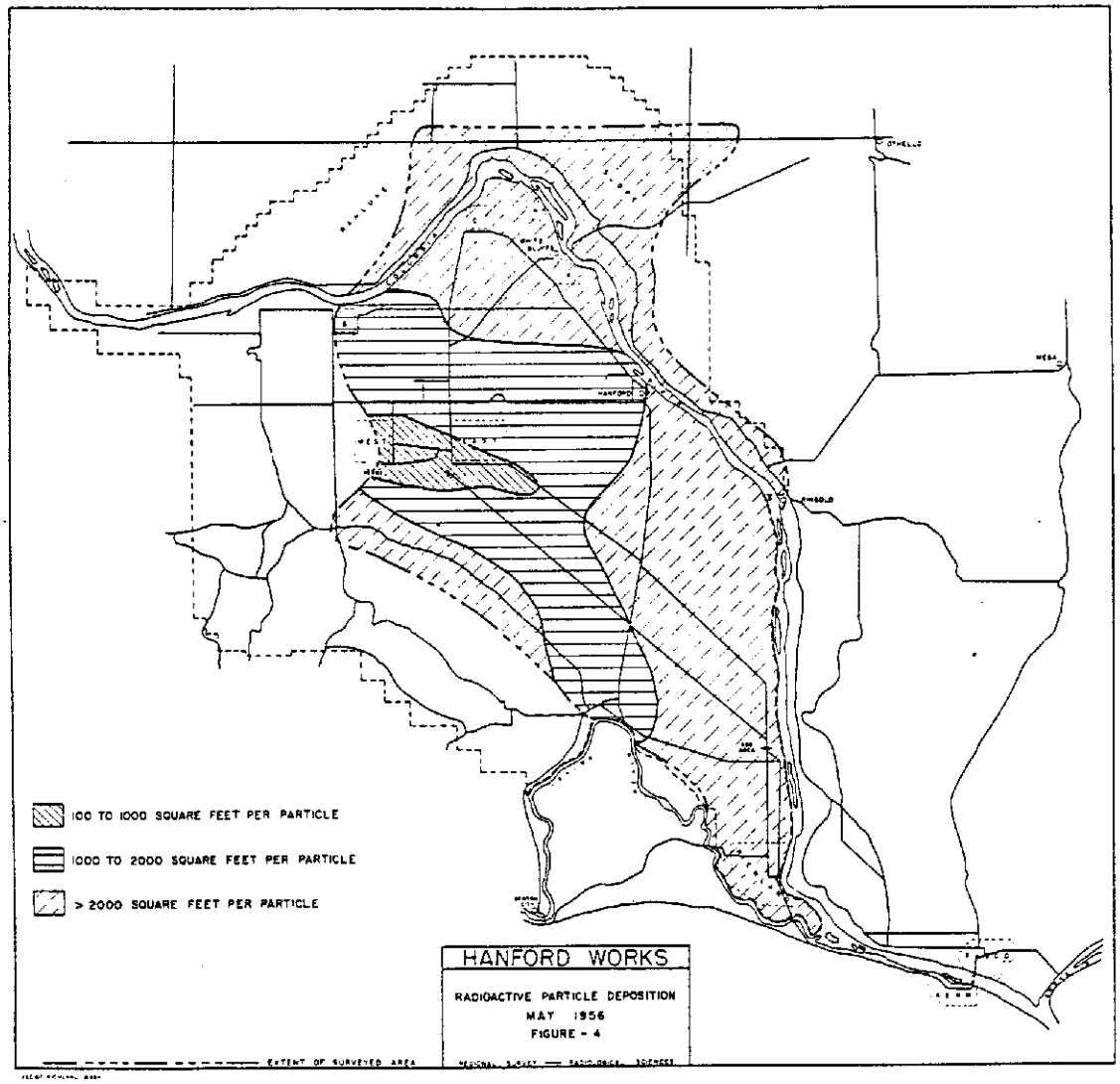

Figure C-37. Radioactive particle deposition density on and around the Hanford site, May 1956. Figure 4 from HW-44215.

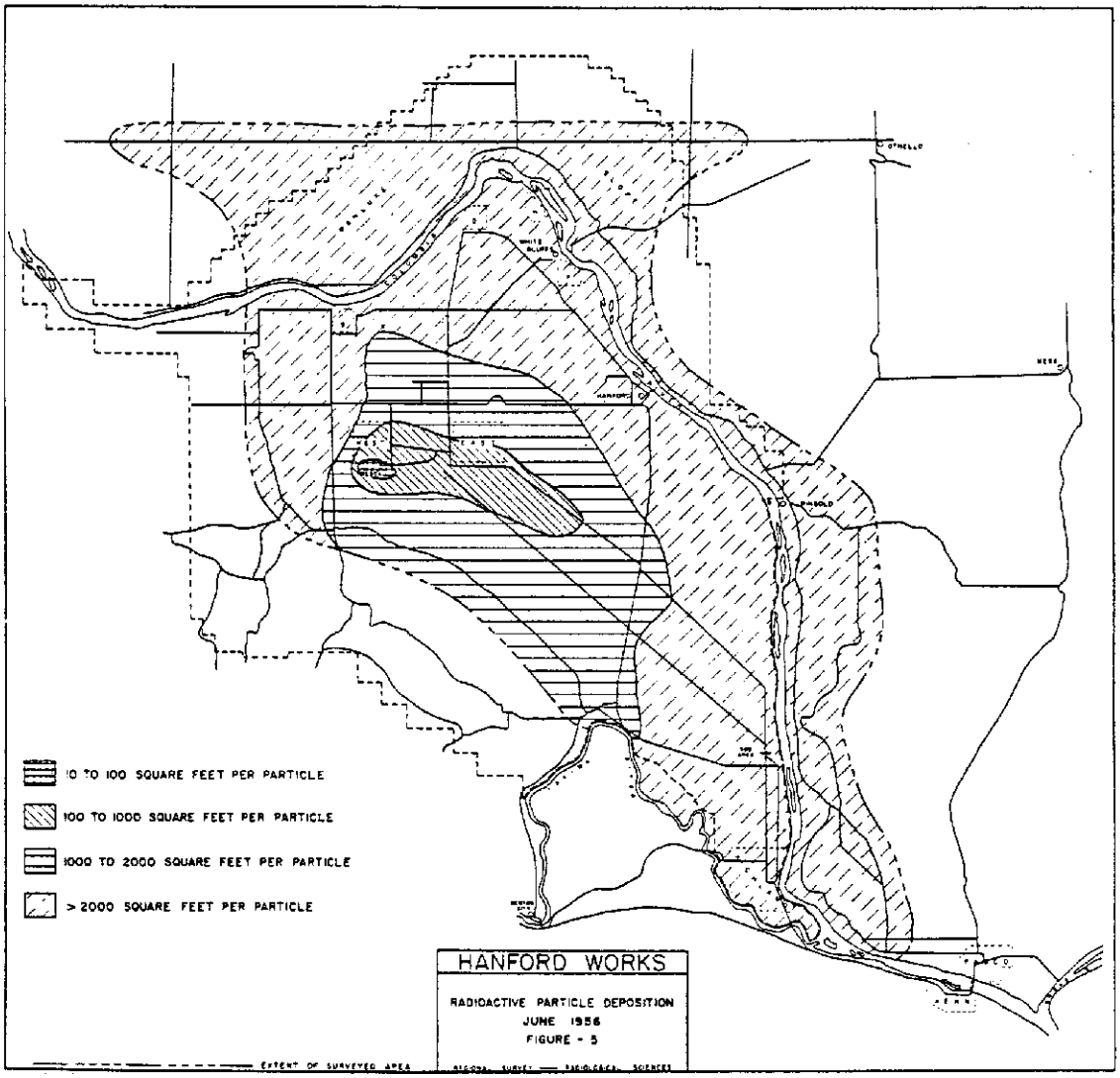

Figure C-38. Radioactive particle deposition density on and around the Hanford site, June 1956. Figure 5 from HW-44215.

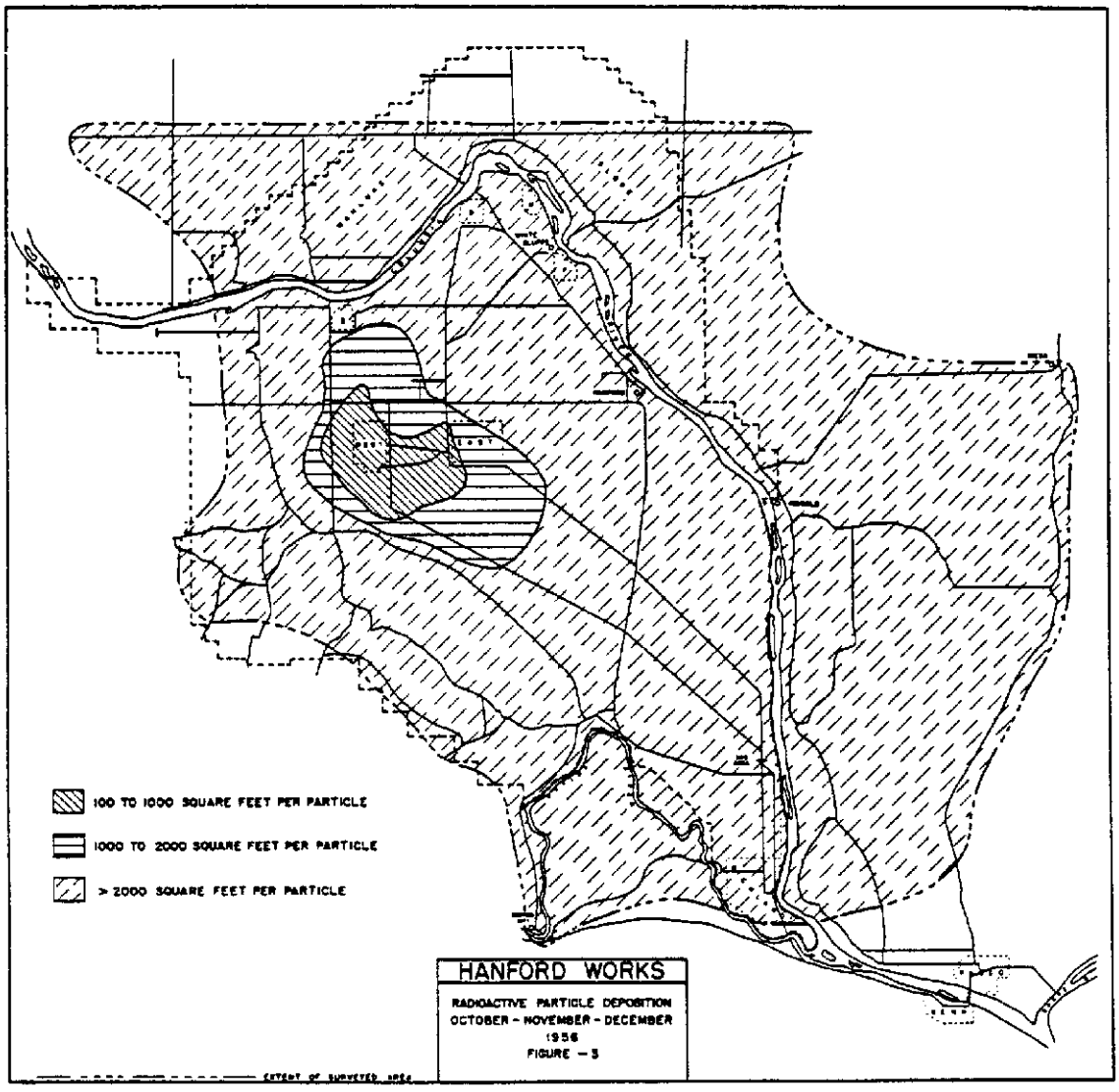

Figure C-39. Radioactive particle deposition density on and around the Hanford site, October–December 1956. Figure 3 from HW-48374.

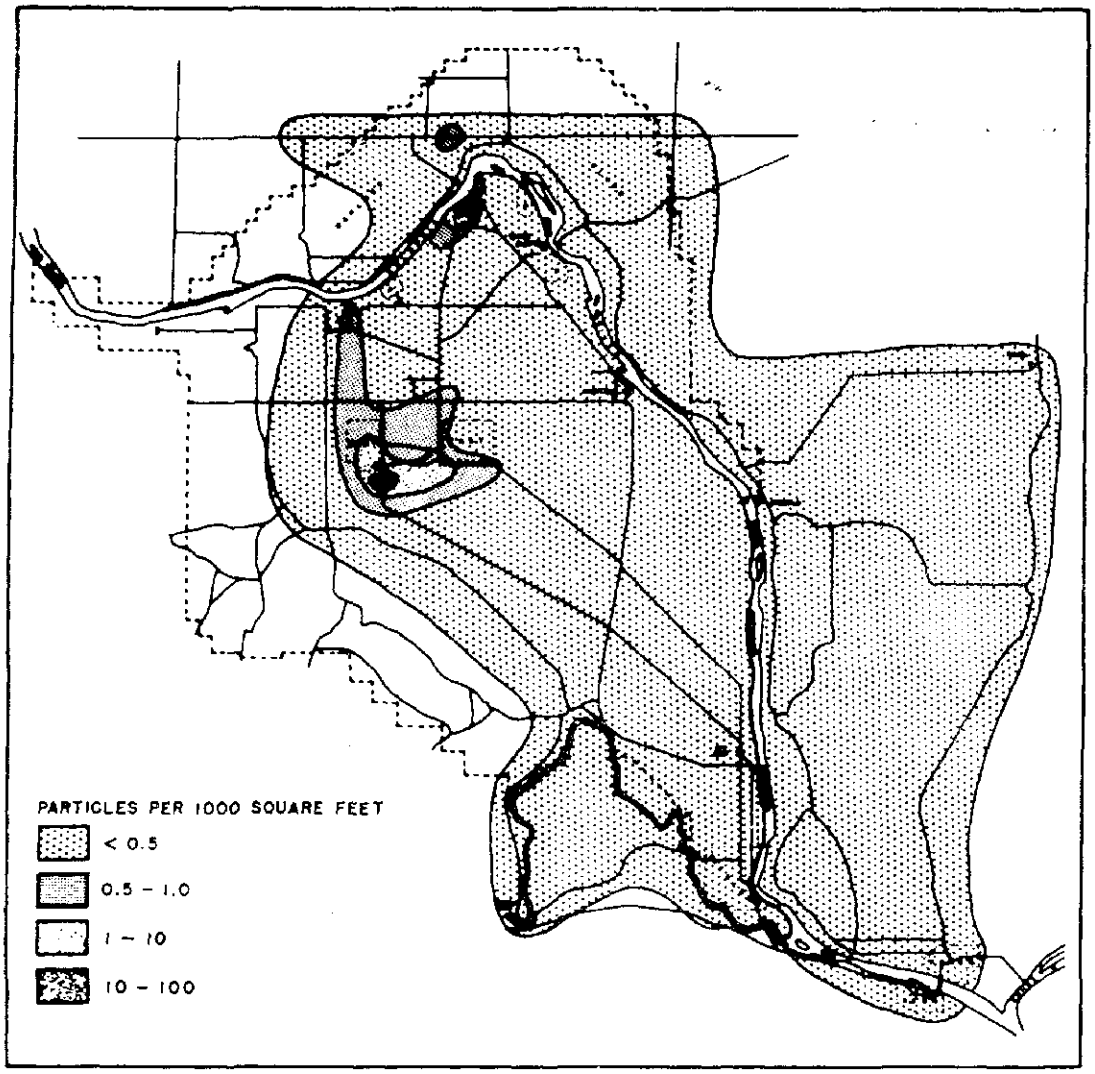

FIGURE 35
GROUND CONTAMINATION PATTERN
HANFORD AND VICINITY
FEBRUARY, 1957

Figure C-40. Radioactive particle deposition density on and around the Hanford site, February 1957. Figure 35 from HW-54636.

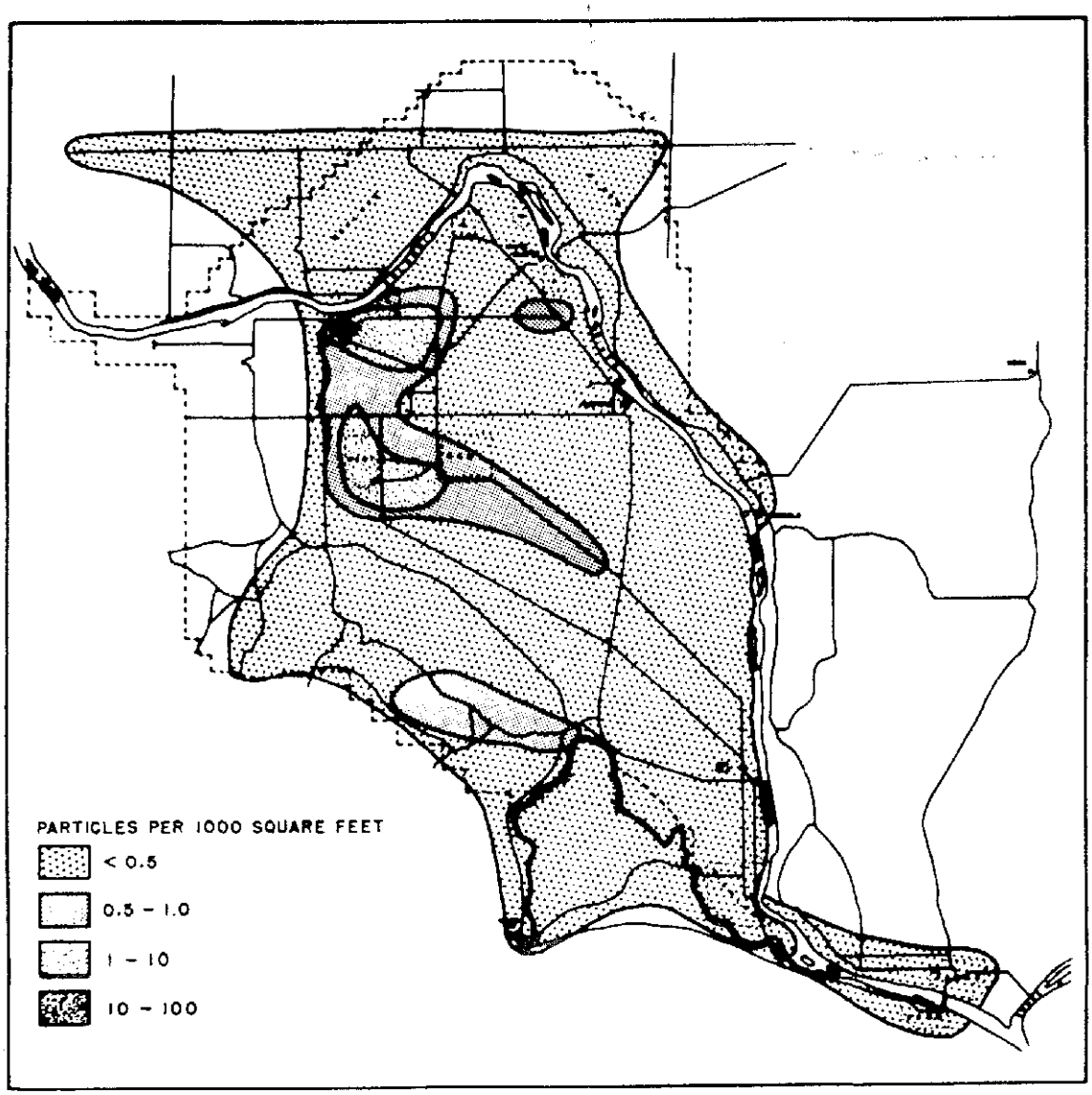

FIGURE 36
GROUND CONTAMINATION PATTERN
HANFORD AND VICINITY
APRIL, 1957

Figure C-41. Radioactive particle deposition density on and around the Hanford site, April 1957. Figure 36 from HW-54636.

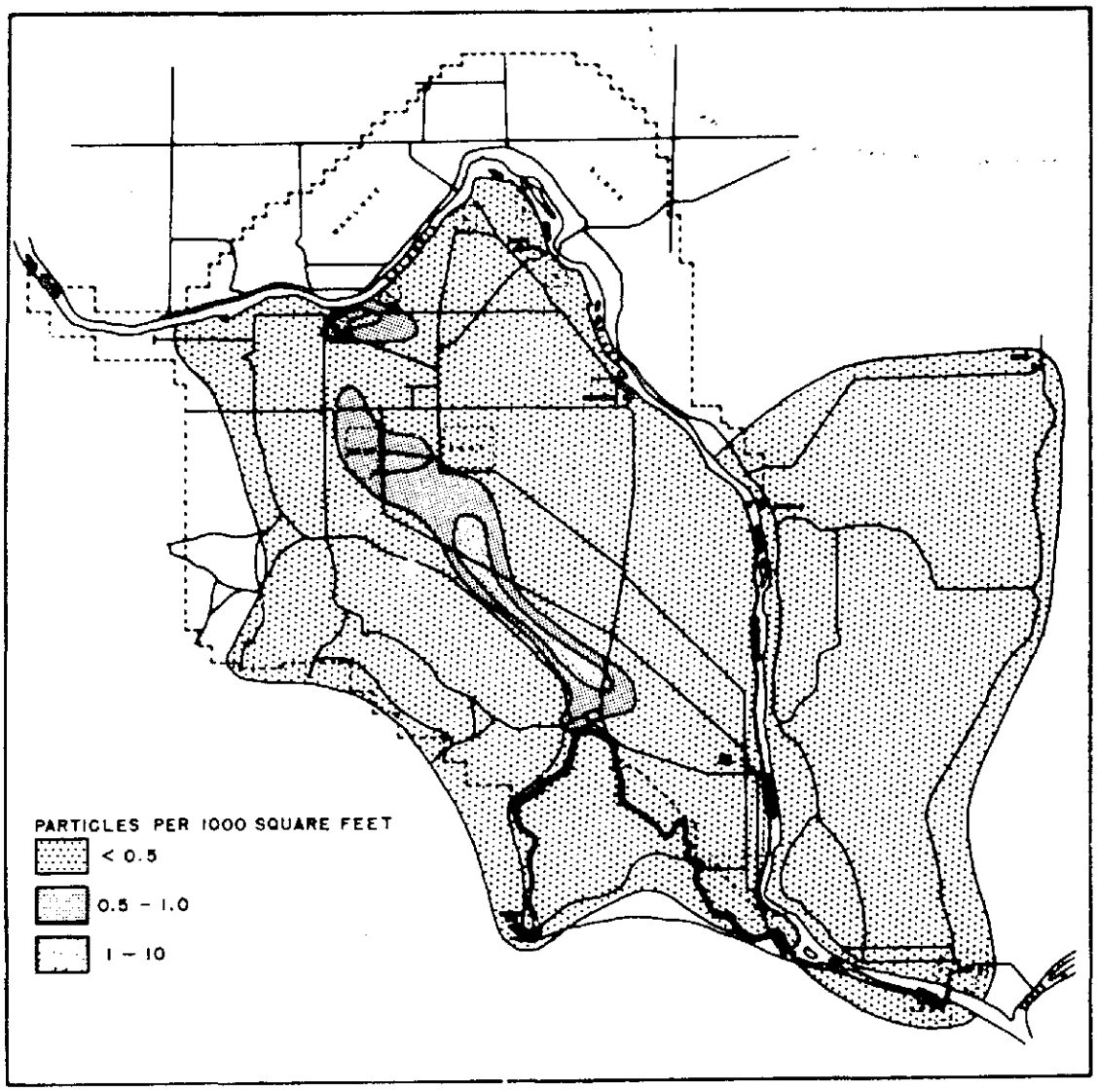

FIGURE 37
GROUND CONTAMINATION PATTERN
HANFORD AND VICINITY
AUGUST, 1957

Figure C-42. Radioactive particle deposition density on and around the Hanford site, August 1957. Figure 37 from HW-54636.

APPENDIX D

STOCHASTIC ESTIMATES OF AIR CONCENTRATION UNCERTAINTIES

D-1. INTRODUCTION

The draft version of this report described a methodology for estimating radiation dose from releases of radionuclides to the atmosphere from nuclear fuel processing plants and nuclear reactors on the Hanford reservation near Richland, Washington. Of particular concern were exposures of people on and near the site during the period 1945–1955 to short-lived airborne particulates. The Centers for Disease Control and Prevention (CDC) Radiation Studies Branch issued a task order for its contractor, Risk Assessment Corporation (RAC), to develop models and methods that could be applied to estimating radiation dose to individuals with known or assumed patterns of exposure during the specified period. The approach that was agreed upon involved the use of deterministic models of atmospheric diffusion and deposition of released radionuclides, with certain assumptions that would tend to increase the estimates, providing a deliberately conservative bias. For individuals residing near the site, the models were extended to include the ingestion of radionuclides associated with plant and animal products raised on their land. By agreement with the CDC, no stochastic modeling or analysis was undertaken, except that an indication of uncertainty (50th and 95th percentile) was provided for each month's release of each radionuclide from each facility.

In its review of the draft report, a committee of the National Research Council (NRC) criticized the approach, which the CDC had characterized in terms of the goal of "worst-case" estimates. This term can have quite different meanings, and the NRC committee referred to two of them. The first interpretation would be based on the behavior of a category of exposed subjects (e.g., military personnel on site) and would consider possible patterns of activity that would tend to maximize the dose estimate. The second interpretation concerns the methods for predicting exposure, particularly time-integrated concentrations of released radionuclides in the atmosphere at various locations on and near the site, with the range of the integration determined by an individual's presence at a particular location. The objective of this interpretation would be to construct models and methods that would tend to maximize estimates of dose for any specified subject behavior.

The NRC committee criticized what it considered the CDC's failure to provide more-realistic scenarios of exposure, although the draft report explained that the scenarios included were illustrations and did not correspond to known exposures of real people. RAC had proceeded with the understanding that the CDC would apply the models to its own data from the site and its own exposure scenarios. The committee also criticized the report for not estimating a high (e.g., 95th) percentile of dose corresponding to the expressed uncertainty in the source term, which was the only element of models or data that the report presented with a stochastic interpretation. The committee recommended extending the source term data into a model of the joint distribution of releases, together with a Monte Carlo implementation that presumably would convolute this model with the deterministic estimates of environmental transport and thus provide a distribution, for which the designated high percentile would furnish the desired "worst case."

RAC had originally discussed with the CDC the possible development of a full Monte Carlo analysis that would include parametric uncertainty for all parts of the release and transport models, together with an extended data analysis that would provide a basis for calibrating the atmospheric transport models, but this approach was rejected as too expensive for the scope of the task order. The deterministic approach taken is similar to many radiological assessments carried out in the 1970s for siting and licensing nuclear facilities. RAC adapted parts of the screening models of the National Council on Radiation Protection and Measurements (NCRP), which have been extensively reviewed and tend toward conservative estimates. But nothing in the approach for Task Order 3 was intended to provide stochastic estimates of uncertainty in calculated dose. We know no easy or completely straightforward way to reconcile the deterministic estimates that the adopted deterministic approach provides with the "worst-case" interpretation (second sense described in the previous paragraph) recommended by the NRC committee.

In paying attention only to the source term, the NRC committee appears to have overlooked the uncertainty in the Gaussian plume atmospheric diffusion model and in the use of 25-year-composite meteorological data from a period later than the one represented by the calculations. If the committee proposes to introduce stochastic analysis into the calculations, it must recognize that these other contributions to uncertainty in predicted air concentrations (on which all dose estimates proportionately depend) may be significant relative to the source-term uncertainties and should not be neglected. Other uncertain parameters affect the food pathway and must also be acknowledged as potential contributors to uncertainty, but (1) the quantification of these pathways in the Hanford assessment is still unclear and (2) we do not judge the magnitude of this uncertainty component to be competitive with the release-transport component for individuals whose primary exposure occurred on site. For the time being, at least, we set uncertainty for this pathway aside.

The purpose of this appendix is to propose a retrofitted stochastic analysis that considers the release and atmospheric transport of the set of radionuclides mentioned in the report, and estimates an uncertainty distribution for the time-integrated atmospheric concentration of each radionuclide for a specified period of exposure (no less than one year in the illustrations given here). The methods do not necessarily depend on Monte Carlo methods, although Monte Carlo calculations have been used to check them. No computer programs are provided; analysts will need to develop their own computational software.

In the coming sections, we frequently use the term "conservative" in what we feel should be obvious ways to readers having some familiarity with environmental dose and risk assessment. A deterministic estimate of exposure, dose, or risk is conservative relative to a standard counterpart if it exceeds the standard estimate (which may or may not have been actually computed). HCalc estimates, for example (Section 3.2), may neglect plume depletion due to deposition of airborne radioactivity from the plume, leading to a higher estimate of concentrtion of radioactivity in the air than would have been the case if depletion had been calculated. In this respect, the HCalc estimate of air concentration is conservative, even if the alternative to which a comparison is implied was never carried out.

For the stochastic modeling described in this appendix, the term takes on a different meaning. In this context, an estimate is a calculated probability distribution corresponding to a conceptual counterpart or target, usually represented by a model parameter or a component of exogenous input to the model (source term). We consider such a stochastic estimate conservative if a selected measure of its variance exceeds the corresponding variance of a standard stochastic estimate of its target

(which may be explicit or implied). But in making conservative estimates of model parameters and source term components by possibly increasing their variances, we also choose our procedures so that they tend to minimize bias in the chosen central statistic (for this work, the central statisitc is the 50th percentile). However, increasing the variances of model parameters and source term components can increase both the variance and the 50th percentile of the output distribution, and this phenomenon will be discussed and illustrated in this appendix.

The reader should be aware that it was necessary to base the illustrative calculations shown in this appendix on preliminary release estimates from most of the Hanford facilities. We have added cautionary footnotes to tables that present information that depends on the preliminary estimates. Since the primary purpose of the calculations is to illustrate the methods, we hope the preliminary estimates provide a sufficient basis. In an ideal world, development of this appendix would have been put off until the final data were ready, but the time required both tasks precluded that approach. We apologize for any inconvenience this might cause.

D-2. COMPONENTS OF UNCERTAINTY

In our analysis of uncertainty in source term and environmental transport, we first take the time-integrated air concentration of each released radionuclide as the endpoint. Combining air concentrations for different radionuclides and different points of release introduces complications involving correlations of random variables. We will discuss these complications in a later section (D-2.6), but we first lay the groundwork in a simpler context. We begin by considering the time integrated air concentration C of a single radionuclide released from a specific plant (or reactor), with the concentration being estimated at a fixed location. We represent the calculation by the equation

$$C = QX\zeta \tag{D-1}$$

where

C = time-integrated concentration (Bq s m^{-3}) of radionuclide at receptor location
Q = cumulative release (Bq) from the plant during the time considered
X = atmospheric diffusion factor (s m^{-3}), often called “Chi over Q”
ζ = random variable representing uncertainty associated with the use of available composite meteorological data for a recent period to represent earlier years for which data are sparse or lacking altogether (dimensionless).

The quantities Q and X are assumed to be random variables. The distribution of Q is based on our stochastic characterization of the monthly releases of radionuclides from the Hanford plants and reactors. The distribution of X is based on an extensive review of validation studies of Gaussian plume atmospheric diffusion models (Miller and Hively 1987). The random factor ζ is based on an analysis of 40 years of data from the Cincinnati Airport, in which predictions for all years using year specific data and a five-year composite for the late 1980s were compared (Killough and Schmidt 2000).

It has been necessary to confine the analysis in this appendix to exposure durations that are integral multiples of one year. In particular, the uncertainty analysis cannot be easily extended to exposures of less than one year. Although the source term distributions (Q) were worked out for each month, it is not straightforward to put the distributions of X and ζ on a similar time scale.

The study of Miller and Hively (1987) did consider some sampling times of one hour and others labeled as "short term" (unspecified), along with annual averages for various conditions, but it did not report experiments with sampling times approximating one month, and interpolation of the given distributions to estimate one for a one-month sampling time is not obvious. Moreover, for estimating ζ, we have no compilation comparable to the one of Killough and Schmidt (2000) to suggest the uncertainty of using a composite of annually-averaged meteorological data for specific periods of one month. However, the restriction to a series of year-long exposures should not be a serious limitation for the uncertainty analysis. Although the relative uncertainty for a fraction-of-a-year exposure may be large (and unknown), the level of exposure is relatively small and presumably less important than longer exposures that would fit into the "worst-case" concerns for scenarios of interest. Accordingly, our henceforth unstated assumption is that the time variable for exposure is an integer and counts years, and that all distributions are based on annual data. As we will see below, it is fairly straightforward to provide credible one-year distributions from the monthly source term compilations.

D-2.1 Stochastic Representation of the Source Term

The source term distributions are broken down by radionuclide, plant (or reactor, and hereafter we use "plant" generically for either), and month between November 1945 and February 1956. They are compiled in separate computer files that give, for each month, the 50th and 95th percentiles of an empirical distribution. For this appendix, we assumed that the distribution for each month is lognormal, and we used the two given percentiles to compute the geometric mean (GM) and geometric standard deviation (GSD):

$$\mathrm{GM} = n_{50\%}, \quad \mathrm{GSD} = (n_{95\%}/n_{50\%})^{1/1.64} \tag{D-2a}$$

where
1.64 = 95th percentile of the standard normal distribution (mean 0 and standard deviation 1)
$n_{x\%}$ = percentile x of the lognormal distribution, where $0 < x < 100$.

To summarize a file for each calendar year, we first computed the (arithmetic) mean α_i and (arithmetic) standard deviation β_i for each month ($i = 1, \ldots, 12$) by the formulas

$$\alpha_i = \mathrm{GM}_i \exp\left((1/2)\ln^2 \mathrm{GSD}_i\right), \quad \beta_i = \alpha_i \sqrt{\exp(\ln^2 \mathrm{GSD}_i) - 1} \tag{D-2b}$$

which are based on relationships given by Aitchison and Brown (1969). The notations α and β for the (arithmetic) mean and standard deviation of a lognormal distribution are adopted from the same reference. Assuming stochastic independence of the monthly distributions, we computed the mean and standard deviation of each year's release as the sum of the monthly means, and the square root of the sum of squares of the monthly standard deviations, respectively:

$$\alpha = \sum_{i=1}^{N} \alpha_i, \quad \beta = \left(\sum_{i=1}^{N} \beta_i^2\right)^{\frac{1}{2}} \tag{D-3}$$

where, for now, $N = 12$. The lack of correlation from month to month is intrinsic to the development of the distributions and is discussed elsewhere (Section 2.4). We mention here that for a particular

month and plant, releases of different radionuclides are highly correlated, but releases from different plants of the same or different radionuclides are assumed independent.

The distribution of a sum of lognormally distributed random variables is not, in general, lognormal. We know of no explicit analytic representation of this distribution. Some readers might be tempted to suggest an approximation based on the Central Limit Theorem, but in our experience such approximations based on a relatively small number of highly skewed distributions are very poor, and normal approximations have the added inconvenience of assigning nonzero probability to the negative numbers. In fact, for our purposes, a much better approximation is obtained from the lognormal distribution defined by the mean and standard deviation of the sum (Eq. (D-3)), even though we stress that this cannot be the exact distribution of the sum. The formulas for the GM and GSD of the sum, given the assumption of lognormality, are based on the inversion of Eq. (D-2b):

$$\mathrm{GM} = \frac{\alpha}{\sqrt{1 + (\beta/\alpha)^2}}, \quad \mathrm{GSD} = \exp\left(\sqrt{\ln\left(1 + (\beta/\alpha)^2\right)}\right) \tag{D-4}$$

where all symbols GM, GSD, α, and β are associated with the sum of the monthly random variables. We note that it often occurs that zero releases are recorded for some months; in such cases, the sum considers only the nonzero releases, and the number N of terms in the sum is less than 12.

As an example of the lognormal approximation for the sum of independently and lognormally distributed terms, Figure D-1 shows plots for sums of 12 monthly releases of ^{103}Ru from T Plant during 1945. The dashed line shows the lognormal approximation, based on the application of Eq. (D-4) to the analytically calculated mean (α) and standard deviation (β) of the sum. The irregular line is the empirical distribution of 1000 Monte Carlo trials for the sum (i.e., at each trial, the twelve monthly distributions are sampled independently, and the sample values are added; the sum is the sample for the trial). Comparison of an approximation with a single Monte Carlo realization leaves out of account the inherent variability of the Monte Carlo sampling procedure. To compensate for this shortcoming, we have computed nonparametric 99% confidence intervals about the Monte Carlo estimates of the 50th and 95th percentiles, using tables from Hahn and Meeker (1991). Table D-1 shows the data for the monthly release distributions, the lognormal approximation for the sum, and the 99% confidence intervals for the corresponding Monte Carlo estimates. The lognormal approximation estimates lie within the confidence intervals for the Monte Carlo percentiles, and there is good qualitative agreement between the two distributions, particularly between the 50th and 99th percentiles.

Table D-2 exhibits the annual lognormal release parameters (GM and GSD) for all radionuclides originating from B Plant, T Plant, Plant Z, and the REDOX Plant. These releases are tabulated for the calendar years 1945–1955. The tabulated parameters are based on the lognormal approximation discussed above for sums of months in which releases occurred, with lognormality being assumed for each month with a release. Table D-2 accounts for all radionuclides studied except ^{41}Ar, which was released from the Hanford reactors. Table D-3 shows annual lognormal parameters for releases of ^{41}Ar from Reactors B, C, D, DR, F, H, KE, and KW for the calendar years 1945–1955. Less stochastic detail is available for ^{41}Ar releases from the reactors. For each period indicated in Table D-3, the distribution shown should be interpreted as an annual rate for the entire period, and not a set of independent distributions for the individual years. This point is illustrated at the end of Section D-2.6.

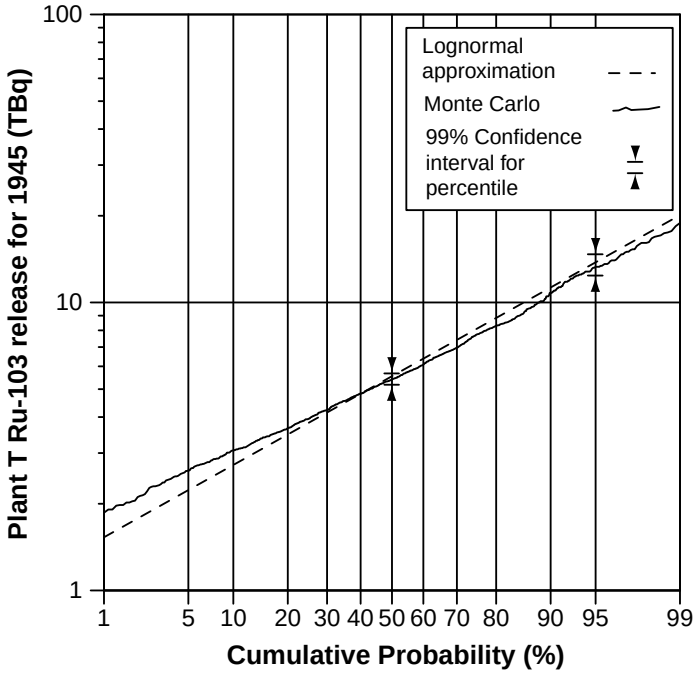

Figure D-1. Lognormal approximation to the sum of independent lognormal distributions for monthly releases of ^{103}Ru from T Plant during 1945 (dashed line). The irregular line represents the empirical Monte Carlo distribution for the same sum, with 1000 realizations. Confidence limits (99%) are indicated for the 50th and 95th percentiles of the Monte Carlo estimate. Table D-1 shows the data and numeric results.

D-2.2 Uncertainty Distribution for Atmospheric Dispersion

The factor X in Eq. (D-1) (sometimes denoted as χ/Q) has units s m^{-3} and represents, for specified source and receptor locations, the air concentration of a radionuclide divided by the release rate. The equivalent interpretation, and the one that we are mostly concerned with in this appendix, is the time-integrated air concentration divided by the cumulative release of the radionuclide during the specified time interval. The factor is specific to the source-receptor pair, the radionuclide released, and meteorological conditions during the release period (wind speed, wind direction, and atmospheric stability).

The Gaussian plume model used to estimate X is subject to error in predictions of an average value over a specified period. The distribution of error varies according to the length of the period, the terrain, the presence of peculiar meteorological regimes (such as conditions along a seacoast), distance from source to receptor, and possibly other factors. Miller and Hively (1987) compiled predicted-to-observed (P/O) ranges for Gaussian plume validations from many references representing a variety of observational conditions. Their study makes possible some quantification of the uncertainty attached to making atmospheric transport predictions such as the ones that come from the methodology developed in this report. The averaging period best covered by the sources of Miller and Hively (1987) is one year. Although they included some information for observatonal periods of one hour and some results from unspecified periods less than one year, this information is not a sufficient basis for the analysis we are attempting here, and it is difficult to see how it might serve as an inferential basis for uncertainty distributions for periods such as one month.

Table D-1. Monthly Release Estimates of ^{103}Ru from T Plant during 1945

Month	GM of Release (TBq)	GSD
Jan	0.0333	3.21
Feb	0.0481	3.23
Mar	0.0481	3.3
Apr	0.192	3.31
May	0.259	3.28
Jun	0.174	3.22
Jul	0.207	3.32
Aug	0.366	3.27
Sep	0.37	3.28
Oct	0.592	3.24
Nov	0.481	3.28
Dec	0.444	3.2

Lognormal approximation to sum:
GM (50th %ile) of sum: 5.54 TBq
GSD of sum: 1.74
95th %ile of sum: $5.54 \times 1.74^{1.64} = 13.7$

Monte Carlo simulation of sum:
99% CI for 50th %ile of sum: $(5.18, 5.67)$
99% CI for 95th %ile of sum: $(12.4, 14.7)$

[a] The ^{103}Ru releases shown in this table are based on preliminary estimates and may be inconsistent with releases or derived quantities presented in other parts of this report.

Accepting one year as the observational period, we find in Table 1 of Miller and Hively (1987) a P/O range of 0.5 to 2 for "annual average for a specific point, flat terrain, within 10 km downwind of the release point." This factor-of-two uncertainty seems reasonably applicable to the Hanford situation. The data are reported with a variance for their log-transformed data of 0.16. If the distribution is assumed to be lognormal, this would correspond to GSD 1.49. If the range limits of 0.5 and 2 are placed (conservatively) at the 5th and 95th percentiles of a lognormal distribution with GM = 1, the GSD is $2^{1/1.64} = 1.53$, just marginally larger than the value reported for the data (the chosen lognormal distribution has a five-percent tail above 2). We take this modification as the definition of uncertainty for the random variable X:

$$X = X_0 \cdot \eta, \quad \eta = \Lambda(1, 1.53) \tag{D-5}$$

where X_0 is the deterministically calculated dispersion factor and $\eta = \Lambda(1, 1.53)$ is a lognormally distributed random variable with GM = 1 and GSD = 1.53. The product is lognormally distributed

Table D-2. Annual Releases of Radionuclides 1945–1955 from Hanford Plants[a]

	B Plant GM (TBq)	GSD	T Plant GM (TBq)	GSD	Z Plant GM (TBq)	GSD	REDOX GM (TBq)	GSD
Ba-137m								
1945	1.95×10^{-1}	1.81	2.12×10^{-1}	1.80	0	—	0	—
1946	4.09×10^{-1}	1.62	2.39×10^{-1}	1.72	0	—	0	—
1947	2.45×10^{-1}	1.62	2.14×10^{-1}	1.61	0	—	0	—
1948	7.59×10^{-2}	2.10	6.56×10^{-2}	2.10	0	—	0	—
1949	2.00×10^{-3}	1.66	2.51×10^{-3}	1.62	0	—	0	—
1950	4.22×10^{-3}	1.62	3.90×10^{-3}	1.61	0	—	0	—
1951	5.64×10^{-3}	1.62	6.01×10^{-3}	1.61	0	—	0	—
1952	1.28×10^{-3}	2.16	3.79×10^{-3}	1.71	0	—	1.09×10^{-2}	1.68
1953	0	—	2.84×10^{-3}	1.65	0	—	1.86×10^{-2}	1.66
1954	0	—	5.60×10^{-3}	1.62	0	—	2.21×10^{-2}	1.65
1955	0	—	6.78×10^{-3}	1.62	0	—	2.51×10^{-2}	1.71
Ce-144								
1945	5.77	1.81	6.31	1.78	0	—	0	—
1946	1.15×10^{1}	1.62	6.35	1.69	0	—	0	—
1947	6.68	1.62	5.85	1.61	0	—	0	—
1948	1.94	2.12	1.67	2.10	0	—	0	—
1949	5.35×10^{-2}	1.65	5.98×10^{-2}	1.63	0	—	0	—
1950	1.01×10^{-1}	1.63	9.08×10^{-2}	1.62	0	—	0	—
1951	1.50×10^{-1}	1.62	1.64×10^{-1}	1.60	0	—	0	—
1952	3.47×10^{-2}	2.16	1.01×10^{-1}	1.71	0	—	2.81×10^{-1}	1.66
1953	0	—	7.65×10^{-2}	1.64	0	—	8.80×10^{-1}	2.33
1954	0	—	1.70×10^{-1}	1.62	0	—	5.79×10^{-1}	1.64
1955	0	—	1.96×10^{-1}	1.65	0	—	5.96×10^{-1}	1.66
Cs-137								
1945	1.95×10^{-1}	1.81	2.12×10^{-1}	1.80	0	—	0	—
1946	4.09×10^{-1}	1.62	2.39×10^{-1}	1.72	0	—	0	—
1947	2.45×10^{-1}	1.62	2.14×10^{-1}	1.61	0	—	0	—
1948	7.59×10^{-2}	2.10	6.56×10^{-2}	2.10	0	—	0	—
1949	2.00×10^{-3}	1.66	2.51×10^{-3}	1.62	0	—	0	—
1950	4.22×10^{-3}	1.62	3.90×10^{-3}	1.61	0	—	0	—
1951	5.64×10^{-3}	1.62	6.01×10^{-3}	1.61	0	—	0	—
1952	1.28×10^{-3}	2.16	3.79×10^{-3}	1.71	0	—	1.09×10^{-2}	1.68
1953	0	—	2.84×10^{-3}	1.65	0	—	1.86×10^{-2}	1.66
1954	0	—	5.60×10^{-3}	1.62	0	—	2.21×10^{-2}	1.65
1955	0	—	6.78×10^{-3}	1.62	0	—	2.51×10^{-2}	1.71

Continued next page.

with GM = X_0 and unchanged GSD = 1.53 (Aitchison and Brown 1969).

Table D-2. Annual Releases of Radionuclides 1945–1955 from Hanford Plants[a] (continued)

	B Plant GM (TBq)	GSD	T Plant GM (TBq)	GSD	Z Plant GM (TBq)	GSD	REDOX GM (TBq)	GSD
I-131								
1945	1.09×10^{4}	1.03	9.68×10^{3}	1.03	0	—	0	—
1946	2.75×10^{3}	1.03	8.36×10^{2}	1.03	0	—	0	—
1947	6.99×10^{2}	1.04	4.88×10^{2}	1.03	0	—	0	—
1948	3.59×10^{1}	1.03	3.26×10^{1}	1.03	0	—	0	—
1949	2.43×10^{1}	1.03	2.99×10^{2}	1.09	0	—	0	—
1950	1.43×10^{2}	1.49	1.94×10^{2}	1.40	0	—	0	—
1951	7.01×10^{2}	1.45	9.97×10^{2}	1.49	0	—	0	—
1952	5.69×10^{1}	1.63	1.30×10^{2}	1.45	0	—	1.31×10^{2}	1.38
1953	0	—	3.63×10^{1}	1.37	0	—	7.55×10^{1}	1.34
1954	0	—	2.97×10^{1}	1.40	0	—	2.29×10^{1}	1.35
1955	0	—	1.12×10^{1}	1.36	0	—	3.11×10^{1}	1.48
Pr-144								
1945	5.77	1.81	6.31	1.78	0	—	0	—
1946	1.15×10^{1}	1.62	6.35	1.69	0	—	0	—
1947	6.68	1.62	5.85	1.61	0	—	0	—
1948	1.94	2.12	1.67	2.10	0	—	0	—
1949	5.35×10^{-2}	1.65	5.98×10^{-2}	1.63	0	—	0	—
1950	1.01×10^{-1}	1.63	9.08×10^{-2}	1.62	0	—	0	—
1951	1.50×10^{-1}	1.62	1.64×10^{-1}	1.60	0	—	0	—
1952	3.47×10^{-2}	2.16	1.01×10^{-1}	1.71	0	—	2.81×10^{-1}	1.66
1953	0	—	7.65×10^{-2}	1.64	0	—	8.80×10^{-1}	2.33
1954	0	—	1.70×10^{-1}	1.62	0	—	5.79×10^{-1}	1.64
1955	0	—	1.96×10^{-1}	1.65	0	—	5.96×10^{-1}	1.66
Pu-239								
1945	6.32×10^{-3}	1.83	6.91×10^{-3}	1.79	0	—	0	—
1946	1.31×10^{-2}	1.63	7.58×10^{-3}	1.72	0	—	0	—
1947	7.95×10^{-3}	1.62	6.95×10^{-3}	1.62	0	—	0	—
1948	2.48×10^{-3}	2.14	2.11×10^{-3}	2.09	0	—	0	—
1949	7.20×10^{-5}	1.64	7.94×10^{-5}	1.63	7.27×10^{-5}	1.34	0	—
1950	1.30×10^{-4}	1.61	1.20×10^{-4}	1.61	1.12×10^{-4}	1.33	0	—
1951	1.70×10^{-4}	1.63	1.81×10^{-4}	1.61	1.81×10^{-4}	1.31	0	—
1952	3.82×10^{-5}	2.20	1.12×10^{-4}	1.70	2.06×10^{-4}	1.34	3.23×10^{-4}	1.66
1953	0	—	8.23×10^{-5}	1.66	3.09×10^{-4}	1.33	5.50×10^{-4}	1.64
1954	0	—	1.79×10^{-4}	1.61	3.53×10^{-4}	1.35	6.43×10^{-4}	1.65
1955	0	—	2.20×10^{-4}	1.64	4.70×10^{-4}	1.35	7.45×10^{-4}	1.68

Continued next page.

D-2.3 Uncertainty from Use of Composite Meteorological Data

The factor ζ in Eq. (D-1) may seem strange to the reader. Predictions of air concentrations by the program HCalc depend on a joint frequency table (JFT) that correlates discrete categories

Table D-2. Annual Releases of Radionuclides 1945–1955 from Hanford Plants[a] (continued)

	B Plant GM (TBq)	GSD	T Plant GM (TBq)	GSD	Z Plant GM (TBq)	GSD	REDOX GM (TBq)	GSD
Rh-103m								
1945	5.46	1.79	5.55	1.74	0	—	0	—
1946	7.76	1.61	3.59	1.73	0	—	0	—
1947	3.60	1.65	3.11	1.63	0	—	0	—
1948	6.60×10^{-1}	2.11	5.74×10^{-1}	2.09	0	—	0	—
1949	1.69×10^{-2}	1.65	2.00×10^{-2}	1.65	0	—	0	—
1950	3.62×10^{-2}	1.66	3.40×10^{-2}	1.64	0	—	0	—
1951	9.78×10^{-2}	1.62	1.10×10^{-1}	1.61	0	—	0	—
1952	2.33×10^{-2}	2.23	6.35×10^{-2}	1.77	0	—	2.03	2.19
1953	0	—	4.69×10^{-2}	1.63	0	—	1.83×10^{1}	2.89
1954	0	—	1.18×10^{-1}	1.64	0	—	4.34×10^{1}	2.97
1955	0	—	1.11×10^{-1}	1.67	0	—	1.63	1.61
Rh-106								
1945	6.41×10^{-1}	1.81	6.99×10^{-1}	1.80	0	—	0	—
1946	1.29	1.62	7.67×10^{-1}	1.73	0	—	0	—
1947	7.56×10^{-1}	1.63	6.62×10^{-1}	1.62	0	—	0	—
1948	2.24×10^{-1}	2.14	1.92×10^{-1}	2.12	0	—	0	—
1949	6.83×10^{-3}	1.65	7.57×10^{-3}	1.64	0	—	0	—
1950	1.41×10^{-2}	1.64	1.30×10^{-2}	1.63	0	—	0	—
1951	2.19×10^{-2}	1.63	2.33×10^{-2}	1.61	0	—	0	—
1952	5.29×10^{-3}	2.20	1.55×10^{-2}	1.72	0	—	8.09×10^{-1}	2.03
1953	0	—	1.10×10^{-2}	1.65	0	—	6.97	2.72
1954	0	—	1.99×10^{-2}	1.62	0	—	1.45×10^{1}	2.70
1955	0	—	2.22×10^{-2}	1.65	0	—	6.19×10^{-1}	1.62
Ru-103								
1945	5.46	1.79	5.55	1.74	0	—	0	—
1946	7.76	1.61	3.59	1.73	0	—	0	—
1947	3.60	1.65	3.11	1.63	0	—	0	—
1948	6.60×10^{-1}	2.11	5.74×10^{-1}	2.09	0	—	0	—
1949	1.69×10^{-2}	1.65	2.00×10^{-2}	1.65	0	—	0	—
1950	3.62×10^{-2}	1.66	3.40×10^{-2}	1.64	0	—	0	—
1951	9.78×10^{-2}	1.62	1.10×10^{-1}	1.61	0	—	0	—
1952	2.33×10^{-2}	2.23	6.35×10^{-2}	1.77	0	—	2.03	2.19
1953	0	—	4.69×10^{-2}	1.63	0	—	1.83×10^{1}	2.89
1954	0	—	1.18×10^{-1}	1.64	0	—	4.34×10^{1}	2.97
1955	0	—	1.11×10^{-1}	1.67	0	—	1.63	1.61

Continued next page.

of wind speed, wind direction, and atmospheric stability on the basis of hourly data taken during the period 1955–1980. Available published JFTs for Hanford are seasonal and annual (Stone et al. 1983), and the latter have been used for our calculations.

Table D-2. Annual Releases of Radionuclides 1945–1955 from Hanford Plants[a] (continued)

	B Plant GM (TBq)	GSD	T Plant GM (TBq)	GSD	Z Plant GM (TBq)	GSD	REDOX GM (TBq)	GSD
Ru-106								
1945	6.41×10^{-1}	1.81	6.99×10^{-1}	1.80	0	—	0	—
1946	1.29	1.62	7.67×10^{-1}	1.73	0	—	0	—
1947	7.56×10^{-1}	1.63	6.62×10^{-1}	1.62	0	—	0	—
1948	2.24×10^{-1}	2.14	1.92×10^{-1}	2.12	0	—	0	—
1949	6.83×10^{-3}	1.65	7.57×10^{-3}	1.64	0	—	0	—
1950	1.41×10^{-2}	1.64	1.30×10^{-2}	1.63	0	—	0	—
1951	2.19×10^{-2}	1.63	2.33×10^{-2}	1.61	0	—	0	—
1952	5.29×10^{-3}	2.20	1.55×10^{-2}	1.72	0	—	8.09×10^{-1}	2.03
1953	0	—	1.10×10^{-2}	1.65	0	—	6.97	2.72
1954	0	—	1.99×10^{-2}	1.62	0	—	1.45×10^{1}	2.70
1955	0	—	2.22×10^{-2}	1.65	0	—	6.19×10^{-1}	1.62
Sr-90								
1945	2.21×10^{-1}	1.83	2.41×10^{-1}	1.79	0	—	0	—
1946	4.64×10^{-1}	1.63	2.73×10^{-1}	1.71	0	—	0	—
1947	2.78×10^{-1}	1.62	2.45×10^{-1}	1.61	0	—	0	—
1948	8.76×10^{-2}	2.09	7.44×10^{-2}	2.10	0	—	0	—
1949	2.27×10^{-3}	1.66	2.83×10^{-3}	1.63	0	—	0	—
1950	4.78×10^{-3}	1.62	4.42×10^{-3}	1.61	0	—	0	—
1951	6.38×10^{-3}	1.62	6.90×10^{-3}	1.60	0	—	0	—
1952	1.47×10^{-3}	2.17	4.30×10^{-3}	1.71	0	—	1.25×10^{-2}	1.65
1953	0	—	3.23×10^{-3}	1.66	0	—	2.11×10^{-2}	1.65
1954	0	—	6.36×10^{-3}	1.62	0	—	2.51×10^{-2}	1.64
1955	0	—	7.80×10^{-3}	1.62	0	—	2.84×10^{-2}	1.70
Xe-131m								
1945	1.09×10^{4}	1.03	9.68×10^{3}	1.03	0	—	0	—
1946	2.75×10^{3}	1.03	8.36×10^{2}	1.03	0	—	0	—
1947	6.99×10^{2}	1.04	4.88×10^{2}	1.03	0	—	0	—
1948	3.59×10^{1}	1.03	3.26×10^{1}	1.03	0	—	0	—
1949	2.43×10^{1}	1.03	2.99×10^{2}	1.09	0	—	0	—
1950	1.43×10^{2}	1.49	1.94×10^{2}	1.40	0	—	0	—
1951	7.01×10^{2}	1.45	9.97×10^{2}	1.49	0	—	0	—
1952	5.69×10^{1}	1.63	1.30×10^{2}	1.45	0	—	1.31×10^{2}	1.38
1953	0	—	3.63×10^{1}	1.37	0	—	7.55×10^{1}	1.34
1954	0	—	2.97×10^{1}	1.40	0	—	2.29×10^{1}	1.35
1955	0	—	1.12×10^{1}	1.36	0	—	3.11×10^{1}	1.48

Continued next page.

An uncertainty analysis must take into account, in some way, the error introduced into predictions by the use of such data, rather than using a JFT based on the specific year in which a year's exposure occurred. The latter procedure, though seemingly the preferred approach, is often

Table D-2. Annual Releases of Radionuclides 1945–1955 from Hanford Plants[a] (continued)

	B Plant GM (TBq)	GSD	T Plant GM (TBq)	GSD	Z Plant GM (TBq)	GSD	REDOX GM (TBq)	GSD
Y-90								
1945	2.21×10^{-1}	1.83	2.41×10^{-1}	1.79	0	—	0	—
1946	4.64×10^{-1}	1.63	2.73×10^{-1}	1.71	0	—	0	—
1947	2.78×10^{-1}	1.62	2.45×10^{-1}	1.61	0	—	0	—
1948	8.76×10^{-2}	2.09	7.44×10^{-2}	2.10	0	—	0	—
1949	2.27×10^{-3}	1.66	2.83×10^{-3}	1.63	0	—	0	—
1950	4.78×10^{-3}	1.62	4.42×10^{-3}	1.61	0	—	0	—
1951	6.38×10^{-3}	1.62	6.90×10^{-3}	1.60	0	—	0	—
1952	1.47×10^{-3}	2.17	4.30×10^{-3}	1.71	0	—	1.25×10^{-2}	1.65
1953	0	—	3.23×10^{-3}	1.66	0	—	2.11×10^{-2}	1.65
1954	0	—	6.36×10^{-3}	1.62	0	—	2.51×10^{-2}	1.64
1955	0	—	7.80×10^{-3}	1.62	0	—	2.84×10^{-2}	1.70

[a] The releases shown in this table are based on preliminary estimates and may not be consistent with releases or derived quantities that appear in other parts of this report. Their use in this appendix is to illustrate the methods.

Table D-3. Annual Release of ^{41}Ar from Hanford Reactors

Reactor	Period	GM (TBq)	GSD
B	1945–1955	1.05×10^3	1.12
C	1952–1955	5.29×10^2	1.22
D	1945–1955	1.06×10^3	1.12
DR	1950–1955	2.60×10^2	1.25
F	1945	8.81×10^2	1.13
	1946–1955	1.05×10^3	1.12
H	1949	9.64×10^2	1.11
	1950–1955	3.88×10^3	1.05
KE	1955	2.51×10^3	1.08
KW	1955	3.22×10^3	1.09

impossible because of the unavailability of the desired data. In the case of Hanford, we know of no published source of individual JFTs for the years 1945–1955. It might have been possible to acquire unpublished hourly data taken at the site, but processing the voluminous data sets (even assuming they were in computer-readable form) would be a considerable task, and we were not asked to attempt this kind of resolution for this task order. Even so, a treatment of uncertainty should deal with this component in some way.

A similar problem — but one with different parameters — arose in connection with an earlier study, the Fernald Dosimetry Reconstruction Project. Data from the site of the former Feed Materials

Production Center (FMPC) had been collected for only about five years at the time the study began, and the calculations were based on an annual JFT that represented a composite of those five years' data. Killough and Schmidt (2000) used a 41-year surrogate data set from the Cincinnati Airport and a recent five-year composite JFT from that surrogate data set to compare composite predictions of past years with corresponding predictions based on JFTs for the specific years (such JFTs were available with the Cincinnati data, but not with the FMPC data). It was assumed that the uncertainty distribution so derived was applicable to the calculation with the five-year composite JFT from the FMPC site. The empirical distribution derived was represented by a lognormal distribution, with 95th/50th-percentile ratio equal to 2.

Application of the work of Killough and Schmidt (2000) to the present problem is not entirely straightforward. The Hanford JFT represents a composite of 25 years of hourly data rather than 5 years. The longer period offers less danger of bias for the long-term average, but it would reduce variability only for years of interest within the 1955–1980 period (and of the years considered here, only 1955 is within that period). Thus, it seems unlikely that the longer composite period would tend to reduce the uncertainty of estimates for specific years outside the composite range.

Some readers might also argue that the application to Hanford of a result based on Cincinnati data is questionable. If such a calculation had been carried out for Hanford, good practice would of course favor using the site-specific data. But in the absence of such data, we would argue that the results are likely more dependent on large-scale meteorological phenomena than on local meteorological characteristics. Although we might not expect close year-for-year correspondences between the two locations if Hanford had been analyzed in the same way as Cincinnati, we would expect no greater error in the overall result from the 25-year Hanford data set than from the 5-year data set from the Cincinnati Airport — i.e., we would consider the error factor based on the Cincinnati data likely to be conservative, and we proceed on that assumption.

Therefore, for this analysis, we adopt the factor-of-two lognormal distribution suggested by Killough and Schmidt (2000):

$$\zeta = \Lambda(1, 1.53)$$

where GSD $1.53 = 2^{1/1.64}$. This distribution for ζ gives 90% of observations within a factor of 2 of the geometric mean, which is taken as 1 because ζ is to be multiplied by another random variable that sets the magnitude of the product.

In applying the factor ζ, we assume that realizations of it are independent from year to year and from one receptor location to another. We will also consider realizations of ζ independent for two source-receptor pairs with the same receptor.

D-2.4 Uncertainty of Exposure for Specific Years and Sums of Years

Equation (D-1) may now be written

$$C_t = Q_t X_t \zeta_t, \quad \tilde{C} = \sum_{t=1}^{N} C_t \tag{D-6}$$

where t denotes the year of exposure and $\tilde{C}$ represents the time-integrated concentration over a given sequence of years. In taking the sum of random variables, as we indicate in the second equation of Eq. (D-6), we have to consider the possibility of correlations among terms representing (in our case) different years (autocorrelation). We have already mentioned the independence of different

realizations of the random variables ζ_t, and releases for different years — even the same radionuclide from the same plant — are assumed independent. The question is not so easily answered for the atmospheric dispersion factor X_t. Nothing in the information analyzed by Miller and Hively (1987) is likely to answer this question, and indeed, the question is fraught with difficulties about its exact meaning. For the time being, however, we prefer to postpone these difficulties and assume that X_{t_1} and X_{t_2} are independent for $t_1 \neq t_2$. We take up the question of correlations in Section D-2.5.

With these assumptions in mind, we state some relationships for the coefficient of variation (CV). These relationships provide useful interpretations for our results. The coefficient of variation, given by the ratio of the standard deviation to the mean (CV = β/α in the notation of Eqs. (D-2b), (D-3), and (D-4)) is ordinarily applied only to nonnegative random variables. For the lognormal distribution, the coefficient of variation depends only on the GSD and is given by

$$\mathrm{CV}^2 = \left(\frac{\beta}{\alpha}\right)^2 = \exp(\ln^2 \mathrm{GSD}) - 1 \tag{D-7}$$

which follows from the second member of Eq. (D-4). The coefficient of variation is useful as a measure of variability for distributions of nonnegative random variables. The CV of a sum of nonnegative and nonnegatively correlated random variables cannot exceed the maximum CV of any term of the sum:

$$\mathrm{CV}_{\mathrm{sum}} \leq \max_i \mathrm{CV}_i \tag{D-8}$$

If the terms are independent with equal means, the CV of the sum cannot exceed the maximum CV of any term divided by the square root of the number of terms:

$$\mathrm{CV}_{\mathrm{sum}} \leq \frac{1}{\sqrt{N}} \max_i \mathrm{CV}_i \tag{D-9a}$$

If, in addition to the assumptions for Eq. (D-9a), all GSDs (and therefore all CVs) for the terms are equal, we have

$$\mathrm{CV}_{\mathrm{sum}} = \frac{\mathrm{CV}}{\sqrt{N}} \tag{D-9b}$$

These results are sufficient for the time being.

Let us consider Eq. (D-6) applied to a succession $t = 1, \ldots, N$ years, with the assumption of independence of the terms for any pair of (distinct) years. Let us assume further that the release Q_t is the same constant $Q_t = q$ for all years considered, with a fixed GSD= g. Equation (D-5) gives us GM X_0 for the dispersion factor, with GSD 1.53. Let us factor out the product qX_0 and work with lognormal terms that have GM = 1. We have for the GSD of the product

$$\mathrm{GSD} = \exp\left(\sqrt{\ln^2 g + 2\ln^2 1.53}\right), \quad \mathrm{CV} = \sqrt{\exp(\ln^2 \mathrm{GSD}) - 1} \tag{D-10}$$

with the second equation coming from Eq. (D-7).

We work out an example of an application for some of the foregoing theory. Using ^{103}Ru releases from T Plant during 1945–1955, with a nominal X_0 value of 5.0×10^{-6} s m^{-3}, we have calculated the term for each year from the release distributions of Table D-2. Table D-4 shows the GM and GSD for each year. Each GM is the product of the annual release (Table D-2), dispersion factor X_0, and a conversion factor from TBq to Bq (10^{12}) to give units of Bq s m^{-3} at the receptor

Table D-4. Example: Air Concentration of ^{103}Ru From T Plant during 1945–1955[a]

Year	GM (Bq s m^{-3})	GSD
1945	2.77×10^7	2.3
1946	1.80×10^7	2.3
1947	1.55×10^7	2.2
1948	2.87×10^6	2.6
1949	9.98×10^4	2.2
1950	1.70×10^5	2.2
1951	5.49×10^5	2.2
1952	3.18×10^5	2.3
1953	2.35×10^5	2.2
1954	5.89×10^5	2.2
1955	5.57×10^5	2.2

A nominal dispersion factor $X_0 = 5 \times 10^{-6}$ s m^{-3} was used for this calculation. Plant-T release estimates for ^{103}Ru are given in Table D-2.

Distribution of the sum (lognormal approximation):
GM (50th %ile) = 8.19×10^7 Bq s m^{-3}, GSD = 1.64
95th %ile: $8.19 \times 10^7 \times 1.64^{1.64} = 1.84 \times 10^8$.

Monte Carlo–estimated percentiles for comparison

Percentile	Estimate	(99% confidence interval)
50th	8.23×10^7	$(7.84 \times 10^7, 8.64 \times 10^7)$
95th	1.86×10^8	$(1.69 \times 10^8, 2.06 \times 10^8)$

[a] The ^{103}Ru air concentrations shown in this table are derived from preliminary release estimates of ^{103}Ru from T Plant during the indicated period and thus may not be consistent with release estimates or derived quantities that appear in other parts of this report.

point. The GSD for each year is computed from the first equation of Eq. (D-10), with the value of g taken from the appropriate GSD entry in Table D-2.

To calculate the sum, we convert the GM and GSD for each term to a mean and standard deviation with Eq. (D-2b) and use Eq. (D-3) for the mean (α) and standard deviation (β) of the sum. Note that the calculated mean and standard deviation are correct for the exact distribution of the sum. It is when we use Eq. (D-4) to convert them to GM and GSD that we invoke the assumption of lognormality, which is approximate for the sum. However, the approximation in this case is very good, as we see from the addenda at the bottom of Table D-4. The approximations of the

50th and 95th percentiles match up well with their counterparts that we estimated with 1000 Monte Carlo trials. Confidence intervals (99%) for these Monte Carlo percentiles are given and include the respective lognormal approximations.

Notice that in the example just discussed, the sum of the geometric means is less than the geometric mean of the sum. This is a general property of sets of numbers. For example, if a sample of M measurements of air concentration is taken each year for N years, and arranged in N rows and M columns (with each row representing the sample for a year), then excluding very narrow exceptions, the sum of the sample geometric means is less than the geometric mean of the column sums (Hardy et al. 1959, Theorem 10). This is an important practical result for applying the uncertainty distributions we derive to the output of HCalc, for that output would frequently have the interpretation of a sum of geometric means, and *not* the geometric mean of the sum as desired. Thus, a method for adjusting the raw numbers will be needed for such cases. We develop this point further is Section D-2.6.

D-2.5 Effect of Correlations among Years on the Sum

In the previous sections, we have considered the distribution of a sum of independently distributed random variables representing one-year time-integrated air concentrations of a released radionuclide. The hypothesis of stochastic independence of the random variables implies that they are uncorrelated. The converse, in general, is not true, although it does hold for random variables with a multivariate normal distribution and in some other special cases. However, in this appendix, we have usually hypothesized that random variables be independent when uncorrelated would have been sufficient for the result.

We consider correlations among the atmospheric dispersion factors X_{t_1} and X_{t_2}, where $t_1 \neq t_2$. Previous discussion has indicated that the corresponding source term factors Q_t and meteorological data uncertainty factors ζ_t are assumed independent. Even so, the correlation of X_{t_1} and X_{t_2} induces a correlation of the respective terms C_{t_1} and C_{t_2} (Eq. (D-6)). Later in the section, we give a theorem that quantifies the relationship of these correlations, but for now we consider the correlation of the pairs of terms C_{t_1} and C_{t_2} generally.

Data for Hanford give little information about these correlations. We propose to study the effect of patterns of correlation on the distribution of the sum of C_t terms for a succession of years. There are many assumptions that we might make, but we will concentrate on a particular model of positive autocorrelation. We will assume that for a fixed coefficient $0 < \rho \leq 1$, the terms C_t and C_{t+k} ($k > 0$) have correlation coefficient ρ^k:

$$\rho_{C_t, C_{t+k}} = \rho^k, \quad k = 1, 2, \ldots \tag{D-11}$$

This assumption has physical plausibility, in that it implies that the correlation of terms decreases as their separation in time increases. This pattern is derived from a discrete Markov process by Kendall and Stuart (1968, Chapter 47). A continuous counterpart is often used as an approximation to unknown autocorrelation of wind speed over time in discussions of atmospheric diffusion: for two events separated by time $t > 0$, the autocorrelation is defined by $R(t) = \exp(-t/T)$, where T is a time-scaling factor (Hanna et al. 1982, Chapter 5).

When the terms of a sum of $N \geq 2$ random variables Y_i, $i = 1, \ldots, N$ are correlated, the mean

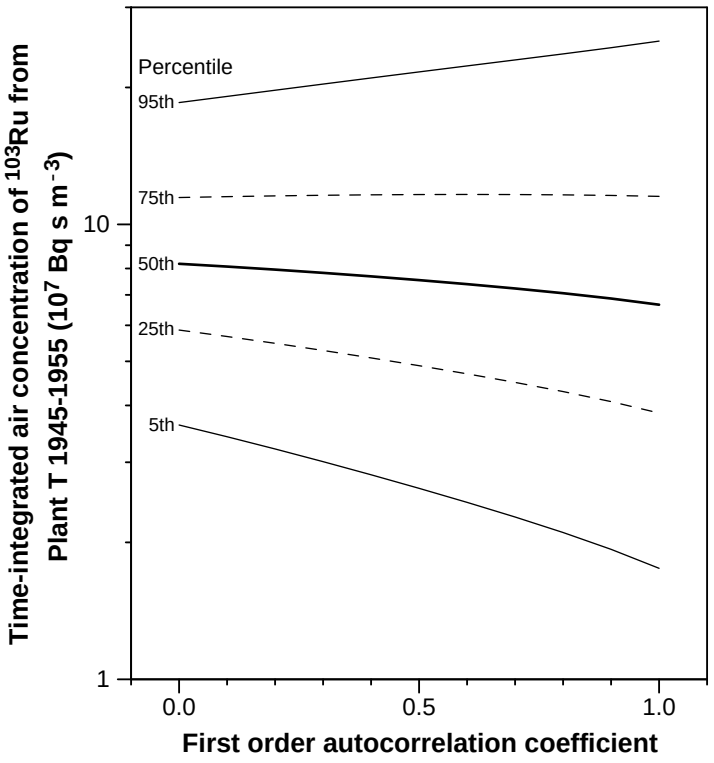

Figure D-2. Percentiles of the sum of annual time-integrated concentrations of ^{103}Ru from T Plant, 1945–1955, plotted against first-order autocorrelation coefficient ρ. Order k autocorrelation (between year t and year $t + k$) is assumed to be ρ^k. Calculations were made with a nominal atmospheric dispersion factor of 5×10^{-6} s m^{-3}. Table D-4 gives the GM and GSD for each year, which are based on preliminary data (see the footnote to Table D-4).

of the sum remains the sum of the means, but the variance of the sum is given by the equation

$$\sigma^2_{\text{sum}} = \sum_{i=1}^{N} \sigma_i^2 + 2 \sum_{i=2}^{N} \sum_{j=1}^{i-1} \rho_{i,j} \sigma_i \sigma_j \qquad \text{(D-12a)}$$

where σ_i denotes the standard deviation of Y_i. The formula in Eq. (D-12a) appears in textbooks of mathematical statistics (e.g., Wilks 1962) and is easily derived from manipulations with the expectation operator E. We use the σ notation to remind the reader that this result is general, and not restricted to the lognormal distribution as the β notation (adopted from Aitchison and Brown 1969) would suggest. We apply Eq. (D-12a) to compute the standard deviation of the sum and (as before) Eq. (D-4) to approximate the GM and GSD, assuming lognormality of the sum. Figure D-2 shows the percentiles of the sum of the annual time-integrated air concentrations of ^{103}Ru from T Plant (1945–1955) as a function of the first-order autocorrelation coefficient ρ, with values between 0 and 1 inclusive. We used the autocorrelation pattern given by Eq. (D-11) for the calculation.

The quantities graphed in Figure D-2 are an extension of the lognormal approximation discussed previously for the sum of independently distributed lognormal random variables. We were able to compare previous instances of this lognormal approximation to Monte Carlo–derived empirical

distributions based on the exact sampling distribution for the sum, but we are unable to provide a similar check for this extension of the approximation. An analogous Monte Carlo procedure is possible for the autocorrelated case, but the sampling distribution for each month is itself approximate. The mean, computed as the sum of the means of the terms, and the standard deviation, computed from Eq. (D-12a), are exact if the component means and standard deviations of the terms are. We still expect the lognormal assumption (Eqs. (D-3) and (D-4)) to lead to a qualitatively good approximation to the distribution of the sum, but we are unable to provide the same empirical checking as we could for the case with independent terms.

Figure D-2 shows clearly the evolution of the distribution of the sum as the autocorrelation coefficient of the terms increases from 0 through 1. Note that the 50th percentile decreases as the 95th percentile increases. However, our assumption that the first-order autocorrelation coefficient could be as large as 1 is overly pessimistic, given the structure of the terms. The following theorem quantifies the relationship:

Theorem D-1. *If random variables x_1 and x_2 are jointly distributed with correlation coefficient ρ_{x_1,x_2} and random variables y_1 and y_2 are independent of each other and of x_1 and x_2, then the products x_1y_1 and x_2y_2 are jointly distributed with correlation coefficient*

$$\rho_{x_1y_1,x_2y_2} = \frac{\rho_{x_1,x_2}\sigma_{x_1}\sigma_{x_2}\mu_{y_1}\mu_{y_2}}{[\sigma_{x_1}^2\sigma_{y_1}^2 + \sigma_{x_1}^2\mu_{y_1}^2 + \sigma_{y_1}^2\mu_{x_1}^2]^{1/2}[\sigma_{x_2}^2\sigma_{y_2}^2 + \sigma_{x_2}^2\mu_{y_2}^2 + \sigma_{y_2}^2\mu_{x_2}^2]^{1/2}}$$

where the symbols μ and σ represent the mean and standard deviation, respectively, of the random variables indicated by the subscripts. When the coefficients of variation exist and are positive, the formula can be rewritten as follows:

$$\rho_{x_1y_1,x_2y_2} = \frac{\rho_{x_1,x_2}\mathrm{CV}_{x_1}\mathrm{CV}_{x_2}}{[\mathrm{CV}_{x_1}^2\mathrm{CV}_{y_1}^2 + \mathrm{CV}_{x_1}^2 + \mathrm{CV}_{y_1}^2]^{1/2}[\mathrm{CV}_{x_2}^2\mathrm{CV}_{y_2}^2 + \mathrm{CV}_{x_2}^2 + \mathrm{CV}_{y_2}^2]^{1/2}}$$

where CV = σ/μ, *with corresponding subscripts.*

We know of no reference for Theorem D-1 in the literature, but it can be derived by elementary (if somewhat tedious) manipulations with the properties of the expectation operator E. It is useful to realize that the second formula of Theorem 1 shows that the correlation coefficient depends only on the CVs of the two random variables, and therefore, for lognormal distributions, only on the GSDs (Eq. (D-7)).

We apply Theorem D-1 by identifying x_1 and x_2 with the atmospheric dispersion factors X_t and X_{t+1} for successive years, and y_1 and y_2 with the products $Q_t\zeta_t$ and $Q_{t+1}\zeta_{t+1}$. To estimate the maximum autocorrelation for a pair of years, we put $\rho_{x_1,x_2} = 1$ and compute the remaining quantities on the right side of the equation. We have done this for each pair of successive years (1945–1955) for air concentration of ^{103}Ru from T Plant (annual data from Table D-4). The maximum correlation between terms for this radionuclide and plant is between 0.25 and 0.3. The latter value corresponds to GSD = 1.79 and 95th percentile $n_{95\%} = 7.82\times10^7\times1.79^{1.64} = 2.03\times10^8$ Bq s m^{-3} (cf. Figure D-2 for first-order autocorrelation coefficient = 0.3). For comparison, the GSD and 95th percentile for independent terms are 1.64 and $n_{95\%} = 8.19\times10^7\times1.64^{1.64} = 1.84\times10^8$ Bq s m^{-3} (cf. Figure D-2 with first order autocorrelation coefficient = 0). In the correlated case, the ratio $n_{95\%}/n_{50\%} = 2.60$; in the case of independent terms the corresponding ratio is 2.25. For this example, the proposed

autocorrelation model has a moderate effect on the uncertainty estimate, increasing $n_{95\%}/n_{50\%}$ by 16%.

We note two important special cases of Eq. (D-12a). If all $\rho_{i,j} = 0$, the equation reduces to

$$\sigma^2_{\text{sum}} = \sum_{i=1}^{N} \sigma_i^2 \tag{D-12b}$$

(uncorrelated terms) which, as we have previously noted, is implied by (but not equivalent to) pairwise stochastic independence of the terms. The second special case occurs if all pairs of terms are perfectly correlated, i.e. all $\rho_{i,j} = 1$:

$$\sigma^2_{\text{sum}} = \left(\sum_{i=1}^{N} \sigma_i \right)^2 \tag{D-12c}$$

Equations (D-12b) and (D-12c) correspond to the left and right endpoints, respectively, of the curves in Figure D-2.

D-2.6 An Extended Example

The collection of methods we have assembled so far falls short of an algorithm that will give an unambiguous set of steps for deriving any needed uncertainty distribution for quantities computed with HCalc. Such an algorithm will not be forthcoming in this appendix. Rather, we give here an illustration of the way an analyst might use the tools that we have derived to convert the outputs of HCalc into uncertainty distributions for a few quantities of particular interest. With more experience, some generalizations about related uncertainties are sure to emerge, and fewer explicit calculations should be necessary.

The data for the sample calculations are contained in Tables D-5 (Plant B) and D-6 (T Plant). They were calculated for receptor location H-61, which was a military anti-aircraft site on the Hanford reservation. The period of exposure is the years 1945 through 1948. The atmospheric dispersion factors for releases from B Plant and T Plant to this receptor are given in footnote a of Tables D-5 and D-6, respectively. We will show first how the theory and formulas discussed previously in this appendix were applied to the releases for each year to compute the time-integrated concentration for each radionuclide for the four-year period. Then we will consider the problem of combining receptor results for the two component sources to obtain the total time-integrated air concentration for each radionuclide. Finally, we will illustrate the procedure for combining an equivalent dose to an organ for each of the radionuclides into a total for the organ. In a non-stochastic calculation, this would be a simple matter of adding the component radionuclide doses, but we must consider the uncertainty distributions that are implicit in each component organ dose.

For each radionuclide in Tables D-5 and D-6, each year's release is converted to a time-integrated concentration (Bq s m^{-3}). We use the 1945 release of ^{103}Ru from B Plant in our example. The geometric mean is the product of the cumulative release for 1945 (5.46 TBq, taken originally from Table D-2) and the atmospheric dispersion factor 1.02×10^{-7} s m^{-3} (footnote a of Table D-5):

$$\text{GM} = 5.46 \text{ TBq} \times 1.02 \times 10^{-7} \text{ s m}^{-3} = 5.57 \times 10^{-7} \text{ TBq s m}^{-3}$$

The geometric standard deviation is calculated with Eq. (D-10) with $g = 1.79$ (= GSD of the release):

$$\text{GSD} = \exp\left(\sqrt{\ln^2 1.79 + 2 \ln^2 1.53} \right) = 2.31$$

Table D-5. B Plant Releases and Time-Integrated Concentrations of Radionuclides at Site H-61 (Military Anti-aircraft Site) 1945–1948[a,b]

	Release (TBq)		TBq s m^{-3}			
Year	GM	GSD	GM	GSD	Mean	Std. Dev.
Ru-103						
1945	5.46	1.79	5.57×10^{-7}	2.31	7.91×10^{-7}	7.97×10^{-7}
1946	7.76	1.61	7.92×10^{-7}	2.15	1.06×10^{-6}	9.51×10^{-7}
1947	3.60	1.65	3.67×10^{-7}	2.19	4.99×10^{-7}	4.58×10^{-7}
1948	6.60×10^{-1}	2.11	6.73×10^{-8}	2.61	1.07×10^{-7}	1.31×10^{-7}
Sum			2.16×10^{-6}	1.66	2.46×10^{-6}	1.33×10^{-6}
Ru-106						
1945	6.41×10^{-1}	1.81	6.54×10^{-8}	2.33	9.34×10^{-8}	9.53×10^{-8}
1946	1.29	1.62	1.32×10^{-7}	2.16	1.77×10^{-7}	1.60×10^{-7}
1947	7.56×10^{-1}	1.63	7.71×10^{-8}	2.17	1.04×10^{-7}	9.44×10^{-8}
1948	2.24×10^{-1}	2.14	2.28×10^{-8}	2.64	3.66×10^{-8}	4.57×10^{-8}
Sum			3.65×10^{-7}	1.63	4.11×10^{-7}	2.13×10^{-7}
I-131						
1945	1.09×10^{4}	1.03	1.11×10^{-3}	1.83	1.33×10^{-3}	8.81×10^{-4}
1946	2.75×10^{3}	1.03	2.80×10^{-4}	1.83	3.36×10^{-4}	2.22×10^{-4}
1947	6.99×10^{2}	1.04	7.13×10^{-5}	1.83	8.55×10^{-5}	5.66×10^{-5}
1948	3.59×10^{1}	1.03	3.66×10^{-6}	1.83	4.39×10^{-6}	2.90×10^{-6}
Sum			1.56×10^{-3}	1.63	1.76×10^{-3}	9.10×10^{-4}
Ce-144						
1945	5.77	1.81	5.89×10^{-7}	2.33	8.41×10^{-7}	8.58×10^{-7}
1946	1.15×10^{1}	1.62	1.17×10^{-6}	2.16	1.58×10^{-6}	1.42×10^{-6}
1947	6.68	1.62	6.81×10^{-7}	2.16	9.17×10^{-7}	8.26×10^{-7}
1948	1.94	2.12	1.98×10^{-7}	2.62	3.14×10^{-7}	3.88×10^{-7}
Sum			3.24×10^{-6}	1.63	3.65×10^{-6}	1.90×10^{-6}
Pu-239						
1945	6.32×10^{-3}	1.83	6.45×10^{-10}	2.35	9.27×10^{-10}	9.58×10^{-10}
1946	1.31×10^{-2}	1.63	1.34×10^{-9}	2.17	1.80×10^{-9}	1.64×10^{-9}
1947	7.95×10^{-3}	1.62	8.11×10^{-10}	2.16	1.09×10^{-9}	9.84×10^{-10}
1948	2.48×10^{-3}	2.14	2.53×10^{-10}	2.64	4.05×10^{-10}	5.06×10^{-10}
Sum			3.75×10^{-9}	1.63	4.23×10^{-9}	2.20×10^{-9}

[a] The dispersion coefficient (χ/Q) for emissions from B Plant to Site H-61 is 1.02×10^{-7} s m^{-3}.

[b] The releases in this table are based on preliminary estimates and may not be consistent with corresponding estimates shown elsewhere in this report.

Recall that 1.53 is the GSD of a factor-of-two lognormal distribution (i.e., $\chi_{95\%}/\chi_{50\%} = 2$). One such distribution represents the uncertainty of the atmospheric dispersion factor applied to the current year; the other represents uncertainty from applying composite meteorological data from a later period to the current year. The results of these calculations appear in the same line of Table D-5 with the 1945 release of ^{103}Ru.

The next step is the calculation of the (arithmetic) mean and standard deviation of the time-integrated air concentration. We continue with the same plant, radionuclide, and year. We apply the formulas of Eq. (D-2b):

$$\begin{aligned}\hat{\alpha}_{1945} &= 5.57 \times 10^{-7} \text{ TBq s m}^{-3} \times \exp\left(\tfrac{1}{2}\ln^2 2.31\right)\\ &= 7.91 \times 10^{-7} \text{ TBq s m}^{-3}\\ \hat{\beta}_{1945} &= 7.91 \times 10^{-7} \text{ TBq s m}^{-3} \times \sqrt{\exp(\ln^2 2.31) - 1}\\ &= 7.97 \times 10^{-7} \text{ TBq s m}^{-3}\end{aligned}$$

and repeat for years 1946–1948.

Now we compute the (arithmetic) mean and standard deviation for the sum of the years 1945–1948, using Eq. (D-3):

$$\begin{aligned}\hat{\alpha}_{\text{sum}} &= 7.91 \times 10^{-7} + 1.06 \times 10^{-6} + 4.99 \times 10^{-7} + 1.07 \times 10^{-7}\\ &= 2.46 \times 10^{-6} \text{ TBq s m}^{-3}\\ \hat{\beta}_{\text{sum}} &= \sqrt{(7.97 \times 10^{-7})^2 + (9.51 \times 10^{-7})^2 + (4.58 \times 10^{-7})^2 + (1.31 \times 10^{-7})^2}\\ &= 1.33 \times 10^{-6} \text{ TBq s m}^{-3}\end{aligned}$$

Note that the calculation of $\hat{\beta}_{\text{sum}}$ invokes the assumption of independence of the distributions for different years by using the second member of Eq. (D-3) or (D-12b).

The geometric mean and geometric standard deviation of the sum are estimated by approximating the sum of the lognormally distributed random variables for the years 1945–1948 with the lognormal distribution having the (arithmetic) mean and standard deviation just calculated. Using Eq. (D-4) gives

$$\begin{aligned}\text{GM}_{\text{sum}} &= 2.46 \times 10^{-6} \Big/ \sqrt{1 + (1.33 \times 10^{-6}/2.46 \times 10^{-6})^2}\\ &= 2.16 \times 10^{-6} \text{ TBq s m}^{-3}\\ \text{GSD}_{\text{sum}} &= \exp\left(\sqrt{\ln\left(1 + (1.33 \times 10^{-6}/2.46 \times 10^{-6})^2\right)}\right)\\ &= 1.66\end{aligned}$$

We repeat the warning that the exact distribution of the sum is not lognormal, but experience indicates that the approximation is acceptable (Table D-4).

For most applications, we will require the total time-integrated air concentation of each radionuclide at the receptor point, and thus we need to sum the component distributions from B Plant and T Plant. This is easily accomplished by applying Eq. (D-3) to the appropriate (arithmetic)

Table D-6. T Plant Releases and Time-Integrated Concentrations of Radionuclides at Site H-61 (Military Anti-aircraft Site) 1945–1948[a,b]

	Release (TBq)			TBq s m^{-3}					
Year	GM		GSD	GM		GSD	Mean		Std. Dev.	
Ru-103										
1945	5.55		1.74	1.10	10^{-6}	2.27	1.54	10^{-6}	1.50	10^{-6}
1946	3.59		1.73	7.14	10^{-7}	2.26	9.95	10^{-7}	9.64	10^{-7}
1947	3.11		1.63	6.19	10^{-7}	2.17	8.36	10^{-7}	7.58	10^{-7}
1948	5.74	10^{-1}	2.09	1.14	10^{-7}	2.59	1.80	10^{-7}	2.18	10^{-7}
Sum				3.11	10^{-6}	1.67	3.55	10^{-6}	1.95	10^{-6}
Ru-106										
1945	6.99	10^{-1}	1.80	1.39	10^{-7}	2.32	1.98	10^{-7}	2.01	10^{-7}
1946	7.67	10^{-1}	1.73	1.53	10^{-7}	2.26	2.13	10^{-7}	2.06	10^{-7}
1947	6.62	10^{-1}	1.62	1.32	10^{-7}	2.16	1.77	10^{-7}	1.60	10^{-7}
1948	1.92	10^{-1}	2.12	3.82	10^{-8}	2.62	6.07	10^{-8}	7.50	10^{-8}
Sum				5.75	10^{-7}	1.63	6.49	10^{-7}	3.38	10^{-7}
I-131										
1945	9.68	10^{3}	1.03	1.93	10^{-3}	1.83	2.31	10^{-3}	1.53	10^{-3}
1946	8.36	10^{2}	1.03	1.66	10^{-4}	1.83	1.99	10^{-4}	1.32	10^{-4}
1947	4.88	10^{2}	1.03	9.71	10^{-5}	1.83	1.16	10^{-4}	7.70	10^{-5}
1948	3.26	10^{1}	1.03	6.49	10^{-6}	1.83	7.78	10^{-6}	5.14	10^{-6}
Sum				2.27	10^{-3}	1.72	2.63	10^{-3}	1.53	10^{-3}
Ce-144										
1945	6.31		1.78	1.26	10^{-6}	2.30	1.78	10^{-6}	1.78	10^{-6}
1946	6.35		1.69	1.26	10^{-6}	2.22	1.74	10^{-6}	1.64	10^{-6}
1947	5.85		1.61	1.16	10^{-6}	2.15	1.56	10^{-6}	1.40	10^{-6}
1948	1.67		2.10	3.32	10^{-7}	2.60	5.24	10^{-7}	6.40	10^{-7}
Sum				4.99	10^{-6}	1.62	5.60	10^{-6}	2.87	10^{-6}
Pu-239										
1945	6.91	10^{-3}	1.79	1.38	10^{-9}	2.31	1.95	10^{-9}	1.97	10^{-9}
1946	7.58	10^{-3}	1.72	1.51	10^{-9}	2.25	2.09	10^{-9}	2.02	10^{-9}
1947	6.95	10^{-3}	1.62	1.38	10^{-9}	2.16	1.86	10^{-9}	1.68	10^{-9}
1948	2.11	10^{-3}	2.09	4.20	10^{-10}	2.59	6.60	10^{-10}	8.01	10^{-10}
Sum				5.84	10^{-9}	1.62	6.57	10^{-9}	3.37	10^{-9}

[a] The dispersion coefficient (χ/Q) for emissions from T Plant to Site H-61 is 1.99 10^{-7} s m^{-3}.

[b] The numbers in this table are based on preliminary release estimates and may not be consistent with estimates used elsewhere in this report.

Table D-7. Time-integrated Air Concentrations at Receptor H-61: Composite for B Plant and T Plant[a]

Radionuclide	GM (TBq s m^{-3})	GSD
Ru-103	5.59×10^{-6}	1.46
Ru-106	9.92×10^{-7}	1.44
I-131	4.07×10^{-3}	1.48
Ce-144	8.67×10^{-6}	1.43
Pu-239	1.01×10^{-8}	1.43

[a] The time-integrated air concentrations shown in this table are based on preliminary release estimates from B Plant and T Plant and may not be consistent with releases or derived quantities presented in other parts of this report.

mean and standard deviation of the sum from each of Tables D-5 and D-6. For ^{103}Ru, the following table gives the means α and standard deviations β for each of B Plant and T Plant and for the sum (in TBq s m^{-3}):

	α	β
B Plant	2.46×10^{-6}	1.33×10^{-6}
T Plant	3.55×10^{-6}	1.95×10^{-6}
Sum	6.01×10^{-6}	2.36×10^{-6}

Using the lognormal approximation (Eq. (D-4)) gives the composite distribution parameters

$$\begin{aligned} \text{GM} &= 6.01 \times 10^{-6} \Big/ \sqrt{1 + (2.36 \times 10^{-6}/6.01 \times 10^{-6})^2} \\ &= 5.59 \times 10^{-6} \text{ TBq s m}^{-3} \\ \text{GSD} &= \exp\left(\sqrt{\ln\left(1 + (2.36 \times 10^{-6}/6.01 \times 10^{-6})^2\right)}\right) \\ &= 1.46 \end{aligned}$$

for ^{103}Ru. Table D-7 summarizes these composite parameters for the two plants for the radionuclides shown in Tables D-5 and D-6.

A complication that arises in these calculations is the formation of radioactive decay products before release and as the released radionuclides move through the environment. HCalc handles these relationships automatically in the deterministic calculation, but it is necessary to look explicitly at the decay chains for this stochastic treatment. A complete discussion of the background is far beyond our scope in this appendix, and we have to rely on inferences the reader may draw from the examples shown here.

Table D-8 shows the decay chain for each of the radionuclides of Tables D-5 and D-6 (^{103}Ru, ^{106}Ru, ^{131}I, ^{144}Ce, and ^{239}Pu). This is not an exhaustive list of the repertory of HCalc, but it includes

Table D-8. Radionuclides and Decay Products for Examples[a]

Parent				Decay product		
Radionuclide	Half-life	Decay type	Branching fraction (%)	Radionuclide	Half-life	Decay type
Ru-103	39.35 d	β^-, γ	99.7	Rh-103m	56.119 m	IT
Ru-106	386.2 d	β^-	100	Rh-106	29.92 s	β^-, γ
I-131	8.04 d	β^-, γ	1.086	Xe-131m	11.84 d	IT
Ce-144	284.3 d	β^-, γ	98.57	Pr-144	17.28 m	β^-, γ
Pu-239	24,131 y	α, γ	100	U-235	7.038×10^8 y	α, γ

[a] Kocher (1981).

the radionuclides which, together with their decay chains, are likely to account for most of the dose by inhalation during the period covered by this example (1945–1948).

Radionuclide decay chains that are in equilibrium at the point of release tend to remain in secular equilibrium as they move downwind in the plume. The HCalc output table labeled "Exposure matrix for the scenario" shows the time-integrated air concentration for each radionuclide (in the "Primary air" column), and members of the same decay chain are grouped together in successive rows. The ruthenium-rhodium entries clearly indicate the equilibrium for this pair. Rhodium-106, formed from ^{106}Ru, however, is considered to give zero dose for the inhalation pathway because of the 30-s half-life of the rhodium decay product; the assumption is that there is insufficient time for significant absorption into body fluids to occur before the isotope decays to a stable element. For ^{131}I, the ^{131}Xe noble gas decay product is not considered important in the inhalation dose (relative to the iodine precursor), which is assumed to be negligibly absorbed in the body. ICRP dose coefficients assign zero inhalation dose to ^{131}Xe, although it is potentially important for external exposure. Plutonium-239 decays to ^{235}U, but the kinetics of the process are such that the amount of uranium produced in the time scale of the assessment is dosimetrically negligible. Thus, we neglect the uranium decay product. Cerium-144 decays to ^{144}Pr in 99% of its nuclear transformations; in the remainder, a metastable isomer of praseodymium is formed (^{144m}Pr), which promptly decays to ^{144}Pr. HCalc is not programmed to account for multiple branches, and the metastable branch is ignored (it is not shown in Table D-8).

In general, we adopt the principle of applying the same GSD to the time-integrated air concentrations of the parent radionuclide and its decay product, and moreover, assuming that the two are perfectly correlated. This point will be important in computing the distribution of dose to an organ from inhalation of the radionuclides or from external exposure to them in the ambient air. Table D-9 gives ICRP dose coefficients for inhalation and external dose from submersion in contaminated air for the radionuclides in Table D-8. We will show how to use these coefficients and the distributions of time-integrated air concentrations of the parent radionuclides to construct distributions of dose to each of several organs.

The dose coefficients in Table D-9 for external exposure convert time-integrated air concentrations of radionuclides directly to external dose accumulated during the exposure period. For

Table D-9. Dose Coefficients for Inhalation of and External Exposure to Airborne Radionuclides[a]

Radionuclide		Lungs	Bone Surface	Liver	Thyroid
Ru-103	Inhalation[b]	1.8×10^{4}	2.0×10^{2}	3.2×10^{2}	1.9×10^{2}
	External[c]	2.2×10^{-2}	3.9×10^{-2}	2.1×10^{-2}	2.2×10^{-2}
Rh-103m	Inhalation[b]	1.6×10^{1}	1.3×10^{-2}	1.2×10^{-2}	9.9×10^{-3}
	External[c]	1.9×10^{-6}	1.8×10^{-5}	3.7×10^{-6}	8.6×10^{-6}
Ru-106	Inhalation[b]	2.0×10^{5}	2.8×10^{3}	2.9×10^{3}	2.7×10^{3}
	External[c]	0	0	0	0
Rh-106	Inhalation[b,d]	0	0	0	0
	External[c]	1.0×10^{-2}	1.7×10^{-2}	9.6×10^{-3}	1.0×10^{-2}
I-131	Inhalation[b]	6.9×10^{2}	1.2×10^{2}	4.4×10^{1}	3.9×10^{5}
	External[c]	1.8×10^{-2}	3.5×10^{-2}	1.7×10^{-2}	1.8×10^{-2}
Xe-131m	Inhalation[b,e]	0	0	0	0
	External[c]	2.7×10^{-4}	1.1×10^{-3}	2.7×10^{-4}	3.9×10^{-4}
Ce-144	Inhalation[b]	1.9×10^{5}	4.9×10^{4}	1.4×10^{5}	1.8×10^{3}
	External[c]	7.7×10^{-4}	2.5×10^{-3}	7.2×10^{-4}	8.3×10^{-4}
Pr-144	Inhalation[b]	5.4×10^{1}	8.9×10^{-2}	1.6×10^{-1}	8.2×10^{-2}
	External[c]	1.9×10^{-3}	3.0×10^{-3}	1.8×10^{-3}	2.0×10^{-3}
Pu-239	Inhalation[b]	3.3×10^{7}	1.5×10^{9}	3.3×10^{8}	2.7×10^{6}
	External[c]	2.7×10^{-6}	9.5×10^{-6}	2.7×10^{-6}	3.9×10^{-6}
Ar-41	External[c]	6.38×10^{-2}	9.08×10^{-2}	6.16×10^{-2}	6.52×10^{-2}

[a] International Commission on Radiological Protection (ICRP).
[b] Sv TBq^{-1}.
[c] Sv s^{-1} (TBq m^{-3})$^{-1}$.
[d] Rh-106 is considered to deliver negligible internal dose from direct inhalation because its 30-s half-life is insufficient for significant absorption into body fluids. However, when it is formed from the decay of internalized ^{106}Ru, it contributes to dose, and this component is included in the dose coefficient of the parent.
[e] Xe-131m, like other noble gases, is considered to deliver negligible internal dose from inhalation because little of it is absorbed into body fluids during a breathing cycle.

inhalation, it is necessary first to assume an air-volume inhalation rate. For purposes of this example, we use B = 23 m^3 day^{-1} = 2.7×10^{-4} m^3 s^{-1}. The computations are

$$H_{\text{inhal}} = B \cdot D_{\text{inhal}} \cdot \tilde{C}_{\text{air}} \cdot U \quad \text{and} \quad H_{\text{extern}} = D_{\text{extern}} \cdot \tilde{C}_{\text{air}} \cdot U \tag{D-13}$$

where D_{inhal} and D_{extern} denote the appropriate dose coefficient from Table D-9, $\tilde{C}_{\text{air}}$ is the time-integrated air concentration of the radionuclide (TBq s m^{-3}), and B is air-volume inhalation rate (m^3 s^{-1}). The factor U accounts for the fraction of the exposure period that the subject is assumed to have been exposed (e.g., U = (8/24) × (6/7) × (50/52) for a subject who was at the receptor

location 8 hours per day, 6 days per week, 52 weeks per year). The factor U could also include other attenuations, such as for indoor locations.

We treat the dose coefficients as physical constants, even though they are calculated from model assumptions and parameters that are themselves uncertain. At this time, however, scientific consensus about the quantification and treatment of this source of uncertainty is lacking, and the questions involved are still under active discussion and debate. It is a subject that we cannot deal with in this task order. However, calculations performed with the principles outlined in this appendix could subsequently be extended to include probability distributions for the dose coefficients if that course seemed desirable.

The next phase of this extended example requires data from the output of the HCalc program, with input location, exposure period, and air-volume breathing rate identical to the values we have assumed. Tables D-10a, D-10b, and D-10c contain excerpts from the HCalc output that are relevant to the example. Some additional material has been left intact in the tables, even though it does not contribute.

Table D-10a shows the χ/Q values for Plants B and T and the radionuclides and decay products chosen for the example. Only the column of "Chi/Q" under the label "Radioactive" is relevant. Note that each parent radionuclide is followed by two lines for its decay product. For ^{103}Ru, the next line (which omits the plant identification) represents the quantity of ^{103m}Rh that would form in the plume from a unit release rate of the parent ^{103}Ru with no release of ^{103m}Rh. The following line, with the plant identification, refers to a release of the decay product itself without regard to the parent radionuclide. Both components of the decay product are necessary for accurate determination of the relative proportions of the activity of parent and decay product at the specified receptor location downwind. In this example, we have the parent and decay product in secular equilibrium at the point and time of release, which (for the decay chains involved) implies that approximately equal amounts of their radioactivity are released per unit time.

Note that the sum of the Chi/Q components of decay product ^{103m}Rh from B Plant (Table D-10a) is nearly equal to the value for ^{103}Ru from B Plant:

$$\underbrace{8.258 \times 10^{-8}}_{\text{formed in plume}} + \underbrace{1.948 \times 10^{-8}}_{\text{released}} \times \overbrace{\quad}^{^{103m}\text{Rh}} \approx \overbrace{1.022 \times 10^{-7}}^{^{103}\text{Ru}}$$

The small discrepancy is explained by the branching fraction 99.7% for ^{103}Ru $\rightarrow$ ^{103m}Rh shown in Table D-8 (the complementary fraction decays directly to nonradioactive ^{103}Rh). For this particular chain, if only ^{103}Ru were released, secular equilibrium would not be established during the time the plume takes to travel to receptor H-61. If it were, the first component in the sum would equal 99.7% of the ^{103}Ru on the right, and the second component on the left would be negligible. For this source term, the concentrations of parent and decay product should be considered perfectly correlated. From Table D-7, we see that the time-integrated concentration of ^{103}Ru from Plants B and T is GM = 5.59×10^{-6} with GSD = 1.46. For decay product ^{103m}Rh, we use GM = $0.997 \times 5.59 \times 10^{-6} = 5.57 \times 10^{-6}$ and GSD = 1.46.

We have laid the groundwork for estimating the distribution of dose to the receptor from releases of ^{103}Ru$\rightarrow$ ^{103m}Rh from Plants B and T.

Table D-10a. Excerpt of χ/Q from HCalc Output

Table of chi/Q and deposition/Q for scenario

Source ID	Nuclide	Radioactive Chi/Q s m^(-3)	Radioactive Dep/Q m^(-2)	Nonradioactive Chi/Q s m^(-3)	Nonradioactive Dep/Q m^(-2)
B-Plant	Ru-103	1.022E-07	1.508E-10	1.024E-07	1.511E-10
	Rh-103m	8.258E-08	1.243E-10		
B-Plant	Rh-103m	1.948E-08	2.623E-11	1.024E-07	1.511E-10
T-Plant	Ru-103	1.993E-07	2.844E-10	1.994E-07	2.846E-10
	Rh-103m	1.037E-07	1.542E-10		
T-Plant	Rh-103m	9.538E-08	1.299E-10	1.994E-07	2.846E-10
B-Plant	Ru-106	1.024E-07	1.51E-10	1.024E-07	1.511E-10
	Rh-106	1.024E-07	1.51E-10		
B-Plant	Rh-106	4.751E-24	3.18E-27	1.024E-07	1.511E-10
T-Plant	Ru-106	1.994E-07	2.846E-10	1.994E-07	2.846E-10
	Rh-106	1.994E-07	2.846E-10		
T-Plant	Rh-106	1.947E-15	1.344E-18	1.994E-07	2.846E-10
B-Plant	I-131	1.015E-07	1.496E-10	1.024E-07	1.511E-10
	Xe-131m	6.969E-12	1.061E-14		
B-Plant	Xe-131m	1.018E-07	1.501E-10	1.024E-07	1.511E-10
T-Plant	I-131	1.987E-07	2.835E-10	1.994E-07	2.846E-10
	Xe-131m	5.505E-12	8.245E-15		
T-Plant	Xe-131m	1.989E-07	2.839E-10	1.994E-07	2.846E-10
B-Plant	Ce-144	1.024E-07	1.51E-10	1.024E-07	1.511E-10
	Pr-144	9.977E-08	1.481E-10		
B-Plant	Pr-144	2.621E-09	2.971E-12	1.024E-07	1.511E-10
T-Plant	Ce-144	1.994E-07	2.846E-10	1.994E-07	2.846E-10
	Pr-144	1.739E-07	2.546E-10		
T-Plant	Pr-144	2.555E-08	3E-11	1.994E-07	2.846E-10
B-Plant	Pu-239	1.024E-07	1.511E-10	1.024E-07	1.511E-10
T-Plant	Pu-239	1.994E-07	2.846E-10	1.994E-07	2.846E-10

The inhalation dose GM for the pair ^{103}Ru↔^{103m}Rh is computed as follows, using dose coefficients from Table D-9 and air-volume inhalation rate $B = 2.7 \times 10^{-4}$ m^3 s^{-1}:

$$2.7 \times 10^{-4} \times (1.8 \times 10^{4} \times 5.59 \times 10^{-6} + 16 \times 5.57 \times 10^{-6}) = 2.72 \times 10^{-5} \quad \text{Sv}$$

The calculation for external dose to the lungs from ^{103}Ru↔^{103m}Rh is similar but without the breathing rate factor:

$$2.2 \times 10^{-2} \times 5.59 \times 10^{-6} + 1.9 \times 10^{-6} \times 5.57 \times 10^{-6} = 1.23 \times 10^{-7} \quad \text{Sv}$$

Table D-10b. Excerpt of Time-Integrated Radioactivity from HCalc Output[a]

Duration of exposure for the scenario: 1.26144E+08 s (48 months)
Exposure matrix for the scenario

	Time-integrated radionuclide concentrations					
Radionuclide	Primary air (Bq s m^(-3))	Resuspended air (Bq s m^(-3))	Surface soil (Bq s m^(-2))	Fresh vegetables (Bq s kg^(-1))	Milk (Bq s L^(-1))	Meat (Bq s kg^(-1))
Sr-90	1.58E+05	32.2	1.61E+10	1.3E+04	3.06E+07	1.53E+08
Y-90	1.58E+05	32.2	1.61E+10	103	2.25E+03	2E+04
Ru-103	2.49E+06	35.4	1.77E+10	4.19E+04	1.08E+06	3.86E+07
Rh-103m	2.49E+06	35.4	1.77E+10	2.67E+04	2.67E+04	2.67E+04
Ru-106	4.4E+05	44.4	2.22E+10	1.15E+04	2.8E+05	2.77E+07
Rh-106	4.4E+05	44.4	2.22E+10	1.15E+04	1.15E+04	1.15E+04
I-131	3.64E+09	1.06E+04	5.29E+12	1.44E+07	1.81E+11	4.7E+11
Xe-131m	3.65E+09	1.56E+04	7.8E+12	2.46E+07	722	722
Cs-137	1.39E+05	28.4	1.42E+10	8.89E+03	6.81E+07	3.4E+08
Ba-137m	1.39E+05	28.4	1.42E+10	3.96E+03	3.96E+03	3.96E+03
Ce-144	3.86E+06	329	1.65E+11	9.62E+04	3.6E+06	2.37E+06
Pr-144	3.86E+06	329	1.65E+11	8.77E+04	8.77E+04	8.77E+04
Pu-239	4.48E+03	0.939	4.7E+08	120	155	1.55E+04
Ar-41	3.51E+08	0	0	1.69E-39	0	0

[a] The calculation results shown in this table are based on preliminary release estimates and may not be consistent with results shown in other parts of this report.

The GSD of the time-integrated concentration of the parent radionuclide (1.46) should be used for the dose delivered by the chain.

At this point, we need to call attention to what may appear to the reader to be an error. Table D-7 shows time-integrated air concentrations (geometric means) that differ markedly from the corresponding deterministic HCalc-computed quantities in Table D-10b (after units conversion). For example, the value shown in Table D-7 for ^{103}Ru is 5.59×10^{-6} TBq s m^{-3}, whereas the counterpart in Table D-10b is equivalent to 2.49×10^{-6} TBq s m^{-3}. However, we have previously alluded to the fact that the sum of geometric means is in general less than the geometric mean of the sum. HCalc proceeds in monthly increments, and its sums depend on sums of geometric means of the monthly releases for each year. We will continue the example of this section by analyzing such a calculation and showing how an adjustment factor may be developed for application to the deterministic sums.

First we need some theory for estimating the ratio of the geometric mean of the sum of independent lognormally distributed variables (GM_{sum}) to the sum of the geometric means ($\sum_i GM_i$). We consider the case for which the GSDs (and therefore the CVs) of the terms are all equal. We have from Eq. (D-9b) and Eq. (D-4)

$$GM_{sum} = \frac{\sum_{i=1}^{N} \alpha_i}{\sqrt{1 + CV_{sum}^2}}, \quad GM_i = \frac{\alpha_i}{\sqrt{1 + CV^2}} \tag{D-14}$$

where CV (without subscript) is the common value of the coefficients of variation of the terms. The desired ratio can be expressed as

$$\frac{GM_{sum}}{\sum_{i=1}^{N} GM_i} = \frac{\sum_{i=1}^{N} \alpha_i \Big/ \sqrt{1 + CV_{sum}^2}}{\sum_{i=1}^{N} \alpha_i \Big/ \sqrt{1 + CV^2}} = \sqrt{\frac{1 + CV^2}{1 + CV_{sum}^2}} \tag{D-15}$$

We wish to find the maximum value of this ratio under the given hypotheses, i.e., to determine the minimum value of CV_{sum}, leaving CV fixed and allowing the geometric means (and therefore the arithmetic means α_i) to vary. From Eq. (D-12b), we may derive

$$CV_{sum}^2 = \frac{\beta^2}{\alpha^2} = \sum_{i=1}^{N} \varphi_i^2 \left(\frac{\beta_i}{\alpha_i}\right)^2 = CV^2 \sum_{i=1}^{N} \varphi_i^2 \qquad \text{(D-16a)}$$

where

$$\varphi_i = \frac{\alpha_i}{\sum_{j=1}^{N} \alpha_j} \quad \text{so that} \quad \sum_{i=1}^{N} \varphi_i = 1\,. \qquad \text{(D-16b)}$$

Thus CV_{sum}^2 is minimum for the set of means $\{\alpha_i: 1 \le i \le N\}$ for which $\sum_{i=1}^{N} \varphi_i^2$ is minimum subject to the constraint that the sum of the φ_i is 1. The answer is well known to be $\varphi_1 = \cdots = \varphi_N = 1/N$, which implies $\alpha_1 = \cdots = \alpha_N$. One can derive this result by a formal technique such as Lagrange multipliers. One can also verify the assertion directly by showing that any set of perturbations $\{1/N + \epsilon_i\}$ satisfying the constraint of Eq. (D-16b) has a sum of squares greater than $\sum 1/N^2 = 1/N$ unless all $\epsilon_i = 0$.

Substitution of $\varphi_i = 1/N$ in Eq. (D-16a) gives the minimum value $CV_{sum}^2 = CV^2/N$. Thus we may substitute in Eq. (D-15) and write the inequality

$$\frac{GM_{sum}}{\sum_{i=1}^{N} GM_i} \le \left(\frac{1 + CV^2}{1 + CV^2/N}\right)^{1/2} \qquad \text{(D-17)}$$

which can serve to adjust deterministically calculated sums of geometric means. In applications where the condition of equal coefficients of variation is not exactly fulfilled, one might take the common value CV as the mean of the CV_i.

There is another case that supports a conservative shortcut. We have already assumed equality of the coefficients of variation: $CV_i = CV$, $i = 1, \ldots, N$. If, in addition, all terms are perfectly correlated ($\rho_{C_t, C_{t+k}} = 1$), then from Eq. (D-12c), we see that

$$CV_{sum}^2 = \left(\frac{\beta}{\alpha}\right)^2 = \left(\sum_{i=1}^{N} \varphi_i CV\right)^2 = CV^2 \left(\sum_{i=1}^{N} \varphi_i\right)^2 = CV^2 \qquad \text{(D-18)}$$

where the definition of φ_i is given by Eq. (D-16b). Substituting $CV_{sum}^2 = CV^2$ in Eq. (D-15) gives

$$\frac{GM_{sum}}{\sum_{i=1}^{N} GM_i} = 1 \qquad \text{(D-19)}$$

i.e., the geometric mean of the sum of perfectly correlated terms with equal coefficients of variation equals the sum of the geometric means. We would apply this result as an approximation to cases where the CV_i (and therefore the GSD_i) vary moderately for near–perfectly correlated terms. However, we have already demonstrated that near-perfect correlation of the C_t, C_{t+k} is unlikely for the stochastic model we are using (Section D-2.5, text following Theorem D-2). Of the three factors Q_t, X_t, and ζ_t (Eq. (D-6)), our model considers correlation of only the X_t factors from year to year and temporal independence of Q_t and ζ_t. Therefore, using Eqs. (D-18) and (D-19) as a lognormal distribution for a time-integrated air concentration will give a somewhatt higher estimate of CV_{sum}

Table D-10c. Excerpt of Committed Effective Dose from HCalc Output[a]

Table of committed EFFECTIVE dose (Sv)

Radionuclide	Inhalation	Ingestion: Food	Soil	External exposure: Air	Ground
Sr-90	1.37E-06	0	0	9.94E-13	7.92E-10
Y-90	5.32E-08	0	0	2.51E-11	2.23E-08
Ru-103	1.43E-06	0	0	4.67E-08	2.54E-06
Rh-103m	1.49E-09	0	0	1.68E-11	3.83E-10
Ru-106	2.95E-06	0	0	0	0
Rh-106	0	0	0	3.81E-09	1.45E-06
I-131	0.0174	0	0	5.52E-05	0.000616
Xe-131m	0	0	0	1.18E-06	1.26E-05
Cs-137	1.54E-07	0	0	8.99E-13	7.27E-10
Ba-137m	0	0	0	3.35E-09	2.58E-06
Ce-144	3.33E-05	0	0	2.75E-09	7.91E-07
Pr-144	1.67E-08	0	0	6.28E-09	1.92E-06
Pu-239	5.37E-05	0	0	1.58E-14	1.18E-11
Ar-41	0	0	0	1.9E-05	0
Totals	0.0175	0	0	7.55E-05	0.000638

Grand total (all pathways): 0.0182427 Sv

[a] The dose estimates shown in this table are based on preliminary release estimates and may not be consistent with doses appearing in other parts of this report.

(or GSD_{sum}) than other methods developed in this appendix. We will illustrate this point in Section 3.2.

We consider the deterministic time-integrated air concentration from Table D-10b for ^{103}Ru ("Primary air" column): 2.49×10^{6} Bq s m^{-3} = 2.49×10^{-6} TBq s m^{-3}. For the period considered (1945–1948), this quantity is the result of releases from Plant B and T Plant. Table D-11 gives, for ^{103}Ru releases from B Plant and T Plant for each of these years, the number of months for which a release was recorded (12 in all cases except B Plant in 1945), the average of monthly coefficients of variation, the composite coefficient of variation for the year (i.e., for the sum of the months), and the value of the right member of Eq. (D-11), which bounds the geometric mean of the sum divided by the sum of the geometric means. We will use some of the information in Table D-11 to estimate an adjustment factor for the deterministically calculated 2.49×10^{-6} TBq s m^{-3}. Note first that from Table D-7, the stochastic counterpart of this number is 5.59×10^{-6} TBq s m^{-3}, giving a ratio of 2.24. This value is a direct calculation of the left member of Eq. (D-17).

We are going to make some approximations to shorten the calculation of an upper bound for the ratio. The maximum bound for the ratio for any year and plant (last column of Table D-11) is 1.81. Let us settle on this value as representative for all years' releases from both plants.

Now we must consider the stochastic properties of the atmospheric dispersion (factors X and ζ in our previous notation, Eq. (D-6)). We are adding results for two plants and four years = 8 terms. The composite CVs for the releases fall in the range 0.5–0.9, and we will use the larger for the bounding ratio. The corresponding GSD = $\exp\sqrt{\ln(1+0.9^2)}$ = 2.16 (Eq. (D-4)). The

composite GSD for the three factors is GSD = $\exp\sqrt{\ln^2 2.16 + 2\ln^2 1.53}$ = 2.66 (Eq. (D-10)). The corresponding CV = $\sqrt{\exp(\ln^2 2.66) - 1}$ = 1.27 (Eq. D-7). And thus, for the eight terms,

$$\left(\frac{1 + 1.27^2}{1 + 1.27^2/8}\right)^{1/2} = 1.47$$

Finally, our bound for the ratio of Eq. (D-17) is 1.81 × 1.47 = 2.66. This compares with the accurately calculated ratio of 2.24 given in the previous paragraph. This example suggests that similar computations might be expected to produce a somewhat conservative adjustment to the deterministically calculated results from HCalc.

The reader might wonder about the composite CVs for 1948 in Table D-11. What might seem an anomaly is due to an abrupt decrease in the magnitudes of releases after April. The decrease is roughly two orders of magnitude, leaving a sum that is dominated by the first four terms. This significantly affects the composite CV for the year. Since we used an upper bound composite CV influenced by this situation (0.9), our computed bound for the ratio is larger than it might otherwise have been. If we give less weight to the 1948 composite CVs and settle on an intermediate effective composite CV of 0.6, the result of calculating the bound by the method shown above is 2.39, which may be compared with the directly calculated ratio 2.24.

We close this example section with some remarks about ^{41}Ar releases. The reader will note in Table D-3 that the annual reactor releases of ^{41}Ar show GSDs that are generally smaller than those for other radionuclides released from the (non-reactor) plants. This phenomenon is a function of the level of detail in which the ^{41}Ar releases were treated during the main phase of the dose reconstruction. Even though the tabulation presents the distribution parameters for ^{41}Ar as annual quantities, we recommend that they be handled as representative of a longer term, and that (for a given reactor) they be considered perfectly correlated from year to year.

For example, let us consider releases from Reactor B from 1945 through 1948 (Table D-3). For the H-61 location we are considering, HCalc gives the χ/Q value of 7.00×10^{-8} s m^{-3}. For 4 years, the GM is $1.05 \times 10^3 \times 4 = 4.20 \times 10^3$ TBq released. The time-integrated concentration is $4.20 \times 10^3 \times 7.00 \times 10^{-8} = 2.94 \times 10^{-4}$ TBq s m^{-3}, with GSD 1.12. We are treating the release distribution as if it represented a long-term parameter, which effectively it does, even though it is tabulated as if it represented a sequence of annual distributions.

The extended example of this section covers a lot of ground, suggesting several ways of inferring stochastic estimates from the deterministic outputs of HCalc (these methods are summarized in Section D-3.3). To be sure, these procedures would be quite laborious for hand calculation, and one would expect some use of a computer to be necessary for most analyses. One might develop spreadsheet templates for typical conversions, using release data tabulated in this appendix (Table D-2). Or one might use a scripting language, such as PERL, with the capability of searching the files of release quantities. We have made no attempt to design such a process, because we believe it cannot be done usefully without more knowledge of how it would be used.

The deterministic outputs of HCalc are quite useful in providing extensive breakdowns of dose estimates that would possibly become prohibitively voluminous and unmanageable if most output quantities were treated stochastically. It is often necessary to see which radionuclides and pathways are major and minor contributors to dose and risk, and risk calculations require knowledge of dose to specific sets of organs. Deterministic estimates can also be very useful in comparing exposures

Table D-11. Ruthenium-103 Data for the Example of the Ratio $GM_{sum}/\sum GM$ [a]

Year	Number N of months	Average of CVs	Composite CV	$\sqrt{(1+CV^2)/(1+CV^2/N)}$
B Plant				
1945	9	1.77	0.635	1.75
1946	12	1.74	0.507	1.79
1947	12	1.76	0.530	1.80
1948	12	1.72	0.866	1.78
T Plant				
1945	12	1.75	0.600	1.80
1946	12	1.76	0.595	1.81
1947	12	1.75	0.521	1.80
1948	12	1.73	0.855	1.79

[a] The numbers in this table depend on preliminary release estimates of ^{103}Ru from T Plant and B Plant.

associated with different scenarios of behavior and in discovering what might be "worst case" behavior for hypothetical individuals.

D-3. DISCUSSION AND CONCLUSIONS

The subject of stochastic modeling, even in the limited context that this appendix treats, is large, and we have been unable to approach it in any comprehensive way. Even so, we believe the discussion and examples given here point the way toward extending the fundamental calculations performed by HCalc, and perhaps beyond that immediate goal.

D-3.1 The Relationship between Deterministic and Stochastic Simulations

We believe the analysis given in this appendix sheds some light on the relationship between deterministic and stochastic simulations for radionuclide releases and their atmospheric transport to a receptor location. Output numbers from a deterministic model, with nominal parameter values, in general do not coincide with central values from corresponding distributions produced by a Monte Carlo simulation based on the same model, using input parameter distributions centered near the aforementioned nominal values. The differences are often sufficient to send analysts looking for explanations or errors to account for them, whereas in fact, there may be nothing technically wrong with either simulation. Rather, the difficulty is one of interpreting two (sometimes) deceptively different ways of looking at the same set of problems (i.e., the environmental assessment).

Stochastic simulations seem to be the current tool of choice for environmental assessments, and we endorse that preference, provided the tool is applied with care and tailored to each situation. But it would be a mistake to assume that deterministic simulations have no further role to play, particularly in preliminary calculations for exploration and screening, where the emphasis is on trends and internal comparisons (e.g., radiation dose to each organ from each radionuclide).

Our theory and examples should indicate that from one point of view, the two approaches are quite compatible, since we have shown how deterministically derived results from HCalc can be related to their stochastic counterparts. Yet from another point of view, the two approaches might be viewed as incompatible, representing as they do different frames of reference. Experienced analysts can make good use of both.

D-3.2 A Long-Term Anomaly and a Conservative Shortcut

Our analysis of sums of (annual) independently lognormally distributed random variables shows the decrease of variability, as measured by the GSD or CV, as the number of terms in a sum increases. In the special case where all distributions of the terms are the same, the coefficient of variation of the sum is $\mathrm{CV}/\sqrt{N}$ (Eq. (D-9b)). Thus, the limit of $\mathrm{CV}_{\mathrm{sum}}$ as $N \to \infty$ is zero. The corresponding limit of $\mathrm{GM}_{\mathrm{sum}}$ is 1, which corresponds to a degenerate lognormal distribution with all probability density concentrated at the GM (in effect, a constant). Does this mean that the sum of many years of time-integrated air concentration would be essentially exact?

The apparent anomaly is the result of our dependence on data at the scale of one year (primarily the information from Miller and Hively (1987)), to the exclusion of a component based on a longer-term average of data (preferably a period at least as great as the 11 years of our temporal scope). If the right kind of long-term data were available, special regression techniques might be able to separate annual and long-term components for better realism. Assuming autocorrelation of the X_t factors of the annual time-integrated air concentrations (Section D-2.5) avoids the anomalous zero limit of $\mathrm{CV}_{\mathrm{sum}}$, although we lack the data to quantify the joint distributions of the terms.

A more conservative way of avoiding this problem is to treat the lognormally distributed terms as if they were perfectly correlated ($\rho_{C_t,C_{t+k}} = 1$). In this case, $\mathrm{CV}_{\mathrm{sum}}$ can be shown to be a weighted average of the CVs of the terms, where the (unnormalized) weights are the means (α_i), and $\mathrm{CV}_{\mathrm{sum}}$ cannot be less than the minimum of the CV_i. If the CV_i are all of comparable magnitude, $\mathrm{CV}_{\mathrm{sum}}$ would be of similar magnitude. In particular, if all CV_i (and therefore, all GSD_i) are assumed equal, $\mathrm{CV}_{\mathrm{sum}}$ has the common value and the sum of the GM_i is the GM of the sum (Eqs. (D-18) and (D-19)). It is for the analyst to determine whether such a shortcut gives too great an exaggeration of the exposure uncertainty. The following table illustrates the point using the accurate calculation shown in Table D-4 for comparison (note that the calculations are based on preliminary release estimates):

Quantity	Shortcut ($\rho_{C_t,C_{t+k}} = 1$)	Table D-4 [a]
$\mathrm{GM}_{\mathrm{sum}}$ Bq s m^{-3}	6.66×10^7 [b]	8.19×10^7
$\mathrm{GSD}_{\mathrm{sum}}$	2.6	1.64
$\mathrm{CV}_{\mathrm{sum}}$	1.22	0.527
$n_{95\%}$ (95th percentile) Bq s m^{-3}	3.19×10^8	1.84×10^8
$n_{95\%}/n_{50\%}$	4.79	2.25

[a] Annual terms are assumed independent.
[b] For this case, $\mathrm{GM}_{\mathrm{sum}}$ is estimated as $\sum_i \mathrm{GM}_i$.

Notice that the ratio $n_{95\%}/n_{50\%}$ of the shortcut method is more than twice that of the calculation given by Table D-4, suggesting that the shortcut method might be quite conservative. We cannot be

sure of the extent of its conservatism, however, without knowing the effect of our missing long-term estimate of Gaussian plume uncertainty. However, if we consider perfect correlation of only the χ/Q (X) factors for different years (and not of the complete products $XQ\zeta$), the example worked out in Section D-2.5 below Theorem D-1, with data also from Table D-4, shows that the maximum effect would produce $n_{95\%} = 2.03 \times 10^8$, with $n_{95\%}/n_{50\%} = 2.60$. It seems likely that long-term data would not lead to a higher estimate of uncertainty. Again, it is for the analyst to decide whether the refined correlation estimate, using Theorem D-1, is worth the extra complexity.

D-3.3 Review of the Methods

The theory and examples discussed in this appendix fit, more or less, into three basic methods for deriving an uncertainty distribution for the time-integrated air concentration of a radionuclide for lognormally distributed annual releases. Additional observations point the way to combining sums of annual terms for the same radionuclide released from different plants, and to combining time-integrated air concentrations for different radionuclides with dose coefficients to develop a distribution of dose to an organ. In this section, we give a brief summary of the three principal methods, with references to earlier sections.

A. Independent years: Tables D-6 and D-7 with accompanying text, using Eq. (D-12b) to compute β_{sum} for each plant and radionuclide.
B. Correlated years:
   1. For each pair of years t and $t + k$, compute $\rho_{C_t, C_{t+k}}$ from Theorem D-1.
   2. Use the method of Tables D-6 and D-7 and accompanying text, applying Eq. D-12a and the correlations $\rho_{C_t, C_{t+k}}$ to compute β_{sum} for each plant and radionuclide.
C. Conservative shortcut (Section D-3.2):
   1. Set $\text{GM}_{\text{sum}} = \sum_{i=1}^{N} \text{GM}_i$.
   2. Set $\text{GSD}_{\text{sum}} = \max_i \text{GSD}_i$.
      (Alternatively, and less conservatively, set GSD_{sum} = arithmetic average of the GSD_i.)

D-3.4 Limitations

We close by mentioning several limitations and anticipated criticisms of the approach developed in this appendix.

1. The analysis is confined to lognormal distributions. Lognormal distributions have been chosen generically for the monthly releases of radionuclides and used to approximate the corresponding annual releases. On the basis of these assumptions, we have shown by example that the lognormal distribution serves to approximate sums of annual time-integrated air concentrations. For the type of analysis provided here, the assumption of lognormality makes possible procedures that are mathematically tractable, leading to specific distributions from which specific percentiles may be calculated. For a full Monte Carlo analysis, assumptions of lognormality would not be essential, although they might remain appropriate in the absence of contradictory data. Critics often suggest that small inaccuracies in the shape of input distributions lead to unacceptable results, but in our experience the output distributions are qualitatively robust with respect to differences between, for example, lognormal and similarly skewed nonlognormal inputs. Rarely are input distributions so accurately characterized that objections of this kind are a central issue. Of course, when the data strongly indicate a departure from lognormality, the simulation usually should not ignore it.

2. All of this analysis might have been implemented within the HCalc program. As we pointed out in the introduction (Section D-1), initial discussions of the task order raised a Monte Carlo program as a possibility, but this approach was judged to be too expensive. The task order did not envision a stochastic approach of any kind. It is true that some of the approaches developed here could be made to work within a revised version of HCalc, but substantial effort would be required to implement this kind of retrofit. Much of the untility of the output arrangements in HCalc could be lost or overwhelmed by the added space requirements for showing parameters of output distributions for many quantities. At this stage of the task order work, we believe the CDC is not receptive to such an option.

3. The appendix should give tables of results that would enable the reader to find distributions of dose without having to carry out these calculations. Such a tabulation would be very large, since there are many possible exposure intervals. Moreover, since there are multiple release sources contributing to each dose, it would not be possible to normalize the tabular entries so that one might multiply by a chi-over-Q factor. Readers who require "quick and dirty" results can fairly easily avail themselves of method C in Section D-3.

4. Some possible sources of uncertainty are not explicitly accounted for. This subject is far too complex to deal with exhaustively in this appendix. We list here and comment on two categories that might be (or seem to be) overlooked:

Dispersion model parameters (e.g., deposition velocity, dispersion coefficient σ_z, plume rise). The deterministic simulations were based on assuming no plume depletion from deposition. If we follow the same procedure in the stochastic modeling, the result will be an exaggerated GM for time-integrated air concentration. Deposition is calculated for external exposure to contaminated ground. An uncertainty component for the deposition velocity is not explicitly included. This is offset to an unknown extent by the higher air concentration estimate from neglect of plume depletion. In the early years treated by our example (1945–1948) this component of dose is small by several orders of magnitude relative to inhalation from direct exposure to the plume. If we consider the year 1954, however (Section 5.1), after additional buildup of radionuclides in the soil, the external component of dose from exposure to contaminated ground is between 21% and 28% of the total. Explicit consideration of uncertainty in deposition velocity could increase uncertainty in total dose in some degree, but we are unable to provide an estimate of the dependence at this time. The reader should remember that both external pathways are counting, in the total dose, radioactivity from an undepleted plume and from material on the ground that would have contributed to the plume's depletion. Uncertainty of the dispersion coefficient σ_z is implicitly considered in the information of Miller and Hively (1987), from which we derived the distribution of the χ/Q atmospheric dispersion factor. Plume rise was neglected as a measure of conservatism, and this step would exaggerate the GM of time-integrated air concentration of each radionuclide. Plume downwash was not considered because of the height of the release stacks above the building roofs.

Meteorological variables (category frequencies of wind speed, wind direction, atmospheric stability). The frequency tables were computed from annually averaged data taken at the site at release height (61 m) during the years 1955–1980 (Stone et al. 1983). Setting aside problems with the measurements themselves (for which we have no indication), questions of model applicability can always be raised. Much of the uncertainty of this variety would be implicit in the

information of Miller and Hively (1987). Applicability of a composite data set from a period other than the one under study has been discussed in the main text (D-2.3) and is addressed by the factor ζ_t in the time-integrated air concentration estimate for year t. Applicability of a straight-line model with meteorological data measured at the point of release to receptor locations at large distances is treated in dichotomous fashion by Miller and Hively (1987). The factor-of-two we employed is suggested for source-to-receptor distances no greater than 10 km. For distances 10 to 150 km, a factor of four is indicated by their study (GSD = 2.33). This refinement is easily incorporated into the methodology of this appendix. Critics of this modeling approach often cite short-term events, such as inversions or high winds, that they believe would influence results one way or another if they were explicitly included. If such events tend to occur in an annual pattern, they are accounted for in the annual averages (assuming that they affect the pattern of frequencies given by the joint frequency table), in proportion to the time they occupy. But a model at annual resolution cannot, for example, estimate a higher dose for a subject who happens to be unduly affected by exposure to an event of this kind (e.g., someone whose only time on site was during an inversion). One-time events are, of course, not considered in the general methodology, but some of them might require separate analysis.

REFERENCES

Aitchison, J., and J.A.C. Brown. 1969. *The Lognormal Distribution.* Cambridge University Press, Cambridge, UK.

Hahn, G.J., and W.Q. Meeker. 1991. *Statistical Intervals — A Guide for Practitioners.* John Wiley and Sons, Inc., New York.

Hanna, S.R., G.A. Briggs, and R.P. Hosker. 1982. *Handbook on Atmospheric Diffusion.* Report DOE/TIC-11223, Technical Information Center, U.S. Department of Energy.

Hardy, G.H., J.E. Littlewood, and G. Pólya. 1959. *Inequalities.* The University Press, Cambridge, UK.

Kendall, M.G., and A. Stuart. 1968. *The Advanced Theory of Statistics. Volume 3. Design and Analysis and Time-Series.* Hafner Publishing Company, New York.

Killough, G.G., and D.W. Schmidt. 2000. "Uncertainty Analysis of Exposure to Radon Released from the Former Feed Materials Production Center." *J. Environmental Radioactivity* 49: 127–156.

Kocher, D.C. 1981. *Radioactive Decay Data Tables — A Handbook of Decay Data for Application to Radiation Dosimetry and Radiological Assessments.* Report DOE/TIC-11026, Technical Information Center, U.S. Department of Energy.

Miller, C.W., and L.M. Hively. 1987. "A Review of Validation Studies for the Gaussian Plume Atmospheric Dispersion Model." *Nuclear Safety* 28(4): 522–531.

Stone, W.A., J.M. Thorp, O.P. Gifford, and D.J. Hoitink. 1983. *Climatological Summary for the Hanford Area.* Report PNL-4622, Pacific Northwest Laboratory, Richland, Washington.

Wilks, S.S. 1962. *Mathematical Statistics.* John Wiley and Sons, New York and London.

APPENDIX E

PROBABILITY OF CONTACT WITH DISCRETE AIRBORNE PARTICLES CONTAMINATED WITH RADIONUCLIDES

E-1. INTRODUCTION

Standard interpretations of the air dispersion and deposition models discussed in Sections 3.2.1 and 3.2.2 usually construe the plume of transported radioactive pollutant as a fluid-like continuum of tracer within the air, leading to nonzero dose to any person exposed to any region of the plume for any time, however brief, or however slight the concentration of tracer the person was exposed to. Although aerosol physics of discrete particles is brought to bear on the theory of deposition, the continuum interpretation persists for plume transport. This interpretation is convenient for dose estimation, but reasonable questions can be raised about parametric boundaries beyond which its applicability would break down.

Specifically, if a substantial airborne release of radioactivity to the atmosphere is carried by a finite number of particles, what is the probability that a person (receptor) standing in the plume for a specified time would have contact with one or more of the particles? If one neglects gamma and beta dose from passing particles that do not touch the receptor (near misses), the calculated dose would be nonzero only in the event of contact of the receptor with one or more particles. (External dose from penetrating radiations from ambient particles not in contact with the subject is usually estimated as a separate component, based on the continuum theory of the plume.)

If an airborne particle is inhaled, the dose (given the radioactivity carried by the particle) may be analyzed either as a distribution that depends on many events and variables associated with the respiratory model used, or it may be estimated as the expected value of a random variable associated with such a distribution. For the present discussion, we take the latter option and make use of ICRP dose coefficients that embody the respiratory model and provide the expected value. If the particle is not inhaled but strikes and adheres to the skin or attaches itself to clothing, the dose depends on the degree of contact and the length of time the particle remains on the body or clothing. Methods and data are available to estimate dose to subcutaneous tissue at various levels when the skin is exposed to such radioactive particles (see Section 3.6.4).

Our present investigation of this topic is limited to the problem of estimating the probability of initial contact of an exposed receptor to one or more of the particles in an airborne release. We make the simplifying and cautious assumption that any particle coming near enough to the skin or clothing of the receptor attaches itself. By "near enough," we mean the following. The receptor is assumed to stand in the plume facing the source. The receptor's body shape is projected on a vertical plane that is perpendicular to the wind flow. Any particle that is predicted to pass through this projected shape ("shadow") is assumed either to be inhaled or to stick to the receptor's skin or clothing. This assumption is cautious because many of the smaller particles would follow the airflow around the receptor and pass off without contact. Particles with greater mass would possess momentum that would resist the air's tendency to carry them parallel to the body's surface. Those with sufficient momentum would fail to follow the curvilinear airflow and instead would cross the

streamlines and strike the body. The interaction with the air disturbances caused by the receptor's breathing is more complex, but our assumption should still tend not to underestimate the fraction of particles inhaled, given the physiological assumptions of breathing mentioned below.

The basic formulas that express the rates of contact with the airborne particles by external collision and inhalation are the following:

$$n_s = n_r[\chi/Q]uA = \frac{\tilde{\chi}}{T} \cdot uA \tag{E-1a}$$

and

$$n_b = n_r[\chi/Q]b = \frac{\tilde{\chi}}{T} \cdot b \tag{E-2a}$$

The quantity n_s is the number of released particles per second that would pass through the shadow projection of the receptor's body on a vertical plane perpendicular to the wind, corresponding to a constant release rate n_r. The second quantity, n_b, is the gross number of released particles per second that would be inhaled from the airstream at the receptor's position, corresponding to constant release rate n_r. The remaining notations are defined in the next paragraph. We specify gross for n_b because this number is not adjusted to exclude particles that are promptly returned to the airstream with exhalation (the adjustment for the net of radioactivity inhaled is incorporated in the dose coefficients for the inhalation pathway). The two quantities n_s and n_b do not represent an exact partition of particles between the two exposure pathways, because n_s counts particles as sticking to the body surface that would also be available to inhalation. Combining the two component estimates would give a higher estimate of total dose than a more detailed modeling effort might lead to, but we accept this overestimate.

In Equations (E-1) and (E-2), the symbols χ and $\tilde{\chi}$ denote, respectively, the particle concentration at the receptor location (number m^{-3}) and the time integral of that quantity over the period T (s) of exposure. The symbol Q generically denotes the cumulative release or release rate, depending on the meaning of χ, and $[\chi/Q]$ stands for a normalized quantity (s m^{-3}) that may be applied with either interpretation. The wind speed is u (m s^{-1}), and A is the area (m^2) of the receptor's shadow projection on a vertical plane perpendicular to the wind direction. The breathing rate of the receptor subject is b (m^3 s^{-1}).

Equations (E-1a) and (E-2a) would predict the number of particle contacts per unit time for a receptor, given a constant rate of release. The presence of the time T in each equation suggests a knowledge of the duration of the release. In general, however, the release may not occur at a constant rate, and its duration may be unknown. It is useful to rewrite Eqs. (E-1a) and (E-2a) in terms of total numbers of contacts when a cumulative estimate N_r of the number of released particles is available:

$$N_s = N_r[\chi/Q]uA = \tilde{\chi}uA \tag{E-1b}$$

and

$$N_b = N_r[\chi/Q]b = \tilde{\chi}b \tag{E-2b}$$

where N_s and N_b are cumulative quantities (numbers of particles) for the entire release (assuming an exposure of the same duration); N_s is taken as the total number of particles to have contacted the skin or clothing of a constantly exposed receptor, and N_b is the total number of particles such a receptor would breathe (we remind the reader of the overlap of these quantities that was mentioned above).

One choice of probability model is the Poisson distribution, which (for our interpretation) represents the number of independent particle encounters with the receptor. Under this model, the probability of n encounters ($n = 0, 1, 2, \ldots$) is

$$p_n = \exp(-\mu)\mu^n / n! \tag{E-3}$$

where μ, the mean number of particle encounters, is whichever of N_s or N_b is applicable. Independently Poisson-distributed random variables have the useful property that their sum also has the Poisson distribution. If we consider M independent Poisson-distributed random variables with means μ_i, $i = 1, \ldots, M$, their sum has the Poisson distribution with probabilities p_n given by Eq. (E-3), where

$$\mu = \mu_1 + \cdots + \mu_M \tag{E-4}$$

(Kendall and Stuart, 1969). Notice that the Poisson distribution has no upper bound for the number of particle encounters. It could be applied to a random process where the rate of independent occurrences has been estimated as λ (s^{-1}) and the mean number for a time T (s) is $\mu = \lambda T$, with no implied maximum number of occurrences.

Another distribution, the binomial, has a useful intuitive appeal for this application, in addition to a more exact interpretation. We consider trajectories of released particles independent events, for which the probability p that a trajectory will pass through the receptor subject's "shadow" (or the probability p_b that the subject will inhale the particle) is meaningful and may be estimated as

$$p = N_s/N_r = [\chi/Q]uA \quad \text{or} \quad p_b = [\chi/Q]b \tag{E-5}$$

where (as before) b ($m^3\ s^{-1}$) is the mean breathing rate of the subject. Thus, we are considering N_r independent trials with probability of "success" in each trial equal to p. This model leads to the binomial distribution, with cumulative distribution function

$$F(n \mid p, N) = \sum_{k=0}^{n} \binom{N}{k} p^k (1-p)^{N-k}, \quad n = 0, \ldots, N \tag{E-6}$$

giving the probability of n or fewer successes in N trials. The probability of exactly n successes in N trials is given by the term for $k = n$:

$$\Pr[n \text{ "successes" in } N \text{ trials}] = \binom{N}{n} p^n (1-p)^{N-n} \tag{E-7}$$

The binomial coefficient $\binom{N}{k}$ is defined as $N!/(k!(N-k)!)$ and is sometimes spoken of as "the number of combinations of N things taken k at a time." Of particular interest to us are the following special cases of the binomial and Poisson distributions:

Number of successes in N trials:	None	Exactly one	One or more
Binomial probability:	$(1-p)^N$	$Np(1-p)^{N-1}$	$1-(1-p)^N$
Poisson probability	$e^{-\mu}$	$\mu e^{-\mu}$	$1-e^{-\mu}$

(E-8)

The Poisson distribution can be derived from the binomial distribution as a limiting case for $p \to 0$ with Np held constant. This interpretation makes it useful in treating rare events. It is also useful

for treating sums of independent random variables from different binomial distributions, all with small p, and we will apply this property in connection with an example in Section E-4. The Poisson and binomial distributions are discussed in statistics textbooks (e.g., Snedecor and Cochran 1967).

It is not possible to provide extensive accounts of the risk of particle encounters for subjects with various assumed exposure conditions at Hanford. Rather, it is our intention in this appendix to provide sufficient information for a reader to make exploratory estimates. The information is based on a simplified methodology relative to the one implemented in HCalc, although the two are similar. Much of the numeric information is given in tables and graphs, and where possible, we have chosen models with formulas that are easily computed. We have chosen to use only Class D meteorological assumptions, because the resulting predictions of concentration are intermediate and are often taken as representative of (but not identical to) longer-term averages. In all relevant cases, the effective release height is assumed to be 61 m (the physical stack height of all release sources considered in the study). Other generic values of variables will be pointed out in the sections that follow. We will illustrate the methods in Secton E-4, using data for ruthenium-particle releases from the REDOX plant in the early 1950s.

E-2. METEOROLOGICAL MODELS AND DATA

We summarize the models needed to estimate χ/Q as it appears in Eqs. (E-1a,b) and (E-2a,b).

E-2.1 The Gaussian Plume Model for Class D Stability

We have chosen the centerline form of the Gaussian plume formula for a ground-level receptor (Hanna et al. 1982):

$$\frac{\chi}{Q} = \frac{\exp\left(-h^2/(2\sigma_z^2)\right)}{\pi\sigma_y\sigma_z} \cdot \frac{f}{u} = D \cdot \frac{f}{u} \tag{E-9}$$

where the release height h = 61 m for this application. We include the fractional frequence f to represent the fraction of the exposure time that the wind blows toward the receptor (meaning into the 22.5° sector where the receptor is located). The quantity D in the alternative formula is called the diffusion and has units m^{-2}. The wind speed is u (m s^{-1}). The diffusion coefficients σ_y and σ_z (m) are estimated by the Briggs formulas for Class D stability in open country:

$$\sigma_y = 0.08x(1 + 0.0001x)^{-1/2}, \quad \sigma_z = 0.06x(1 + 0.0015x)^{-1/2} \tag{E-10}$$

These formulas represent a departure from the more complicated ones of Section 3.2.2 of this report.

It is useful to plot and tabulate the diffusion D from Eq. (E-9). This normalized form, which may be written as $\chi u/(Qf)$, has been plotted and tabulated as Figure E-1 and Table E-1, respectively. The normalized values can then be converted to the desired χ/Q by multiplication by the ratio f/u. Wind direction frequencies f and the corresponding average wind speeds u for the various sectors are shown in Table E-2, based on Hanford meteorology for 1946–1980.

The reader should note that χ/Q values estimated from the information in this subsection do not take into account depletion of the plume concentration that results from wet and dry deposition. Consideration of these processes complicates matters considerably, and Section E-2.2 provides the necessary information.

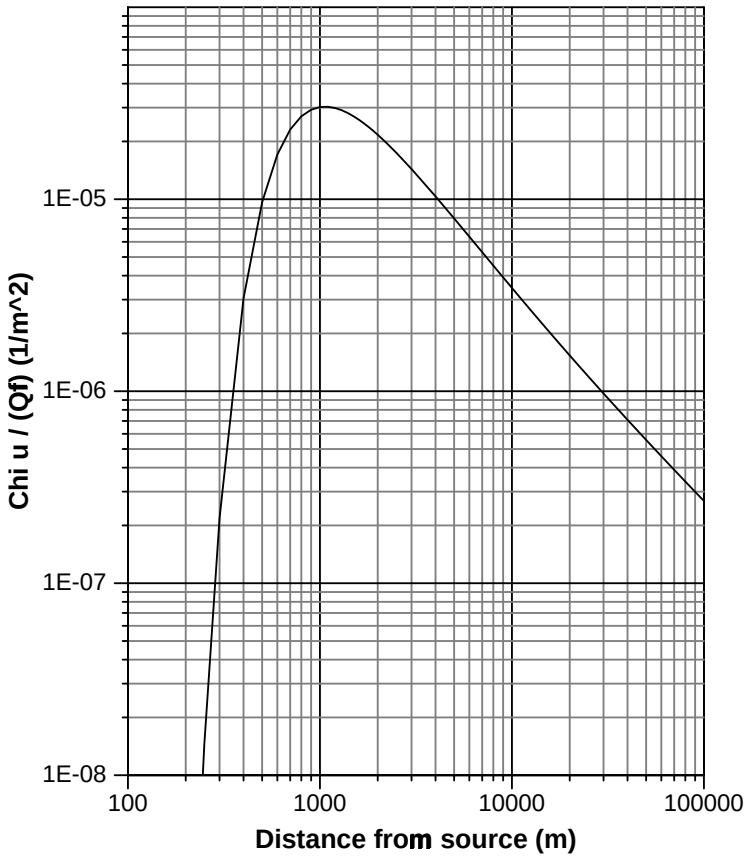

Figure E-1. Diffusion (m^{-2}) for 61-m release height and Class-D atmospheric stability for source-to-receptor distances ranging to 10^5 m. The product of the normalized diffusion quantity with the ratio f/u — where f is the fraction of time the wind blows from the sector of interest and u is the wind speed (m s^{-1}) — gives the concentration per unit release rate χ/Q (s m^{-3}).

E-2.2 Plume Depletion from Deposition

We characterize total deposition from the plume by a deposition velocity — denoted by v (m s^{-1}) — equal to the sum of two component deposition velocities for dry and wet deposition, denoted by v_d and v_w, respectively. We assume that dry deposition occurs at all times, and the deposition velocity v_d is treated as a time average that depends on wind speed and aerodynamic diameter (AD) of the airborne particles. For wet deposition, the formula depends on the interpretation. If the event of interest occurs entirely during a period of precipitation, we use $v = v_d + v_w$ as the total deposition velocity. But if the event spans a longer period, we introduce a coefficient f_w representing the fraction of the time precipitation occurs and write $v = v_d + f_w v_w$.

The wet deposition velocity v_w is based on a rainfall rate J (m s^{-1}) which represents an average for times of precipitation. The wet deposition velocity is estimated as $v_w = JW_r$, where the washout ratio W_r is taken as 6×10^5 (dimensionless). This value is a median given by Hanna et al. (1982)

Table E-1. Diffusion as a Function of Distance [a]

Distance (m)	(m^{-2})	Distance (m)	(m^{-2})
100	1.10×10^{-28}	2,200	1.98×10^{-5}
110	1.46×10^{-24}	2,500	1.75×10^{-5}
120	2.04×10^{-21}	3,000	1.44×10^{-5}
130	5.82×10^{-19}	4,000	1.03×10^{-5}
140	5.22×10^{-17}	5,000	7.95×10^{-6}
150	1.98×10^{-15}	6,000	6.38×10^{-6}
160	3.91×10^{-14}	7,000	5.30×10^{-6}
170	4.65×10^{-13}	8,000	4.51×10^{-6}
180	3.71×10^{-12}	9,000	3.92×10^{-6}
190	2.15×10^{-11}	10,000	3.45×10^{-6}
200	9.69×10^{-11}	11,000	3.08×10^{-6}
220	1.09×10^{-9}	12,000	2.78×10^{-6}
250	1.45×10^{-8}	13,000	2.53×10^{-6}
300	2.18×10^{-7}	14,000	2.32×10^{-6}
400	3.05×10^{-6}	15,000	2.14×10^{-6}
500	9.65×10^{-6}	16,000	1.99×10^{-6}
600	1.71×10^{-5}	17,000	1.85×10^{-6}
700	2.31×10^{-5}	18,000	1.73×10^{-6}
800	2.70×10^{-5}	19,000	1.63×10^{-6}
900	2.93×10^{-5}	20,000	1.54×10^{-6}
1,000	3.02×10^{-5}	22,000	1.38×10^{-6}
1,100	3.03×10^{-5}	25,000	1.19×10^{-6}
1,200	2.99×10^{-5}	30,000	9.73×10^{-7}
1,300	2.91×10^{-5}	40,000	7.10×10^{-7}
1,400	2.81×10^{-5}	50,000	5.58×10^{-7}
1,500	2.70×10^{-5}	60,000	4.59×10^{-7}
1,600	2.59×10^{-5}	70,000	3.90×10^{-7}
1,700	2.48×10^{-5}	80,000	3.39×10^{-7}
1,800	2.37×10^{-5}	90,000	2.99×10^{-7}
1,900	2.27×10^{-5}	100,000	2.68×10^{-7}
2,000	2.17×10^{-5}	—	—

[a] Diffusion estimates are based on a release height of 61 m and Class D atmospheric stability.

from their survey of existing literature. Table E-3 shows monthly and annual hours of rainfall, f_w, J, and v_w, based on Hanford data from 1946 through 1980 (Stone et al. 1983).

Dry deposition velocity is discussed in Section 3 of this report. The calculation of specific values is somewhat complicated, and we provide a graph and a table to assist the reader. Figure E-2 and Table E-4 provide values of v_d for particle aerodynamic diameters 0.03–100 μm (the range of the table omits 0.03–0.09 μm) and wind speeds 1, 2, . . ., 7 m s^{-1}. Linear interpolation in the table

Table E-2. Wind Speed Frequencies for Class D [a]

Wind from [b]	f [c]	u (m s^{-1})[d]
N	0.05716	2.592
NNE	0.04255	2.767
NE	0.03947	2.216
ENE	0.03101	1.778
E	0.03639	1.685
ESE	0.04332	1.817
SE	0.05639	1.990
SSE	0.03793	2.514
S	0.03255	3.458
SSW	0.03639	5.105
SW	0.05639	6.560
WSW	0.06409	6.017
W	0.05793	4.365
WNW	0.13180	5.931
NW	0.20560	5.628
NNW	0.07101	2.723
Summary	1.00000	4.195 [e]

[a] The tabulated values are based on a joint frequency table in Stone et al. (1983). Although the frequencies shown are relative to the occurrence of Class D conditions at Hanford, in this appendix they are used generically as representative of an average (Class D conditions occurred about 13% of the time).

[b] Direction from which the wind blows, as determined by the source-to-receptor geometry (e.g., if the receptor is due east from the source, the relevant wind would be from the west (W)).

[c] Fraction of the time the wind is assumed to blow from the indicated direction (based only on Class D conditions).

[d] Mean wind speed for wind blowing from the indicated direction (based only on Class D conditions).

[e] This entry is the average wind speed for Class D conditions over all wind directions ($\sum_{i=1}^{16} f_i u_i$).

is adequate for most purposes. The values given in Figure E-2 and Table E-4 are specific to stability Class D.

For plume depletion resulting from deposition, we use the method given by Van der Hoven (1968), which treats the source Q as a function of distance x and adjusts it to account for the cumulative loss of material in the plume. This so-called source depletion method seems to have been superseded by surface depletion methods, which are considered more physically plausible, and which are also more complicated to implement. We have retained the source depletion model

Table E-3. Monthly Rainfall Intensities and Wet Deposition Coefficients [a]

Month	Mean hours of rainfall	f [b]	J (m s^{-1}) [c]	v_w (m s^{-1}) [d]
Jan	98.8	0.133	7.06×10^{-8}	0.0423
Feb	60.3	0.090	7.13×10^{-8}	0.0428
Mar	38.7	0.052	7.90×10^{-8}	0.0474
Apr	31.3	0.043	9.74×10^{-8}	0.0584
May	35.2	0.047	1.02×10^{-7}	0.0610
Jun	31.2	0.043	1.35×10^{-7}	0.0809
Jul	10.7	0.014	1.21×10^{-7}	0.0728
Aug	15.8	0.021	1.35×10^{-7}	0.0809
Sep	17.4	0.024	1.19×10^{-7}	0.0711
Oct	36.2	0.049	1.09×10^{-7}	0.0656
Nov	65.7	0.091	8.40×10^{-8}	0.0504
Dec	89.7	0.121	6.77×10^{-8}	0.0406
Annual	531.0	0.061	—	0.0522 [e]

[a] Based on Stone et al. (1983), Figure 16 and Table 12, using data from July 1946 through June 1971 and July 1974 through 1980.
[b] Mean fraction of the month precipitation is falling.
[c] Mean rainfall rate during precipitation periods.
[d] The wet deposition velocity $v_w = JW_r$, where the washout ratio W_r is estimated as 6×10^5 (median value given by Hanna et al. (1982) based on a survey of literature). This value of v_w is is interpreted as an average for periods of precipitation within the indicated month. The total deposition velocity, averaged over the month, is $fv_w + v_d$.
[e] Average weighted by the monthly hours of rainfall.

in the HCalc methodology and in this appendix because (1) it is much simpler for calculations and (2) as far as we are aware, data are lacking to indicate a clear preference for one approach or the other (or rejection of both).

Figure E-3 and Table E-5 provide the depletion factor Q/Q_0 for Class D conditions as a function of the source-to-receptor distance x. The calculation depends on the ratio $r = v/u$, where v is the total deposition velocity, u is the wind speed, and both are in the same units. For purposes of the graph and table, the value $r = 0.01$ has been used. The form of the solution derived by Van der Hoven (1968) shows that one may convert the tabular value to one suitable for any other ratio r' by raising the tabular value to the power $r'/0.01$.

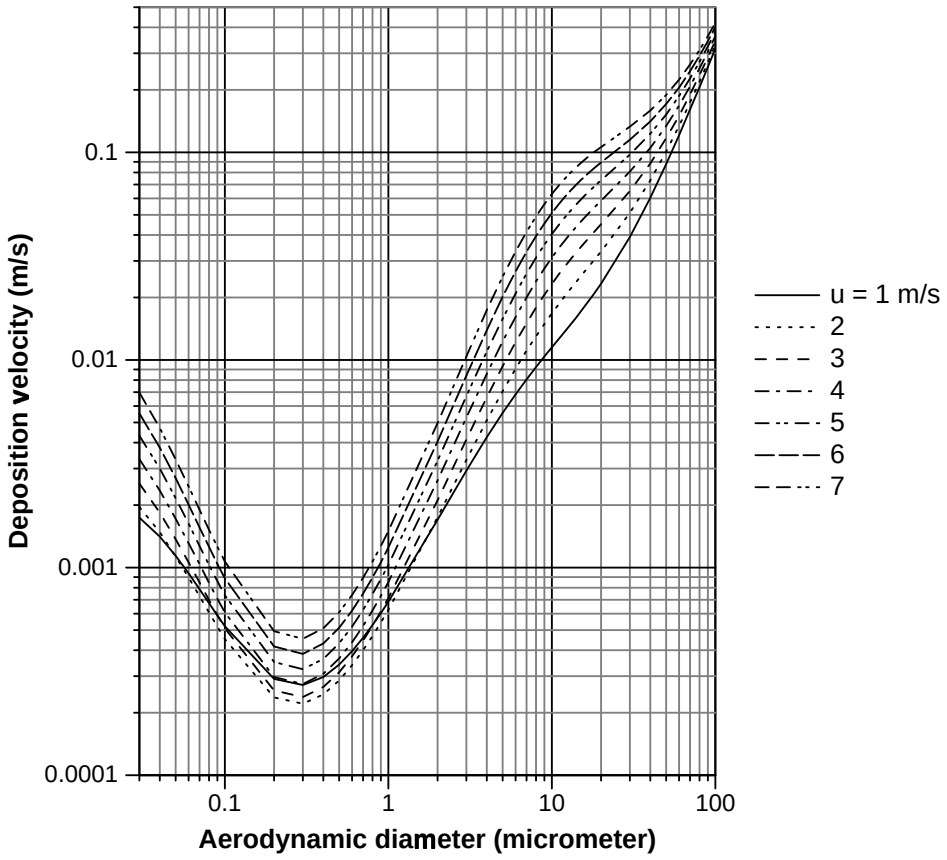

Figure E-2. Dry deposition velocity curves for several wind speeds and particle aerodynamic diameters ranging from 0.03 to 100 μm. Atmospheric stability is Class D. The estimates are based on a surface layer model of Sehmel and Hodgson (1980). A subset of the same data is presented in Table E-4 for the reader's convenience in making computations.

E-3. PARTICLE DISTRIBUTIONS

We use a discrete representation of the distribution of particle aerodynamic diameters. At the point of release, the count distribution is assumed to be lognormal with a specified geometric mean (GM) and geometric standard deviation (GSD). On the basis of this distribution, we divide the aerodynamic diameter–ranked particles into ten compartments with equal numbers of particles. Each compartment is represented by the median diameter of the particles that it contains. For a lognormal distribution, calculating such a partition is simple. One begins with the probability intervals $0 \le p < 0.1$, $0.1 \le p < 0.2$, . . ., $0.9 \le p \le 1$ and takes the midpoints p_k = 0.05, 0.15, . . ., 0.95 ($k = 1, \ldots, 10$). Using inverse tables of the standard normal distribution (e.g., Abramowitz and Stegun 1965), one finds the corresponding quantiles z_k, defined implicitly by the equation

$$p_k = \Pr[Z \le z_k] \tag{E-11}$$

Table E-4. Dry Deposition Velocity (m s^{-1}) as a Function of Aerodynamic Diameter (Class D)

Aerodynamic diameter (μm)	Wind speed (m s^{-1})						
	1	2	3	4	5	6	7
0.1	0.000522	0.000453	0.00051	0.000608	0.000735	0.000888	0.00107
0.2	0.000291	0.000237	0.000256	0.000297	0.000351	0.000417	0.000494
0.3	0.000272	0.000221	0.000238	0.000275	0.000324	0.000384	0.000454
0.4	0.000297	0.000245	0.000266	0.000308	0.000363	0.000431	0.00051
0.5	0.000341	0.000286	0.000313	0.000365	0.000432	0.000513	0.000609
0.6	0.000396	0.000339	0.000374	0.000437	0.00052	0.000621	0.000738
0.7	0.000459	0.0004	0.000445	0.000523	0.000625	0.000749	0.000893
0.8	0.000529	0.000468	0.000525	0.000622	0.000746	0.000896	0.00107
0.9	0.000604	0.000544	0.000615	0.000731	0.000881	0.00106	0.00127
1	0.000685	0.000626	0.000713	0.000852	0.00103	0.00125	0.0015
2	0.0017	0.00175	0.00211	0.00263	0.00327	0.00405	0.00497
3	0.00293	0.0033	0.00414	0.00528	0.0067	0.00841	0.0104
4	0.00425	0.00512	0.00661	0.00857	0.011	0.0139	0.0174
5	0.00556	0.00707	0.00933	0.0123	0.0158	0.0202	0.0252
6	0.00683	0.00907	0.0122	0.0161	0.0209	0.0267	0.0333
7	0.00806	0.0111	0.015	0.02	0.0261	0.0332	0.0414
8	0.00924	0.013	0.0179	0.0239	0.0311	0.0395	0.0491
9	0.0104	0.0149	0.0206	0.0276	0.0359	0.0454	0.0563
10	0.0115	0.0168	0.0232	0.0311	0.0404	0.051	0.063
11	0.0126	0.0185	0.0258	0.0345	0.0446	0.0562	0.0691
12	0.0137	0.0203	0.0282	0.0376	0.0486	0.061	0.0747
13	0.0148	0.022	0.0305	0.0407	0.0523	0.0654	0.0798
14	0.0159	0.0236	0.0328	0.0435	0.0558	0.0695	0.0844
15	0.0171	0.0253	0.0349	0.0463	0.0591	0.0734	0.0887
16	0.0183	0.0269	0.037	0.0489	0.0623	0.0769	0.0927
17	0.0195	0.0285	0.0391	0.0514	0.0652	0.0803	0.0965
18	0.0207	0.0301	0.0411	0.0538	0.068	0.0835	0.0999
19	0.022	0.0317	0.0431	0.0562	0.0708	0.0865	0.103
20	0.0233	0.0333	0.0451	0.0585	0.0734	0.0894	0.106
30	0.0391	0.0511	0.0651	0.0808	0.0975	0.115	0.133
40	0.0604	0.0733	0.0884	0.105	0.123	0.141	0.159
50	0.0878	0.101	0.117	0.134	0.152	0.171	0.189
60	0.121	0.134	0.15	0.168	0.187	0.205	0.224
70	0.161	0.174	0.19	0.208	0.227	0.246	0.265
80	0.206	0.219	0.236	0.254	0.273	0.292	0.311
90	0.258	0.271	0.287	0.305	0.324	0.344	0.363
100	0.316	0.329	0.345	0.363	0.382	0.402	0.421

This gives ten numbers z_k that are symmetric about zero.

To find the representative aerodynamic diameters for the lognormal distribution, with $\mu = \ln \mathrm{GM}$ and $\sigma = \ln \mathrm{GSD}$, we use the formula

$$\zeta_k = \exp(\sigma z_k + \mu) \tag{E-12}$$

Table E-6 shows the results for the lognormal distribution with GM = 2 μm and GSD = 3.

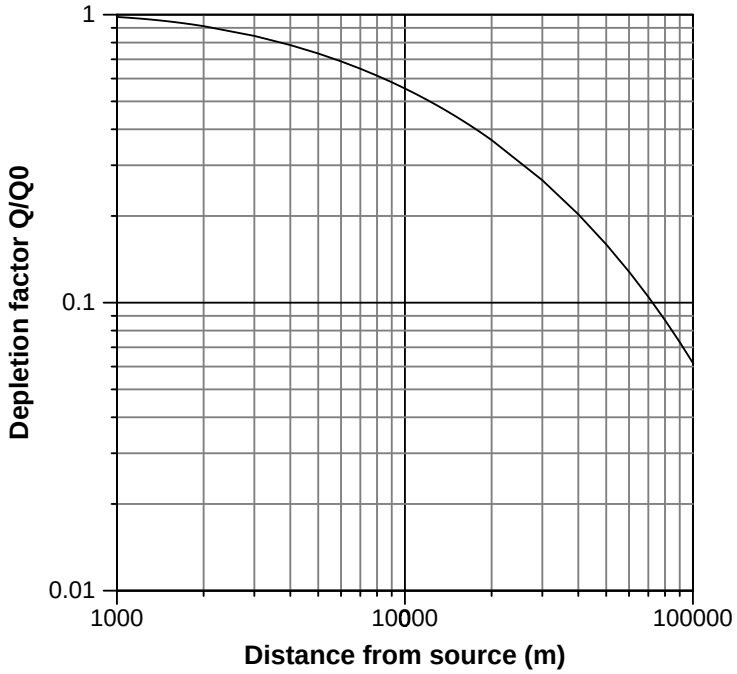

Figure E-3. Plume depletion factor for deposition processes, plotted as a function of distance from the source. The release height is 61 m, and atmospheric stability is Class D. The curve is based on a source-depletion model and was calculated by numerical integration, using the method described by Van der Hoven (1968).

For each representative aerodynamic diameter shown in Table E-6, we estimate χ/Q as follows:

$$[\chi/Q]_k = D \cdot \frac{f}{u} \cdot (Q/Q_0)_k \tag{E-13}$$

where $(Q/Q_0)_k$ is the tabular value (Table E-5) raised to the power $r = (v/u)/0.01$. The dry deposition component v_d of v is interpolated from Table E-4 in accordance with aerodynamic diameter ζ_k and mean wind speed u for the wind direction implied by the source-receptor relationship. We will compute χ/Q and the corresponding particle fluxes for each representative particle aerodynamic diameter.

It is also useful to have a χ/Q quantity for the complete ensemble of particles that move through the airstream at the receptor location. Since our model considers 10 sets of particles with equal numbers, we assume that a total of N particles was released and thus have (at the source) $N/10$ particles represented by each AD ζ_k. Multiplying Eq. (E-13) by $N/10$ and summing over k, we find when we associate the factor $1/10$ with $(Q/Q_0)_k$ and divide by $Q = N$ (for the entire ensemble) that

$$[\chi/Q] = D \cdot \frac{f}{u} \cdot \overline{Q/Q_0} \tag{E-14}$$

where we obtain χ/Q for the ensemble of particles by replacing $(Q/Q_0)_k$ in Eq. (E-13) with the

Table E-5. Plume Depletion Factor with Distance from Source [a]

Distance (m)	Depletion factor (Q/Q_0)	Distance (m)	Depletion factor (Q/Q_0)
300	1.00000	7,000	0.64918
400	0.99991	8,000	0.61415
500	0.99935	9,000	0.58268
600	0.99790	10,000	0.55421
700	0.99534	11,000	0.52827
800	0.99170	12,000	0.50452
900	0.98712	13,000	0.48266
1,000	0.98178	14,000	0.46245
1,100	0.97584	15,000	0.44371
1,200	0.96944	16,000	0.42627
1,300	0.96271	17,000	0.40998
1,400	0.95574	18,000	0.39474
1,500	0.94862	19,000	0.38044
1,600	0.94139	20,000	0.36699
1,700	0.93410	30,000	0.26617
1,800	0.92680	40,000	0.20271
1,900	0.91951	50,000	0.15934
2,000	0.91226	60,000	0.12813
3,000	0.84377	70,000	0.10482
4,000	0.78439	80,000	0.08694
5,000	0.73316	90,000	0.07293
6,000	0.68852	100,000	0.06175

[a] These values are based on a source-depletion model with release height 61 m, atmospheric stability Class D, and $r = v/u = 0.01$, where v is total deposition velocity and u is wind speed, both in the same units. To convert the tabular value to a different v/u ratio r', use $(Q/Q_0)^{r'/0.01}$. The table was calculated by numerical integration using a method described by Van der Hoven (1968).

arithmetic mean of the ten plume depletion factorbs. A corresponding total deposition velocity for the ensemble of particles can be estimated from the equation

$$v = 0.01u \cdot \frac{\ln \overline{Q/Q_0}}{\ln(Q/Q_0)_{\text{tab}}} \qquad \text{(E-15)}$$

where the subscript “tab” refers to the tabulated value in Table E-5 corresponding to the source-to-receptor distance. Equations (E-14) and (E-15) provide the means of applying the earlier probability theory (Eqs. (E-1a, 2a) or (E-1b, 2b)) collectively to the ensemble of particles without considering the ten compartments individually.

Table E-6. Representative Aerodynamic Diameters (μm): Midpoints of Ten Equal-Activity Intervals (Lognormal Distribution of Activity with Respect to Surface Area)

Cumulative probability p_k [a]	Standard normal z_k [b]	Scrubber failure ζ_k [c]
0.05	−1.64485	0.591
0.15	−1.03643	1.15
0.25	−0.67449	1.72
0.35	−0.38532	2.36
0.45	−0.12566	3.14
0.55	0.12566	4.13
0.65	0.38532	5.50
0.75	0.67449	7.55
0.85	1.03643	11.2
0.95	1.64485	21.9

[a] Cumulative probabilities for the midpoints of ten equal-probability intervals, $0 \le p < 0.1$, $0.1 \le p < 0.2, \ldots,$ $0.9 \le p \le 1.0$.

[b] Quantile points for the standard normal distribution, defined implicitly by $p_k = \Pr[Z \le z_k]$. These values are found in standard tables such as Abramowitz and Stegun (1965).

[c] Representative diameters for the lognormal distribution estimated for particle releases following REDOX scrubber failures, with GM = 3.6 μm and GSD = 3. These diameters are calculated from the standard normal quantile points as $\zeta_k = \exp(\sigma z_k + \mu)$, where $\mu = \ln \mathrm{GM}$ and $\sigma = \ln \mathrm{GSD}$. The same technique can be applied to other lognormally-distributed particle releases.

E-4. AN EXTENDED EXAMPLE

The durations of episodic releases of ruthenium particles, which dominated the median releases estimated for some months, are generally not well documented. For some releases, there was no operational effluent sampling system and the release was discovered when particles were found in the environment. Other releases occurred from the stack walls and were likely not reliably assessed, even though effluent sampling was being performed. Durations of these episodic releases are believed to be between a few hours and a few days, periods shorter than those used in the source term estimates and the intervals for which we have detailed meteorological data. Thus, only generalized assessments are provided here. For those who may wish to make more detailed investigations of particular releases, the effort to find and compile original meteorological data appropriate for the specific episode may prove worthwhile.

We consider an incident at the REDOX Plant in March 1952, when a scrubber failure led to a release of ruthenium-bearing particles. The release consisted of both ^{103}Ru and ^{106}Ru. The median estimate for the total release is 5.37 TBq (145 Ci). Using the number of particles per unit activity

release given in Section 2.2.2 (5.4×10^7 TBq^{-1} or 2×10^6 Ci^{-1}), we estimate that the number of particles released $N_r = 2.9 \times 10^8$.

We estimate that the distribution of these particles with respect to count had physical GM diameter 2 μm, with GSD 3. Using the assumption of effective density 4.9 g cm^{-3} and default shape factor 1.5 (Section 2.2.2), we calculate for the GM aerodynamic diameter $2 \times \sqrt{4.9/1.5} = 3.6$ μm (GSD = 3 remains unchanged).

We first compute the probabilities of particle encounter for a receptor in Richland, and we begin by assuming around-the-clock potential exposure for the duration of the event in the month of March 1952. We assume for the exercise that the receptor's projected area $A = 1$ m^2.

We include Table E-7 to provide locations of sources and receptors of interest and distances and directions between them. We round the distance from the REDOX Plant to Richland to 38,700 m. Richland is in the plume when the wind blows from NW; Table E-2 gives the frequency $f = 0.20560$ and the mean wind speed for that direction as $u = 5.628$ m s^{-1}.

The diffusion for the Richland receptor is $D = \chi u/(Qf) = 7.357 \times 10^{-7}$ m^{-2}, which can be approximated by interpolation in Table E-1. The tabular value of the plume depletion factor is $(Q/Q_0)_{tab} = 0.20958$, which can be estimated by interpolation in Table E-5. Before adjusting this tabular value to the example, we need the deposition velocity.

Using GM = 3.6 μm as the count median aerodynamic diameter for the released particles, we find a dry deposition value $v_d = 0.0107$ m s^{-1}, which the reader may approximate from Table E-4, interpolating between wind speeds of 5 and 6 m s^{-1} and aerodynamic diameters 3 and 4 μm. Wet deposition velocity for March (Table E-3) is $v_w = 0.0474$ m s^{-1} with precipitation fraction $f_w = 0.052$ for that month. Combining wet and dry components, we obtain $v = v_d + f_w v_w = 0.0132$ m s^{-1}. Note that for this example we have forgone the partitioning of the distribution into ten parts with equal numbers of released particles.

Now we may adjust the plume depletion factor:

$$Q/Q_0 = (Q/Q_0)_{tab}^{v/u/0.01} = 0.20958^{\frac{0.0132/5.628}{0.01}} = 0.6932$$

This permits us to calculate χ/Q for the NW wind direction (i.e., with directional frequency $f = 0.2056$), and with plume depletion included:

$$\chi/Q = 7.357 \times 10^{-7} \times \frac{0.2056}{5.628} \times 0.6932 = 1.86 \times 10^{-8} \text{ s m}^{-3}$$

Putting $A = 1$ m^2, we now compute, using Eq. (E-5), the binomial probability p of a "success," i.e., that a randomly selected released particle will pass through the receptor's shadow:

$$p = 1.86 \times 10^{-8} \text{ s m}^{-3} \times 5.628 \text{ m s}^{-1} \times 1 \text{ m}^2 = 1.05 \times 10^{-7} \text{ (dimensionless)}$$

For breathing, we use the rate $b = 23$ m^3 day^{-1} $= 2.66 \times 10^{-4}$ m^3 s^{-1}, and from Eq. (E-5) we find

$$p_b = 1.86 \times 10^{-8} \text{ s m}^{-3} \times 2.66 \times 10^{-4} \text{ m}^3 \text{ s}^{-1} = 4.95 \times 10^{-12} \text{ (dimensionless)}$$

which represents the probability that a randomly selected released particle will be inhaled by the receptor.

Table E-7. Coordinates for Hanford Sources and Receptors [a]

Sources	Also known as	East (m)	North (m)
291-S-1	Redox stack	567530	134034
291-B-1	B Plant stack	573576	136383
291-T-1	T Plant stack	567696	136877
Receptors			
H-61	Antiaircraft site	563950	138100
H-51	PSN 310 D Battery	564120	132330
H-42	A Battery	573750	128320
H-40	PSN330	576460	134450
H-50	PSN320	568220	130884
Guard towers:			
200-East[c]		575252	134845
200-West[d]		568379	136024
Hanford townsite	Camp Hanford	585450	139050
Ringold		595500	132000
Richland		594000	105800

	REDOX stack [b]			B Plant stack [b]			T Plant stack [b]		
Receptors	Distance (m)	Angle (°) from N	Sector	Distance (m)	Angle (°) from N	Sector	Distance (m)	Angle (°) from N	Sector
H-61	5417	319	NW	9778	280	W	3941	288	WNW
H-51	3812	243	WSW	10288	247	WSW	5785	218	SW
H-42	8446	133	SE	8065	179	S	10482	145	SE
H-40	8940	87	E	3472	124	SE	9094	105	ESE
H-50	3225	168	SSE	7676	224	SW	6016	175	S
Guard towers:									
200-East[c]	7763	84	E	2282	133	SE	7827	105	ESE
200-West[d]	2164	23	NNE	5209	266	W	1093	141	SE
Hanford townsite	18609	74	ENE	12170	77	ENE	17886	83	E
Ringold	28044	94	E	22358	101	ESE	28228	100	E
Richland	38702	137	SE	36776	146	SSE	40715	140	SE

[a] Obtained from Hanford Site Atlas. The Internet address for the Hanford Geographic Information System is currently http://www.bhi-erc.com/projects/p_m/eis/hgis/hgis.htm. For security purposes, password/user registration is required. Projection coordinate system is Washington State Plane, and units are meters.

[b] The indicated angle from north and the sector refer to the location of the receptor relative to the source, and *not* to the wind direction. The correct sector for the direction the wind blows *from* is the reciprocal of the one given. For example, receptor H-61 is NW from the REDOX stack; but the wind direction that would place H-61 downwind from the REDOX stack is (from) SE.

[c] 200-East perimeter at the southeast entrance (intersection of Route 4 South and existing perimeter fence at Canton Avenue).

[d] 200-West perimeter at the east entrance (intersection of Route 3 and existing perimeter fence at 20th Street).

Given these probabilities, we are interested in the subject's risk of contacting or inhaling one or more particles from this release. From Eq. (E-8), we have

$$\Pr[\text{one or more}] = 1 - (1-p)^N = 1 - (1 - 1.05 \times 10^{-7})^{2.9\times10^8} = 1.000 \text{ contact}$$
$$= 1 - (1 - 4.94 \times 10^{-12})^{2.9\times10^8} = 1.43 \times 10^{-3} \text{ inhalation}$$

The contrast in these two probabilities may astonish some readers. Coming into external contact with at least one particle is effectively certain under the assumed (extreme) conditions of exposure, but inhaling one or more particles under the same exposure conditions is less than two chances in one thousand. How could this be?

Let us consider a single particle that is destined to pass through the subject's shadow. As the particle arrives, in one second, 5.628 m^3 of air flows through the shadow (i.e., around the subject). In the same time, the subject breathes 2.66×10^{-4} m^3 of that volume. The ratio of the latter to the former number is the probability that the particle will be inhaled, given that it is in the larger volume (i.e., given that it arrives at the subject):

$$\Pr[\text{particle inhaled} \mid \text{arrival}] = \frac{2.66 \times 10^{-4}}{5.628} = 4.73 \times 10^{-5}$$

Thus if the particle arrives at the subject, its probability of being inhaled is only about 50 chances in one million. Now multiplying this conditional probability by the probability of encounter p gives

$$\Pr[\text{particle inhaled}] = 4.73 \times 10^{-5} \times 1.05 \times 10^{-7} = 4.96 \times 10^{-12}$$

the same (except for rounding) as we calculated directly from Eq. (E-5). How many particles would we expect the subject to be exposed to?

$$N_r p = 2.9 \times 10^8 \times 1.05 \times 10^{-7} = 30.5 \approx 31$$

for the event we are discussing. We emphasize that this is the mean or "expected" number; the model allows the possibility of more or fewer in random repetitions of the release-dispersion event.

Since we assumed an extreme potential exposure regimen (around-the-clock outdoor exposure for the duration of the event), it is reasonable to inquire about the extent of mitigation that would occur for a less exposed subject. Let us assume that the subject is outdoors only one-tenth of the time during the course of the release event. We need only multiply the probabilities p and p_b by a factor $U = 0.1$ and recalculate:

$$\Pr[\text{one or more}] = 1 - (1 - Up)^N = 1 - (1 - 1.05 \times 10^{-8})^{2.9\times10^8} = 0.952 \text{ contact}$$
$$= 1 - (1 - 4.94 \times 10^{-13})^{2.9\times10^8} = 1.43 \times 10^{-4} \text{ inhalation}$$

Thus the exposure reduction gains a small decrease in the probability of encountering one or more of the particles and an order-of-magnitude reduction in the already small probability of inhaling one or more. Even so, the subject is still likely to have contact with particles on clothes or skin, even with less than two and one-half hours of outdoor time each day.

An application of the Poisson distribution might begin with the expected number of particle encounters N_s (or N_b):

$N_s = \mu_s = 2.9 \times 10^8 \times 1.86 \times 10^{-8} \times 5.628 = 30.4$ (rounding difference with previous value)

$N_b = \mu_b = 2.9 \times 10^8 \times 1.86 \times 10^{-8} \times 2.66 \times 10^{-4} = 1.46 \times 10^{-3}$

Table E-8. Comparison of Poisson and Binomial Probabilities for Example [a]

k	Poisson: $(\mu^k/k!)e^{-\mu}$	Binomial: $\binom{N}{k}p^k(1-p)^{N-k}$
0	6.2726×10^{-14}	5.9667×10^{-14}
1	1.9069×10^{-12}	1.8169×10^{-12}
2	2.8984×10^{-11}	2.7662×10^{-11}
3	2.9371×10^{-10}	2.8077×10^{-10}
4	2.2322×10^{-9}	2.1373×10^{-9}
5	1.3572×10^{-8}	1.3016×10^{-8}
6	6.8763×10^{-8}	6.6058×10^{-8}
7	2.9863×10^{-7}	2.8735×10^{-7}
8	1.1348×10^{-6}	1.0937×10^{-6}
9	3.8331×10^{-6}	3.7005×10^{-6}
10	1.1653×10^{-5}	1.1268×10^{-5}
11	3.2203×10^{-5}	3.1192×10^{-5}
12	8.1582×10^{-5}	7.9149×10^{-5}
13	1.9078×10^{-4}	1.8539×10^{-4}
14	4.1426×10^{-4}	4.0322×10^{-4}
15	8.3956×10^{-4}	8.1855×10^{-4}

[a] Parameter values: Poisson — μ = 30.4; Binomial — $N = 2.9 \times 10^8$, $p = 1.05 \times 10^{-7}$. The probabilities increase until k = 30, with maximum values 0.07244 for Poisson and 0.07239 for binomial.

The corresponding estimates of Poisson probabilities for one or more encounters are

$$\Pr[\text{one or more}\,|\,s] = 1 - \exp(-30.4) = 1.000$$
$$\Pr[\text{one or more}\,|\,b] = 1 - \exp(-1.43 \times 10^{-3}) = 1.43 \times 10^{-3}$$

which agree with previous results.

We need to point out, however, that the two distributions are not strictly equivalent in this application. As we indicated in Section E-1, the Poisson distribution does not depend explicitly on the number of particles in the release, whereas the binomial distribution does. We also explained that the Poisson distribution is often applied to rare events and may be thought of as a limiting form of the binomial distribtuion as $p \to 0$ in such a way that the mean $\mu = Np$ remains constant. Table E-8 shows the degree of approximation for this example. If the table were extended, it would show maximum individual probabilities for k = 30, with Poisson equal to 0.07244 and binomial equal to 0.07239. The good agreement for small numbers of particle encounters that may at first seem surprising comes from the derivation of the Poisson parameter μ from the binomial parameters N_r and p. Properties and other applications of these distributions are given in statistics textbooks (e.g., Snedecor and Cochran 1967).

It is possible that the same subject may be exposed to multiple particle-release events with different numbers N_r of released particles and different probabilities p and p_b of encounter. One would be interested in the collective effect of such encounters, and the theory needs to be extended for the more complex exposure potential.

We have the following general suggestion. Suppose the M events involve release numbers N_i, $i = 1, \ldots, M$ and respective encounter probabilities p_i (these might be either clothing-skin or inhalation, but all of the same type for a particular analysis). Use the binomial means $\mu_i = N_i p_i$, $i = 1, \ldots, M$ and sum them (these are assumed to be independent release events):

$$\mu = \sum_{i=1}^{M} \mu_i = \sum_{i=1}^{M} N_i p_i$$

Then use this mean μ of the number of encounters for all exposure events as the parameter of the Poisson distribution, which can be used for approximate individual or cumulative probabilities of encounters (e.g., Pr[one or more] = $1 - \exp(-\mu)$). This is a common type of application of the Poisson distribution, and its utility is that it works for sums of independent binomial random variables having different individual distribution parameters. The application works well if each individual binomial distribution $\mathrm{Bi}(N_i, p_i)$ is well approximated by its Poisson counterpart $\mathrm{Po}(\mu_i)$, because the sum of the independent Poisson random variables also has the Poisson distribution $\mathrm{Po}(\sum_{i=1}^{M} \mu_i)$ with mean equal to the sum of the individual means (Kendall and Stuart 1969).

We illustrate this approach by calculating the probability of encounter with particles from ten unusual ruthenium release events at the REDOX plant from March 1952 through June 1954. We consider a subject at each of five military locations (designated H-61, H-51, H-42, H-40, and H-50), two guard towers (200-E and 200-W), the Hanford Townsite, and the towns of Ringold and Richland. For each receptor location and each incident, we compute the expected number of particle interactions with the subject for body surface and inhalation. We assume that the incidents are stochastically independent and sum the expected numbers over all ten events for each receptor location. The sum for a given subject represents the expected number of encounters if the subject is exposed to all ten events. In carrying out these calculations, we calculate the maximum potential numbers of encounters by assuming that each subject remains outdoors 24 hours per day throughout the month of each release event. But attenuation of exposure times or reduction of exposure by partial shelter or both can be considered by introducing a fractional use factor U. For example, if $U = 0.1$, each expected number of interactions is one-tenth of the unadjusted value. Table E-9 shows the results of these calculations.

We continue with the assumption that each subject is exposed to all ten events and estimate the probabilities of encounters with one or more particles for each exposure mode (contact with body surface or inhalation). Table E-10 presents these results for both maximum potential exposure and for attenuation by use factor $U = 0.1$. The computation uses the Poisson probability corresponding to the sum of the expected numbers of encounters over all ten events: Pr[one or more] = $1 - \exp(-\mu)$ where $\mu = \mu_1 + \cdots + \mu_{10}$ and μ_i is the expected number of encounters for incident i. To apply the use factor U, replace μ by $U\mu$. The μ_i are, of course, different for the two exposure modes.

The results shown in Table E-10 raise some points of interest. Even with the attenuated exposure implied by the 10-percent use factor (last two columns), and even at the more-distant Ringold and Richland locations, body surface contact with one or more released particles is virtually certain, but inhalation of one or more is very unlikely. The reduction of the maximum potential inhalation probabilities by the ten-percent use factor is approximately a factor of ten, whereas the reduction for the body contact mode is insignificant. (For $|\mu|$ much less than 1, $1 - \exp(-\mu) \approx \mu$, so that reduction of μ by a factor of ten would correspond to about the same reduction of the Poisson probability; but

Table E-9. Expected Numbers of Radioactive Particle Encounters for Several Receptor Locations and Unusual Ruthenium Particle Release Incidents from the REDOX Plant during the Early 1950s [a]

Month	Particles released	H-61[b]		H-51[b]		H-42[b]		H-40[b]		H-50[b]	
		Body	Inhalation	Body	Inhalation	Body	Inhalation	Body	Inhalation	Body	Inhalation
Mar-52	2.9×10^{8}	1.1×10^{2}	1.4×10^{-2}	9.2×10^{1}	1.4×10^{-2}	2.3×10^{2}	1.1×10^{-2}	5.9×10^{1}	3.6×10^{-3}	2.6×10^{2}	2.6×10^{-2}
Apr-52	2.1×10^{7}	7.5	1.0×10^{-3}	6.5	9.7×10^{-4}	1.6×10^{1}	7.6×10^{-4}	4.2	2.6×10^{-4}	1.9×10^{1}	1.8×10^{-3}
Jun-52	1.8×10^{5}	6.7×10^{-2}	8.9×10^{-6}	5.7×10^{-2}	8.5×10^{-6}	1.5×10^{-1}	6.9×10^{-6}	3.8×10^{-2}	2.3×10^{-6}	1.6×10^{-1}	1.6×10^{-5}
Sep-52	9.9×10^{5}	3.9×10^{-1}	5.2×10^{-5}	3.3×10^{-1}	4.9×10^{-5}	8.5×10^{-1}	4.0×10^{-5}	2.2×10^{-1}	1.3×10^{-5}	9.2×10^{-1}	9.0×10^{-5}
Aug-53	1.3×10^{6}	5.3×10^{-1}	7.0×10^{-5}	4.4×10^{-1}	6.6×10^{-5}	1.1	5.4×10^{-5}	3.0×10^{-1}	1.8×10^{-5}	1.243	1.2×10^{-4}
Sep-53	1.9×10^{8}	7.4×10^{1}	9.9×10^{-3}	6.2×10^{1}	9.3×10^{-3}	1.6×10^{2}	7.6×10^{-3}	4.2×10^{1}	2.6×10^{-3}	1.7×10^{2}	1.7×10^{-2}
Jan-54	4.3×10^{8}	1.5×10^{2}	2.0×10^{-2}	1.3×10^{2}	1.9×10^{-2}	3.2×10^{2}	1.5×10^{-2}	8.3×10^{1}	5.1×10^{-3}	3.7×10^{2}	3.7×10^{-2}
Apr-54	2.9×10^{5}	1.1×10^{-1}	1.5×10^{-5}	9.6×10^{-2}	1.4×10^{-5}	2.5×10^{-1}	1.2×10^{-5}	6.5×10^{-2}	4.0×10^{-6}	2.7×10^{-1}	2.7×10^{-5}
May-54	7.1×10^{5}	2.7×10^{-1}	3.7×10^{-5}	2.3×10^{-1}	3.5×10^{-5}	6.0×10^{-1}	2.8×10^{-5}	1.6×10^{-1}	9.5×10^{-6}	6.6×10^{-1}	6.4×10^{-5}
Jun-54	1.1×10^{5}	4.3×10^{-2}	5.8×10^{-6}	3.7×10^{-2}	5.5×10^{-6}	9.5×10^{-2}	4.5×10^{-6}	2.5×10^{-2}	1.5×10^{-6}	1.0×10^{-1}	1.0×10^{-5}
Total		3.4×10^{2}	4.5×10^{-2}	2.9×10^{2}	4.3×10^{-2}	7.3×10^{2}	3.4×10^{-2}	1.9×10^{2}	1.2×10^{-2}	8.3×10^{2}	8.1×10^{-2}

Month	Particles released	200-East guard tower[c]		200-West guard tower[d]		Townsite		Ringold		Richland	
		Body	Inhalation	Body	Inhalation	Body	Inhalation	Body	Inhalation	Body	Inhalation
Mar-52	2.9×10^{8}	7.1×10^{1}	4.3×10^{-3}	2.1×10^{2}	1.1×10^{-2}	2.5×10^{1}	1.1×10^{-3}	1.3×10^{1}	8.1×10^{-4}	3.1×10^{1}	1.5×10^{-3}
Apr-52	2.1×10^{7}	5.0	3.1×10^{-4}	1.5×10^{1}	7.8×10^{-4}	1.8	7.9×10^{-5}	9.4×10^{-1}	5.7×10^{-5}	2.2	1.0×10^{-4}
Jun-52	1.8×10^{5}	4.5×10^{-2}	2.8×10^{-6}	1.3×10^{-1}	6.7×10^{-6}	1.8×10^{-2}	7.7×10^{-7}	9.5×10^{-3}	5.8×10^{-7}	2.4×10^{-2}	1.1×10^{-6}
Sep-52	9.9×10^{5}	2.6×10^{-1}	1.6×10^{-5}	7.3×10^{-1}	3.8×10^{-5}	1.0×10^{-1}	4.5×10^{-6}	5.7×10^{-2}	3.5×10^{-6}	1.4×10^{-1}	6.7×10^{-6}
Aug-53	1.3×10^{6}	3.5×10^{-1}	2.2×10^{-5}	9.8×10^{-1}	5.1×10^{-5}	1.4×10^{-1}	6.1×10^{-6}	7.6×10^{-2}	4.7×10^{-6}	1.9×10^{-1}	9.0×10^{-6}
Sep-53	1.9×10^{8}	5.0×10^{1}	3.0×10^{-3}	1.4×10^{2}	7.1×10^{-3}	1.9×10^{1}	8.6×10^{-4}	1.1×10^{1}	6.5×10^{-4}	2.7×10^{1}	1.3×10^{-3}
Jan-54	4.3×10^{8}	1.0×10^{2}	6.1×10^{-3}	3.0×10^{2}	1.6×10^{-2}	3.5×10^{1}	1.5×10^{-3}	1.8×10^{1}	1.1×10^{-3}	4.1×10^{1}	1.9×10^{-3}
Apr-54	2.9×10^{5}	7.7×10^{-2}	4.7×10^{-6}	2.1×10^{-1}	1.1×10^{-5}	3.0×10^{-2}	1.3×10^{-6}	1.6×10^{-2}	1.0×10^{-6}	4.1×10^{-2}	1.9×10^{-6}
May-54	7.1×10^{5}	1.9×10^{-1}	1.1×10^{-5}	5.2×10^{-1}	2.7×10^{-5}	7.2×10^{-2}	3.2×10^{-6}	3.9×10^{-2}	2.4×10^{-6}	9.8×10^{-2}	4.6×10^{-6}
Jun-54	1.1×10^{5}	3.0×10^{-2}	1.8×10^{-6}	8.3×10^{-2}	4.3×10^{-6}	1.1×10^{-2}	5.0×10^{-7}	6.2×10^{-3}	3.8×10^{-7}	1.5×10^{-2}	7.3×10^{-7}
Total		2.3×10^{2}	1.4×10^{-2}	6.7×10^{2}	3.5×10^{-2}	8.1×10^{1}	3.6×10^{-3}	4.3×10^{1}	2.6×10^{-3}	1.0×10^{2}	4.8×10^{-3}

[a] Each expected number of particle encounters shown in the table represents the maximum potential number, given the estimated number of particles released and the dispersion model as parameterized, i.e., the number corresponds to outdoor around-the-clock exposure of the subject for the entire month of the release incident. Exposure may be attenuated by a fractional use factor U. For example, if $U = 0.1$, each expected number of particle encounters is reduced to one-tenth of its value. This could account for reduced exposure times or partial sheltering or both.

[b] Location of military personnel; see Figure 1-2.

[c] Tower is located near the southeast corner of 200-E; see Figure 1-2.

[d] Tower is located near the center of the east side of 200-W; see Figure 1-2.

the accuracy of this approximation decreases as $|\mu|$ increases, and thus the effect is minor for large $|\mu|$ corresponding to body surface contact.) For persons at some receptor locations, the maximum potential columns may be more nearly applicable than those reduced by the use factor. It is perhaps more likely that the individuals manning some military stations spent extended periods outdoors, with only partial shelter such as tents during off-watch times. Note that the maximum probability of inhaling one or more particles is 0.078 for the receptor at the military post H-50. Of course, it would be necessary to construct realistic scenarios for such exposures to estimate appropriate use factors. It could turn out to be unlikely that any one individual would have been at H-50 during all of the incidents. This level of detail was beyond the scope of this task order.

Table E-10. Probabilities of Particle Contact with Body Surface and of Particle Inhalation during Unusual REDOX Ruthenium Particle Releases, March 1952–June 1954

	Maximum potential for exposure		Exposure for use factor 0.1	
Exposure Location	Probability of particle contact[a] with body surface	Probability of particle inhalation[a]	Probability of particle contact[a] with body surface	Probability of particle inhalation[a]
H-61[b]	1.0	0.044	1.0	0.0045
H-51[b]	1.0	0.042	1.0	0.0043
H-42[b]	1.0	0.034	1.0	0.0034
H-40[b]	1.0	0.011	1.0	0.0012
H-50[b]	1.0	0.078	1.0	0.0081
200-E guard tower[c]	1.0	0.014	1.0	0.0014
200-W guard tower[d]	1.0	0.034	1.0	0.0035
Hanford Townsite	1.0	0.0036	0.9997	0.00036
Ringold	1.0	0.0026	0.9860	0.00026
Richland	1.0	0.0048	0.99996	0.00048

[a] Interaction of subject with one or more particles.
[b] Location of military personnel; see Figure 1-2.
[c] Tower is located near the southeast corner of 200-E; see Figure 1-2.
[d] Tower is located near the center of the east side of 200-W; see Figure 1-2.

E-5. DISCUSSION AND CONCLUSIONS

This appendix presents methods for estimating the probability of encounter of an exposed subject on or near the Hanford site in the 1940s or 1950s with airborne radioactive particles released routinely or during unusual events during that period. The modes of encounter illustrated are contact of the particle with the body surface (clothing or exposed skin) and inhalation. The latter mode of contact with one or more released particles was shown to be generally much less likely than the former.

The methods depend on (a) atmospheric diffusion and deposition models similar to those programmed in HCalc for generic application to the Hanford site during the period of interest and (b) elementary theory of the binomial and Poisson probability distributions for discrete events. As with any simulation, the reader must bear in mind that the applicability of results depends on the applicability of the models that are linked together to produce the results. We feel confident that the approach we have outlined and illustrated will lead to results that are conservative if the interpretations are carefully considered. Note, however, the cautions and complications discussed below.

In using the atmospheric diffusion and deposition models to estimate expected numbers of particle encounters and probabilities of one or more encounters, we have not burdened the discussion with the formalisms of uncertainty that we developed in Appendix D, although these methods

certainly are applicable. But most readers are likely to find that a probability of particle encounters that possesses its own uncertainty distribution with median and 95th percentile requires a level of interpretation that they would prefer to avoid at a first reading. Specialists may quietly deal with the added complexities and, for example, present the 95th percentiles of the desired probabilities in the tables (a conservative practice), with disclosures in the footnotes.

Other questions remain, such as dealing with the dosimetric consequences of an encounter with particles. These questions can quickly become complicated, and interpreting them and discussing them with the public may prove difficult until a sufficient base of experience is established. The universe of possibilities is large for an encounter with "one or more" particles, because there can be few or many, and they are a random sample (with random sample size) from a particle size distribution. In each case, the amount of radioactivity carried by each particle must be covered by a reasonable assumption (e.g., uniformly distributed with respect to the particle's surface area — which is randomly determined by the particle size distribution, or controlled by some other probability distribution that might allow discrete and varying amounts on the individual carrier particles). What would likely arise from such an analysis is yet another distribution of effect (such as respiratory dose or risk for the inhalation mode) *given* the exposure consequent to the encounter. Thus one might be considering the 95th percentile of a lung cancer risk *given* a particle encounter with probability, say, 0.001 (95th percentile, as in the previous paragraph). The risk estimate for lung cancer would then be the product of the conditional risk given the particle encounter and the probability of the encounter (0.001 in our example). Even more complexity arises as the tree of consequences branches into ever more possibilities (for inhalation microdosimetry: which respiratory region the particle deposits in, if it is not exhaled; for body surface contact: where the particle deposits — on the back of the hand, in the ear, in the eye, lodged in clothing, and so on).

Applications of these methods require, as much as anything else, reasonable scenarios for the specific doses and risks being assessed. In our experience, this is one of the most difficult parts of the task. Even so, beyond the need for illustration, this function was mostly excluded from this task order. Without doubt, pursuing it further would have demonstrated the need for some extensions of the theory and implementation tools. But we believe we have at least anticipated the starting point for most needs.

REFERENCES

Abramowitz, M., and I.A. Stegun. 1965. *Handbook of Mathematical Functions.* Dover Publications, Inc., New York.

Hanna, S.R., G.A. Briggs, and R.P. Hosker, Jr. 1982. *Handbook on Atmospheric Diffusion.* Report DOE/TIC-11223 (DE82002045), Technical Information Center, U.S. Department of Energy.

Kendall, M.G., and A. Stuart. 1969. *The Advanced Theory of Statistics — Volume 1. Distribution Theory.* Hafner Publishing Company, New York.

Sehmel, G.A., and W.H. Hodgson. 1980. "A Model for Predicting Dry Deposition of Particles and Gases to Environmental Surfaces," in *Implications of Clean Air Amendments of 1977 and of Energy Considerations for Air Pollution Control.* Symposium Series #196, vol. 76, American Institute of Chemical Engineers Symposium Series.

Snedecor, G.W., and W.G. Cochran. 1967. *Statistical Methods,* Sixth Edition. The Iowa State University Press, Ames, Iowa.

Stone, W.A., J.M. Thorp, O.P. Gifford, and D.J. Hoitink. 1983. *Climatological Summary for the Hanford Area.* Report PNL-4622, Pacific Northwest Laboratory, Richland, Washington.

Van der Hoven, I. 1968. "Deposition of Particles and Gases," Section 5–3 in *Meteorology and Atomic Energy 1968,* D. Slade, Ed. Report TID-24190, Office of Information Services, U.S. Atomic Energy Commission.